

Insights in alzheimer's disease and related dementias

Edited by

Agustin Ibanez, Allison B. Reiss, Suvarna Alladi and Nilton Custodio

Published in

Frontiers in Aging Neuroscience



FRONTIERS EBOOK COPYRIGHT STATEMENT

The copyright in the text of individual articles in this ebook is the property of their respective authors or their respective institutions or funders. The copyright in graphics and images within each article may be subject to copyright of other parties. In both cases this is subject to a license granted to Frontiers.

The compilation of articles constituting this ebook is the property of Frontiers.

Each article within this ebook, and the ebook itself, are published under the most recent version of the Creative Commons CC-BY licence. The version current at the date of publication of this ebook is CC-BY 4.0. If the CC-BY licence is updated, the licence granted by Frontiers is automatically updated to the new version.

When exercising any right under the CC-BY licence, Frontiers must be attributed as the original publisher of the article or ebook, as applicable.

Authors have the responsibility of ensuring that any graphics or other materials which are the property of others may be included in the CC-BY licence, but this should be checked before relying on the CC-BY licence to reproduce those materials. Any copyright notices relating to those materials must be complied with.

Copyright and source acknowledgement notices may not be removed and must be displayed in any copy, derivative work or partial copy which includes the elements in question.

All copyright, and all rights therein, are protected by national and international copyright laws. The above represents a summary only. For further information please read Frontiers' Conditions for Website Use and Copyright Statement, and the applicable CC-BY licence.

ISSN 1664-8714
ISBN 978-2-83250-985-2
DOI 10.3389/978-2-83250-985-2

About Frontiers

Frontiers is more than just an open access publisher of scholarly articles: it is a pioneering approach to the world of academia, radically improving the way scholarly research is managed. The grand vision of Frontiers is a world where all people have an equal opportunity to seek, share and generate knowledge. Frontiers provides immediate and permanent online open access to all its publications, but this alone is not enough to realize our grand goals.

Frontiers journal series

The Frontiers journal series is a multi-tier and interdisciplinary set of open-access, online journals, promising a paradigm shift from the current review, selection and dissemination processes in academic publishing. All Frontiers journals are driven by researchers for researchers; therefore, they constitute a service to the scholarly community. At the same time, the *Frontiers journal series* operates on a revolutionary invention, the tiered publishing system, initially addressing specific communities of scholars, and gradually climbing up to broader public understanding, thus serving the interests of the lay society, too.

Dedication to quality

Each Frontiers article is a landmark of the highest quality, thanks to genuinely collaborative interactions between authors and review editors, who include some of the world's best academicians. Research must be certified by peers before entering a stream of knowledge that may eventually reach the public - and shape society; therefore, Frontiers only applies the most rigorous and unbiased reviews. Frontiers revolutionizes research publishing by freely delivering the most outstanding research, evaluated with no bias from both the academic and social point of view. By applying the most advanced information technologies, Frontiers is catapulting scholarly publishing into a new generation.

What are Frontiers Research Topics?

Frontiers Research Topics are very popular trademarks of the *Frontiers journals series*: they are collections of at least ten articles, all centered on a particular subject. With their unique mix of varied contributions from Original Research to Review Articles, Frontiers Research Topics unify the most influential researchers, the latest key findings and historical advances in a hot research area.

Find out more on how to host your own Frontiers Research Topic or contribute to one as an author by contacting the Frontiers editorial office: frontiersin.org/about/contact

Insights in alzheimer's disease and related dementias

Topic editors

Agustin Ibanez — Latin American Brain Health Institute (BrainLat), Chile

Allison B. Reiss — New York University, United States

Suvarna Alladi — National Institute of Mental Health and Neurosciences (NIMHANS), India

Nilton Custodio — Peruvian Institute of Neurosciences (IPN), Peru

Citation

Ibanez, A., Reiss, A. B., Alladi, S., Custodio, N., eds. (2022). *Insights in alzheimer's disease and related dementias*. Lausanne: Frontiers Media SA.
doi: 10.3389/978-2-83250-985-2

Table of contents

| | |
|-----|--|
| 06 | Editorial: Insights in Alzheimer's disease and related dementias Agustín Ibáñez, Allison B. Reiss, Nilton Custodio and Suvarna Alladi |
| 11 | Moderate increase of serum uric acid within a normal range is associated with improved cognitive function in a non-normotensive population: A nationally representative cohort study Jinqi Wang, Rui Jin, Zhiyuan Wu, Yueruijing Liu, Xiaohan Jin, Ze Han, Yue Liu, Zongkai Xu, Xiuhua Guo and Lixin Tao |
| 24 | Identification and immunological characterization of cuproptosis-related molecular clusters in Alzheimer's disease Yongxing Lai, Chunjin Lin, Xing Lin, Lijuan Wu, Yinan Zhao and Fan Lin |
| 40 | Alzheimer's disease and epilepsy: The top 100 cited papers Gui-Fen Zhang, Wen-Xin Gong, Zheng-Yan-Ran Xu and Yi Guo |
| 57 | Independent effect of body mass index variation on amyloid-β positivity Sung Hoon Kang, Jong Hyuk Kim, Yoosoo Chang, Bo Kyoung Cheon, Yeong Sim Choe, Hyemin Jang, Hee Jin Kim, Seong-Beom Koh, Duk L. Na, Kyunga Kim and Sang Won Seo |
| 67 | Excessive/Aberrant and Maladaptive Synaptic Plasticity: A Hypothesis for the Pathogenesis of Alzheimer's Disease Shigeki Kawabata |
| 77 | Investigation of coenzyme Q10 status, serum amyloid-β, and tau protein in patients with dementia Po-Sheng Chang, Hsi-Hsien Chou, Te-Jen Lai, Chi-Hua Yen, Ji-Cyun Pan and Ping-Ting Lin |
| 91 | Presenilin Deficiency Increases Susceptibility to Oxidative Damage in Fibroblasts Kun Zou, Sadequl Islam, Yang Sun, Yuan Gao, Tomohisa Nakamura, Hiroto Komano, Taisuke Tomita and Makoto Michikawa |
| 100 | Extraversion Is Associated With Lower Brain Beta-Amyloid Deposition in Cognitively Normal Older Adults Hwamee Oh |
| 110 | Genome Sequencing Variations in the Octodon degus, an Unconventional Natural Model of Aging and Alzheimer's Disease Michael J. Hurley, Claudio Urra, B. Maximiliano Garduno, Agostino Bruno, Allison Kimbell, Brent Wilkinson, Cristina Marino-Buslje, Marcelo Ezquer, Fernando Ezquer, Pedro F. Aburto, Elie Poulin, Rodrigo A. Vasquez, Robert Deacon, Ariel Avila, Francisco Altimiras, Peter Whitney Vanderklisch, Guido Zampieri, Claudio Angione, Gabriele Constantino, Todd C. Holmes, Marcelo P. Coba, Xiangmin Xu and Patricia Cogram |

- 126 **Different Profiles of Spatial Navigation Deficits In Alzheimer's Disease Biomarker-Positive Versus Biomarker-Negative Older Adults With Amnesic Mild Cognitive Impairment**
Martina Laczó, Lukas Martinkovic, Ondrej Lerch, Jan M. Wiener, Jana Kalinova, Veronika Matuskova, Zuzana Nedelska, Martin Vyhnaek, Jakub Hort and Jan Laczó
- 150 **Endophenotypic effects of the *SORL1* variant rs2298813 on regional brain volume in patients with late-onset Alzheimer's disease**
Chun-Yu Chen, Yung-Shuan Lin, Wei-Ju Lee, Yi-Chu Liao, Yu-Shan Kuo, Albert C. Yang and Jong-Ling Fuh
- 160 **Differential Abnormality in Functional Connectivity Density in Preclinical and Early-Stage Alzheimer's Disease**
Yu Song, Huimin Wu, Shanshan Chen, Honglin Ge, Zheng Yan, Chen Xue, Wenzhang Qi, Qianqian Yuan, Xuhong Liang, Xingjian Lin and Jiu Chen
- 173 **Cortical neuroanatomical changes related to specific language impairments in primary progressive aphasia**
Sung Hoon Kang, Yu Hyun Park, Jiho Shin, Hang-Rai Kim, Jihwan Yun, Hyemin Jang, Hee Jin Kim, Seong-Beom Koh, Duk L. Na, Mee Kyung Suh and Sang Won Seo
- 184 **Autophagy Impairment in *App* Knock-in Alzheimer's Model Mice**
Richeng Jiang, Makoto Shimozaawa, Johanna Mayer, Simone Tambaro, Rakesh Kumar, Axel Abelein, Bengt Winblad, Nenad Bogdanovic and Per Nilsson
- 194 **Phenotypic Displays of Cholinergic Enzymes Associate With Markers of Inflammation, Neurofibrillary Tangles, and Neurodegeneration in Pre- and Early Symptomatic Dementia Subjects**
Unnur D. Teitsdottir, Taher Darreh-Shori, Sigrun H. Lund, Maria K. Jonsdottir, Jon Snaedal and Petur H. Petersen
- 208 **The Effects of Brain Magnetic Resonance Imaging Indices in the Association of Olfactory Identification and Cognition in Chinese Older Adults**
Ziyi Tan, Yingzhe Wang, Heyang Lu, Weizhong Tian, Kelin Xu, Min Fan, Xiaolan Zhao, Li Jin, Mei Cui, Yanfeng Jiang and Xingdong Chen
- 216 **Characterizing Differences in Functional Connectivity Between Posterior Cortical Atrophy and Semantic Dementia by Seed-Based Approach**
Yi Chen, Qingze Zeng, Yunyun Wang, Xiao Luo, Yan Sun, Lumi Zhang, Xiaoyan Liu, Kaicheng Li, Minming Zhang and Guoping Peng

229 Distinctive Temporal Trajectories of Alzheimer's Disease Biomarkers According to Sex and APOE Genotype: Importance of Striatal Amyloid

Jun Pyo Kim, Min Young Chun, Soo-Jong Kim, Hyemin Jang, Hee Jin Kim, Jee Hyang Jeong, Duk L. Na and Sang Won Seo for the Alzheimer's Disease Neuroimaging Initiative

238 Aged Cattle Brain Displays Alzheimer's Disease-Like Pathology and Promotes Brain Amyloidosis in a Transgenic Animal Model

Ines Moreno-Gonzalez, George Edwards III, Rodrigo Morales, Claudia Duran-Aniotz, Gabriel Escobedo Jr., Mercedes Marquez, Marti Pumarola and Claudio Soto



OPEN ACCESS

EDITED BY

Stephen D. Ginsberg,
Nathan Kline Institute for Psychiatric
Research, United States

REVIEWED BY

Sylvia Eva Perez,
Barrow Neurological Institute (BNI),
United States

*CORRESPONDENCE

Agustín Ibáñez
agustin.ibanez@gbhi.org

SPECIALTY SECTION

This article was submitted to
Alzheimer's Disease and Related
Dementias,
a section of the journal
Frontiers in Aging Neuroscience

RECEIVED 12 October 2022

ACCEPTED 14 November 2022

PUBLISHED 23 November 2022

CITATION

Ibáñez A, Reiss AB, Custodio N and
Alladi S (2022) Editorial: Insights in
Alzheimer's disease and related
dementias.
Front. Aging Neurosci. 14:1068156.
doi: 10.3389/fnagi.2022.1068156

COPYRIGHT

© 2022 Ibáñez, Reiss, Custodio and
Alladi. This is an open-access article
distributed under the terms of the
[Creative Commons Attribution License](#)
(CC BY). The use, distribution or
reproduction in other forums is
permitted, provided the original
author(s) and the copyright owner(s)
are credited and that the original
publication in this journal is cited, in
accordance with accepted academic
practice. No use, distribution or
reproduction is permitted which does
not comply with these terms.

Editorial: Insights in Alzheimer's disease and related dementias

Agustín Ibáñez^{1,2,3,4*}, Allison B. Reiss⁵, Nilton Custodio^{6,7} and
Suvarna Alladi⁸

¹Latin American Brain Health Institute (BrainLat), Universidad Adolfo Ibáñez, Santiago, Chile, ²Cognitive Neuroscience Center (CNC), Universidad de San Andrés and CONICET, Buenos Aires, Argentina, ³Global Brain Health Institute (GBHI), University of California, San Francisco (UCSF), San Francisco, CA, United States, ⁴Trinity College Dublin (TCD), Dublin, Ireland, ⁵Department of Medicine and Biomedical Research Institute, NYU Long Island School of Medicine, Mineola, NY, United States, ⁶Department of Neurology, Instituto Peruano de Neurociencias, Lima, Peru, ⁷Unit of Diagnosis of Cognitive Impairment and Dementia Prevention, Instituto Peruano de Neurociencias, Lima, Peru, ⁸Department of Neurology, National Institute of Mental Health and Neurosciences, Bengaluru, India

KEYWORDS

dementia, Alzheimer's disease (AD), ADRD, research, clinical, imaging, genetics

Editorial on the Research Topic

Insights in Alzheimer's disease and related dementias

Introduction

According to the World Alzheimer's Report ([Alzheimer's Disease International, 2022](#)) and the Global status report on the public health response to dementia ([WHO, 2022](#)), 55+ million people live with dementia, a condition characterized by deterioration in cognition and functionality beyond the expected effects of normal aging. WHO has recognized dementia as a public health priority. Alzheimer's disease and related dementias (ADRD) may result from a disparate combination of processes, including genetic and environmental factors (fiscal, social, economic), pathological processes, and injuries that primarily or secondarily affect the brain. Dementia is a leading cause of disability, dependence and death among older people globally. The impact of dementia at personal and societal levels is unequally distributed, usually following a distribution similar to that of the inequality index of the corresponding country.

Current dementia research is transitioning from more simplistic and universal models toward complex, multilevel, heterogeneity-sensitive, and diversity-oriented frameworks. These landscapes of dementia science are changing rapidly, creating novel bridges across disciplines, diverse populations, regions, scales, methods and approaches. Some of these reconfigurations are driven by animal and human research focused in multiple emerging areas such as diversity contributions to genetic traits ([Dehghani et al., 2021](#)); heterogeneity and variation in protein misfolding and aggregation ([Frisoni et al., 2022](#)); explanatory models based on excitation/inhibition synaptic activity ([Babiloni et al., 2020](#)); impact of multiple sources of disparities (gender, admixtures, cultural, socioeconomic) ([Alladi and Hachinski, 2018](#); [Parra et al., 2018, 2021](#)); development

of multimodal and region-specific biomarkers (Moguilner et al., 2022; Parra et al., 2022; Maito et al., 2023) and initiatives (Ibanez et al., 2021; Parra et al., 2021; Duran-Aniotz et al., 2022); interactions between environmental stressors and physiopathological mechanisms of allostatic overload (Birba et al., 2022; De Felice et al., 2022; Migeot et al., 2022); and going beyond universal models toward non-stereotypical samples (Greene et al., 2022) and designs (Ibanez, 2022) in neuroscience and dementia (Alladi and Hachinski, 2018). Notably, many of these key matters are being covered in this special issue.

The contributions to ADRD

This Research Topic comprises 20 articles, involving >150 authors across the globe, and organized into four main areas: (a) animal studies, and human studies of (b) biomarkers and basic approaches, (c) neurocognition, and (d) clinically relevant assessments. These contributions are briefly summarized in the following sections.

Animal studies

Moreno-Gonzalez et al. were interested in testing the hypothesis that protein misfolding and aggregation can be induced by administration of small quantities of preformed aggregates. They model their hypothesis on a principle similar to that of prion diseases, which are transmitted by a proteinaceous infectious agent that seeds misfolding and aggregation of the human prion protein. Using transgenic animal models of AD, they assessed how the intra-cerebrally inoculated A β aggregates in the brain of aged cattle promote AD pathological features. Results suggest that aged cattle can develop AD-like neuropathological abnormalities (amyloid plaques). Also, bovine-derived aggregates accelerate A β amyloid deposition.

Jiang et al. compared AD postmortem brain tissue with brains from two types (AppNL-F and AppNL-G-F) of APP knock-in mice, which typically exhibit robust A β pathology. They found an increase of both p62 and LC3-II levels in the brains of the knock-in mice compared to wild type mice, signaling inhibited autophagy, and discovered LC3-positive puncta in the hippocampus of AppNL-F mice around the A β plaques. They posit that APP knock-in mouse models are a promising platform for aiding in the correlation of A β and autophagy.

Zou et al. researched amyloid plaques and neuronal loss in AD murine models. They found an increase in reactive oxygen species (ROS) in pre-senilin (PS) deficient fibroblasts, while H2O2 and ferrous sulfate treatments produced more ROS in PS deficient fibroblasts over wild-type fibroblasts. Their results also suggest reduced iron sequestration in PS deficient cells, as well as a key role of γ -secretase activity in maintaining ferritin levels. Overexpression of PS1 mutants in

wild type fibroblasts decreased ferritin light chain levels while increasing intracellular ROS levels. Their results suggest how PS dysfunction can reduce intracellular ferritin levels, resulting in free iron-induced oxidative stress which may play an important role in AD pathogenesis.

Hurley et al. reported the whole-genome sequencing and analysis of the degu genome. The degu is a diurnal long-living rodent that can develop changes analogous to human aging and AD. Their results revealed unique features and molecular adaptations similar to aging and AD in humans. Particularly, they identified a novel APOE gene variant that correlated with an increase in the amyloid plaques of the brain. Their results could help further advance biomedical treatments for AD.

Human studies of biomarkers and basic advances

Kim et al. looked at the issue of whether A β accumulation in the cortex and striatum, as well as tau accumulation, differ depending on sex and APOE genotypes. Using a sample of subjects from the Alzheimer's Disease Neuroimaging Initiative database, they selected 534 subjects who had undergone 18F-florbetapir PET and 163 subjects who had undergone 18F-flortaucipir PET. They performed trajectory analysis of A β and tau protein deposition and obtained predictions of SUVR curves across time. They found no differences of cortical A β accumulation depending on sex, but did find striatal A β accumulation was faster for women than for men. This difference was even more pronounced for tau accumulation. Still, APOE ϵ 4 carriers showed greater progression than non-carriers, regardless of the biomarkers' trajectories.

Unnur et al. evaluated the association between CSF cholinergic enzymes with AD-related biomarkers and cognitive functioning. They measured enzyme activity of AChE and BuChE in the CSF, as well as amyloid- β 1–42 (A β 42), phosphorylated tau (P-tau), total-tau (T-tau), neurofilament light (NFL), YKL-40, S100 calcium-binding protein B (S100B), and glial fibrillary acidic protein (GFAP). They also evaluated verbal episodic memory with behavioral batteries. Although they did not find a relationship between CSF A β 42 and AChE or BuChE activity, they did find a positive correlation between higher activity of ACh-degrading cholinergic enzymes and increased neurodegeneration, neurofibrillary tangles and inflammation in pre- and early dementia.

Lai et al. explored the cuproptosis-related molecular clusters in AD and also developed a predictive model with a sample of 310 AD patients from the GSE33000 microarray dataset. They found cluster-specific differentially expressed genes in 2 clusters. Cluster1 was related to synapse and axon regulation while Cluster2 was involved in immune responses. High diagnostic value subtype-specific genes were identified with a random forest machine learning model and the 5 genes found were externally validated with two datasets. All of the

five model-related genes were significantly associated with A β -42 levels and β -secretase activity, illustrating the complex interaction of cuproptosis and AD.

The amyloid hypothesis of AD pathogenesis is still one of the main drivers of research. However, the results of the anti-A β antibody, aducanumab, are still uncertain. Accounting for divided opinions on A β as a major causal factor of AD, Kawabata et al. proposed a novel hypothesis on how excessive/aberrant and maladaptive synaptic plasticity are the basis for AD pathophysiology.

Human studies of neurocognition in ADRD

Chen et al. assessed abnormal functional connectivity in posterior cortical atrophy (PCA) and semantic dementia (SD). They evaluated seed-based functional connectivity in PCA, SD, and control subjects, along with detailed clinical, physical and neuropsychological assessments. Their results revealed abnormal connectivity within the cortex in the language and salience networks for both PCA and SD patients. Meanwhile, functional connectivity changes in the visual networks were unique for PCA patients. All FC changes were matched for cognitive deficits and accounted for abnormal metabolism.

Tan et al. evaluated the behavioral and neural associations between olfactory identification and cognitive functioning in a sample of 645 adults (AD and MCI) from the Taizhou Imaging Study. They found that higher olfactory identification score on smell testing was associated with better scores on a battery of neuropsychological tests of cognitive function. Higher olfactory identification was correlated with lower likelihood of MCI and dementia. Amygdala volume was significantly correlated with olfactory identification and the results from the cognition batteries, thus, highlighting a key role of the amygdala in the link between olfactory identification and cognitive function.

Hoong Kang et al. evaluated the correlation between performance in language tests and cortical thickness in order to determine neural substrates of 96 Korean patients with primary progressive aphasia. Poor performance on language tests (object naming, semantic generative naming, phonemic generative naming and comprehension) was correlated to lower cortical thickness in key cortical regions. Specifically, the neural substrates of the semantic generative naming test (midportion of the lateral and basal temporal regions) significantly differed from control patients with other dementia subtypes.

Song et al. assessed alterations in resting-state functional connectivity density (FCD) in subjective cognitive decline (SCD), amnesic MCI (aMCI), and controls ($N = 194$) in order to further define how these changes can help to distinguish preclinical and early-stage AD. Their results revealed global FCD in the left parahippocampal gyrus and increased FCD

in the left hippocampus for SCD patients. Meanwhile, aMCI patients exhibited decreased global and long-range FCD in the left parahippocampal gyrus. Follow-up FC analysis revealed significant variations between the left parahippocampal gyrus and occipital lobe in SCD and aMCI patients. These results can help understand the progression of SCD and aMCI to AD.

Chen et al. determined whether Sortilin-related receptor 1 (SORL1) polymorphisms were associated with volume differences in brain regions in late-onset AD in patients of Han Chinese descent. They recruited 200 late-onset AD patients (Taipei Veterans General Hospital) for MR imaging and neurocognitive assessment, with 77.5% of patients receiving follow-up Mini-Mental State Examination 2 years after enrollment to assess changes longitudinally. They found that the homozygous rs2298813 allele was associated with larger volumes in the right putamen and pallidum (which was correlated with verbal fluency). The major and minor alleles of rs2298813 predicted clinical progression in the 2-year follow-up, while putaminal volume was associated with verbal fluency.

Laczó et al. examined spatial navigation as a cognitive marker of clinical and preclinical AD. For this study, they assessed spatial navigation performance in older adults with AD aMCI (positive amyloid PET and/or CSF AD biomarkers) vs. non-AD aMCI (negative amyloid PET and/or normal CSF amyloid- β 1–42), and assessed navigation performance and MRI measures of regional brain volumetry. Their results revealed that AD aMCI adults performed worse than non-AD aMCI adults in route learning. Meanwhile, spatial navigation impairments were associated with posterior medial temporal lobe and parietal atrophy and reflected AD pathology.

Oh et al. looked for the pathological and functional correlates of extraversion and neuroticism in healthy adults and older participants in order to gain better understanding of how personality traits can be crucial for vulnerability to or protection from AD. They measured brain imaging *via* a task-switching fMRI paradigm in young adults, while they obtained data on A β deposition in older individuals *via* PET. They found that extraversion was significantly associated with lower A β across brain regions in older individuals, while high extraversion in young adults was associated with lower activity in the anterior cingulate cortex, left anterior insular cortex, left putamen, and medial frontal gyrus. Higher neuroticism was overall associated with increased global brain activity. Results suggest that extraversion, *via* efficient neuronal activity, may confer protection against A β pathology.

Human studies assessing ADRD clinically relevant measures

Zhang et al. studied the top 100 published papers on AD and epilepsy. They found a substantial increase in publications

between the years 2000 to 2021, with a mean of 67.4 citations for these 100 papers. The US, and Columbia University were the most influential country and institution, respectively, while Journal of Alzheimer's Disease accounted for the highest number of papers in this area ($n = 8$). Their results point toward the increasing importance of this topic and the need for fruitful collaborations and cooperation going forward.

Kang et al. aimed to determine the association of BMI changes and variability with A β positivity. They conducted a large retrospective cohort study with participants 50 years of age and above using multivariable logistic regression. They found that decreased or increased BMI, as well as BMI variability, were positively correlated with greater A β positivity. Their results showcase how BMI changes, and particularly BMI variability, make the brain more prone to A β deposition, as well as signaling important interventions in preventing A β deposition with weight control and stabilization.

Chang et al. looked at the relationship of coenzyme Q10 with dementia biomarkers and antioxidant capacity in 80 dementia patients. They found a majority of patients (73%) presented with low coenzyme Q10 levels. Coenzyme Q10 was inversely correlated with plasma amyloid β -42 and amyloid β -42/40 ratio, but not with tau level. Coenzyme Q10 levels correlated positively with antioxidant capacity. Their results show that it may be beneficial to monitor and maintain adequate levels of coenzyme Q10 in patients with dementia.

Finally, Wang et al. examined the effects on cognitive function of serum uric acid (SUA) at baseline and with change after 4 years in a non-normotensive population from the China Health and Retirement Longitudinal Study (CHARLS; $N = 3,905$). They highlighted four single-trajectories of global cognitive performance, executive function and episodic memory. Overall, higher SUA levels were associated with favorable cognitive trajectories and a moderate increase of SUA over time was good for cognitive function as long as SUA was in the normal range. However, persistent hyperurcemia resulted in increased risk of cognitive dysfunction. This indicates the importance of maintaining normal SUA levels.

Conclusions

We are now entering the third decade of the 21st century, and, especially in the last years, the achievements made by scientists have been exceptional, leading to major advancements in the fast-growing field of ADRD. The present Research Topic highlights some of the latest advancements, new insights, novel developments, current challenges, latest discoveries, and future

perspectives in ADRD research. We hope these contributions may shed light on the progress made in the past and in the forthcoming challenges of the field. We are proud of the diversity of our authors, topics, and editorial team and hope they will contribute to a more diverse and robust science of dementia.

Author contributions

AI prepared the initial draft of this editorial. AR, SA, and NC carefully revised the draft. All authors contributed to the contents of this article and approved the final version.

Funding

AI is partially supported by grants from CONICET; ANID/FONDECYT Regular (1210195, 1210176, and 1220995); ANID/FONDAP/15150012; ANID/PIA/ANILLOS ACT210096; FONDEF ID20I10152, ID22I10029; ANID/FONDAP 15150012; Takeda CW2680521 and the MULTI-PARTNER CONSORTIUM TO EXPAND DEMENTIA RESEARCH IN LATIN AMERICA [ReDLat, supported by National Institutes of Health, National Institutes of Aging (R01 AG057234), Alzheimer's Association (SG-20-725707), Rainwater Charitable foundation – Tau Consortium, and Global Brain Health Institute]. AR is supported by the Alzheimer's Foundation of America (Award AWD00004772) and The Herb and Evelyn Abrams Family Amyloid Research Fund. The contents of this publication are solely the responsibility of the authors and do not represent the official views of these Institutions.

Conflict of interest

The authors declare that the research was conducted in the absence of any commercial or financial relationships that could be construed as a potential conflict of interest.

Publisher's note

All claims expressed in this article are solely those of the authors and do not necessarily represent those of their affiliated organizations, or those of the publisher, the editors and the reviewers. Any product that may be evaluated in this article, or claim that may be made by its manufacturer, is not guaranteed or endorsed by the publisher.

References

- Alladi, S., and Hachinski, V. (2018). World dementia: One approach does not fit all. *Neurology* 91, 264–270. doi: 10.1212/WNL.0000000000005941
- Alzheimer's Disease International, A. (2022). *World Alzheimer Report 2022*. London, England: Alzheimer's Disease International.
- Babiloni, C., Blinowska, K., Bonanni, L., Cichocki, A., De Haan, W., Del Percio, C., et al. (2020). What electrophysiology tells us about Alzheimer's disease: a window into the synchronization and connectivity of brain neurons. *Neurobiol. Aging* 85, 58–73. doi: 10.1016/j.neurobiolaging.2019.09.008
- Birba, A., Santamaria-Garcia, H., Prado, P., Cruzat, J., Ballesteros, A. S., Legaz, A., et al. (2022). Allostatic-interoceptive overload in frontotemporal dementia. *Biol. Psychiatry* 92, 54–67. doi: 10.1016/j.biopsych.2022.02.955
- De Felice, F. G., Gonçalves, R. A., and Ferreira, S. T. (2022). Impaired insulin signalling and allostatic load in Alzheimer disease. *Nat. Rev. Neurosci.* 23, 215–230. doi: 10.1038/s41583-022-00558-9
- Dehghani, N., Bras, J., and Guerreiro, R. (2021). How understudied populations have contributed to our understanding of Alzheimer's disease genetics. *Brain* 144, 1067–1081. doi: 10.1093/brain/awab028
- Duran-Aniotz, C., Sanhueza, J., Grinberg, L. T., Slachevsky, A., Valcour, V., Robertson, I., et al. (2022). The Latin American Brain Health Institute, a regional initiative to reduce the scale and impact of dementia. *Alzheimers Dement.* 18, 1696–1698. doi: 10.1002/alz.12710
- Frisoni, G. B., Altomare, D., Thal, D. R., Ribaldi, F., Van Der Kant, R., Ossenkoppele, R., et al. (2022). The probabilistic model of Alzheimer disease: the amyloid hypothesis revised. *Nat. Rev. Neurosci.* 23, 53–66. doi: 10.1038/s41583-021-00533-w
- Greene, A. S., Shen, X., Noble, S., Horien, C., Hahn, C. A., Arora, J., et al. (2022). Brain-phenotype models fail for individuals who defy sample stereotypes. *Nature* 609, 109–118. doi: 10.1038/s41586-022-05118-w
- Ibanez, A. (2022). The mind's golden cage and cognition in the wild. *Trends Cogn. Sci.* 26, 1031–1034. doi: 10.1016/j.tics.2022.07.008
- Ibanez, A., Yokoyama, J. S., Possin, K. L., Matallana, D., Lopera, F., Nitrini, R., et al. (2021). The multi-partner consortium to expand dementia research in latin America (ReDLat): Driving multicentric research and implementation science. *Front. Neurol.* 12, 631722. doi: 10.3389/fneur.2021.631722
- Maito, M. A., Santamaria-Garcia, H., Moguilner, S., Possin, K. L., Godoy, M. E., Avila-Funes, J. A., et al. (2023). Classification of Alzheimer's disease and frontotemporal dementia using routine clinical and cognitive measures across multicentric underrepresented samples: A cross sectional observational study. *Lancet Reg. Health Am.* 17, 100387. doi: 10.1016/j.lana.2022.100387
- Migeot, J. A., Duran-Aniotz, C. A., Signorelli, C. M., Piguet, O., and Ibáñez, A. (2022). A predictive coding framework of allostatic-interoceptive overload in frontotemporal dementia. *Trends Neurosci.* 45, 838–853. doi: 10.1016/j.tins.2022.08.005
- Moguilner, S., Birba, A., Fittipaldi, S., Gonzalez-Campo, C., Tagliazucchi, E., Reyes, P., et al. (2022). Multi-feature computational framework for combined signatures of dementia in underrepresented settings. *J. Neural. Eng.* 19, 046048. doi: 10.1088/1741-2552/ac87d0
- Parra, M. A., Baez, S., Allegri, R., Nitrini, R., Lopera, F., Slachevsky, A., et al. (2018). Dementia in Latin America: Assessing the present and envisioning the future. *Neurology* 90, 222–231. doi: 10.1212/WNL.0000000000004897
- Parra, M. A., Baez, S., Sedeño, L., Gonzalez Campo, C., Santamaria-Garcia, H., Aprahamian, I., et al. (2021). Dementia in Latin America: Paving the way toward a regional action plan. *Alzheimers Dement.* 17, 295–313. doi: 10.1002/alz.12202
- Parra, M. A., Orellana, P., Leon, T., Victoria, C. G., Henriquez, F., Gomez, R., et al. (2022). Biomarkers for dementia in Latin American countries: Gaps and opportunities. *Alzheimers Dement.* 17, 295–313. doi: 10.1002/alz.12757
- WHO (2022). *Global Status Report on the Public Health Response to Dementia 2017-2025*. Geneva: World Health Organization.



OPEN ACCESS

EDITED BY

Agustin Ibanez,
Latin American Brain Health Institute
(BrainLat), Chile

REVIEWED BY

Yutang Wang,
Federation University Australia,
Australia
Francesca Viazzi,
San Martino Hospital (IRCCS), Italy

*CORRESPONDENCE

Lixin Tao
taolixin@ccmu.edu.cn

SPECIALTY SECTION

This article was submitted to
Alzheimer's Disease and Related
Dementias,
a section of the journal
Frontiers in Aging Neuroscience

RECEIVED 15 May 2022

ACCEPTED 26 July 2022

PUBLISHED 01 September 2022

CITATION

Wang J, Jin R, Wu Z, Liu Y, Jin X, Han Z,
Liu Y, Xu Z, Guo X and Tao L (2022)
Moderate increase of serum uric acid
within a normal range is associated
with improved cognitive function in a
non-normotensive population:
A nationally representative cohort
study.
Front. Aging Neurosci. 14:944341.
doi: 10.3389/fnagi.2022.944341

COPYRIGHT

© 2022 Wang, Jin, Wu, Liu, Jin, Han,
Liu, Xu, Guo and Tao. This is an
open-access article distributed under
the terms of the [Creative Commons
Attribution License \(CC BY\)](#). The use,
distribution or reproduction in other
forums is permitted, provided the
original author(s) and the copyright
owner(s) are credited and that the
original publication in this journal is
cited, in accordance with accepted
academic practice. No use, distribution
or reproduction is permitted which
does not comply with these terms.

Moderate increase of serum uric acid within a normal range is associated with improved cognitive function in a non-normotensive population: A nationally representative cohort study

Jinqi Wang¹, Rui Jin¹, Zhiyuan Wu^{1,2}, Yueruijing Liu¹,
Xiaohan Jin¹, Ze Han¹, Yue Liu¹, Zongkai Xu¹, Xiuhua Guo¹
and Lixin Tao^{1*}

¹Beijing Municipal Key Laboratory of Clinical Epidemiology, Department of Epidemiology and Health Statistics, School of Public Health, Capital Medical University, Beijing, China,

²Department of Public Health, School of Medical and Health Sciences, Edith Cowan University, Perth, WA, Australia

Background: Associations between serum uric acid (SUA) and changes in cognitive function are understudied in non-normotensive populations, and many previous studies only considered the baseline SUA at a single time point. We aimed to examine the effects of baseline SUA and 4-year changes in SUA on cognitive changes in the non-normotensive population.

Materials and methods: In the China Health and Retirement Longitudinal Study (CHARLS), cognitive function was measured based on executive function and episodic memory in four visits (years: 2011, 2013, 2015, and 2018). We identified two study cohorts from CHARLS. The first cohort included 3,905 non-normotensive participants. Group-based single-trajectory and multi-trajectory models were applied to identify 7-year cognitive trajectories. Adjusted ordinal logistics models were performed to assess the association between baseline SUA and 7-year cognitive trajectories, and subgroup analyses were conducted according to the presence of hyperuricemia or SUA levels. The second cohort included 2,077 eligible participants. Multiple linear regression was used to explore the effect of a 4-year change in SUA on cognitive change during the subsequent 3-year follow-up.

Results: Four distinct single-trajectories of global cognitive performance and four multi-trajectories of executive function and episodic memory were identified. Higher baseline SUA levels were significantly associated with more favorable cognitive single-trajectories ($OR_{Q4 \text{ vs. } Q1}$: 0.755; 95% CI: 0.643, 0.900) and multi-trajectories ($OR_{Q4 \text{ vs. } Q1}$: 0.784; 95% CI: 0.659, 0.933). Subgroup analyses revealed that the protective effect of SUA was

significant in the non-hyperuricemia groups or the low-level SUA groups. Additionally, changes in SUA could influence future cognitive changes. Compared with non-hyperuricemia participants with elevated SUA, non-hyperuricemia participants with decreased SUA and patients with persistent hyperuricemia had a higher risk for cognitive decline. Furthermore, only the Q3 group of changes in SUA could enhance global cognitive function compared with the Q1 group (β : 0.449; 95% CI: 0.073, 0.826).

Conclusion: Our study indicates that the maintenance of normal SUA levels and a moderate increase of SUA were advantageous in improving cognitive function or trajectories in a non-normotensive population. Conversely, SUA may impair cognitive function in patients with persistent hyperuricemia.

KEYWORDS

cognitive trajectory, cognitive function, serum uric acid, changes in serum uric acid, hypertension, cohort study

Introduction

Cognitive impairment and dementia have become major and increasing global health challenges that reduce the quality of life and cause a huge economic burden (Jia et al., 2018; Nichols et al., 2019; Davis et al., 2022). Due to the aging population, the global number of people living with dementia or cognitive impairment has dramatically increased (Nichols et al., 2019). Approximately, more than 15% of Chinese older people are suffering from cognitive impairment (Xue et al., 2018). Several studies suggested that people with hypertension, even under prehypertensive conditions, were more likely to have cognitive decline or dementia (Gottesman et al., 2014; Chen et al., 2015; Iadecola and Gottesman, 2019; de Menezes et al., 2021). Considering that there is no effective disease-modifying treatment for cognitive impairment or dementia (Li et al., 2020; Davis et al., 2022), early identification of possible modifiable risk factors of rapid cognitive decline is crucial to prevent or delay the incidence of cognitive impairment among the prehypertensive and hypertensive populations.

As a natural antioxidant, serum uric acid (SUA) is thought to exert a neuroprotective effect by acting as a free radical scavenger to prevent the development of cognitive dysfunction (Bowman et al., 2010; Tuven et al., 2017; Kim et al., 2020). However, urate-lowering therapy plays an important role in

the management of hypertension to prevent diabetes, chronic kidney disease, stroke, and adverse cardiovascular outcomes (Kawai et al., 2012; Sharaf El Din et al., 2017; Cassano et al., 2020; Viridis et al., 2020). Hypertension with other chronic diseases co-occurring in the same individuals may result in a more severe and accelerated decline in cognitive function (Iadecola and Gottesman, 2019). Previous epidemiological studies and meta-analyses found the association of the lower SUA level with poorer cognitive function and dementia (Wang F. et al., 2017; Wang T. et al., 2017; Huang et al., 2019; Scheepers et al., 2019; Chen et al., 2021; Zhou et al., 2021; Huang Y. et al., 2022), but whether SUA plays a neuroprotective role among prehypertensive and hypertensive populations remains unclear. Additionally, the potential protective effects of SUA on cognition were controversial in other studies. The opposite association (Beydoun et al., 2016; Suzuki et al., 2016; Latourte et al., 2018b; Singh and Cleveland, 2018; Alam et al., 2020) or no association (Richard et al., 2021) between SUA and cognitive performance have been reported. As for the reason, most previous studies included participants with hyperuricemia. Patients with hyperuricemia may have different underlying etiology pathways due to the impact of higher levels of SUA on adverse health outcomes as compared to the non-hyperuricemia population (Huang Y. et al., 2022). The different effects of SUA on cognition among both non-hyperuricemia and hyperuricemia populations still need further exploration.

Several other limitations were present in previous studies. Most previous studies only recorded the SUA levels at baseline, failing to take into account the potential effect of changes in SUA in follow-up on subsequent cognitive function (Qiao et al., 2021). Moreover, these studies neglected the longitudinal change pattern of cognitive function during the follow-up period. An advanced statistical method, group-based trajectory models

Abbreviations: SUA, serum uric acid; GBTM, group-based trajectory model; CHARLS, China Health and Retirement Longitudinal Study; BMI, body mass index; eGFR, estimated glomerular filtration rate; CMD, cardiometabolic diseases; SBP, systolic blood pressure; DBP, diastolic blood pressure; SD, standard deviation; GBMTM, group-based multi-trajectory modeling; BIC, Bayesian information criteria; AIC, Akaike information criterion; APP, average posterior probabilities; CI, confidence interval; RCS, restricted cubic spline; GEE, generalized estimating equation; OR, odds ratio.

(GBTM), allowed us to identify subgroups that share common developmental trajectories over time (Nagin and Odgers, 2010).

Thus, the present study was conducted in the non-normotensive population, including prehypertensive and hypertensive individuals, to: (1) identify different 7-year cognitive trajectories and investigate the association between the baseline SUA levels and cognitive trajectories; (2) assess the above associations among both the non-hyperuricemia and hyperuricemia populations; and (3) examine the effect of 4-year changes in SUA on subsequent 3-year changes in cognitive performance.

Materials and methods

Study population

China Health and Retirement Longitudinal Study (CHARLS) is a nationwide survey that was conducted among Chinese adults aged 45 years or older (Zhao et al., 2014), which is a prospective cohort collecting data on social and economic information, anthropometric and laboratory measurements, demographic characteristics, health-related behaviors, and health conditions. A total of 17,707 participants from 150 county-level units distributed in 28 provinces of China were recruited at baseline (wave 1: 2011–2012), and the subsequent three follow-up visits were carried out (wave 2 in 2013, wave 3 in 2015, wave 4 in 2018). Details about the data were previously described in an earlier publication (Zhao et al., 2014). The protocols of CHARLS were approved by the Biomedical Ethics Review Committee of Peking University (IRB00001052-11015). All participants provided their signed informed consents. We identified two study cohorts from CHARLS.

The first cohort was constructed to explore the longitudinal association between baseline SUA and 7-year cognitive trajectories. Participants were excluded if they had missing data on gender, age, SUA, and cognitive function; had self-reported the previous diagnosis of brain damage, intellectual disability, and memory-related disease (Alzheimer's disease, brain atrophy, Parkinson's disease); or were normotensive at baseline in 2011. Finally, a total of 3,905 participants with two or more subsequent follow-up visits were enrolled for the analyses (Supplementary Figure 1).

The second cohort was constructed to examine the effect of changes in SUA on the future 3-year cognitive changes. We calculated changes in SUA using the SUA levels in 2011 and 2015 to predict the risk of developing cognitive decline from 2015 to 2018. Participants were excluded if they had missing data on gender, age, SUA, and cognitive function at baseline or the survey in 2015; had self-reported the previous diagnosis of brain damage, intellectual disability, or memory-related disease; or were normotensive in or before 2015. Ultimately, a total of 2,077 participants who attended the last survey in 2018 (wave

4) were enrolled in the study (Supplementary Figure 2). The timeline of the study is presented in Supplementary Figure 3.

Cognitive function

Cognitive function was assessed by two measures: episodic memory and executive function according to previous studies (Lei et al., 2012; Li et al., 2020; Huang Y. et al., 2022). In the episodic memory test, participants were instructed to recall words immediately (immediate recall) and 5 min later (delayed recall) after examiners read 10 Chinese words to them. The number of correctly recalled words was scored. The episodic memory score was the average score of the immediate and delayed recall tests and ranged from 0 to 10 (Hua et al., 2020). In the executive function test, participants were shown a figure and asked to redraw it. If the participant succeeded, the score was 1. They also were asked to subtract 7 from 100 serially five times and to identify the date (month, day, and year), season, and day of the week. Answers to these questions were summed into the executive function score ranging from 0 to 11 (Wu et al., 2021a). The global cognition score was calculated as the sum of episodic memory score and executive function score and ranged from 0 to 21.

Measurements of serum uric acid and serum uric acid changes

Venous blood was collected from participants with their fasting status recorded. The blood samples were first kept in local hospitals, then transported to Peking University in Beijing, and stored at -80°C until measurement. The level of SUA was analyzed using the UA Plus method (Wang T. et al., 2017; Chen et al., 2019). Hyperuricemia was defined as SUA > 6.0 mg/dL in women and > 7.0 mg/dL in men (Huang Y. et al., 2022). Sex-specific quartiles of baseline SUA were constructed and used for subsequent analysis.

Participants were divided into five categories according to the changes in SUA from baseline in 2011 to the follow-up survey in 2015: “non-hyperuricemia with elevated SUA,” “non-hyperuricemia with decreased SUA,” “incident hyperuricemia,” “remittent hyperuricemia,” and “persistent hyperuricemia.” “Non-hyperuricemia with elevated SUA” was defined as hyperuricemia absent both in 2011 and 2015 and an increase in SUA levels. “Non-hyperuricemia with decreased SUA” was defined as hyperuricemia absent both in 2011 and 2015 and a decrease in the SUA levels. Remittent hyperuricemia was defined as hyperuricemia that was present only in 2011 but not hyperuricemia in 2015. Incident hyperuricemia was defined as hyperuricemia that was present only in the follow-up survey in 2015. Persistent hyperuricemia was defined as hyperuricemia present both

in 2011 and 2015 (Liu et al., 2018). The first group was set as the reference group. Then, changes in SUA were calculated as the SUA level in 2015 minus that in 2011: $Changes\ in\ SUA = SUA_{2015} - SUA_{2011}$. Both continuous and categorical (quartiles) types were constructed and used in analyses.

Measurements of non-normotensive status

Systolic blood pressure (SBP) and diastolic blood pressure (DBP) were measured three times repeatedly by trained medical staff using an Omron HEM-7200 Monitor. We used the average of the three measured results as the final blood pressure. Past medical history and medication history of hypertension were obtained from self-reports.

The non-normotensive status included prehypertensive and hypertensive statuses (Wu et al., 2021b). Hypertension status was defined as SBP ≥ 140 mmHg or DBP ≥ 90 mmHg, the use of anti-hypertensive medication, or self-reported history of hypertension (Chobanian et al., 2003). Prehypertension status was defined as SBP of 120–139 mmHg or DBP of 80–89 mmHg (Chobanian et al., 2003).

Covariates

Several covariates were included in our analyses. Sociodemographic characteristics included age, gender (men and women), marital status (married and others), and educational level (no formal education, junior high school or below, and high school or above). Health-related lifestyles included self-reported smoking status (non-smoker, former smoker, and current smoker) and drinking status (drink more than once a month, drink but less than once a month, and none of these). Body mass index (BMI) was calculated as weight in kilograms divided by height in meters squared and was categorized as follows: < 18.5 , $18.5\text{--}23.9$, ≥ 24.0 (Wang and Zhai, 2013). Depressive symptoms were assessed using the 10-item Center for Epidemiological Studies Depression Scale (CES-D-10). A score of ≥ 12 indicated the presence of depressive symptoms (Chen and Mui, 2014). Self-reported history of cardiometabolic diseases (CMD) included diabetes, dyslipidemia, stroke, and heart-related diseases (Huang Z. T. et al., 2022). We calculated the estimated glomerular filtration rate (eGFR) using the Chronic Kidney Disease Epidemiology Collaboration's 2009 creatinine equation (Levey et al., 2009). Finally, physical activity was assessed by the questionnaires among a randomly selected subsample of the study population. Physical activity was defined as ≥ 150 min/week of moderate, or ≥ 75 min/week of vigorous activity, or a combination (≥ 600 metabolic equivalents [METs]) (Lloyd-Jones et al., 2010;

Ding et al., 2020). Otherwise, they were categorized as physically inactive.

Statistical analysis

Baseline characteristics were presented as the mean (standard deviation, SD), median [interquartile range, IQR], or number (percentage), as appropriate.

Single trajectories of global cognitive function were determined using GBTM to map the developmental course of cognitive performance from the baseline survey to three follow-up visits. The jointly longitudinal changes in episodic memory and executive function over time were estimated using group-based multi-trajectory modeling (GBMTM). GBMTM is a new application of GBTM and allows the joint modeling of the trajectories of multiple outcomes (Nagin et al., 2018). GBTM and GBMTM can identify clusters of individuals following similar change patterns through multiple visits. Varied models were considered to choose the optimal number of distinct groups and trajectory shape parameters (e.g., linear, quadratic, and cubic) based on Bayesian information criteria (BIC), Akaike information criterion (AIC), and average posterior probabilities (APP) of each trajectory group (≥ 0.70) (Li et al., 2020). In addition, the sufficient sample size in each trajectory group ($> 5\%$ of the sample) and clinical interpretation are important elements when determining the best model. Finally, trajectories of cognitive function were plotted over a 7-year follow-up time.

Ordinal logistics regression models were used to assess the associations between baseline SUA and 7-year cognitive trajectories. The final multivariable model was adjusted for age, gender, marital status, education level, smoking status, drinking status, BMI, depressive symptoms, CMD, and the presence of prehypertension at baseline. We evaluated the dose-response relationship between SUA, as a continuous change, and each trajectory of cognitive function using restricted cubic splines (RCS) with four knots (at the 5th, 35th, 65th, and 95th percentiles). Then, subgroup analyses based on the hyperuricemia status were performed. Considering the relatively small sample size of the population with hyperuricemia ($N = 262$), other subgroup analyses by the SUA levels were conducted to test the robustness of the results. Participants were divided into the high-level SUA and low-level SUA groups based on the sex-specific median and 75th quartile of SUA. Both continuous and categorical (sex-specific median of SUA in each subgroup) types were constructed and used in subgroup analyses (lower SUA level as a reference category).

Subsequently, we used multiple linear regression models to explore the effect of changes in SUA on 3-year cognitive change, adjusting for the same abovementioned covariates and SUA in 2015. The regression coefficient (β) and its 95% confidence interval (CI) were presented. The cognitive change was calculated by differences in

cognitive scores between 2015 and 2018: $\text{Cognitive changes} = \text{cognitive score}_{2018} - \text{cognitive score}_{2015}$. RCS with four knots was used to capture the dose–response relationship between changes in SUA and cognitive changes.

Sensitivity analyses were also conducted as follows: (1) eGFR was further adjusted to explore the stability of our findings; (2) the models were further adjusted for physical activity in the subpopulations of two study cohorts who underwent physical activity assessments; (3) the generalized estimating equation (GEE) models were used to examine the longitudinal association between the SUA levels and cognitive function in the following several years; (4) the effect of baseline SUA on cognitive trajectories in subgroups, according to age, gender, depression status, and the presence of prehypertension and non-normotensive combined with other CMD were analyzed; (5) cognitive scores in 2018 were used as the secondary outcome to explore the effect of changes in SUA on cognitive function, adjusting for the abovementioned covariates plus cognitive scores in 2015.

Group-based trajectory models and GBMTM techniques were implemented using the Proc Traj in Stata software version 15.1. Other statistical analyses above were performed with the R software version 4.1.0. A two-sided p -value < 0.05 was considered statistically significant.

Results

Baseline characteristics

The mean age of the 3,905 participants was 58.48 ± 8.54 years and 50.4% of participants were men. The mean age of the 2,077 participants was 57.78 ± 8.06 years and 50.4% of participants were men. The distribution of baseline SUA, changes in SUA, baseline covariates, and cognitive scores is shown in [Table 1](#).

Estimated cognitive trajectories

[Supplementary Table 1](#) shows the procedure of choosing the optimal group number and shape parameter for the final single-trajectory model. The BIC was lower for the model with six trajectories (BIC = -33582.86). However, APP was less than 0.7 for the two trajectories group. Additionally, the average APP of all groups for the model with five trajectories was less than with four trajectories. Thus, we determined four single trajectories of global cognitive function reflected the longitudinal change patterns over 7 years ([Figure 1A](#)): class 1, “low-declining” ($n = 293$, 7.50%); class 2, “moderate low-declining” ($n = 769$, 19.69%); class 3, “moderate high-stable” ($n = 1,472$, 37.70%); and class 4, “high-stable” ($n = 1,371$,

TABLE 1 Baseline characteristics of the study population in two cohorts.

| Characteristics | The first cohort | The second cohort |
|--|------------------|-------------------|
| No. of participants | 3905 | 2077 |
| Age(years), mean (SD) | 58.48 (8.54) | 57.78 (8.06) |
| Male, n (%) | 1968 (50.4) | 1046 (50.4) |
| Married, n (%) | 3383 (86.6) | 1833 (88.3) |
| Educational level, n (%) | | |
| No formal education | 1400 (35.9) | 654 (31.5) |
| Junior high school or below | 1997 (51.1) | 1136 (54.7) |
| High school or above | 508 (13.0) | 287 (13.8) |
| Smoking status, n (%) | | |
| Non-smoker | 2309 (59.1) | 1243 (59.8) |
| Former smoker | 391 (10.0) | 206 (9.9) |
| Current smoker | 1205 (30.9) | 628 (30.2) |
| Drinking status, n (%) | | |
| More than once a month | 1072 (27.5) | 569 (27.4) |
| Less than once a month | 312 (8.0) | 177 (8.5) |
| None of these | 2521 (64.6) | 1331 (64.1) |
| Depressive symptoms, n (%) | 875 (22.4) | 504 (24.3) |
| BMI (kg/m^2), n (%) | | |
| <18.5 | 160 (4.1) | 81 (3.9) |
| $18.5\text{--}23.9$ | 1829 (46.8) | 897 (43.2) |
| ≥ 24.0 | 1916 (49.1) | 1099 (52.9) |
| CMD, n (%) | | |
| Diabetes | 295 (7.6) | 154 (7.4) |
| Dyslipidemia | 510 (13.1) | 273 (13.1) |
| Stroke | 76 (1.9) | 31 (1.5) |
| Heart-related diseases | 559 (14.3) | 295 (14.2) |
| At least 1 CMD, n (%) | 1080 (27.7) | 573 (27.6) |
| Prehypertension, n (%) | 1596 (40.9) | 1011 (48.7) |
| eGFR ($\text{mL}/\text{min}/1.73 \text{ m}^2$), mean (SD) | 91.97 (14.86) | 92.77 (14.43) |
| SUA (mg/dL), mean (SD) | 4.61 (1.29) | 5.11 (1.41) |
| Cognitive scores, mean (SD) | | |
| Global cognitive function | 12.23 (3.50) | 12.32 (3.57) |
| Executive function | 8.45 (2.55) | 8.54 (2.56) |
| Episodic memory | 3.78 (1.67) | 3.79 (1.67) |
| Changes in SUA | – | |
| No hyperuricemia and increased SUA | – | 1258 (60.6) |
| No hyperuricemia and decreased SUA | – | 499 (24.0) |
| Incident hyperuricemia | – | 199 (9.6) |
| Remittent hyperuricemia | – | 50 (2.4) |
| Persistent hyperuricemia | – | 71 (3.4) |
| Changes in SUA (mg/dL), mean (SD) | – | 0.57 (1.10) |

Data are presented as the mean (SD), median [IQR] or number (%), as appropriate. BMI, body mass index; CMD, cardiometabolic diseases; eGFR, estimated glomerular filtration rate; SUA, serum uric acid.

35.11%). The four groups represented a trend of increasingly better cognitive trajectories.

Using the same criteria and procedure ([Supplementary Table 2](#)), we determined four groups using GBMTM that

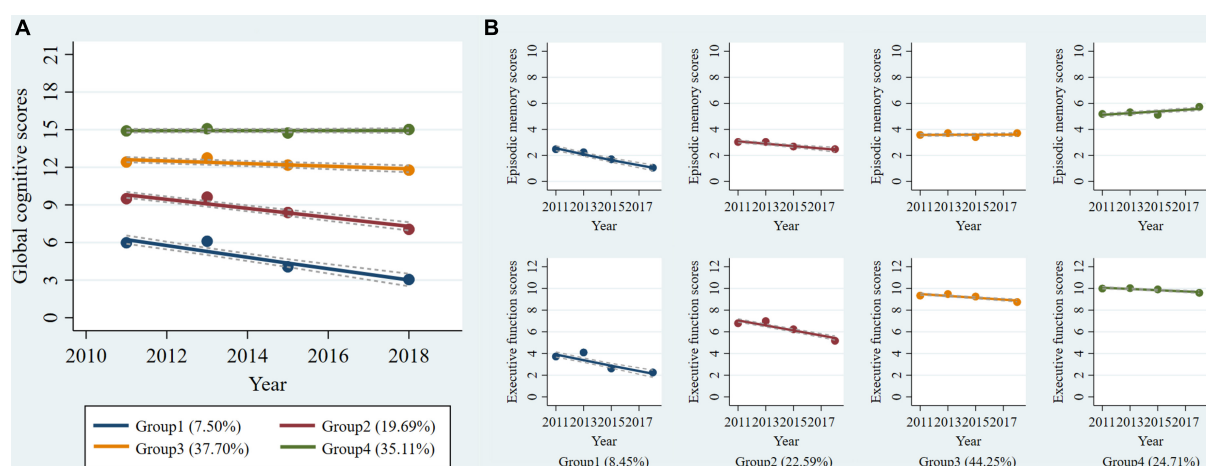


FIGURE 1

Trajectories of cognitive function from 2011 to 2018 among non-normotensive populations. Graphs show four trajectories of global cognitive function (A) and four multi-trajectories of executive function and episodic memory (B). Descriptions of the trajectory groups are as follow: (A) group 1: “low-declining,” group 2: “moderate low-declining,” group 3: “moderate high-stable,” group 4: “high-stable”; (B) group 1: “episodic memory: low-rapid declining + executive function: low-declining,” group 2: “episodic memory: low-minimal declining + executive function: moderate-declining,” group 3: “episodic memory: moderate-stable + executive function: high-declining,” group 4: “episodic memory: high-rising + executive function: high-stable.”

showed the longitudinal joint changes of episodic memory and executive function (Figure 1B): class 1, “episodic memory: low-rapid declining + executive function: low-declining” ($n = 330$, 8.45%); class 2, “episodic memory: low-minimal declining + executive function: moderate-declining” ($n = 882$, 22.59%); class 3, “episodic memory: moderate-stable + executive function: high-declining” ($n = 1,728$, 44.25%); class 4, “episodic memory: high-rising + executive function: high-stable” ($n = 965$, 24.71%). The four groups also can represent a trend of increasingly better cognitive multi-trajectories. The maximum likelihood estimates for the final trajectory models are summarized in Supplementary Tables 3, 4.

Associations between the baseline serum uric acid and 7-year cognitive trajectories

We found that higher baseline SUA levels had a lower risk of poorer global cognitive single-trajectories in three adjusted models (Table 2). The odds ratio (OR) of the highest SUA of less optimal trajectories was 0.755 (95% CI: 0.634 - 0.900, P for trend = 0.002) as compared with those with the lowest levels of SUA after full adjustment of covariates in model 3. Similarly, higher baseline SUA was negatively associated with worse and declining memory and executive function multi-trajectories. The OR was 0.940 (95% CI: 0.894, 0.990) for SUA per 1 mg/dL increase in model 3. We used RCS to estimate the trend in the risk for each poor trajectory relative to the best trajectory. The spline function for SUA confirmed the non-linear, U-shaped,

or J-shaped relationship with the risk of each poor cognitive trajectory. As seen in Figure 2, the protective effect of SUA disappeared when the SUA level was excessively higher.

In subgroup analyses based on SUA levels (Table 3), we observed that the negative association of baseline SUA with poorer global cognitive single-trajectories (OR: 0.890; 95% CI: 0.834, 0.950) and worse cognitive multi-trajectories (OR: 0.911; 95% CI: 0.853, 0.973) remained statistically significant among those without hyperuricemia. However, no significant association was found among those with hyperuricemia. Choosing different cut-points for SUA levels to perform other subgroup analyses yielded similar results (sex-specific median or 75th percentile). Notably, among those with ≥ 75 th percentile level of SUA, higher SUA levels were positively correlated with poor global cognitive trajectories (OR: 1.048; 95% CI: 0.821, 1.337). Although this result was not statistically significant, it still suggested the adverse effect of higher SUA levels on cognition among those with hyperuricemia.

Associations between changes in serum uric acid and 3-year cognitive change

Table 4 shows the association between changes in SUA and future 3-year cognitive change. Compared with participants in the “non-hyperuricemia with elevated SUA” group, participants in the “non-hyperuricemia with decreased SUA” group had a higher risk for decline in global cognitive function (β : -0.387; 95% CI: -0.696, -0.078) and executive function (β : -0.335; 95%

TABLE 2 Associations between baseline SUA and risk of poorer cognitive trajectories.

| | Model 1 | | Model 2 | | Model 3 | |
|--|----------------------|--------------|----------------------|--------------|----------------------|--------------|
| | OR (95% CI) | P-value | OR (95% CI) | P-value | OR (95% CI) | P-value |
| Global cognitive trajectories | | | | | | |
| SUA, +1 mg/dL | 0.907 (0.865, 0.952) | <0.001 | 0.946 (0.899, 0.995) | 0.032 | 0.948 (0.901, 0.998) | 0.043 |
| By sex-specific quartiles^a | | | | | | |
| Q1 | Ref. | | Ref. | | Ref. | |
| Q2 | 0.829 (0.703, 0.977) | 0.025 | 0.843 (0.710, 1.000) | 0.051 | 0.855 (0.720, 1.016) | 0.076 |
| Q3 | 0.773 (0.656, 0.911) | 0.002 | 0.808 (0.680, 0.960) | 0.015 | 0.821 (0.690, 0.977) | 0.026 |
| Q4 | 0.661 (0.560, 0.780) | <0.001 | 0.747 (0.628, 0.889) | 0.001 | 0.755 (0.634, 0.900) | 0.002 |
| P for trend | | <0.001 | | 0.001 | | 0.002 |
| Multi-trajectories | | | | | | |
| SUA, +1 mg/dL | 0.904 (0.861, 0.948) | <0.001 | 0.938 (0.892, 0.987) | 0.013 | 0.940 (0.894, 0.990) | 0.018 |
| By sex-specific quartiles^a | | | | | | |
| Q1 | Ref. | | Ref. | | Ref. | |
| Q2 | 0.807 (0.684, 0.952) | 0.011 | 0.809 (0.681, 0.961) | 0.016 | 0.816 (0.687, 0.970) | 0.021 |
| Q3 | 0.732 (0.621, 0.864) | <0.001 | 0.748 (0.629, 0.889) | 0.001 | 0.761 (0.639, 0.905) | 0.002 |
| Q4 | 0.691 (0.585, 0.815) | <0.001 | 0.777 (0.654, 0.924) | 0.004 | 0.784 (0.659, 0.933) | 0.006 |
| P for trend | | <0.001 | | 0.002 | | 0.004 |

CI, confidence interval; OR, Odds ratios; SUA, serum uric acid; ref., reference. Model 1: adjusted for age, gender. Model 2: adjusted for age, gender, marital status, education level, smoking status, drinking status, depressive symptoms. Model 3: adjusted for age, gender, marital status, education level, smoking status, drinking status, depressive symptoms, BMI, diabetes, dyslipidemia, stroke, heart-related diseases and prehypertension.

^aThe cutoff values were sex-specific quartiles of SUA (3.399, 4.008, and 4.733 mg/dL for women, 4.188, 4.964, and 5.818 mg/dL for men). Bold P-value denotes statistical significance ($P < 0.05$).

CI: -0.555, -0.114). Additionally, the “persistent hyperuricemia” group was negatively associated with improved global cognitive function (β : -0.851; 95% CI: -1.562, -0.140) and enhanced executive function (β : -0.672; 95% CI: -1.180, -0.164). The risk of cognitive decline was higher in the persistent hyperuricemia group. Both the remittent and incident hyperuricemia groups were not significantly associated with cognitive decline.

When the changes in SUA were calculated as the difference of both SUA measurements, only the Q3 group of change was related to improved global cognitive function compared with the Q1 group (β : 0.449; 95% CI: 0.073, 0.826). Moreover, there was a non-linear relationship between changes in SUA and cognitive change. The dose-response relationship indicated that moderate increases in the level of SUA were beneficial to enhance cognitive function (Figure 3).

Sensitivity analyses

First, we repeated the analyses after further adjusting for eGFR. The results remained almost consistent, as seen in Supplementary Tables 5, 6.

Second, we excluded 2,198 participants without information on physical activity in the first cohort, and the comparison of baseline characteristics between participants included and those who were not included in this analysis is shown in Supplementary Table 7. All variables were not

significantly different between groups. The results did not significantly change after further adjusting for physical activity (Supplementary Table 8). Similarly, the SUA levels were significantly negatively associated with worse cognitive trajectories, especially in the non-hyperuricemia group and the low-level SUA group. Conversely, higher SUA levels were significantly positively associated with poorer cognitive trajectories among the hyperuricemia group and the high-level SUA group (75th percentile as cut-points). In the second cohort, 872 participants with assessments of physical activity were included. There was also no significant difference in all variables between the included and excluded populations (Supplementary Table 9). Only the Q4 group of changes in SUA was related to improved global cognitive function compared with the Q1 group (β : 0.629; 95% CI: 0.002, 1.255) (Supplementary Table 10). However, the associations of “non-hyperuricemia with decreased SUA” and “persistent hyperuricemia” with cognitive changes became non-significant, probably due to the reduced sample size.

Moreover, the associations between the SUA levels and cognitive scores over time based on GEE models are shown in Supplementary Table 11. With each 1 mg/dl increase of SUA, the global cognitive score increased by 0.071 (95%CI: 0.015, 0.128) and the executive function score increased by 0.077 (95%CI: 0.035, 0.118). Similarly, a protective role for SUA was only found among those with normal or lower SUA. Interestingly, it seems that higher SUA levels

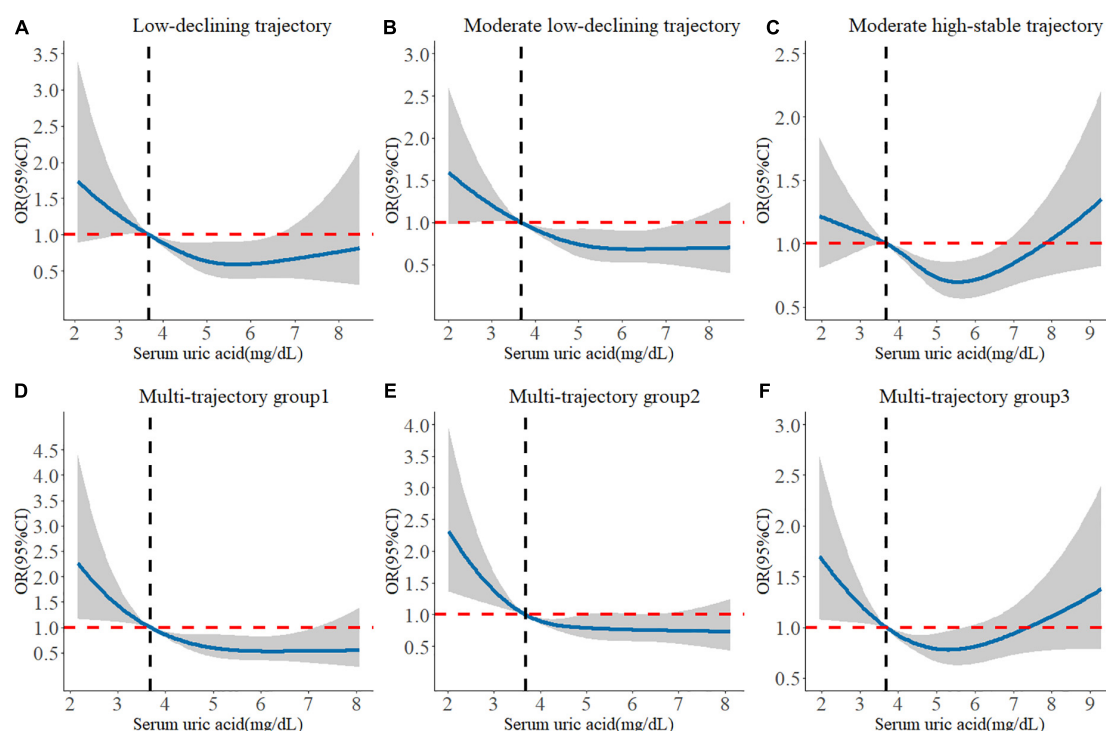


FIGURE 2

Longitudinal dose-response relationship between baseline SUA levels and poorer cognitive trajectories. The curve was estimated by a restricted cubic spline function with four knots. Solid lines indicate OR. The reference was set to 3.686 mg/dL (25th quantile). The shadow represents 95% confidence intervals. (A) Longitudinal dose-response relationship between baseline SUA levels and low-declining global cognitive trajectory. (B) Longitudinal dose-response relationship between baseline SUA levels and moderate low-declining global cognitive trajectory. (C) Longitudinal dose-response relationship between baseline SUA levels and moderate high-stable global cognitive trajectory. (D) Longitudinal dose-response relationship between baseline SUA levels and “episodic memory: low-rapid declining + executive function: low-declining” trajectory. (E) Longitudinal dose-response relationship between baseline SUA levels and “episodic memory: low-minimal declining + executive function: moderate-declining” trajectory. (F) Longitudinal dose-response relationship between baseline SUA levels and “episodic memory: moderate-stable + executive function: high-declining” trajectory.

could significantly impair episodic memory function among those with hyperuricemia [clinical diagnosis criteria for hyperuricemia (Huang Y. et al., 2022), sex-specific median, and 75th percentile as cut-points].

In addition, the results of subgroup analyses are presented in **Supplementary Figure 4**. The protective effects of SUA on better cognitive trajectories were significant in all subgroups by age, depression status, and the presence of prehypertension. Such association was observed among women but not among men. When non-normotensive patients were complicated by at least 1 CMD, the protective effect of SUA also disappeared.

Finally, the results were similar when the cognitive score in 2018 was used as the secondary outcome, which are shown in **Supplementary Table 12**.

Discussion

In this cohort study, four single-trajectories of global cognitive performance and four multi-trajectories of

executive function and episodic memory were identified in prehypertensive and hypertensive populations. We demonstrated that higher baseline SUA levels were negatively associated with a declining and poorer 7-year cognitive performance trajectory in a non-normotensive population. In subgroup analyses, the associations only existed among those with normal or lower levels of SUA. Reciprocally, higher baseline SUA may impair cognitive function among patients with hyperuricemia. Additionally, 4-year changes in SUA could influence future 3-year cognitive changes. Maintenance of the normal SUA levels and decreased levels of SUA at the same time can disrupt cognitive function. For patients with hyperuricemia in 2011, when SUA levels decreased to the normal range in 2015, no adverse effects on cognitive performance were found. Reversely, the persistent presence of hyperuricemia increased the risk of cognitive decline. In summary, our findings confirm the neuroprotective effect of SUA. However, under only the normal levels of SUA, moderate increases in SUA can prevent a decline in cognitive function among the non-normotensive population.

TABLE 3 Associations between baseline SUA and cognitive trajectories in subgroups by SUA levels.

| Subgroups | Global cognitive trajectories | | Multi-trajectories | |
|--|-------------------------------|------------------|----------------------|--------------|
| | OR (95% CI) | P-value | OR (95% CI) | P-value |
| Cut-points: clinical diagnosis criteria^a | | | | |
| Non-hyperuricemia group | | | | |
| SUA, +1 mg/dL | 0.890 (0.834, 0.950) | <0.001 | 0.911 (0.853, 0.973) | 0.006 |
| Lower-level SUA (by sex-specific median) | Ref. | | Ref. | |
| Higher-level SUA | 0.823 (0.721, 0.939) | 0.004 | 0.856 (0.748, 0.979) | 0.023 |
| Hyperuricemia group | | | | |
| SUA, +1 mg/dL | 1.169 (0.875, 1.561) | 0.289 | 1.194 (0.884, 1.615) | 0.247 |
| Lower-level SUA (by sex-specific median) | Ref. | | Ref. | |
| Higher-level SUA | 0.983 (0.531, 1.825) | 0.956 | 1.235 (0.647, 2.366) | 0.522 |
| Cut-points: sex-specific median^b | | | | |
| Low-level SUA group | | | | |
| SUA, +1 mg/dL | 0.896 (0.774, 1.038) | 0.144 | 0.838 (0.722, 0.973) | 0.021 |
| Lower-level SUA (by sex-specific median) | Ref. | | Ref. | |
| Higher-level SUA | 0.825 (0.697, 0.978) | 0.026 | 0.825 (0.694, 0.981) | 0.029 |
| High-level SUA group | | | | |
| SUA, +1 mg/dL | 0.996 (0.907, 1.092) | 0.927 | 1.005 (0.915, 1.104) | 0.913 |
| Lower-level SUA (by sex-specific median) | Ref. | | Ref. | |
| Higher-level SUA | 0.902 (0.760, 1.070) | 0.238 | 1.023 (0.859, 1.218) | 0.800 |
| Cut-points: sex-specific 75th quantile^c | | | | |
| Low-level SUA group | | | | |
| SUA, +1 mg/dL | 0.901 (0.821, 0.989) | 0.028 | 0.870 (0.791, 0.957) | 0.004 |
| Lower-level SUA (by sex-specific median) | Ref. | | Ref. | |
| Higher-level SUA | 0.859 (0.748, 0.987) | 0.032 | 0.851 (0.739, 0.980) | 0.025 |
| High-level SUA group | | | | |
| SUA, +1 mg/dL | 1.081 (0.938, 1.245) | 0.279 | 0.983 (0.852, 1.134) | 0.815 |
| Lower-level SUA (by sex-specific median) | Ref. | | Ref. | |
| Higher-level SUA | 1.048 (0.821, 1.337) | 0.707 | 0.900 (0.704, 1.151) | 0.400 |

CI, confidence interval; OR, Odds ratios; SUA, serum uric acid; ref., reference. Adjusted for: age, gender, marital status, education level, smoking status, drinking status, depressive symptoms, BMI, diabetes, dyslipidemia, stroke, heart-related diseases and prehypertension.

^aThe clinical diagnosis criteria for hyperuricemia were > 6.0 mg/dL for women and > 7.0 mg/dL for men.

^bThe sex-specific median of SUA were 4.008 mg/dL for women, 4.964 mg/dL for men.

^cThe sex-specific 75th percentile of SUA was 4.733 mg/dL for women, 5.818 mg/dL for men. Bold *P*-value denotes statistical significance (*P* < 0.05).

Based on our results, 27.19% of individuals with prehypertension and hypertension had a significant trend of decline in global cognitive function. Meanwhile, 31.04% of non-normotensive populations had a marked decreasing trend in both episodic memory and executive function. Non-normotensive patients had a high risk of incident cognitive decline. Then, we found that the non-normotensive population with high levels of SUA still had more favorable 7-year cognitive trajectories than those with low levels of SUA, which is similar to previous studies in the general population (Wang T. et al., 2017; Xiu et al., 2017; Scheepers et al., 2019; Chen et al., 2021). One potential protection mechanism may be the antioxidant effects of SUA (Tana et al., 2018). Oxidative stress or low antioxidant levels in the brain may exert an important role in the pathogenesis of cognitive impairment or dementia, leading to free radical generation, lipid peroxidation,

and mitochondrial dysfunction (Zhou et al., 2021). While higher SUA could protect the blood-brain barrier against oxidative stress (Tana et al., 2018). Moreover, patients with congenital SUA disorder may have a genetic tendency to cognitive dysfunction (Qiao et al., 2021). Then, hypouricemia is often accompanied by poor nutritional status, which results in cognitive impairment (Sanders et al., 2016; Zhou et al., 2021). Thus, people with higher SUA levels would show better cognitive performance.

However, the results of some previous studies are contradictory. A study reported that higher levels of SUA were associated with faster cognitive decline (Alam et al., 2020). Another finding of a 12-year cohort study demonstrated that high SUA levels may increase the risk of dementia, especially vascular or mixed dementia (Latourte et al., 2018b). This inconsistency could be explained by the included patient with

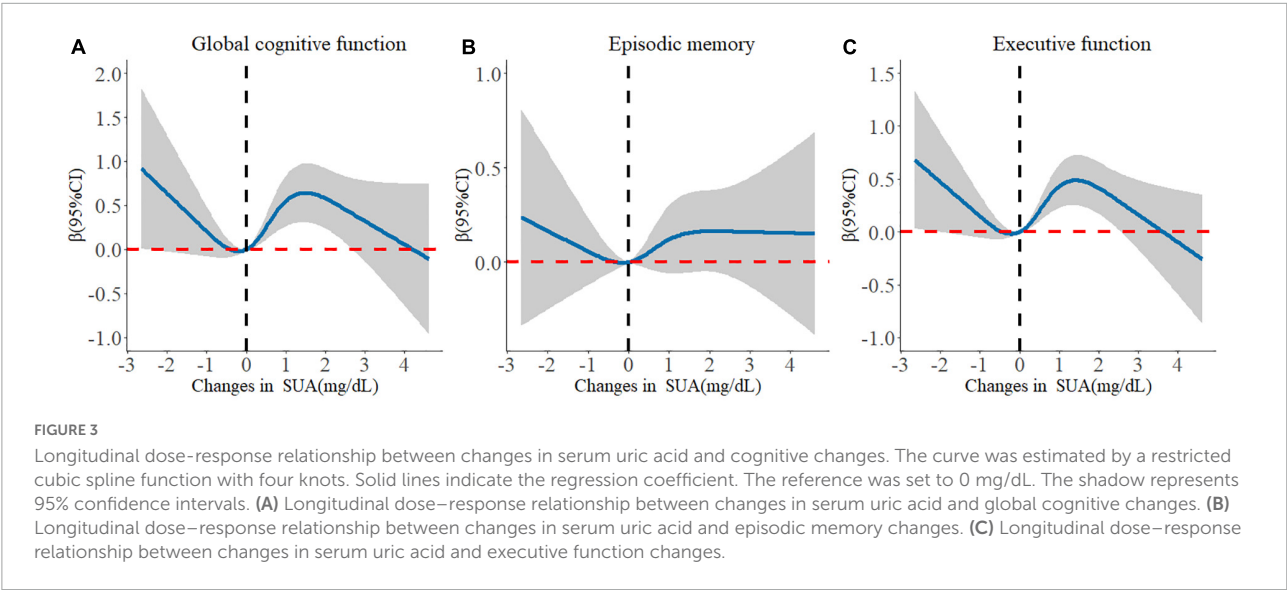
TABLE 4 Associations between changes in SUA and 3-year cognitive changes.

| | Global cognitive function | | Episodic memory | | Executive function | |
|--------------------------------------|---------------------------|--------------|------------------------|----------|-------------------------|--------------|
| | β (95% CI) | <i>P</i> | β (95% CI) | <i>P</i> | β (95% CI) | <i>P</i> |
| Non-hyperuricemia with elevated SUA | Ref. | | Ref. | | Ref. | |
| Non-hyperuricemia with decreased SUA | −0.387 (−0.696, −0.078) | 0.014 | −0.053 (−0.247, 0.142) | 0.595 | −0.335 (−0.555, −0.114) | 0.003 |
| Incident hyperuricemia | 0.007 (−0.440, 0.454) | 0.976 | 0.035 (−0.246, 0.317) | 0.806 | −0.029 (−0.348, 0.291) | 0.861 |
| Remittent hyperuricemia | 0.055 (−0.789, 0.900) | 0.898 | −0.074 (−0.606, 0.458) | 0.785 | 0.129 (−0.474, 0.733) | 0.674 |
| Persistent hyperuricemia | −0.851 (−1.562, −0.140) | 0.019 | −0.179 (−0.626, 0.269) | 0.434 | −0.672 (−1.180, −0.164) | 0.010 |
| Changes in SUA ^a | | | | | | |
| Changes in SUA, +1 mg/dL | 0.075 (−0.049, 0.199) | 0.235 | 0.025 (−0.053, 0.103) | 0.528 | 0.050 (−0.039, 0.138) | 0.270 |
| By quartiles ^b | | | | | | |
| Q1 | Ref. | | Ref. | | Ref. | |
| Q2 | −0.067 (−0.436, 0.303) | 0.723 | −0.094 (−0.327, 0.138) | 0.426 | 0.029 (−0.236, 0.293) | 0.832 |
| Q3 | 0.449 (0.073, 0.826) | 0.019 | 0.002 (−0.235, 0.239) | 0.987 | 0.447 (0.178, 0.717) | 0.001 |
| Q4 | 0.375 (−0.006, 0.757) | 0.054 | 0.089 (−0.152, 0.329) | 0.470 | 0.287 (0.014, 0.560) | 0.040 |

CI, confidence interval; β , regression coefficient; SUA, serum uric acid; ref., reference. Adjusted for: age, gender, marital status, education level, smoking status, drinking status, depressive symptoms, BMI, diabetes, dyslipidemia, stroke, heart-related diseases, prehypertension, and SUA levels in 2015.

^aChanges in SUA was also calculated as the SUA level in 2015 minus that at baseline in 2011.

^bThe cutoff values were quartiles of changes in SUA (−0.073, 0.492, 1.150). Bold *P*-value denotes statistical significance (*P* < 0.05).



hyperuricemia. Cardiometabolic disorders, inflammation, vascular damage, and the pro-arteriosclerotic effect caused by higher SUA levels may counteract its neuroprotective role, resulting in cognitive decline and increasing the risk of vascular dementia (Tana et al., 2018; Zhou et al., 2021; Huang Y. et al., 2022). Thus, we performed several subgroup analyses with different SUA levels. We found that the non-normotensive population with higher SUA levels has more stable and better cognitive trajectories only in non-hyperuricemia groups, which is similar to one previous study (Chen et al., 2021). The sample size of adults with hyperuricemia in both our study and of the study of Chen et al. (2021) was relatively small. Considering this limitation, subgroups were divided by different cut-points

for SUA levels (sex-specific median and 75th percentile) and similar results were obtained. The significant protective effect of SUA on cognitive function was found only in low-level SUA subgroups. Notably, among those with higher or abnormal levels of SUA, SUA could impair their cognitive function, especially memory function. The optimum cut-points of the abnormal levels of SUA to balance the integrated prevention of cognitive impairment and cardiovascular and cerebrovascular diseases should be further explored. Besides, the dose-response relationship test further confirmed our results.

In sensitivity analyses, the protective effect of SUA also disappeared when non-normotensive patients were complicated by at least 1 CMD, which could further verify our conjecture

mentioned above. Additionally, the finding of this association only in women, rather than in men, may be explained by the higher risk of cerebrovascular disease in men and the estrogen effects after menopause in women (Lee et al., 2021). Some studies reported similar research conclusions (Scheepers et al., 2019; Lee et al., 2021). Our findings suggested that the neuroprotective role of SUA should be emphasized in female patients with hypertension without other CMD.

Innovatively, we also provide evidence that the changes in SUA can influence future cognitive performance. When SUA was maintained at normal levels over a period of time, decreased levels of SUA are strongly associated with worse cognitive performance. However, the persistent presence of hyperuricemia may result in more severe cognitive decline. Additionally, we analyzed the changes in SUA as a continuous variable and the dose-response relationship. We proved that a moderate increase in SUA levels may improve cognitive function, rather than an excessive increase. When SUA increased to abnormal levels, the protective effect of SUA may disappear. SUA appears to be a double-edged sword due to both the harmful effect on patients with hypertension and the neuroprotective role (Latourte et al., 2018a; Yang et al., 2021). In clinical practice, it also remains unknown whether urate-lowering therapy has adverse effects on cognitive performance, which is of great concern (Singh, 2018; Latourte et al., 2021). To a certain extent, our study could provide supporting evidence that remittent hyperuricemia was not associated with cognitive decline. Conversely, the risk for cognitive decline may be even higher if left untreated or if higher SUA levels are not controlled. Decreased SUA may result in poorer cognitive changes only in those without hyperuricemia. Our findings provide some inspiration for balancing the urate-lowering therapy against the prevention of cognitive impairment or dementia. The maintenance of normal SUA levels is a primary condition to prevent cognitive impairment and dementia. Thus, the treatment of hyperuricemia should still be a priority in daily life and clinical practice for non-normotensive populations.

Strengths and limitations

First, our findings extend and refine evidence that higher SUA levels within the normal range could still protect cognitive functions in the prehypertensive and hypertensive populations. Additionally, single-time point measures of SUA and changes in SUA over time were all considered. Furthermore, our study fully considered different situations among both patients with non-hyperuricemia and hyperuricemia, which provides specific guidance to balance urate-lowering therapy against the prevention of cognitive impairment or dementia. The other strength is the use of GBTM and GBMTM to identify groups of individuals who experienced similar levels and change patterns of cognitive functions over time (Li et al., 2020), while the traditional statistical approaches for repeated

measures data, such as GEE or linear mixed models, only focus on mean population trajectories (Li et al., 2020). However, the conventional method, GEE, was also used to validate the robustness of our results. Finally, the strengths of our study also include the prospective cohort design and the use of a large nationwide representative sample covering 28 provinces in China.

We acknowledge several limitations of this study. First, the physical activity investigation was limited to a randomly selected subgroup in the CHARLS study and had a large number of missing values. In the sensitivity analysis, physical activity was adjusted for only in the subpopulation with a small sample size. Second, residual confounding factors were not fully controlled. Dietary intake, nutrients, and urate-lowering medications were also not incorporated in the final model due to the lack of related data. Additionally, the assessment tool for cognition performance used was relatively simple and limited. The cutoff values of cognitive impairment of this test were lacking, but the moderate-to-high validity of this cognitive test was reported compared with the Mini-Mental State Examination (MMSE) and the Clinical Dementia Rating Scale (CDR) (Meng et al., 2019). Finally, more time point measurements of the SUA levels need to be conducted to capture the longitudinal patterns of SUA over a period more accurately.

Conclusion

In brief, our findings indicate that baseline SUA and changes in SUA can affect future cognitive trajectories or changes in a non-normotensive population. The maintenance of normal SUA levels and a moderate increase of SUA may be beneficial for enhanced cognitive function. However, the persistent presence of hyperuricemia may result in cognitive decline. Although the neuroprotective role of high levels of SUA was confirmed in our study, the maintenance of normal SUA levels is a primary condition to prevent cognitive impairment and dementia.

Data availability statement

The raw data supporting the conclusions of this article will be made available by the authors, without undue reservation.

Ethics statement

The studies involving human participants were reviewed and approved by Ethical approval for all the CHARLS waves was granted from the Institutional Review Board at Peking University. The IRB approval number for the main household survey, including anthropometrics, is IRB00001052-11015. The patients/participants provided their written informed consent to participate in this study.

Author contributions

LT: full access to all of the data in the study and takes responsibility for the integrity of the data and the accuracy of the data analysis. JW, XG, and LT: study conception and design. JW, RJ, ZH, ZX, and LT: data collection. JW, ZW, YL, YJL, XJ, and LT: data analysis and interpretation. JW and LT: manuscript writing and reviewing. XG and LT: study supervision. All authors read and approved the final manuscript.

Funding

This work was funded by the National Natural Science Foundation of China (numbers: 82073668 and 81872708 to LT).

Acknowledgments

The National School of Development at Peking University provided the data in the China Health and Retirement Longitudinal Survey. We thank the staff of the China Health and Retirement Longitudinal Study team for their invaluable contributions.

References

- Alam, A. B., Wu, A., Power, M. C., West, N. A., and Alonso, A. (2020). Associations of serum uric acid with incident dementia and cognitive decline in the ARIC-NCS cohort. *J. Neurol. Sci.* 414:116866. doi: 10.1016/j.jns.2020.116866
- Beydoun, M. A., Canas, J. A., Dore, G. A., Beydoun, H. A., Rostant, O. S., Fanelli-Kuczmarski, M. T., et al. (2016). Serum Uric Acid and Its Association with Longitudinal Cognitive Change Among Urban Adults. *J. Alzheimers Dis.* 52, 1415–1430. doi: 10.3233/jad-160028
- Bowman, G. L., Shannon, J., Frei, B., Kaye, J. A., and Quinn, J. F. (2010). Uric acid as a CNS antioxidant. *J. Alzheimers Dis.* 19, 1331–1336. doi: 10.3233/jad-2010-1330
- Cassano, V., Crescibene, D., Hribal, M. L., Pelaia, C., Armentaro, G., Magurno, M., et al. (2020). Uric Acid and Vascular Damage in Essential Hypertension: Role of Insulin Resistance. *Nutrients* 12:2509. doi: 10.3390/nu12092509
- Chen, C., Li, X., Lv, Y., Yin, Z., Zhao, F., Liu, Y., et al. (2021). High Blood Uric Acid Is Associated With Reduced Risks of Mild Cognitive Impairment Among Older Adults in China: A 9-Year Prospective Cohort Study. *Front. Aging Neurosci.* 13:747686. doi: 10.3389/fnagi.2021.747686
- Chen, H., and Mui, A. C. (2014). Factorial validity of the Center for Epidemiologic Studies Depression Scale short form in older population in China. *Int. Psychogeriatr.* 26, 49–57. doi: 10.1017/s1041610213001701
- Chen, K. H., Henderson, V. W., Stolwyk, R. J., Dennerstein, L., and Szoek, C. (2015). Prehypertension in midlife is associated with worse cognition a decade later in middle-aged and older women. *Age Ageing* 44, 439–445. doi: 10.1093/ageing/afv026
- Chen, X., Crimmins, E., Hu, P. P., Kim, J. K., Meng, Q., Strauss, J., et al. (2019). Venous Blood-Based Biomarkers in the China Health and Retirement Longitudinal Study: Rationale, Design, and Results From the 2015 Wave. *Am. J. Epidemiol.* 188, 1871–1877. doi: 10.1093/aje/kwz170
- Chobanian, A. V., Bakris, G. L., Black, H. R., Cushman, W. C., Green, L. A., Izzo, J. L. Jr., et al. (2003). The Seventh Report of the Joint National Committee on Prevention, Detection, Evaluation, and Treatment of High Blood Pressure: The JNC 7 report. *JAMA* 289, 2560–2572. doi: 10.1001/jama.289.19.2560
- Davis, M. A., Chang, C.-H., Simonton, S., and Bynum, J. P. W. (2022). Trends in US Medicare Decedents' Diagnosis of Dementia From 2004 to 2017. *JAMA Health Forum* 3:e220346–e220346. doi: 10.1001/jamahealthforum.2022.0346
- de Menezes, S. T., Giatti, L., Brant, L. C. C., Griep, R. H., Schmidt, M. I., Duncan, B. B., et al. (2021). Hypertension, Prehypertension, and Hypertension Control: Association With Decline in Cognitive Performance in the ELSA-Brasil Cohort. *Hypertension* 77, 672–681. doi: 10.1161/hypertensionaha.120.16080
- Ding, L., Liang, Y., Tan, E. C. K., Hu, Y., Zhang, C., Liu, Y., et al. (2020). Smoking, heavy drinking, physical inactivity, and obesity among middle-aged and older adults in China: Cross-sectional findings from the baseline survey of CHARLS 2011–2012. *BMC Public Health* 20:1062. doi: 10.1186/s12889-020-08625-5
- Gottesman, R. F., Schneider, A. L., Albert, M., Alonso, A., Bandeen-Roche, K., Coker, L., et al. (2014). Midlife hypertension and 20-year cognitive change: The atherosclerosis risk in communities neurocognitive study. *JAMA Neurol.* 71, 1218–1227. doi: 10.1001/jamaneurol.2014.1646
- Hua, J., Sun, H., and Shen, Y. (2020). Improvement in sleep duration was associated with higher cognitive function: A new association. *Aging* 12, 20623–20644. doi: 10.18632/aging.103948
- Huang, R., Tian, S., Han, J., Lin, H., Guo, D., Wang, J., et al. (2019). U-Shaped Association Between Serum Uric Acid Levels and Cognitive Functions in Patients with Type 2 Diabetes: A Cross-Sectional Study. *J. Alzheimers Dis.* 69, 135–144. doi: 10.3233/jad-181126
- Huang, Y., Zhang, S., Shen, J., Yang, J., Chen, X., Li, W., et al. (2022). Association of plasma uric acid levels with cognitive function among non-hyperuricemia adults: A prospective study. *Clin. Nutr.* 41, 645–652. doi: 10.1016/j.clnu.2021.12.039
- Huang, Z. T., Luo, Y., Han, L., Wang, K., Yao, S. S., Su, H. X., et al. (2022). Patterns of cardiometabolic multimorbidity and the risk of depressive symptoms in a longitudinal cohort of middle-aged and older Chinese. *J. Affect. Disord.* 301, 1–7. doi: 10.1016/j.jad.2022.01.030

Conflict of interest

The authors declare that the research was conducted in the absence of any commercial or financial relationships that could be construed as a potential conflict of interest.

Publisher's note

All claims expressed in this article are solely those of the authors and do not necessarily represent those of their affiliated organizations, or those of the publisher, the editors and the reviewers. Any product that may be evaluated in this article, or claim that may be made by its manufacturer, is not guaranteed or endorsed by the publisher.

Supplementary material

The Supplementary Material for this article can be found online at: <https://www.frontiersin.org/articles/10.3389/fnagi.2022.944341/full#supplementary-material>

- Iadecola, C., and Gottesman, R. F. (2019). Neurovascular and Cognitive Dysfunction in Hypertension. *Circ. Res.* 124, 1025–1044. doi: 10.1161/circresaha.118.313260
- Jia, J., Wei, C., Chen, S., Li, F., Tang, Y., Qin, W., et al. (2018). The cost of Alzheimer's disease in China and re-estimation of costs worldwide. *Alzheimers Dement.* 14, 483–491. doi: 10.1016/j.jalz.2017.12.006
- Kawai, T., Ohishi, M., Takeya, Y., Onishi, M., Ito, N., Yamamoto, K., et al. (2012). Serum uric acid is an independent risk factor for cardiovascular disease and mortality in hypertensive patients. *Hypertens Res.* 35, 1087–1092. doi: 10.1038/hr.2012.99
- Kim, J. W., Byun, M. S., Yi, D., Lee, J. H., Jeon, S. Y., Ko, K., et al. (2020). Serum Uric Acid, Alzheimer-Related Brain Changes, and Cognitive Impairment. *Front. Aging Neurosci.* 12:160. doi: 10.3389/fnagi.2020.00160
- Latourte, A., Bardin, T., and Richette, P. (2018a). Uric acid and cognitive decline: A double-edge sword? *Curr. Opin Rheumatol.* 30, 183–187. doi: 10.1097/bor.0000000000000472
- Latourte, A., Soumaré, A., Bardin, T., Perez-Ruiz, F., Debette, S., and Richette, P. (2018b). Uric acid and incident dementia over 12 years of follow-up: A population-based cohort study. *Ann. Rheum. Dis.* 77, 328–335. doi: 10.1136/annrheumdis-2016-210767
- Latourte, A., Dumurgier, J., Paquet, C., and Richette, P. (2021). Hyperuricemia, Gout, and the Brain—an Update. *Curr. Rheumatol. Rep.* 23:82. doi: 10.1007/s11926-021-01050-6
- Lee, Y. G., Park, M., Jeong, S. H., Kang, S. W., Baik, K., Jung, J. H., et al. (2021). Effects of baseline serum uric acid and apolipoprotein E4 on longitudinal cognition and cerebral metabolism. *Neurobiol. Aging* 106, 223–231. doi: 10.1016/j.neurobiolaging.2021.05.003
- Lei, X., Hu, Y., McArdle, J. J., Smith, J. P., and Zhao, Y. (2012). Gender Differences in Cognition among Older Adults in China. *J. Hum. Resour.* 47, 951–971. doi: 10.3368/jhr.47.4.951
- Levey, A. S., Stevens, L. A., Schmid, C. H., Zhang, Y. L., Castro, A. F. III, Feldman, H. I., et al. (2009). A new equation to estimate glomerular filtration rate. *Ann. Intern. Med.* 150, 604–612. doi: 10.7326/0003-4819-150-9-200905050-00006
- Li, H., Li, C., Wang, A., Qi, Y., Feng, W., Hou, C., et al. (2020). Associations between social and intellectual activities with cognitive trajectories in Chinese middle-aged and older adults: A nationally representative cohort study. *Alzheimers Res. Ther.* 12:115. doi: 10.1186/s13195-020-00691-6
- Liu, J., Tao, L., Zhao, Z., Mu, Y., Zou, D., Zhang, J., et al. (2018). Two-Year Changes in Hyperuricemia and Risk of Diabetes: A Five-Year Prospective Cohort Study. *J. Diabetes Res.* 2018:6905720. doi: 10.1155/2018/6905720
- Lloyd-Jones, D. M., Hong, Y., Labarthe, D., Mozaffarian, D., Appel, L. J., Van Horn, L., et al. (2010). Defining and setting national goals for cardiovascular health promotion and disease reduction: The American Heart Association's strategic Impact Goal through 2020 and beyond. *Circulation* 121, 586–613. doi: 10.1161/circulationaha.109.192703
- Meng, Q., Wang, H., Strauss, J., Langa, K. M., Chen, X., Wang, M., et al. (2019). Validation of neuropsychological tests for the China Health and Retirement Longitudinal Study Harmonized Cognitive Assessment Protocol. *Int. Psychogeriatr.* 31, 1709–1719. doi: 10.1017/s1041610219000693
- Nagin, D. S., Jones, B. L., Passos, V. L., and Tremblay, R. E. (2018). Group-based multi-trajectory modeling. *Stat. Methods Med. Res.* 27, 2015–2023. doi: 10.1177/0962280216673085
- Nagin, D. S., and Odgers, C. L. (2010). Group-based trajectory modeling in clinical research. *Annu. Rev. Clin. Psychol.* 6, 109–138. doi: 10.1146/annurev.clinpsy.121208.131413
- Nichols, E., Szoek, C. E., Vollset, S. E., Abbasi, N., Abd-Allah, F., Abdela, J., et al. (2019). Global, regional, and national burden of neurological disorders, 1990–2016: A systematic analysis for the Global Burden of Disease Study 2016. *Lancet Neurol.* 18, 459–480. doi: 10.1016/s1474-4422(18)30499-x
- Qiao, M., Chen, C., Liang, Y., Luo, Y., and Wu, W. (2021). The Influence of Serum Uric Acid Level on Alzheimer's Disease: A Narrative Review. *Biomed. Res. Int.* 2021:5525710. doi: 10.1155/2021/5525710
- Richard, E. L., McEvoy, L. K., Cao, S. Y., Oren, E., Alcaraz, J. E., LaCroix, A. Z., et al. (2021). Biomarkers of kidney function and cognitive ability: A Mendelian randomization study. *J. Neurol. Sci.* 430:118071. doi: 10.1016/j.jns.2021.11.8071
- Sanders, C., Behrens, S., Schwartz, S., Wengreen, H., Corcoran, C. D., Lyketsos, C. G., et al. (2016). Nutritional Status is Associated with Faster Cognitive Decline and Worse Functional Impairment in the Progression of Dementia: The Cache County Dementia Progression Study1. *J. Alzheimers Dis.* 52, 33–42. doi: 10.3233/jad-150528
- Scheepers, L., Jacobsson, L. T. H., Kern, S., Johansson, L., Dehlin, M., and Skoog, I. (2019). Urate and risk of Alzheimer's disease and vascular dementia: A population-based study. *Alzheimers Dement.* 15, 754–763. doi: 10.1016/j.jalz.2019.01.014
- Sharaf El Din, U. A. A., Salem, M. M., and Abdulazim, D. O. (2017). Uric acid in the pathogenesis of metabolic, renal, and cardiovascular diseases: A review. *J. Adv. Res.* 8, 537–548. doi: 10.1016/j.jare.2016.11.004
- Singh, J. A. (2018). Role of serum urate in neurocognitive function and dementia: New evidence contradicts old thinking. *Ann. Rheum. Dis.* 77, 317–318. doi: 10.1136/annrheumdis-2017-211975
- Singh, J. A., and Cleveland, J. D. (2018). Gout and dementia in the elderly: A cohort study of Medicare claims. *BMC Geriatr.* 18:281. doi: 10.1186/s12877-018-0975-0
- Suzuki, K., Koide, D., Fujii, K., Yamazaki, T., Tsuji, S., and Iwata, A. (2016). Elevated Serum Uric Acid Levels Are Related to Cognitive Deterioration in an Elderly Japanese Population. *Dement. Geriatr. Cogn. Dis. Extra.* 6, 580–588. doi: 10.1159/000454660
- Tana, C., Ticinesi, A., Prati, B., Nouvenne, A., and Meschi, T. (2018). Uric Acid and Cognitive Function in Older Individuals. *Nutrients* 10:975. doi: 10.3390/nu10080975
- Tuven, B., Soysal, P., Unutmaz, G., Kaya, D., and Isik, A. T. (2017). Uric acid may be protective against cognitive impairment in older adults, but only in those without cardiovascular risk factors. *Exp. Gerontol.* 89, 15–19. doi: 10.1016/j.exger.2017.01.002
- Viridis, A., Masi, S., Casiglia, E., Tikhonoff, V., Cicero, A. F. G., Ungar, A., et al. (2020). Identification of the Uric Acid Thresholds Predicting an Increased Total and Cardiovascular Mortality Over 20 Years. *Hypertension* 75, 302–308. doi: 10.1161/hypertensionaha.119.13643
- Wang, F., Zhao, M., Han, Z., Li, D., Zhang, S., Zhang, Y., et al. (2017). Hyperuricemia as a Protective Factor for Mild Cognitive Impairment in Non-Obese Elderly. *Tohoku J. Exp. Med.* 242, 37–42. doi: 10.1620/tjem.242.37
- Wang, T., Wu, Y., Sun, Y., Zhai, L., and Zhang, D. (2017). A Prospective Study on the Association between Uric Acid and Cognitive Function among Middle-Aged and Older Chinese. *J. Alzheimers Dis.* 58, 79–86. doi: 10.3233/jad-161243
- Wang, H., and Zhai, F. (2013). Programme and policy options for preventing obesity in China. *Obes. Rev.* 14, 134–140. doi: 10.1111/obr.12106
- Wu, Z., Zhang, H., Miao, X., Li, H., Pan, H., Zhou, D., et al. (2021a). High-intensity physical activity is not associated with better cognition in the elder: Evidence from the China Health and Retirement Longitudinal Study. *Alzheimers Res. Ther.* 13:182. doi: 10.1186/s13195-021-00923-3
- Wu, Z., Zhou, D., Liu, Y., Li, Z., Wang, J., Han, Z., et al. (2021b). Association of TyG index and TG/HDL-C ratio with arterial stiffness progression in a non-normotensive population. *Cardiovasc Diabetol.* 20:134. doi: 10.1186/s12933-021-01330-6
- Xiu, S., Zheng, Z., Guan, S., Zhang, J., Ma, J., and Chan, P. (2017). Serum uric acid and impaired cognitive function in community-dwelling elderly in Beijing. *Neurosci. Lett.* 637, 182–187. doi: 10.1016/j.neulet.2016.11.013
- Xue, J., Li, J., Liang, J., and Chen, S. (2018). The Prevalence of Mild Cognitive Impairment in China: A Systematic Review. *Aging Dis.* 9, 706–715. doi: 10.14336/ad.2017.0928
- Yang, Y., Zhang, X., Jin, Z., and Zhao, Q. (2021). Association of serum uric acid with mortality and cardiovascular outcomes in patients with hypertension: A meta-analysis. *J. Thromb. Thrombolysis* 52, 1084–1093. doi: 10.1007/s11239-021-02453-z
- Zhao, Y., Hu, Y., Smith, J. P., Strauss, J., and Yang, G. (2014). Cohort profile: The China Health and Retirement Longitudinal Study (CHARLS). *Int. J. Epidemiol.* 43, 61–68. doi: 10.1093/ije/dys203
- Zhou, Z., Zhong, S., Liang, Y., Zhang, X., Zhang, R., Kang, K., et al. (2021). Serum Uric Acid and the Risk of Dementia: A Systematic Review and Meta-Analysis. *Front. Aging Neurosci.* 13:625690. doi: 10.3389/fnagi.2021.625690



OPEN ACCESS

EDITED BY

Agustin Ibanez,
Latin American Brain Health Institute
(BrainLat), Chile

REVIEWED BY

Chao Zhou,
University of Pittsburgh, United States
Chun Chen,
Newcastle University, United Kingdom
Chenlong Liao,
Shanghai Jiao Tong University, China

*CORRESPONDENCE

Fan Lin
linfan@fjmu.edu.cn

†These authors have contributed
equally to this work

SPECIALTY SECTION

This article was submitted to
Alzheimer's Disease and Related
Dementias,
a section of the journal
Frontiers in Aging Neuroscience

RECEIVED 30 April 2022

ACCEPTED 28 June 2022

PUBLISHED 28 July 2022

CITATION

Lai Y, Lin C, Lin X, Wu L, Zhao Y and
Lin F (2022) Identification and
immunological characterization of
cuproptosis-related molecular clusters
in Alzheimer's disease.
Front. Aging Neurosci. 14:932676.
doi: 10.3389/fnagi.2022.932676

COPYRIGHT

© 2022 Lai, Lin, Lin, Wu, Zhao and Lin.
This is an open-access article
distributed under the terms of the
Creative Commons Attribution License
(CC BY). The use, distribution or
reproduction in other forums is
permitted, provided the original
author(s) and the copyright owner(s)
are credited and that the original
publication in this journal is cited, in
accordance with accepted academic
practice. No use, distribution or
reproduction is permitted which does
not comply with these terms.

Identification and immunological characterization of cuproptosis-related molecular clusters in Alzheimer's disease

Yongxing Lai^{1,2†}, Chunjin Lin^{1,2†}, Xing Lin^{1,2}, Lijuan Wu^{1,2},
Yinan Zhao^{1,2} and Fan Lin^{1,2*}

¹Department of Geriatric Medicine, Shengli Clinical Medical College of Fujian Medical University, Fuzhou, China, ²Fujian Provincial Center for Geriatrics, Fujian Provincial Hospital, Fuzhou, China

Introduction: Alzheimer's disease is the most common dementia with clinical and pathological heterogeneity. Cuproptosis is a recently reported form of cell death, which appears to result in the progression of various diseases. Therefore, our study aimed to explore cuproptosis-related molecular clusters in Alzheimer's disease and construct a prediction model.

Methods: Based on the GSE33000 dataset, we analyzed the expression profiles of cuproptosis regulators and immune characteristics in Alzheimer's disease. Using 310 Alzheimer's disease samples, we explored the molecular clusters based on cuproptosis-related genes, along with the related immune cell infiltration. Cluster-specific differentially expressed genes were identified using the WGCNA algorithm. Subsequently, the optimal machine model was chosen by comparing the performance of the random forest model, support vector machine model, generalized linear model, and eXtreme Gradient Boosting. Nomogram, calibration curve, decision curve analysis, and three external datasets were applied for validating the predictive efficiency.

Results: The dysregulated cuproptosis-related genes and activated immune responses were determined between Alzheimer's disease and non-Alzheimer's disease controls. Two cuproptosis-related molecular clusters were defined in Alzheimer's disease. Analysis of immune infiltration suggested the significant heterogeneity of immunity between distinct clusters. Cluster2 was characterized by elevated immune scores and relatively higher levels of immune infiltration. Functional analysis showed that cluster-specific differentially expressed genes in Cluster2 were closely related to various immune responses. The Random forest machine model presented the best discriminative performance with relatively lower residual and root mean square error, and a higher area under the curve (AUC = 0.9829). A final 5-gene-based random forest model was constructed, exhibiting satisfactory performance in two external validation datasets (AUC = 0.8529 and 0.8333). The nomogram, calibration curve, and decision curve analysis also demonstrated the accuracy to predict Alzheimer's disease subtypes. Further analysis revealed that these five model-related genes were significantly associated with the A β -42 levels and β -secretase activity.

Conclusion: Our study systematically illustrated the complicated relationship between cuproptosis and Alzheimer's disease, and developed a promising prediction model to evaluate the risk of cuproptosis subtypes and the pathological outcome of Alzheimer's disease patients.

KEYWORDS

Alzheimer's disease, cuproptosis, molecular clusters, immune infiltration, machine learning, prediction model

Introduction

Alzheimer's disease (AD) is the most common form of age-related neurodegenerative disease. It is reported that approximately more than 42.3 million people worldwide suffer from progressive cognitive impairment caused by AD (Ambrogio et al., 2019), and data from epidemiological analyses suggest that the number of people with AD will be more than twice the current number in 2060 (Matthews et al., 2019). As the disease progresses, AD patients may experience varying degrees of cognitive and memory insult, such as language, visuospatial, motor, and executive function deficits (McKhann et al., 2011). The increasing number of AD patients, therefore, places a huge burden on families and society. Unfortunately, due to the clinical heterogeneity of AD and the complexity of pathological types, satisfactory treatment for AD was lacking and no effective strategy was proven to prevent the occurrence of AD (Nandigam, 2008; Rahimi and Kovacs, 2014). Recently, a growing number of biomarkers are associated with AD, yet a single dataset or relatively small sample sizes may make these results unconvincing (Zheng et al., 2018; Liu et al., 2022). In addition, the efficacy of biomarker-based univariate prediction models has also been challenged (Jack et al., 2014). Therefore, further accurate identification of molecular subtypes of AD at the molecular level and establishing a multivariate predictive model would be of great clinical importance.

As cofactors for enzymes, the maintenance of copper ions (Cu^{2+}), copper homeostasis, mainly depends on the regulation of mitochondria (Baker et al., 2017). Copper exists mainly in the form of cytochrome C oxidase (COX) and superoxide dismutase (SOD1) in mitochondria, thus acting as a vital regulator in the tricarboxylic acid cycle (TCA) and eventually playing a critical role in various biological processes including redox balance, iron utilization, oxidative phosphorylation, and cell growth (Soto et al., 2012; Dennerlein and Rehling, 2015). However, dysregulation of copper homeostasis has been proven to be associated with neurodegenerative diseases (Gromadzka et al., 2020). Cuproptosis is a recently discovered novel form of cell death that differs from other oxidative stress-regulated deaths such as pyroptosis, ferroptosis, and necroptosis. It is reported that mitochondrial stress characterized by over-accumulation of lipoylated mitochondrial enzymes and the depletion of Fe-S cluster proteins are the primary mechanisms causing

cuproptosis (Oliveri, 2022; Wang et al., 2022b). Cu^{2+} entering the cell can be reduced to Cu^+ by FDX1, which in turn promotes lipid acylation of mitochondrial proteins and overproduction of key enzymes associated with the mitochondrial tricarboxylic acid (TCA) cycle (DBT, GCSH, DLST, and DLAT). In addition, the instability of Fe-S cluster proteins is also closely related to FDX1. Moreover, critical genes implicated in the Cu^{2+} transport, such as SLC31A1 and ATP7B, may play a vital role in regulating the occurrence of cuproptosis. Furthermore, it was found that the inhibition of mitochondrial pyruvate carrier and electron transport chain activity could alleviate the damage caused by cuproptosis (Cobine and Brady, 2022; Tang et al., 2022; Tsvetkov et al., 2022). In addition, an increasing number of studies demonstrate that mitochondria dysfunction-induced deficiency of energy metabolism and oxidative stress may be the critical pathogenesis involved in AD progression (Chen and Zhong, 2014; Murphy and Hartley, 2018; Tang et al., 2019). Therefore, it would be reasonable to infer that cuproptosis is closely associated with the development of AD. However, the potential regulatory mechanisms of cuproptosis in AD remain unknown and require further exploration. Therefore, further illustrating the molecular characteristics of cuproptosis-related genes (CRGs) may be able to explain the cause of heterogeneity in AD.

In the present study, we systematically examined the differentially expressed CRGs and immune characteristics for the first time between normal and AD individuals. Based on the 13 CRGs expression landscapes, we classified 310 AD patients into two cuproptosis-related clusters, and immune cell differences between the two clusters were further evaluated. Subsequently, cluster-specific DEGs were identified using the WGCNA algorithm, and the enriched biological functions and pathways were elucidated based on cluster-specific DEGs. In addition, a prediction model for disclosing patients with different molecular clusters was established by comparing multiple machine learning algorithms. The nomogram, calibration curve, decision curve analysis (DCA), and two external datasets were used to validate the performance of the predictive model. Finally, we further investigated the correlation between model-related genes with β -secretase activity and A β -42 levels in another external AD cohort, thus providing novel insights into the prediction of AD clusters and risk.

Materials

Data acquisition and pre-processing

Four microarray datasets (GSE33000, GSE5281, GSE122063, and GSE106241) related to AD were obtained from the GEO website database (GEO, www.ncbi.nlm.nih.gov/geo) using the “GEOquery” R package (version 2.60) (Davis and Meltzer, 2007). The GSE33000 dataset (GPL4372 platform) including 157 healthy (age: 22 to 106 years) and 310 AD (age: 53 to 100 years) cortex tissue samples were selected for further analysis. The GSE5281 dataset (GPL570 platform), which included brain tissues from 74 normal (age: 68 to 97 years) subjects and 87 AD (age: 63 to 102 years) samples; the GSE122063 dataset (GPL16699 platform), which included cortex tissues from 44 normal (age: 60 to 91 years) samples and 56 AD (age: 63–91 years) samples, and the GSE106241 dataset (GPL24170 platform), which included cortex tissues from 40 AD (age: 50–100 years) samples, were selected for validation analysis. The raw gene expression profiles of these GEO datasets were processed and normalized using the Robust Multiarray Average (RMA) method (“affy” R package, version 1.70.0).

Evaluating the immune cell infiltration

The CIBERSORT algorithm (<https://cibersort.stanford.edu/>) and LM22 signature matrix were applied for estimating the relative abundances of 22 types of immune cells in each sample based on the proceeded gene expression data. CIBERSORT uses Monte Carlo sampling to obtain an inverse fold product *p*-value for each sample. Only samples with *p*-values <0.05 were considered to be accurate immune cell fractions. The sum of the 22 immune cells proportions in each sample was 1 (Newman et al., 2015).

Correlation analysis between CRGs and infiltrated immune cells

To further demonstrate the association between CRGs and AD-related immune cell properties, we analyzed the correlation coefficients between the CRGs expression and the relative percentage of immune cells. According to the spearman correlation coefficient, *p*-values below 0.05 represented a significant correlation. Finally, the results were exhibited using the “corrplot” R package (version 0.92).

Unsupervised clustering of AD patients

Initially, a total of 13 CRGs were obtained according to the previous report by Tsvetkov et al. (2022). Based on 13 CRGs

expression profiles, we applied the unsupervised clustering analysis (“ConsensusClusterPlus” R package, version 2.60) (Wilkerson and Hayes, 2010) classifying the 310 AD samples into different clusters by using the k-means algorithm with 1,000 iterations. We chose a maximum subtype number *k* (*k* = 6) and the optimal cluster number was comprehensively evaluated based on the cumulative distribution function (CDF) curve, consensus matrix, and consistent cluster score (>0.9).

Gene set variation analysis (GSVA) analysis

GSVA enrichment analysis was conducted to elucidate the differences in enriched gene sets between different CRGs clusters using the R package of “GSVA” (version 2.11). The “c2.cp.kegg.v7.4.symbols” and “c5.go.bp.v7.5.1.symbols” files were obtained from the MSigDB website database for further GSVA analysis. The “limma” R package (version 3.52.1) was utilized to identify the differentially expressed pathways and biological functions by comparing GSVA scores between different CRGs clusters. The |*t* value of GSVA score| more than 2 was considered as significantly altered.

Weighted gene co-expression network analysis (WGCNA)

WGCNA was performed to identify co-expression modules using the R package of “WGCNA” (version 1.70.3) (Langfelder and Horvath, 2008). The top 25% of genes with the highest variance were applied for subsequent WGCNA analyses to guarantee the accuracy of quality results. We selected an optimal soft power to construct a weighted adjacency matrix and further transformed it into a topological overlap matrix (TOM). Modules were obtained using the TOM dissimilarity measure (1-TOM) based on the hierarchical clustering tree algorithm when the minimum module size was set to 100. Each module was assigned a random color. Module eigengene represented the global gene expression profiles in each module. The relationship between modules and disease status was exhibited by the modular significance (MS). Gene significance (GS) was described as the correlation between a gene with clinical phenotype.

Construction of predictive model based on multiple machine learning methods

Based on two different CRGs clusters, we applied the “caret” R packages (version 6.0.91) for establishing machine learning

models including random forest model (RF), support vector machine model (SVM), generalized linear model (GLM), and eXtreme Gradient Boosting (XGB). RF is an ensemble machine learning approach utilizing various independent decision trees for the prediction of classification or regression (Rigatti, 2017). SVM algorithm enables to generate a hyperplane in the characteristic space with a maximum margin to distinguish between positive and negative instances (Gold and Sollich, 2003). GLM, an extension of multiple linear regression models, could flexibly evaluate the relationship between normally distributed dependent features and categorical or continuous independent features (Nelder and Wedderburn, 1972). XGB is an ensemble of boosted trees based on gradient boosting, which can make a careful comparison between classification error and model complexity (Chen et al., 2015). The distinct clusters were considered as the response variable, and the cluster-specific DEGs were selected as explanatory variables. The 310 AD samples were randomly classified into a training set (70%, $N = 217$) and a validation set (30%, $N = 93$). The caret package automatically tuned the parameters in these models by grid search, and all of these machine learning models were performed with default parameters and assessed via 5-fold cross-validation. The “DALEX” package (version 2.4.0) was carried out to interpret the aforementioned four machine learning models and visualize the residual distribution and feature importance among these machine learning models. The “pROC” R package (version 1.18.0) was performed to visualize the area under ROC curves. Consequently, the optimal machine learning model was determined and the top five important variables were considered as the key predictive genes associated with AD. Finally, The ROC curves analysis were performed in GSE5281 and GSE122063 datasets to verify the diagnostic value of the diagnostic model.

Construction and validation of a nomogram model

A nomogram model was established to evaluate the occurrence of AD clusters using the “rms” R package (version 6.2.0). Each predictor has a corresponding score, and the “total score” represents the sum of the scores of the above predictors. The calibration curve and DCA were utilized to estimate the predictive power of the nomogram model.

Independent validation analysis

Two external brain tissue datasets, GSE5281 and GSE122063, were applied for validating the ability of the prediction model to distinguish AD from non-AD controls

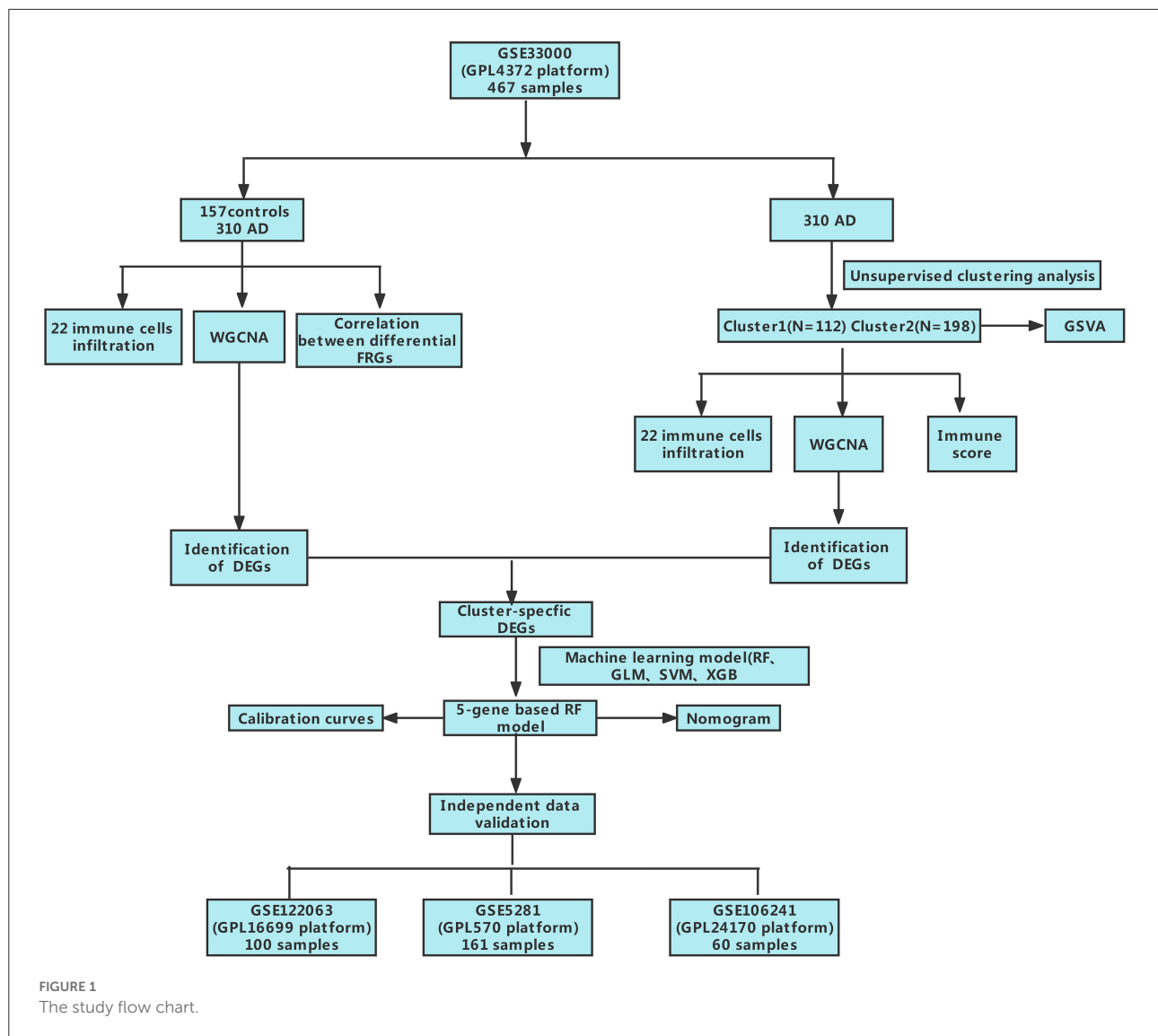
by using the ROC analyses. ROC curves were visualized using the “pROC” R package. In addition, we performed the spearman correlation analysis to explore the associations between prediction model-related genes with A β -42 levels and β -secretase activity. A value of $p < 0.05$ was considered as statistically significant.

Results

Dysregulation of cuproptosis regulators and activation of the immune responses in AD patients

To clarify the biological functions of cuproptosis regulators in the occurrence and progression of AD, we first systematically evaluated the expression profiles of 13 CRGs between AD and non-AD controls using the GSE33000 dataset. A detailed flow chart of the study process was exhibited in Figure 1. A total of 12 CRGs were determined as the differentially expressed cuproptosis genes. Among them, the expression levels of CDKN2A, SLC31A1, ATP7B, LIPT1, and MTF1 were higher, whereas FDX1, GLS, PDHA1, DLD, DLAT, PDHB, and LIAS gene expression levels were largely lower in AD cortex tissues than that in non-AD controls (Figures 2A–C). Subsequently, we performed the correlation analysis between these differentially expressed CRGs to explore whether cuproptosis regulators functioned essentially in the progression of AD. Surprisingly, some cuproptosis modulators, such as PDHB and DLAT, presented a strong synergistic effect (coefficient = 0.83). Simultaneously, CDKN2A and DLAT exhibited an apparent antagonistic action (coefficient = 0.54). In addition, we further investigated the correlation patterns of these CRGs and found both DLAT and DLD were significantly correlated with other regulators (Figure 2D). The gene relationship network diagram further demonstrated the closeness of the relationship among these differentially expressed CRGs (Figure 2E).

To elucidate whether there is variation in the immune system between the AD and non-AD controls, immune infiltration analysis was performed to show a difference in the proportions of 22 infiltrated immune cell types between AD and non-AD control subjects based on the CIBERSORT algorithm (Figure 2F). The results revealed that AD patients presented higher infiltration levels of naïve B cells, resting memory CD4⁺ T cells, gamma delta T cells, resting NK cells, Monocytes, M1 macrophages, M2 macrophages, activated dendritic cells, and neutrophils (Figure 2G), suggesting that the alternations in the immune system may be a major cause for the occurrence of AD. Meanwhile, correlation analysis results indicated that both resting NK cells and CD8⁺ T cells were correlated with cuproptosis modulators (Figure 2H). These results suggested



that CRGs may be the critical factors involved in regulating the molecular and immune infiltration status of AD patients.

Identification of cuproptosis clusters in AD

To elucidate the cuproptosis-related expression patterns in ASD, we grouped the 310 AD samples based on the expression profiles of 13 CRGs using a consensus clustering algorithm. The cluster numbers were most stable when the k value was set to two ($k = 2$), and the CDF curves fluctuated within a minimum range at a consensus index of 0.2 to 0.6 (Figures 3A,B). When $k = 2$ to 6, the area under the CDF curves exhibited the difference between the two CDF curves (k and $k-1$) (Figure 3C). Furthermore, the consistency score of each subtype was >0.9

only when $k = 2$ (Figure 3D). Conjoined with the heatmap of the consensus matrix, we finally grouped 310 AD patients into two clusters, including Cluster1 ($n = 112$) and Cluster2 ($n = 198$) (Figure 3E). The results of the t-Distributed Stochastic Neighbor Embedding (tSNE) analysis demonstrated that there was a significant difference between these two clusters (Figure 3F).

Differentiation of cuproptosis regulators and immune infiltration characteristics between cuproptosis clusters

To explore the molecular characteristics between clusters, we first comprehensively assessed the expression differences of 13 CRGs between Cluster1 and Cluster2. Distinct CRGs expression landscapes were observed between the two cuproptosis patterns

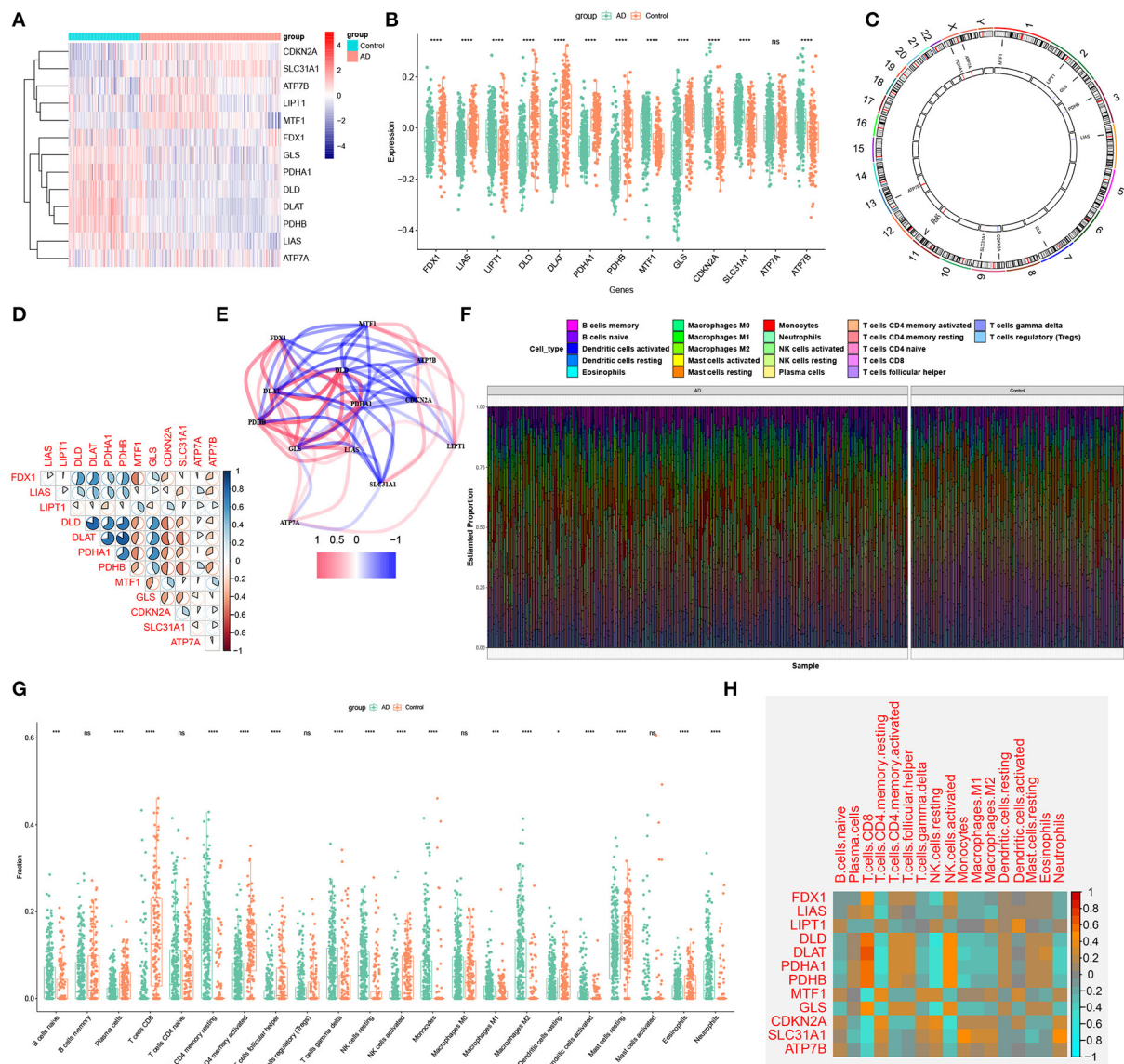


FIGURE 2

Identification of dysregulated CRGs in AD. (A) The expression patterns of 13 CRGs were presented in the heatmap. (B) Boxplots showed the expression of 13 CRGs between AD and non-AD controls. **** $p < 0.0001$, ns, no significance. (C) The location of 13 CRGs on chromosomes. (D) Correlation analysis of 12 differentially expressed CRGs. Blue and Red colors represent positive and negative correlations, respectively. The correlation coefficients were marked with the area of the pie chart. (E) Gene relationship network diagram of 12 differentially expressed CRGs. (F) The relative abundances of 22 infiltrated immune cells between AD and non-AD controls. (G) Boxplots showed the differences in immune infiltrating between AD and non-AD controls. * $p < 0.05$, *** $p < 0.001$, **** $p < 0.0001$, ns, no significance. (H) correlation analysis between 12 differentially expressed CRGs and infiltrated immune cells.

(Figure 4A). Cuproptosis Cluster1 revealed high expression levels of FDX1, DLD, DLAT, PDHA1, PDHB, and GLS, while cuproptosis Cluster2 was characterized by enhanced expressions of LIPT1, MTF1, CDKN2A, and SLC31A1 (Figure 4B). Moreover, the results of immune infiltration analysis showed that an altered immune microenvironment was presented between cuproptosis Cluster1 and Cluster2 (Figure 4C). Cluster1 exhibited higher proportions of CD8+

T cells, follicular helper T cells, activated NK cells, resting dendritic cells, and eosinophils, whereas the abundance of naïve B cells, Plasma cells, naïve CD4+ T cells, resting memory CD4+ T cells, resting NK cells, Monocytes, M0 macrophages, and M1 macrophages were relatively greater in Cluster2 (Figure 4D). Consistently, Cluster2 also presented elevated immune scores (Figure 4E), which revealed that cuproptosis Cluster2 might possess a more dominant level of immune infiltration.

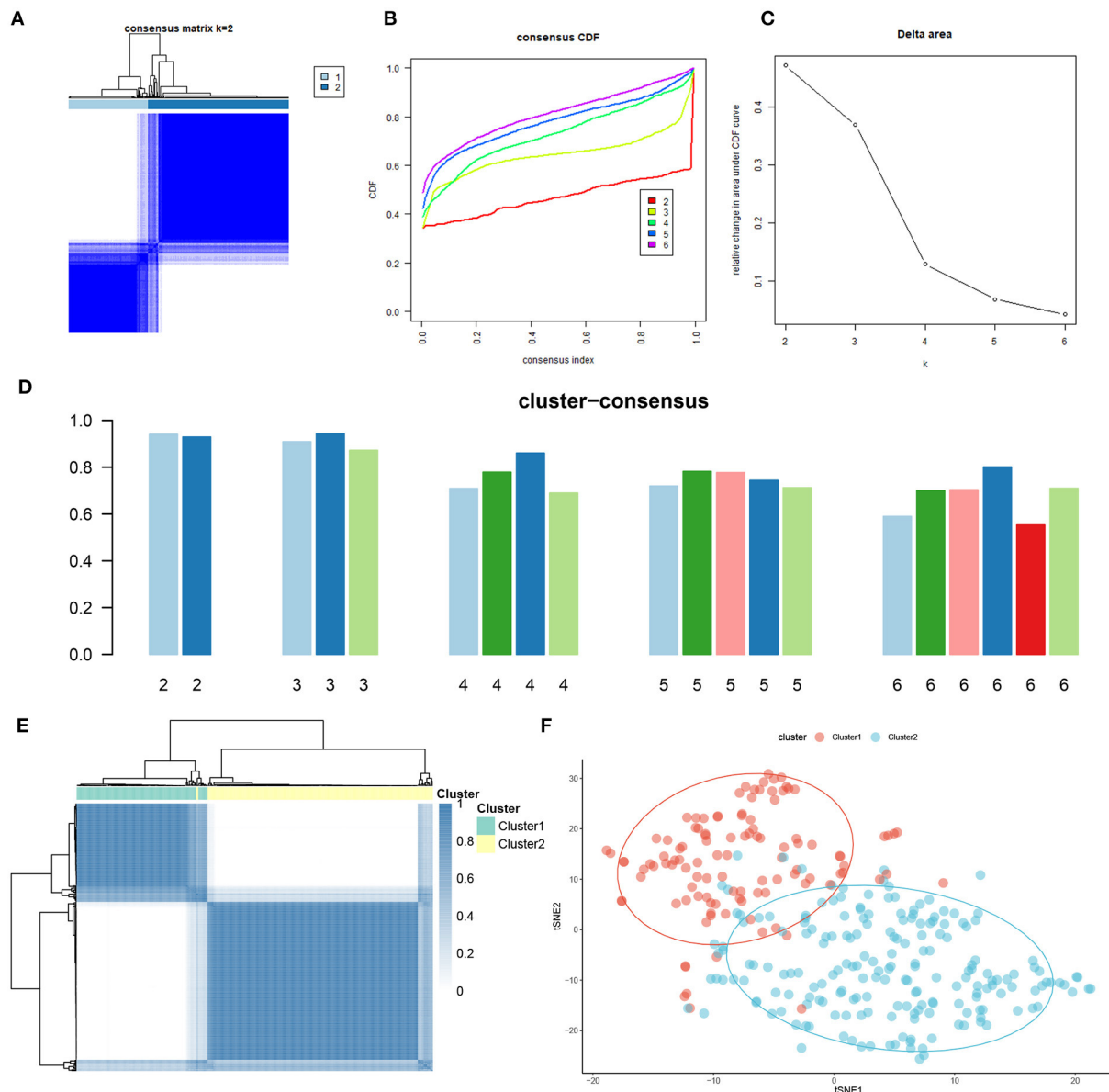


FIGURE 3
Identification of cuproptosis-related molecular clusters in AD. (A) Consensus clustering matrix when $k = 2$. (B–E) Representative cumulative distribution function (CDF) curves (B), CDF delta area curves (C), the score of consensus clustering (D), and heatmap of non-negative matrix (E). (F) t-SNE visualizes the distribution of two subtypes.

Gene modules screening and co-expression network construction

To identify the key gene modules associated with AD, we utilized the WGCNA algorithm to establish a co-expression network and modules for the normal and AD subjects. We calculated the variance of each gene expression in GSE33000 and then selected the top 25% genes with the highest variance to further analysis. Co-expressed gene modules were identified when the value of soft power was set to 9 and the scale-free

R^2 was equal to 0.9 (Figure 5A). A total of 10 distinct co-expression modules with different colors were acquired using the dynamic cutting algorithm and the heatmap of the topological overlap matrix (TOM) was also presented (Figures 5B–D). Subsequently, these genes in the 10 color modules were continuously applied for analyzing the similarity and adjacency of module-clinical features (Control and AD) co-expression. Finally, the turquoise module exhibited the strongest relationship with AD, which included 1,609 genes (Figure 5E). Moreover, we observed a positive association

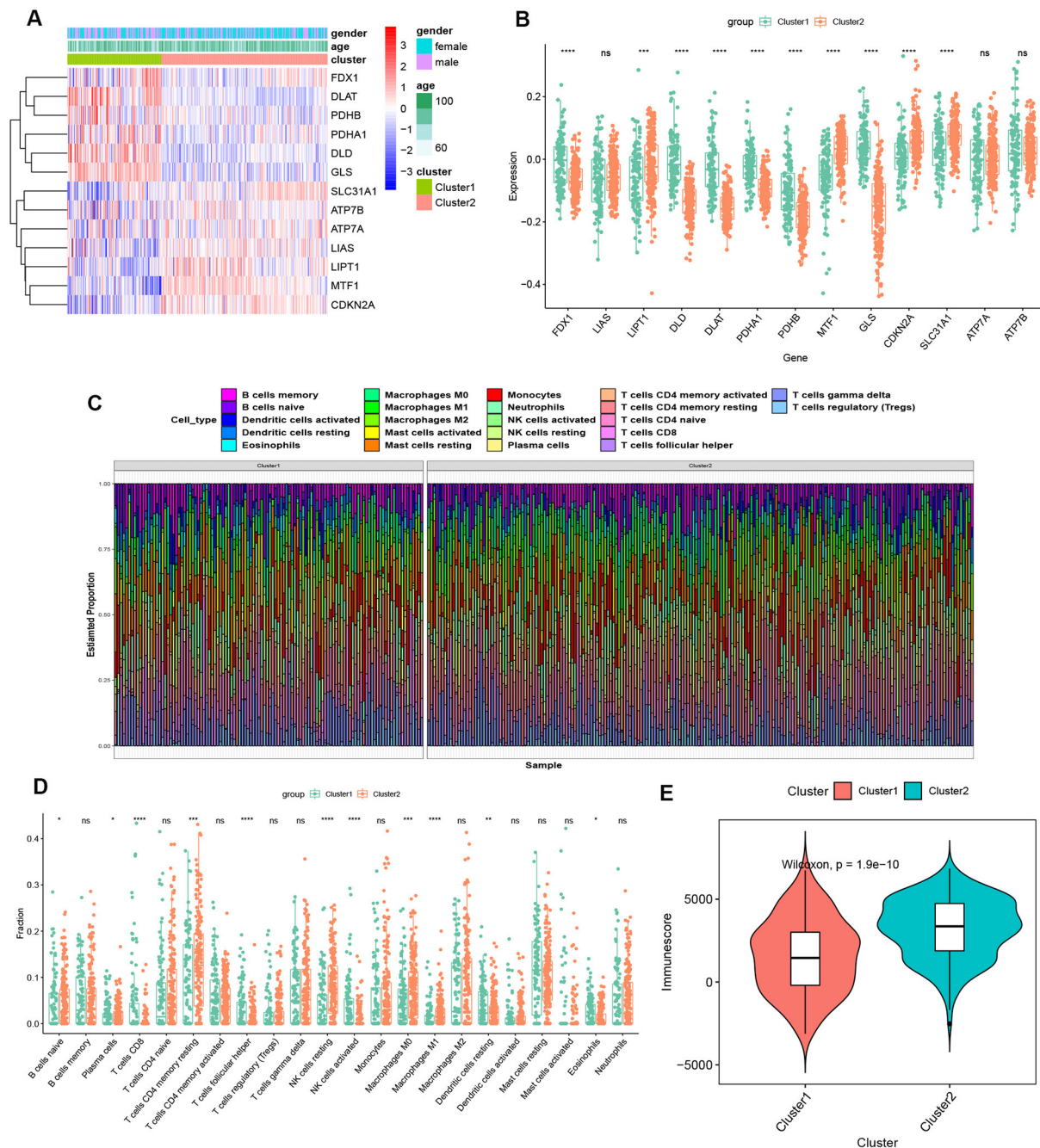


FIGURE 4 Identification of molecular and immune characteristics between the two cuproptosis clusters. **(A)** Clinical features and expression patterns of 13 CRGs between two cuproptosis clusters were presented in the heatmap. **(B)** Boxplots showed the expression of 13 CRGs between two cuproptosis clusters. **** $p < 0.0001$, ns, no significance. **(C)** the relative abundances of 22 infiltrated immune cells between two cuproptosis clusters. **(D)** Boxplots showed the differences in immune infiltrating between two cuproptosis clusters. * $p < 0.05$, ** $p < 0.01$ *** $p < 0.001$, **** $p < 0.0001$, ns, no significance. **(E)** Boxplots showed the estimated immune score between the two cuproptosis subtypes.

between the turquoise module and module-related genes (Figure 5F).

In addition, we also analyzed the critical gene modules closely related to cuproptosis clusters using the WGCNA algorithm. We screened $\beta = 7$ and $R^2 = 0.9$ as the most

suitable soft threshold parameters to construct a scale-free network (Figure 6A). Specifically, 11 modules containing 4,422 genes were determined as significant modules and the heatmap portrayed the TOM of all module-related genes (Figures 6B–D). Module-clinical features (Cluster1 and Cluster2) relationship

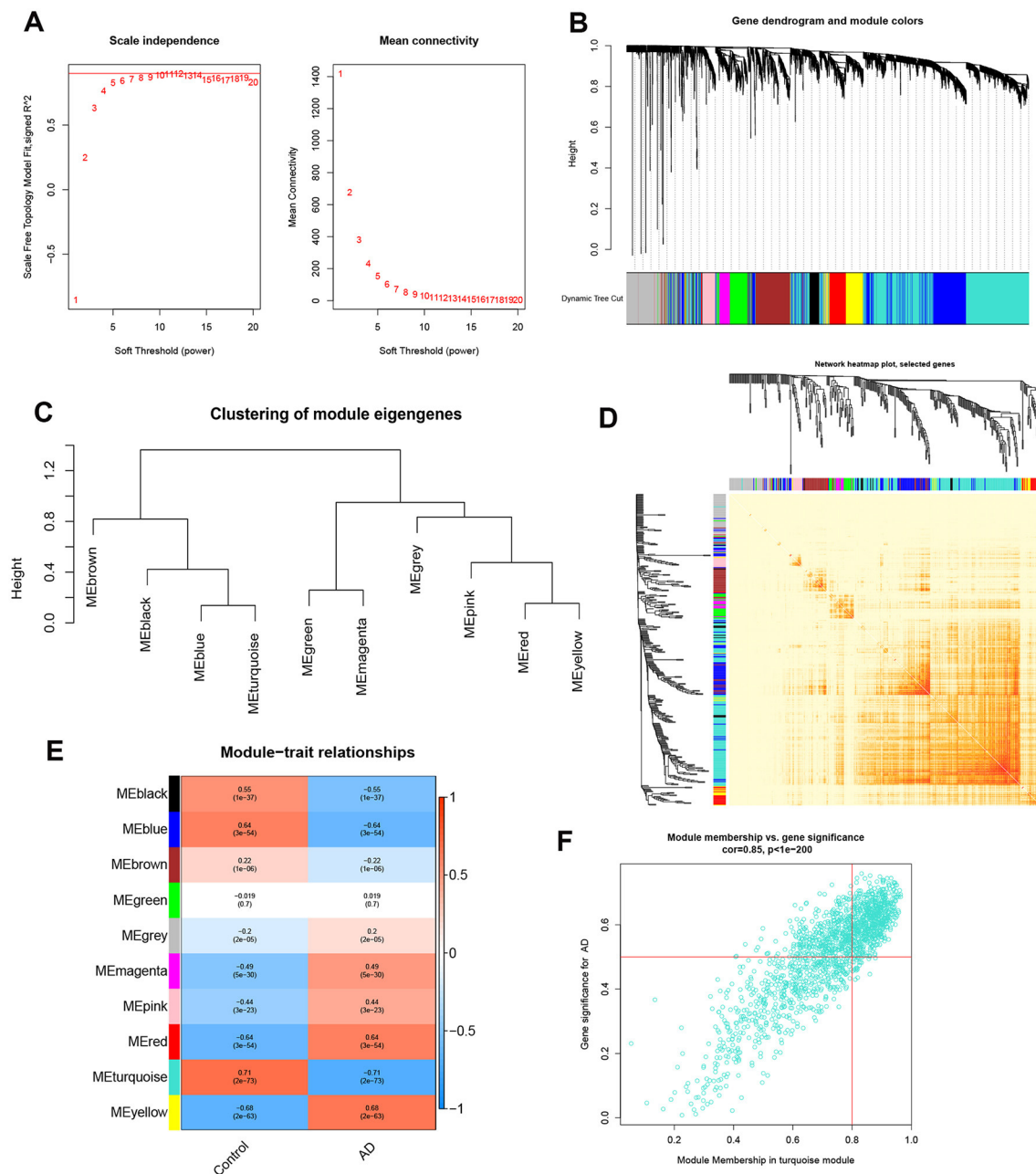


FIGURE 5

Co-expression network of differentially expressed genes in AD. (A) The selection of soft threshold power. (B) Cluster tree dendrogram of co-expression modules. Different colors represent distinct co-expression modules. (C) Representative of clustering of module eigengenes. (D) Representative heatmap of the correlations among 10 modules. (E) Correlation analysis between module eigengenes and clinical status. Each row represents a module; each column represents a clinical status. (F) Scatter plot between module membership in turquoise module and the gene significance for AD.

analysis demonstrated the high correlation between the turquoise module (1,115 genes) and AD clusters (Figure 6E). The correlation analysis suggested that turquoise module genes had a significant relationship with the selected module (Figure 6F).

Identification of cluster-specific DEGs and functional annotation

A total of 909 cluster-specific DEGs were identified by analyzing the intersections between module-related genes of

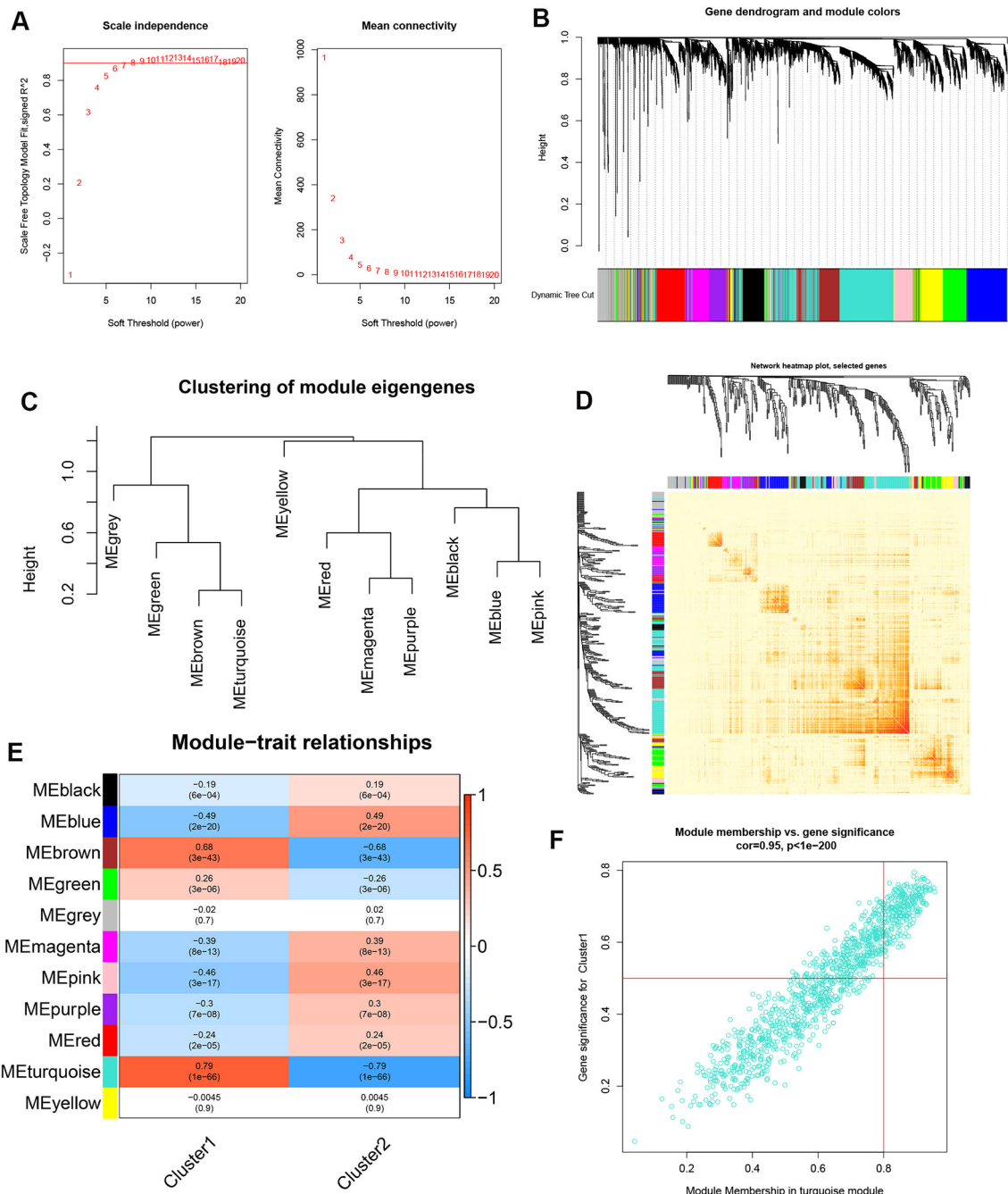
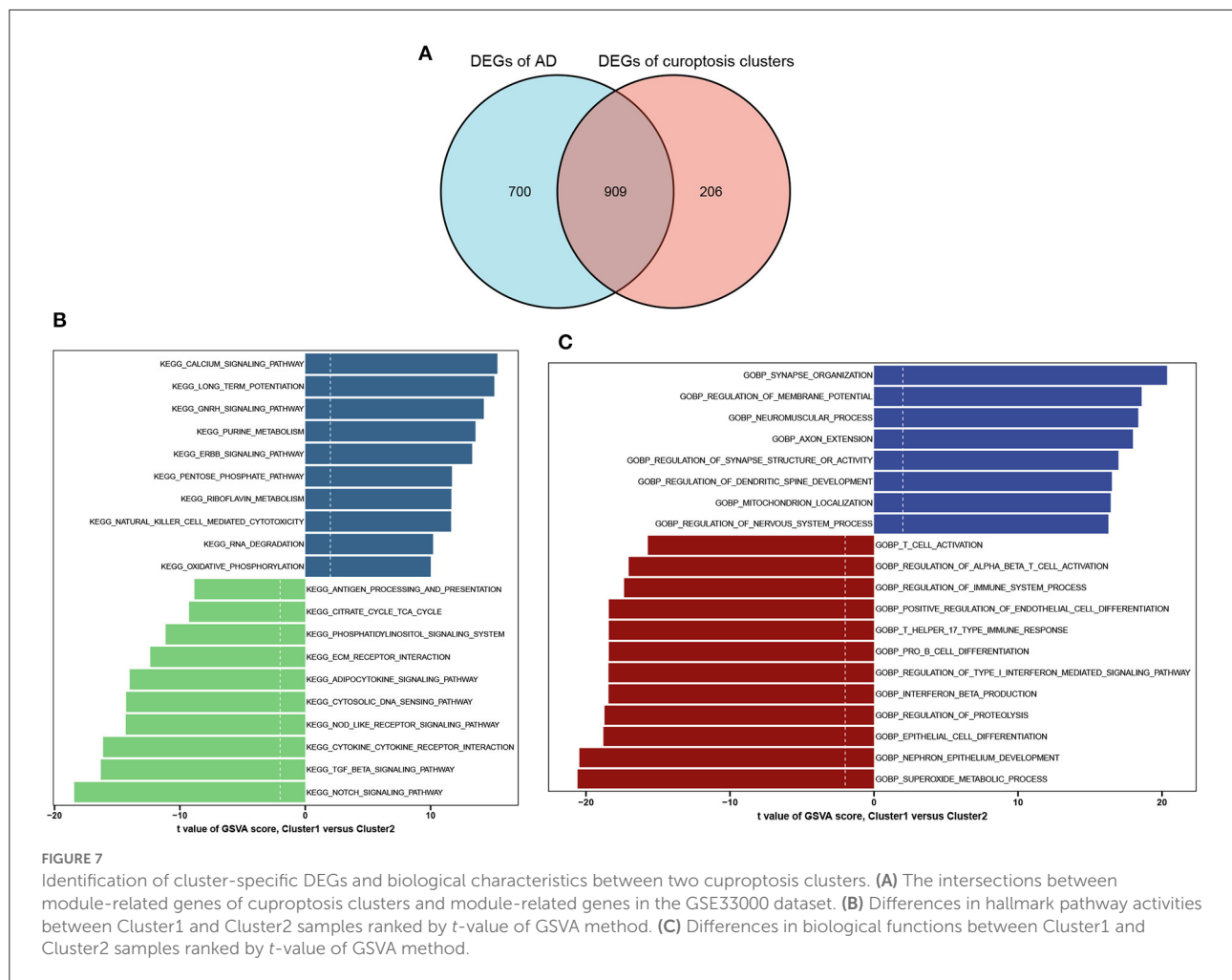


FIGURE 6 Co-expression network of differentially expressed genes between the two cuproptosis clusters. **(A)** The selection of soft threshold power. **(B)** Cluster tree dendrogram of co-expression modules. Different colors represent distinct co-expression modules. **(C)** Representative of clustering of module eigengenes. **(D)** Representative heatmap of the correlations among 11 modules. **(E)** Correlation analysis between module eigengenes and clinical status. Each row represents a module; each column represents a clinical status. **(F)** Scatter plot between module membership in turquoise module and the gene significance for Cluster1.

cuproptosis clusters and module-related genes of AD and non-AD individuals (Figure 7A). The GSVA analysis was utilized to further explore the functional differences associated with cluster-specific DEGs between the two clusters. The results

indicated that oxidative phosphorylation, RNA degradation, long-time potentiation, and metabolism signaling activity were reinforced in Cluster1, while the TCA cycle, immune responses, cytokine receptor, TGF- β , and Notch signaling



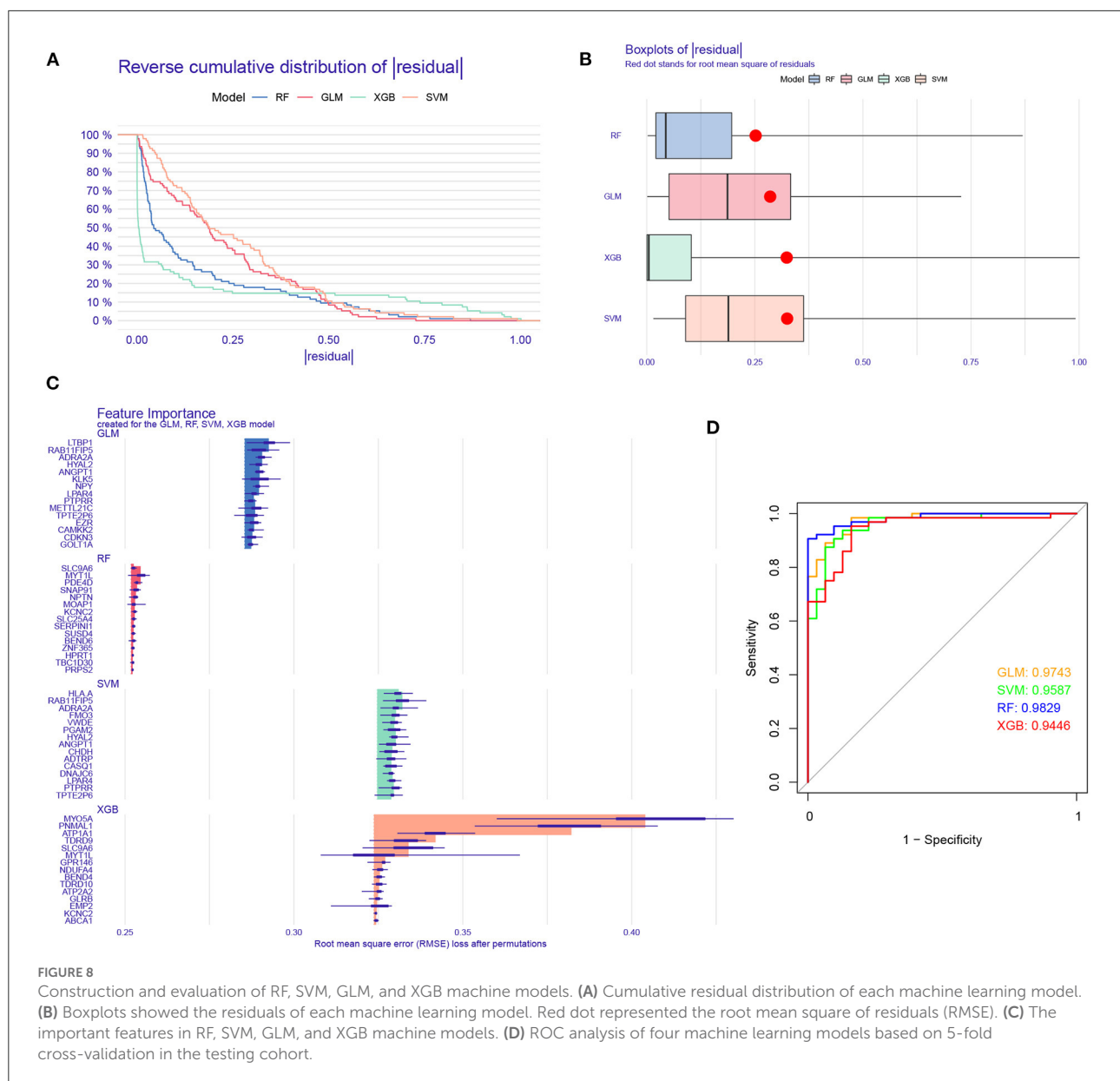
activity were upregulated in Cluster2 (Figure 7B). Otherwise, functional enrichment results revealed that Cluster1 was remarkably related to the regulation of synapse and axon outgrowth, the development of the dendritic spine development, and mitochondrial localization. However, immune-related pathways, such as T-cell activation, B-cell differentiation, and beta-interferon production, were enriched in Cluster2 (Figure 7C). Thus, we hypothesized that Cluster2 may be involved in various immune responses.

Construction and assessment of machine learning models

To further identify subtype-specific genes with high diagnostic value, we established four proven machine learning models [random forest model (RF), support vector machine model (SVM), generalized linear model (GLM), and eXtreme Gradient Boosting (XGB)] based on the expression profiles of 909 cluster-specific DEGs in the AD training cohort. The

“DALEX” package was applied for explaining the four models and plotting the residual distribution of each model in the test set. RF and GLM machine learning models presented a relatively lower residual (Figures 8A,B). Subsequently, the top 15 important feature variables of each model were ranked according to the root mean square error (RMSE) (Figure 8C). Moreover, we evaluated the discriminative performance of the four machine learning algorithms in the testing set by calculating receiver operating characteristic (ROC) curves based on 5-fold cross-validation. The RF machine learning model displayed the highest area under the ROC curve (AUC) (GLM, AUC = 0.9743; SVM, AUC = 0.9587; RF, AUC = 0.9829; XGB, AUC = 0.9446, Figure 8D). Overall, combined with these results, the RF model was demonstrated to best distinguish patients with different clusters. Finally, the top five most important variables (MYT1L, PDE4D, SNAP91, NPTN, and KCNC2) from the RF model were selected as predictor genes for further analysis.

To further assess the predictive efficiency of the RF model, we first constructed a nomogram to estimate the risk of cuproptosis clusters in 310 AD patients (Figure 9A). The



calibration curve and decision curve analysis (DCA) were applied for assessing the predictive efficiency of the nomogram model. According to the calibration curve, the error between the actual AD clusters risk and the predicted risk was very small (Figure 9B), and the DCA indicates that our nomogram has a high accuracy, which may provide a basis for clinical decision-making (Figure 9C). Subsequently, we validated our 5-gene prediction model on two external brain tissue datasets including normal subjects and AD patients. ROC curves showed satisfactory performance of the 5-gene prediction model with an AUC value of 0.8529 in the GSE5281 dataset and 0.8333 in the GSE122063 dataset (Figures 9D,E), indicating our

diagnosis model is equally efficacious in distinguishing AD from normal individuals.

Furthermore, we enrolled another external dataset (GSE106241) to validate the correlation between the predictor genes and biomarkers of AD that have been widely reported ($A\beta$ -42 levels and β -secretase activity). We found that MYT1L, PED4D, SNAP91, and KCNC2 were negatively correlated with $A\beta$ -42 levels (MYT1L, $R = -0.27$; PED4D, $R = -0.31$; SNAP91, $R = -0.27$; KCNC2, $R = -0.31$) and β -secretase activity (MYT1L, $R = -0.52$; PED4D, $R = -0.58$; SNAP91, $R = -0.59$; KCNC2, $R = -0.57$), while NPTN was only negatively associated with β -secretase activity ($R = -0.29$, Figures 10A–J).

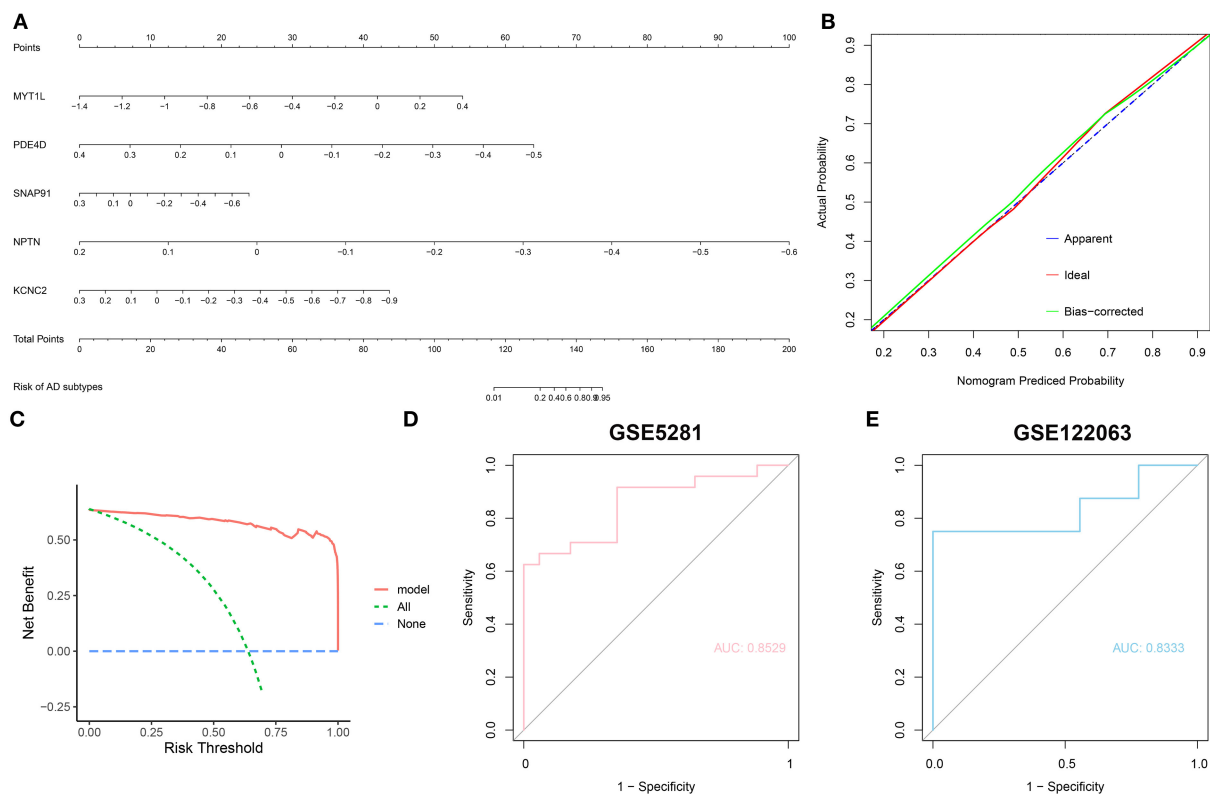


FIGURE 9

Validation of the 5-gene-based RF model. **(A)** Construction of a nomogram for predicting the risk of AD clusters based on the 5-gene-based RF model. **(B,C)** Construction of calibration curve **(B)** and DCA **(C)** for assessing the predictive efficiency of the nomogram model. **(D,E)** ROC analysis of the 5-gene-based RF model based on 5-fold cross-validation in GSE5281 **(D)** and GSE122063 **(E)** datasets.

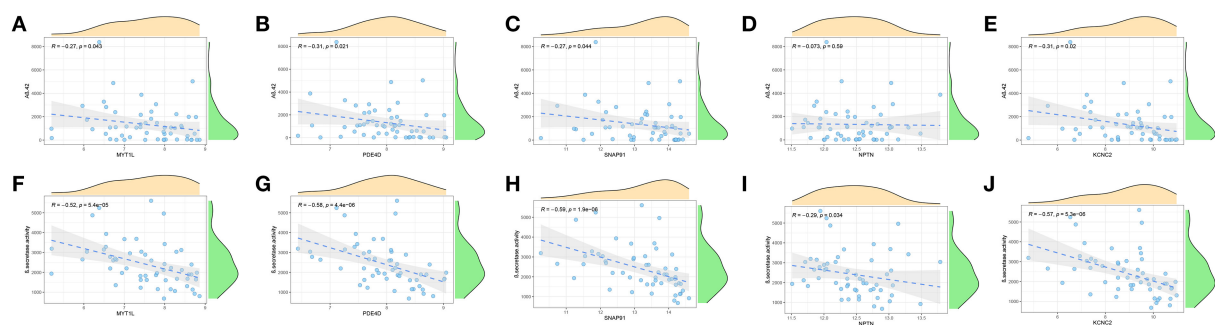


FIGURE 10

Validation of correlation analysis based on GSE106241 dataset. **(A-E)** Correlation between MYT1L **(A)**, PDE4D **(B)**, SNAP91 **(C)**, NPTN **(D)**, KCNC2 **(E)**, and $A\beta$ -42 levels. **(F-J)** Correlation between MYT1L **(F)**, PDE4D **(G)**, SNAP91 **(H)**, NPTN **(I)**, KCNC2 **(J)**, and β -secretase activity.

This result has proven the outstanding pathological diagnostic value of the 5-gene prediction model.

Discussion

Due to the heterogeneity of AD pathology, the current treatment for AD lacks adequate efficacy (Lam et al., 2013;

Byun et al., 2015). In the past decades, increasing advances have been made in anti-neurodegenerative therapy for AD, whereas the conventional classification based on histology allows for frequent drug resistance (Nandigam, 2008). Therefore, the identification of more appropriate molecular clusters is essential to guide the individualized treatment of AD. Cuproptosis, a recently reported form of copper-dependent cell death mainly evidenced by the aggregation of lipoylated mitochondrial

enzymes, has been strongly implicated in the progression of the disease (Tang et al., 2022; Tsvetkov et al., 2022). However, the specific mechanisms of cuproptosis and its regulatory roles in various diseases have not been further investigated. Therefore, we attempted to elucidate the specific role of cuproptosis-related genes in AD phenotyping and the immune microenvironment. Additionally, gene signatures related to cuproptosis were utilized to predict the AD subtypes.

In this study, we comprehensively analyzed the expression profiles of cuproptosis regulators for the first time in brain tissues between normal subjects and AD patients. The dysregulated CRGs were found in AD patients more than those in normal individuals, suggesting a critical role of CRGs in the occurrence of AD. Subsequently, we calculated the correlation among CRGs to clarify the association between cuproptosis regulators and AD. We discovered that some cuproptosis modulators presented significant synergistic or antagonistic effects, which are evidenced by the existence of CRG interactions in AD patients. The abundance of immune cells were altered between control subjects and patients with AD. AD patients exhibited higher infiltration levels of B cells, T cells, neutrophils, resting NK cells, and macrophages, which were consensus with the previous studies verified in blood or brain tissues (Dey and Hankey Giblin, 2018; Dai and Shen, 2021; Paranjpe et al., 2021; Wang et al., 2022a). Further, we utilized unsupervised cluster analysis to illustrate the different cuproptosis regulation patterns in AD patients based on the expression landscapes of CRGs, and two distinct cuproptosis-related clusters were identified. Cluster2 exhibited elevated immune scores and relatively higher levels of immune infiltration. Cluster-specific DEGs indicated that Cluster1 was primarily enriched in mitochondrial localization, nerve growth, and development-related biological processes, while Cluster2 was characterized by immune cell activation and differentiation. It was reported that TGF- β signaling and Notch signaling were essential for the activation and differentiation of B cells and T cells (Cortez et al., 2016; Tsukumo and Yasutomo, 2018; Garis and Garrett-Sinha, 2020). Consistently, Cluster2 had a stronger activity of TGF- β signaling and Notch signaling. Taken together, it would be reasonable to believe that Cluster2 may possess more activated B cells and T cells to counteract the progression of AD and therefore showed a better prognosis.

In recent years, machine learning models based on demographic and imaging metrics have been increasingly applied for the prediction of AD prevalence (Falahati et al., 2014), and these studies confirm that multifactorial analyses have taken into account the relationships between variables, thus having a lower error rate and more reliable results compared to univariate analysis. In our current study, we compared the predictive performance of four selected machine learning classifiers (RF, SVM, GLM, and XGB) based on the expression profiles of cluster-specific DEGs and established an RF-based prediction model, which presented the highest predictive

efficacy in the testing cohort (AUC = 0.9829), suggesting the RF-based machine learning has satisfactory performance in predicting the subtypes of AD. Subsequently, we selected five important variables (MYT1L, PDE4D, SNAP91, NPTN, and KCNC2) to construct a 5-gene-based RF model. MYT1L is a gene expressed exclusively in neurons that reprograms embryonic and infant fibroblasts into functional neurons and therefore acts as the critical regulator in the development of the nervous system, suggesting that MYT1L might be a potential treatment strategy for AD patients (Li et al., 2012). PDE4D is a member of the cAMP phosphodiesterase superfamily and is mainly involved in the regulation of cAMP activity. The role of PDE4D in AD is still controversial. It is reported that PDE4D inhibitors can improve cognitive function in the elderly and have mild gastrointestinal side effects, suggesting that PDE4D may be an effective therapeutic target for age-related neurodegenerative diseases (Bruno et al., 2011). However, another study demonstrated that the expression levels of PDE4D protein are negatively correlated with age and phosphorylated tau and positively correlated with the performance on frontal association cortex-related working memory tasks. Inhibition of PDE4D would make the frontal association cortex more vulnerable to degeneration (Leslie et al., 2020). Bioinformatics analysis indicated that SNAP91 could serve as a primary biomarker for Parkinson's disease and AD (Yemni et al., 2019; Hu et al., 2020). As a housekeeper of neuroplasticity, NPTN is closely associated with the regulation of synaptic plasticity, thus playing an important role in facilitating learning and memory. Studies have found that elevated KCNC2 might be implicated in the maturation of neuronal electrical activity during nervous system development, and a decrease in KCNC2 may aggravate the impairment of cognitive function in AD patients (Boda et al., 2012).

The 5-gene-based RF model can accurately predict AD in two external validation datasets (AUC = 0.8529 and 0.8333), which provides new insights into the diagnosis of AD. More importantly, we then constructed a nomogram model for the diagnosis of AD subtypes by using the MYT1L, PDE4D, SNAP91, NPTN, and KCNC2. We found this model exhibited remarkable predictive efficacy, indicating the value of this prediction model for clinical applications. Additionally, an increasing number of studies have confirmed that A β -42 levels and β -secretase activity are key pathological mechanisms contributing to the progression and poor prognosis of AD (Hampel et al., 2021; Cho et al., 2022). Therefore, we performed the correlation analysis between these five predictor genes with A β -42 levels and β -secretase activity in 60 AD samples from another external dataset. The results suggested that NPTN was negatively associated with β -secretase activity, while the other four predictor genes were negatively correlated with A β -42 levels and β -secretase activity. Taken together, the 5-gene-based RF model is a satisfactory indicator to assess AD subtypes and the pathological outcome of AD patients.

Some limitations need to be emphasized in this study. First, our current study was performed based on comprehensive bioinformatics analysis, and additional clinical or experimental assessment would be necessary to validate the expression levels of CRGs. Furthermore, more detailed clinical characteristics are required to confirm the performance of the prediction model. In addition, a greater number of AD samples are needed to clarify the accuracy of cuproptosis-related clusters and the potential correlation between CRGs and immune responses requires further exploration. Furthermore, though we applied an external dataset for additional validation, more experiments are necessary to prove the association between feature genes and A β -42 levels and β -secretase activity in AD pathology.

Conclusion

In total, our study disclosed the correlation between CRGs and infiltrated immune cells and elucidated the significant heterogeneity of immune between AD patients with distinct cuproptosis clusters. A 5-gene-based RF model was selected as the optimal machine learning model, which can accurately assess AD subtypes and the pathological outcome of AD patients. Our study identifies for the first time the role of cuproptosis in AD and further elucidates the underlying molecular mechanisms leading to AD heterogeneity.

Data availability statement

The datasets supporting the conclusions of this article are available in the GEO website (<https://www.ncbi.nlm.nih.gov/geo/>), with the following data accession identifiers: GSE33000, GSE5281, GSE122063, and GSE106241.

References

- Ambrogio, F., Martella, L. A., Odetti, P., and Monacelli, F. (2019). Behavioral disturbances in dementia and beyond: time for a new conceptual frame? *Int. J. Mol. Sci.* 20:3647. doi: 10.3390/ijms20153647
- Baker, Z. N., Cobine, P. A., and Leary, S. C. (2017). The mitochondrion: a central architect of copper homeostasis. *Metallomics* 9, 1501–1512. doi: 10.1039/C7MT00221A
- Boda, E., Hoxha, E., Pini, A., Montarolo, F., and Tempia, F. (2012). Brain expression of Kv3 subunits during development, adulthood and aging and in a murine model of Alzheimer's disease. *J. Mol. Neurosci.* 46, 606–615. doi: 10.1007/s12031-011-9648-6
- Bruno, O., Fedele, E., Prickaerts, J., Parker, L. A., Canepa, E., Brullo, C., et al. (2011). GEBR-7b, a novel PDE4D selective inhibitor that improves memory in rodents at non-emetic doses. *Br. J. Pharmacol.* 164, 2054–2063. doi: 10.1111/j.1476-5381.2011.01524.x
- Byun, M. S., Kim, S. E., Park, J., Yi, D., Choe, Y. M., Sohn, B. K., et al. (2015). Heterogeneity of regional brain atrophy patterns associated with distinct progression rates in Alzheimer's disease. *PLoS ONE* 10:e0142756. doi: 10.1371/journal.pone.0142756
- Chen, T., He, T., Benesty, M., Khotilovich, V., Tang, Y., Cho, H., et al. (2015). Xgboost: extreme gradient boosting. *R Package Version 0.4-2*. 1, 1–4.
- Chen, Z., and Zhong, C. (2014). Oxidative stress in Alzheimer's disease. *Neurosci. Bull.* 30, 271–281. doi: 10.1007/s12264-013-1423-y
- Cho, Y., Bae, H. G., Okun, E., Arumugam, T. V., and Jo, D. G. (2022). Physiology and pharmacology of amyloid precursor protein. *Pharmacol. Ther.* 235:108122. doi: 10.1016/j.pharmthera.2022.108122
- Cobine, P. A., and Brady, D. C. (2022). Cuproptosis: cellular and molecular mechanisms underlying copper-induced cell death. *Mol. Cell* 82, 1786–1787. doi: 10.1016/j.molcel.2022.05.001
- Cortez, V. S., Cervantes-Barragan, L., Robinette, M. L., Bando, J. K., Wang, Y., Geiger, T. L., et al. (2016). Transforming growth factor- β signaling guides the differentiation of innate lymphoid cells in salivary glands. *Immunity* 44, 1127–1139. doi: 10.1016/j.immuni.2016.03.007
- Dai, L., and Shen, Y. (2021). Insights into T-cell dysfunction in Alzheimer's disease. *Aging Cell* 20:e13511. doi: 10.1111/acer.13511

Author contributions

YL designed the study, collected the original data, and drafted the initial manuscript. XL, CL, and LW searched related literature, finished the analysis, and visualized the final results. CL and YZ helped revise the manuscript. FL provided the funding and supervised the study. The final manuscript was read and approved by all authors. All authors contributed to the article and approved the submitted version.

Funding

This work was supported by the High-level hospital foster grants from Fujian Provincial Hospital, Fujian province, China (Grant number: 2019HSJJ17), and the National Health and Family Planning Commission Grant (Grant number: WKJ-FJ-20).

Conflict of interest

The authors declare that the research was conducted in the absence of any commercial or financial relationships that could be construed as a potential conflict of interest.

Publisher's note

All claims expressed in this article are solely those of the authors and do not necessarily represent those of their affiliated organizations, or those of the publisher, the editors and the reviewers. Any product that may be evaluated in this article, or claim that may be made by its manufacturer, is not guaranteed or endorsed by the publisher.

- Davis, S., and Meltzer, P. S. (2007). GEOquery: a bridge between the Gene Expression Omnibus (GEO) and BioConductor. *Bioinformatics* 23, 1846–1847. doi: 10.1093/bioinformatics/btm254
- Dennerlein, S., and Rehling, P. (2015). Human mitochondrial COX1 assembly into cytochrome c oxidase at a glance. *J. Cell Sci.* 128, 833–837. doi: 10.1242/jcs.161729
- Dey, A., and Hankey Giblin, P. A. (2018). Insights into macrophage heterogeneity and cytokine-induced neuroinflammation in major depressive disorder. *Pharmaceuticals* 11:64. doi: 10.3390/ph11030064
- Falahati, F., Westman, E., and Simmons, A. (2014). Multivariate data analysis and machine learning in Alzheimer's disease with a focus on structural magnetic resonance imaging. *J. Alzheimers. Dis.* 41, 685–708. doi: 10.3233/JAD-131928
- Garis, M., and Garrett-Sinha, L. A. (2020). Notch signaling in B cell immune responses. *Front. Immunol.* 11:609324. doi: 10.3389/fimmu.2020.609324
- Gold, C., and Sollich, P. (2003). Model selection for support vector machine classification. *Neurocomputing* 55, 221–249. doi: 10.1016/S0925-2312(03)00375-8
- Gromadzka, G., Tarnacka, B., Flaga, A., and Adamczyk, A. (2020). Copper dyshomeostasis in neurodegenerative diseases-therapeutic implications. *Int. J. Mol. Sci.* 21:9259. doi: 10.3390/ijms21239259
- Hampel, H., Vassar, R., De Strooper, B., Hardy, J., Willem, M., Singh, N., et al. (2021). The β -Secretase BACE1 in Alzheimer's disease. *Biol. Psychiatry* 89, 745–756. doi: 10.1016/j.biopsych.2020.02.001
- Hu, R. T., Yu, Q., Zhou, S. D., Yin, Y. X., Hu, R. G., Lu, H. P., et al. (2020). Co-expression network analysis reveals novel genes underlying alzheimer's disease pathogenesis. *Front. Aging Neurosci.* 12:605961. doi: 10.3389/fnagi.2020.605961
- Jack, C. R. Jr., Wiste, H. J., Weigand, S. D., Rocca, W. A., Knopman, D. S., Mielke, M. M., et al. (2014). Age-specific population frequencies of cerebral β -amyloidosis and neurodegeneration among people with normal cognitive function aged 50–89 years: a cross-sectional study. *Lancet Neurol.* 13, 997–1005. doi: 10.1016/S1474-4422(14)70194-2
- Lam, B., Masellis, M., Freedman, M., Stuss, D. T., and Black, S. E. (2013). Clinical, imaging, and pathological heterogeneity of the Alzheimer's disease syndrome. *Alzheimers. Res. Ther.* 5:1. doi: 10.1186/alzrt155
- Langfelder, P., and Horvath, S. (2008). WGCNA: an R package for weighted correlation network analysis. *BMC Bioinformatics* 9:559. doi: 10.1186/1471-2105-9-559
- Leslie, S. N., Datta, D., Christensen, K. R., van Dyck, C. H., Arnsten, A. F. T., and Nairn, A. C. (2020). Phosphodiesterase PDE4D is decreased in frontal cortex of aged rats and positively correlated with working memory performance and inversely correlated with PKA phosphorylation of tau. *Front. Aging Neurosci.* 12:576723. doi: 10.3389/fnagi.2020.576723
- Li, W., Wang, X., Zhao, J., Lin, J., Song, X. Q., Yang, Y., et al. (2012). Association study of myelin transcription factor 1-like polymorphisms with schizophrenia in Han Chinese population. *Genes Brain Behav.* 11, 87–93. doi: 10.1111/j.1601-183X.2011.00734.x
- Liu, C., Zhang, X., Chai, H., Xu, S., Liu, Q., Luo, Y., et al. (2022). Identification of immune cells and key genes associated with Alzheimer's disease. *Int. J. Med. Sci.* 19, 112–125. doi: 10.7150/ijms.66422
- Matthews, K. A., Xu, W., Gaglioti, A. H., Holt, J. B., Croft, J. B., Mack, D., et al. (2019). Racial and ethnic estimates of Alzheimer's disease and related dementias in the United States (2015–2060) in adults aged ≥ 65 years. *Alzheimers. Dement.* 15, 17–24. doi: 10.1016/j.jalz.2018.06.3063
- McKhann, G. M., Knopman, D. S., Chertkow, H., Hyman, B. T., Jack, C. R. Jr., Kawas, C. H., et al. (2011). The diagnosis of dementia due to Alzheimer's disease: recommendations from the National Institute on Aging-Alzheimer's Association workgroups on diagnostic guidelines for Alzheimer's disease. *Alzheimers. Dement.* 7, 263–269. doi: 10.1016/j.jalz.2011.03.005
- Murphy, M. P., and Hartley, R. C. (2018). Mitochondria as a therapeutic target for common pathologies. *Nat. Rev. Drug Discov.* 17, 865–886. doi: 10.1038/nrd.2018.174
- Nandigam, R. N. (2008). Mixed brain pathologies account for most dementia cases in community-dwelling older persons. *Neurology* 70:816; author reply 816–817. doi: 10.1212/01.wnl.0000307675.38908.39
- Nelder, J. A., and Wedderburn, R. W. (1972). Generalized linear models. *J. R. Stat. Soc. Ser. A* 135, 370–384. doi: 10.2307/2344614
- Newman, A. M., Liu, C. L., Green, M. R., Gentles, A. J., Feng, W., Xu, Y., et al. (2015). Robust enumeration of cell subsets from tissue expression profiles. *Nat. Methods* 12, 453–457. doi: 10.1038/nmeth.3337
- Oliveri, V. (2022). Selective targeting of cancer cells by copper ionophores: an overview. *Front. Mol. Biosci.* 9:841814. doi: 10.3389/fmolb.2022.841814
- Paranjpe, M. D., Belonwu, S., Wang, J. K., Oskotsky, T., Gupta, A., Taubes, A., et al. (2021). Sex-specific cross tissue meta-analysis identifies immune dysregulation in women with Alzheimer's disease. *Front. Aging Neurosci.* 13:735611. doi: 10.3389/fnagi.2021.735611
- Rahimi, J., and Kovacs, G. G. (2014). Prevalence of mixed pathologies in the aging brain. *Alzheimers. Res. Ther.* 6:82. doi: 10.1186/s13195-014-0082-1
- Rigatti, S. J. (2017). Random forest. *J. Insur. Med.* 47, 31–39. doi: 10.17849/inm-47-01-31-39.1
- Soto, I. C., Fontanesi, F., Liu, J., and Barrientos, A. (2012). Biogenesis and assembly of eukaryotic cytochrome c oxidase catalytic core. *Biochim. Biophys. Acta* 1817, 883–897. doi: 10.1016/j.bbabi.2011.09.005
- Tang, D., Chen, X., and Kroemer, G. (2022). Cuproptosis: a copper-triggered modality of mitochondrial cell death. *Cell Res.* 32, 417–418. doi: 10.1038/s41422-022-00653-7
- Tang, J., Oliveros, A., and Jang, M. H. (2019). Dysfunctional mitochondrial bioenergetics and synaptic degeneration in Alzheimer disease. *Int. Neurol.* 101, S5–S10. doi: 10.5213/inj.1938036.018
- Tsukumo, S. I., and Yasutomo, K. (2018). Regulation of CD8(+) T cells and antitumor immunity by notch signaling. *Front. Immunol.* 9:101. doi: 10.3389/fimmu.2018.00101
- Tsvetkov, P., Coy, S., Petrova, B., Dreishpoon, M., Verma, A., Abdusamad, M., et al. (2022). Copper induces cell death by targeting lipoylated TCA cycle proteins. *Science* 375, 1254–1261. doi: 10.1126/science.abf0529
- Wang, X., Wang, D., Su, F., Li, C., and Chen, M. (2022a). Immune abnormalities and differential gene expression in the hippocampus and peripheral blood of patients with Alzheimer's disease. *Ann. Transl. Med.* 10:29. doi: 10.21037/atm-21-4974
- Wang, Y., Zhang, L., and Zhou, F. (2022b). Cuproptosis: a new form of programmed cell death. *Cell. Mol. Immunol.* doi: 10.1038/s41423-022-00866-1. [Epub ahead of print].
- Wilkerson, M. D., and Hayes, D. N. (2010). ConsensusClusterPlus: a class discovery tool with confidence assessments and item tracking. *Bioinformatics* 26, 1572–1573. doi: 10.1093/bioinformatics/btq170
- Yemni, E. A., Monies, D., Alkhairallah, T., Bohlega, S., Abouelhoda, M., Magrashi, A., et al. (2019). Integrated analysis of whole exome sequencing and copy number evaluation in Parkinson's disease. *Sci. Rep.* 9:3344. doi: 10.1038/s41598-019-40102-x
- Zheng, J. J., Li, W. X., Liu, J. Q., Guo, Y. C., Wang, Q., Li, G. H., et al. (2018). Low expression of aging-related NRXN3 is associated with Alzheimer disease: a systematic review and meta-analysis. *Medicine* 97:e11343. doi: 10.1097/MD.00000000000011343



OPEN ACCESS

EDITED BY

Suvarna Alladi,
National Institute of Mental Health
and Neurosciences (NIMHANS), India

REVIEWED BY

Yuri Zilberter,
INSERM U1106 Institut
de Neurosciences des Systèmes,
France
Benjamin Creton,
Hôpitaux Universitaires de Strasbourg,
France

*CORRESPONDENCE

Yi Guo
yiguo@zju.edu.cn

SPECIALTY SECTION

This article was submitted to
Alzheimer's Disease and Related
Dementias,
a section of the journal
Frontiers in Aging Neuroscience

RECEIVED 23 April 2022

ACCEPTED 30 June 2022

PUBLISHED 22 July 2022

CITATION

Zhang G-F, Gong W-X, Xu Z-Y-R and
Guo Y (2022) Alzheimer's disease
and epilepsy: The top 100 cited
papers.
Front. Aging Neurosci. 14:926982.
doi: 10.3389/fnagi.2022.926982

COPYRIGHT

© 2022 Zhang, Gong, Xu and Guo. This
is an open-access article distributed
under the terms of the [Creative
Commons Attribution License \(CC BY\)](#).
The use, distribution or reproduction in
other forums is permitted, provided
the original author(s) and the copyright
owner(s) are credited and that the
original publication in this journal is
cited, in accordance with accepted
academic practice. No use, distribution
or reproduction is permitted which
does not comply with these terms.

Alzheimer's disease and epilepsy: The top 100 cited papers

Gui-Fen Zhang¹, Wen-Xin Gong¹, Zheng-Yan-Ran Xu² and Yi Guo^{1,2*}

¹Department of General Practice and International Medicine, Second Affiliated Hospital, School of Medicine, Zhejiang University, Hangzhou, China, ²Department of Neurology, Epilepsy Center, Second Affiliated Hospital, School of Medicine, Zhejiang University, Hangzhou, China

Background: Alzheimer's disease (AD) is one of the common neurodegenerative diseases, which often coexists with epilepsy. It is very significant to study the treatment options and the relationship between AD and epilepsy.

Aims: The purpose of this study was to analyze the top 100 cited papers about AD and epilepsy using bibliometrics, and to describe the current situation and predict research hot spots.

Methods: Top 100 papers were obtained from the Web of Science Core Collection (WoSCC). The WoSCC was used to analyze the author, institution, country, title, keywords, abstract, citation, subject category, publication year, impact factor (IF), and other functions. SPSS25 software was used for statistical analysis and CiteSpace V.5.7.R2 was used to visualize the information through collaborative networks.

Results: The number of publications gradually increased from 2000 to 2021. The total citation count for the top 100 papers ranged from 15 to 433 (mean = 67.43). The largest number of papers were published in 2016 ($n = 11$). Meanwhile, USA (centrality: 0.93) and Columbia University (centrality: 0.06) were the most influential research country and institutions, respectively. The top contributing journals was Journal of Alzheimer's Disease (8%). The IF for journals ranged from 1.819 to 53.44. A network analysis of the author's keywords showed that "beta" (centrality: 0.39), "amyloid beta" (centrality: 0.29), "hyperexcitability" (centrality: 0.29) and "disease" (centrality: 0.29) had a high degree of centrality.

Conclusion: AD and epilepsy have been intensively studied in the past few years. The relationships, mechanisms and treatment of AD and epilepsy will be subjects of active research hotspots in future. These findings provide valuable information for clinicians and scientists to identify new perspectives with potential collaborators and cooperative countries.

KEYWORDS

Alzheimer's disease, epilepsy, bibliometric study, top-cited, citation

Introduction

Alzheimer's disease (AD) and epilepsy are common neurological diseases. The number of patients with dementia and epilepsy in the global population is increasing, representing a growing problem for global health. The overall lifetime prevalence of epilepsy is 7.60 per 1,000 population [95% confidence interval (CI) 6.17–9.38] and the prevalence of epilepsy tends to peak in the elderly (Beghi, 2020). The prevalence of AD in Europe was estimated at 5.05% (95% CI, 4.73–5.39), and similar to epilepsy, AD prevalence increases with age (Niu et al., 2017). In fact, these two diseases are related. Epilepsy occurs more frequently in patients with AD than in those with non-Alzheimer's disease (Samson et al., 1996). Recent findings showed that seizures could accelerate the decline of cognitive ability in patients with AD and that there might be an important bidirectional relationship between epilepsy and AD (Sen et al., 2018). AD and Epilepsy also share many pathological similarities (Lehmann et al., 2021), e.g., temporal lobe atrophy, neuronal death, gliosis, neuritic alterations, and neuroinflammation (Struble et al., 2010). In addition, AD plus epilepsy would lead to more serious clinical consequences, such as cognitive decline, weakness, anxiety, depression, social withdrawal, psychological and behavioral comorbidity, and poor treatment compliance (Cretin, 2021). Overtime, a large amount of literature has been published comprising a wide range of relevant research and clinical themes. However, the precise mechanisms leading to the development of seizures in the setting of AD are still under investigation and require further study. A meta-analysis showed that the quality of evidence on the treatment outcome of epilepsy in patients with AD was very low (Liu and Wang, 2021).

As a discipline emerging since its formal foundation, a bibliometric review of the literature was warranted to aid the synthesis and implementation of the evidence base. Despite citation analysis across a broad range of neurosciences (Yeung et al., 2017), there is limited information in the field of AD and epilepsy, with few published studies. Citation counting is an important metric to understand the significance of the contribution of research to a research field (Fox et al., 2021). Previous reviews only relied on individuals to study the research through literature summary and extraction, and thus cannot fully reflect the temporal and spatial distribution of researchers, institutions, and journals. Moreover, it is difficult to visualize the internal structure of the knowledge base and research focus, and systematic, comprehensive, and visual research are rarely found. Therefore, the present study aims to comprehensively analyze the current status, research hotspots, and development trends through a bibliometric analysis of the top 100 papers on AD and epilepsy published from 2000 to 2021. The findings may help follow-up researchers study the association between AD and epilepsy, identify journal publications and collaborators, and analyze keywords and research trends, which might promote

research aiming to determine the cause, mechanism, and treatment of the disease.

Materials and methods

Data source

The retrieval data for measurement and statistical analysis were screened from the Web of Science Core Collection (WoSCC), which provided the citation search, giving access to multiple databases that reference cross-disciplinary research and allowing an in-depth exploration of specialized subfields (Wu et al., 2021). We conducted a literature search from the WoSCC on June 5th, 2022. In this study, the search criteria in the WoSCC database were as follows: ((TI = (epilep* OR seizure* OR convuls*)) OR KP = (epilep* OR seizure* OR convuls*)) AND ((TI = (dement* OR Alzheimer* OR "cognit* impair*" OR AD)) OR KP = (dement* OR Alzheimer* OR "cognit* impair*" OR AD)). Timespan: 2000-01-01 to 2021-12-31 (Publication Date). Document type: articles and reviews; Language: English. A total of 2601 records were retrieved. Then, two independent investigators reviewed the titles and abstracts and deleted studies that were not associated with AD and epilepsy, which excluded 1237 papers according to the criteria (Guo et al., 2021). And 1264 papers were excluded after the 100th rank from the selected literature. Finally, the top 100 studies were determined. A Preferred Reporting Items for Systematic Reviews and Meta-Analyses (PRISMA) flow diagram for the WoSCC results is provided in Figure 1.

Data analysis

In the present study, WoSCC was used to analyze the author, institution, country, title, keywords, abstract, citation, subject category, publication year, impact factor (IF), and other functions. The selected documents were imported into Excel (Microsoft Corporation, Redmond, WA, United States) and CiteSpace 5.8.R3 (64-bit) (Palop and Mucke, 2009). SPSS 25.0 statistical software (IBM Corp., Armonk, NY, United States) was used for statistical analysis. Continuous variables were expressed as the mean \pm SD. Categorical variables were expressed as a percentage. CiteSpace, a bibliometric analysis tool, was created by Dr. Chaomei Chen (School of Information Science and Technology, Drexel University, Philadelphia, PA, United States) and his team. It visualizes countries/regions, institutions, authors and their cooperative relationships, co-cited references, and co-occurrence words through collaborative networks, which has been widely used in biomedical research fields.

Three folders of the research were created, including input folder placing the data downloaded from WoSCC, a data folder containing the data after deleting duplicate documents, and a

TABLE 1 The 100 most-cited publications.

| Rank | Article title | Journal | IF (2020) | Times Cited | Times Cited, in 2021 | Times Cited, per year |
|------|---|---|-----------|-------------|----------------------|-----------------------|
| 1 | Epilepsy and Cognitive Impairments in Alzheimer Disease | ARCHIVES OF NEUROLOGY | 7.419 | 433 | 39 | 31 |
| 2 | Amyloid beta-Induced Neuronal Hyperexcitability Triggers Progressive Epilepsy | JOURNAL OF NEUROSCIENCE | 6.167 | 405 | 54 | 28.93 |
| 3 | Incidence and predictors of seizures in patients with Alzheimer's disease | EPILEPSIA | 5.886 | 391 | 37 | 23 |
| 4 | Seizures and Epileptiform Activity in the Early Stages of Alzheimer's Disease | JAMA NEUROLOGY | 18.302 | 357 | 56 | 35.7 |
| 5 | Epileptic activity in Alzheimer's disease: causes and clinical relevance | LANCET NEUROLOGY | 44.182 | 213 | 64 | 35.5 |
| 6 | Incidence and Impact of Subclinical Epileptiform Activity in Alzheimer's Disease | ANNALS OF NEUROLOGY | 10.442 | 201 | 43 | 28.71 |
| 7 | Antisense Reduction of Tau in Adult Mice Protects against Seizures | JOURNAL OF THE INTERNATIONAL NEUROPSYCHOLOGICAL SOCIETY | 6.167 | 192 | 31 | 19.2 |
| 8 | Seizures in Alzheimer Disease Who, When, and How Common? | ARCHIVES OF NEUROLOGY | 7.419 | 187 | 21 | 13.36 |
| 9 | Silent hippocampal seizures and spikes identified by foramen ovale electrodes in Alzheimer's disease | NATURE MEDICINE | 53.44 | 172 | 54 | 28.67 |
| 10 | A perfect storm: Converging paths of epilepsy and Alzheimer's dementia intersect in the hippocampal formation | EPILEPSIA | 5.886 | 167 | 15 | 13.92 |
| 11 | Tau Loss Attenuates Neuronal Network Hyperexcitability in Mouse and Drosophila Genetic Models of Epilepsy | JOURNAL OF NEUROSCIENCE | 6.167 | 148 | 26 | 14.8 |
| 12 | Seizures and Epilepsy in Alzheimer's Disease | CNS NEUROSCIENCE AND THERAPEUTICS | 5.243 | 135 | 23 | 12.27 |
| 13 | Seizures in elderly patients with dementia - Epidemiology and management | DRUGS AND AGING | 3.923 | 132 | 8 | 6.6 |
| 14 | Down syndrome, Alzheimer's disease, and seizures | BRAIN AND DEVELOPMENT | 1.961 | 128 | 8 | 7.11 |
| 15 | Hyperphosphorylated tau in patients with refractory epilepsy correlates with cognitive decline: a study of temporal lobe resections | BRAIN | 13.501 | 123 | 28 | 17.57 |
| 16 | Levetiracetam, lamotrigine, and phenobarbital in patients with epileptic seizures and Alzheimer's disease | EPILEPSY AND BEHAVIOR | 2.937 | 113 | 23 | 8.69 |
| 17 | Septal networks: relevance to theta rhythm, epilepsy and Alzheimer's disease | JOURNAL OF NEUROCHEMISTRY | 5.372 | 105 | 9 | 6.18 |
| 18 | Prevalence and causes of seizures at the time of diagnosis of probable Alzheimer's disease | DEMENTIA AND GERIATRIC COGNITIVE DISORDERS | 2.959 | 94 | 8 | 5.53 |
| 19 | Cognition and dementia in older patients with epilepsy | BRAIN | 7.419 | 93 | 31 | 18.6 |
| 20 | Seizures in patients with Alzheimer's disease or vascular dementia: A population-based nested casecontrol analysis | EPILEPSIA | 5.886 | 89 | 14 | 8.9 |
| 21 | Incidence of New-Onset Seizures in Mild to Moderate Alzheimer Disease | ARCHIVES OF NEUROLOGY | 7.419 | 82 | 11 | 7.45 |
| 22 | Seizures in Alzheimer's disease | NEUROSCIENCE | 3.59 | 81 | 13 | 10.13 |
| 23 | Shared cognitive and behavioral impairments in epilepsy and Alzheimer's disease and potential underlying mechanisms | EPILEPSY AND BEHAVIOR | 2.937 | 80 | 9 | 8 |

(Continued)

TABLE 1 (Continued)

| Rank | Article title | Journal | IF (2020) | Times Cited | Times Cited, in 2021 | Times Cited, per year |
|------|--|--|-----------|-------------|----------------------|-----------------------|
| 24 | Epileptic Seizures in AD Patients | NEUROMOLECULAR MEDICINE | 3.843 | 78 | 3 | 6 |
| 25 | Seizures in Alzheimer's Disease: Clinical and Epidemiological Data | EPILEPSY CURRENTS | 7.5 | 71 | 11 | 6.45 |
| 26 | Spontaneous epileptiform discharges in a mouse model of Alzheimer's disease are suppressed by antiepileptic drugs that block sodium channels | EPILEPSY RESEARCH | 3.045 | 65 | 9 | 5.42 |
| 27 | Relative Incidence of Seizures and Myoclonus in Alzheimer's Disease, Dementia with Lewy Bodies, and Frontotemporal Dementia | JOURNAL OF ALZHEIMER'S DISEASE | 4.472 | 59 | 22 | 9.83 |
| 28 | Epileptic Seizures in Alzheimer Disease A Review | ALZHEIMER DISEASE AND ASSOCIATED DISORDERS | 2.703 | 59 | 11 | 8.43 |
| 29 | Interictal spikes during sleep are an early defect in the Tg2576 mouse model of beta-amyloid neuropathology | SCIENTIFIC REPORTS | 4.38 | 59 | 11 | 8.43 |
| 30 | Epileptic Prodromal Alzheimer's Disease, a Retrospective Study of 13 New Cases: Expanding the Spectrum of Alzheimer's Disease to an Epileptic Variant? | JOURNAL OF ALZHEIMER'S DISEASE | 4.472 | 58 | 13 | 8.29 |
| 31 | Levetiracetam monotherapy in Alzheimer patients with late-onset seizures: a prospective observational study | EUROPEAN JOURNAL OF NEUROLOGY | 6.089 | 58 | 8 | 3.63 |
| 32 | Common factors among Alzheimer's disease, Parkinson's disease, and epilepsy: Possible role of the noradrenergic nervous system | EPILEPSIA | 5.886 | 57 | 3 | 5.18 |
| 33 | Dietary energy substrates reverse early neuronal hyperactivity in a mouse model of Alzheimer's disease | JOURNAL OF NEUROCHEMISTRY | 5.372 | 56 | 5 | 5.6 |
| 34 | Brivaracetam, but not ethosuximide, reverses memory impairments in an Alzheimer's disease mouse model | ALZHEIMER'S RESEARCH AND THERAPY | 6.982 | 54 | 12 | 6.75 |
| 35 | Increased Cortical and Thalamic Excitability in Freely Moving APPswe/PS1dE9 Mice Modeling Epileptic Activity Associated with Alzheimer's Disease | CEREBRAL CORTEX | 5.357 | 51 | 8 | 5.1 |
| 36 | Down Syndrome and Dementia: Seizures and Cognitive Decline | JOURNAL OF ALZHEIMER'S DISEASE | 4.472 | 51 | 8 | 4.64 |
| 37 | The efficacy of a voxel-based morphometry on the analysis of imaging in schizophrenia, temporal lobe epilepsy, and Alzheimer's disease/mild cognitive impairment: a review | NEURORADIOLOGY | 2.804 | 48 | 2 | 3.69 |
| 38 | CA1 hippocampal neuronal loss in familial Alzheimer's disease – Presenilin-1 E280A mutation is related to epilepsy | EPILEPSIA | 5.886 | 48 | 3 | 2.53 |
| 39 | Bexarotene reduces network excitability in models of Alzheimer's disease and epilepsy | NEUROBIOLOGY OF AGING | 4.673 | 46 | 4 | 5.11 |
| 40 | Seizure resistance without parkinsonism in aged mice after tau reduction | NEUROBIOLOGY OF AGING | 4.673 | 45 | 5 | 5 |
| 41 | Early-Onset Network Hyperexcitability in Presymptomatic Alzheimer's Disease Transgenic Mice Is Suppressed by Passive Immunization with Anti-Human APP/A beta Antibody and by mGluR5 Blockade | FRONTIERS IN AGING NEUROSCIENCE | 5.75 | 43 | 11 | 7.17 |
| 42 | Epigenetic suppression of hippocampal calbindin-D28k by Delta FosB drives seizure-related cognitive deficits | NATURE MEDICINE | 53.44 | 42 | 17 | 7 |

(Continued)

TABLE 1 (Continued)

| Rank | Article title | Journal | IF (2020) | Times Cited | Times Cited, in 2021 | fTimes Cited, per year |
|------|---|--|-----------|-------------|----------------------|------------------------|
| 43 | Seizures in dominantly inherited Alzheimer disease | NEUROLOGY | 9.91 | 42 | 9 | 6 |
| 44 | Seizures in Alzheimer's disease: a retrospective study of a cohort of outpatients | EPILEPTIC DISORDERS | 1.819 | 41 | 7 | 3.15 |
| 45 | Epilepsy presenting as AD: Neuroimaging, electroclinical features, and response to treatment | NEUROLOGY | 9.91 | 41 | 0 | 1.95 |
| 46 | Ectopic white matter neurons, a developmental abnormality that may be caused by the PSEN1 S169L mutation in a case of familial AD with myoclonus and seizures | JOURNAL OF NEUROPATHOLOGY AND EXPERIMENTAL NEUROLOGY | 3.685 | 41 | 0 | 1.86 |
| 47 | Alzheimer's disease and late-onset epilepsy of unknown origin: two faces of beta amyloid pathology | NEUROBIOLOGY OF AGING | 4.673 | 40 | 16 | 10 |
| 48 | From here to epilepsy: the risk of seizure in patients with Alzheimer's disease | EPILEPTIC DISORDERS | 1.819 | 40 | 6 | 5.71 |
| 49 | Alzheimer's disease underlies some cases of complex partial status epilepticus - Clinical, radiologic, EEG, and pathologic correlations | JOURNAL OF CLINICAL NEUROPHYSIOLOGY | 2.177 | 40 | 2 | 1.74 |
| 50 | Early Onset of Hypersynchronous Network Activity and Expression of a Marker of Chronic Seizures in the Tg2576 Mouse Model of Alzheimer's Disease | PLOS ONE | 3.24 | 39 | 10 | 4.88 |
| 51 | Chronic Temporal Lobe Epilepsy Is Associated with Enhanced Alzheimer-Like Neuropathology in 36 x Tg-AD Mice | PLOS ONE | 3.24 | 39 | 6 | 3.55 |
| 52 | Overview of cannabidiol (CBD) and its analogs: Structures, biological activities, and neuroprotective mechanisms in epilepsy and Alzheimer's disease | EUROPEAN JOURNAL OF MEDICINAL CHEMISTRY | 6.514 | 38 | 24 | 12.67 |
| 53 | Adult-Onset Epilepsy in Presymptomatic Alzheimer's Disease: A Retrospective Study | JOURNAL OF ALZHEIMER'S DISEASE | 4.472 | 38 | 9 | 6.33 |
| 54 | Seizures and dementia in the elderly: Nationwide Inpatient Sample 1999–2008 | EPILEPSY AND BEHAVIOR | 2.937 | 38 | 4 | 4.22 |
| 55 | Senile myoclonic epilepsy: Delineation of a common condition associated with Alzheimer's disease in Down syndrome | SEIZURE-EUROPEAN JOURNAL OF EPILEPSY | 3.184 | 38 | 2 | 2.92 |
| 56 | Presenilin-1 mutation Alzheimer's disease: A genetic epilepsy syndrome? | EPILEPSY AND BEHAVIOR | 2.937 | 37 | 4 | 3.08 |
| 57 | Sleep EEG Detects Epileptiform Activity in Alzheimer's Disease with High Sensitivity | JOURNAL OF ALZHEIMER'S DISEASE | 4.472 | 36 | 9 | 6 |
| 58 | Incidence and risk of seizures in Alzheimer's disease: A nationwide population-based cohort study | EPILEPSY RESEARCH | 3.045 | 33 | 11 | 4.13 |
| 59 | Low brain ascorbic acid increases susceptibility to seizures in mouse models of decreased brain ascorbic acid transport and Alzheimer's disease | EPILEPSY RESEARCH | 3.045 | 33 | 2 | 4.13 |
| 60 | Alzheimer's Disease and Down Syndrome Rodent Models Exhibit Audiogenic Seizures | JOURNAL OF ALZHEIMER'S DISEASE | 4.472 | 33 | 3 | 2.54 |

(Continued)

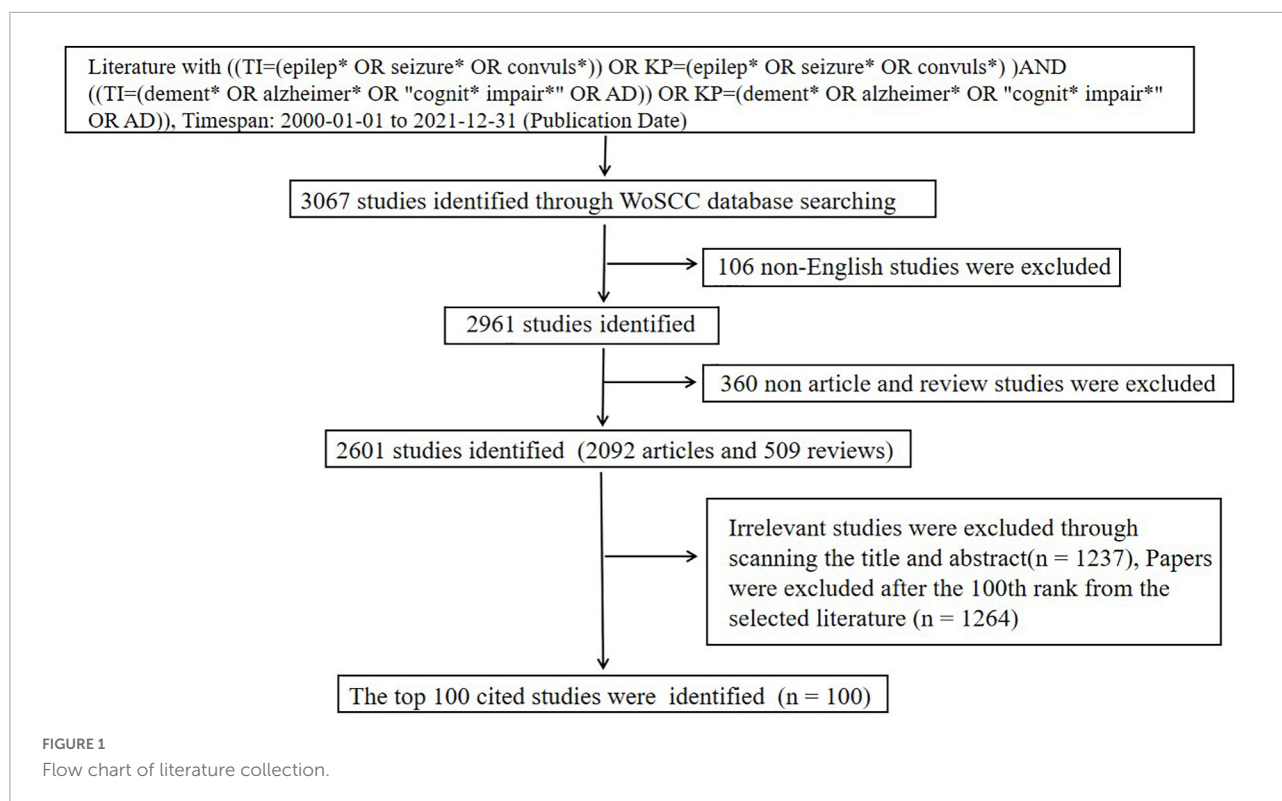
TABLE 1 (Continued)

| Rank | Article title | Journal | IF (2020) | Times Cited | Times Cited, in 2021 | Times Cited, per year |
|------|--|---|-----------|-------------|----------------------|-----------------------|
| 61 | Paroxysmal slow cortical activity in Alzheimer's disease and epilepsy is associated with blood-brain barrier dysfunction | SCIENCE TRANSLATIONAL MEDICINE | 17.992 | 31 | 14 | 7.75 |
| 62 | Prevalence, Semiology, and Risk Factors of Epilepsy in Alzheimer's Disease: An Ambulatory EEG Study | JOURNAL OF ALZHEIMER'S DISEASE | 4.472 | 30 | 12 | 6 |
| 63 | Incidence of stroke and seizure in Alzheimer's disease dementia | AGE AND AGEING | 10.668 | 30 | 7 | 3.75 |
| 64 | A presenilin 1 mutation (L420R) in a family with early onset Alzheimer disease, seizures and cotton wool plaques, but not spastic paraparesis | NEUROPATHOLOGY | 1.906 | 30 | 1 | 1.88 |
| 65 | Association of epileptiform abnormalities and seizures in Alzheimer disease | NEUROLOGY | 9.91 | 29 | 16 | 9.67 |
| 66 | Alzheimer-like amyloid and tau alterations associated with cognitive deficit in temporal lobe epilepsy | BRAIN | 13.501 | 28 | 15 | 9.33 |
| 67 | Tau-Induced Pathology in Epilepsy and Dementia: Notions from Patients and Animal Models | INTERNATIONAL JOURNAL OF MOLECULAR SCIENCES | 5.924 | 28 | 10 | 5.6 |
| 68 | A mouse model of Alzheimer's disease displays increased susceptibility to kindling and seizure-associated death | EPILEPSIA | 5.886 | 28 | 3 | 3.5 |
| 69 | Early Seizure Activity Accelerates Depletion of Hippocampal Neural Stem Cells and Impairs Spatial Discrimination in an Alzheimer's Disease Model | CELL REPORTS | 9.423 | 27 | 14 | 6.75 |
| 70 | Traumatic Brain Injury Increases the Expression of Nos1, A beta Clearance, and Epileptogenesis in APP/PS1 Mouse Model of Alzheimer's Disease | MOLECULAR NEUROBIOLOGY | 5.59 | 27 | 9 | 3.86 |
| 71 | Alternative ion channel splicing in mesial temporal lobe epilepsy and Alzheimer's disease | GENOME BIOLOGY | 2.763 | 27 | 2 | 1.69 |
| 72 | Hyperpolarization-activated cyclic nucleotide gated channels: a potential molecular link between epileptic seizures and A beta generation in Alzheimer's disease | MOLECULAR NEURODEGENERATION | 14.195 | 26 | 4 | 2.36 |
| 73 | Untangling Alzheimer's Disease and Epilepsy | EPILEPSY CURRENTS | 7.5 | 26 | 2 | 2.36 |
| 74 | Increased Epileptiform EEG Activity and Decreased Seizure Threshold in Arctic APP Transgenic Mouse Model of Alzheimer's Disease | CURRENT ALZHEIMER'S RESEARCH | 3.498 | 25 | 7 | 3.57 |
| 75 | GSK3 beta and Tau Protein in Alzheimer's Disease and Epilepsy | FRONTIERS IN CELLULAR NEUROSCIENCE | 5.505 | 24 | 12 | 8 |
| 76 | Alterations of Coherent Theta and Gamma Network Oscillations as an Early Biomarker of Temporal Lobe Epilepsy and Alzheimer's Disease | FRONTIERS IN INTEGRATIVE NEUROSCIENCE | 2.763 | 24 | 11 | 4.8 |
| 77 | Seizure susceptibility in the APP/PS1 mouse' model of Alzheimer's disease and relationship with amyloid beta plaques | BRAIN RESEARCH | 3.252 | 24 | 9 | 4 |
| 78 | A possible significant role of zinc and GPR39 zinc sensing receptor in Alzheimer disease and epilepsy | BIOMEDICINE AND PHARMACOTHERAPY | 6.53 | 24 | 2 | 3.43 |
| 79 | Early onset familial Alzheimer disease with spastic paraparesis, dysarthria, and seizures and N135S mutation in PSEN1 | ALZHEIMER DISEASE AND ASSOCIATED DISORDERS | 2.703 | 22 | 5 | 1.47 |

(Continued)

TABLE 1 (Continued)

| Rank | Article title | Journal | IF (2020) | Times Cited | Times Cited, in 2021 | Times Cited, per year |
|------|--|---|-----------|-------------|----------------------|-----------------------|
| 80 | Epilepsy and antiepileptic drug use in elderly people as risk factors for dementia | JOURNAL OF THE NEUROLOGICAL SCIENCES | 3.181 | 22 | 4 | 1.38 |
| 81 | Do we know how to diagnose epilepsy early in Alzheimer's disease? | REVUE NEUROLOGIQUE | 2.607 | 21 | 3 | 3.5 |
| 82 | Increased risk of epilepsy in patients registered in the Swedish Dementia Registry | EUROPEAN JOURNAL OF NEUROLOGY | 6.089 | 20 | 8 | 5 |
| 83 | Seizures as an early symptom of autosomal dominant Alzheimer's disease | NEUROBIOLOGY OF AGING | 4.673 | 20 | 7 | 5 |
| 84 | Inflammasome-derived cytokine IL18 suppresses amyloid-induced seizures in Alzheimer-prone mice | PROCEEDINGS OF THE NATIONAL ACADEMY OF SCIENCES OF THE UNITED STATES OF AMERICA | 11.205 | 20 | 7 | 4 |
| 85 | Epileptic Amnesic Syndrome revealing Alzheimer's disease | EPILEPSY RESEARCH | 3.045 | 20 | 0 | 1.82 |
| 86 | <i>In Silico</i> Analyses for Key Genes and Molecular Genetic Mechanism in Epilepsy and Alzheimer's Disease | CNS AND NEUROLOGICAL DISORDERS-DRUG TARGETS | 4.388 | 19 | 4 | 3.8 |
| 87 | Seizures Can Precede Cognitive Symptoms in Late-Onset Alzheimer's Disease | JOURNAL OF ALZHEIMER'S DISEASE | 4.472 | 19 | 0 | 1.58 |
| 88 | Dementia, delusions and seizures: storage disease or genetic AD? | EUROPEAN JOURNAL OF NEUROLOGY | 6.089 | 19 | 1 | 1.19 |
| 89 | A Case Series of Epilepsy-derived Memory Impairment Resembling Alzheimer Disease | ALZHEIMER DISEASE AND ASSOCIATED DISORDERS | 2.703 | 18 | 2 | 1.29 |
| 90 | A novel mutation (L250V) in the presenilin 1 gene in a Japanese familial Alzheimer's disease with myoclonus and generalized convulsion | JOURNAL OF THE NEUROLOGICAL SCIENCES | 3.181 | 18 | 0 | 0.9 |
| 91 | Epilepsy and Alzheimer's Disease: Potential mechanisms for an association | BRAIN RESEARCH BULLETIN | 4.079 | 17 | 7 | 5.67 |
| 92 | Subclinical epileptiform activity during sleep in Alzheimer's disease and mild cognitive impairment | CLINICAL NEUROPHYSIOLOGY | 3.708 | 17 | 7 | 5.67 |
| 93 | A Longitudinal Study of Epileptic Seizures in Alzheimer's Disease | FRONTIERS IN NEUROLOGY | 4.003 | 17 | 7 | 4.25 |
| 94 | Seizures in Alzheimer's disease are highly recurrent and associated with a poor disease course | JOURNAL OF NEUROLOGY | 4.849 | 16 | 9 | 5.33 |
| 95 | Pharmacotherapeutic strategies for treating epilepsy in patients with Alzheimer's disease | EXPERT OPINION ON PHARMACOTHERAPY | 3.889 | 16 | 5 | 3.2 |
| 96 | From Molecular Circuit Dysfunction to Disease: Case Studies in Epilepsy, Traumatic Brain Injury, and Alzheimer's Disease | NEUROSCIENTIST | 7.519 | 16 | 1 | 2.29 |
| 97 | Alzheimer beta-amyloid blocks epileptiform activity in hippocampal neurons | MOLECULAR AND CELLULAR NEUROSCIENCE | 4.314 | 16 | 0 | 1.14 |
| 98 | Memory disturbances and temporal lobe epilepsy simulating Alzheimer's disease: a case report | FUNCTIONAL NEUROLOGY | 1.855 | 16 | 0 | 0.8 |
| 99 | Epileptic seizures in autosomal dominant forms of Alzheimer's disease | SEIZURE-EUROPEAN JOURNAL OF EPILEPSY | 3.184 | 15 | 3 | 3 |
| 100 | DBA/2J Genetic Background Exacerbates Spontaneous Lethal Seizures but Lessens Amyloid Deposition in a Mouse Model of Alzheimer's Disease | PLOS ONE | 4.24 | 15 | 0 | 1.88 |



project folder containing the data processed by cite. We did not find duplicate documents that needed to be deleted. The overall selected time span was from January 2000 to December 2021. Then, the slice length was set as 2 years. The node type was selected according to the type of analysis performed. The link lines between the nodes indicated the collaborative relationships. The size of the circles represented the number of papers published by the country/region, institute, or author. Purple rings indicated that these countries/regions, institutes, or authors had greater centrality.

Results

The 100 most-cited publications

We retrieved the 100 most frequently cited papers related to AD and epilepsy. The results were ranked according to citation counts to represent the 100 most-cited publications (76 articles and 24 reviews). A comprehensive list of the 100 publications and a citation details are presented in the **Table 1**.

As shown in **Table 1**, The 100 most-cited articles received a total of 6743 citations (according to Web of science, WOS). The median number citations was 39, with a range of 15–433. For annual citations, the mean value was 7.41 with a range of 0.8–35.70. Seventeen papers were cited more than 100 times, and 36 were cited more than 50 times. The review entitled “Epilepsy and

Cognitive Impairments in Alzheimer Disease” from **Palop and Mucke (2009)** was the most-cited publication ($n = 433$).

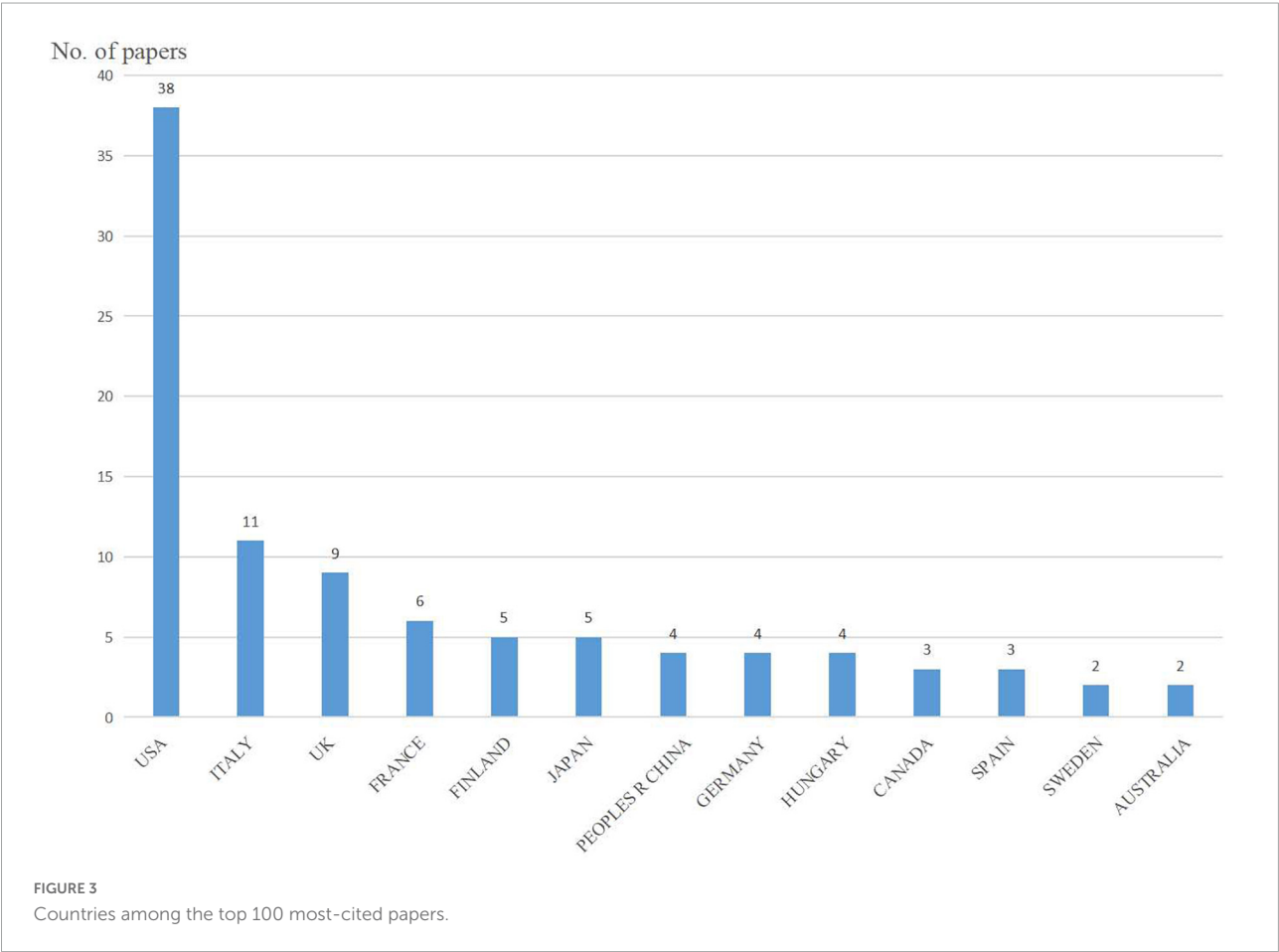
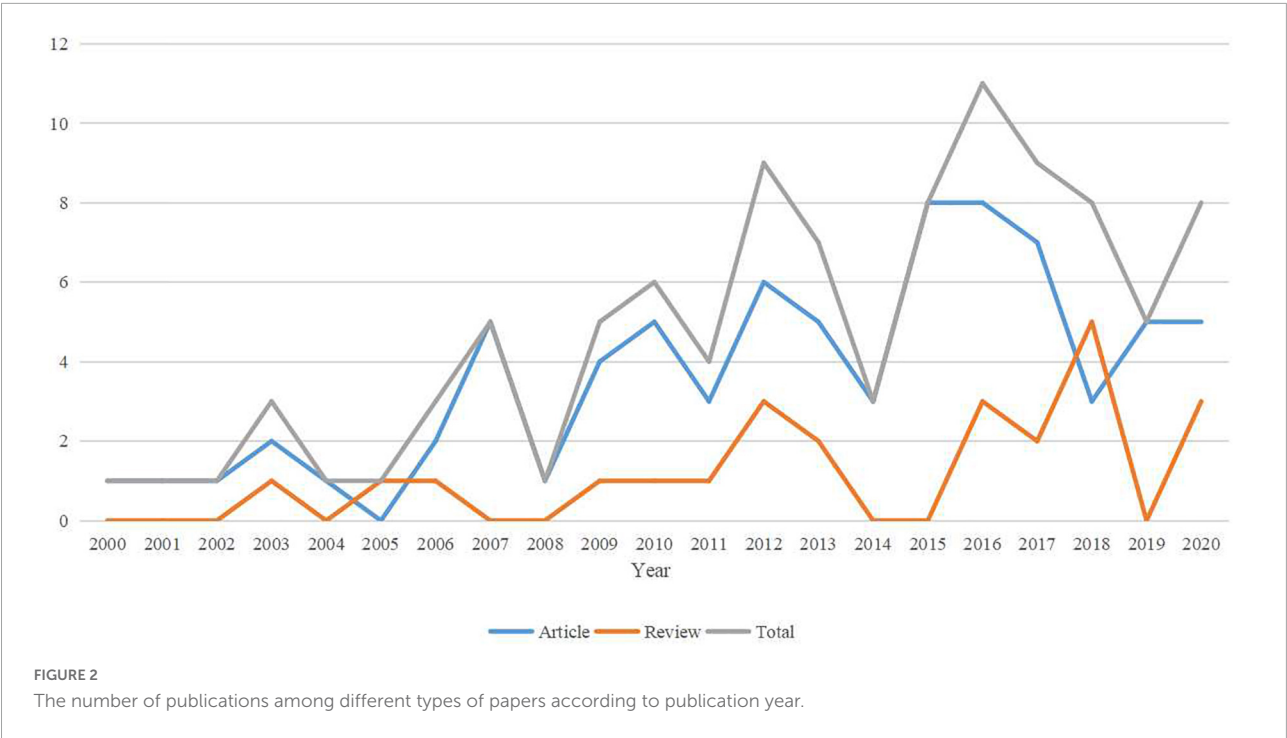
Publication years

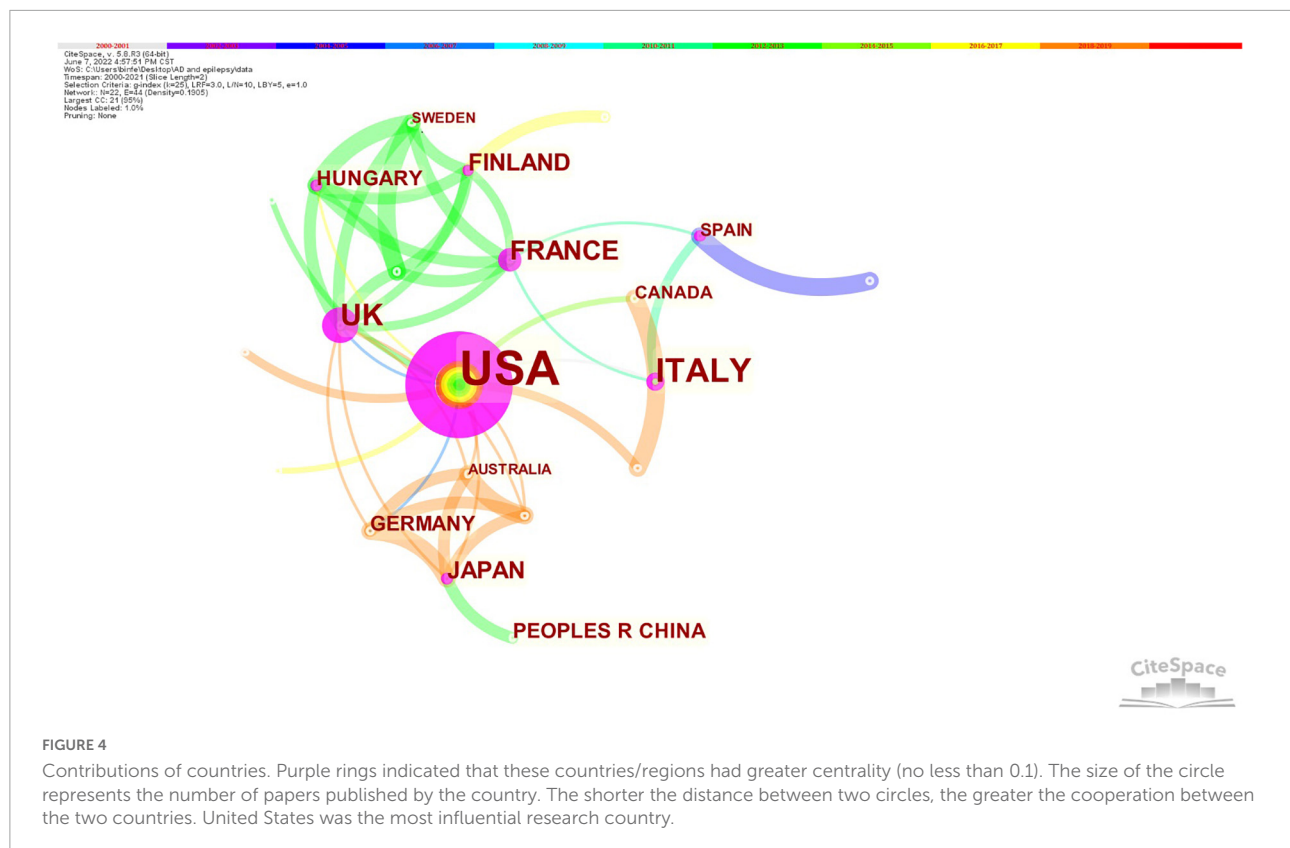
As shown in **Figure 2**, the top 100 most-cited papers were published from 2000 to 2020. Overall, publications showed a fluctuating upward trend. The largest number of studies was published in 2016 ($n = 11$), including eight articles and three reviews. The number of papers published in 2011 was higher than the number of papers published between 2000 and 2010.

Contributions of countries

Overall, 22 countries contributed to the included studies, with nine countries publishing only one study. The United States was the largest contributor of studies (38%), followed by Italy (11%) and the United Kingdom (9%). The contributing countries are shown in **Figure 3**.

Generating a country map using CiteSpace resulted in 22 nodes and 44 links (**Figure 4**). The 100 papers were published by research groups in 22 countries. The top five countries were the United States, Italy, the United Kingdom, France, and Finland. The top three countries in terms of centrality were the United States (0.93), the United Kingdom (0.44), and France (0.21). An analysis in terms of publication and centrality





indicated that the United States, the United Kingdom, Italy, and France were the main research powers in this research. United States has established cooperation with 12 countries, and the strongest collaborations were identified between United States, Canada, Israel, Greece, India, and Switzerland.

Contributions of institutions

A total of 178 institutions published at least one top-cited paper, the distribution of institutions was very scattered, with 21 (11.80%) institutions publishing two papers and 148 (83.15%) institutions publishing only one paper. A small number of institutions accounted for a high proportion of the highest cited papers. **Table 2** shows that the top nine institutions collectively published at least three papers. Baylor College of Medicine from United States topped the list with eight papers.

Figure 5 shows that generating an institution map resulted in 149 nodes and 308 links. The top 100 publications were distributed among 149 research institutions. The top five institutions were Baylor College Medicine, University of Eastern Finland, Columbia University, and Johns Hopkins University and Kuopio University Hospital. The top four institutions in terms of centrality were Columbia University (0.06), Baylor College of Medicine (0.04), Johns Hopkins University (0.04) and Indiana University (0.03). Analysis in terms of centrality

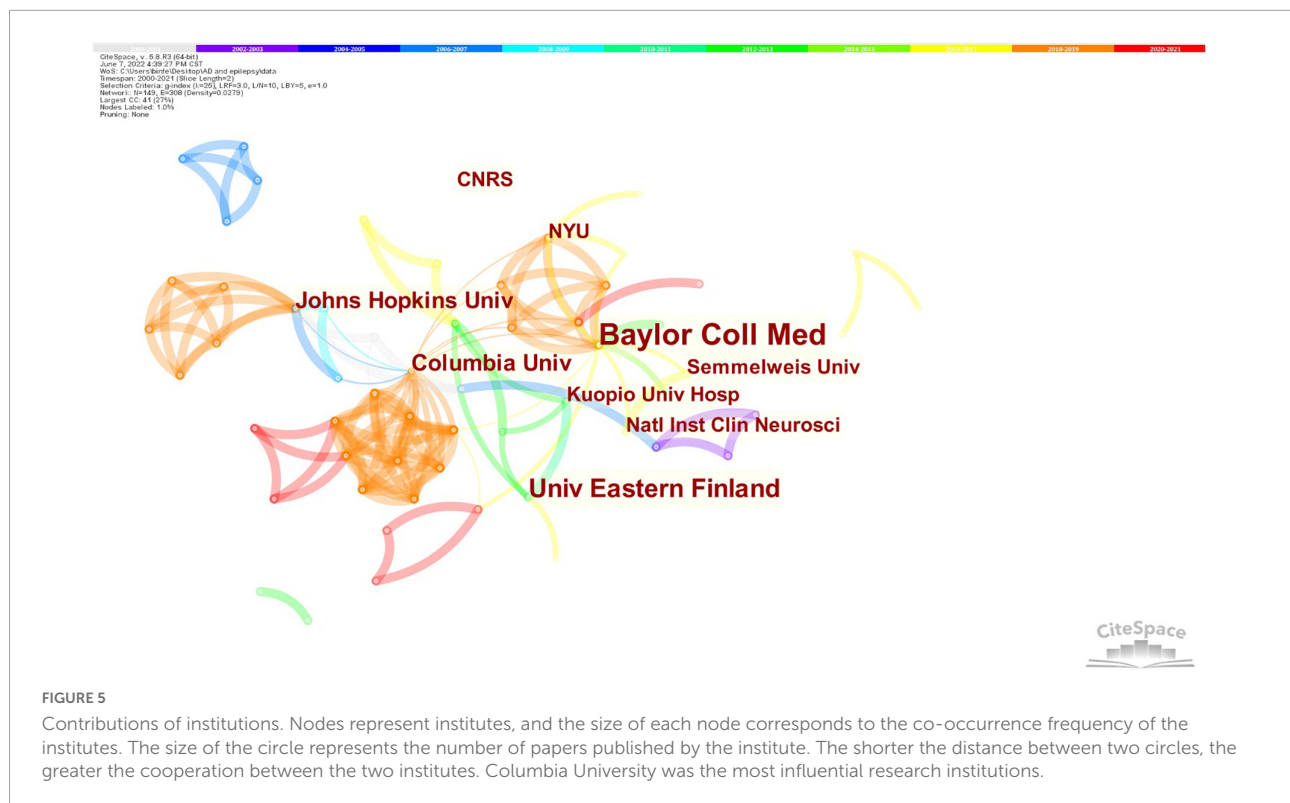
indicated that Columbia University was the most influential research institution.

Distribution of journals

The 100 most-cited articles were published in 59 journals; 18 journals published more than one study, which were distributed in the four partitions of Journal Citation Reports (JCR) (McVeigh, 2008). The JCR data provide both detailed journal information and flexible context, and category information to

TABLE 2 Top nine institutions with at least three papers in the top 100 most-cited papers.

| Rank | Institution | No. of papers | Centrality |
|------|--|---------------|------------|
| 1 | Baylor College of Medicine | 8 | 0.04 |
| 2 | University of Eastern Finland | 5 | 0 |
| 3 | Columbia University | 4 | 0.06 |
| 4 | Johns Hopkins University | 4 | 0.04 |
| 5 | Kuopio University Hospital | 3 | 0 |
| 6 | Semmelweis University | 3 | 0 |
| 7 | National Institute of Clinical Neurosciences | 3 | 0 |
| 8 | New York University | 3 | 0.01 |
| 9 | Centre National de la Recherche Scientifique | 3 | 0 |



allow people to understand the way each journal functions in the literature. The major contributing journals are presented in **Table 3**. The top five journals that published the 100 most-cited AD and epilepsy studies included Journal of Alzheimer's Disease ($n = 8$), Epilepsia ($n = 6$), Epilepsy and Behavior ($n = 4$), Neurobiology of Aging ($n = 4$) and Epilepsy Research ($n = 4$). With regard to the average citation number per paper, Journal of Neuroscience ranked first with a mean of 20.98 citations per paper, followed by Nature Medicine, with a mean of 17.84.

The IF for journals in the top 100 most-cited papers ranged from 1.819 to 53.44, among which 37 journals had an IF between 3 and 5, 34 journals had an IF between 5 and 10, and 3 journals had an IF above 20 (**Figure 6**).

In **Table 4**, the top 100 papers were classified into different study fields on the basis of WOS categories. The leading WOS category was "Clinical Neurology" ($n = 54$), following by "Neurosciences" ($n = 49$) and "Behavioral Sciences" ($n = 10$).

Major contributing authors

Overall, a total of 606 authors contributed to the 100 studies. There was wide, disparate authorship of first authors, with 90 different first authors represented in the 100 included publications. A total of four contributors published the most articles, namely Tanila Heikki, Noebels Jeffrey, Pitkänen, Asla and Scharfman, Helen E, who all published five publications,

the total number of citations for the papers were 629, 592, 578, and 234 respectively. Only three authors have published three studies as a first author. Keith A. Vossel from the University of California, as a first author and corresponding author, had the largest number of total citations in 2021 ($n = 185$). **Table 5** presents results for authors who contributed three or more of the 100 most-cited papers.

Analysis of co-occurring keywords

CiteSpace was used to extract the keywords from the top 100 papers on AD and epilepsy. A network analysis of the author's keywords or subject words was carried out during the publication time of the articles, namely, 2000–2021. **Table 6** shows that the top five keywords are epilepsy ($n = 41$), dementia ($n = 21$), mouse model ($n = 21$), mild cognitive impairment ($n = 13$), and Alzheimer's disease ($n = 11$). The greater the centrality value, the more cooperation between the node and other nodes. **Figure 7** shows that "beta" (centrality: 0.39), "amyloid beta" (centrality: 0.29), "hyperexcitability" (centrality: 0.29) and "disease" (centrality: 0.29) had a high degree of centrality during this period. A comprehensive analysis of centrality showed that "beta" ($n = 7$, centrality: 0.39), "disease" ($n = 3$, centrality: 0.29), "dementia" ($n = 21$, centrality: 0.25) and "brain" ($n = 4$, centrality: 0.25) are the most influential keywords in this field.

TABLE 3 Journals contributed ≥ 2 papers in the top 100 most-cited papers.

| Journal | JCR category | Frequency | JCR partition | IF (2020) | IF (5 year) | Citations WOS Mean \pm SD | Citations in 2021 Mean \pm SD | Citations per year Mean \pm SD |
|--|--|-----------|---------------|-----------|-------------|-----------------------------|---------------------------------|----------------------------------|
| JOURNAL OF ALZHEIMER'S DISEASE | Neurosciences | 8 | Q2 | 4.472 | 4.851 | 40.50 \pm 14.21 | 9.5 \pm 6.66 | 5.65 \pm 2.74 |
| EPILEPSIA | Clinical Neurology | 6 | Q1 | 5.886 | 7.1211 | 130 \pm 136.84 | 12.5 \pm 13.26 | 9.51 \pm 7.82 |
| EPILEPSY AND BEHAVIOR | Behavioral Sciences; Clinical Neurology; Psychiatry | 4 | Q2, Q3, Q3 | 2.937 | 3.224 | 67 \pm 36.63 | 10 \pm 8.98 | 6.0 \pm 2.76 |
| EPILEPSY RESEARCH | Clinical Neurology | 4 | Q3 | 3.045 | 3.143 | 37.75 \pm 19.17 | 5.5 \pm 5.32 | 3.88 \pm 1.50 |
| NEUROBIOLOGY OF AGING | Geriatrics and Gerontology; Neurosciences | 4 | Q2, Q2 | 4.673 | 5.164 | 37.75 \pm 12.12 | 8 \pm 5.48 | 6.28 \pm 2.48 |
| ALZHEIMER DISEASE AND ASSOCIATED DISORDERS | Clinical Neurology; Pathology | 3 | Q3, Q3 | 2.703 | 3.007 | 33 \pm 22.61 | 6 \pm 4.58 | 3.73 \pm 4.07 |
| ARCHIVES OF NEUROLOGY | Clinical Neurology | 3 | Q1 | 7.419 | 7.249 | 234 \pm 180.16 | 23.67 \pm 14.19 | 17.27 \pm 12.25 |
| BRAIN | Clinical Neurology; Neurosciences | 3 | Q1, Q1 | 13.501 | 14.25 | 81.33 \pm 48.56 | 24.67 \pm 8.51 | 15.17 \pm 5.08 |
| EUROPEAN JOURNAL OF NEUROLOGY | Clinical Neurology; Neurosciences | 3 | Q1, Q1 | 6.089 | 5.308 | 32.33 \pm 22.23 | 5.67 \pm 4.04 | 3.27 \pm 1.93 |
| JOURNAL OF NEUROSCIENCE | Neurosciences | 3 | Q1 | 6.167 | 6.993 | 248.33 \pm 137.45 | 37 \pm 14.93 | 20.98 \pm 7.23 |
| NEUROLOGY | Clinical Neurology | 3 | Q1 | 9.91 | 10.664 | 37.33 \pm 12.12 | 8.33 \pm 8.02 | 5.87 \pm 3.86 |
| PLOS ONE | Multidisciplinary Sciences | 3 | Q3 | 3.24 | 3.788 | 31 \pm 13.86 | 5.33 \pm 5.03 | 3.44 \pm 1.50 |
| EPILEPSY CURRENTS | Clinical Neurology | 2 | Q1 | 7.5 | 8.772 | 48.50 \pm 31.82 | 6.50 \pm 6.36 | 4.41 \pm 2.89 |
| EPILEPTIC DISORDERS | Clinical Neurology | 2 | Q4 | 1.819 | 2.352 | 40.50 \pm 0.71 | 6.50 \pm 0.71 | 4.43 \pm 1.81 |
| JOURNAL OF NEUROCHEMISTRY | Biochemistry and Molecular Biology; Neurosciences | 2 | Q2, Q1 | 5.372 | 5.69 | 80.50 \pm 34.65 | 7 \pm 2.83 | 5.89 \pm 0.41 |
| JOURNAL OF THE NEUROLOGICAL SCIENCES | Clinical Neurology; Neurosciences | 2 | Q3, Q3 | 3.181 | 3.403 | 20 \pm 2.83 | 2 \pm 2.83 | 1.14 \pm 0.34 |
| NATURE MEDICINE | Biochemistry and Molecular Biology; Cell Biology; Research and Experimental Medicine | 2 | Q1, Q1, Q1 | 53.44 | 49.248 | 107.00 \pm 91.92 | 35.50 \pm 26.16 | 17.84 \pm 15.32 |
| SEIZURE-EUROPEAN JOURNAL OF EPILEPSY | Clinical Neurology; Neurosciences | 2 | Q3, Q3 | 3.184 | 3.729 | 26.50 \pm 16.26 | 2.50 \pm 0.71 | 2.96 \pm 0.06 |

Discussion

The aim of this paper was to perform a bibliometric study of the top 100 most-cited publications on AD and epilepsy over the last 22 years. To the best of our knowledge, this was the first study to provide an overview the current main status of development, hot spots of study, and the future

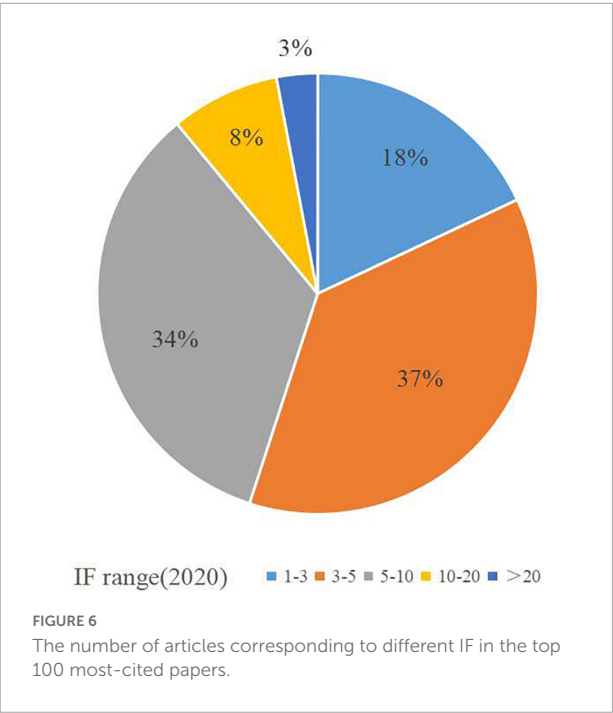
trends in AD and epilepsy. Our study is of great significance for students, researchers, and clinicians working in the field. Here, we summarize several characteristics of these papers to help understand the history and professional prospects comprehensively.

The average number of citations for the 100 most-cited clinical trials in AD and epilepsy was 67.43 (range: 15–433), well

TABLE 4 The number of study fields on the basis of WOS categories.

| WoS Categories | Frequency |
|------------------------------------|-----------|
| Clinical Neurology | 54 |
| Neurosciences | 49 |
| Behavioral Sciences | 10 |
| Geriatrics and Gerontology | 8 |
| Multidisciplinary Sciences | 5 |
| Psychiatry | 5 |
| Pathology | 5 |
| Biochemistry and Molecular Biology | 5 |

below the number of citations observed in general neuroscience articles (3,087) (Yeung et al., 2017). However, citation counts are not a direct measure of scientific quality and importance. The number of citations can be regarded as a relatively reasonable index to evaluate the quality of papers, which varies in different sub disciplines and depends on the size of the scientific community. Citation count analysis might be related to journal IF, publication frequency, and publication year. In general, an article with 100 or more citations is considered a “classic” in the research field and might even be a seminal paper (Xiong et al., 2021). However, our study showed that only 17 papers were cited more than 100 times, this can possibly come from the fact that comorbid epilepsy in AD may not be an interesting topic for



many clinicians. In fact, cognitivists dealing with AD patients are not highly aware of epilepsy and, inversely, epileptologists may be poorly informed of dementing diseases. Therefore, the

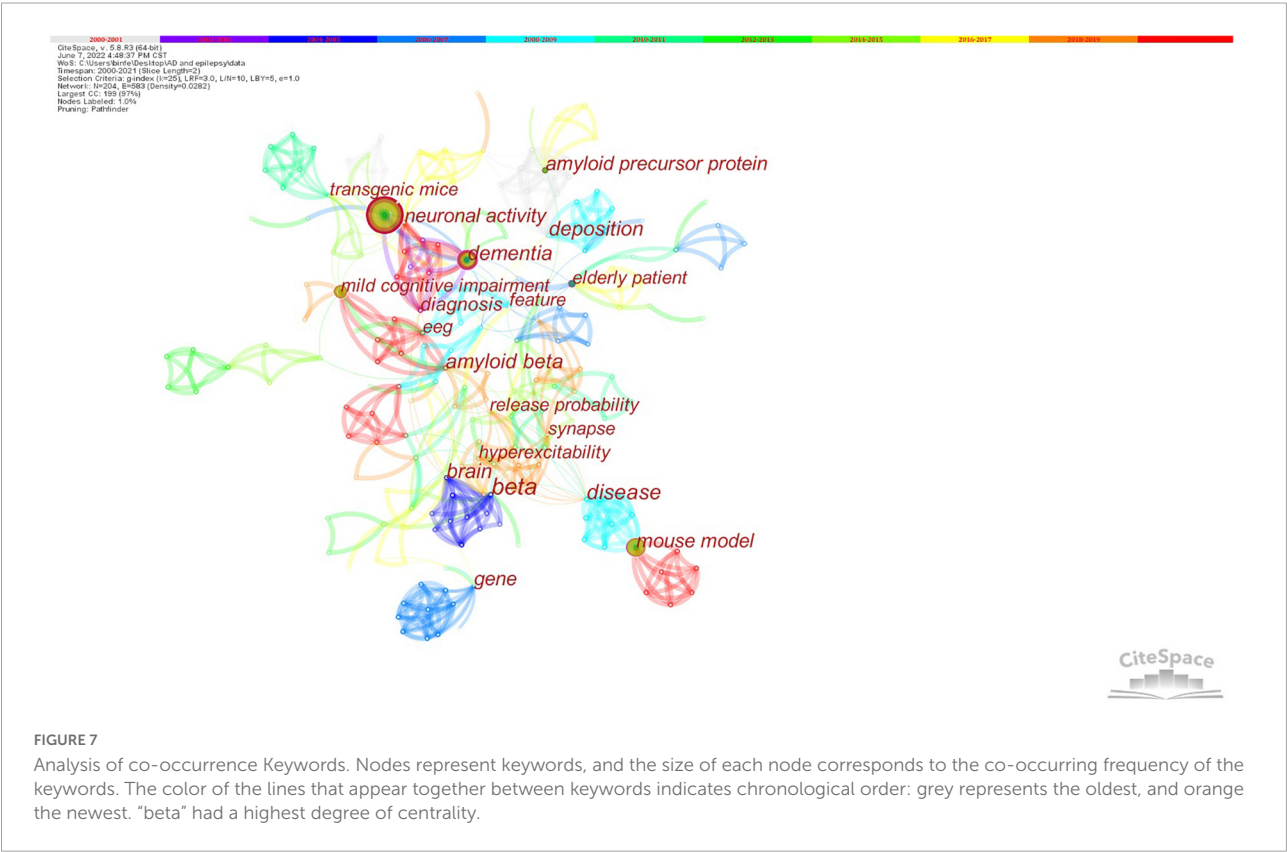


TABLE 5 Major contributing authors in the top 100 most-cited list.

| Author | Frequency | Total citations WOS | Total citation in 2021 | First author | Correspond author | Co-author | Constitution | Country |
|----------------------|-----------|---------------------|------------------------|--------------|-------------------|-----------|--|----------------|
| Tanila, Heikki | 5 | 629 | 92 | 0 | 2 | 4 | Kuopio University Hospital | Finland |
| Noebels, Jeffrey | 5 | 592 | 110 | 1 | 2 | 3 | Baylor Coll Medicine | United States |
| Pitkänen, Asla | 5 | 578 | 84 | 0 | 2 | 3 | Kuopio University Hospital | Finland |
| Scharfman, Helen E. | 5 | 234 | 33 | 1 | 2 | 3 | New York University Langone Medical Center | United States |
| Vossel, Keith A. | 4 | 830 | 185 | 3 | 4 | 0 | University of California | United States |
| Beagle, Alexander J. | 3 | 617 | 121 | 1 | 0 | 2 | University of California | United States |
| Miller, Bruce L. | 3 | 701 | 163 | 0 | 0 | 3 | University of California | United States |
| Mucke, Lennart | 3 | 991 | 138 | 0 | 0 | 3 | University of California | United States |
| Scarmeas, Nikolaos | 3 | 393 | 55 | 1 | 2 | 1 | University of California | United States |
| Szűcs, Anna | 3 | 128 | 31 | 0 | 0 | 3 | Semmelweis University | Hungary |
| Barcs, Gábor | 3 | 128 | 31 | 0 | 0 | 3 | Semmelweis University | Hungary |
| Horváth, András | 3 | 128 | 31 | 3 | 3 | 0 | Semmelweis University | Hungary |
| Kamondi, Anita | 3 | 128 | 31 | 0 | 0 | 3 | Semmelweis University | Hungary |
| Blanc, Frédéric | 3 | 120 | 22 | 0 | 0 | 3 | University of Strasbourg | France |
| Cretin, Benjamin | 3 | 94 | 18 | 3 | 3 | 0 | University of Strasbourg | France |
| Sellal, Francois | 3 | 120 | 22 | 0 | 0 | 3 | University of Strasbourg | France |
| Gurevicius, Kestutis | 3 | 172 | 22 | 1 | 1 | 2 | Kuopio University Hospital | Finland |
| Ziyatdinova, Sofya | 3 | 146 | 21 | 2 | 1 | 1 | University of Eastern Finland | Finland |
| Larner, A. J. | 3 | 214 | 15 | 2 | 3 | 0 | Walton Centre for Neurology and Neurosurgery | United Kingdom |

AD-epilepsy topic may have interest only for a small research community, which can result in a relatively low citation index.

The most-cited publication was “Epilepsy and Cognitive Impairments in Alzheimer’s Disease” (Palop and Mucke, 2009),

wrote by Palop and Mucke (2009), with 433 total citations, 31 annual citations, and 39 citations in 2021. It may be relevant to current research and have far-reaching implications. However, in general, consensus and position papers, guides,

TABLE 6 Frequency of co-occurring keywords.

| Keyword | Frequency | Centrality |
|---------------------------|-----------|------------|
| Epilepsy | 41 | 0.13 |
| Dementia | 21 | 0.25 |
| Mouse model | 21 | 0.11 |
| Mild cognitive impairment | 13 | 0.14 |
| Alzheimer's disease | 11 | 0.17 |
| Amyloid precursor protein | 10 | 0.13 |
| Diagnosis | 8 | 0.23 |
| Elderly patient | 8 | 0.2 |
| Neuronal activity | 7 | 0.23 |
| Beta | 7 | 0.39 |
| EEG | 6 | 0.09 |
| Transgenic mice | 6 | 0.12 |
| Amyloid beta | 6 | 0.29 |

and systematic reviews receive more citations than original articles, which is a bias that must be considered in citation analysis. The article that ranked second, which was based on a “Amyloid beta-Induced Neuronal Hyperexcitability Triggers Progressive Epilepsy” (Minkeviciene et al., 2009) had a total of 405 citations, 28.93 annual citations and 54 citations in 2021; it was published in *Journal of Neuroscience* in 2009 and written by Minkeviciene et al. (2009). The team performed video-EEG recordings in mice carrying mutant human APP^{swe} and PS1^{dE9} genes (APdE9 mice) and their wild-type littermates, identifying fibrillar Aβ may be the cause of epileptiform activity.

The number of papers published has increased in recent years. Although the most cited publications tend to be from the first few years (2000–2010), the number of highly cited articles published from 2011–2020 is nearly three times that published from 2000–2010. In 2016, the number of publications was the largest, reaching 11, which showed that a recently published article is likely to gradually improve the quality of research in recent years and have a potential academic importance in the future.

The majority of research originated from the United States (38%). A bibliometric analysis of the most cited articles in neurocritical care research showed that United States was the country with most articles (60, 35 primary research) and citations (6115) among the top 100 (Ramos et al., 2019). Baylor College of Medicine from United States topped the list with eight papers. The distribution of country and institutions was very scattered. The United States and its institutions have played a leading role in AD and epilepsy research. The United States was also ranked first in other fields of neurology (Xiong et al., 2021), and it is also a research leader in terms of quality and quantity. However, compared with other studies, our study showed that the cooperation between countries and institutions was not close

(Yin et al., 2019). In fact, just like the study of Parkinson's disease (Li et al., 2008), more cooperation between different countries and institutions might be an effective way to promote the development of AD and epilepsy research worldwide. Contrastingly, distribution analysis showed that research was widespread all over the world and the diseases had research value.

Baylor College of Medicine and Columbia University played important roles in the field of AD and epilepsy research. Baylor College of Medicine, as one of the top colleges and universities in Texas, United States, focused on cooperative research programs, discovered basic insights into human health and diseases through extensive interdisciplinary and interdisciplinary cooperation, and applied their findings to develop new diagnostic tools and treatments. Columbia University is a world-class private research university located in Manhattan, NY, United States. It carried out extensive research in the field of neuroscience.

The 100 included articles were published in 59 journals, among which 18 journals published more than one study. The papers were distributed in four partitions of JCR. The IF of the top five journals was less than six. The top journal among the list of the 100 most-cited studies was *Journal of Alzheimer's Disease* (IF = 4.472). The leading WOS categories focused on “Clinical Neurology” and “Neurosciences,” with few interdisciplinary studies. Resulting from its interdisciplinary nature, Psycho-Oncology has been subject to extensive interdisciplinary research, which has provided great help for the development of the discipline (Fox et al., 2021). Therefore, we look forward to more interdisciplinary research.

Author analysis revealed a network of core author collaborations in the field of AD and epilepsy research. This information might be relevant to clinical researchers and research institutions who are searching for a network of research leaders in the field to explore potential collaborations. Our authorship analysis does not show as many authors as other areas in research. The most contributing author was Tanila, Heikki from Kuopio University Hospital from Finland. Related research focuses on the pathogenesis of epilepsy in mouse models of AD, which is a research hotspot in this field.

Keyword analysis showed that “beta,” “amyloid beta,” “hyperexcitability,” “disease,” “dementia,” and “brain” had high influential, indicating that these research directions are very significant. This result showed that researchers have begun to extend their research to the pathogenesis. These results also show that AD and epilepsy is still a disease that requires to be solved urgently. We must explore the deficiencies and innovations in this field, such as treatment, pathological mechanism, and disease management on improve the quality of life of patients.

Limitations

The present study has some limitations. First, there are several intrinsic limitations of using citation analysis to evaluate the academic importance of a specific article, author, or journal. There is a certain bias in citation analysis, such as the fact that papers written in English, papers that can be accessed through open access, and papers published in journals with high IFs are more likely to be cited. In addition, through a “snowball effect,” people tended to cite publications that are already highly cited (Yeung et al., 2017). We selected the top 100 papers, but citation searches are “time-dependent,” older articles are likely to be cited more often, and the newest list of highly cited articles may be dominated by some older articles. Furthermore, citation analysis might severely underestimate the impact of clinical research as compared to basic research (van Eck et al., 2013). Second, the search was limited to the WOS database. It did not record citations by textbooks and other databases. Our study only selected papers written in English, which might have yielded an incomplete search.

Conclusion

We identified the 100 most cited papers in the field of AD and epilepsy. By reviewing these top cited papers, researchers can immediately understand the hot topics and research collaborations on AD and epilepsy, and improve their work. This study shows that the relationship, mechanism, and treatment of AD and epilepsy have been widely studied, and in recent years, this field has shown new vitality; however, there is a general lack of cooperation between countries, and the mechanism of epilepsy and AD is unclear, which deserves further study.

References

- Beghi, E. (2020). The Epidemiology of Epilepsy. *Neuroepidemiology* 54, 185–191. doi: 10.1159/000503831
- Cretin, B. (2021). Treatment of Seizures in Older Patients with Dementia. *Drugs Aging* 38, 181–192. doi: 10.1007/s40266-020-00826-2
- Fox, S., Lynch, J., D’Alton, P., and Carr, A. (2021). Psycho-Oncology: a Bibliometric Review of the 100 Most-Cited Articles. *Healthcare* 9:1008. doi: 10.3390/healthcare9081008
- Guo, Y., Xu, Z. Y. R., Cai, M. T., Gong, W. X., and Shen, C. H. (2021). Epilepsy With Suicide: a Bibliometrics Study and Visualization Analysis via CiteSpace. *Front. Neurol.* 12:823474. doi: 10.3389/fneur.2021.823474
- Lehmann, L., Lo, A., Knox, K. M., and Barker-Haliski, M. (2021). Alzheimer’s Disease and Epilepsy: a Perspective on the Opportunities for Overlapping Therapeutic Innovation. *Neurochem. Res.* 46, 1895–1912. doi: 10.1007/s11064-021-03332-y
- Li, T., Ho, Y. S., and Li, C. Y. (2008). Bibliometric analysis on global Parkinson’s disease research trends during 1991–2006. *Neurosci. Lett.* 441, 248–252. doi: 10.1016/j.neulet.2008.06.044
- Liu, J., and Wang, L. N. (2021). Treatment of epilepsy for people with Alzheimer’s disease. *Cochrane Database Syst. Rev.* 12:CD011922. doi: 10.1002/14651858.CD011922.pub4
- McVeigh, M. E. (2008). Neurology in the journal citation reports. *Neurology* 71, 1848–1849. doi: 10.1212/01.wnl.0000338902.81462.88
- Minkeviciene, R., Rheims, S., Dobszay, M. B., Zilberter, M., Hartikainen, J., and Fülöp, L. (2009). Amyloid beta-induced neuronal hyperexcitability triggers

Data availability statement

The datasets presented in this study can be found in online repositories. The names of the repository/repositories and accession number(s) can be found in the article/supplementary material.

Author contributions

G-FZ and YG designed the study. G-FZ drafted and edited the manuscript. G-FZ and W-XG analyzed the data. G-FZ, Z-Y-RX, YG, and W-XG revised the manuscript. All authors contributed to the article and approved the submitted version.

Funding

This study was supported by the National Natural Science Foundation of China (Grant No. 81871010).

Conflict of interest

The authors declare that the research was conducted in the absence of any commercial or financial relationships that could be construed as a potential conflict of interest.

Publisher’s note

All claims expressed in this article are solely those of the authors and do not necessarily represent those of their affiliated organizations, or those of the publisher, the editors and the reviewers. Any product that may be evaluated in this article, or claim that may be made by its manufacturer, is not guaranteed or endorsed by the publisher.

progressive epilepsy. *J. Neurosci.* 29, 3453–3462. doi: 10.1523/JNEUROSCI.5215-08.2009

Niu, H., Álvarez-Álvarez, I., Guillén-Grima, F., and Aguinaga-Ontoso, I. (2017). Prevalence and incidence of Alzheimer's disease in Europe: a meta-analysis. *Neurologia* 32, 523–532. doi: 10.1016/j.nrl.2016.02.016

Palop, J. J., and Mucke, L. (2009). Epilepsy and Cognitive Impairments in Alzheimer Disease. *Arch. Neurol.* 66, 435–440. doi: 10.1001/archneurol.2009.15

Ramos, M. B., Koterba, E., Rosi Júnior, J., Teixeira, M. J., and Figueiredo, E. G. A. (2019). Bibliometric Analysis of the Most Cited Articles in Neurocritical Care Research. *Neurocrit. Care* 31, 365–372. doi: 10.1007/s12028-019-00731-6

Samson, W. N., van Duijn, C. M., Hop, W. C., and Hofman, A. (1996). Clinical features and mortality in patients with early-onset Alzheimer's disease. *Eur. Neurol.* 36, 103–106. doi: 10.1159/000117218

Sen, A., Capelli, V., and Husain, M. (2018). Cognition and dementia in older patients with epilepsy. *Brain* 141, 1592–1608. doi: 10.1093/brain/awy022

Struble, R. G., Ala, T., Patrylo, P. R., Brewer, G. J., and Yan, X. X. (2010). Is brain amyloid production a cause or a result of dementia of the Alzheimer's type? *J. Alzheimers Dis.* 22, 393–399. doi: 10.3233/JAD-2010-100846

van Eck, N. J., Waltman, L., van Raan, A. F., Klautz, R. J., and Peul, W. C. (2013). Citation analysis may severely underestimate the impact of clinical research as compared to basic research. *PLoS One*. 8:e62395. doi: 10.1371/journal.pone.0062395

Wu, M. Q., Wu, D. Q., Hu, C. P., and Iao, L. S. (2021). Studies on Children With Developmental Coordination Disorder in the Past 20 Years: a Bibliometric Analysis via CiteSpace. *Front Psychiatry* 12:776883. doi: 10.3389/fpsy.2021.776883

Xiong, H. Y., Liu, H., and Wang, X. Q. (2021). Top 100 Most-Cited Papers in Neuropathic Pain From 2000 to 2020: a Bibliometric Study. *Front. Neurol.* 12:765193. doi: 10.3389/fneur.2021.765193

Yeung, A. W. K., Goto, T. K., and Leung, W. K. (2017). At the Leading Front of Neuroscience: a Bibliometric Study of the 100 Most-Cited Articles. *Front. Hum. Neurosci.* 11:363. doi: 10.3389/fnhum.2017.00363

Yin, X., Cheng, F., Wang, X., Mu, J., Ma, C., Zhai, C., et al. (2019). Top 100 cited articles on rheumatoid arthritis: a bibliometric analysis. *Medicine* 98:e14523. doi: 10.1097/md.00000000000014523



OPEN ACCESS

EDITED BY

Agustin Ibanez,
Latin American Brain Health Institute
(BrainLat), Chile

REVIEWED BY

Gefei Chen,
Karolinska Institutet (KI), Sweden
Ian James Martins,
University of Western Australia,
Australia

*CORRESPONDENCE

Kyunga Kim
kyunga.j.kim@samsung.com
Sang Won Seo
sw72.seo@samsung.com

†These authors have contributed
equally to this work

SPECIALTY SECTION

This article was submitted to
Alzheimer's Disease and Related
Dementias,
a section of the journal
Frontiers in Aging Neuroscience

RECEIVED 20 April 2022

ACCEPTED 04 July 2022

PUBLISHED 22 July 2022

CITATION

Kang SH, Kim JH, Chang Y, Cheon BK,
Choe YS, Jang H, Kim HJ, Koh S-B,
Na DL, Kim K and Seo SW (2022)
Independent effect of body mass index
variation on amyloid- β positivity.
Front. Aging Neurosci. 14:924550.
doi: 10.3389/fnagi.2022.924550

COPYRIGHT

© 2022 Kang, Kim, Chang, Cheon,
Choe, Jang, Kim, Koh, Na, Kim and
Seo. This is an open-access article
distributed under the terms of the
[Creative Commons Attribution License](#)
(CC BY). The use, distribution or
reproduction in other forums is
permitted, provided the original
author(s) and the copyright owner(s)
are credited and that the original
publication in this journal is cited, in
accordance with accepted academic
practice. No use, distribution or
reproduction is permitted which does
not comply with these terms.

Independent effect of body mass index variation on amyloid- β positivity

Sung Hoon Kang^{1,2,3†}, Jong Hyuk Kim^{4†}, Yoosoo Chang⁵,
Bo Kyoung Cheon^{1,2,4}, Yeong Sim Choe^{1,2,6}, Hyemin Jang^{1,2},
Hee Jin Kim^{1,2}, Seong-Beom Koh³, Duk L. Na^{1,2},
Kyunga Kim^{4,7,8*} and Sang Won Seo^{1,2,6,9,10*}

¹Department of Neurology, Samsung Medical Center, School of Medicine, Sungkyunkwan University, Seoul, South Korea, ²Neuroscience Center, Samsung Medical Center, Seoul, South Korea, ³Department of Neurology, Korea University Guro Hospital, Korea University College of Medicine, Seoul, South Korea, ⁴Department of Digital Health, SAHST, Sungkyunkwan University, Seoul, South Korea, ⁵Center for Cohort Studies, Total Healthcare Center, Kangbuk Samsung Hospital, School of Medicine, Sungkyunkwan University, Seoul, South Korea, ⁶Department of Health Sciences & Technology, SAHST, Sungkyunkwan University, Seoul, South Korea, ⁷Biomedical Statistics Center, Research Institute for Future Medicine, Samsung Medical Center, Seoul, South Korea, ⁸Department of Data Convergence and Future Medicine, School of Medicine, Sungkyunkwan University, Seoul, South Korea, ⁹Samsung Alzheimer Research Center, Center for Clinical Epidemiology Medical Center, Seoul, South Korea, ¹⁰Department of Intelligent Precision Healthcare Convergence, SAHST, Sungkyunkwan University, Seoul, South Korea

Objectives: The relationship of body mass index (BMI) changes and variability with amyloid- β (A β) deposition remained unclear, although there were growing evidence that BMI is associated with the risk of developing cognitive impairment or AD dementia. To determine whether BMI changes and BMI variability affected A β positivity, we investigated the association of BMI changes and BMI variability with A β positivity, as assessed by PET in a non-demented population.

Methods: We retrospectively recruited 1,035 non-demented participants ≥ 50 years of age who underwent A β PET and had at least three BMI measurements in the memory clinic at Samsung Medical Center. To investigate the association between BMI change and variability with A β deposition, we performed multivariable logistic regression. Further distinctive underlying features of BMI subgroups were examined by employing a cluster analysis model.

Results: Decreased (odds ratio [OR] = 1.68, 95% confidence interval [CI] 1.16–2.42) or increased BMI (OR = 1.60, 95% CI 1.11–2.32) was associated with a greater risk of A β positivity after controlling for age, sex, APOE e4 genotype, years of education, hypertension, diabetes, baseline BMI, and BMI variability. A greater BMI variability (OR = 1.73, 95% CI 1.07–2.80) was associated with a greater risk of A β positivity after controlling for age, sex, APOE e4 genotype, years of education, hypertension, diabetes, baseline BMI, and BMI change. We also identified BMI subgroups showing a greater risk of A β positivity.

Conclusion: Our findings suggest that participants with BMI change, especially those with greater BMI variability, are more vulnerable to A β deposition regardless of baseline BMI. Furthermore, our results may contribute to the design of strategies to prevent A β deposition with respect to weight control.

KEYWORDS

amyloid- β (A β), body mass index (BMI), BMI change, BMI variability, Alzheimer's disease

Introduction

A large amount of evidence suggests that body mass index (BMI) is associated with the risk of developing cognitive impairment. Specifically, mid-life obesity increases the risk of cognitive impairment (Kivipelto et al., 2005; Fitzpatrick et al., 2009; Tolppanen et al., 2014). Previous studies have also shown that being underweight in later life may be associated with an increased risk of dementia (Tolppanen et al., 2014; Bell et al., 2017), and the acceleration of cortical atrophy (Kim H. et al., 2015; Kim et al., 2019). Furthermore, larger BMI changes were also associated with a higher risk of conversion to dementia in patients with mild cognitive impairment (MCI), (Ye et al., 2016) and these changes had deleterious effects on the cognitive function in the non-demented elderly (Giudici et al., 2019).

Amyloid- β (A β) deposition in the brain is an important pathological hallmark of Alzheimer's disease (AD), which is the most common cause of dementia. According to the A β cascade hypothesis, A β deposition in the brain occurs at a very early stage. In fact, A β deposition in the brain precedes the development of AD dementia by 10–20 years. Furthermore, non-demented participants with A β deposition were more converted to dementia than those without A β deposition (Villemagne et al., 2011; Rowe et al., 2013; Ye et al., 2018). Therefore, A β positivity is a crucial predictor of AD prognosis in non-demented individuals.

Recently, being underweight or obese in mid-life was found to be associated with an increased risk of A β deposition (Gottesman et al., 2017; Lee et al., 2020; Möllers et al., 2021), and individuals who are underweight in later life were also at an increased risk of A β deposition (Vidoni et al., 2011; Ewers et al., 2012; Hsu et al., 2016; Thirunavu et al., 2019). However, since previous studies investigated the association of BMI with A β deposition at a single time point, these studies could not evaluate the effects of BMI variability on A β deposition. Considering that BMI changes and variability is closely associated with a new onset of diabetes, cardiovascular disease, atrial fibrillation, and higher mortality (Bangalore et al., 2017; Lim et al., 2019; Sponholtz et al., 2019), it is reasonable to expect that BMI changes and

variability may be important risk factors for A β deposition. Therefore, by studying the association of BMI changes and variability with A β deposition, it could be identified whether BMI changes and variability is specifically related to AD, especially in the early stage of AD pathobiology. Furthermore, this study may provide the importance of rigorous strategies for weight maintenance to prevent A β deposition in non-demented individuals.

Thus, the goal of our study was to investigate the influence of BMI changes and BMI variability on A β positivity in a non-demented population. Furthermore, to determine the complex relationships among BMI changes, BMI variability, and A β positivity, we evaluated the distinguishable BMI subgroups classified by the cluster analysis model. We hypothesized that decreased BMI and greater BMI variability would have deleterious effects on A β deposition.

Materials and methods

Participants

Our study was designed as a retrospective cohort study. We recruited 1,546 non-demented participants ≥ 50 years of age [611 with normal cognition and 935 with mild cognitive impairment (MCI)] from the memory clinic in the Department of Neurology at Samsung Medical Center (SMC) in Seoul, Korea. The participants had undergone A β PET between August 2015 and August 2020. All participants underwent a comprehensive dementia work-up including the standardized cognitive assessment battery (Kang et al., 2019), APOE genotyping, and brain MRI. We excluded participants who had any of the following conditions: severe white matter hyperintensities based on the Fazekas scale; structural lesions such as brain tumor, large territorial infarct, and intracranial hemorrhage; other causes of neurodegenerative diseases including Lewy body dementia, Parkinson's disease, cortico-basal syndrome, progressive supranuclear palsy, and frontotemporal dementia.

All participants with normal cognition fulfilled the following conditions: (1) no medical history that is likely to affect cognitive function based on Christensen's criteria (Christensen et al., 1991); (2) no objective cognitive impairment from a comprehensive neuropsychological test battery on any cognitive domain (at least -1.0 SD above age-adjusted norms on any cognitive tests); and (3) independence in activities of daily living. All participants with MCI fulfilled Petersen's criteria with the following modifications (Petersen, 2011; Jeong et al., 2020): (1) subjective cognitive complaints by the participants or caregiver; (2) objective memory impairment below -1.0 SD on verbal or visual memory tests; (3) no significant impairment in activities of daily living; (4) non-demented.

The institutional review board of the SMC approved this study. Written informed consent was obtained from all participants.

Amyloid- β PET acquisition

All participants underwent A β PET (^{18}F -florbetaben [FBB] PET and ^{18}F -flutemetamol [FMM] PET) scans at SMC using a Discovery STe PET/CT scanner (GE Medical Systems, Milwaukee, WI, United States). For FBB or FMM PET, a 20-min emission PET scan in dynamic mode (consisting of 4 min \times 5 min frames) was performed 90 min after an injection of a mean dose of 311.5 MBq FBB and 197.7 MBq FMM, respectively. Three-dimensional PET images were reconstructed in a 128 \times 128 \times 48 matrix with a 2 mm \times 2 mm \times 3.27 mm voxel size using the ordered-subsets expectation maximization algorithm (FBB, iteration = 4 and subset = 20; FMM, iteration = 4 and subset = 20).

Amyloid- β PET assessment

A β positivity on PET scans was determined using visual reads in the primary analyses. Specifically, A β PET images were rated by two experienced doctors (one nuclear medicine physician and one neurologist) who were blinded to the clinical information, and the images were dichotomized as either A β -positive (A β +) or A β -negative (A β -) using visual reads. They discussed any discordant results regarding A β positivity to achieve consensus. The FBB PET scan was regarded as positive if the A β plaque load was visually rated as 2 or 3 on the brain amyloid plaque load scoring system, and the FMM PET scan was considered positive if one of five brain regions (frontal, parietal, posterior cingulate and precuneus, striatum, and lateral temporal lobes) systematically reviewed using FMM PET was positive in either hemisphere (Kang et al., 2021). Representative PET images in participants with A β + and A β - were shown in **Supplementary Figure 1**. Inter-rater agreement of PET interpretation was excellent for A β positivity at the subject level (kappa score = 0.84). In addition, visual rating was highly concordant with a standardized uptake value ratio (SUVR)

cutoff categorization for A β positivity (93.5% for FBB and 91.6% for FMM).

Amyloid- β PET quantification using Centiloid values

For the sensitivity analyses, A β positivity on PET scans was determined using Centiloid (CL) cutoff-based categorization. We used a CL method previously developed by our group (Cho et al., 2020) to standardize the quantification of A β PET images obtained using different ligands. The CL method for FBB and FMM PET enables the transformation of the SUVR of FBB and FMM PET to CL values directly without conversion to the ^{11}C -labeled Pittsburgh compound SUVR.

There are three steps to obtain CL values (Cho et al., 2020): (1) preprocessing of PET images, (2) determination of CL global cortical target volume of interest (CTX VOI), and (3) conversion of SUVR to CL values. First, to preprocess the A β PET images, PET images were co-registered to each participant's MR image and then normalized to a T1-weighted MNI-152 template using the SPM8 unified segmentation method (Klunk et al., 2015). We used T1-weighted MRI correction with the N3 algorithm only for intensity non-uniformities (Sled et al., 1998), without applying corrections to the PET images for brain atrophy or partial volume effects. Second, we used the FBB-FMM CTX VOI defined as areas of AD-specific brain A β deposition in our previous study (Cho et al., 2020). Briefly, to exclude areas of aging-related brain A β deposition, the FBB-FMM CTX VOI was generated by comparing SUVR parametric images (with the whole cerebellum as a reference area) between 20 typical patients with AD-related cognitive impairment (AD-CTX) and 16 healthy elderly participants (EH-CTX) who underwent both FBB and FMM PET scans. To generate the FBB-FMM CTX VOI, the average EH-CTX image was subtracted from the average AD-CTX image. We then defined the FBB-FMM CTX VOI as areas of AD-related brain A β accumulation common to both FBB and FMM PET. Finally, the SUVR values of the FBB-FMM CTX VOI were converted to CL units using the CL conversion equation. The CL equation was derived from the FBB-FMM CTX VOI separately for FBB and FMM PET and applied to FBB and FMM SUVR.

To determine the participants' CL cutoff-based A β positivity, we applied the optimal cutoff value derived using a k-means cluster analysis in 527 independent samples of participants with normal cognition. The cutoff value was set at 27.08, representing the 95th percentile of the lower cluster (Villeneuve et al., 2015), and the whole cerebellum was used as a reference region (Kim et al., 2021).

Body mass index acquisition

For each participant, BMI data were obtained by backtracking their weight and height records in clinical data warehouse of SMC, which were measured at all visits

within 3 years after inspecting A β PET until March 2000 (**Supplementary Figure 2**). We excluded 511 participants who did not have at least three BMI measurements. A total of 1,035 non-demented participants (409 with normal cognition and 626 with MCI) were included in the present study.

Body mass index assessment

Baseline BMIs was defined as the farthest past measurement from the A β PET scan (**Supplementary Figure 3**). Participants were then categorized into three subgroups according to their baseline BMI values based on the World Health Organization's recommendations for Asian populations: underweight (BMI < 18.5 kg/m²), normal weight (18.5–24.9 kg/m²), obesity (BMI \geq 25 kg/m²) (WHO Expert Consultation, 2004).

Follow-up BMI was defined as the closest measurement to the A β PET scan (**Supplementary Figure 3**). We calculated BMI change as the change rate by taking the difference between baseline and follow-up BMIs and dividing it by duration. Using the 1st and 3rd quantiles (Q1 and Q3) of BMI changes, we characterized participants as increased (\geq Q3), stable, and decreased (\leq Q1).

$$BMI\ change = \frac{BMI_f - BMI_b}{Duration}$$

B_b : baseline BMI, B_f : follow-up BMI, Duration: period between B_b and B_f .

BMI values at three or more time points were used to obtain BMI variability (**Supplementary Figure 3**). Six measures of variability were considered: standard deviation (SD), coefficient of variation (CV), variability independent of the mean (VIM), residual standard deviation (RSD), average real variability (ARV), and successive variability (SV). These variability measures have different characteristics, and their formulae are shown in **Supplementary Table 1**. While SD was known to suffer from the bias due to the correlation with the mean value, CV and VIM were developed to avoid this bias. RSD was designed to take the time effect into account when assessing variability among longitudinal measurements. ARV and SV were calculated based on the differences between the consecutive measurements. BMI variability values were obtained based on each of six variability measures. While we used VIM-based variability for the primary association analysis, we considered all six measures to identify underlying patterns in longitudinal BMI values *via* the cluster analysis. In the association analysis, participants were classified into subgroups with non-high variability versus with high variability according to the upper 15-percentile of BMI variability values as a threshold.

Statistical analyses

We used independent *t*-tests and chi-square tests to compare the demographic and clinical characteristics of A β – and A β – groups. To investigate the association between BMI

change and variability with A β deposition, we performed multivariable logistic regression using BMI change and variability as predictors after controlling for age, sex, APOE e4 genotype, years of education, hypertension, diabetes, and baseline BMI. To further validate the association between BMI change and variability with A β deposition, we performed multivariable logistic regression using CL cutoff-based A β positivity as an outcome rather than visually rated A β positivity.

Further distinctive underlying patterns in longitudinal BMI values were recognized by employing clustering algorithms including Gaussian mixture model (GMM), k-means clustering, and self-organizing map (Bilmes, 1998; Yang et al., 2012). First, we examined the correlations among BMI features, such as baseline BMI, BMI change and six BMI variability measures, to select features that would play complementary roles in clustering (**Supplementary Figure 4**). Second, the similarity between participants was assessed *via* the Euclidean distance after each selected feature was scaled through standardization. Finally, we used GMM to identify clusters, each of which consisted of participants with similar BMI patterns, because it can be used when more fine-grained workload characterization and analysis are required (Patel and Kushwaha, 2020). The optimal number of clusters was determined by validating clustering results with clinical interpretability as well as the silhouette index, Akaike information criterion (AIC) and Bayesian information criterion (BIC) measures. The identified clusters were further validated by examining the consistency with clustering results from the other algorithms. To investigate the association between the identified clusters (called as BMI subgroups) and A β deposition, we used multivariable logistic regression after controlling for age, sex, APOE e4 genotype, years of education, hypertension, and diabetes.

All reported *p*-values were two-sided, and the significance level was set at 0.05. All analyses were performed using SPSS version 25.0 and R version 4.3.0 (Institute for Statistics and Mathematics, Vienna, Austria¹).

Data availability

Anonymized data for our analyses presented in the present report are available upon request from the corresponding authors.

Results

Clinical characteristics of participants

Among the 1,035 participants, 579 individuals were A β – and 456 were A β – (Table 1). Participants who were A β – were

¹ www.R-project.org

TABLE 1 Demographic and clinical characteristics of study participants.

| | A β (–) (<i>n</i> = 579) | A β (+) (<i>n</i> = 456) | <i>P</i> -value |
|---------------------------------|---------------------------------|---------------------------------|-----------------|
| Demographics | | | |
| Gender, females | 306 (52.8%) | 261 (57.2%) | 0.179 |
| Age, years | 68.5 \pm 8.6 | 70.5 \pm 7.4 | 0.001 |
| Education, years | 12.1 \pm 4.8 | 12.0 \pm 4.5 | 0.843 |
| Clinical characteristics | | | |
| APOE e4 carrier | 127 (21.9%) | 286 (62.7%) | <0.001 |
| Hypertension | 281 (48.5%) | 178 (39.0%) | 0.003 |
| Diabetes | 141 (24.4%) | 60 (13.2%) | <0.001 |
| Follow-up years | 6.1 \pm 4.8 | 4.8 \pm 4.2 | <0.001 |
| Baseline BMI | | | <0.001 |
| Normal | 334 (57.7%) | 317 (69.5%) | |
| Obese | 238 (41.1%) | 121 (26.5%) | |
| Underweight | 7 (1.2%) | 18 (3.9%) | |

A β , amyloid- β ; BMI, body mass index. Values are presented as mean \pm SD or *n* (%).

more likely to be older (age, 70.6 \pm 7.4 years) than those who were A β – (age, 68.5 \pm 8.6 years, *p* < 0.001). Participants who were A β – had a higher frequency of APOE e4 genotype (62.7% vs. 48.5%, *p* < 0.001) but a lower frequency of hypertension (39.0% vs. 48.5%, *p* = 0.003) and diabetes (13.2% vs. 24.4%, *p* < 0.001) than those who were A β –.

Association of amyloid- β positivity with body mass index change and variability

Decreased BMI (odds ratio [OR] = 1.68, 95% confidence interval [CI] 1.16–2.42) was associated with a greater risk of A β positivity after controlling for age, sex, APOE e4 genotype, years of education, hypertension, diabetes, baseline BMI, and BMI variability (Table 2). Increased BMI (OR = 1.60, 95% CI 1.11–2.32) was also associated with a greater risk of A β positivity (Table 2).

A greater BMI variability (OR = 1.73, 95% CI 1.07–2.80) was associated with a greater risk of A β positivity after controlling for age, sex, APOE e4 genotype, years of education, hypertension, diabetes, baseline BMI, and BMI change (Table 2).

Body mass index subgroups using Gaussian mixture model cluster analysis

Based on BMI baseline, change, and variability measures, four subgroups were created by GMM and validated with the Silhouette index, AIC and BIC (Supplementary Figure 5). The BMI characteristics for each subgroup were summarized in Supplementary Table 2. While the BMI baselines were

very similar across all subgroups, BMI change and variability measures were different between subgroups. Because the mean change and variability measures were relatively small in subgroup 1 compared to other subgroups, we characterized subgroup 1 as the stable subgroup. Likewise, subgroups 2, 3, and 4 were characterized, respectively, as the subgroup having stable change with some variability; the subgroup having slightly increased BMI with some variability; the subgroup having decreased BMI with more variability. Longitudinal BMI patterns of representative patients in each subgroup are shown in Figure 1.

Compared to the stable subgroup 1, the subgroups showing greater BMI variability had a greater risk of A β positivity, especially when BMI was decreasing: subgroup 2 (OR = 1.49, 95% CI 1.05–2.13), subgroup 3 (OR = 1.49, 95% CI 1.01–2.20), and subgroup 4 (OR = 2.39, 95% CI 1.37–4.16) (Table 3).

Association of Centiloid cutoff-based amyloid- β positivity with body mass index change and variability

For CL cutoff-based A β positivity, decreased BMI (OR = 1.56, 95% CI 1.06–2.29) was associated with a greater risk of A β positivity after controlling for age, sex, APOE e4 genotype, years of education, hypertension, diabetes, baseline BMI, and BMI variability (Table 2). Increased BMI (OR = 1.58, 95% CI 1.06–2.34) was also associated with a greater risk of A β positivity (Table 2). Higher BMI variability (OR = 2.12,

TABLE 2 Association of A β positivity with BMI change and variability.

| | OR (95% CI)* | <i>p</i> |
|---|------------------|----------|
| Visually rated Aβ positivity | | |
| BMI change | | |
| Stable | 1 (ref.) | |
| Decreased | 1.68 (1.16–2.42) | 0.006 |
| Increased | 1.60 (1.11–2.32) | 0.012 |
| BMI variability | | |
| Normal | 1 (ref.) | |
| High | 1.73 (1.07–2.80) | 0.025 |
| CL cutoff-based Aβ positivity | | |
| BMI change | | |
| Stable | 1 (ref.) | |
| Decreased | 1.56 (1.06–2.29) | 0.025 |
| Increased | 1.58 (1.06–2.34) | 0.024 |
| BMI variability | | |
| Normal | 1 (ref.) | |
| High | 2.12 (1.28–3.51) | 0.003 |

A β , amyloid- β ; BMI, body mass index; OR, odds ratio; CI, confidence; CL, Centiloid.

*Adjusted ORs for A β positivity were obtained by logistic regression analysis with BMI change and BMI variability together as predictors after controlling for age, sex, APOE e4 genotype, years of education, hypertension, diabetes, and baseline BMI.

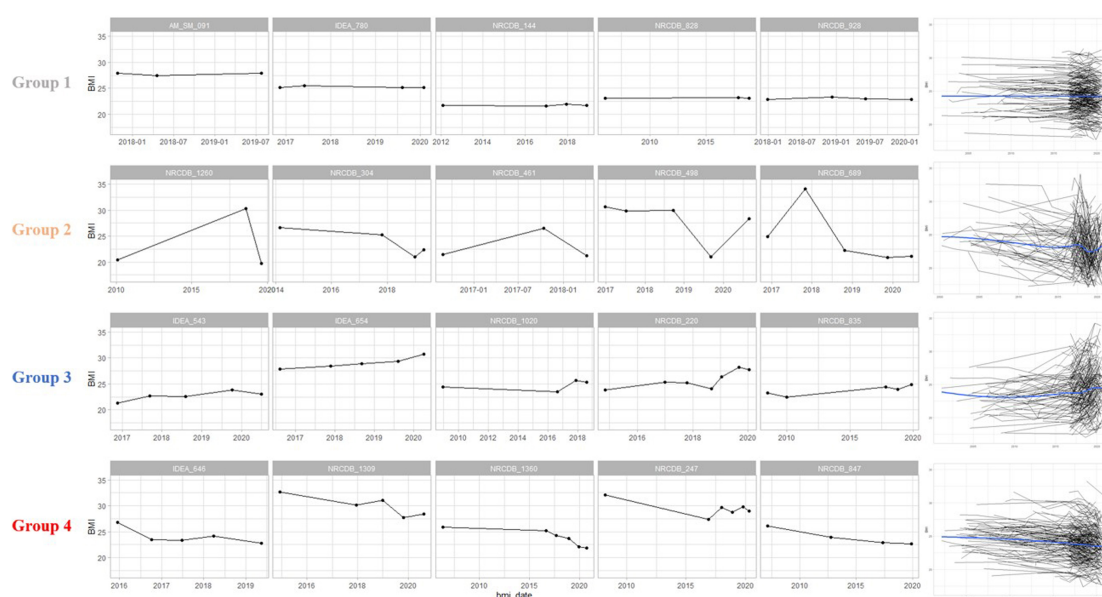


FIGURE 1

Body mass index (BMI) patterns of representative participants in each group. Group 1 had a constant pattern of both BMI change and variability. Group 2 showed a constant BMI change and some variability. Group 3 was a cluster with increasing BMI changes and high variability. Group 4 was a cluster with a decreasing BMI changes and high variability. The graphs on the right are spaghetti plots representing the BMI pattern of all patients in each group, and a blue line representing the trend of the group. BMI, body mass index.

95% CI 1.28–3.51) was associated with a greater risk of A β positivity after controlling for age, sex, APOE e4 genotype, years of education, hypertension, diabetes, baseline BMI, and BMI change (Table 2).

Discussion

We systematically investigated the association of A β positivity with BMI change and variability in a relatively large group of participants who did not have dementia. In the present study, we found that BMI change (increased or decreased) was associated with a greater risk of A β positivity, regardless of baseline BMI status. Furthermore, we noted that greater variability in BMI predicted a greater risk of A β positivity despite baseline BMI status and BMI change. Finally, our cluster analysis identified BMI subgroups with specific patterns of BMI change and variability, which eventually showed a greater risk of A β positivity. Taken together, our findings suggest that participants with BMI change, especially those with greater BMI variability, are more vulnerable to A β deposition regardless of baseline BMI. Furthermore, given the paucity of modifiable risk factors for the development of A β , our results may contribute to the design of strategies to prevent A β deposition with respect to weight control.

Our major finding was that BMI change (increased or decreased) was associated with a greater risk of A β positivity, regardless of baseline BMI status. Considering that A β

deposition is associated with the development of dementia, our findings are supported by previous epidemiologic studies (Ye et al., 2016; Giudici et al., 2019). Specifically, a previous study suggested that patients with MCI who had larger BMI changes are more likely to convert to probable AD dementia regardless of baseline BMI status (Ye et al., 2016). In another study, cognitively unimpaired individuals with decreased BMI were also reported to be at an increased risk of cognitive decline over a 5-year follow-up (Giudici et al., 2019). Furthermore, in agreement with our finding, recent study identified that decreased BMI or unstable BMI was associated with A β positivity in non-demented individuals (Buchman et al., 2021; Lane et al., 2021). Altogether, there is no exact pathobiology to explain these associations. However, as the elderly age, there is a loss of muscle mass and gain in visceral fat (Al-Sofiani et al., 2019). Therefore, it is reasonable to expect that participants with decreased BMI and increased BMI might reflect decreased muscle mass and increased visceral fat, respectively. In fact, some studies have investigated the relationship between the progression of sarcopenia and A β deposition (Maltais et al., 2019). A β deposition was found to be associated with sarcopenia, which might be mediated by an increased systemic inflammatory reaction (Yaffe et al., 2004; Maltais et al., 2019). Alternatively, decreased BMI might be an early reflective symptom of A β pathology (Grundman et al., 1996). In fact, a recent study revealed that the A β burden was associated with a prospective BMI decline in individuals with normal cognition (Rabin et al., 2020). On the other hand,

regarding increased BMI, increased visceral fat deposition might affect brain atrophy and A β deposition (Kim H. J. et al., 2015) through several potential mechanisms, including increased insulin resistance (Jack et al., 2013; Luchsinger et al., 2013), lower levels of adipose-derived hormones (Montague et al., 1998), and a larger pattern of proatherogenic gene expression (Yao et al., 2012). Further studies are needed to examine the independent effects of specific body composition on A β deposition.

Another major novel finding was that greater BMI variability was associated with a greater risk of A β positivity, regardless of baseline BMI status and BMI changes. For example, even if the BMI measured 5 years ago and the current BMI are at the same level, there is a higher possibility of A β deposition if there is a high variation in BMI within the 5 years. We reviewed the literature regarding between BMI and AD related outcome (Supplementary Table 3). To the best of our knowledge, the association between BMI variability and A β positivity has not been thoroughly investigated. These findings offer new insight into an important role of BMI change and variability in non-demented individuals, and evidence that unstable and higher variability in BMI may be early manifestation related to A β deposition before developing dementia. The exact pathobiology of why greater BMI variation is detrimental to A β deposition remains unclear. However, there has been growing evidence that greater BMI variation is closely associated with a new onset of diabetes, cardiovascular disease, atrial fibrillation, and higher mortality (Bangalore et al., 2017; Lim et al., 2019; Sponholtz et al., 2019). One possible mechanism of these findings might be gene alternation. Specifically, the anti-aging gene Sirtuin 1 repression is associated with the onset of diabetes, cardiovascular disease and sarcopenia (Martins, 2016, 2017, 2018), which in turn leads to BMI variation, eventually resulting in A β deposition. Another possible explanation is that these medical diseases might result in both greater BMI variation and A β positivity, although we excluded participants with severe medical diseases using Christensen's criteria (Christensen et al., 1991). Alternatively, regarding the greater BMI variability without medical diseases, even though there is a repeated occurrence and recovery of sarcopenia and visceral obesity, the accumulation of the remaining detrimental effects might affect

A β deposition through the possible mechanisms mentioned in the previous paragraph.

Finally, our cluster analysis identified BMI subgroups with specific patterns of BMI change and variability, which eventually showed a greater risk of A β positivity. Specifically, a subgroup with decreased BMI and a greater variability in BMI was predictive of a higher risk of A β positivity. This was again replicated in cluster analyses with various BMI measures and A β positivity, a prior finding suggestive of the importance of decreased BMI with greater variability in A β positivity.

The strength of this study is that we investigated the associations between A β positivity and BMI changes and BMI variability in a large cohort. However, our study has several limitations that need to be addressed. First, due to the inherent challenges of a retrospective cohort study, we did not provide information about the participants' amyloid status at baseline. Thus, we were not able to show their causal relationships. However, a retrospective cohort study was considered a realistic alternative given that the change in amyloid appears very slowly and the cost of amyloid PET is very expensive. Second, because we used the Asia-Pacific BMI criteria for participants who are obese and underweight, caution should be taken when generalizing our findings to other races. Third, BMI values were collected from March 2020 until 3 years after the A β PET scan, and several BMI values were recorded at 3 years after the A β PET scan. This limitation might be mitigated to a certain extent with the existing findings that the annual rate of increasing A β deposition is very low (Ossenkoppele et al., 2012; Kemppainen et al., 2014; Kim et al., 2016). Fourth, we did not assess the body composition that might explain the associations we reported, such as muscle mass and fat mass. Fifth, we lacked information on whether the BMI change and fluctuations were intentional or unintentional, although these factors may have different effects on A β deposition. Sixth, we could not consider the alterations of dietary habit, although these factors might be associated with BMI change and A β positivity. Finally, because BMI data were retrospectively derived from the clinical data warehouse, there were differences in the duration of follow-up among participants despite controlling for the duration of follow-up in the process of calculating BMI changes. Instead, the results of the study with data from the clinical data warehouse could reflect the clinical situation in real-world settings, which were considered as real-world evidence for healthcare decisions.

TABLE 3 Association of A β positivity with BMI subgroup.

| BMI subgroup* | OR (95% CI)* | p |
|---------------|------------------|-------|
| 1 | 1 (ref.) | |
| 2 | 1.49 (1.05–2.13) | 0.027 |
| 3 | 1.49 (1.01–2.20) | 0.044 |
| 4 | 2.39 (1.37–4.16) | 0.002 |

A β , amyloid- β ; BMI, body mass index; OR, odds ratio; CI, confidence interval. *Adjusted ORs for A β positivity were obtained by logistic regression analysis with BMI subgroup as a predictor after controlling for age, sex, APOE e4 genotype, years of education, hypertension, and diabetes.

Conclusion

We provide a comprehensive understanding of the marked influences of BMI change and variability on the risk of A β positivity in non-demented individuals. Furthermore, our findings suggest that rigorous strategies for weight maintenance are required to prevent A β deposition in non-demented individuals.

Data availability statement

The raw data supporting the conclusions of this article will be made available by the authors, without undue reservation.

Ethics statement

The studies involving human participants were reviewed and approved by the Institutional Review Board of the Samsung Medical Center. Written informed consent was obtained from all participants. The patients/participants provided their written informed consent to participate in this study.

Author contributions

SHK: writing – original draft, review and editing, formal analysis, and data curation. JHK: writing – review and editing, formal analysis, and data curation. YC: conceptualization. BKC, YSC, HJ, HJK, S-BK, and DLN: data curation. KK: methodology, formal analysis, writing – review and editing, and conceptualization. SWS: methodology, writing – review and editing, and conceptualization. All authors contributed to the article and approved the submitted version.

Funding

This research was supported by a grant of the Korean Health Technology R&D Project, Ministry of Health and Welfare, South Korea (HI19C1132); a grant of the Korea Health Technology R&D Project through the Korea Health Industry Development Institute (KHIDI), funded by the Ministry of Health and Welfare and Ministry of science and ICT, Republic of Korea (grant numbers: HU20C0111 and HU22C0170); the National Research Foundation of Korea (NRF) grant funded

by the Korea government (MSIT) (NRF-2019R1A5A2027340); Institute of Information and communications Technology Planning and Evaluation (IITP) grant funded by the Korea government (MSIT) (No. 2021-0-02068, Artificial Intelligence Innovation Hub); Future Medicine 20*30 Project of the Samsung Medical Center (#SMX1220021); the “National Institute of Health” research project (2021-ER1002-01 and 2021-ER1006-01); Korea University Guro Hospital (KOREA RESEARCH-DRIVEN HOSPITAL) and grant funded by Korea University Medicine (K2210201); and Basic Science Research Program through the National Research Foundation of Korea (NRF) funded by the Ministry of Education (grant number: 2022R111A1A01056956).

Conflict of interest

The authors declare that the research was conducted in the absence of any commercial or financial relationships that could be construed as a potential conflict of interest.

Publisher's note

All claims expressed in this article are solely those of the authors and do not necessarily represent those of their affiliated organizations, or those of the publisher, the editors and the reviewers. Any product that may be evaluated in this article, or claim that may be made by its manufacturer, is not guaranteed or endorsed by the publisher.

Supplementary material

The Supplementary Material for this article can be found online at: <https://www.frontiersin.org/articles/10.3389/fnagi.2022.924550/full#supplementary-material>

References

- Al-Sofiani, M. E., Ganji, S. S., and Kalyani, R. R. (2019). Body composition changes in diabetes and aging. *J. Diabetes Complications* 33, 451–459. doi: 10.1016/j.jdiacomp.2019.03.007
- Bangalore, S., Fayyad, R., Laskey, R., DeMicco, D. A., Messerli, F. H., and Waters, D. D. (2017). Body-weight fluctuations and outcomes in coronary disease. *N. Engl. J. Med.* 376, 1332–1340. doi: 10.1056/NEJMoa1606148
- Bell, S. P., Liu, D., Samuels, L. R., Shah, A. S., Gifford, K. A., Hohman, T. J., et al. (2017). Late-life body mass index, rapid weight loss, apolipoprotein e ε4 and the risk of cognitive decline and incident dementia. *J. Nutr. Health Aging* 21, 1259–1267. doi: 10.1007/s12603-017-0906-3
- Bilmes, J. (1998). A Gentle Tutorial of the EM Algorithm and its Application to Parameter Estimation for Gaussian Mixture and Hidden Markov Models.
- Buchman, A. S., Capuano, A. W., VanderHorst, V., Wilson, R. S., Oveisgharan, S., Schneider, J. A., et al. (2021). Brain β-amyloid links the association of change in BMI with cognitive decline in community-dwelling older adults. *J. Gerontol. A Biol. Sci. Med. Sci.* Online ahead of print. doi: 10.1093/gerona/glab320
- Cho, S. H., Choe, Y. S., Kim, H. J., Jang, H., Kim, Y., Kim, S. E., et al. (2020). A new Centiloid method for (18)F-florbetaben and (18)F-flutemetamol PET without conversion to PiB. *Eur. J. Nucl. Med. Mol. Imaging* 47, 1938–1948. doi: 10.1007/s00259-019-04596-x
- Christensen, K. J., Multhaup, K. S., Nordstrom, S., and Voss, K. (1991). A cognitive battery for dementia: development and measurement characteristics. *Psychol. Assessment J. Consulting Clin. Psychol.* 3, 168–174. doi: 10.1037/1040-3590.3.2.168

- Ewers, M., Schmitz, S., Hansson, O., Walsh, C., Fitzpatrick, A., Bennett, D., et al. (2012). Body mass index is associated with biological CSF markers of core brain pathology of Alzheimer's disease. *Neurobiol. Aging* 33, 1599–1608. doi: 10.1016/j.neurobiolaging.2011.05.005
- Fitzpatrick, A. L., Kuller, L. H., Lopez, O. L., Diehr, P., O'Meara, E. S., Longstreth, W. T., et al. (2009). Midlife and late-life obesity and the risk of dementia: cardiovascular health study. *Arch. Neurol.* 66, 336–342. doi: 10.1001/archneurol.2008.582
- Giudici, K. V., Guyonnet, S., Rolland, Y., Vellas, B., de Souto Barreto, P., and Nourhashemi, F. (2019). Body weight variation patterns as predictors of cognitive decline over a 5 year follow-up among community-dwelling elderly (MAPT Study). *Nutrients* 11:1371. doi: 10.3390/nu11061371
- Gottesman, R. F., Schneider, A. L., Zhou, Y., Coresh, J., Green, E., Gupta, N., et al. (2017). Association between midlife vascular risk factors and estimated brain amyloid deposition. *JAMA* 317, 1443–1450. doi: 10.1001/jama.2017.3090
- Grundman, M., Corey-Bloom, J., Jernigan, T., Archibald, S., and Thal, L. J. (1996). Low body weight in Alzheimer's disease is associated with mesial temporal cortex atrophy. *Neurology* 46, 1585–1591. doi: 10.1212/wnl.46.6.1585
- Hsu, D. C., Mormino, E. C., Schultz, A. P., Amariglio, R. E., Donovan, N. J., Rentz, D. M., et al. (2016). Lower late-life body-mass index is associated with higher cortical amyloid burden in clinically normal elderly. *J. Alzheimer's Dis.* 53, 1097–1105. doi: 10.3233/JAD-150987
- Jack, C. R., Knopman, D. S., Jagust, W. J., Petersen, R. C., Weiner, M. W., Aisen, P. S., et al. (2013). Tracking pathophysiological processes in Alzheimer's disease: an updated hypothetical model of dynamic biomarkers. *Lancet Neurol.* 12, 207–216. doi: 10.1016/S1474-4422(12)70291-0
- Jeong, H. J., Lee, H., Lee, S.-Y., Seo, S., Park, K. H., Lee, Y.-B., et al. (2020). [18F]THK5351 PET imaging in patients with mild cognitive impairment. *J. Clin. Neurol.* 16, 202–214. doi: 10.3988/jcn.2020.16.2.202
- Kang, S. H., Park, Y. H., Lee, D., Kim, J. P., Chin, J., Ahn, Y., et al. (2019). The cortical neuroanatomy related to specific neuropsychological deficits in Alzheimer's continuum. *Dement. Neurocogn. Disord.* 18, 77–95. doi: 10.12779/dnd.2019.18.3.77
- Kang, S. H., Kim, M. E., Jang, H., Kwon, H., Lee, H., Kim, H. J., et al. (2021). Amyloid positivity in the Alzheimer/subcortical-vascular spectrum. *Neurology* 96, e2201–e2211. doi: 10.1212/WNL.00000000000011833
- Kemppainen, N. M., Scheinin, N. M., Koivunen, J., Johansson, J., Toivonen, J. T., Nägren, K., et al. (2014). Five-year follow-up of 11C-PIB uptake in Alzheimer's disease and MCI. *Eur. J. Nuclear Med. Mol. Imaging* 41, 283–289. doi: 10.1007/s00259-013-2562-0
- Kim, H., Kim, C., Seo, S. W., Na, D. L., Kim, H. J., Kang, M., et al. (2015). Association between body mass index and cortical thickness: among elderly cognitively normal men and women. *Int. Psychogeriatrics* 27, 121–130. doi: 10.1017/S1041610214001744
- Kim, H. J., Kim, C., Jeon, S., Kang, M., Kim, Y. J., Lee, J. M., et al. (2015). Association of body fat percentage and waist-hip ratio with brain cortical thickness: a study among 1777 cognitively normal subjects. *Alzheimer Dis. Assoc. Disorders* 29, 279–286. doi: 10.1097/WAD.0000000000000079
- Kim, H. J., Yang, J. J., Kwon, H., Kim, C., Lee, J. M., Chun, P., et al. (2016). Relative impact of amyloid- β , lacunes, and downstream imaging markers on cognitive trajectories. *Brain J. Neurol.* 139, 2516–2527. doi: 10.1093/brain/aww148
- Kim, H. R., Choe, Y. S., Moon, S. H., Kim, H. J., Jang, H. L., Na, D., et al. (2021). Finding the optimal cutoff value for amyloid β positivity using the iterative outlier method and concordance rate. *Precis. Future Med.* 5, 83–89. doi: 10.23838/pfm.2021.00023
- Kim, S. E., Lee, J. S., Woo, S., Kim, S., Kim, H. J., Park, S., et al. (2019). Sex-specific relationship of cardiometabolic syndrome with lower cortical thickness. *Neurology* 93, e1045–e1057. doi: 10.1212/WNL.0000000000000804
- Kivipelto, M., Ngandu, T., Fratiglioni, L., Viitanen, M., Kåreholt, I., Winblad, B., et al. (2005). Obesity and vascular risk factors at midlife and the risk of dementia and Alzheimer disease. *Arch. Neurol.* 62, 1556–1560. doi: 10.1001/archneur.62.10.1556
- Klunk, W. E., Koeppe, R. A., Price, J. C., Benzinger, T. L., Devous, M. D. Sr., Jagust, W. J., et al. (2015). The Centiloid Project: standardizing quantitative amyloid plaque estimation by PET. *Alzheimers Dement.* 11, 1–15.e4. doi: 10.1016/j.jalz.2014.07.003
- Lane, C. A., Barnes, J., Nicholas, J. M., Baker, J. W., Sudre, C. H., Cash, D. M., et al. (2021). Investigating the relationship between BMI across adulthood and late life brain pathologies. *Alzheimer's Res. Therapy* 13:91. doi: 10.1186/s13195-021-00830-7
- Lee, S. H., Byun, M. S., Lee, J. H., Yi, D., Sohn, B. K., Lee, J. Y., et al. (2020). Sex-specific association of lifetime body mass index with Alzheimer's disease neuroimaging biomarkers. *J. Alzheimer's Dis.* 75, 767–777.
- Lim, Y. M., Yang, P. S., Jang, E., Yu, H. T., Kim, T. H., Uhm, J. S., et al. (2019). Body mass index variability and long-term risk of new-onset atrial fibrillation in the general population: a Korean nationwide cohort study. *Mayo Clin. Proc.* 94, 225–235. doi: 10.1016/j.mayocp.2018.10.019
- Luchsinger, J. A., Biggs, M. L., Kizer, J. R., Barzilay, J., Fitzpatrick, A., Newman, A., et al. (2013). Adiposity and cognitive decline in the cardiovascular health study. *Neuroepidemiology* 40, 274–281. doi: 10.1159/000345136
- Maltais, M., De Souto Barreto, P., Hooper, C., Payoux, P., Rolland, Y., and Vellas, B. (2019). Association between brain β -Amyloid and frailty in older adults. *J. Gerontology. Ser. A Biol. Sci. Med. Sci.* 74, 1747–1752. doi: 10.1093/gerona/glz009
- Martins, I. (2016). Anti-aging genes improve appetite regulation and reverse cell senescence and apoptosis in global populations. *Adv. Aging Res.* 5, 9–26. doi: 10.4236/aar.2016.51002
- Martins, I. (2017). Single gene inactivation with implications to diabetes and multiple organ dysfunction syndrome. *J. Clin. Epigenet.* 3:24.
- Martins, I. (2018). *Appetite Regulation and the Peripheral Sink Amyloid Beta Clearance Pathway in Diabetes and Alzheimer's Disease*.
- Möllers, T., Stocker, H., Perna, L., Nabers, A., Rujescu, D., Hartmann, A. M., et al. (2021). A β misfolding in blood plasma is inversely associated with body mass index even in middle adulthood. *Alzheimer's Res. Therapy* 13:145. doi: 10.1186/s13195-021-00889-2
- Montague, C. T., Prins, J. B., Sanders, L., Zhang, J., Sewter, C. P., Digby, J., et al. (1998). Depot-related gene expression in human subcutaneous and omental adipocytes. *Diabetes* 47, 1384–1391.
- Ossenkoppele, R., Tolboom, N., Foster-Dingley, J. C., Adriaanse, S. F., Boellaard, R., Yaqub, M., et al. (2012). Longitudinal imaging of Alzheimer pathology using [11C]PIB, [18F]FDDNP and [18F]FDG PET. *Eur. J. Nuclear Med. Mol. Imaging* 39, 990–1000. doi: 10.1007/s00259-012-2102-3
- Patel, E., and Kushwaha, D. S. J. P. C. S. (2020). Clustering cloud workloads: K-means vs gaussian mixture model. *Proc. Comput. Sci.* 171, 158–167.
- Petersen, R. C. (2011). Clinical practice. mild cognitive impairment. *N. Engl. J. Med.* 364, 2227–2234.
- Rabin, J. S., Shirzadi, Z., Swardfager, W., MacIntosh, B. J., Schultz, A., Yang, H. S., et al. (2020). Amyloid-beta burden predicts prospective decline in body mass index in clinically normal adults. *Neurobiol. Aging* 93, 124–130. doi: 10.1016/j.neurobiolaging.2020.03.002
- Rowe, C. C., Bourgeat, P., Ellis, K. A., Brown, B., Lim, Y. Y., Mulligan, R., et al. (2013). Predicting Alzheimer disease with β -amyloid imaging: results from the Australian imaging, biomarkers, and lifestyle study of ageing. *Ann. Neurol.* 74, 905–913. doi: 10.1002/ana.24040
- Sled, J. G., Zijdenbos, A. P., and Evans, A. C. (1998). A nonparametric method for automatic correction of intensity nonuniformity in MRI data. *IEEE Trans. Med. Imaging* 17, 87–97.
- Sponholtz, T. R., van den Heuvel, E. R., Xanthakis, V., and Vasan, R. S. (2019). Association of Variability in body mass index and metabolic health with cardiometabolic disease risk. *J. Am. Heart Assoc.* 8:e010793.
- Thirunavu, V., McCullough, A., Su, Y., Flores, S., Dincer, A., Morris, J. C., et al. (2019). Higher body mass index is associated with lower cortical Amyloid- β burden in cognitively normal individuals in late-life. *J. Alzheimer's Dis.* 69, 817–827. doi: 10.3233/JAD-190154
- Tolppanen, A. M., Ngandu, T., Kåreholt, I., Laatikainen, T., Rusanen, M., Soininen, H., et al. (2014). Midlife and late-life body mass index and late-life dementia: results from a prospective population-based cohort. *J. Alzheimer's Dis.* 38, 201–209.
- Vidoni, E. D., Townley, R. A., Honea, R. A., and Burns, J. M. (2011). Alzheimer disease biomarkers are associated with body mass index. *Neurology* 77, 1913–1920.
- Villemagne, V. L., Pike, K. E., Chételat, G., Ellis, K. A., Mulligan, R. S., Bourgeat, P., et al. (2011). Longitudinal assessment of A β and cognition in aging and Alzheimer disease. *Ann. Neurol.* 69, 181–192.
- Villeneuve, S., Rabinovici, G. D., Cohn-Sheehy, B. I., Madison, C., Ayakta, N., Ghosh, P. M., et al. (2015). Existing pittsburgh compound-B positron emission tomography thresholds are too high: statistical and pathological evaluation. *Brain J. Neurol.* 138, 2020–2033. doi: 10.1093/brain/aww112
- WHO Expert Consultation, (2004). Appropriate bodymass index for Asian populations and its implications for policy and intervention strategies. *Lancet* 363, 157–163. doi: 10.1016/S0140-6736(03)15268-3

Yaffe, K., Kanaya, A., Lindquist, K., Simonsick, E. M., Harris, T., Shorr, R. I., et al. (2004). The metabolic syndrome, inflammation, and risk of cognitive decline. *JAMA* 292, 2237–2242.

Yang, M.-S., Lai, C.-Y., and Lin, C.-Y. (2012). A robust EM clustering algorithm for Gaussian mixture models. *Pattern Recognition* 45, 3950–3961.

Yao, Z., Hu, B., Liang, C., Zhao, L., Jackson, M., Alzheimer's Disease, et al. (2012). A longitudinal study of atrophy in amnesic mild cognitive impairment and normal aging revealed by cortical thickness. *PLoS One* 7:e48973. doi: 10.1371/journal.pone.0048973

Ye, B. S., Jang, E. Y., Kim, S. Y., Kim, E. J., Park, S. A., Lee, Y., et al. (2016). Unstable body mass index and progression to probable Alzheimer's disease dementia in patients with amnesic mild cognitive impairment. *J. Alzheimer's Dis.* 49, 483–491. doi: 10.3233/JAD-150556

Ye, B. S., Kim, H. J., Kim, Y. J., Jung, N. Y., Lee, J. S., Lee, J., et al. (2018). Longitudinal outcomes of amyloid positive versus negative amnesic mild cognitive impairments: a three-year longitudinal study. *Sci. Rep.* 8:5557. doi: 10.1038/s41598-018-23676-w



Excessive/Aberrant and Maladaptive Synaptic Plasticity: A Hypothesis for the Pathogenesis of Alzheimer's Disease

Shigeki Kawabata*

Dementia Project Promotion Office, Sampo Care Inc., Tokyo, Japan

OPEN ACCESS

Edited by:

Allison B. Reiss,
New York University, United States

Reviewed by:

Alejandro O. Sodero,
CONICET Institute for Biomedical
Research (BIOMED), Argentina
Hwamee Oh,
Brown University, United States

*Correspondence:

Shigeki Kawabata
sc6s-kwbt@asahi-net.or.jp

Specialty section:

This article was submitted to
Alzheimer's Disease and Related
Dementias,
a section of the journal
Frontiers in Aging Neuroscience

Received: 06 April 2022

Accepted: 08 June 2022

Published: 05 July 2022

Citation:

Kawabata S (2022)
Excessive/Aberrant and Maladaptive
Synaptic Plasticity: A Hypothesis
for the Pathogenesis of Alzheimer's
Disease.
Front. Aging Neurosci. 14:913693.
doi: 10.3389/fnagi.2022.913693

The amyloid hypothesis for the pathogenesis of Alzheimer's disease (AD) is widely accepted. Last year, the US Food and Drug Administration considered amyloid- β peptide ($A\beta$) as a surrogate biomarker and approved an anti- $A\beta$ antibody, aducanumab, although its effectiveness in slowing the progression of AD is still uncertain. This approval has caused a great deal of controversy. Opinions are divided about whether there is enough evidence to definitely consider $A\beta$ as a causative substance of AD. To develop this discussion constructively and to discover the most suitable therapeutic interventions in the end, an alternative persuasive hypothesis needs to emerge to better explain the facts. In this paper, I propose a hypothesis that excessive/aberrant and maladaptive synaptic plasticity is the pathophysiological basis for AD.

Keywords: Alzheimer's disease, synapse, plasticity, Amyloid - beta, APP – amyloid precursor protein, presenilin, ApoE4

INTRODUCTION

Research on Alzheimer's disease (AD) began with the elucidation of its pathological features. Once the amyloid plaque (AP) substance was identified as amyloid- β peptide ($A\beta$), which is produced from amyloid β precursor protein (APP), the amyloid hypothesis became scientific orthodoxy in academia and has remained so for many years. APP is processed through two enzymatic pathways, namely non-amyloidogenic α -pathway and amyloidogenic β -pathway. Within α -pathway, the first step of the proteolysis is performed by α -secretase and the large ectodomain, so-called sAPP α , and the C-terminal fragment (CTF) which remains anchored to the membrane (CTF α) are produced. In β -pathway, β -secretase cleaves APP and generates sAPP β and CTF β . At the second step of the proteolysis, CTF α and CTF β are both cleaved by γ -secretase, but $A\beta$ is only produced from CTF β (Carrillo-Mora et al., 2014). The striking discoveries, which moved the amyloid theory forward, are the linkage of the gene mutations in APP and presenilin, the catalytic core of γ -secretase complex (PSEN1 and PSEN2) to Familial Alzheimer's disease (FAD). The amyloid hypothesis states that $A\beta$ is toxic to neurons and that FAD-linked mutations in the APP and presenilin genes lead to the production of more toxic $A\beta$ such as $A\beta_{42}$ and other longer species of $A\beta$ (Selkoe and Hardy, 2016). However, when analyzing more than a hundred types of gene mutation found in FAD, the produced $A\beta$ was found to vary in length and amount among the mutations (Li et al., 2016; Sun et al., 2017; Devkota et al., 2021). Such variability raises the question of which types of $A\beta$ exert toxicity. A debatable fact is that some FAD-linked PSEN1 mutations drastically reduce the production of $A\beta_{42}$, a type of $A\beta$ that have been widely studied in the context of AD causality

(Sun et al., 2017). Various mechanisms of AD causation have also been reported (Carrillo-Mora et al., 2014), such as oxidative stress, glutamate toxicity as well as impairment of various signal transductions and several intracellular mechanisms. It is not well understood how A β acquires multiple functions, and which mechanism of action contributes to the causal neurotoxicity. Issues raised by the amyloid hypothesis are still unresolved.

In this paper, I integrate the past research findings from a different angle from what has been discussed in connection with the amyloid theory, and propose a hypothesis that excessive/aberrant and maladaptive synaptic plasticity is the cause of AD.

THE GENES ASSOCIATED WITH FAMILIAL ALZHEIMER'S DISEASE

Research on APP and presenilin has been focused on how mutations found in FAD alter the mode of A β production. However, when a gene mutation is linked to the disease, questions arise including what the original function of the gene is, whether the mutation affects that function, and if so, whether the functional abnormality causes the disease. The function of APP has been elucidated by studies in mice and *Drosophila* (Torroja et al., 1999; Leyssen et al., 2005; Soldano et al., 2013; Klevanski et al., 2015). *Drosophila* has an APP homolog called APPL. These studies have shown that APP plays an important role in synaptic plasticity such as neurite extension and synaptogenesis and that the CTF, especially the cytoplasmic domain of APP is critical for the function of APP. In *Drosophila*, axonal arborization of the small ventral lateral neurons is induced by full-length APPL or the CTF only, but not by APPL lacking the intracellular region (Leyssen et al., 2005). Accumulation of membrane-tethered intracellular domain of APP in rodent neuronal cultures also results in marked increase in neurite extension (Deyts et al., 2012). The importance of APP or APPL in synaptic plasticity has also been shown in the Mushroom Bodies, a *Drosophila* center of olfactory learning (Soldano et al., 2013) and the neuromuscular junction of *Drosophila* (Torroja et al., 1999), and in the central nervous system and the neuromuscular junction of mice (Klevanski et al., 2015). Although a large ectodomain of APP also has important roles, these studies demonstrate that the intracellular region of APP or APPL is indispensable to these functions.

Many strains of AD model mice (I refer to these mice collectively as AD mice) have been developed by inducing expression of FAD-linked mutant APP and presenilin. In these mice with aging, there is a loss of neurons and synapses as well as development of APs accompanied by dystrophic neurites (DNs), which is reminiscent of AD. Hyperphosphorylated tau, which is a constituent of neurofibrillary tangles (NFTs), is accumulated in DNs in a variety of AD mice (Sasaguri et al., 2017). At a young age, AD mice present network abnormalities. In a functional magnetic resonance imaging (fMRI) study, hypersynchrony of the default mode network (DMN)-like network is observed at the pre-plaque stage in APP^{NL-F/NL-F} knock-in mice (Shah et al., 2018). Conversely, at 7 months of age when A β deposition appears,

the DMN-like network is hyposynchronous in these mice. This dynamic pattern of resting-state network hypersynchrony before A β deposition and subsequent hyposynchrony at a later age is consistent with other studies in AD mice, specifically in Tet-off APP (TG) mice (Ben-Nejma et al., 2019) and in APP^{sw}/PS1dE9 mice (Bero et al., 2012). In addition, network hyperexcitability and seizure susceptibility are common manifestations in AD mice, preceding A β pathology in 3XTg-AD mice (Kazim et al., 2017) and in Tg2576 mice (Bezzina et al., 2015).

In mice expressing M146V PSEN1 mutant as well as presenilin knockout mice, exuberant neurite outgrowth and hippocampal axonal sprouting are seen (Deyts et al., 2016). These changes are abrogated when APP expression is absent. The level of CTF of APP increases significantly in these mice, which is believed to be a mechanism for aberrant plasticity (Deyts et al., 2016). Mutations in FAD linked PSEN1 impair its function as γ -secretase (Zhou et al., 2017), and then CTF accumulation occurs. It should be noted that an increase in the CTF level is commonly observed among mice expressing various PSEN1 mutants (Li et al., 2016), suggesting that aberrant plasticity is a common manifestation among the mutants. fMRI studies revealed hypersynchrony in key regions of the DMN and a decrease in DMN deactivation in children with FAD-linked E280A PSEN1 mutant when compared with non-carrier children (mean age of participants: 13 y) (Quiroz et al., 2015). The DMN is most active during inwardly oriented mental activity and deactivated during memory tasks. The degree of task induced DMN deactivation is correlated with cognitive performance (Sperling et al., 2010). The DMN is rather impaired in the course of disease onset (Chhatwal et al., 2013). Earlier hypersynchronization and subsequent decline are similarly observed in AD mice (Bero et al., 2012; Shah et al., 2018; Ben-Nejma et al., 2019). During a face-name associative encoding task, neurons in the hippocampus are hyperactivated in presymptomatic E280A PSEN1 mutation carriers (age: 33.7 y) (Quiroz et al., 2010). Epileptic activity is also prominent among FAD pedigrees harboring the mutation in PSEN1, PSEN2, or APP (Zarea et al., 2016). Gray matter volume increases in children with PSEN1 mutant (Quiroz et al., 2015). It is conceivable that the volume of gray matter reflects the number of synapses, because gray matter volume and synapse number are well correlated at puberty (Blakemore and Choudhury, 2006).

Altogether, these observations suggest that network abnormalities are commonly present from an early stage of life in FAD mutant carriers and in AD mice.

THE MECHANISM OF NETWORK ABNORMALITIES

Synchronous firing of large groups of neurons can be elicited by the enhancement of excitatory synaptic connections or loss of inhibitory GABAergic drive onto principal neurons. Subgroups of GABAergic interneurons generate oscillatory rhythms through controlling the spike timing in neighboring principal neurons. Network abnormalities are often caused by synaptic remodeling of these inhibitory/excitatory neuronal circuits. APP and presenilin play important roles in synaptic plasticity, implying

that network abnormalities seen in FAD patients and AD mice (abnormal DMN, decreased deactivation of DMN, seizure-like hyperexcitation and hippocampal hyperactivation during memory task) may result from aberrant plasticity caused by abnormal functions of these mutants. Indeed, hyperconnectivity and hyperexcitability of principal neurons have been observed at a young age in AD mice. In APP^{NL-F/NL-F} knock-in mice, pyramidal neurons show persistent hyperexcitation by imbalance of excitation and inhibition (E/I), which originally occurs in the entorhinal cortex at 1-2 months of age (Petrache et al., 2019). In these mice, the function of parvalbumin-positive interneurons (PV cells) is impaired in the entorhinal cortex, and a network-driven component contributes to the E/I imbalance (Petrache et al., 2019). APP is highly expressed in GABAergic interneurons, especially in PV cells (Rice et al., 2020), enhances inhibitory tone to granule cells by regulating the formation of GABAergic synapses onto these cells (Wang et al., 2014), implying that dysregulation of GABAergic synapses caused by the mutant APP-induced disruption of PV cell microcircuitry leads to the E/I imbalance and hyperexcitation. In APP^{swe}/PS1dE9 mice, at postnatal day 21, an increase in the number of medial apical synapses (CA3-CA1 connections) is seen in CA1 pyramidal neurons (Ray et al., 2020). Noting that the number of synapses simultaneously decreases at the distal apical tuft, the site for entorhinal inputs, an aberrant increase in the number of excitatory CA3-CA1 connections may reflect compensatory reweighting of synaptic connections. In aged transgenic mice (13-14 months), the number of synapses decreases uniformly across all dendritic and somatic compartments (Ray et al., 2020). Similarly, in Tg2576 mice, spine densities in hippocampal CA1 and cortical pyramidal neurons increase at 1 month of age before A β pathology and later decrease at 12 months of age (Lee et al., 2010).

PV cells are involved in forming gamma oscillations. Increasing the firing rate of PV cells enhances the power of gamma oscillations (Sohal et al., 2009). Conversely, impairment of PV cells is associated with aberrant hypersynchronization such as occurs in schizophrenia and epilepsy (Freund and Katona, 2007). In hAPPJ20 mice, it is demonstrated that functional deficit of PV cells causes network hypersynchrony during reduced gamma oscillatory activity (Verret et al., 2012). In APP^{swe}/PS1dE9 mice, hippocampal PV cells are hyperexcitable at 4 months of age, but rather hypoexcitable at 6 months of age (Hijazi et al., 2020). It was also reported that the electroencephalogram power in gamma-band oscillations increases in the frontal cortex and the thalamus of APP^{swe}/PS1dE9 mice at 16-17 weeks of age (Gurevicius et al., 2013). The pattern of early hyperexcitation and subsequent decline in PV cell activity is correlated with early network hypersynchrony and hyposynchrony at later age (Bero et al., 2012; Shah et al., 2018). It is proposed that a coupled set of local gamma oscillations at multiple brain regions leads to long-distance synchrony of the resting-state network (Cabral et al., 2014; Koelewijn et al., 2019). In patients with cingulate gyrus epilepsy, gamma oscillations may be a key contributor to DMN connectivity (Leng et al., 2020), and transient suppression of gamma oscillations is associated with DMN deactivation

(Ossandón et al., 2011), implying that PV cells may regulate DMN activity through controlling local gamma oscillations. The number of PV cells increases (Verdaguer et al., 2015) or decreases (Petrache et al., 2019) depending on the strain of AD mice. Similarly, the number of PV cells increases in the rat kindling model (Kamphuis et al., 1989), but decreases in the pilocarpine-induced epileptic model (Kobayashi and Buckmaster, 2003).

Differential phenotypes among AD mice may be due to distinct patterns and levels of transgene expression. Dysregulation of GABAergic synapses, increased spine density in principal neurons and increased/dysregulated gamma oscillations are differentially seen among AD mice, but all can be the molecular basis of network abnormalities. Results also depend on the age of examined mice. As is well known, hyperexcitability in principal neurons causes neuronal impairment and neuron loss, which eventually lead to hypoactivity of the neuronal network. As a compensatory response for hyperexcitation, remodeling of inhibitory circuits also occurs in AD mice (Palop et al., 2007). PV cells express α -Amino-3-hydroxy-5-methyl-4-isoxazolepropionic Acid (AMPA) receptors and are vulnerable to glutamate hyperexcitability (Moga et al., 2002). Increase or decrease in the number/activity of PV cells may depend on how inhibitory PV cell microcircuitry is remodeled.

Direct soluble A β administration into the hippocampus of mice can induce neuronal hyperexcitability (Busche et al., 2012). Soluble A β triggers hyperexcitation by suppressing glutamate reuptake (Zott et al., 2019), but paradoxically A β reduces glutamatergic transmission at the synaptic level (Kamenetz et al., 2003; Snyder et al., 2005). A β increases hippocampal PV cell excitability but not pyramidal neuron excitability (Hijazi et al., 2020). On the contrary, A β disrupts hippocampal gamma oscillations (Kurudenkandy et al., 2014). It is suggested that A β monomers, oligomers, fibrils, and APs behave differentially, by which multifunctional actions of A β are understood. Nonetheless, it is not conclusive that A β triggers the network abnormalities which are seen earlier than A β deposition. All in all, it can be proposed that network abnormalities seen at early stage of life results from FAD mutant-driven aberrant synaptic plasticity. The mechanism of how aberrant synaptic plasticity causes AD will be discussed later in this paper.

Individuals with Down's syndrome develop AD pathology. Findings of different segmental duplications of chromosome 21 subregions in Down's syndrome conclusively show that lifelong overexpression of wild-type APP causes AD (Selkoe and Hardy, 2016). If a hypothesis based on synaptic plasticity is correct, it follows that the cause of AD in Down's syndrome is hyperfunction of APP. Nonetheless, it is uncertain whether the functional abnormality of FAD mutants can be simply described as excessive. In this paper, the word "aberrant" is preferably used to explain the pathogenesis of FAD.

APOLIPOPROTEIN E ϵ 4 AND SPORADIC ALZHEIMER'S DISEASE

Apolipoprotein E (APOE) has three isoforms, APOE ϵ 2, 3, and 4, and individuals with APOE ϵ 4 are more likely to develop

AD. Thus, APOE $\epsilon 4$ is the genetic risk factor for sporadic Alzheimer's disease (SAD) (Farrer et al., 1997). Numerous reports have indicated the roles of APOE in AD pathogenesis, but the underlying mechanism by which APOE $\epsilon 4$ increases the risk of AD is not fully understood. In mouse studies, the effects of APOE $\epsilon 4$ on neuronal plasticity are inconsistent. Both negative and beneficial effects have been associated with APOE $\epsilon 4$ (Kim et al., 2014). More essentially, it has been shown that inherent functional differences may exist between mouse and human APOE isoforms (Brendza et al., 2002), suggesting that much importance should be placed on studies in humans. In fMRI studies on healthy young adults, network abnormalities are commonly observed in APOE $\epsilon 4$ carriers. Just like individuals with presenilin mutant, DMN enhancement (mean age of participants: 28.4 y) (Filippini et al., 2009), (24 y) (Su et al., 2015), decreased DMN inactivation (19.7 y) (Shine et al., 2015) and increased hippocampal activation during memory tasks (23.2 y) (Dennis et al., 2010), (28.4 y) (Filippini et al., 2009) are observed in APOE $\epsilon 4$ carriers when compared with non-carriers. Hyperactivity in gamma-band oscillations is also seen in young APOE $\epsilon 4$ carriers (25.2 y) (Koelewijn et al., 2019). Alterations of DMN activity precede abnormalities in brain structure, blood flow, and memory performance (Filippini et al., 2009; Su et al., 2015), and probably A β deposition (Shine et al., 2015). According to studies in human derived neuronal cultures (Huang et al., 2017, 2019; Lin et al., 2018), APOE modulates APP expression (Huang et al., 2017, 2019) or metabolism (Lin et al., 2018), and promotes synaptic plasticity, which is substantiated by the number of synapses (Lin et al., 2018; Huang et al., 2019). The consensus of these reports is that APOE $\epsilon 4$ has the strongest effects on APP expression or metabolism, and synaptic plasticity, which is in line with neuronal network enhancement seen in young APOE $\epsilon 4$ carriers. Again, the DMN, once enhanced in young APOE $\epsilon 4$ carriers, is decreased in older carriers (Badhwar et al., 2017).

EXCESSIVE AND MALADAPTIVE SYNAPTIC PLASTICITY WITH AGING

It has been reported that during memory tasks, the activity of neurons in the medial temporal lobe or the hippocampus is greater in patients with early-stage mild cognitive impairment (MCI) than in healthy subjects, and that greater activation of neurons is associated with poorer performance (Dickerson et al., 2004; Yassa et al., 2010; Corriveau-Lecavalier et al., 2021a), indicating that such hyperactivation is detrimental to brain function. In fact, the drug levetiracetam ameliorates the lowered memory performance as well as hyperactive state in the hippocampus of MCI patients (Bakker et al., 2012, 2015). A β induces neuronal hyperexcitability in the hippocampus and hyperactive neurons are found preferentially (Busche et al., 2012) or exclusively (Busche et al., 2008) near the APs in AD mice. Thus, hyperactivation seen in the hippocampus of early MCI may simply reflect A β pathology. However, hippocampal hyperactivation during memory task is already detectable in healthy young APOE $\epsilon 4$ carriers who are unlikely to have A β deposition (Filippini et al., 2009; Dennis et al., 2010). Besides,

hyperactivation is task-dependent, implying that it is associated with altered patterns of functional connectivity (Corriveau-Lecavalier et al., 2021a). Although remodeling of the neuronal network compensates for loss of brain function which declines with aging, it has also become evident that plastic remodeling is sometimes detrimental. Namely, greater activation of neurons in the newly constructed neural network in older adults is found to be correlated with poorer, not better task performance (Grady, 2012). As aging increases the demand for neuronal plastic remodeling, it is a tall order to fulfill it perpetually. Errors may arise during this process. If plastic remodeling, which is basically a compensatory mechanism for overcoming age-related functional decline, occurs excessively, it may lead to maladaptive, neural over-recruitment.

The activity of neurons in the hippocampus increases in early MCI and then decreases as the disease progresses. The shape of this temporal change in neuronal activity is described by the inverse U-shape model (Zott et al., 2018; Corriveau-Lecavalier et al., 2021b). If the activity of neurons increases in early MCI, how will cognitive function change thereafter? Follow-up studies for a period of 2 years or more demonstrate that cognitive function declines significantly and the rate of AD development increases when the baseline neuronal activity is greater (Dickerson et al., 2004; Dickerson and Sperling, 2008; Miller et al., 2008; O'Brien et al., 2010; Huijbers et al., 2015).

THE FUNCTION OF TREM2 AND ITS IMPLICATION FOR ALZHEIMER'S DISEASE

A closer look at SAD risk genes found by genome wide association studies highlights the link between microglial cells and AD. Of particular interest is triggering receptor expressed on myeloid cells-2 (TREM2) (Guerreiro et al., 2013; Jonsson et al., 2013), a gene expressed in microglial cells. The R47H mutation in TREM2 has a similar risk as APOE $\epsilon 4$. Functional studies revealed that TREM2 variants related to AD reduce function, suggesting that the functional deficit of TREM2 increases the risk of AD (Song et al., 2018). It has been reported that in AD mice, APs are morphologically less compact and more damaging to surrounding neurites when TREM2 function is impaired (Wang et al., 2016; Yuan et al., 2016). In these papers, it is proposed that TREM2 has the function of protecting neurites from the toxicity of A β by wrapping A β compactly to block contact with neurites. Nonetheless, the assumption that the toxicity of A β causes neurodegeneration is not in accord with the fact that in rare cases DNs are present outside of APs (Blazquez-Llorca et al., 2017).

Staining with anti-GAP-43 antibody has shown that DNs associated with APs form growth cones with abnormal extension of neurites (Masliah et al., 1991). This pathological feature is called aberrant sprouting. GAP-43 is also present in DNs in AD mice. In APP23 mice, AP-associated DNs, which are identified as entorhinal axons or commissural axons, extend beyond boundaries and ectopically invade the inner molecular layer or the outer molecular layer of the dentate gyrus, respectively (Phinney et al., 1999). Although A β may not only damage neurites but also attract

neurite outgrowth beyond normal boundaries, an alternative explanation is that aberrant plasticity caused by the mutant APP leads to axon terminal invasion of the ectopic region, and neurodegeneration itself is caused by the mutant APP-driven aberrant plasticity.

The long-known function of microglial cells is phagocytosis, but this classic notion has already been overturned (Andoh

and Koyama, 2021). They act on neurons and play important roles in modulating neuronal functions, one of which is neuronal plasticity. They are engaged in several processes of synaptic plasticity, such as synapse formation, maturation, and elimination (pruning) (Andoh and Koyama, 2021). TREM2 plays an important role in the dynamics of synapse formation. In mice lacking TREM2, an increased number of synapses is

Familial Alzheimer's Disease

Mutations in the APP and presenilin

Aberrant synaptic plasticity

Alzheimer's disease

Sporadic Alzheimer's Disease

Compensation for age-related functional decline

Excessive synaptic plasticity

Remodeling promoted by APOE $\epsilon 4$

Remodeling exaggerated by TREM2 variants?

Described in Figure 2 in detail

FIGURE 1 | Summary of the synaptic plasticity hypothesis of Alzheimer's disease.

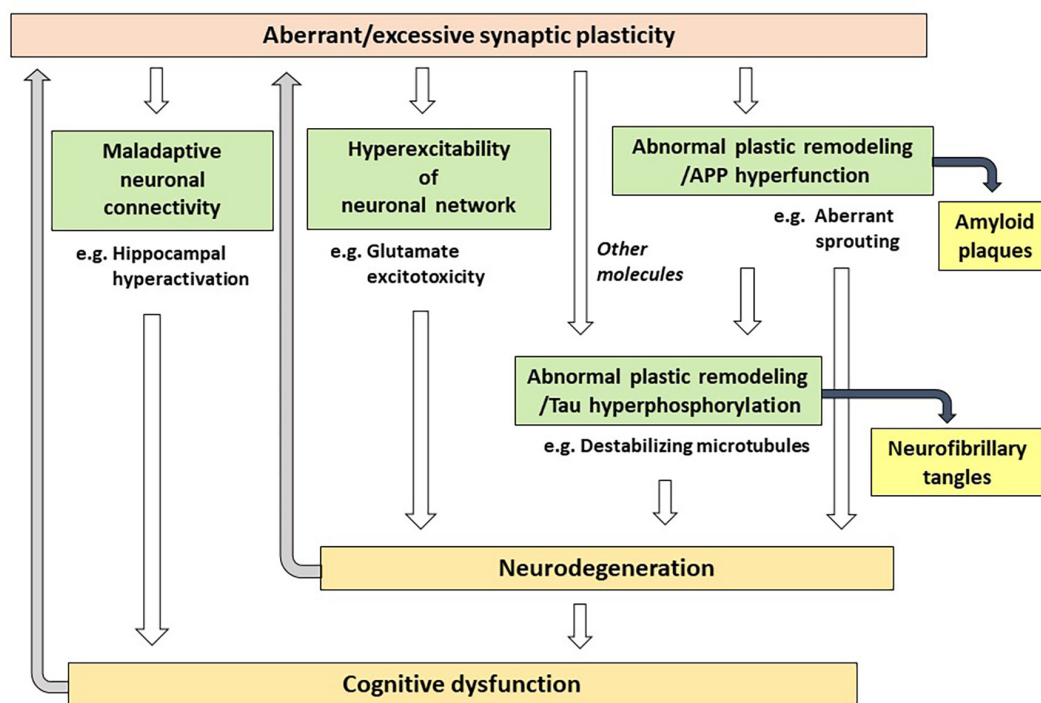


FIGURE 2 | Possible mechanisms of how aberrant/excessive plasticity causes cognitive dysfunction in Alzheimer's disease.

observed in both histological and biochemical studies (Filipello et al., 2018; Qu and Li, 2020). The increased number of synapses may be due to impaired synaptic elimination (Filipello et al., 2018). Thus, it is plausible that TREM2 deficiency exacerbated neurite abnormalities in AD mice by leading to more prominent hyperconnectivity when the mutant APP drives synaptic remodeling aberrantly. It is also suggested that the synaptic maturation process is accelerated in mice deficient in TREM2 signaling (Andoh and Koyama, 2021). Further investigations are needed to elucidate the process of synaptic plasticity and the involvement of TREM2 especially at the aged stage, and thereby provide important clues to AD pathogenesis.

CONCLUSION

AD is pathologically characterized by the existence of APs and NFTs, and symptoms of AD typically begin with mild memory loss and eventually lead to loss of the ability to carry on a conversation and respond to the environment. This sequence of clinical manifestations is consistent with the anatomic progression of the neurodegeneration. Lesions of AD begin in the hippocampus and spread to the temporal, frontal, and parietal lobes within the cerebral cortex. Numerous studies have been attempted to link AD-related molecules to the pathogenesis of AD: APOE ϵ 4-associated mechanisms (Yamazaki et al., 2019) such as A β clearance and aggregation, cerebral energy metabolism, neuroinflammation, neurovascular function, and synaptic plasticity, and presenilin-related ones such as A β production (Selkoe and Hardy, 2016), calcium homeostasis (Honarnejad and Herms, 2012) and neurogenesis (Hernandez-Sapiens et al., 2022). Such heterogeneous and multiple mechanistic pathways may work cumulatively over a lifetime to increase an individual's risk of AD. Nonetheless, the pathogenesis hypothesis needs to make logical connections with several confirmed findings, that is, the existence of both APs and NFTs, anatomical characteristics of neurodegeneration, and the similarity in pathology between FAD and SAD. The amyloid hypothesis has long been at the center of discussions. A β is believed to be toxic to neurons and have various mechanisms of action. It is also suggested that A β triggers tau aggregation and that the tau aggregate becomes a seed for further aggregation, leading to tau aggregate spread along neurons that are anatomically connected (Silva and Haggarty, 2020). Although this notion is not conclusive because of lack of evidence for the existence of a seed-competent form of extracellular tau and the mechanism of transcellular propagation (Silva and Haggarty, 2020), it can bridge the gap between APs and NFTs and provide a possible explanation for how the pathology spreads anatomically.

As an alternative to the A β hypothesis, in this paper, I propose that excessive (or aberrant) and maladaptive synaptic plasticity is the cause of AD (Figure 1). Previously, plasticity failure was proposed as a cause of AD (Mesulam, 1999). In this hypothesis, AD results if the demand for plastic remodeling exceeds the biological capacity to fulfill it. The author explains that FAD causing mutations of APP increase the demand for plastic remodeling by shifting the balance of

its processing toward more toxic form of A β . Another example is the malignant synaptic growth hypothesis, which suggests that AD develops if the positive feedback mechanism during synaptic modification is dysregulated (Newman et al., 2012). The authors suggest that A β prevents neurons from malignant synaptic growth by impairing the function of plasticity-related synaptic molecules and that FAD-linked mutations produce types of A β which have a weaker neuroprotective effect against it. Network abnormalities have also been discussed as potential mechanisms of cognitive dysfunction in AD (Palop and Mucke, 2016; Harris et al., 2020). In these papers, A β is considered to be a central molecule causing network abnormalities. In contrast to the previous discussions, hypothesis proposed here states that excessive/aberrant synaptic plasticity is a root cause for cognitive dysfunction in AD and that cognitive dysfunction is developed through maladaptive neuronal connections, hyperexcitability of neuronal network and abnormal process of synaptic remodeling (Figure 2). APP is a key player in synaptic plasticity, and in FAD, the mutant APP or presenilin leads to aberrant plasticity through altered APP metabolism and function, which initially manifest as neuronal network abnormalities. Such aberrant and maladaptive synaptic plasticity is burdensome on neurons and renders them vulnerable. Hyperexcitability of neuronal network leads to glutamate excitotoxicity that has been hypothesized to play a role in the progressive neuronal loss that underlies AD (Rogawski and Wenk, 2003). It was also reported that neurons enriched with processes related to remodeling connections with adjacent neurons are vulnerable to AD (Roussarie et al., 2020). Tau is a key regulator for microtubule dynamics, which is fundamental in the formation and remodeling of synaptic structures. Phosphorylation of tau reduces its binding affinity to microtubules, by which tau regulates the stability of microtubule bundles. Accordingly, errors during burdensome bursts of exuberant plastic remodeling may cumulatively disturb the dynamics of microtubule formation. If tau is hyperphosphorylated concomitantly, it no longer can bind to microtubules allowing neurodegeneration to progress and hyperphosphorylated tau to accumulate. Thus, a perturbation of plasticity-associated activities stemming from functional abnormalities of the mutant APP or presenilin may lie at the heart of FAD pathogenesis. As described previously (Mesulam, 1999), it is conceivable that two pathological hallmarks of AD, APs and NFTs, represent byproducts of excessive/aberrant synaptic plasticity seen in the AD brain. If APs and NFTs are byproducts of excessive/aberrant synaptic plasticity, distinctive topographic distributions of APs and NFTs and individually variable patterns of them can be explained by the likelihood that the pathological appearances depend on several independent factors, such as intrinsic neuronal properties, properties of neighboring neurons and glial cells, the extracellular environments and how excessive/aberrant synaptic plasticity takes place. The baseline activities for plastic remodeling are rising with aging, in which plasticity-related molecules other than APP come to participate. These molecules like Nerve Growth Factor are known to upregulate the expression of tau and favors its phosphorylation (Mesulam, 1999), suggesting that they may also be involved in the degenerative process by accelerating hyperphosphorylation of tau (Figure 2).

AD pathology starts in a region of high plastic remodeling activity and progresses to regions of descending order of such activity (the entorhinal cortex and the hippocampus > the association neocortex > primary sensory-motor areas) (Arendt et al., 1998). The entorhinal cortex is the area of the brain in which AD pathology is first detectable in old age in individuals with or without MCI and AD. A compensatory response in the hippocampus is triggered by the damage in the entorhinal cortex (Geddes et al., 1985; Hyman et al., 1987). If plastic remodeling occurs excessively and maladaptively in the hippocampus, it may lead to the cognitive decline significantly and the rate of AD development may increase (Dickerson et al., 2004; Dickerson and Sperling, 2008; Miller et al., 2008; O'Brien et al., 2010; Huijbers et al., 2015). Among isoforms, APOE $\epsilon 4$, a genetic risk factor of SAD, exercises the strongest plasticity-promoting effect through an APP-related mechanism (Huang et al., 2017, 2019; Lin et al., 2018). The magnitude and the extent of brain activation during memory tasks in regions affected by AD including the left hippocampus, parietal, and prefrontal regions, are greater among APOE $\epsilon 4$ carriers than among APOE $\epsilon 3$ carriers (Bookheimer et al., 2000). If one has this risk factor, plastic remodeling which occurs with aging tends to become excessive and the risk of SAD may increase. Hyperactivation of neuronal networks seems to occur at different times for different brain regions. Task-related parietal hyperactivation is seen in individuals with late-stage MCI who already show hippocampal hypoactivation (Corriveau-Lecavalier et al., 2019). Excessive plasticity seems to be involved not only in disease onset but also in disease progression. AD patients are at risk for accelerated cognitive decline, if they show epileptiform activity, which is an indicator of network hypersynchrony (Vossel et al., 2016; Horvath et al., 2021).

As discussed in this paper, decades of research do not necessarily support only the amyloid hypothesis, but also can be utilized to hypothesize excessive/aberrant and maladaptive synaptic plasticity as the cause of AD. If this hypothesis is correct, an important goal aimed at delaying the onset of AD and slowing or halting the disease progression is to find ways to adaptively regulate synaptic remodeling without interfering with necessary changes. This requires an understanding of the fundamental mechanism of synapse dynamics, and the characteristics of the stage of synaptic plasticity (formation, maturation, or elimination) at which a person developing AD is affected. Because of heterogeneity between individuals, identifying the stage of synaptic plasticity at which individuals are prone to error is a prerequisite for providing each person the appropriate intervention.

CLINICAL APPLICATION

Neuronal synchrony regulates the functional state of brain network and supports cognition. Because the network activities

are altered before the clinical onset of AD, therapeutic interventions which counteract such network abnormalities may be able to ameliorate the cognitive dysfunction seen in persons with MCI and AD. However, this strategy of therapeutic intervention may only provide symptomatic effects and for the disease modification, it may be necessary to inhibit excessive synaptic remodeling, which is the basis of network abnormalities. Interestingly, levetiracetam attenuates expression of genes known to regulate synaptic remodeling (Christensen et al., 2010), suggesting that it does not only improve cognitive performance of MCI patients (Bakker et al., 2012, 2015), but can also palliates excessive synaptic plasticity and then prevent or delay disease progression.

The use of fMRI may allow early detection of hyperactive state in the hippocampus and the presence of excessive synaptic remodeling in MCI patients. However, it may be difficult to utilize fMRI as a biomarker because of its cost and scalability as well as the need for validation and normalization of the procedure. Recent progress has been made in use of blood biomarkers for the early recognition of persons at high risk for development of AD, especially measurement of phosphorylated tau (P-tau) species such as P-tau181, P-tau217, and P-tau231 (Verde, 2022). The gradual rise in plasma levels of P-tau species may be able to predict the age at which a person develops clinically recognized AD (Verde, 2022). When synaptic remodeling takes place, tau is phosphorylated and its binding affinity to microtubules is reduced, implying that an increase in the P-tau levels may be a sign of a perturbation of excessive plasticity-associated activities. Thus, the plasma level of P-tau species may be able to identify persons who may benefit from early therapeutic intervention.

DATA AVAILABILITY STATEMENT

The original contributions presented in this study are included in the article/supplementary material, further inquiries can be directed to the corresponding author.

AUTHOR CONTRIBUTIONS

SK contributed to the conceptualization and wrote the manuscript.

ACKNOWLEDGMENTS

I thank Myron Miller, Johns Hopkins University School of Medicine and Sinai Hospital of Baltimore for his invaluable comments on the manuscript.

REFERENCES

Andoh, M., and Koyama, R. (2021). Microglia regulate synaptic development and plasticity. *Dev. Neurobiol.* 81, 568–590. doi: 10.1002/dneu.22814

Arendt, T., Brückner, M. K., Gertz, H. J., and Marcova, L. (1998). Cortical distribution of neurofibrillary tangles in Alzheimer's disease matches the pattern of neurons that retain their capacity of plastic remodeling in the adult brain. *Neuroscience* 83, 991–1002. doi: 10.1016/s0306-4522(97)00509-5

- Badhwar, A. P., Tam, A., Dansereau, C., Orban, P., Hoffstaedter, F., and Bellec, P. (2017). Resting-state network dysfunction in Alzheimer's disease: a systematic review and meta-analysis. *Alzheimers Dement.* 18, 73–85. doi: 10.1016/j.dadm.2017.03.007
- Bakker, A., Albert, M. S., Krauss, G., Speck, C. L., and Gallagher, M. (2015). Response of the medial temporal lobe network in amnesic mild cognitive impairment to therapeutic intervention assessed by fMRI and memory task performance. *Neuroimage Clin.* 7, 688–698. doi: 10.1016/j.nicl.2015.02.009
- Bakker, A., Krauss, G. L., Albert, M. S., Speck, C. L., Jones, L. R., Stark, C. E., et al. (2012). Reduction of hippocampal hyperactivity improves cognition in amnesic mild cognitive impairment. *Neuron* 74, 467–474. doi: 10.1016/j.neuron.2012.03.023
- Ben-Nejma, I. R. H., Keliris, A. J., Daans, J., Ponsaerts, P., Verhoye, M., Van der Linden, A., et al. (2019). Increased soluble amyloid-beta causes early aberrant brain network hypersynchronisation in a mature-onset mouse model of amyloidosis. *Acta Neuropathol. Commun.* 7:180. doi: 10.1186/s40478-019-0810-7
- Bero, A. W., Bauer, A. Q., Stewart, F. R., White, B. R., Cirrito, J. R., Raichle, M. E., et al. (2012). Bidirectional relationship between functional connectivity and amyloid- β deposition in mouse brain. *J. Neurosci.* 32, 4334–4340. doi: 10.1523/JNEUROSCI.5845-11.2012
- Bezzina, C., Verret, L., Juan, C., Remaud, J., Halley, H., Rampon, C., et al. (2015). Early onset of hypersynchronous network activity and expression of a marker of chronic seizures in the Tg2576 mouse model of Alzheimer's disease. *PLoS One* 10:e0119910. doi: 10.1371/journal.pone.0119910
- Blakemore, S.-J., and Choudhury, S. (2006). Development of the adolescent brain: implications for executive function and social cognition. *J. Child Psychol. Psychiatry* 47, 296–312. doi: 10.1111/j.1469-7610.2006.01611.x
- Blazquez-Llorca, L., Valero-Freitag, S., Rodríguez, E. F., Merchán-Pérez, Á., Rodríguez, J. R., Dorostkar, M. M., et al. (2017). High plasticity of axonal pathology in Alzheimer's disease mouse models. *Acta Neuropathol. Commun.* 5, 14. doi: 10.1186/s40478-017-0415-y
- Bookheimer, S. Y., Strojwas, M. H., Cohen, M. S., Saunders, A. M., Pericak-Vance, M. A., Mazziotta, J. C., et al. (2000). Patterns of brain activation in people at risk for Alzheimer's disease. *N. Engl. J. Med.* 343, 450–456. doi: 10.1056/NEJM200008173430701
- Brendza, R. P., Bales, K. R., Paul, S. M., and Holtzman, D. M. (2002). Role of apoE/A β interactions in Alzheimer's disease: insights from transgenic mouse models. *Mol. Psychiatry* 7, 132–135. doi: 10.1038/sj.mp.4001006
- Busche, M. A., Chen, X., Henning, H. A., Reichwald, J., Staufenbiel, M., Sakmann, B., et al. (2012). Critical role of soluble amyloid- β for early hippocampal hyperactivity in a mouse model of Alzheimer's disease. *Proc. Natl. Acad. Sci. U.S.A.* 109, 8740–8745. doi: 10.1073/pnas.1206171109
- Busche, M. A., Eichhoff, G., Adelsberger, H., Abramowski, D., Wiederhold, K.-H., Haass, C., et al. (2008). Clusters of hyperactive neurons near amyloid plaques in a mouse model of Alzheimer's disease. *Science* 319, 1686–1689. doi: 10.1126/science.1162844
- Cabral, J., Luckhoo, H., Woolrich, M., Joensson, M., Mohseni, H., Baker, A., et al. (2014). Exploring mechanisms of spontaneous functional connectivity in MEG: how delayed network interactions lead to structured amplitude envelopes of band-pass filtered oscillations. *Neuroimage* 90, 423–435. doi: 10.1016/j.neuroimage.2013.11.047
- Carrillo-Mora, P., Luna, R., and Colín-Barenque, L. (2014). Amyloid beta: multiple mechanisms of toxicity and only some protective effects? *Oxid. Med. Cell. Longev.* 2014:795375. doi: 10.1155/2014/795375
- Chhatwal, J. P., Schultz, A. P., Johnson, K., Benzinger, T. L. S., Jack, C. Jr., Ances, B. M., et al. (2013). Impaired default network functional connectivity in autosomal dominant Alzheimer disease. *Neurology* 81, 736–744. doi: 10.1212/WNL.0b013e3182a1aaf6
- Christensen, K. V., Leffers, H., Watson, W. P., Sánchez, C., Kallunki, P., and Egebjerg, J. (2010). Levetiracetam attenuates hippocampal expression of synaptic plasticity-related immediate early and late response genes in amygdala-kindled rats. *BMC Neurosci.* 11:9. doi: 10.1186/1471-2202-11-9
- Corriveau-Lecavalier, N., Mellah, S., Clément, F., and Belleville, S. (2019). Evidence of parietal hyperactivation in individuals with mild cognitive impairment who progressed to dementia: a longitudinal fMRI study. *Neuroimage Clin.* 24:101958. doi: 10.1016/j.nicl.2019.101958
- Corriveau-Lecavalier, N., Rajah, M. N., Mellah, S., and Belleville, S. (2021a). Latent patterns of task-related functional connectivity in relation to regions of hyperactivation in individuals at risk of Alzheimer's disease. *Neuroimage Clin.* 30, 102643. doi: 10.1016/j.nicl.2021.102643
- Corriveau-Lecavalier, N., Duchesne, S., Gauthier, S., Hudon, G., Kergoat, M.-J., Mellah, S., et al. (2021b). A quadratic function of activation in individuals at risk of Alzheimer's disease. *Alzheimers Dement.* 12:e12139. doi: 10.1002/dad2.12139
- Dennis, N. A., Shine, J. P., Williams, H., Postans, M., Sims, R., Williams, J., et al. (2010). Temporal lobe functional activity and connectivity in young adult APOE ϵ 4 carriers. *Alzheimers Dement.* 6, 303–311. doi: 10.1016/j.neurobiolaging.2018.08.026
- Devkota, S., Williams, T. D., and Wolfe, M. S. (2021). Familial Alzheimer's disease mutations in amyloid protein precursor alter proteolysis by γ -secretase to increase A β -peptides of ≥ 45 residues. *J. Biol. Chem.* 296:100281. doi: 10.1016/j.jbc.2021.100281
- Deyts, C., Clutter, M., Herrera, S., Jovanovic, N., Goddi, A., and Parent, A. T. (2016). Loss of presenilin function is associated with a selective gain of APP function. *eLife* 5:e15645. doi: 10.7554/eLife.15645
- Deyts, C., Vetrivel, K. S., Das, S., Shepherd, Y. M., Dupré, D. J., Thinakaran, G., et al. (2012). Novel G α S-protein signaling associated with membrane-tethered amyloid precursor protein intracellular domain. *J. Neurosci.* 32, 1714–1729. doi: 10.1523/JNEUROSCI.5433-11.2012
- Dickerson, B. C., Salat, D. H., Bates, J. F., Atiya, M., Killiany, R. J., Greve, D. N., et al. (2004). Medial temporal lobe function and structure in mild cognitive impairment. *Ann. Neurol.* 56, 27–35. doi: 10.1002/ana.20163
- Dickerson, B. C., and Sperling, R. A. (2008). Functional abnormalities of the medial temporal lobe memory system in mild cognitive impairment and Alzheimer's disease: insights from functional MRI studies. *Neuropsychologia* 46, 1624–1635. doi: 10.1016/j.neuropsychologia.2007.11.030
- Farrer, L. A., Cupples, L. A., Haines, J. L., Hyman, B., Kukull, W. A., Mayeux, R., et al. (1997). Effects of age, sex, and ethnicity on the association between apolipoprotein E genotype and Alzheimer disease. A meta-analysis. APOE and Alzheimer Disease Meta Analysis Consortium. *JAMA* 278, 1349–1356. doi: 10.1001/jama.278.16.1349
- Filipello, F., Morini, R., Corradini, I., Zerbi, V., Canzi, A., Michalski, B., et al. (2018). The Microglial Innate Immune Receptor TREM2 Is Required for Synapse Elimination and Normal Brain Connectivity. *Immunity* 48, 979–991. doi: 10.1016/j.immuni.2018.04.016
- Filippini, N., MacIntosh, B. J., Hough, M. G., Goodwin, G. M., Frisoni, G. B., Smith, S. M., et al. (2009). Distinct patterns of brain activity in young carriers of the APOE- ϵ 4 allele. *Proc. Natl. Acad. Sci. U.S.A.* 106, 7209–7214. doi: 10.1073/pnas.0811879106
- Freund, T. F., and Katona, I. (2007). Perisomatic inhibition. *Neuron* 56, 33–42. doi: 10.1016/j.neuron.2007.09.012
- Geddes, J. W., Monaghan, D. T., Cotman, C. W., Lott, I. T., Kim, R. C., and Chui, H. C. (1985). Plasticity of hippocampal circuitry in Alzheimer's disease. *Science* 230, 1179–1181. doi: 10.1126/science.4071042
- Grady, C. (2012). The cognitive neuroscience of ageing. *Nat. Rev. Neurosci.* 13, 491–505. doi: 10.1038/nrn3256
- Guerreiro, R., Wojtas, A., Bras, J., Carrasquillo, M., Rogaeva, E., Majounie, E., et al. (2013). TREM2 variants in Alzheimer's disease. *N. Engl. J. Med.* 368, 117–127. doi: 10.1056/NEJMoa1211851
- Gurevicius, K., Lipponen, A., and Tanila, H. (2013). Increased cortical and thalamic excitability in freely moving APPswe/PS1dE9 mice modeling epileptic activity associated with Alzheimer's disease. *Cereb. Cortex* 23, 1148–1158. doi: 10.1093/cercor/bhs105
- Harris, S. S., Wolf, F., De Strooper, B., and Busche, M. A. (2020). Tipping the scales: peptide-dependent dysregulation of neural circuit dynamics in Alzheimer's disease. *Neuron* 107, 417–435. doi: 10.1016/j.neuron.2020.06.005
- Hernandez-Sapiens, M. A., Reza-Zaldivar, E. E., Aguirre, A. L., Gómez-Pinedo, U., Matias-Guiu, J., Cevallos, R. R., et al. (2022). Presenilin mutations and their impact on neuronal differentiation in Alzheimer's disease. *Neural Regen. Res.* 17, 31–37. doi: 10.4103/1673-5374.313016
- Hijazi, S., Heistek, T. S., Scheltens, P., Neumann, U., Shimshek, D. R., Mansvelder, H. D., et al. (2020). Early restoration of parvalbumin interneuron activity prevents memory loss and network hyperexcitability in a mouse model of

- Alzheimer's disease. *Mol. Psychiatry* 25, 3380–3398. doi: 10.1038/s41380-019-0483-4
- Honarnejad, K., and Herms, J. (2012). Presenilins: role in calcium homeostasis. *Int. J. Biochem. Cell Biol.* 44, 1983–1986. doi: 10.1016/j.biocel.2012.07.019
- Horvath, A. A., Papp, A., Zsuffa, J., Szucs, A., Luckl, J., Radai, F., et al. (2021). Subclinical epileptiform activity accelerates the progression of Alzheimer's disease: a long-term EEG study. *Clin. Neurophysiol.* 132, 1982–1989. doi: 10.1016/j.clinph.2021.03.050
- Huang, Y.-W. A., Zhou, B., Nabat, A. M., Wernig, M., and Südhof, T. C. (2019). Differential Signaling Mediated by ApoE2, ApoE3, and ApoE4 in Human Neurons Parallels Alzheimer's Disease Risk. *J. Neurosci.* 39, 7408–7427. doi: 10.1523/JNEUROSCI.2994-18.2019
- Huang, Y.-W. A., Zhou, B., Wernig, M., and Südhof, T. C. (2017). ApoE2, ApoE3, and ApoE4 Differentially Stimulate APP Transcription and A β Secretion. *Cell* 168, 427–441. doi: 10.1016/j.cell.2016.12.044
- Huijbers, W., Mormino, E. C., Schultz, A. P., Wigman, S., Ward, A. M., Larvie, M., et al. (2015). Amyloid- β deposition in mild cognitive impairment is associated with increased hippocampal activity, atrophy and clinical progression. *Brain* 138, 1023–1035. doi: 10.1093/brain/awv007
- Hyman, B. T., Kromer, L. J., and Van Hoesen, G. W. (1987). Reinnervation of the hippocampal perforant pathway zone in Alzheimer's disease. *Ann. Neurol.* 21, 259–267. doi: 10.1002/ana.410210307
- Jonsson, T., Stefansson, H., Steinberg, S., Jonsson, P. V., Snaedal, J., et al. (2013). Variant of TREM2 associated with the risk of Alzheimer's disease. *N. Engl. J. Med.* 368, 107–116. doi: 10.1056/NEJMoa1211103
- Kamenetz, E., Tomita, T., Hsieh, H., Seabrook, G., Borchelt, D., Iwatsubo, T., et al. (2003). APP processing and synaptic function. *Neuron* 37, 925–937. doi: 10.1016/s0896-6273(03)00124-7
- Kamphuis, W., Huisman, E., Wadman, W. J., Heizmann, C. W., and Lopes da Silva, F. H. (1989). Kindling induced changes in parvalbumin immunoreactivity in rat hippocampus and its relation to long-term decrease in GABA-immunoreactivity. *Brain Res.* 479, 23–34. doi: 10.1016/0006-8993(89)91331-0
- Kazim, S. F., Chuang, S.-C., Zhao, W., Wong, R. K. S., Bianchi, R., and Iqbal, K. (2017). Early-Onset Network Hyperexcitability in Presymptomatic Alzheimer's disease transgenic mice is suppressed by passive immunization with anti-human APP/A β Antibody and by mGluR5 Blockade. *Front. Aging Neurosci.* 9:71. doi: 10.3389/fnagi.2017.00071
- Kim, J., Yoon, H., Basak, J., and Kim, J. (2014). Apolipoprotein E in synaptic plasticity and Alzheimer's disease: potential cellular and molecular mechanisms. *Mol. Cells* 37, 767–776. doi: 10.14348/molcells.2014.0248
- Klevanski, M., Herrmann, U., Weyer, S. W., Fol, B., Cartier, N., Wolfer, D. P., et al. (2015). The APP intracellular domain is required for normal synaptic morphology, synaptic plasticity, and hippocampus-dependent behavior. *J. Neurosci.* 35, 16018–16033. doi: 10.1523/JNEUROSCI.2009-15.2015
- Kobayashi, M., and Buckmaster, P. S. (2003). Reduced inhibition of dentate granule cells in a model of temporal lobe epilepsy. *J. Neurosci.* 23, 2440–2452. doi: 10.1523/JNEUROSCI.23-06-02440.2003
- Koelewijn, L., Lancaster, T. M., Linden, D., Dima, D. C., Routley, B. C., Magazzini, L., et al. (2019). Oscillatory hyperactivity and hyperconnectivity in young APOE- ϵ 4 carriers and hypoconnectivity in Alzheimer's disease. *eLife* 8:e36011. doi: 10.7554/eLife.36011
- Kurudenkandy, F. R., Zilberter, N., Biverstål, H., Presto, J., Honcharenko, D., Strömberg, R., et al. (2014). Amyloid- β -induced action potential desynchronization and degradation of hippocampal gamma oscillations is prevented by interference with peptide conformation change and aggregation. *J. Neurosci.* 34, 11416–11425. doi: 10.1523/JNEUROSCI.1195-14.2014
- Lee, K. L., Moussa, C. E. H., Lee, Y., Sung, Y., Howell, B. W., Turner, R. S., et al. (2010). Beta amyloid-independent role of amyloid precursor protein in generation and maintenance of dendritic spines. *Neuroscience* 169, 344–356. doi: 10.1016/j.neuroscience.2010.04.078
- Leng, X., Xiang, J., Yang, Y., Yu, T., Qi, X., Zhang, X., et al. (2020). Frequency-specific changes in the default mode network in patients with cingulate gyrus epilepsy. *Hum. Brain Mapp.* 41, 2447–2459. doi: 10.1002/hbm.24956
- Leyssen, M., Ayaz, D., Hébert, S. S., Reeve, S., De Strooper, B., and Hassan, B. A. (2005). Amyloid precursor protein promotes post-developmental neurite arborization in the Drosophila brain. *EMBO J.* 24, 2944–2955. doi: 10.1038/sj-emboj.7600757
- Li, N., Liu, K., Qiu, Y., Ren, Z., Dai, R., Deng, Y., et al. (2016). Effect of Presenilin Mutations on APP Cleavage; Insights into the Pathogenesis of FAD. *Front Aging Neurosci.* 8:51. doi: 10.3389/fnagi.2016.00051
- Lin, Y.-T., Seo, J., Gao, F., Feldman, H. M., Wen, H.-L., Penney, J., et al. (2018). APOE4 Causes Widespread Molecular and Cellular Alterations Associated with Alzheimer's Disease Phenotypes in Human iPSC-Derived Brain Cell Types. *Neuron* 98, 1141–1154. doi: 10.1016/j.neuron.2018.06.011
- Masliah, E., Mallory, M., Hansen, L., Alford, M., Albright, T., DeTeresa, R., et al. (1991). Patterns of aberrant sprouting in Alzheimer's disease. *Neuron* 6, 729–739. doi: 10.1016/0896-6273(91)90170-5
- Mesulam, M. M. (1999). Neuroplasticity failure in Alzheimer's disease: bridging the gap between plaques and tangles. *Neuron* 24, 521–529. doi: 10.1016/s0896-6273(00)81109-5
- Miller, S. L., Fenstermacher, E., Bates, J., Blacker, D., Sperling, R. A., and Dickerson, B. C. (2008). Hippocampal activation in adults with mild cognitive impairment predicts subsequent cognitive decline. *J. Neurol. Neurosurg. Psychiatry* 79, 630–635. doi: 10.1136/jnnp.2007.124149
- Moga, D., Hof, P. R., Vissavajhala, P., Moran, T. M., and Morrison, J. H. (2002). Parvalbumin-containing interneurons in rat hippocampus have an AMPA receptor profile suggestive of vulnerability to excitotoxicity. *J. Chem. Neuroanat.* 23, 249–253. doi: 10.1016/s0891-0618(02)00012-1
- Newman, F. L., Shay, C. F., and Hasselmo, M. E. (2012). Malignant synaptic growth and Alzheimer's disease. *Future Neurol.* 7, 557–571. doi: 10.2217/fnl.12.47
- O'Brien, J. L., O'Keefe, K. M., LaViolette, P. S., DeLuca, A. N., Blacker, D., Dickerson, B. C., et al. (2010). Longitudinal fMRI in elderly reveals loss of hippocampal activation with clinical decline. *Neurology* 74, 1969–1976. doi: 10.1212/WNL.0b013e3181e3966e
- Ossandón, T., Jerbi, K., Vidal, J. R., Bayle, D. J., Henaff, M.-A., Jung, J., et al. (2011). Transient suppression of broadband gamma power in the default-mode network is correlated with task complexity and subject performance. *J. Neurosci.* 31, 14521–14530. doi: 10.1523/JNEUROSCI.2483-11.2011
- Palop, J. J., Chin, J., Roberson, E. D., Wang, J., Thwin, M. T., Bien-Ly, N., et al. (2007). Aberrant excitatory neuronal activity and compensatory remodeling of inhibitory hippocampal circuits in mouse models of Alzheimer's disease. *Neuron* 55, 697–711. doi: 10.1016/j.neuron.2007.07.025
- Palop, J. J., and Mucke, L. (2016). Network abnormalities and interneuron dysfunction in Alzheimer disease. *Nat. Rev. Neurosci.* 17, 777–792. doi: 10.1038/nrn.2016.141
- Petrache, A. L., Rajulawalla, A., Shi, A., Wetzel, A., Saito, T., Saido, T. C., et al. (2019). Aberrant Excitatory-Inhibitory Synaptic Mechanisms in Entorhinal Cortex Microcircuits During the Pathogenesis of Alzheimer's Disease. *Cereb. Cortex* 29, 1834–1850. doi: 10.1093/cercor/bhz016
- Phinney, A. L., Deller, T., Stalder, M., Calhoun, M. E., Frotscher, M., Sommer, B., et al. (1999). Cerebral amyloid induces aberrant axonal sprouting and ectopic terminal formation in amyloid precursor protein transgenic mice. *J. Neurosci.* 19, 8552–8559. doi: 10.1523/JNEUROSCI.19-19-08552.1999
- Qu, W., and Li, L. (2020). Loss of TREM2 confers resilience to synaptic and cognitive impairment in aged mice. *J. Neurosci.* 40, 9552–9563. doi: 10.1523/JNEUROSCI.2193-20.2020
- Quiroz, Y. T., Budson, A. E., Celone, K., Ruiz, A., Newmark, R., Castrillón, G., et al. (2010). Hippocampal hyperactivation in presymptomatic familial Alzheimer's disease. *Ann. Neurol.* 68, 865–875. doi: 10.1002/ana.22105
- Quiroz, Y. T., Schultz, A. P., Chen, K., Protas, H. D., Brickhouse, M., Fleisher, A. S., et al. (2015). Brain imaging and blood biomarker abnormalities in children with autosomal dominant Alzheimer disease: a cross-sectional study. *JAMA Neurol.* 72, 912–919. doi: 10.1001/jamaneurol.2015.1099
- Ray, A., Bernhard, S. M., Kuljis, D. A., Bruchez, M. P., and Barth, A. L. (2020). Early developmental abnormalities in hippocampal synapse distribution in a mouse model of Alzheimer's disease. *Alzheimers Dement.* 16:e044118. doi: 10.1002/alz.044118
- Rice, H. C., Marcassa, G., Chrysidou, I., Horré, K., Young-Pearse, T. L., Müller, U. C., et al. (2020). Contribution of GABAergic interneurons to amyloid- β plaque pathology in an APP knock-in mouse model. *Mol. Neurodegener.* 15:3. doi: 10.1186/s13024-019-0356-y

- Rogawski, M. A., and Wenk, G. L. (2003). The neuropharmacological basis for the use of memantine in the treatment of Alzheimer's disease. *CNS Drug Rev.* 9, 275–308. doi: 10.1111/j.1527-3458.2003.tb00254.x
- Roussarie, J.-P., Yao, V., Rodriguez-Rodriguez, P., Oughtred, R., Rust, J., Plautz, Z., et al. (2020). Selective neuronal vulnerability in Alzheimer's disease: a network-based analysis. *Neuron* 107, 821–835. doi: 10.1016/j.neuron.2020.06.010
- Sasaguri, H., Nilsson, H. P., Hashimoto, S., Nagata, K., Saito, T., De Strooper, B., et al. (2017). APP mouse models for Alzheimer's disease preclinical studies. *EMBO J.* 36, 2473–2487. doi: 10.15252/embj.201797397
- Selkoe, D. J., and Hardy, J. (2016). The amyloid hypothesis of Alzheimer's disease at 25 years. *EMBO Mol. Med.* 8, 595–608. doi: 10.15252/emmm.201606210
- Shah, D., Latif-Hernandez, A., De Strooper, B., Saito, T., Saido, T., Verhoye, M., et al. (2018). Spatial reversal learning defect coincides with hypersynchronous telencephalic BOLD functional connectivity in APP NL-F/NL-F knock-in mice. *Sci. Rep.* 8:6264. doi: 10.1038/s41598-018-24657-9
- Shine, J. P., Hodgetts, C. J., Postans, M., Lawrence, A. D., and Graham, K. S. (2015). APOE-ε4 selectively modulates posteromedial cortex activity during scene perception and short-term memory in young healthy adults. *Sci. Rep.* 5:16322. doi: 10.1038/srep16322
- Silva, M. C., and Haggarty, S. J. (2020). Tauopathies: deciphering disease mechanisms to develop effective therapies. *Int. J. Mol. Sci.* 21:8948. doi: 10.3390/ijms21238948
- Snyder, E. M., Nong, Y., Almeida, C. G., Paul, S., Moran, T., Choi, E. Y., et al. (2005). Regulation of NMDA receptor trafficking by amyloid-beta. *Nat. Neurosci.* 8, 1051–1058. doi: 10.1038/nn1503
- Sohal, V. S., Zhang, F., Yizhar, O., and Deisseroth, K. (2009). Parvalbumin neurons and gamma rhythms enhance cortical circuit performance. *Nature* 459, 698–702. doi: 10.1038/nature07991
- Soldano, A., Okray, Z., Janovska, P., Tmejová, K., Reynaud, E., Claeys, A., et al. (2013). The Drosophila homologue of the amyloid precursor protein is a conserved modulator of Wnt PCP signaling. *PLoS Biol.* 11:e1001562. doi: 10.1371/journal.pbio.1001562
- Song, W. M., Joshita, S., Zhou, Y., Ulland, T. K., Gilfillan, S., and Colonna, M. (2018). Humanized TREM2 mice reveal microglia-intrinsic and -extrinsic effects of R47H polymorphism. *J. Exp. Med.* 215, 745–760. doi: 10.1084/jem.20171529
- Sperling, R. A., Dickerson, B. C., Pihlajamäki, M., Vannini, P., LaViolette, P. S., Vitolo, O. V., et al. (2010). Functional alterations in memory networks in early Alzheimer's disease. *Neuromol. Med.* 12, 27–43. doi: 10.1007/s12017-009-8109-7
- Su, Y. Y., Liang, X., Schoepf, U. J., Varga-Szemes, A., West, H. C., Qi, R., et al. (2015). APOE polymorphism affects brain default mode network in healthy young adults. *Medicine* 94:e1734. doi: 10.1097/MD.0000000000001734
- Sun, L., Zhou, R., Yang, G., and Shiet, Y. (2017). Analysis of 138 pathogenic mutations in presenilin-1 on the in vitro production of Aβ42 and Aβ40 peptides by γ-secretase. *Proc. Natl. Acad. Sci. U.S.A.* 114, E476–E485. doi: 10.1073/pnas.1618657114
- Torres, L., Packard, M., Gorczyca, M., White, K., and Budnik, V. (1999). The Drosophila beta-amyloid precursor protein homolog promotes synapse differentiation at the neuromuscular junction. *J. Neurosci.* 19, 7793–7803. doi: 10.1523/JNEUROSCI.19-18-07793.1999
- Verdaguer, E., Brox, S., Petrov, D., Olloquequi, J., Romero, R., de Lemos, M. L., et al. (2015). Vulnerability of calbindin, calretinin and parvalbumin in a transgenic/knock-in APPsw/PS1dE9 mouse model of Alzheimer disease together with disruption of hippocampal neurogenesis. *Exp. Gerontol.* 69, 176–188. doi: 10.1016/j.exger.2015.06.013
- Verde, F. (2022). Tau proteins in blood as biomarkers of Alzheimer's disease and other proteinopathies. *J. Neural. Transm.* 129, 239–259. doi: 10.1007/s00702-022-02471-y
- Verret, L., Mann, E. O., Hang, G. B., Barth, A. M. I., Cobos, I., Ho, K., et al. (2012). Inhibitory interneuron deficit links altered network activity and cognitive dysfunction in Alzheimer model. *Cell* 149, 708–721. doi: 10.1016/j.cell.2012.02.046
- Vossel, K. A., Ranasinghe, K. G., Beagle, A. J., Mizuiri, D., Honma, S. M., Dowling, A. F., et al. (2016). Incidence and impact of subclinical epileptiform activity in Alzheimer's disease. *Ann. Neurol.* 80, 858–870. doi: 10.1002/ana.24794
- Wang, B., Wang, Z., Sun, L., Yang, L., Li, H., Cole, A. L., et al. (2014). The amyloid precursor protein controls adult hippocampal neurogenesis through GABAergic interneurons. *J. Neurosci.* 34, 13314–13325. doi: 10.1523/JNEUROSCI.2848-14.2014
- Wang, S., Ulland, T. K., Ulrich, J. D., Song, W., Tzaferis, J. A., Hole, J. T., et al. (2016). TREM2-mediated early microglial response limits diffusion and toxicity of amyloid plaques. *J. Exp. Med.* 213, 667–675. doi: 10.1084/jem.20151948
- Yamazaki, Y., Zhao, N., Caulfield, T. R., Liu, C.-C., and Bu, G. (2019). Apolipoprotein E and Alzheimer disease: pathobiology and targeting strategies. *Nat. Rev. Neurol.* 15, 501–518. doi: 10.1038/s41582-019-0228-7
- Yassa, M. A., Stark, S. M., Bakker, A., Albert, M. S., Gallagher, M., and Stark, C. E. L. (2010). High-resolution structural and functional MRI of hippocampal CA3 and dentate gyrus in patients with amnesic Mild Cognitive Impairment. *Neuroimage* 51, 1242–1252. doi: 10.1016/j.neuroimage.2010.03.040
- Yuan, P., Condello, C., Keene, C. D., Wang, Y., Bird, T. D., Paul, S. M., et al. (2016). TREM2 haploinsufficiency in mice and humans impairs the microglia barrier function leading to decreased amyloid compaction and severe axonal dystrophy. *Neuron* 92, 252–264. doi: 10.1016/j.neuron.2016.09.016
- Zarea, A., Charbonnier, C., Rovelet-Lecrux, A., Nicolas, G., Rousseau, S., Borden, A., et al. (2016). Seizures in dominantly inherited Alzheimer disease. *Neurology* 87, 912–919. doi: 10.1212/WNL.0000000000003048
- Zhou, R., Yang, G., and Shi, Y. (2017). Dominant negative effect of the loss-of-function γ-secretase mutants on the wild-type enzyme through heterooligomerization. *Proc. Natl. Acad. Sci. U.S.A.* 114, 12731–12736. doi: 10.1073/pnas.1713605114
- Zott, B., Busche, M. A., Sperling, R. A., and Konnerth, A. (2018). What happens with the circuit in Alzheimer's disease in mice and humans? *Annu. Rev. Neurosci.* 41, 277–297. doi: 10.1146/annurev-neuro-080317-061725
- Zott, B., Simon, M. M., Hong, W., Unger, F., Chen-Engerer, H.-J., Froesch, M. P., et al. (2019). A vicious cycle of β amyloid-dependent neuronal hyperactivation. *Science* 365, 559–565. doi: 10.1126/science.aay0198

Conflict of Interest: SK was employed by Somp Care Inc.

Publisher's Note: All claims expressed in this article are solely those of the authors and do not necessarily represent those of their affiliated organizations, or those of the publisher, the editors and the reviewers. Any product that may be evaluated in this article, or claim that may be made by its manufacturer, is not guaranteed or endorsed by the publisher.

Copyright © 2022 Kawabata. This is an open-access article distributed under the terms of the Creative Commons Attribution License (CC BY). The use, distribution or reproduction in other forums is permitted, provided the original author(s) and the copyright owner(s) are credited and that the original publication in this journal is cited, in accordance with accepted academic practice. No use, distribution or reproduction is permitted which does not comply with these terms.



OPEN ACCESS

EDITED BY

Nilton Custodio,
Peruvian Institute of Neurosciences
(IPN), Peru

REVIEWED BY

Iain Hargreaves,
University of Liverpool,
United Kingdom
Mateusz Maciejczyk,
Medical University of Białystok, Poland

*CORRESPONDENCE

Ping-Ting Lin
apt810@csmu.edu.tw

SPECIALTY SECTION

This article was submitted to
Alzheimer's Disease and Related
Dementias,
a section of the journal
Frontiers in Aging Neuroscience

RECEIVED 01 April 2022

ACCEPTED 06 July 2022

PUBLISHED 25 July 2022

CITATION

Chang P-S, Chou H-H, Lai T-J,
Yen C-H, Pan J-C and Lin P-T (2022)
Investigation of coenzyme Q10 status,
serum amyloid- β , and tau protein
in patients with dementia.
Front. Aging Neurosci. 14:910289.
doi: 10.3389/fnagi.2022.910289

COPYRIGHT

© 2022 Chang, Chou, Lai, Yen, Pan
and Lin. This is an open-access article
distributed under the terms of the
[Creative Commons Attribution License
\(CC BY\)](#). The use, distribution or
reproduction in other forums is
permitted, provided the original
author(s) and the copyright owner(s)
are credited and that the original
publication in this journal is cited, in
accordance with accepted academic
practice. No use, distribution or
reproduction is permitted which does
not comply with these terms.

Investigation of coenzyme Q10 status, serum amyloid- β , and tau protein in patients with dementia

Po-Sheng Chang^{1,2}, Hsi-Hsien Chou^{3,4}, Te-Jen Lai^{5,6},
Chi-Hua Yen^{3,7}, Ji-Cyun Pan¹ and Ping-Ting Lin^{1,8*}

¹Department of Nutrition, Chung Shan Medical University, Taichung, Taiwan, ²Graduate Program in Nutrition, Chung Shan Medical University, Taichung, Taiwan, ³School of Medicine, Chung Shan Medical University, Taichung, Taiwan, ⁴Department of Neurology, Chung Shan Medical University Hospital, Taichung, Taiwan, ⁵Institute of Medicine, Chung Shan Medical University, Taichung, Taiwan, ⁶Department of Psychiatry, Chung Shan Medical University Hospital, Taichung, Taiwan, ⁷Department of Family and Community Medicine, Chung Shan Medical University Hospital, Taichung, Taiwan, ⁸Department of Nutrition, Chung Shan Medical University Hospital, Taichung, Taiwan

Objectives: Dementia is an oxidative stress-related disease. Coenzyme Q10 is a nutrient that occurs naturally in the human body and acts as an antioxidant. The purpose of this study was to investigate the relationships of coenzyme Q10 status, biomarkers for dementia (amyloid β and tau protein), and antioxidant capacity in patients with dementia.

Methods: Eighty dementia patients aged ≥ 60 years and with a mini mental state examination (MMSE) score ≤ 26 were enrolled. The levels of coenzyme Q10, total antioxidant capacity (TAC), amyloid β , and tau protein were measured.

Results: A total of 73% of patients had a low coenzyme Q10 status. Patients with low coenzyme Q10 status had a significantly higher level of serum amyloid β -42 and amyloid β -42/40 ratio ($p < 0.05$). Coenzyme Q10 status was significantly correlated with the values of TAC, MMSE score, amyloid β -42, and amyloid β -42/40 ratio ($p < 0.05$) but not with tau protein. Additionally, a high proportion of moderate dementia patients were found to have low coenzyme Q10 status ($p = 0.07$).

Conclusion: Patients with dementia suffered from coenzyme Q10 deficiency, and the degree of deficiency was related to the level of amyloid- β and antioxidant capacity. Since adequate level of coenzyme Q10 may delay the progression of dementia, monitoring coenzyme Q10 status in patients with dementia is necessary.

KEYWORDS

coenzyme Q10, antioxidant capacity, amyloid- β , tau protein, dementia

Introduction

Dementia has become a critical public health issue. The latest report of the World Health Organization estimated that more than 55 million people are living with dementia worldwide, and the number is growing every year (WHO, 2021). The pathophysiology of dementia is credited to the extracellular growth of amyloid- β oligomers causing insoluble plaques and the hyperphosphorylation of tau protein that produces neurofibrillary tangles within neuron cells, which damages synapses that mediate memory and cognition (Bloom, 2014). Dementia is also an oxidative stress-related and mitochondrial dysfunction disease (Cabezas-Opazo et al., 2015; Tönnies and Trushina, 2017). Patients with dementia have a higher level of oxidative stress and reduced antioxidant defenses, which changes the synaptic activity and neurotransmitter release (Tönnies and Trushina, 2017). Thus, researchers have suggested that antioxidants play the role in delaying the progression of dementia (Sinyor et al., 2020). Antioxidant nutrients, such as vitamins C and E have been shown to reduce amyloid- β -induced oxidative stress (Basambombo et al., 2017; Gugliandolo et al., 2017). Lipophilic antioxidants, such as vitamin A, vitamin E, and carotenoids, play the role of preventing cell membranes from damage by free radicals and may aid in halting the progression of neurodegeneration (Chang et al., 2018). A review of human studies indicated that lipid peroxidation involved with mitochondrial dysfunction was a factor in the pathogenesis of neurodegenerative diseases, which may be decreased by the lipophilic antioxidants to reduce the severity of neurodegenerative diseases (Petrovic et al., 2020). Coenzyme Q10 is also a lipophilic antioxidant in the mitochondria, which may react with reactive oxygen species directly. In addition to traditional antioxidants (vitamins), the effect of coenzyme Q10 on neurodegenerative disease has begun to be discussed (Spindler et al., 2009; Yang et al., 2016).

Coenzyme Q10 is an essential electron carrier in the mitochondrial electron transport chain for the generation of adenosine triphosphate (Bentinger et al., 2010). Coenzyme Q10 can act as an antioxidant against the increase in reactive oxygen species during the development of chronic diseases (Tönnies and Trushina, 2017). Studies have shown that patients with chronic diseases including, neurodegenerative diseases, cardiovascular disease, and cancer, have lower coenzyme Q10 status (Arenas-Jal et al., 2020). Yamagishi et al. (2014) were the first to observe that the level of coenzyme Q10 was associated with the risk of dementia. The neuroprotective effect of coenzyme Q10 has been demonstrated in animal models

(Komaki et al., 2019; Ibrahim Fouad, 2020). However, few human studies have examined the correlation between the level of coenzyme Q10 and biomarkers for dementia (such as amyloid β and tau protein) in clinical setting. Therefore, the purpose of this study was to investigate the relationships of coenzyme Q10 status, amyloid β and tau protein, and antioxidant capacity in patients with dementia.

Materials and methods

Participants and study design

Eighty patients with dementia were recruited from the Chung Shan Medical University Hospital, which is a medical center in Taiwan. Patients with dementia were diagnosed by a neurologist and psychiatrist based on brain magnetic resonance imaging or computed tomography scan to confirm the absence of structural lesions. The inclusion criteria were age ≥ 60 years and mini mental state examination (MMSE) score ≤ 26 . The MMSE questionnaire included six domains, such as orientation, registration, attention and calculation, recall, language, and visual construction. The sum of all item scores on the MMSE was 30, with higher scores indicating better cognitive function. As an MMSE score > 20 was defined as mild dementia and an MMSE score ≤ 20 was defined as moderate dementia (Folstein et al., 1975; Nolan et al., 2018). We excluded patients who were diagnosed with cancer, severe heart, lung, liver, and kidney disease, severe disability or aphasia, and the use of coenzyme Q10 supplements. A total of eighty patients with dementia met the criteria of the study, and all of them completed the measurement and examination. This study was approved by the Institutional Review Board of Chung Shan Medical University Hospital, Taiwan (CSMUH No: CS2-18147). Informed consent was obtained from each subject before participating in the present study.

Demographic data collection

The demographic data of patients with dementia, including age and gender, were collected by a questionnaire. A digital electronic sphygmomanometer (Hartmann Tensoval® duo control, Heidenheim, Germany) was used to measure blood pressure. Height and weight were measured to calculate body mass index (BMI). Waist circumference was measured with a tape measure. In addition, we used vacutainers with K2-EDTA anticoagulant (Becton Dickinson, Franklin Lakes, NJ, United States) or without anticoagulant to collect the venous blood sample after 12 h of fasting in patients with dementia. Plasma, serum, and red blood cell (RBC) samples were separated after centrifugation at 3,000 rpm for 15 min at 4°C. The white blood cell (WBC) sample was

Abbreviations: BMI, body mass index; HDL-C, high density lipoprotein-cholesterol; HPLC, high performance liquid chromatography; MMSE, mini mental state examination; RBC, red blood cell; TAC, total antioxidant capacity; TC, total cholesterol; TG, triglycerides; WBC, white blood cell.

collected by using RBC lysis buffer and stored at -80°C until analysis. An automated chemistry analyzer (Roche, Cobas c501, Risch-Rotkreuz, Switzerland) was used to analyze the levels of triglycerides (TG), total cholesterol (TC), low density lipoprotein-cholesterol, high density lipoprotein-cholesterol (HDL-C), fasting glucose, glycated hemoglobin, and high-sensitivity C-reactive protein.

Measurement of coenzyme Q10 status

High performance liquid chromatography (HPLC) with an ultraviolet detector was used to measure the level of coenzyme Q10 in plasma and WBC (Littarru et al., 2007). The WBC pellet was homogenized by adding 1-propanol in preparation for coenzyme Q10 measurement. The coenzyme Q10 in plasma and homogeneous fluid of WBC was extracted by 1-propanol. After centrifugation at 12,000 rpm for 15 min, the supernatant was mixed with methanol for a ratio of 1:1 and then filtered with a PTFE syringe filter, $0.45\ \mu\text{m} \times 13\ \text{mm}$ (Branch Billion Lung, Tianjin, China) for analysis. Mixed methanol and ethanol were used as the mobile phase, and the flow rate was set at 0.8 mL/min. The analysis column was a LiChroCART®RP-18 (Merck, Darmstadt, Germany), and the wavelength of the detector was set at 275 nm. The standard of coenzyme Q10 was purchased from Sigma-Aldrich (Merck, Germany) as the external standard to apply the calibration curve to measure the level of coenzyme Q10. In the method of coenzyme Q10 in this study, the linearity with correlation coefficients of the standard curve was 0.9999. The mean of intra- and inter-assay coefficients of variability for coenzyme Q10 were 3.4 and 2.8%, respectively. The mean analytical recovery of coenzyme Q10 was 102.0%. The reference range of plasma coenzyme Q10 was 0.5–1.7 μM in adults, and the individuals with plasma coenzyme Q10 level lower than 0.50 μM were defined as having plasma coenzyme Q10 deficiency (Molyneux et al., 2008).

Total antioxidant capacity measurement

A Trolox equivalent antioxidant capacity assay was used to analyze the total antioxidant capacity (TAC) in serum and RBC (Re et al., 1999). The 2,2'-azinobis (3-ethylbenzothiazoline-6-sulfonic acid) radical was prepared, which exhibited a blue-green color. The level of TAC was measured through the neutralized reaction between antioxidants in serum or free radicals in RBC. A vitamin E analog, Trolox, was used as a standard in the calculation of the level of TAC, which was expressed as mM Trolox. A spectrophotometer was used to measure the absorbance at 730 nm.

Biomarkers for dementia measurements

We used an enzyme-linked immunosorbent assay kit to quantify the levels of amyloid β -42 (KHB3441, Thermo Fisher Scientific, MA, United States), amyloid β -40 (KHB3481, Thermo Fisher Scientific, MA, United States), and tau protein (KHB0041, Thermo Fisher Scientific, MA, United States) in serum, and followed the manufacturer's instructions.

Statistical analysis

All data were analyzed by using SigmaPlot software (version 12.0, Systat, San Jose, CA, United States) in the present study. The mean \pm standard deviation (median) or percentages are shown for continuous variables or categorical variables, respectively. The Shapiro–Wilk test was used to examine the normality of distribution for the data. The differences in demographic data, antioxidant capacity, and biomarkers for dementia between the two groups stratified by coenzyme Q10 status were examined by Student's *t*-test or the Mann–Whitney rank sum test. Spearman's rank order correlation coefficient was calculated to examine the correlations between coenzyme Q10 status and antioxidant capacity and biomarkers for dementia in patients with dementia. The differences in coenzyme Q10 status between mild and moderate dementia patients were examined by the Mann–Whitney rank sum test; the differences in the proportion of moderate dementia between low and high coenzyme Q10 status were examined by the Chi-square test and the Fisher's exact test. Statistical significance was set at $p \leq 0.05$.

Results

Demographic data and coenzyme Q10 status in patients with dementia

Table 1 shows the demographic data and coenzyme Q10 status in patients with dementia. In these patients, the median age was 77.0 years, the male to female ratio was 1:3, and the median BMI was 23.8 kg/m^2 . The median values of waist circumference were 91.8 and 89.3 cm in male and female, respectively, which were higher than the reference values for waist circumference (male: $< 90\ \text{cm}$, female: $< 80\ \text{cm}$). In hematology, the fasting glucose level was higher than the normal reference value (fasting glucose $< 5.6\ \text{mmol}/\text{L}$). Regarding coenzyme Q10 status, the median level of plasma coenzyme Q10 was 0.36 μM . Approximately 73% of patients with dementia had plasma coenzyme Q10 deficiency, with coenzyme Q10 level lower than 0.50 μM . We therefore stratified by coenzyme Q10 status based on plasma coenzyme Q10 (0.5 μM) and found that

TABLE 1 Demographic data and coenzyme Q10 status in patients with dementia.

| Patients with dementia (N = 80) | |
|---|----------------------|
| Age (years) | 76.5 ± 6.3 (77.0) |
| Gender (male/female) | 22/58 |
| Physical features | |
| SBP (mmHg) | 129.6 ± 17.4 (130.0) |
| DBP (mmHg) | 73.0 ± 10.3 (72.5) |
| BMI (kg/m ²) | 24.2 ± 3.9 (23.8) |
| Waist circumference (cm) | 90.7 ± 10.0 (90.4) |
| Male | 91.3 ± 7.1 (91.8) |
| Female | 90.4 ± 10.9 (89.3) |
| Clinical characteristics | |
| Triglycerides (mmol/L) | 1.4 ± 1.0 (1.3) |
| Total cholesterol (mmol/L) | 4.8 ± 1.0 (4.6) |
| LDL-C (mmol/L) | 3.0 ± 1.0 (2.8) |
| HDL-C (mmol/L) | 1.6 ± 0.5 (1.6) |
| Male | 1.4 ± 0.4 (1.3) |
| Female | 1.7 ± 0.5 (1.6) |
| Fasting glucose (mmol/L) | 6.6 ± 1.6 (6.1) |
| Glycated hemoglobin (%) | 6.3 ± 1.0 (6.0) |
| Hs-CRP (mg/L) | 2.1 ± 5.2 (0.8) |
| GOT (U/L) | 25.7 ± 12.4 (23.0) |
| GPT (U/L) | 19.7 ± 10.8 (17.5) |
| WBCs (× 10 ⁹ /L) | 6.1 ± 1.5 (6.0) |
| RBCs (× 10 ¹² /L) | 4.5 ± 0.6 (4.5) |
| Hemoglobin (mmol/L) | 13.5 ± 1.4 (13.5) |
| Hematocrit (%) | 39.9 ± 3.8 (40.1) |
| Platelet (× 10 ⁹ /L) | 221.0 ± 64.9 (218.0) |
| Comorbidities (n, %) | |
| Hypertension | 47 (58.8%) |
| Diabetes | 29 (36.3%) |
| Hyperlipidemia | 29 (36.3%) |
| Heart disease | 16 (20.0%) |
| Liver disease | 6 (7.5%) |
| Chronic kidney disease | 5 (6.3%) |
| Education (n, %) | |
| None | 15 (18.8%) |
| Elementary school | 33 (41.3%) |
| Junior high school | 15 (18.8%) |
| Senior high school | 14 (17.5%) |
| University or above | 3 (3.8%) |
| Place of residence (n, %) | |
| Center | 78 (97.5%) |
| Southern | 2 (2.5%) |
| Use of supplement (n, %) | 42 (52.5%) |
| Use of hypolipidemic agents (n, %) | |
| HMG-CoA reductase inhibitors | 30 (37.5%) |
| Fibric acid derivatives | 4 (5.0%) |
| Cholesterol absorption inhibitor | 2 (2.5%) |
| Nicotinic acid | 1 (1.3%) |
| Coenzyme Q10 status | |
| Plasma coenzyme Q10 (μM) | 0.41 ± 0.21 (0.36) |
| Plasma coenzyme Q10/TC (μmol/mmol) | 0.09 ± 0.04 (0.08) |
| WBC coenzyme Q10 (nmol/g) | 3.4 ± 1.5 (3.6) |

(Continued)

TABLE 1 (Continued)

| | Low plasma coenzyme Q10 (N = 58) | High plasma coenzyme Q10 (N = 22) | P-value |
|--|----------------------------------|-----------------------------------|--------------------|
| Age (years) | 77.2 ± 6.2 (79.0) | 74.5 ± 6.2 (76.0) | 0.08 [†] |
| Gender (male/female) | 16/42 | 6/16 | 0.80 |
| Physical features | | | |
| SBP (mmHg) | 129.9 ± 17.4 (132.0) | 128.7 ± 18.0 (129.5) | 0.79 [†] |
| DBP (mmHg) | 73.0 ± 11.0 (71.5) | 73.0 ± 8.7 (74.0) | 0.98 [†] |
| BMI (kg/m ²) | 24.3 ± 4.0 (23.9) | 23.8 ± 3.5 (23.5) | 0.58 [†] |
| Waist circumference (cm) | 91.5 ± 9.9 (91.0) | 88.5 ± 9.9 (88.0) | 0.24 [†] |
| Male | 92.6 ± 6.2 (92.6) | 88.1 ± 8.9 (91.0) | 0.20 [†] |
| Female | 91.1 ± 11.1 (90.2) | 88.7 ± 10.6 (86.0) | 0.46 [†] |
| Clinical characteristics | | | |
| Triglycerides (mmol/L) | 1.5 ± 1.1 (1.4) | 1.1 ± 0.5 (1.0) | 0.06 [‡] |
| Total cholesterol (mmol/L) | 4.7 ± 0.9 (4.6) | 5.3 ± 1.1 (5.2) | 0.02 [‡] |
| LDL-C (mmol/L) | 2.9 ± 0.9 (2.7) | 3.3 ± 1.0 (3.1) | 0.08 [‡] |
| HDL-C (mmol/L) | 1.5 ± 0.4 (1.5) | 1.8 ± 0.5 (1.8) | <0.01 [†] |
| Male | 1.3 ± 0.2 (1.3) | 1.7 ± 0.6 (1.7) | 0.25 [‡] |
| Female | 1.6 ± 0.4 (1.6) | 1.9 ± 0.5 (1.9) | 0.06 [†] |
| Fasting glucose (mmol/L) | 6.5 ± 1.5 (6.0) | 6.7 ± 1.9 (6.2) | 0.78 [‡] |
| Glycated hemoglobin (%) | 6.3 ± 0.8 (6.0) | 6.5 ± 1.4 (5.9) | 0.54 [‡] |
| Hs-CRP (mg/L) | 1.6 ± 1.7 (0.9) | 3.5 ± 9.6 (0.8) | 0.95 [‡] |
| GOT (U/L) | 25.0 ± 11.6 (23.0) | 27.5 ± 14.5 (24.5) | 0.29 [‡] |
| GPT (U/L) | 18.8 ± 8.0 (17.0) | 22.0 ± 16.0 (18.0) | 0.82 [‡] |
| Use of hypolipidemic agents (n,%) | | | |
| HMG-CoA reductase inhibitors | 22 (37.9%) | 8 (36.4%) | 0.90 |
| Fibric acid derivatives | 4 (6.9%) | 0 (0.0%) | 0.57 |
| Cholesterol absorption inhibitor | 2 (3.4%) | 0 (0.0%) | 1.00 |
| Nicotinic acid | 1 (1.7%) | 0 (0.0%) | 1.00 |

Data is shown as mean ± SD (median). Low plasma coenzyme Q10: plasma coenzyme Q10 < 0.5 μM; High plasma coenzyme Q10: plasma coenzyme Q10 ≥ 0.5 μM. [†]Parametric tests were performed by Student's *t*-test; [‡]non-parametric tests were performed by the Mann–Whitney rank sum test. BMI, body mass index; DBP, diastolic blood pressure; GOT, glutamic oxaloacetic transaminase; GPT, glutamic pyruvic transaminase; HDL-C, high density lipoprotein-cholesterol; HMG-CoA, 3-hydroxy-3-methyl- glutaryl-coenzyme A; Hs-CRP, high-sensitivity C-reactive protein; LDL-C, low density lipoprotein-cholesterol; MMSE, mini mental state examination; RBC, red blood cell; SBP, systolic blood pressure; TC, total cholesterol; WBC, white blood cell.

patients with low plasma coenzyme Q10 status had significantly lower lipid profiles, such as TC ($p = 0.02$) and HDL-C ($p < 0.01$).

Antioxidant capacity, biomarkers for dementia, and mini mental state examination score of patients

Table 2 shows the antioxidant capacity, biomarkers for dementia, and MMSE scores of patients after stratification by coenzyme Q10 status. A slightly lower level of serum TAC was found in the patients with low plasma coenzyme Q10 level compared with those with high plasma coenzyme Q10 level ($p = 0.06$), similarly shown in patients with low plasma coenzyme Q10/TC ($p = 0.08$) and low WBC coenzyme Q10 levels ($p = 0.07$). In addition, patients with low WBC coenzyme Q10 level exhibited a significantly lower level of RBC TAC than those with a higher level of WBC coenzyme Q10 ($p = 0.04$). Regarding biomarkers for dementia, patients with low plasma coenzyme Q10/TC ($p = 0.05$) or low WBC coenzyme Q10 levels

($p = 0.02$) exhibited a significantly higher level of serum amyloid β -42. A similar trend was found in the serum amyloid β -42/40 ratio in patients with low plasma coenzyme Q10/TC ($p = 0.08$) or low WBC coenzyme Q10 ($p = 0.01$), while patients with low level of WBC coenzyme Q10 had a slightly lower level of serum amyloid β -40 ($p = 0.08$). However, there was no significant difference in the level of tau protein after stratified by coenzyme Q10 status. In the MMSE score, patients with low coenzyme Q10 status had a significantly lower MMSE score than those with high coenzyme Q10 status (plasma coenzyme Q10, $p = 0.01$; coenzyme Q10/TC, $p = 0.02$).

Correlations between biomarkers for dementia and antioxidant capacity

The correlations between biomarkers for dementia and antioxidant capacity are shown in **Figure 1**. The level of serum amyloid β -42 ($r = -0.25$, $p = 0.02$), serum amyloid β -40 ($r = 0.29$, $p = 0.01$), and amyloid β -42/40 ratio ($r = -0.34$, $p < 0.01$) were

TABLE 2 Antioxidant capacity, biomarkers for dementia, and MMSE score of patients after stratified by coenzyme Q10 status.

| | Low plasma coenzyme Q10 (<i>N</i> = 58) | High plasma coenzyme Q10 (<i>N</i> = 22) | <i>P</i> -value |
|--------------------------------|---|--|-------------------|
| Antioxidant capacity | | | |
| Serum TAC (mM Trolox) | 5.0 ± 0.5 (5.1) | 5.2 ± 0.4 (5.3) | 0.06 [†] |
| RBC TAC (mM Trolox) | 9.5 ± 0.9 (9.6) | 9.6 ± 1.1 (9.8) | 0.30 [‡] |
| Biomarkers for dementia | | | |
| Amyloid β-42 (pg/mL) | 37.2 ± 12.4 (33.0) | 33.8 ± 5.8 (33.0) | 0.71 [‡] |
| Amyloid β-40 (pg/mL) | 54.5 ± 26.1 (47.4) | 46.4 ± 24.3 (46.6) | 0.34 [‡] |
| Amyloid β-42/40 ratio | 0.92 ± 0.72 (0.78) | 1.10 ± 0.99 (0.72) | 0.77 [‡] |
| Tau protein (pg/mL) | 37.1 ± 28.5 (30.5) | 39.3 ± 57.6 (27.6) | 0.36 [‡] |
| MMSE score (points) | 18.4 ± 5.5 (20.0) | 21.5 ± 5.2 (24.0) | 0.01 [‡] |
| | Low plasma coenzyme Q10/TC (<i>N</i> = 41) | High plasma coenzyme Q10/TC (<i>N</i> = 39) | <i>P</i> -value |
| Antioxidant capacity | | | |
| Serum TAC (mM Trolox) | 5.0 ± 0.5 (5.1) | 5.1 ± 0.4 (5.2) | 0.08 [†] |
| RBC TAC (mM Trolox) | 9.5 ± 0.8 (9.6) | 9.5 ± 1.0 (9.7) | 0.54 [‡] |
| Biomarkers for dementia | | | |
| Amyloid β-42 (pg/mL) | 38.6 ± 13.2 (34.0) | 33.7 ± 7.3 (32.2) | 0.05 [‡] |
| Amyloid β-40 (pg/mL) | 50.5 ± 25.2 (45.0) | 54.4 ± 26.4 (51.2) | 0.37 [‡] |
| Amyloid β-42/40 ratio | 1.01 ± 0.78 (0.87) | 0.91 ± 0.83 (0.65) | 0.08 [‡] |
| Tau protein (pg/mL) | 35.4 ± 26.1 (33.0) | 40.2 ± 47.6 (27.0) | 0.74 [‡] |
| MMSE score (points) | 17.9 ± 5.7 (18.0) | 20.7 ± 5.1 (23.0) | 0.02 [‡] |
| | Low WBC coenzyme Q10 (<i>N</i> = 39) | High WBC coenzyme Q10 (<i>N</i> = 41) | <i>P</i> -value |
| Antioxidant capacity | | | |
| Serum TAC (mM Trolox) | 5.0 ± 0.5 (5.0) | 5.1 ± 0.4 (5.3) | 0.07 [†] |
| RBC TAC (mM Trolox) | 9.3 ± 0.9 (9.4) | 9.7 ± 0.9 (9.7) | 0.04 [‡] |
| Biomarkers for dementia | | | |
| Amyloid β-42 (pg/mL) | 39.5 ± 13.6 (34.5) | 33.1 ± 6.4 (31.9) | 0.02 [‡] |
| Amyloid β-40 (pg/mL) | 47.3 ± 24.3 (45.5) | 57.3 ± 26.4 (52.2) | 0.08 [‡] |
| Amyloid β-42/40 ratio | 1.13 ± 0.85 (0.86) | 0.80 ± 0.71 (0.64) | 0.01 [‡] |
| Tau protein (pg/mL) | 34.5 ± 24.3 (30.6) | 40.8 ± 47.6 (27.0) | 0.76 [‡] |
| MMSE score (points) | 19.7 ± 5.1 (21.0) | 18.9 ± 6.0 (20.0) | 0.63 [‡] |

Data is shown as mean ± SD (median). Low plasma coenzyme Q10: plasma coenzyme Q10 < 0.5 μM; High plasma coenzyme Q10: plasma coenzyme Q10 ≥ 0.5 μM. Low plasma coenzyme Q10/TC: plasma coenzyme Q10/TC < median value; High plasma coenzyme Q10/TC: plasma coenzyme Q10/TC ≥ median value. Low WBC coenzyme Q10: WBC coenzyme Q10 < median value; High WBC coenzyme Q10: WBC coenzyme Q10 ≥ median value. [†]Parametric tests were performed by Student's *t*-test; [‡]non-parametric tests were performed by the Mann–Whitney rank sum test. MMSE, mini mental state examination; RBC, red blood cell; TAC, total antioxidant capacity; TC, total cholesterol; WBC, white blood cell.

significantly correlated with the level of serum TAC, as well as in the patients with moderate dementia (Figure 1A). In addition, the level of serum amyloid β-40 ($r = 0.33$, $p < 0.01$) and amyloid β-42/40 ratio ($r = -0.29$, $p < 0.01$, Figure 1B) were significantly correlated with the level of RBC TAC, and the significant correlations were also found in patients with mild dementia (Figure 1B). However, there was no significant correlation between tau protein and antioxidant capacity (Figures 1C,D).

Correlations between coenzyme Q10 status and antioxidant capacity

Figure 2 shows the correlations between coenzyme Q10 status and antioxidant capacity in patients with dementia.

Coenzyme Q10 status was significantly positively correlated with the levels of serum TAC (plasma coenzyme Q10, $r = 0.23$, $p < 0.05$, Figure 2A; plasma coenzyme Q10/TC, $r = 0.23$, $p = 0.04$, Figure 2C; WBC coenzyme Q10, $r = 0.24$, $p = 0.03$, Figure 2E) and RBC TAC (WBC coenzyme Q10, $r = 0.30$, $p < 0.01$, Figure 2F). These significant correlations also existed in patients with mild dementia (Figures 2A,E,F).

Correlations between coenzyme Q10 status and biomarkers for dementia

Figure 3 shows the correlations between coenzyme Q10 status and biomarkers for dementia. Coenzyme Q10 status was significantly correlated with the levels of serum amyloid

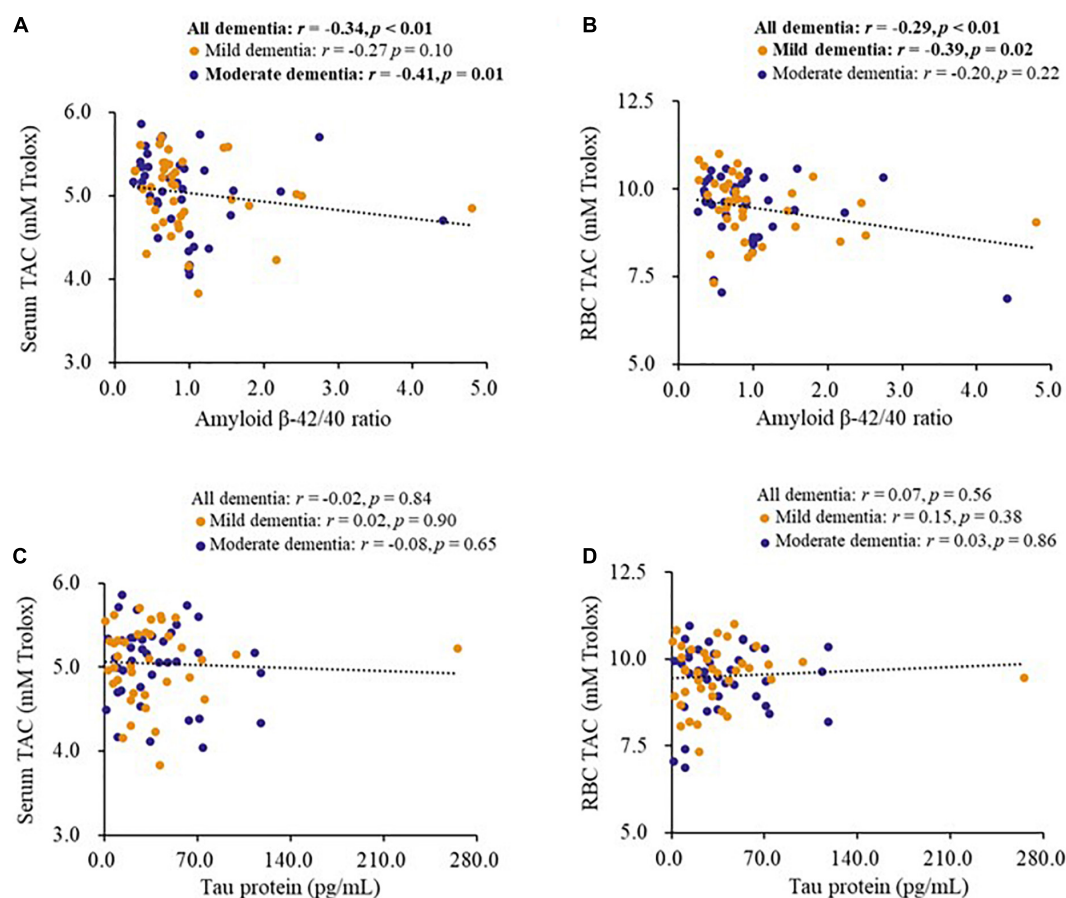


FIGURE 1

Correlations between biomarkers for dementia and antioxidant capacity of patients. (A,B) Correlations between the level of amyloid β -42/40 ratio and antioxidant capacity. (C,D) Correlations between the level of tau protein and antioxidant capacity. CoQ10, A β , Tau in Dementia.

β -42 (plasma coenzyme Q10/TC, $r = -0.28, p = 0.01$; WBC coenzyme Q10, $r = -0.26, p = 0.02$) and the amyloid β -42/40 ratio (plasma coenzyme Q10/TC, $r = -0.22, p = 0.05$, **Figure 3B**; WBC coenzyme Q10, $r = -0.24, p = 0.03$, **Figure 3C**), and these correlations also existed in patients with mild dementia for the amyloid β -42/40 ratio ($r = -0.44, p < 0.01$, **Figure 3C**) or with moderate dementia for the amyloid β -42 ($r = -0.37, p = 0.02$). However, there was no significant correlation between coenzyme Q10 status and tau protein (**Figures 3D–F**).

Correlations between coenzyme Q10 status and mini mental state examination score

Figure 4 shows the correlations between coenzyme Q10 status and MMSE score in patients with dementia. Coenzyme Q10 status was significantly correlated with MMSE score (plasma coenzyme Q10, $r = 0.33, p < 0.01$, **Figure 4A**; plasma

coenzyme Q10/TC, $r = 0.30, p < 0.01$, **Figure 4B**). Plasma coenzyme Q10 level was significantly correlated with MMSE score in patients with mild dementia ($r = 0.31, p < 0.05$, **Figure 4A**).

Coenzyme Q10 status and dementia progression

We further examined coenzyme Q10 status and dementia progression, as shown in **Figure 5**. Patients with moderate dementia had a significantly lower level of coenzyme Q10 status than those with mild dementia (plasma coenzyme Q10, median value: 0.32 vs. 0.45 μ M, $p = 0.01$; plasma coenzyme Q10/TC, median value: 0.07 vs. 0.09 μ mol/mmol, $p = 0.03$, **Figure 5A**). In addition, patients with low level of plasma coenzyme Q10 (56.9 vs. 31.8%, $p = 0.08$) or low level of plasma coenzyme Q10/TC (61.0 vs. 38.5%, $p = 0.07$) showed a slightly higher proportion of moderate dementia than those with high coenzyme Q10 status (**Figure 5B**).

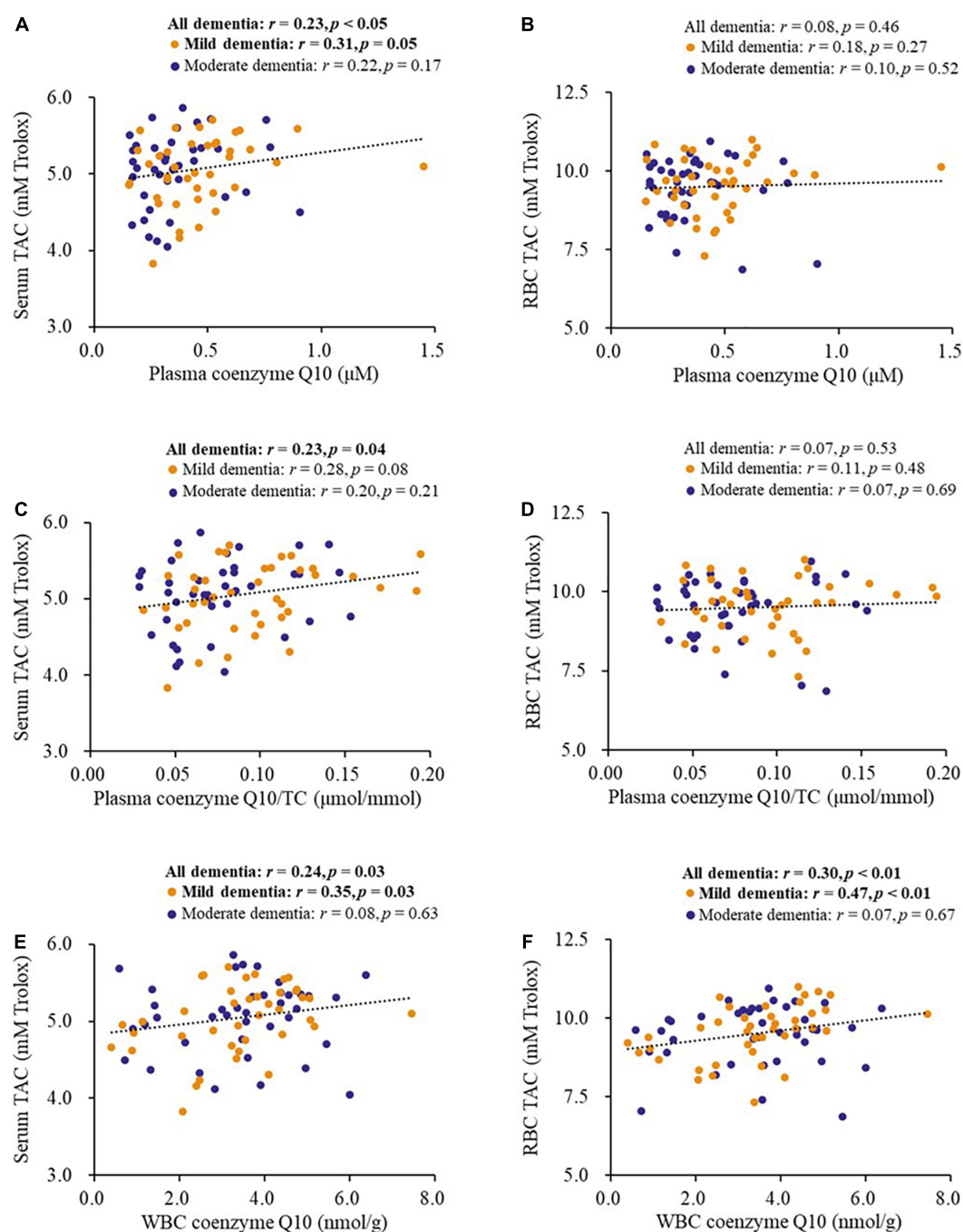


FIGURE 2

Correlations between coenzyme Q10 status and antioxidant capacity of patients. (A,B) Correlations between the level of plasma coenzyme Q10 and antioxidant capacity. (C,D) Correlations between the level of plasma coenzyme Q10/TC and antioxidant capacity. (E,F) Correlations between the level of WBC coenzyme Q10 and antioxidant capacity. CoQ10, A β , Tau in Dementia.

Discussion

This study was the first to investigate the relationship between coenzyme Q10 status and biomarkers in patients with dementia. The amyloid hypothesis of the pathogenesis of

dementia was proposed by John Hardy and David Allsop in 1991 (Hardy and Allsop, 1991). Amyloid β is produced through the amyloidogenic pathway (Coronel et al., 2018), and amyloid β -42 and amyloid β -40 are produced by cleavage of A β precursor protein by γ -secretase (Coronel et al., 2018; Fan et al., 2020).

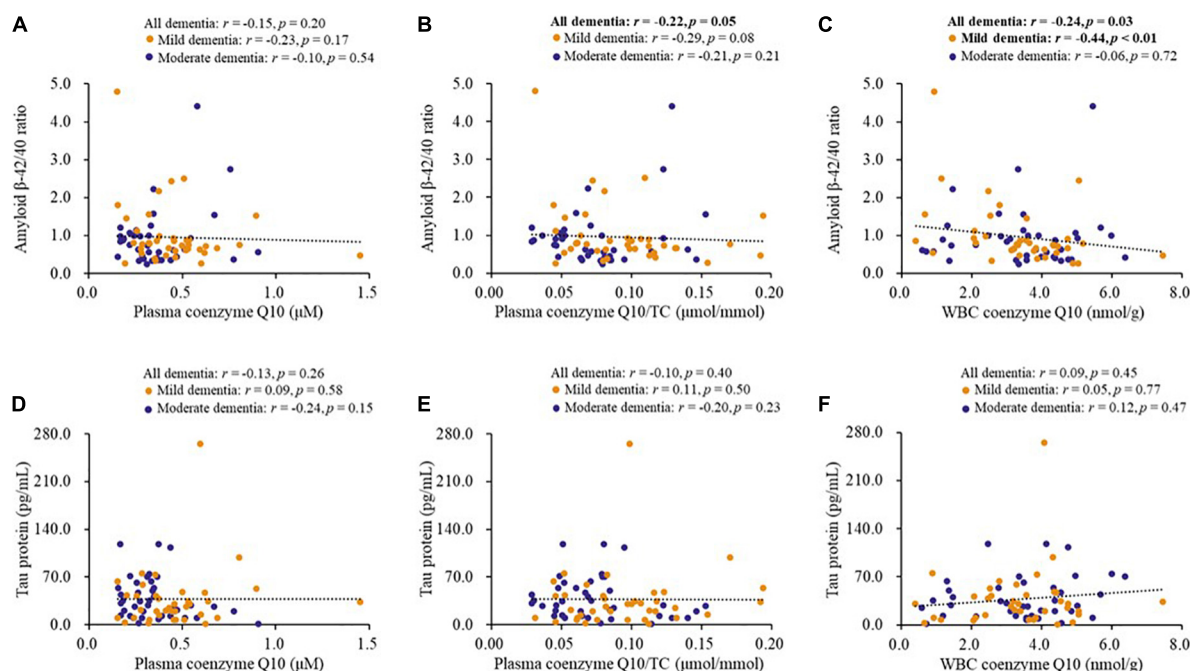


FIGURE 3

Correlations between coenzyme Q10 status and biomarkers for dementia of patients. (A–C) Correlations between coenzyme Q10 status and the level of amyloid β -42/40 ratio. (D–F) Correlations between coenzyme Q10 status and the level of tau protein. CoQ10, A β , Tau in Dementia.

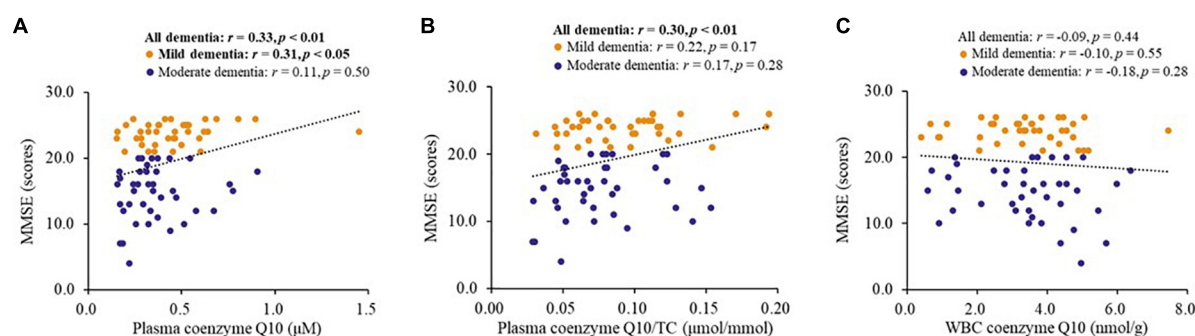


FIGURE 4

Correlations between coenzyme Q10 status and the MMSE score of patients. CoQ10, A β , Tau in Dementia. (A) Correlation between the level of plasma coenzyme Q10 and MMSE score. (B) Correlation between the level of plasma coenzyme Q10/TC and MMSE score. (C) Correlation between the level of WBC coenzyme Q10 and MMSE score.

In this study, we found that patients with higher coenzyme Q10 status had a significantly lower level of serum amyloid β -42 and amyloid β -42/40 ratio (Table 2), and they were significantly correlated with each other (Figure 3). Amyloid β is proposed to induce hyperphosphorylation of tau protein during the pathological severity of dementia (Mocanu et al., 2008; Fan et al., 2020). Studies in the elderly population have found that amyloid β is related to neuropathological performance (Yun et al., 2021; Zecca et al., 2021). The neuroprotective effects of coenzyme Q10 have also been demonstrated in cells and animal models (Elipenhli et al., 2012; Komaki et al., 2019;

Ekicier Acar et al., 2020; Ibrahim Fouad, 2020). Administration of coenzyme Q10 could attenuate amyloid β accumulation and mitigate Alzheimer's-like behavioral and pathological symptoms (Yang et al., 2008; Muthukumaran et al., 2018; Ibrahim Fouad, 2020). Recent published data showed that lower levels of amyloid β -42 and amyloid β -42/40 ratio was found in dementia patients (Hanon et al., 2022; Thijssen et al., 2022), but other researchers found that patients with dementia had higher levels of amyloid β -42, and the level of plasma amyloid β -42/40 ratio was correlated with amyloid positivity in the bilateral frontal, parietal, temporal, and occipital cortices (Manafikhi et al., 2021;

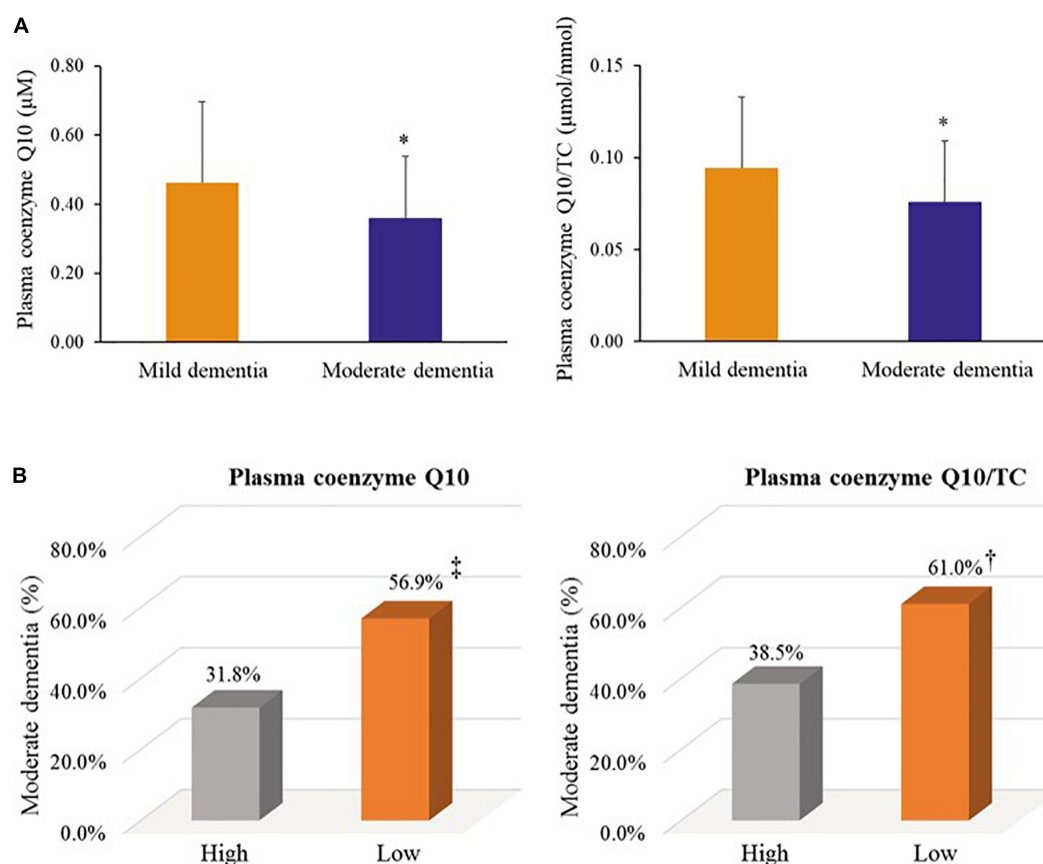


FIGURE 5

Coenzyme Q10 status and dementia progression. (A) Coenzyme Q10 status in patients with mild and moderate dementia. (B) The proportion of moderate dementia by coenzyme Q10 status. Mild dementia: the score of MMSE > 20; Moderate dementia: the score of MMSE ≤ 20. Low plasma coenzyme Q10: plasma coenzyme Q10 < 0.5 μM; High plasma coenzyme Q10: plasma coenzyme Q10 ≥ 0.5 μM. Low plasma coenzyme Q10/TC: plasma coenzyme Q10/TC < median value; High plasma coenzyme Q10/TC: plasma coenzyme Q10/TC ≥ median value. MMSE, mini mental state examination; TC, total cholesterol; WBC, white blood cell. *, $p < 0.05$; †, $p = 0.07$; ‡, $p = 0.08$.

Yun et al., 2021). The levels of amyloid β -42 and β -40 in dementia patients appear to remain uncertain. Administration of coenzyme Q10 reduced the level of serum amyloid β -42 and showed neuroprotective effects in animal experiments (Ibrahim Fouad, 2020). Further human studies are needed to elucidate the effect of CoQ10 supplementation on biomarkers of dementia. Although we did not find a significant correlation between coenzyme Q10 status and tau protein in the present study, Yang et al. (2020) demonstrated that coenzyme Q10 could reduce the expression of phosphorylated tau protein and attenuate neuroinflammation. As plasma total tau protein just partly reflects the pathology of dementia (Mattsson et al., 2016), evidence has indicated that measurements of phosphorylated tau species, P-tau181, P-tau217, and P-tau231, appear to have better performance in discriminating patients with cognitive impairment (Tang et al., 2018; Palmqvist et al., 2021; Tissot et al., 2022; Verde, 2022). Therefore, future studies should attempt to examine the correlation between coenzyme Q10 and phosphorylated tau instead of total tau protein. Additionally, it

is worth noting that 73% of patients in this study suffered from coenzyme Q10 deficiency (plasma coenzyme Q10 < 0.5 μM, Molyneux et al., 2008). In addition to the disease, aging is also a risk factor for impaired coenzyme Q10 status (Díaz-Casado et al., 2019). Because it is not easy to include the age matching healthy controls, so we tried to compare the level of coenzyme Q10 with our previous study that the middle-aged and elderly without osteoarthritis (Chang et al., 2020), and we found that coenzyme Q10 status was lower in the aging and patients with dementia (Median level of plasma coenzyme Q10, Dementia vs. Middle and Elderly, 0.36 vs. 0.45 μM, $p < 0.01$). However, the middle-aged and elderly without osteoarthritis in our previous study without assessing MMSE scores, so we did not make comparisons in the present study. Therefore, it is necessary to monitor coenzyme Q10 status in patients with dementia, and dietary supplementation with coenzyme Q10 could be considered to increase coenzyme Q10 to normal levels.

The oxidative stress hypothesis of dementia pathogenesis has been widely discussed (Butterfield and Halliwell, 2019;

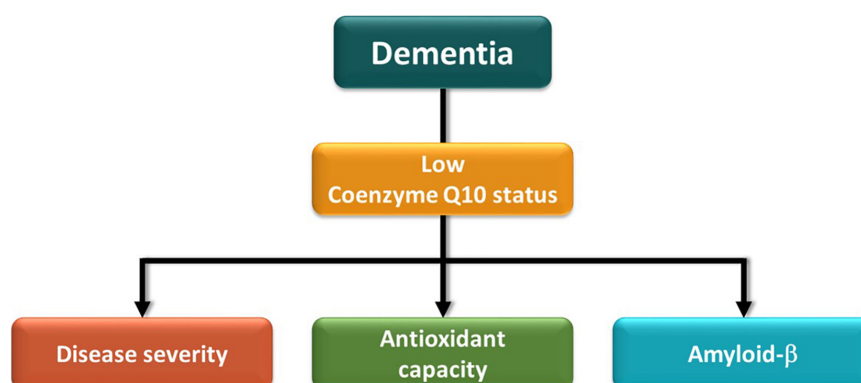


FIGURE 6
Schematic representation of concluding remark.

Fracassi et al., 2021). Growing evidence supports that oxidative stress, such as DNA damage, A β accumulation, tau hyperphosphorylation, subsequent mitochondrial dysfunction, and loss of synapses and neurons, is an essential part of the development of dementia (Chen and Zhong, 2014; Wang et al., 2014; Butterfield and Halliwell, 2019). Antioxidants may be beneficial in complementary therapy for dementia (Chen and Zhong, 2014). Coenzyme Q10 is considered to be a good antioxidant in mitochondria and membranes, which provides its neuroprotective effects by inhibiting oxidative stress (Choi et al., 2012). In human neuronal cells, coenzyme Q10 level is related to neuronal mitochondrial function and oxidative stress, and mitochondrial oxidative stress can be attenuated after coenzyme Q10 supplementation (Duberley et al., 2013, 2014). In this study, we used the WBC sample, which has a nucleus, as an estimate of coenzyme Q10 in tissue (Duncan et al., 2005). In the present study, we found that amyloid β -42 and the amyloid β -42/40 ratio were negatively correlated with TAC (Figure 1), while coenzyme Q10 status was positively correlated with the level of TAC (Table 2 and Figure 2). These results may imply that an improvement in coenzyme Q10 status is related to a good antioxidant capacity in patients with dementia. Notably, most of the significant correlations were also found in patients with mild dementia (Figures 1–3). Coenzyme Q10 may exert neuroprotective effects by its antioxidant capacity against the accumulation of amyloid- β on synaptic plasticity in the hippocampus (Yang et al., 2008; Komaki et al., 2019; Ibrahim Fouad, 2020). Recently, the pathologic development of dementia was associated with free-radical production causing the formation of β -amyloid aggregates, research demonstrated some lipid peroxidation metabolites could be potential biomarkers in patients with dementia (Peña-Bautista et al., 2019). In order to reduce the invasive and expensive diagnosis techniques for the

diagnosis of dementia, a series of plasma lipid peroxidation biomarkers that could reflect brain damage have been validated as a satisfactory early diagnostic model (Zuliani et al., 2018). In addition, high level of lipid peroxidation was usually accompanied with defecting the antioxidants status (Manoharan et al., 2016). Coenzyme Q10 acting as a lipophilic antioxidant could exert its antioxidant capacity in patients (Figure 2) and is beneficial for the progression of dementia (Figures 4, 5). As a result, examining the effects of coenzyme Q10 supplement on these redox biomarkers in patients with dementia can be the next step for the research.

In the present study, we also found that coenzyme Q10 status was correlated with cognitive performance MMSE in patients with dementia (Figure 4). Not only did patients with moderate dementia show a significantly lower coenzyme Q10 status, but a higher proportion of patients with low coenzyme Q10 status suffered from moderate dementia (Figure 5). The results are also supported by the Japanese general population (Community Circulation Risk Study), which reported that low level of coenzyme Q10 was associated with dementia risk and suggested that coenzyme Q10 level may be a predictor for the development of dementia, rather than a biomarker for the presence of dementia (Momiya, 2014; Yamagishi et al., 2014). Recently, two clinical trials have been conducted to investigate the effect of coenzyme Q10 supplementation on cognitive evaluation (Ramezani et al., 2020; García-Carpintero et al., 2021). Patients with acute ischemic stroke treated with coenzyme Q10 supplementation (300 mg/day) for 4 weeks showed an improvement in MMSE score (Ramezani et al., 2020). Another clinical study found that ubiquinol supplementation (200 mg/day) improved cerebral vasoreactivity and ameliorated chronic inflammation in patients with mild cognitive impairment (García-Carpintero et al., 2021). In addition, it is interesting to note that a total of

36.3% of dementia patients suffered from diabetes, 26.3% were suffered from prediabetes in the present study. Moreover, the levels of glucose parameters were correlated with systolic blood pressure (fasting glucose: $r = 0.32$, $p < 0.01$; glycated hemoglobin: $r = 0.28$, $p = 0.01$) and triglycerides (fasting glucose: $r = 0.33$, $p < 0.01$; glycated hemoglobin: $r = 0.41$, $p < 0.01$) in patients with dementia. Glycemic disorders have been identified as a key risk factor for dementia (Pal et al., 2018). Recent clinical studies demonstrated that coenzyme Q10 supplementation is beneficial for glycemic control, especially in diabetes (Yen et al., 2018; Yoo and Yum, 2018; Zhang et al., 2018; Gholami et al., 2019). A dose of 100–200 mg/d of coenzyme Q10 supplement for 8–12 weeks seems could significantly improve the insulin resistance and the level of glucose parameters, in patients with prediabetes, type 2 diabetes (Yen et al., 2018; Yoo and Yum, 2018; Gholami et al., 2019), or in dyslipidemia individuals (Zhang et al., 2018). Since coenzyme Q10 status may be associated with delayed cognitive decline and improved glycemic control, it is worth further interventional studies to verify the dosage and formulation of coenzyme Q10 supplementation and examine the effect on cognitive performance and glycemic control in dementia patients.

The limitations of this study include that we cannot confirm the types of dementia, such as Alzheimer's disease or vascular dementia. Second, this is a single-center, cross-sectional study, and only a correlation but not a causal relationship between coenzyme Q10 and biomarkers for dementia can be established from the results. Third, we did not measure the cerebral level of coenzyme Q10 and amyloid- β in the present study because it is not easy to access in clinical sampling. However, some animal models evidence found that treatment with coenzyme Q10 could provide beneficial effects on the brain (Yang et al., 2008; Muthukumaran et al., 2018; Ibrahim Fouad, 2020). Thus, clinical interventional studies are needed to validate the results in future studies.

Conclusion

The concluding remark of the present study is schematically summarized in **Figure 6**. This study found that patients with dementia suffered from a low coenzyme Q10 status, and the level of coenzyme Q10 was significantly correlated with the level of amyloid β -42 and the amyloid β -42/40 ratio, but not with the level of tau protein. In addition, both coenzyme Q10 status and amyloid- β levels were related to antioxidant capacity in patients with dementia. Since the level of coenzyme Q10 may be associated with delayed the progression of dementia, monitoring the level of coenzyme Q10 in patients with dementia is necessary. Further intervention studies will elucidate the causal effects of coenzyme Q10 supplementation on these parameters for dementia.

Data availability statement

The raw data supporting the conclusions of this article will be made available by the authors, without undue reservation.

Ethics statement

The studies involving human participants were reviewed and approved by the Institutional Review Board of Chung Shan Medical University Hospital, Taiwan (CSMUH No: CS2-18147). The patients/participants provided their written informed consent to participate in this study.

Author contributions

P-SC, H-HC, T-JL, and C-HY performed the study and recruited the subjects. P-SC performed the data analyses. J-CP helped perform the study and analyzed the sample. P-TL conceived the study, participated the design, and coordinated the study. P-SC and P-TL drafted the manuscript. All authors read and approved the final manuscript.

Funding

This study was supported by a grant from the Ministry of Science and Technology, Taiwan (MOST 108-2320-B-040-023).

Acknowledgments

We would like to express our sincere appreciation to the subjects for their participation.

Conflict of interest

The authors declare that the research was conducted in the absence of any commercial or financial relationships that could be construed as a potential conflict of interest.

Publisher's note

All claims expressed in this article are solely those of the authors and do not necessarily represent those of their affiliated organizations, or those of the publisher, the editors and the reviewers. Any product that may be evaluated in this article, or claim that may be made by its manufacturer, is not guaranteed or endorsed by the publisher.

References

- Arenas-Jal, M., Suñé-Negre, J. M., and García-Montoya, E. (2020). Coenzyme Q10 supplementation: efficacy, safety, and formulation challenges. *Compr. Rev. Food Sci. Food Saf.* 19, 574–594. doi: 10.1111/1541-4337.12539
- Basambombo, L. L., Carmichael, P. H., Côté, S., and Laurin, D. (2017). Use of vitamin E and C supplements for the prevention of cognitive decline. *Ann. Pharmacother.* 51, 118–124. doi: 10.1177/1060028016673072
- Bentinger, M., Tekle, M., and Dallner, G. (2010). Coenzyme Q–biosynthesis and functions. *Biochem. Biophys. Res. Commun.* 396, 74–79. doi: 10.1016/j.bbrc.2010.02.147
- Bloom, G. S. (2014). Amyloid- β and tau: the trigger and bullet in Alzheimer disease pathogenesis. *JAMA Neurol.* 71, 505–508. doi: 10.1001/jamaneurol.2013.5847
- Butterfield, D. A., and Halliwell, B. (2019). Oxidative stress, dysfunctional glucose metabolism and Alzheimer disease. *Nat. Rev. Neurosci.* 20, 148–160. doi: 10.1038/s41583-019-0132-6
- Cabezas-Opazo, F. A., Vergara-Pulgar, K., Pérez, M. J., Jara, C., Osorio-Fuentealba, C., and Quintanilla, R. A. (2015). Mitochondrial dysfunction contributes to the pathogenesis of Alzheimer's disease. *Oxid. Med. Cell. Longev.* 2015:509654. doi: 10.1155/2015/509654
- Chang, K. H., Cheng, M. L., Chiang, M. C., and Chen, C. M. (2018). Lipophilic antioxidants in neurodegenerative diseases. *Clin. Chim. Acta.* 485, 79–87. doi: 10.1016/j.cca.2018.06.031
- Chang, P. S., Yen, C. H., Huang, Y. Y., Chiu, C. J., and Lin, P. T. (2020). Associations between coenzyme Q10 status, oxidative stress, and muscle strength and endurance in patients with osteoarthritis. *Antioxidants (Basel)* 9:1275. doi: 10.3390/antiox9121275
- Chen, Z., and Zhong, C. (2014). Oxidative stress in Alzheimer's disease. *Neurosci. Bull.* 30, 271–281. doi: 10.1007/s12264-013-1423-y
- Choi, H., Park, H. H., Koh, S. H., Choi, N. Y., Yu, H. J., Park, J., et al. (2012). Coenzyme Q10 protects against amyloid beta-induced neuronal cell death by inhibiting oxidative stress and activating the PI3K pathway. *Neurotoxicology* 33, 85–90. doi: 10.1016/j.neuro.2011.12.005
- Coronel, R., Bernabeu-Zornoza, A., Palmer, C., Muñiz-Moreno, M., Zambrano, A., Cano, E., et al. (2018). Role of amyloid precursor protein (APP) and its derivatives in the biology and cell fate specification of neural stem cells. *Mol. Neurobiol.* 55, 7107–7117. doi: 10.1007/s12035-018-0914-2
- Díaz-Casado, M. E., Quiles, J. L., Barriocanal-Casado, E., González-García, P., Battino, M., López, L. C., et al. (2019). The paradox of coenzyme Q10 in aging. *Nutrients* 11:2221. doi: 10.3390/nu11092221
- Duberley, K. E., Abramov, A. Y., Chalasani, A., Heales, S. J., Rahman, S., and Hargreaves, I. P. (2013). Human neuronal coenzyme Q10 deficiency results in global loss of mitochondrial respiratory chain activity, increased mitochondrial oxidative stress and reversal of ATP synthase activity: implications for pathogenesis and treatment. *J. Inherit. Metab. Dis.* 36, 63–73. doi: 10.1007/s10545-012-9511-0
- Duberley, K. E., Heales, S. J., Abramov, A. Y., Chalasani, A., Land, J. M., Rahman, S., et al. (2014). Effect of coenzyme Q10 supplementation on mitochondrial electron transport chain activity and mitochondrial oxidative stress in coenzyme Q10 deficient human neuronal cells. *Int. J. Biochem. Cell. Biol.* 50, 60–63. doi: 10.1016/j.biocel.2014.02.003
- Duncan, A. J., Heales, S. J., Mills, K., Eaton, S., Land, J. M., and Hargreaves, I. P. (2005). Determination of coenzyme Q10 status in blood mononuclear cells, skeletal muscle, and plasma by HPLC with di-propoxy-coenzyme Q10 as an internal standard. *Clin. Chem.* 51, 2380–2382. doi: 10.1373/clinchem.2005.054643
- Ekicier Acar, S., Sarıcaoglu, M. S., Çolak, A., Aktaş, Z., and Sepici Dinçel, A. (2020). Neuroprotective effects of topical coenzyme Q10+vitamin E in mechanistic optic nerve injury model. *Eur. J. Ophthalmol.* 30, 714–722. doi: 10.1177/1120672119833271
- Elipenahli, C., Stack, C., Jainuddin, S., Gerges, M., Yang, L., Starkov, A., et al. (2012). Behavioral improvement after chronic administration of coenzyme Q10 in P301S transgenic mice. *J. Alzheimers Dis.* 28, 173–182. doi: 10.3233/JAD-2011-111190
- Fan, L., Mao, C., Hu, X., Zhang, S., Yang, Z., Hu, Z., et al. (2020). New insights into the pathogenesis of Alzheimer's disease. *Front. Neurol.* 10:1312. doi: 10.3389/fneur.2019.01312
- Folstein, M. F., Folstein, S. E., and McHugh, P. R. (1975). "Mini-mental state. A practical method for grading the cognitive state of patients for the clinician. *J. Psychiatr. Res.* 12, 189–198. doi: 10.1016/0022-3956(75)90026-6
- Fracassi, A., Marcatti, M., Zolocheska, O., Tabor, N., Woltjer, R., Moreno, S., et al. (2021). Oxidative damage and antioxidant response in frontal cortex of demented and nondemented individuals with Alzheimer's neuropathology. *J. Neurosci.* 41, 538–554. doi: 10.1523/JNEUROSCI.0295-20.2020
- García-Carpintero, S., Domínguez-Bértalo, J., Pedrero-Prieto, C., Frontiñán-Rubio, J., Amo-Salas, M., Durán-Prado, M., et al. (2021). Ubiquinol supplementation improves gender-dependent cerebral vasoreactivity and ameliorates chronic inflammation and endothelial dysfunction in patients with mild cognitive impairment. *Antioxidants (Basel)* 10:143. doi: 10.3390/antiox10020143
- Gholami, M., Rezvanfar, M. R., Delavar, M., Abdollahi, M., and Khosrowbeygi, A. (2019). Effects of coenzyme Q10 supplementation on serum values of gamma-glutamyl transferase, Pseudocholinesterase, Bilirubin, Ferritin, and High-Sensitivity C-Reactive Protein in Women with Type 2 Diabetes. *Exp. Clin. Endocrinol. Diabetes* 127, 311–319. doi: 10.1055/s-0043-124183
- Gugliandolo, A., Bramanti, P., and Mazzon, E. (2017). Role of vitamin E in the treatment of Alzheimer's disease: evidence from animal models. *Int. J. Mol. Sci.* 18:2504. doi: 10.3390/ijms18122504
- Hanon, O., Vidal, J. S., Lehmann, S., Bombois, S., Allinquant, B., Baret-Rose, C., et al. (2022). Plasma amyloid beta predicts conversion to dementia in subjects with mild cognitive impairment: the BALTAZAR study. *Alzheimers Dement.* doi: 10.1002/alz.12613 [Epub ahead of print].
- Hardy, J., and Allsop, D. (1991). Amyloid deposition as the central event in the aetiology of Alzheimer's disease. *Trends Pharmacol. Sci.* 12, 383–388. doi: 10.1016/0165-6147(91)90609-v
- Ibrahim Fouad, G. (2020). Combination of omega 3 and coenzyme Q10 exerts neuroprotective potential against hypercholesterolemia-induced Alzheimer's-like disease in rats. *Neurochem. Res.* 45, 1142–1155. doi: 10.1007/s11064-020-02996-2
- Komaki, H., Faraji, N., Komaki, A., Shahidi, S., Etaee, F., Raoufi, S., et al. (2019). Investigation of protective effects of coenzyme Q10 on impaired synaptic plasticity in a male rat model of Alzheimer's disease. *Brain Res. Bull.* 147, 14–21. doi: 10.1016/j.brainresbull.2019.01.025
- Littarru, G. P., Mosca, F., Fattorini, D., and Bompadre, S. (2007). *Method to Assay Coenzyme Q10 in Blood Plasma or Blood Serum*. United States Patent 7303921. Available online at: <https://patents.google.com/patent/US7303921B2/en> (accessed November 8, 2010).
- Manafikhi, R., Haik, M. B., Lahdo, R., and AlQuobaili, F. (2021). Plasma amyloid β levels in Alzheimer's disease and cognitively normal controls in Syrian population. *Med. J. Islam. Repub. Iran.* 35:19. doi: 10.47176/mjiri.35.19
- Manoharan, S., Guillemin, G. J., Abiramasundari, R. S., Essa, M. M., Akbar, M., and Akbar, M. D. (2016). The role of reactive oxygen species in the pathogenesis of Alzheimer's disease, Parkinson's disease, and Huntington's disease: a Mini Review. *Oxid. Med. Cell Longev.* 2016:8590578. doi: 10.1155/2016/8590578
- Mattsson, N., Zetterberg, H., Janelidze, S., Insel, P. S., Andreasson, U., Stomrud, E., et al. (2016). Plasma tau in Alzheimer disease. *Neurology* 87, 1827–1835. doi: 10.1212/WNL.0000000000003246
- Mocanu, M. M., Nissen, A., Eckermann, K., Khlistunova, I., Biernat, J., Drexler, D., et al. (2008). The potential for beta-structure in the repeat domain of tau protein determines aggregation, synaptic decay, neuronal loss, and coassembly with endogenous Tau in inducible mouse models of tauopathy. *J. Neurosci.* 28, 737–748. doi: 10.1523/JNEUROSCI.2824-07.2008
- Molyneux, S. L., Young, J. M., Florkowski, C. M., Lever, M., and George, P. M. (2008). Coenzyme Q10: is there a clinical role and a case for measurement? *Clin. Biochem. Rev.* 29, 71–82.
- Momiyama, Y. (2014). Serum coenzyme Q10 levels as a predictor of dementia in a Japanese general population. *Atherosclerosis* 237, 433–434. doi: 10.1016/j.atherosclerosis.2014.08.056
- Muthukumar, K., Kanwar, A., Vegh, C., Marginean, A., Elliott, A., Guilbeault, N., et al. (2018). Ubisol-Q10 (a Nanomicellar water-soluble formulation of CoQ10) treatment inhibits Alzheimer-type behavioral and pathological symptoms in a double transgenic mouse (TgA β ESwe, PSEN1dE9) model of Alzheimer's disease. *J. Alzheimers Dis.* 61, 221–236. doi: 10.3233/JAD-170275
- Nolan, J. M., Mulcahy, R., Power, R., Moran, R., and Howard, A. N. (2018). Nutritional intervention to prevent Alzheimer's disease: potential benefits of xanthophyll carotenoids and omega-3 fatty acids combined. *J. Alzheimers Dis.* 64, 367–378. doi: 10.3233/JAD-180160
- Pal, K., Mukadam, N., Petersen, I., and Cooper, C. (2018). Mild cognitive impairment and progression to dementia in people with diabetes, prediabetes and metabolic syndrome: a systematic review and meta-analysis. *Soc. Psychiatry Psychiatr. Epidemiol.* 53, 1149–1160. doi: 10.1007/s00127-018-1581-3

- Palmqvist, S., Tideman, P., Cullen, N., Zetterberg, H., Blennow, K., Alzheimer's Disease Neuroimaging Initiative et al. (2021). Prediction of future Alzheimer's disease dementia using plasma phospho-tau combined with other accessible measures. *Nat. Med.* 27, 1034–1042. doi: 10.1038/s41591-021-01348-z
- Peña-Bautista, C., Baquero, M., Vento, M., and Cháfer-Pericás, C. (2019). Free radicals in Alzheimer's disease: lipid peroxidation biomarkers. *Clin. Chim. Acta.* 491, 85–90. doi: 10.1016/j.cca.2019.01.021
- Petrovic, S., Arsic, A., Ristic-Medic, D., Cvetkovic, Z., and Vucic, V. (2020). Lipid peroxidation and antioxidant supplementation in neurodegenerative diseases: a review of human studies. *Antioxidants (Basel)* 9:1128. doi: 10.3390/antiox9111128
- Ramezani, M., Sahraei, Z., Simani, L., Heydari, K., and Shahidi, F. (2020). Coenzyme Q10 supplementation in acute ischemic stroke: is it beneficial in short-term administration? *Nutr. Neurosci.* 23, 640–645. doi: 10.1080/1028415X.2018.1541269
- Re, R., Pellegrini, N., Proteggente, A., Pannala, A., Yang, M., and Rice-Evans, C. (1999). Antioxidant activity applying an improved ABTS radical cation decolorization assay. *Free. Radic. Biol. Med.* 26, 1231–1237. doi: 10.1016/s0891-5849(98)00315-3
- Sinyor, B., Mineo, J., and Ochner, C. (2020). Alzheimer's disease, inflammation, and the role of antioxidants. *J. Alzheimers Dis. Rep.* 4, 175–183. doi: 10.3233/ADR-200171
- Spindler, M., Beal, M. F., and Henchcliffe, C. (2009). Coenzyme Q10 effects in neurodegenerative disease. *Neuropsychiatr. Dis. Treat.* 5, 597–610. doi: 10.2147/ndt.s5212
- Tang, S. C., Yang, K. C., Chen, C. H., Yang, S. Y., Chiu, M. J., Wu, C. C., et al. (2018). Plasma β -amyloids and tau proteins in patients with vascular cognitive impairment. *Neuromolecular. Med.* 20, 498–503. doi: 10.1007/s12017-018-8513-y
- Thijssen, E. H., Verberk, I. M. W., Kindermans, J., Abramian, A., Vanbrabant, J., Ball, A. J., et al. (2022). Differential diagnostic performance of a panel of plasma biomarkers for different types of dementia. *Alzheimers Dement. (Amst.)*. 14:e12285. doi: 10.1002/dad2.12285
- Tissot, C., Therriault, J., Kunach, P., L. Benedet, A., Pascoal, T. A., Ashton, N. J., et al. (2022). Comparing tau status determined via plasma pTau181, pTau231 and [18F]MK6240 tau-PET. *EBioMedicine* 76:103837. doi: 10.1016/j.ebiom.2022.103837
- Tönnies, E., and Trushina, E. (2017). Oxidative stress, synaptic dysfunction, and Alzheimer's disease. *J. Alzheimers Dis.* 57, 1105–1121. doi: 10.3233/JAD-161088
- Verde, F. (2022). Tau proteins in blood as biomarkers of Alzheimer's disease and other proteinopathies. *J. Neural. Transm. (Vienna)* 129, 239–259. doi: 10.1007/s00702-022-02471-y
- Wang, X., Wang, W., Li, L., Perry, G., Lee, H. G., and Zhu, X. (2014). Oxidative stress and mitochondrial dysfunction in Alzheimer's disease. *Biochim. Biophys. Acta.* 1842, 240–247. doi: 10.1016/j.bbdis.2013.10.015
- WHO (2021). *Dementia. 2 September*. Available online at: <https://www.who.int/news-room/fact-sheets/detail/dementia> (accessed December 16, 2021).
- Yamagishi, K., Ikeda, A., Moriyama, Y., Chei, C. L., Noda, H., Umesawa, M., et al. (2014). Serum coenzyme Q10 and risk of disabling dementia: the Circulatory Risk in Communities Study (CIRCS). *Atherosclerosis* 237, 400–403. doi: 10.1016/j.atherosclerosis.2014.09.017
- Yang, M., Lian, N., Yu, Y., Wang, Y., Xie, K., and Yu, Y. (2020). Coenzyme Q10 alleviates sevoflurane-induced neuroinflammation by regulating the levels of apolipoprotein E and phosphorylated tau protein in mouse hippocampal neurons. *Mol. Med. Rep.* 22, 445–453. doi: 10.3892/mmr.2020.11131
- Yang, X., Yang, Y., Li, G., Wang, J., and Cheng, E. S. (2008). Coenzyme Q10 attenuates beta-amyloid pathology in the aged transgenic mice with Alzheimer presenilin 1 mutation. *J. Mol. Neurosci.* 34, 165–171. doi: 10.1007/s12031-007-9033-7
- Yang, X., Zhang, Y., Xu, H., Luo, X., Yu, J., Liu, J., et al. (2016). Neuroprotection of coenzyme Q10 in neurodegenerative diseases. *Curr. Top. Med. Chem.* 16, 858–866. doi: 10.2174/1568026615666150827095252
- Yen, C. H., Chu, Y. J., Lee, B. J., Lin, Y. C., and Lin, P. T. (2018). Effect of liquid ubiquinol supplementation on glucose, lipids and antioxidant capacity in type 2 diabetes patients: a double-blind, randomised, placebo-controlled trial. *Br. J. Nutr.* 120, 57–63. doi: 10.1017/S0007114518001241
- Yoo, J. Y., and Yum, K. S. (2018). Effect of coenzyme Q10 on insulin resistance in Korean patients with prediabetes: a pilot single-center, randomized, double-blind, placebo-controlled study. *Biomed. Res. Int.* 2018:1613247. doi: 10.1155/2018/1613247
- Yun, G., Kim, H. J., Kim, H. G., Lee, K. M., Hong, I. K., Kim, S. H., et al. (2021). Association between plasma amyloid- β and neuropsychological performance in patients with cognitive decline. *Front. Aging Neurosci.* 13:736937. doi: 10.3389/fnagi.2021.736937
- Zecca, C., Pasculli, G., Tortelli, R., Dell'Abate, M. T., Capozzo, R., Barulli, M. R., et al. (2021). The role of age on beta-amyloid 1–42 plasma levels in healthy subjects. *Front. Aging Neurosci.* 13:698571. doi: 10.3389/fnagi.2021.698571
- Zhang, P., Yang, C., Guo, H., Wang, J., Lin, S., Li, H., et al. (2018). Treatment of coenzyme Q10 for 24 weeks improves lipid and glycemic profile in dyslipidemic individuals. *J. Clin. Lipidol.* 12, 417–427.e5. doi: 10.1016/j.jacl.2017.12.006
- Zuliani, G., Passaro, A., Bosi, C., Sanz, J. M., Trentini, A., Bergamini, C. M., et al. (2018). Testing a combination of markers of systemic redox status as a possible tool for the diagnosis of late onset Alzheimer's disease. *Dis. Markers.* 2018:2576026. doi: 10.1155/2018/2576026



Presenilin Deficiency Increases Susceptibility to Oxidative Damage in Fibroblasts

Kun Zou^{1*}, Sadequl Islam¹, Yang Sun¹, Yuan Gao¹, Tomohisa Nakamura¹, Hiroto Komano², Taisuke Tomita³ and Makoto Michikawa^{1*}

¹ Department of Biochemistry, Graduate School of Medical Sciences, Nagoya City University, Nagoya, Japan, ² Advanced Prevention and Research Laboratory for Dementia, Faculty of Pharmaceutical Sciences, Hokkaido University, Sapporo, Japan, ³ Laboratory of Neuropathology and Neuroscience, Faculty of Pharmaceutical Sciences, University of Tokyo, Bunkyo City, Japan

OPEN ACCESS

Edited by:

Allison B. Reiss,
New York University, United States

Reviewed by:

Satoru Funamoto,
Doshisha University, Japan
Timothy Y. Huang,
Sanford Burnham Prebys Medical
Discovery Institute, United States

*Correspondence:

Kun Zou
kunzou@med.nagoya-cu.ac.jp
Makoto Michikawa
michi@med.nagoya-cu.ac.jp

Specialty section:

This article was submitted to
Alzheimer's Disease and Related
Dementias,
a section of the journal
Frontiers in Aging Neuroscience

Received: 23 March 2022

Accepted: 27 May 2022

Published: 16 June 2022

Citation:

Zou K, Islam S, Sun Y, Gao Y, Nakamura T, Komano H, Tomita T and Michikawa M (2022) Presenilin Deficiency Increases Susceptibility to Oxidative Damage in Fibroblasts. *Front. Aging Neurosci.* 14:902525. doi: 10.3389/fnagi.2022.902525

Alzheimer's disease (AD) is a genetic and sporadic neurodegenerative disease characterized by extracellular amyloid- β -protein (A β) aggregates as amyloid plaques and neuronal loss in the brain parenchyma of patients. Familial AD (FAD) is found to be genetically linked to missense mutations either in presenilin (PS) or amyloid precursor protein (APP). Most of PS mutations increase A β 42/A β 40 ratio, which is thought to result in early amyloid deposition in brain. However, PS deficiency in the fore brain of adult mouse leads to neuronal loss in an A β independent manner and the underlying mechanism is largely unknown. In this study, we found that reactive oxygen species (ROS) are increased in PS deficient fibroblasts and that H₂O₂ and ferrous sulfate treatment produced more ROS in PS deficient fibroblasts than in wild-type fibroblasts. PS deficient fibroblasts showed significantly decreased cellular ferritin levels compared with wild-type fibroblasts, suggesting reduced iron sequestering capability in PS deficient cells. Blockade of γ -secretase activity by a γ -secretase inhibitor, DAPT, decreased ferritin levels, indicating that γ -secretase activity is important for maintaining its levels. Moreover, overexpression PS1 mutants in wild-type fibroblasts decreased ferritin light chain levels and enhanced intracellular ROS levels. Our results suggest that dysfunction of PS may reduce intracellular ferritin levels and is involved in AD pathogenesis through increasing susceptibility to oxidative damage.

Keywords: presenilin, oxidative, ferritin, iron, Alzheimer's disease

INTRODUCTION

Alzheimer's disease (AD) is a neurodegenerative disease characterized by extracellular amyloid plaques in brain parenchyma, intracellular neurofibrillary tangles and neuronal loss (McKhann et al., 1984; Knopman et al., 2021). The major components of amyloid plaques are amyloid β -proteins (A β) consisting of 40–43 amino acids, which are generated from amyloid precursor protein (APP) by β -secretase and γ -secretase (Shoji et al., 1992; De Strooper et al., 2012). The accumulation of A β occurs 15–20 years prior to AD symptoms and it is one of the earliest pathological events in AD brain (Scheltens et al., 2016). A β is hypothesized to be the causative molecule for AD because it has neurotoxic effects, which is called amyloid cascade hypothesis (Selkoe and Hardy, 2016).

AD is clinically divided into sporadic AD (SAD) caused by multiple risk factors, including lifestyle-related factors, and familial AD (FAD) caused by inherited mutations of specific genes. SAD accounts for more than 95% of all AD cases and it is hypothesized to be induced by reduced

clearance of A β . Genetic causes for FAD include dominantly inherited mutations of the genes encoding amyloid precursor protein (*APP*), presenilin 1 (*PSEN1*, PS1) and *PSEN2* (PS2). PS1 and PS2 provide the catalytic subunit to the γ secretase complex, which contains PS, nicastrin, Aph-1 and PEN-2 (De Strooper et al., 2012). Most of the mutations found in *PSEN* result in increased A β 42 production or decreased A β 40 production, leading to an increased A β 42/A β 40 ratio (Borchelt et al., 1996; De Strooper et al., 2012; Watanabe and Shen, 2017). The findings of amyloid inhibitory effect of A β 40 against A β 42 aggregation and the increased A β 42/A β 40 ratio in most of FAD patients with PS mutations provide molecular mechanisms for the pathogenesis of FAD. However, some of *PSEN* mutations lead to reduce A β 42/A β 40 ratio and PS conditional knockout mice in the forebrain show progressive neurodegeneration without A β deposition, suggesting that loss of PS function could contribute to neuronal damage independently of amyloid cascade (Saura et al., 2004; De Strooper et al., 2012; Watanabe and Shen, 2017).

In addition to amyloid accumulation, oxidative damage in the brain of AD patients also typifies AD pathology and is found to precede A β deposition (Nunomura et al., 2001; Ayton et al., 2013; Chen and Zhong, 2014). Redox-active iron is responsible for inducing oxidative damage and extensively deposits in amyloid plaques and neurofibrillary tangles of AD brain (Smith et al., 1997; Zecca et al., 2004; Belaidi and Bush, 2016). We have found that A β 40 protects neurons against oxidative damage induced by iron, whereas A β 42 enhanced neurotoxicity (Zou et al., 2002; Zou and Michikawa, 2008). These lines of evidence suggest that A β deposition could be a secondary event of oxidative damage in AD brain. Here, we studied whether loss of function of PS is involved in oxidative stress in cells and found that reactive oxygen species (ROS) generation increased in PS deficient fibroblasts compared with wild type fibroblasts. We also found that cellular levels of both ferritin light and heavy chains markedly decreased in PS deficient fibroblasts and that inhibition of γ -secretase activity suppressed cellular levels of ferritin light and heavy chains in the presence of ferrous sulfate. Our results suggest that dysfunction of PS or reduced γ -secretase activity may decrease iron sequestration and enhance oxidative stress.

MATERIALS AND METHODS

Cell Culture and Western Blot Analysis

Wild-type and PS double-knockout (PS-DK) fibroblasts were provided by Dr. Bart De Strooper (Herreman et al., 1999). Cells were cultured in Dulbecco's modified Eagle medium (DMEM; GIBCO) containing 10% fetal bovine serum (FBS). Wild-type and PS-DK fibroblasts were lysed in RIPA buffer [10 mM Tris/HCl (pH 7.5), 150 mM NaCl, 1% Nonidet P-40, 0.1% sodium dodecyl sulfate (SDS) and 0.2% sodium deoxycholate, containing a protease inhibitor cocktail (Roche)]. Equal amounts (20 μ g) of protein from cell lysate were separated by SDS-PAGE in 12% gel and blotted onto polyvinylidene difluoride (PVDF) membranes (Immobilon). The ferritin proteins were detected by Western blotting using rabbit polyclonal anti-ferritin light chain and anti-ferritin heavy chain antibodies (abcam).

The blots were visualized using Super Signal Chemiluminescence solution (Wako) according to the manufacturer's instructions. Membranes were then stripped and re-probed with anti- α -tubulin (Sigma) or anti- β -actin (Proteintec) antibodies. Quantification of protein levels was performed using Image J software (National Institutes of Health).

Fluorescence Microscopy

The levels of intracellular ROS were measured using dihydroethidium (DHE), which interacts with ROS to form ethidium and emits a red fluorescence in the cells, as described previously (Bindokas et al., 1996). A total of 2×10^4 /ml wild-type and PS-DK fibroblasts were seeded and incubated at 37°C in 5% CO₂ for 12 h and then treated with vehicle control or 1 mM H₂O₂. After 30 min, 5 μ M DHE (Cayma Chemical) was added into the cells and the cells were incubated for another 30 min at 37°C in 5% CO₂. Confocal microscopy images were captured using an Olympus FV3000 confocal microscope (Olympus). For quantification of fluorescence intensity, acquired images were imported to Image J software. Threshold intensity was determined using the automatically set thresholding function for all images. Pixel intensity for fluorescence images was expressed as fluorescence mean intensity.

Reactive Oxygen Species Activity Assay

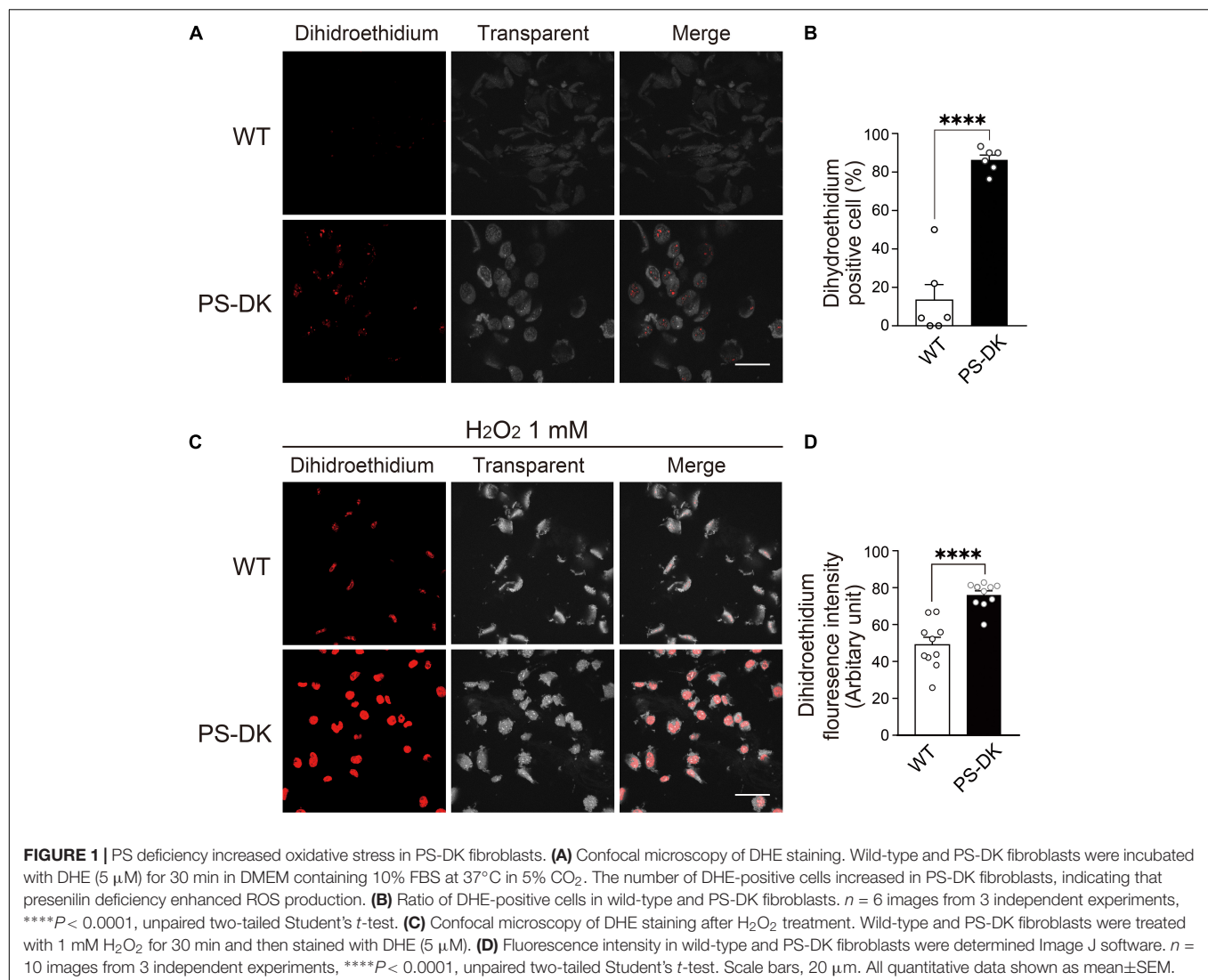
Intracellular total ROS activity in live cells was analyzed using Amplitude Fluorimetric ROS assay kit (AAT Bioquest). WT and PS-DK cells were seeded in a 96 well plate in triplicate and cultured with DMEM containing 10% FBS for 48h. Then the cells were incubated in serum free DMEM and 100 μ l/well of AmplitudeTM ROS Red working solution at 37°C for 1 h. The cells were then treated with 30 and 100 μ M FeSO₄. After 16 h, ROS levels were measured using Amplitude Fluorimetric ROS assay kit according to the manufacturer's protocol. The fluorescence density was measured by plate reader (SPECTRA MAX GEMINI EM) at Ex/Em = 520/605 nm.

Infection of Presenilin Mutants

The expression of human PS mutants (PS1 Δ E9, PS1G384A, PS1D257A, and PS1D385A) was performed as previously described (Islam et al., 2022). Briefly, the retroviral plasmids were transfected into platinum-E cells using FuGENE (Promega) for retroviral packaging. After 24 h, the conditioned medium was collected and used as viral stock. For highly efficient retroviral infection, fibroblasts were cultured with viral stock containing 5 μ g/ml polybrene (Santa Cruz Biotechnology) and allowed to proceed for PS expression.

Statistical Analyses

Prism 7.0 software (GraphPad Software) was used for statistical analyses. All data are shown as the mean \pm SEM of at least three independent experiments with *P*-values. *P*-value < 0.05 was considered to represent a significant difference. Student's *t*-test was used to determine whether the results were significantly different between



two groups. Group differences were analyzed by one-way analysis of variance (ANOVA) followed by Tukey's multiple comparison tests for multiple groups against the control group.

RESULTS

Reactive Oxygen Species Levels in PS Double-Knockout Fibroblasts Increased at Basal Level and After H₂O₂ Treatment

To investigate whether PS function is involved in oxidative stress in cells, wild-type and PS1, 2 double knockout (PS-DK) fibroblasts were stained with DHE, which detects cellular ROS generation by oxidation to form ethidium with red fluorescence. The ratio of DHE-positive PS-DK fibroblasts was significantly higher than wild-type fibroblasts, 13% for wild-type and 86% for PS-DK cells, respectively (**Figures 1A,B**). This result suggests that the basal ROS levels in PS-DK fibroblasts

is higher than wild-type fibroblasts. To examine whether PS-DK fibroblasts are more susceptible to oxidative stress, we treated wild-type and PS-DK fibroblasts with H₂O₂ and found that PS-DK fibroblasts generated markedly more ROS than wild-type fibroblasts (**Figures 1C,D**). This result suggests that PS-DK fibroblasts may have lower antioxidant capabilities than wild-type cells.

Presenilin Deficiency Leads to Increased Susceptibility to Iron-Induced Oxidative Damage and Decreased Cellular Ferritin Levels

Because H₂O₂ generates ROS through Fenton reaction and free iron ion is involved in this reaction, $\text{Fe}^{2+} + \text{H}_2\text{O}_2 \rightarrow \text{Fe}^{3+} + \text{HO}\cdot + \text{OH}^-$, we examined whether iron treatment can also induce more ROS in PS-DK fibroblasts than in wild-type fibroblasts. The cellular ROS level in PS-DK fibroblasts treated with 30 μ M ferrous sulfate showed a

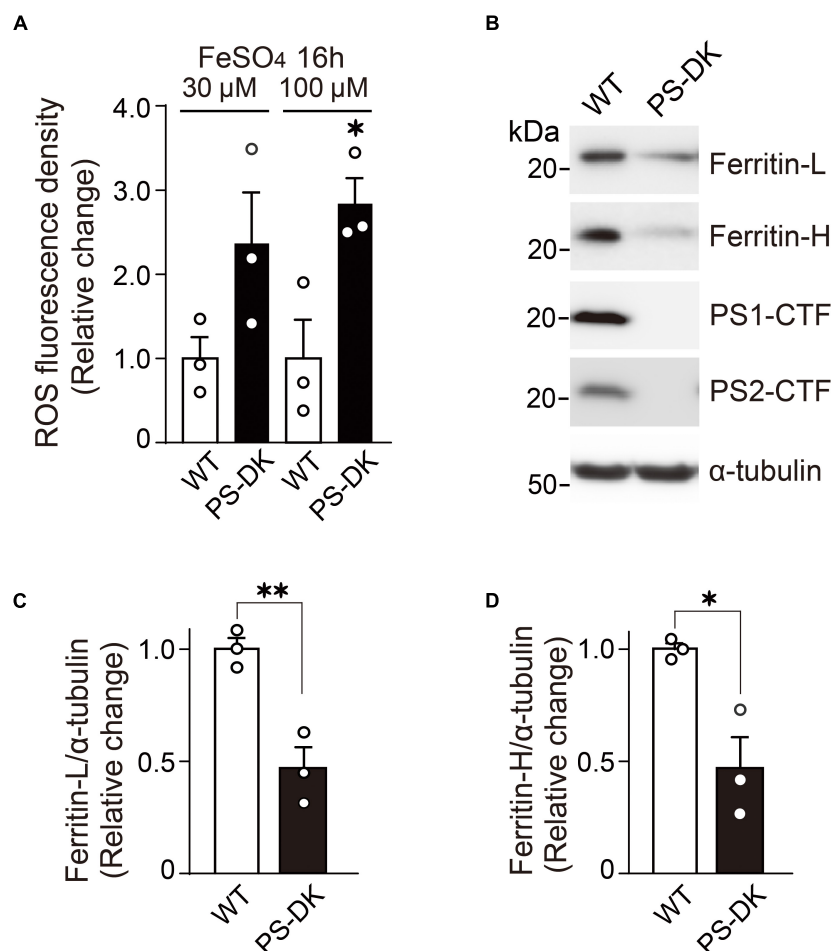


FIGURE 2 | PS-DK fibroblasts generated more ROS by iron-treatment and showed lower intracellular ferritin levels than wild-type fibroblasts. **(A)** ROS fluorescence density were measured 16 h after treatment with ferrous sulfate. PS-DK fibroblasts showed higher ROS levels after iron-treatment. $n = 3$, from 3 independent experiments, $*P < 0.05$, unpaired two-tailed Student's t -test. **(B)** Western blot analysis of intracellular ferritin light and heavy chains, PS1 C-terminal fragment (CTF) and PS2 CTF. **(C,D)** Quantification of intracellular ferritin light and heavy chain levels. Their levels were normalized to α -tubulin protein levels. $n = 3$, from 3 independent experiments, $*P < 0.05$, $**P < 0.01$, unpaired two-tailed Student's t -test. All quantitative data shown as mean \pm SEM. Ferritin-L, ferritin light chain. Ferritin-H, ferritin heavy chain.

tendency toward increase compared with wild-type fibroblasts. The treatment with 100 μ M ferrous sulfate significantly increased the cellular ROS level in PS-DK fibroblasts compared with wild-type fibroblasts (Figure 2A). This result suggests that PS-DK fibroblasts have lower antioxidant molecules against iron-induced free radical generation. Antioxidant molecules include direct ROS scavengers and indirect metal binding proteins that quench metal ions to inhibit secondary generation of free radicals. Ferritin is a major intracellular iron binding and storage protein that provides protective effects to cells against free iron-induced oxidative stress (Philpott et al., 2017). We then examined the cellular levels of ferritin in wild-type and PS-DK fibroblasts. Interestingly, total ferritin, ferritin light chain and ferritin heavy chain markedly decreased in PS-DK fibroblasts compared with wild-type fibroblasts (Figures 2B–D). These results suggest that the decrease in ferritin levels may result in increased

free iron and increased susceptibility to iron-induced oxidative damage.

Ferritin Light and Heavy Chains in Response to Iron Treatment Decreased in PS Double-Knockout Fibroblasts

Ferritin sequesters iron in a non-toxic form and its expression level is regulated by labile iron for protecting cells from damage triggered by excess iron (Picard et al., 1998; Torti and Torti, 2002). We examined whether the regulation of cellular ferritin levels by iron treatment is impaired in PS-DK fibroblasts. Wild-type and PS-DK fibroblasts were treated with 1, 3, and 10 μ M ferrous sulfate, respectively. Both wild-type and PS-DK cells showed iron dose-dependent increases in ferritin light chain and ferritin heavy chain levels (Figures 3A,C). However, the cellular levels of ferritin light chain were significantly lower in PS-DK

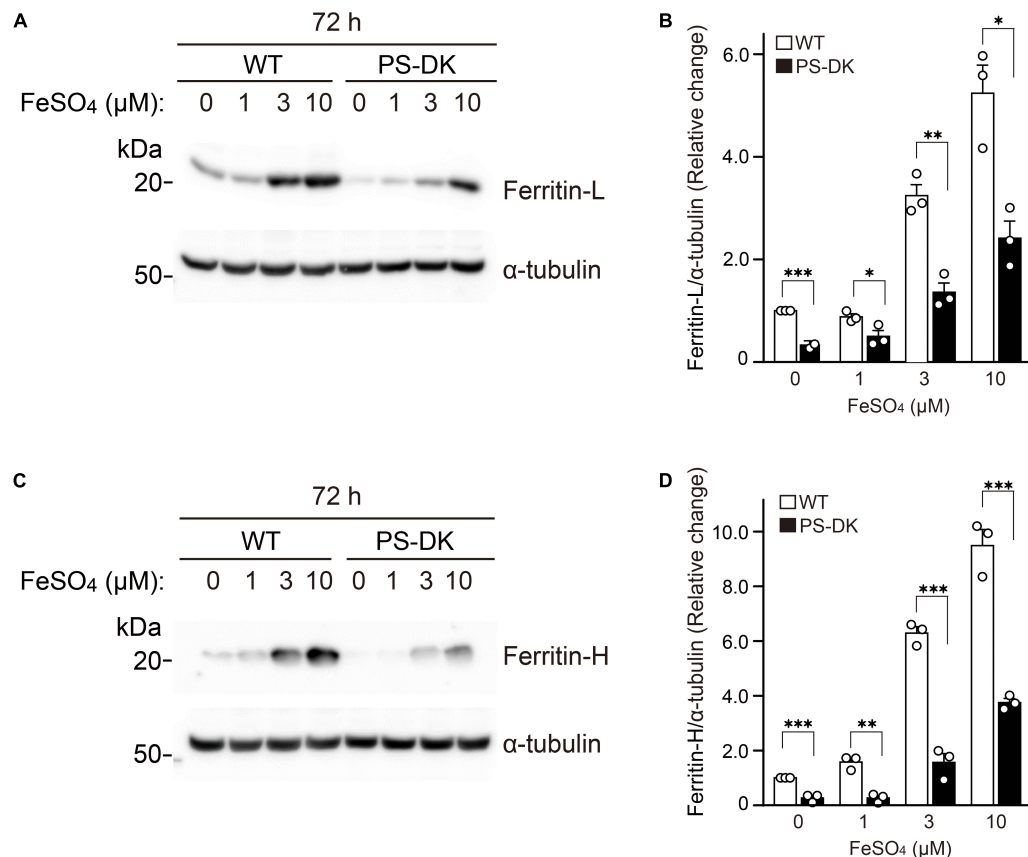


FIGURE 3 | PS deficiency reduced ferritin levels in response to iron treatment. **(A)** Western blot analysis of ferritin light chain in wild-type and PS-DK fibroblasts treated with ferrous sulfate. **(B)** Quantification of intracellular ferritin light chain levels. Their levels were normalized to α -tubulin protein levels. $n = 3$, from 3 independent experiments, $*P < 0.05$, $**P < 0.01$, $***P < 0.001$, one-way ANOVA followed by Tukey's multiple-comparison tests. **(C)** Western blot analysis of ferritin heavy chain in wild-type and PS-DK fibroblasts treated with ferrous sulfate. **(D)** Quantification of intracellular ferritin heavy chain levels. Their levels were normalized to α -tubulin protein levels. $n = 3$, from 3 independent experiments, $**P < 0.01$, $***P < 0.001$, one-way ANOVA followed by Tukey's multiple-comparison tests. All quantitative data shown as mean \pm SEM. Ferritin-L, ferritin light chain. Ferritin-H, ferritin heavy chain.

fibroblasts than wild-type fibroblasts at all concentration of iron treatment. Ferritin light chain levels in PS-DK fibroblasts were 57, 42, and 46% compared with wild fibroblasts at 1, 3, and 10 μ M ferrous sulfate treatment, respectively (**Figure 3B**). Ferritin heavy chain levels in PS-DK fibroblasts were 17, 25, and 40% compared with wild fibroblasts at 1, 3, and 10 μ M ferrous sulfate treatment, respectively (**Figure 3D**). These results suggest that PS deficiency does not only reduce the basal level of cellular ferritin, but also reduce the levels of ferritin in response to iron over load. Thus, the increase of ROS levels in PS-DK fibroblasts may result from decreased cellular ferritin levels and increased labile iron ions.

Inhibition of γ -Secretase Activity Reduced the Increase of Ferritin in Response to Iron Treatment

PS is a multifunctional molecule and its major function is serving as a catalytic component of γ -secretase complex (De Strooper et al., 2012). To examine whether γ -secretase activity is involved in regulating ferritin levels in response to iron treatment, wild-type fibroblasts were treated with a γ -secretase inhibitor, DAPT

(5 μ M), and ferrous sulfate (0, 1, 2, 5, and 10 μ M). In the presence of DAPT, ferritin light and heavy chain levels induced by iron treatment was significantly lower than that without DAPT treatment (**Figures 4A,C**). DAPT treatment suppressed ferritin light chain levels to 37% at 5 μ M ferrous sulfate treatment, and to 56% at 10 μ M ferrous sulfate treatment compared to those without DAPT treatment (**Figure 4B**). Ferritin heavy chain levels were also decreased by DAPT to 82% at 5 μ M ferrous sulfate treatment and to 53% at 10 μ M ferrous sulfate treatment (**Figure 4D**). These results suggest that γ -secretase activity can regulate ferritin levels in response to iron treatment and that impairment of γ -secretase activity may increase susceptibility to iron-induced oxidative damage.

Overexpression of Mutant PS1 Decreased Ferritin Light Chain Levels and Increased Reactive Oxygen Species Levels in Wild-Type Fibroblasts

To examine whether PS mutants found in FAD (PS1 Δ E9 and PS1G384A) or PS mutants without γ -secretase activity

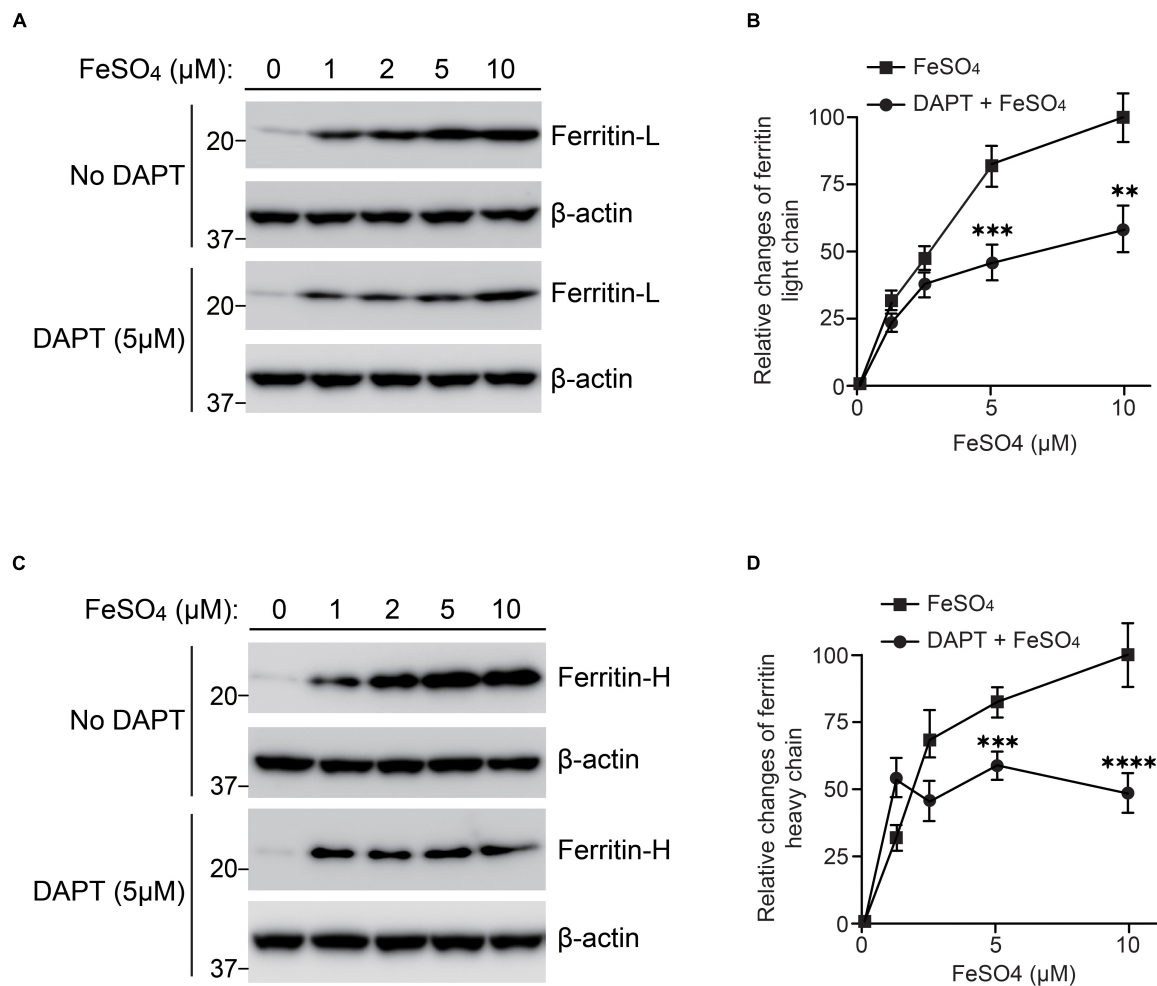


FIGURE 4 | Inhibition of γ -secretase activity reduced ferritin levels in response to iron treatment in wild-type fibroblasts. Wild-type fibroblasts were treated with or without 5 μ M DAPT in DMEM containing 10% FBS after seeding. After 1 h, ferrous sulfate was added and the cells were incubated at 37°C in 5% CO₂ for 72 h. **(A)** Western blot analysis of ferritin light chain in wild-type fibroblasts treated with or without ferrous sulfate or DAPT. **(B)** Quantification of intracellular ferritin light chain levels. Ferritin light chain levels at 10 μ M ferrous sulfate treatment (without DAPT) were normalized to α -tubulin protein levels and adjusted to 100%. The relative change of ferritin light chain at each concentration was calculated. DAPT treatment significantly inhibited intracellular ferritin light chain levels. $n = 3$, from 3 independent experiments, $**P < 0.01$, $***P < 0.001$, one-way ANOVA followed by Tukey's multiple-comparison tests. **(C)** Western blot analysis of ferritin heavy chain in wild-type fibroblasts treated with or without ferrous sulfate or DAPT. **(D)** Quantification of intracellular ferritin heavy chain levels. Ferritin heavy chain levels in wild-type fibroblasts with 10 μ M ferrous sulfate treatment (without DAPT) were normalized to α -tubulin protein levels and adjusted to 100%. The relative change of ferritin light chain at each concentration was calculated. DAPT treatment significantly inhibited intracellular ferritin heavy chain levels. $n = 3$, from 3 independent experiments, $***P < 0.001$, $****P < 0.0001$, one-way ANOVA followed by Tukey's multiple-comparison tests. ■, ferrous sulfate treatment. ●, DAPT and ferrous sulfate treatment. All quantitative data shown as mean \pm SEM. Ferritin-L, ferritin light chain. Ferritin-H, ferritin heavy chain.

(PS1D257A and PS1D385A) can reduce ferritin level and increase ROS level, we overexpressed PS1 Δ E9, PS1G384A, PS1D257A, or PS1D385A in wild-type fibroblasts. PS1 Δ E9, PS1D257A, and PS1D385A significantly decreased ferritin light chain levels, whereas did not affect ferritin heavy chain levels. PS1G384A did not change ferritin light or heavy chain levels (**Figures 5A–D**). ROS levels in fibroblasts overexpressing PS1D257A or PS1D385A are markedly more than control cells (**Figure 5E**). These results suggest that PS mutants with less γ -secretase activity have dominant negative effects on reducing ferritin light chain levels and increasing ROS levels.

DISCUSSION

Neurodegeneration in the brain of patients with AD has long been considered to be caused by the aggregation of toxic form of A β , A β 42. This notion is strongly supported by the findings that most of genetic mutations in *APP*, *PSEN1*, and *PSEN2* found in FAD showed increased A β 42 generation or A β 42/A β 40 ratio (Scheltens et al., 2016; Sun et al., 2017). However, oxidative damage is found to precede A β deposition and iron extensively deposits in amyloid plaques and neurofibrillary tangles in the brain of patient with SAD (Nunomura et al., 2001; Ayton et al., 2013). In support of this oxidative damage pathogenesis

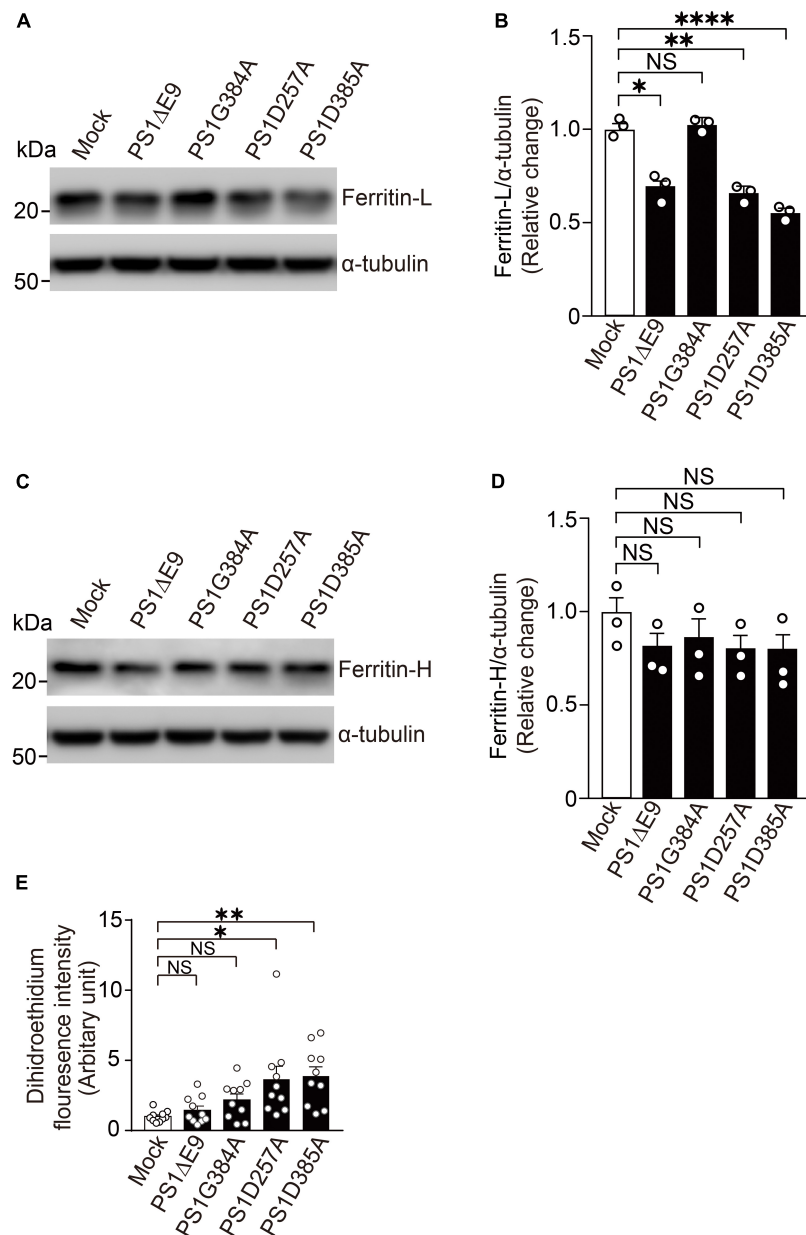


FIGURE 5 | Overexpression of PS1 mutants decreased ferritin light chain levels and increased ROS levels in wild-type fibroblasts. **(A)** Western blot analysis of intracellular ferritin light chain in wild-type fibroblasts overexpressing PS1ΔE9, PS1G384A, PS1D257A, or PS1D385A. **(B)** Quantification of intracellular ferritin light chain levels. Their levels were normalized to α-tubulin protein levels. $n = 3$, from 3 independent experiments, $*P < 0.05$, $**P < 0.01$, $****P < 0.0001$, one-way ANOVA followed by Tukey's multiple-comparison tests. **(C)** Western blot analysis of intracellular ferritin heavy chain in wild-type fibroblasts overexpressing PS1ΔE9, PS1G384A, PS1D257A, or PS1D385A. **(D)** Quantification of intracellular ferritin heavy chain levels. Their levels were normalized to α-tubulin protein levels. $n = 3$, from 3 independent experiments, NS, not significant, one-way ANOVA followed by Tukey's multiple-comparison tests. **(E)** Fluorescence intensity in wild-type fibroblasts infected with retrovirus bearing human PS1 mutations (PS1ΔE9, PS1G384A, PS1D257A, and PS1D385A) were determined by Image J software. $n = 10$ images from 3 independent experiments, $*P < 0.05$, $**P < 0.01$. NS, not significant, by one-way ANOVA followed by Tukey's multiple-comparison tests.

theory for AD, we have found that Aβ₄₀, the major form all secreted Aβ, has neuroprotective effects against iron-induced oxidative damage (Zou et al., 2002; Zou and Michikawa, 2008). The findings that iron overload can accelerate Aβ production also support this notion (Becerril-Ortega et al., 2014; Shen et al., 2019). Here we demonstrated that PS deficiency

leads to increased ROS generation in cells at basal level and after treatment with H₂O₂ or labile iron. In addition, cellular ferritin light and heavy chain levels significantly decreased in PS-DK fibroblasts compared with wild-type fibroblasts, suggesting that the lack of iron sequestration by ferritin increases ROS generation in PS-DK cells.

Multitude of omics studies have characterized expression profiles of thousands of molecular changes and uncovered neuronal gene subnetworks as the most dysregulated in human AD brain and AD mouse models. Interestingly, ferritin heavy and light chain genes, *FTHL* and *FTL*, have been found to be dysregulated in human AD brain and AD mouse models, indicating an important role of ferritin in AD pathophysiology (Bai et al., 2020; Wang et al., 2021). Ferritin plays a key role in maintaining iron homeostasis by capturing and buffering the intracellular labile iron pool (Torti and Torti, 2002). The translation of ferritin is controlled by RNA-binding proteins, iron regulatory protein-1 (IRP1) and IRP2 that interact with iron responsive element (IRE) (Gray and Hentze, 1994; Pantopoulos, 2004; Zhou and Tan, 2017). Microglia highly express *FTL* with increased Iba1 expression, a marker for activated microglia and represented as iron-accumulating microglia, whereas *FTL* expressed to a lower extent in neurons in human brain (Kenkhuis et al., 2021). Microglia are in a constant cross-talk with neurons and are capable of tight regulation of neuronal homeostasis. Activated microglia reacts against disease and injury, protect from chronic neuroinflammation and oxidative damage, a hallmark feature of neurodegenerative diseases (Ndayisaba et al., 2019). Thus, PS may be involved in maintaining neuronal homeostasis by regulating iron metabolism in both microglia and neurons.

We found that suppression of γ -secretase activity significantly inhibited the elevation ferritin light and heavy chains in response to iron treatment (Figure 4), suggesting that γ -secretase activity may be involved in IRP- and IRE-mediated pathway in iron metabolism. Among the *PSEN1* mutations examined in this study, PS1 Δ E9 causes a reduction in A β 40 production, whereas PS1G384A mutant significantly increases A β 42 production, suggesting that PS1 Δ E9 results in a decreased γ -secretase activity (Bentahir et al., 2006). PS1D257A and PS1D385A also greatly reduce γ -secretase activity (Wolfe et al., 1999). Thus, the decreased ferritin light chain levels and increase ROS levels in PS1D257A and PS1D385A overexpressing cells may result from loss of γ -secretase activity (Figure 5). It is possible that γ -secretase inhibitors using in clinical trials may reduce ferritin levels or increase ROS levels. This should be studied in human samples from clinical trials in future. There are more than 100 substrates of γ -secretase were identified (De Strooper et al., 2012), that which substrate is

responsible for regulating cellular ferritin levels needs to be further studied. Although most of mutations of *PSEN* found in FAD result in impaired γ -secretase activity, dysregulated A β 42/40 ratio and APP cleavage, our findings suggest FAD *PSEN* mutations may also lead to increased oxidative damage by affecting cellular ferritin levels and provide a novel molecular mechanism underlying the neuronal degeneration in FAD induced by PS mutations.

DATA AVAILABILITY STATEMENT

The raw data supporting the conclusions of this article will be made available by the authors, without undue reservation.

AUTHOR CONTRIBUTIONS

KZ, SI, YS, YG, TN, HK, and TT: data curation. KZ, SI, and YS: data analysis. KZ: conceptualization and writing the manuscript. KZ and MM: supervision and funding. All authors contributed to the article and approved the submitted version.

FUNDING

This work was supported by the Grant-in-Aid for Scientific Research C 19K07846 and 22K07352 (to KZ), Grant-in-Aid for Scientific Research B 16H05559 (to MM), and Challenging Exploratory Research 15K15712 (to MM) from the Ministry of Education, Culture, Sports, Science, and Technology, Japan. This work was also supported by AMED under grant number JP20dk0207050h001 and JP20de010702 (to MM), and by Grants-in-aid from “the 24th General Assembly of the Japanese Association of Medical Sciences” (to KZ), the Daiko Foundation (to KZ), the Hirose International Scholarship Foundation (to KZ), and the Hori Sciences and Arts Foundation (to KZ).

ACKNOWLEDGMENTS

We thank Bart De Strooper for providing wild-type and PS double knockout (PS-DK) mouse embryonic fibroblasts.

REFERENCES

- Ayton, S., Lei, P., and Bush, A. I. (2013). Metallostasis in alzheimer's disease. *Free Radic. Biol. Med.* 62, 76–89. doi: 10.1016/j.freeradbiomed.2012.10.558
- Bai, B., Wang, X., Li, Y., Chen, P.-C., Yu, K., Dey, K. K., et al. (2020). Deep multilayer brain proteomics identifies molecular networks in alzheimer's disease progression. *Neuron* 105, 975.e–991.e.
- Becerril-Ortega, J., Bordji, K., Freret, T., Rush, T., and Buisson, A. (2014). Iron overload accelerates neuronal amyloid-beta production and cognitive impairment in transgenic mice model of Alzheimer's disease. *Neurobiol. Aging* 35, 2288–2301. doi: 10.1016/j.neurobiolaging.2014.04.019
- Belaidi, A. A., and Bush, A. I. (2016). Iron neurochemistry in alzheimer's disease and parkinson's disease: targets for therapeutics. *J. Neurochem.* 139(Suppl. 1), 179–197. doi: 10.1111/jnc.13425
- Bentahir, M., Nyabi, O., Verhamme, J., Tolia, A., Horre, K., Wiltfang, J., et al. (2006). Presenilin clinical mutations can affect gamma-secretase activity by different mechanisms. *J. Neurochem.* 96, 732–742. doi: 10.1111/j.1471-4159.2005.03578.x
- Bindokas, V. P., Jordan, J., Lee, C. C., and Miller, R. J. (1996). Superoxide production in rat hippocampal neurons: selective imaging with hydroethidine. *J. Neurosci.* 16, 1324–1336. doi: 10.1523/JNEUROSCI.16-04-01324.1996
- Borchelt, D. R., Thinakaran, G., Eckman, C. B., Lee, M. K., Davenport, F., Ratovitsky, T., et al. (1996). Familial alzheimer's disease-linked presenilin 1 variants elevate Abeta1-42/1-40 ratio *in vitro* and *in vivo*. *Neuron* 17, 1005–1013. doi: 10.1016/s0896-6273(00)80230-5
- Chen, Z., and Zhong, C. (2014). Oxidative stress in alzheimer's disease. *Neurosci. Bull.* 30, 271–281.

- De Strooper, B., Iwatsubo, T., and Wolfe, M. S. (2012). Presenilins and gamma-secretase: structure, function, and role in alzheimer disease. *Cold Spring Harb. Perspect. Med.* 2:a006304. doi: 10.1101/cshperspect.a006304
- Gray, N. K., and Hentze, M. W. (1994). Iron regulatory protein prevents binding of the 43S translation pre-initiation complex to ferritin and eALAS mRNAs. *Embo J.* 13, 3882–3891. doi: 10.1002/j.1460-2075.1994.tb06699.x
- Herreman, A., Hartmann, D., Annaert, W., Saftig, P., Craessaerts, K., Serneels, L., et al. (1999). Presenilin 2 deficiency causes a mild pulmonary phenotype and no changes in amyloid precursor protein processing but enhances the embryonic lethal phenotype of presenilin 1 deficiency. *Proc. Natl. Acad. Sci. U.S.A.* 96, 11872–11877. doi: 10.1073/pnas.96.21.11872
- Islam, S., Sun, Y., Gao, Y., Nakamura, T., Noorani, A. A., Li, T., et al. (2022). Presenilin Is essential for ApoE secretion, a novel role of presenilin involved in alzheimer's disease pathogenesis. *J. Neurosci.* 42, 1574–1586. doi: 10.1523/JNEUROSCI.2039-21.2021
- Kenkhuys, B., Somarakis, A., de Haan, L., Dzyubachyk, O., Ijsselstein, M. E., de Miranda, N. F. C. C., et al. (2021). Iron loading is a prominent feature of activated microglia in Alzheimer's disease patients. *Acta Neuropathol. Commun.* 9:27. doi: 10.1186/s40478-021-01126-5
- Knopman, D. S., Amieva, H., Petersen, R. C., Chetelat, G., Holtzman, D. M., Hyman, B. T., et al. (2021). Alzheimer disease. *Nat. Rev. Dis. Primers* 7:33.
- McKhann, G., Drachman, D., Folstein, M., Katzman, R., Price, D., and Stadlan, E. M. (1984). Clinical diagnosis of Alzheimer's disease: report of the NINCDS-ADRDA work group under the auspices of department of health and human services task force on alzheimer's disease. *Neurology* 34, 939–944. doi: 10.1212/wnl.34.7.939
- Ndayisaba, A., Kaindlstorfer, C., and Wenning, G. K. (2019). Iron in neurodegeneration – cause or consequence? *Front. Neurosci.* 13:180. doi: 10.3389/fnins.2019.00180
- Nunomura, A., Perry, G., Aliev, G., Hirai, K., Takeda, A., Balraj, E. K., et al. (2001). Oxidative damage is the earliest event in Alzheimer disease. *J. Neuropathol. Exp. Neurol.* 60, 759–767. doi: 10.1093/jnen/60.8.759
- Pantopoulos, K. (2004). Iron metabolism and the IRE/IRP regulatory system: an update. *Ann. N.Y. Acad. Sci.* 1012, 1–13. doi: 10.1196/annals.1306.001
- Philpott, C. C., Ryu, M. S., Frey, A., and Patel, S. (2017). Cytosolic iron chaperones: proteins delivering iron cofactors in the cytosol of mammalian cells. *J. Biol. Chem.* 292, 12764–12771. doi: 10.1074/jbc.R117.791962
- Picard, V., Epsztejn, S., Santambrogio, P., Cabantchik, Z. I., and Beaumont, C. (1998). Role of ferritin in the control of the labile iron pool in murine erythroleukemia cells*. *J. Biol. Chem.* 273, 15382–15386. doi: 10.1074/jbc.273.25.15382
- Saura, C. A., Choi, S. Y., Beglopoulos, V., Malkani, S., Zhang, D., Shankaranarayana Rao, B. S., et al. (2004). Loss of presenilin function causes impairments of memory and synaptic plasticity followed by age-dependent neurodegeneration. *Neuron* 42, 23–36. doi: 10.1016/s0896-6273(04)00182-5
- Scheltens, P., Blennow, K., Breteler, M. M., de Strooper, B., Frisoni, G. B., Salloway, S., et al. (2016). Alzheimer's disease. *Lancet* 388, 505–517.
- Selkoe, D. J., and Hardy, J. (2016). The amyloid hypothesis of alzheimer's disease at 25 years. *EMBO Mol. Med.* 8, 595–608. doi: 10.15252/emmm.201606210
- Shen, X., Liu, J., Fujita, Y., Liu, S., Maeda, T., Kikuchi, K., et al. (2019). Iron treatment inhibits Abeta42 deposition *in vivo* and reduces Abeta42/Abeta40 ratio. *Biochem. Biophys. Res. Commun.* 512, 653–658. doi: 10.1016/j.bbrc.2019.01.119
- Shoji, M., Golde, T. E., Ghiso, J., Cheung, T. T., Estus, S., Shaffer, L. M., et al. (1992). Production of the Alzheimer amyloid beta protein by normal proteolytic processing. *Science* 258, 126–129. doi: 10.1126/science.1439760
- Smith, M. A., Harris, P. L., Sayre, L. M., and Perry, G. (1997). Iron accumulation in Alzheimer disease is a source of redox-generated free radicals. *Proc. Natl. Acad. Sci. U.S.A.* 94, 9866–9868. doi: 10.1073/pnas.94.18.9866
- Sun, L., Zhou, R., Yang, G., and Shi, Y. (2017). Analysis of 138 pathogenic mutations in presenilin-1 on the *in vitro* production of Aβ₄₂ and Aβ₄₀ peptides by γ-secretase. *Proc. Natl. Acad. Sci. U.S.A.* 114, E476–E485. doi: 10.1073/pnas.1618657114
- Torti, F. M., and Torti, S. V. (2002). Regulation of ferritin genes and protein. *Blood* 99, 3505–3516.
- Wang, M., Li, A., Sekiya, M., Beckmann, N. D., Quan, X., Schrode, N., et al. (2021). Transformative network modeling of multi-omics data reveals detailed circuits, key regulators, and potential therapeutics for alzheimer's disease. *Neuron* 109, 257.e–272.e. doi: 10.1016/j.neuron.2020.11.002
- Watanabe, H., and Shen, J. (2017). Dominant negative mechanism of Presenilin-1 mutations in FAD. *Proc. Natl. Acad. Sci. U.S.A.* 114, 12635–12637. doi: 10.1073/pnas.1717180114
- Wolfe, M. S., Xia, W., Ostaszewski, B. L., Diehl, T. S., Kimberly, W. T., and Selkoe, D. J. (1999). Two transmembrane aspartates in presenilin-1 required for presenilin endoproteolysis and gamma-secretase activity. *Nature* 398, 513–517. doi: 10.1038/19077
- Zecca, L., Youdim, M. B., Riederer, P., Connor, J. R., and Crichton, R. R. (2004). Iron, brain ageing and neurodegenerative disorders. *Nat. Rev. Neurosci.* 5, 863–873.
- Zhou, Z. D., and Tan, E. K. (2017). Iron regulatory protein (IRP)-iron responsive element (IRE) signaling pathway in human neurodegenerative diseases. *Mol. Neurodegener.* 12:75. doi: 10.1186/s13024-017-0218-4
- Zou, K., Gong, J. S., Yanagisawa, K., and Michikawa, M. (2002). A novel function of monomeric amyloid beta-protein serving as an antioxidant molecule against metal-induced oxidative damage. *J. Neurosci.* 22, 4833–4841. doi: 10.1523/JNEUROSCI.22-12-04833.2002
- Zou, K., and Michikawa, M. (2008). Angiotensin-converting enzyme as a potential target for treatment of Alzheimer's disease: inhibition or activation? *Rev. Neurosci.* 19, 203–212. doi: 10.1515/revneuro.2008.19.4-5.203

Conflict of Interest: The authors declare that the research was conducted in the absence of any commercial or financial relationships that could be construed as a potential conflict of interest.

Publisher's Note: All claims expressed in this article are solely those of the authors and do not necessarily represent those of their affiliated organizations, or those of the publisher, the editors and the reviewers. Any product that may be evaluated in this article, or claim that may be made by its manufacturer, is not guaranteed or endorsed by the publisher.

Copyright © 2022 Zou, Islam, Sun, Gao, Nakamura, Komano, Tomita and Michikawa. This is an open-access article distributed under the terms of the Creative Commons Attribution License (CC BY). The use, distribution or reproduction in other forums is permitted, provided the original author(s) and the copyright owner(s) are credited and that the original publication in this journal is cited, in accordance with accepted academic practice. No use, distribution or reproduction is permitted which does not comply with these terms.



Extraversion Is Associated With Lower Brain Beta-Amyloid Deposition in Cognitively Normal Older Adults

Hwamee Oh^{1,2,3,4,5*}

¹Department of Psychiatry and Human Behavior, Warren Alpert Medical School, Brown University, Providence, RI, United States, ²Department of Cognitive, Linguistic, and Psychological Sciences, Brown University, Providence, RI, United States, ³Carney Institute for Brain Science, Brown University, Providence, RI, United States, ⁴Memory and Aging Program, Butler Hospital, Providence, RI, United States, ⁵Division of Cognitive Neuroscience, Department of Neurology, Columbia University College of Physicians and Surgeons, New York, NY, United States

OPEN ACCESS

Edited by:

Agustin Ibanez,
Latin American Brain Health Institute
(BrainLat), Chile

Reviewed by:

Jeremy Andrew Elman,
University of California, San Diego,
United States
Michelle Farrell,
Massachusetts General Hospital and
Harvard Medical School,
United States

*Correspondence:

Hwamee Oh
Hwamee_Oh@brown.edu

Specialty section:

This article was submitted to
Alzheimer's Disease and Related
Dementias,
a section of the journal
Frontiers in Aging Neuroscience

Received: 20 March 2022

Accepted: 08 June 2022

Published: 13 July 2022

Citation:

Oh H (2022) Extraversion Is
Associated With Lower Brain
Beta-Amyloid Deposition in
Cognitively Normal Older Adults.
Front. Aging Neurosci. 14:900581.
doi: 10.3389/fnagi.2022.900581

Emerging evidence suggests that some personality traits may link to the vulnerability to or protection for Alzheimer's disease (AD). A causal mechanism underlying this relationship, however, remains largely unknown. Using ¹⁸F-Florbetaben positron emission tomography (PET) binding to beta-amyloid (A β) plaques, a pathological feature of AD, and functional magnetic resonance imaging (fMRI), we investigated pathological and functional correlates of extraversion and neuroticism in a group of healthy young and older subjects. We quantified the level of brain A β deposition in older individuals. Brain activity was measured in young adults using a task-switching fMRI paradigm. When we correlated personality scores of extraversion and neuroticism with these pathological and functional measures, higher extraversion, but not neuroticism, was significantly associated with lower global A β measures among older adults, accounting for age and sex. This association was present across widespread brain regions. Among young subjects, higher extraversion was associated with lower activity during task switching in the anterior cingulate cortex, left anterior insular cortex, left putamen, and middle frontal gyrus bilaterally, while higher neuroticism was associated with increased activity throughout the brain. The present results suggest that possibly *via* efficient neuronal activity, extraversion, one of the lifelong personality traits, may confer the protective mechanism against the development of A β pathology during aging.

Keywords: beta amyloid deposition, extraversion, neuroticism, personality, Alzheimer's disease risk factor

INTRODUCTION

Alzheimer's disease (AD) is characterized by the pathological accumulation of beta-amyloid (A β) peptides and tau-protein neurofibrillary tangles, followed by neuronal injury and severe cognitive impairment (Hardy and Selkoe, 2002; Jack et al., 2013). Neuropathological and epidemiological studies suggest that lifestyle factors such as education, social network, diet, and cognitive and physical activities, may confer an increased risk or conversely a protective mechanism for the clinical manifestation of AD as well as the development of AD pathology (Bennett et al., 2006, 2014; Stern, 2009). The observed association between lifestyle factors and clinical and pathological manifestation of AD points to the possibility that the vulnerability to AD pathology and onset of AD symptoms may develop over the lifespan. Although relatively less attention has

been given compared to these lifestyle factors, emerging evidence suggests that an individual's personality, a trait that is found to be relatively stable across the lifespan, relates to the increased risk or protection of AD (Wilson et al., 2007; Wang et al., 2009; Terracciano et al., 2013, 2014). A neuro-mechanistic explanation linking the personality traits to AD, however, is largely unknown. Personality often interacts with the proposed lifestyle factors such as cognitive and physical activity and social network (Ackerman and Heggstad, 1997; Bennett et al., 2014). Therefore, the understanding of the neural mechanism linking personality to AD risk will be an important step in disentangling specific effects of complex lifestyle variables that may act simultaneously across the lifespan in the development of resilience or vulnerability to AD.

Personality traits are an individual's styles and tendencies of interacting with external events. There is a general consensus that adult personality can be defined by five factors, known as the Big Five: neuroticism, extraversion, openness to experience, agreeableness, and conscientiousness (McCrae and Costa, 2008). Among personality traits, neuroticism has been mostly linked to an increased risk of dementia, while conscientiousness has been related to healthier lifestyle choices (Wilson et al., 2011; Low et al., 2013). Extraversion and openness have been associated positively with the intellectual ability which in turn moderates the severity of clinical symptoms (Ackerman and Heggstad, 1997; Valenzuela and Sachdev, 2006; Meng and D'Arcy, 2012). Over the course of AD, the level of neuroticism and extraversion has changed, showing a higher level of neuroticism and a lower level of extraversion in AD patients compared to premorbid status. Collectively, personality traits and AD risk have been linked; however, what neural mechanism underlies this relationship remains to be elucidated.

In the process of AD, A β accumulation, a pathological feature of AD, is considered as a relatively early event that antedates more than a decade the appearance of clinical symptoms (Bateman et al., 2012; Jack et al., 2013). Findings from both animal and human studies suggest that A β accumulation relates to neural activity and physiology early in life before plaque accumulation (Yan et al., 2009; Vlassenko et al., 2010; Bero et al., 2011; Oh et al., 2016a). For example, the regional concentration of interstitial fluid A β in young mice was associated with lactate production indicating neuronal activity, and was further related to amyloid- β plaque deposition in the same brain regions in APP transgenic aged mice (Bero et al., 2011). In humans, A β accumulation in older adults topographically overlaps with brain regions showing higher metabolic rates in young adults (Vlassenko et al., 2010; Oh et al., 2016a). Interestingly, neuroimaging studies examining personality trait-based phenotypes have shown differential brain activity patterns in relation to personality types. Among personality traits, introversion/extraversion and neuroticism have been the most influential and frequently studied dimensions of human personality. Across a range of emotional and cognitive tasks, neuroticism has been associated with increased brain activity in the medial frontoparietal network including the medial prefrontal cortex and precuneus (Hariri et al., 2002; Eisenberger et al., 2005; Haas et al., 2007). On the

other hand, extraversion has been associated with decreased activity across the brain reflecting neural processing efficiency or reduced self-consciousness (Eisenberger et al., 2005; Gray et al., 2005). Considering the epidemiological, neuropathological, and neurocognitive findings, personality traits, possibly *via* differential regulation of regional neural activity across the lifespan, may contribute to an individual's risk of the buildup of AD pathology during aging.

Based on the literature linking personality traits, neural activity, and A β deposition, we sought to directly test the relationship between personality and A β pathology and a potential neural mechanism underlying this relationship. Specifically, we tested whether extraversion is associated with lower A β pathology measured by 18 F-Florbetaben PET in cognitively normal older adults and reduced neural activity in the medial frontoparietal cortex during executive control in young adults. To confirm the specificity of the effect of extraversion on A β deposition *via* neural activity, we also examined the relationship between neuroticism and brain activation patterns in young adults. We hypothesized that cognitively normal older adults with higher extraversion scores would show lower A β pathology and that higher extraversion in young adults would be associated with reduced activity in the medial frontoparietal cortices during executive control. With neuroticism, we hypothesized that higher neuroticism scores would be associated with greater A β pathology in cognitively normal elderly and increased task-related brain activity in young adults. Because A β deposition is highly regulated by neural activity, a differential pattern of brain activity in association with extraversion and neuroticism in young adulthood would provide a link between personality and A β pathology, which may form across the lifespan and would be observed among older adults.

MATERIALS AND METHODS

Participants and Neuropsychological Assessment

Thirty-three healthy young (age range: 20–30) and 57 cognitively normal older adults (age range: 60–70) participated in the study. Demographic details are provided in **Table 1**. Participants were a subset of subjects who participated in our previous study (Oh et al., 2016b) and whose personality test measures were available. A detailed description of subject characteristics can be found in our previous report (Oh et al., 2016b). Briefly, all subjects were recruited *via* a market mailing procedure and older subjects were classified as either “Amyloid-positive” (A β +O) or “Amyloid-negative” (A β –O) based on amyloid PET measurements as described below. All subjects provided informed consent in accordance with the Institutional Review Boards of the College of Physicians and Surgeons of Columbia University. Participants were paid for their participation in the study.

A comprehensive battery of neuropsychological tests was administered to all participants to assess cognition. Among cognitive domains, we computed a composite score for processing speed/attention using Wechsler Adult Intelligence Scale-Third Edition (WAIS-III) Digit Symbol

TABLE 1 | Subject characteristics.

| | Young | Amyloid– Old | Amyloid+ Old |
|--------------------|------------|--------------|--------------|
| N | 33 | 43 | 14 |
| Age | 26.4 (3.1) | 65.3 (2.9) | 65.4 (3.7) |
| Sex (F,%) | 15.5 (1.9) | 16.4 (2.5) | 15.9 (1.8) |
| Amyloid index | – | 1.16 (0.05) | 1.36 (0.1) |
| Extraversion | 3.40 (0.8) | 3.34 (0.7) | 2.96 (0.8) |
| Neuroticism* | 2.90 (1.0) | 2.57 (0.7) | 2.17 (0.8) |
| Memory** | 0.5 (0.4) | –0.4 (0.6) | –0.3 (0.8) |
| Processing speed** | 0.8 (0.6) | –0.4 (0.7) | –0.3 (0.6) |

Values (SD). * $p < 0.05$, ** $p < 0.01$.

subtest (Wechsler, 1997), Trail Making Test Part A (Reitan, 1978; inverted value), and Stroop Color Naming test- Color naming in 90 s (Golden, 1978) and a composite score of episodic memory combining scores from Selective Reminding Test (SRT; Buschke and Fuld, 1974)—long term storage, SRT-continued recall, and SRT-recall at the last trial.

For extraversion and neuroticism scores, we used a subset of the international personality item pool (IPIP) Big-Five personality inventory (Goldberg, 1992), which additionally consists of items for openness, agreeableness, and conscientiousness. The IPIP inventory is a 50-item questionnaire, with 10 items for each personality type, on a 5-point Likert scale (1=“Very Inaccurate”, 2 = “Moderately Inaccurate”, 3 = “Neither Inaccurate nor Accurate”, 4 = “Moderately Accurate”, 5 = “Very Accurate”). An averaged score for each personality type represented each subject’s personality score.

As summarized in **Table 1**, older subjects were more educated, although at a trend level, than young subjects ($T_{(88)} = -1.8$, $p = 0.07$). Aβ+O vs. Aβ–O groups did not differ in age, gender, education, dementia rating scale (DRS), or IQ estimated by AMNART. With cognitive composite scores, young subjects showed significantly higher scores in memory than Aβ–O subjects, while no other group differences were found for both memory and processing speed composite scores. For extraversion and neuroticism scores, young subjects showed significantly higher scores in neuroticism compared to Aβ+O subjects. Personality scores for five factor personality domains are summarized for all subjects and by age group in **Supplementary Table 1**.

18F-Florbetaben-PET Acquisition, Image Processing, and Analysis

¹⁸F-Florbetaben was donated by Piramal (Piramal Pharma Inc.). Detailed information on ¹⁸F-Florbetaben PET data acquisition and image processing can be found in our previous report (Oh et al., 2016b). Briefly, scans were performed on a Siemens MCT PET/CT scanner in dynamic, three-dimensional acquisition mode over 20 min (4 × 5 min frames) beginning 50 min following the bolus injection of 10 mCi of ¹⁸F-Florbetaben. Dynamic PET frames (four scans) were aligned and averaged to form a mean PET image that was coregistered to each individual’s structural T1 image in FreeSurfer space. The standardized uptake value ratio (SUVR) was calculated for selected cortical regions encompassing frontal, temporal, parietal, and anterior/posterior cingulate cortices with the cerebellar gray matter as a reference

region (Landau et al., 2013, 2015). Mean SUVR values from these lobar ROIs constituted a global amyloid index for each subject. Amyloid positivity of elderly subjects was determined using a K-means clustering method as previously reported (Oh et al., 2015). Fourteen and 43 older subjects were classified as Aβ+ and Aβ– subjects, respectively. The proportion of Aβ+ subjects in our sample is comparable to the reports from other studies (Mormino, 2014).

In order to assess the relationship between personality traits and Aβ deposition, we performed two analyses: (Hardy and Selkoe, 2002) a multiple regression model using a mean cortical Aβ measure as a dependent variable and personality scores as an independent variable, and (Jack et al., 2013) the whole-brain voxel-wise analysis using general linear model treating voxel-wise Aβ level as a dependent measure and personality scores as an independent measure. The whole-brain family-wise error was cluster corrected to $p < 0.05$ (two-sided) using a cluster forming threshold of $p < 0.05$. Age and sex were controlled in all analyses.

fMRI Experimental Task

To assess a brain activation pattern in association with extraversion and neuroticism, we used the executive contextual task adapted from Koechlin et al. (2003) which is described in detail in our previous report (Oh et al., 2016b). Briefly, the fMRI task was designed to assess executive control function in a block-design in which either single or dual-task condition was assigned (**Supplementary Figure 1**). During fMRI scans, a letter in either red or green appeared on the screen and subjects were asked to do vowel/consonant judgment for a green letter and lower/upper-case judgment for a red letter. For a single task condition, either a green or a red letter appeared throughout a block so that subjects had to do only one type of task throughout the task block. For a dual-task condition, color of the letters changed between green and red so that subjects had to switch between two tasks within a task block accordingly. Twelve letters were presented for a maximum of 2,400 ms each within a block that was 33.5 s in duration. One-third of letters in a block appeared in white, for which no response was required. Each functional run consisted of four tasks (two single-task and two dual-task) blocks and two resting condition blocks during which no stimuli were presented and no response was required; in total, the scan session was composed of six functional runs. The executive contextual task fMRI session lasted approximately 26 min.

Response time (RT) of correct trials and proportion correct for single and dual-task conditions were calculated for each individual and reported as behavioral measures.

MRI Data Acquisition

Participants underwent MRI using a 3T Philips Achieva System equipped with a standard quadrature headcoil. High-resolution T1-weighted magnetization-prepared rapid gradient echo (MPPAGE) scans were collected axially for each subject (TR = 6.6 ms, TE = 3 ms, flip angle = 8°, field of view (FOV) = 256 × 256 mm, matrix size: 256 × 256 mm, slices: 165, voxel size = 1 × 1 × 1 mm³). For the executive context task scans, 111 volumes of functional images were acquired in each

run (six runs in total) using a T2*-weighted gradient-echo echo planar images (EPI) sequence (TR = 2,000 ms; TE = 20 ms; flip angle = 72°; FOV = 224 × 224 mm; voxel size = 2 × 2 mm; slice thickness = 3 mm; duration = 3.5 min). Each functional volume consisted of 41 transverse slices per volume. Four dummy volumes acquired at the beginning of each functional run were discarded from the data set before image processing and analysis.

Structural MRI Image Processing

For each subject, a single structural T1 image was processed through FreeSurfer v5.1 to implement region of interest (ROI) labeling following the FreeSurfer processing pipeline¹. Briefly, structural images were bias field corrected, intensity normalized, and skull stripped using a watershed algorithm, followed by a tissue-based segmentation, defining gray/white matter and pial surfaces, and topology correction (Dale et al., 1999). Subcortical and cortical ROIs spanning the entire brain were defined in each subject's native space (Fischl et al., 2002).

fMRI Image Processing and Analysis

All fMRI analyses were performed with SPM8 (Wellcome Department of Imaging Neuroscience, London, UK). A detailed description of fMRI data preprocessing and subject-level analysis can be found elsewhere (Oh et al., 2016b). To identify brain regions that show task-related activity associated with extraversion and neuroticism in young adults, we focused on task-related activity from three comparisons/contrasts: single-task condition compared with baseline, dual-task condition compared with baseline, dual vs. single task contrast. Using general linear models, each comparison/contrast-related activity was regressed on extraversion and neuroticism scores, with gender as covariates of no interest. The whole-brain family-wise error was cluster corrected to $p < 0.05$ (two-sided) using a cluster forming threshold of $p < 0.05$.

Non-image Data Analysis

All non-image data analysis was conducted using SPSS v.22. The relationship between personality traits and A β deposition was assessed using multiple regression with a mean cortical A β measure as a dependent measure and personality scores as an independent measure. The direct correlation across all older adults was further probed using analysis of covariance (ANCOVA) to assess whether the relationship between personality scores and global A β measures changes as a function of amyloid positivity status (i.e., an interaction effect of amyloid positivity status and personality scores on global A β measures). This analysis can help determine whether the association between levels of amyloid and extraversion is primarily driven by the A β + group or if the effect is seen across all individuals (meaning sub-threshold amyloid levels showed similar associations). The association between personality scores and cognition was assessed using cognitive composite scores of memory and processing speed as well as executive control task performance (e.g., RT and proportion accuracy). Age and sex were controlled as covariates of no interest.

RESULTS

Extraversion Is Associated With Lower Amyloid Deposition Among Cognitively Normal Older Adults

We assessed the relationship between personality traits and A β deposition using a mean cortical and whole-brain voxel-wise A β measures. Using multiple regression model with a mean cortical A β measure, we found that, among cognitively normal older adults, higher extraversion scores were significantly associated with lower global amyloid index ($\beta = -0.31$, $p < 0.05$; **Figure 1B**). In addition to a global A β measure, we found similar results using local amyloid deposition in the posterior cingulate cortex ($\beta = -0.37$, $p < 0.05$; **Figure 1C**). Neuroticism scores, however, were not significantly associated with amyloid burden ($p > 0.1$). A significant relationship between extraversion scores and amyloid burden was mainly driven by a significant association within the A β + group, as revealed by a significant interaction between extraversion scores and amyloid positivity status on the global amyloid index ($F = 4.2$, $p < 0.05$). Next, we performed the whole-brain voxel-wise analysis to further probe regional specificity for A β deposition in relation to extraversion scores. The cortical regions wherein the level of A β deposition is significantly related to extraversion score are shown in **Figure 1A** (cluster $p < 0.05$), indicating that higher extraversion scores are associated with lower A β deposition across frontal, parietal, and temporal cortices. These brain regions highly overlap with regions that typically accumulate more A β than other brain areas.

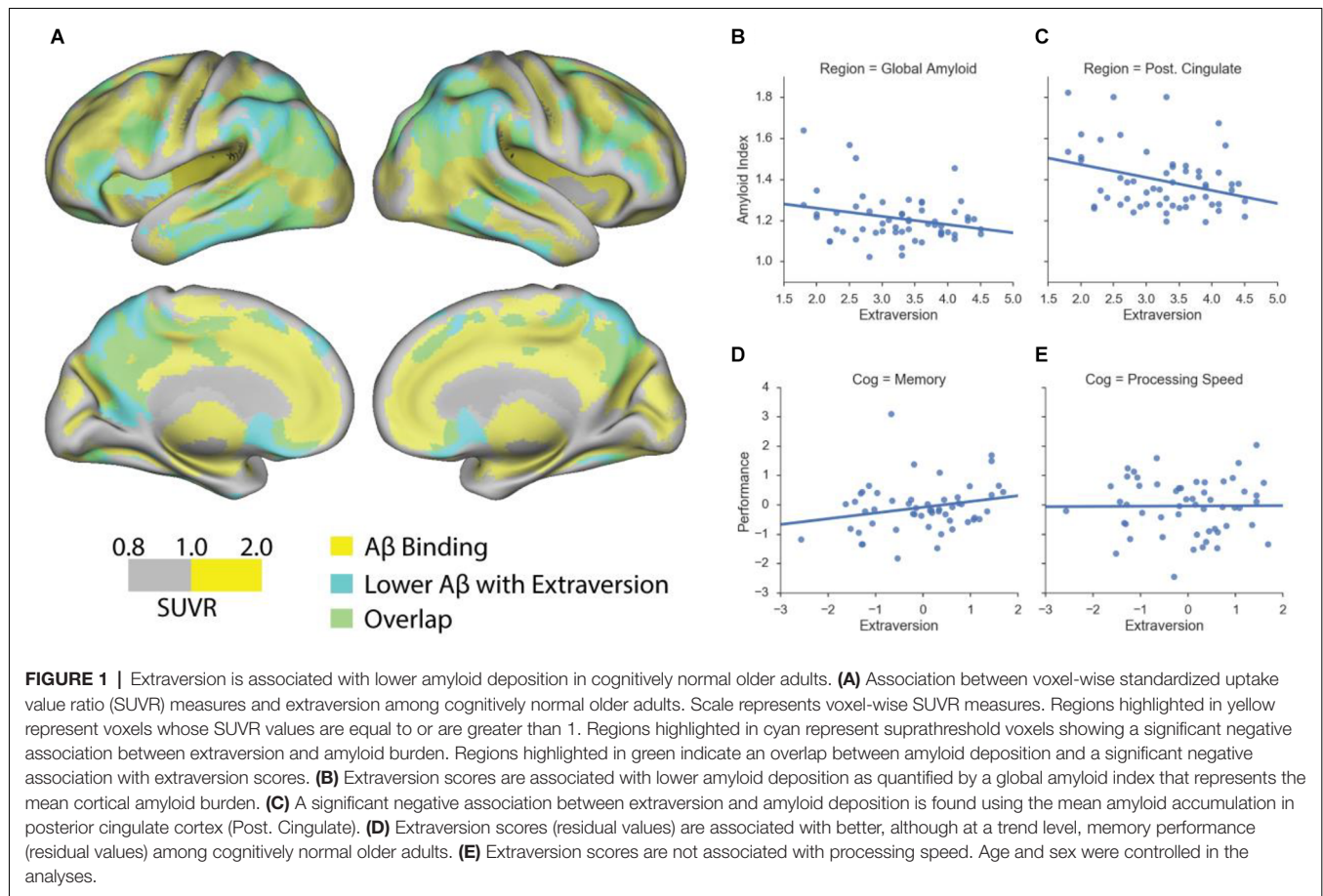
Using the two approaches, we further performed exploratory analyses to test an association between global A β deposition and other personality scores: conscientiousness, openness, and agreeableness. No significant association was found between global A β level and these personality measures ($ps > 0.1$). Age and sex were controlled in all analyses.

Differential Brain Activity Is Associated With Extraversion and Neuroticism in Young Adults

For fMRI task behavioral measures, we examined an association between extraversion/neuroticism scores and response time and proportion correct during single and dual-task conditions. Neither extraversion nor neuroticism was related to any behavioral performance measure ($ps > 0.1$).

For task-evoked brain activation, overall, higher extraversion scores in young adults were related to less brain activation in single task compared to baseline and dual-task compared to baseline (**Figure 2A**). Specifically, in the single task compared to baseline activity, higher extraversion was associated with reduced activation in the anterior cingulate, medial frontal cortex, and lateral middle frontal cortex. In the dual-task compared to baseline activity, a similar but more extended pattern of activity was found in association with extraversion scores. In the dual vs. single task contrast, there was no suprathreshold activity. With neuroticism, we found extensive increases in brain activity in association with higher neuroticism (**Figure 2B**). Across the activation maps, higher neuroticism was associated with

¹<http://surfer.nmr.mgh.harvard.edu/>



increased activity in the anterior cingulate cortex, anterior frontal cortex, right insular cortex, lateral inferior and middle frontal cortex, posterior cingulate cortex, right superior frontal cortex, caudate, and thalamus, while more extensive regions showed a positive association between neuroticism and brain activity for the dual-task compared to baseline activity.

Association Between Personality and Cognitive Performance

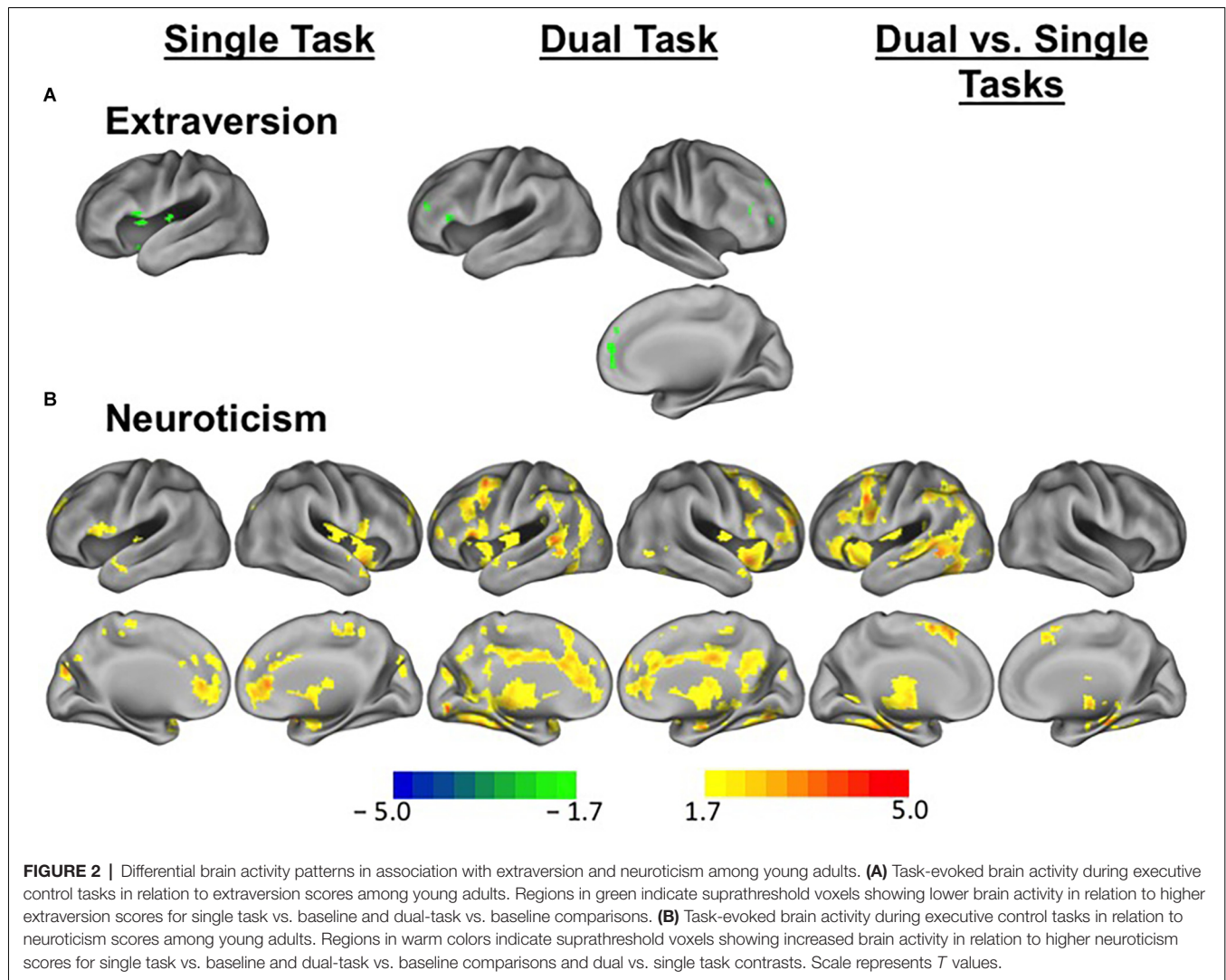
We conducted several exploratory analyses to better understand the demographic and psychosocial factors and cognition that relate to personality traits of extraversion and neuroticism in healthy young and cognitively normal older adults. Among cognitively normal older adults, we found no association between extraversion and neuroticism, controlling for age and sex. Extraversion was not correlated with age, but significantly correlated with sex, such that women showed significantly higher extraversion compared to men ($\beta = 0.4$, $p = 0.003$). Neuroticism was not correlated with sex, but significantly correlated with age, showing that the older the age is, the lower the neuroticism scores are ($\beta = -0.33$, $p = 0.02$). A significant relationship between extraversion and memory composite scores was found at a trend level ($\beta = 0.28$, $p = 0.08$; **Figure 1D**), but no significant relationship was found between extraversion and processing

speed composite score ($\beta = 0.03$, $p > 0.1$; **Figure 1E**). Neuroticism was not related to any cognitive composite measure. In relation to other personality traits, extraversion was significantly associated with openness ($\beta = 0.3$, $p = 0.02$), controlling for age and sex. Neuroticism was significantly negatively associated with agreeableness ($\beta = -0.27$, $p = 0.046$) as well as conscientiousness ($\beta = -0.35$, $p = 0.01$), controlling for age and sex.

Among young subjects, there was no association between extraversion and neuroticism ($p > 0.1$). Neither age nor sex was associated with extraversion or neuroticism ($ps > 0.1$). With neuropsychological composite scores, personality measures were not associated with any neuropsychological score ($ps > 0.1$). In relation to other personality traits, extraversion was significantly associated with agreeableness ($\beta = 0.5$, $p = 0.01$) as well as conscientiousness ($\beta = 0.4$, $p = 0.035$), controlling for age and sex. Neuroticism was not associated with any other personality trait scores ($ps > 0.1$).

DISCUSSION

In the present study, we report a novel finding showing that higher extraversion scores are associated with lower A β deposition across the widespread brain regions among cognitively normal older adults. When we examined personality-



related differences in task-evoked brain activity among young adults, we found a significant dissociation in brain activity as a function of personality traits: extraversion was related to lower brain activity, in particular, in the medial and lateral frontal cortex and anterior cingulate cortex, while neuroticism was associated with increased activity throughout the brain. Our results are consistent with a metabolism hypothesis of A β pathology (Kamenetz et al., 2003), which may, in part, provide neural evidence linking personality traits to a source of risk and protective factors of AD that are formed throughout the lifespan.

Personality as a Risk and/or Protective Factor for AD

There is great interest in understanding individual differences that influence the vulnerability of individuals to age-related neurodegenerative diseases such as AD. A large body of neuropathological and epidemiological studies suggests that lifestyle factors such as education, social network, diet, and

cognitive and physical activities, may affect the clinical manifestation of AD as well as the development of AD pathology. The relationship between lifestyle factors and AD has been commonly investigated with at least three hypothesized pathways. The pathway that received the most attention is its modulatory pathway that acts on the connection between disease pathology and clinical symptoms, which has been termed as cognitive or neural reserve (Stern, 2009; Bennett et al., 2014). The other equally plausible pathways are to influence directly either the buildup of AD pathology or clinical symptoms independent of AD pathology (Landau et al., 2011; Nyberg et al., 2012; Vemuri et al., 2012; Farfel et al., 2013; Terracciano et al., 2013; Wilson et al., 2013; Bennett et al., 2014; Arenaza-Urquijo et al., 2015; Gidicsin et al., 2015). Epidemiological and neuropathological data from large cohort studies are collectively more supportive of the modulatory effect of lifestyle factors on the clinical manifestation of AD both in cognitively normal older adults (Rentz et al., 2010) and AD patients (Bennett et al., 2014; Snitz et al., 2015).

Compared with the role of education and cognitive aspects of lifestyle factors in the occurrence of AD, less attention has been given to the role of personality and related social engagement factors in AD neuropathology and dementia status. The most common model of personality organizes personality traits into five factors: neuroticism, extraversion, openness to experience, agreeableness, and conscientiousness (McCrae and Costa, 2008). Studies have consistently found that measures of these personality traits predict AD risk and important health outcomes of their lives. Neuroticism, an individual's increased tendency to negative affectivity, anxiety, and distress proneness, has been shown to predict higher psychological distress, cognitive decline, mortality, and increased risk of AD (Wilson et al., 2006; Low et al., 2013). Loneliness, which is defined as perceived isolation, was robustly associated with cognitive decline and the development of AD (Wilson et al., 2007). Personality-related risk and beneficial effects on the onset of clinical symptoms and AD pathology were further supported once a possibility of premorbid personality changes has been accounted for (Terracciano et al., 2013). Using a quantitative measure at both global and voxel-wise levels, our results provide evidence showing a significant association between amyloid deposition and extraversion among older adults who are yet clinically intact.

Contrary to our prediction, we did not find any association between neuroticism and A β deposition. Interestingly, however, we found a significant age-related difference in neuroticism scores between older and young subjects, which is consistent with the literature (Terracciano et al., 2005; Donnellan and Lucas, 2008). Therefore, we speculate that the older adults who remain cognitively normal may be individuals whose neuroticism scores were relatively lower across their lifetime. In a similar manner, individuals with higher neuroticism scores during their lifetime might have already developed cognitive impairment, and thus, could not meet the selection criteria to be included in the present study. On the other hand, extraversion scores did not differ between young and older subjects.

Personality and Differential Task-Based Activation

A central motivation of the present study was to elucidate the neural basis underlying the impact of personality traits on AD pathology. Some morphological studies have shown larger gray matter (GM) volume in association with low neuroticism and higher extraversion, openness, agreeableness, and conscientiousness mostly in higher-level association cortices (Kapogiannis et al., 2013). Because these results remained identical across different time points, findings further suggest that distinct personality traits are associated with stable individual differences in GM volume and potentially act as a risk or protective factor by presenting neural reserve during brain aging.

A more direct link in relation to AD pathology can be drawn from brain activation studies showing that personality traits relate to unique patterns of brain activity in response to emotional or cognitive events or stimuli. Neuroticism is associated with negative mood states, sensitivity to negative information, negative appraisal, and vulnerability

to psychopathology, which commonly relate to the sustained processing of negative information. By assessing sustained patterns of activity within a brain region implicated in emotional self-evaluation and appraisal, such as the medial frontal cortex, studies have found that higher scores of neuroticism are associated with greater sustained patterns of brain activity in the medial frontal cortex when responding to blocks of negative facial expressions (Haas et al., 2008). In the cognitive domain, controlled processing mechanisms have been linked to the dorsal anterior cingulate cortex (dACC) and the reactivity of dACC has been directly related to neuroticism, due to its role in discrepancy detection (Eisenberger et al., 2005). With regard to extraversion, studies have consistently shown lower baseline activity with higher extraversion and task-related decreases in the lateral and medial frontoparietal network, typically associated with task-focused controlled processing, reflecting neural-processing efficiency, and reduced self-consciousness (Kumari et al., 2004; Eisenberger et al., 2005; Gray et al., 2005). Using the same personality questionnaire that we used for our older subjects, the present findings of differential activity as a function of extraversion and neuroticism during task-switching in young adults are consistent with findings of other studies and extend its implication to AD pathology possibly *via* differential regulation of neural activity throughout the lifetime, as discussed below.

Personality, Brain Activity, and A β Pathology

Accumulation of A β peptides is considered an initiating event that precipitates downstream neuro/pathological changes in the process of AD (Hardy and Selkoe, 2002; Gandy, 2005). Because of its significant impact on the pathogenesis of AD, there has been great interest in understanding the causal factors of A β accumulation during aging. One of the proposed mechanisms is increased neural activity and physiology early in life before plaque formation during senescence (Cirrito et al., 2005; Jagust and Mormino, 2011). High topographic correspondence between increased metabolism in young people and increased A β deposition in older people has been consistently supported by both animal and human studies (Vlassenko et al., 2010; Bero et al., 2011; Oh et al., 2016a). Incipient amyloid accumulation *via* neural activity may also lead to amyloidosis secondarily in other regions through the prion-like spreading of the A β seed (Gandy, 2005). Therefore, an overall regulation of neural activity across the brain may be protective against brain A β deposition. Brain regions that accumulate brain A β include medial frontal and parietal cortices and anterior cingulate cortex that play a critical role in both cognitive and affective processes (Buckner et al., 2005; Haas et al., 2008). Dysfunction of these brain regions has been implicated in affective and psychiatric disorders such as depression and anxiety that are core personality characteristics associated with neuroticism (Sinha et al., 2016). Abnormal changes in these brain regions may relate to a dysfunction of the serotonergic system, which has been also suggested for amyloid precursor protein metabolism, or serotonin transporter polymorphisms (Pezawas et al., 2005; Fisher et al., 2016). It is important to note that the association of extraversion with lower activity in our executive contextual

fMRI task was fairly circumscribed and showed both overlap but also differences compared to regions where extraversion was associated with amyloid. Thus, rather than complete topographic overlapping between lower brain activity in young adulthood and A β accumulation during aging, the results indicate a directional link between regional neural activity and A β pathology. Taken together, our findings provide evidence linking personality traits to A β pathology by showing differential lifelong regulations of brain activity in association with extraversion and neuroticism.

Limitations and Alternative Explanations

Although we aimed to examine the impact of personality in AD risk *via* the hypothesized relationship across the two personality traits, neural activity, and A β pathology, other psychosocial mechanisms could be considered as a mediator of the observed relationship between personality traits and A β pathology. As personality traits such as extraversion have been significantly related to other personality traits such as openness to experience among older adults and conscientiousness in young subjects, it is possible that other lifelong variables may mediate the observed relationship between extraversion and lower A β pathology. Some genetic factors associated with personality may also explain its relationship with AD pathology *via* prevalent comorbidity associated with the genes (Deuschle et al., 2010). More generally, personality may impact dementia risk and pathology by influencing health habits, number and quality of social relationships, cognitive activity, and reactions to stress over the lifespan, which could collectively have contributed to the observed relationship. Another limitation of the study is that the association of extraversion with each of the other measures of interest come from different groups, so can only provide indirect (yet converging) evidence that brain activity can explain the link between extraversion and amyloid deposition. Longitudinal fMRI and amyloid data from younger age to older age do not yet exist, so by necessity, this is a cross-sectional study. Therefore, the causal and temporal relationships between these measures cannot be determined definitively. In addition, because of the cross-sectional investigation of the current study, the observed association between extraversion and A β pathology in cognitively normal older adults may have reflected premorbid changes as other studies have suggested, although our prediction of A β pathology based on brain activation in young adulthood is against this possibility. Future studies are warranted to address these questions using a larger and longitudinal cohort and multivariate analysis approaches that allow assessing unique contributions of multiple lifetime variables to A β pathology.

Conclusion

The present study is the first to show that extraversion is associated with lower A β pathology among cognitively normal

older adults and is associated with lower brain activity in regions including the medial frontal cortex and anterior cingulate cortex in response to a controlled processing task in young adulthood. Our results provide evidence showing the neural basis underlying the link between extraversion and A β pathology that may develop throughout the lifespan. It is important to note that, although personality can be seen as a trait vs. state, it is potentially modifiable. In addition, while it is possible that life events, especially early stressful life events, may influence the formation of the personality type of individuals, one's personality type also can modify the impact of stressful life events on health outcomes, affect lifestyle choices, and, more directly, impact AD pathology. Our results suggest that personality is an important factor that should be considered for conceptual and biological models of dementia risk and designing clinical trials. Considering its modifiability, personality can be considered for dementia risk reduction strategies that can start early in the lifespan.

DATA AVAILABILITY STATEMENT

The original contributions presented in the study are included in the article/**Supplementary Material**, further inquiries can be directed to the corresponding author.

ETHICS STATEMENT

The studies involving human participants were reviewed and approved by the Institutional Review Boards of the College of Physicians and Surgeons of Columbia University. All methods were carried out in accordance with the approved guidelines. The patients/participants provided their written informed consent to participate in this study.

AUTHOR CONTRIBUTIONS

HO conceptualized the study, contributed to the acquisition of the data, analyzed and interpreted the data, wrote the manuscript, and approved the submitted version.

FUNDING

This research was supported by the National Institute on Aging (grant numbers R01AG026158, R01AG068990).

SUPPLEMENTARY MATERIAL

The Supplementary Material for this article can be found online at: <https://www.frontiersin.org/articles/10.3389/fnagi.2022.900581/full#supplementary-material>.

REFERENCES

- Ackerman, P. L., and Heggestad, E. D. (1997). Intelligence, personality and interests: evidence for overlapping traits. *Psychol. Bull.* 121, 219–245. doi: 10.1037/0033-2909.121.2.219
- Arenaza-Urquijo, E. M., Wirth, M., and Chetelat, G. (2015). Cognitive reserve and lifestyle: moving towards preclinical Alzheimer's disease. *Front. Aging Neurosci.* 7:134. doi: 10.3389/fnagi.2015.00134
- Bateman, R. J., Xiong, C., Benzinger, T. L., Fagan, A. M., Goate, A., Fox, N. C., et al. (2012). Clinical and biomarker changes in dominantly inherited

- Alzheimer's disease. *N. Engl. J. Med.* 367, 795–804. doi: 10.1056/NEJMoa120753
- Bennett, D. A., Arnold, S. E., Valenzuela, M. J., Brayne, C., and Schneider, J. A. (2014). Cognitive and social lifestyle: links with neuropathology and cognition in late life. *Acta Neuropathol.* 127, 137–150. doi: 10.1007/s00401-013-1226-2
- Bennett, D. A., Schneider, J. A., Tang, Y., Arnold, S. E., and Wilson, R. S. (2006). The effect of social networks on the relation between Alzheimer's disease pathology and level of cognitive function in old people: a longitudinal cohort study. *Lancet Neurol.* 5, 406–412. doi: 10.1016/S1474-4422(06)70417-3
- Bero, A. W., Yan, P., Roh, J. H., Cirrito, J. R., Stewart, F. R., Raichle, M. E., et al. (2011). Neuronal activity regulates the regional vulnerability to amyloid-β deposition. *Nat. Neurosci.* 14, 750–756. doi: 10.1038/nn.2801
- Buckner, R. L., Snyder, A. Z., Shannon, B. J., LaRossa, G., Sachs, R., Fotenos, A. F., et al. (2005). Molecular, structural and functional characterization of Alzheimer's disease: evidence for a relationship between default activity, amyloid and memory. *J. Neurosci.* 25, 7709–7717. doi: 10.1523/JNEUROSCI.2177-05.2005
- Buschke, H., and Fuld, P. A. (1974). Evaluating storage, retention and retrieval in disordered memory and learning. *Neurology* 24, 1019–1025. doi: 10.1212/wnl.24.11.1019
- Cirrito, J. R., Yamada, K. A., Finn, M. B., Sloviter, R. S., Bales, K. R., May, P. C., et al. (2005). Synaptic activity regulates interstitial fluid amyloid-β levels *in vivo*. *Neuron* 48, 913–922. doi: 10.1016/j.neuron.2005.10.028
- Dale, A. M., Fischl, B., and Sereno, M. I. (1999). Cortical surface-based analysis. I. Segmentation and surface reconstruction. *Neuroimage* 9, 179–194. doi: 10.1006/nimg.1998.0395
- Deuschle, M., Schredl, M., Schilling, C., Wust, S., Frank, J., Witt, S. H., et al. (2010). Association between a serotonin transporter length polymorphism and primary insomnia. *Sleep* 33, 343–347. doi: 10.1093/sleep/33.3.343
- Donnellan, M. B., and Lucas, R. E. (2008). Age differences in the Big Five across the life span: evidence from two national samples. *Psychol. Aging* 23, 558–566. doi: 10.1037/a0012897
- Eisenberger, N. I., Lieberman, M. D., and Satpute, A. B. (2005). Personality from a controlled processing perspective: an fMRI study of neuroticism, extraversion and self-consciousness. *Cogn. Affect. Behav. Neurosci.* 5, 169–181. doi: 10.3758/cabn.5.2.169
- Farfel, J. M., Nitritni, R., Suemoto, C. K., Grinberg, L. T., Ferretti, R. E., Leite, R. E., et al. (2013). Very low levels of education and cognitive reserve: a clinicopathologic study. *Neurology* 81, 650–657. doi: 10.1212/WNL.0b013e3182a08f1b
- Fischl, B., Salat, D. H., Busa, E., Albert, M., Dieterich, M., Haselgrove, C., et al. (2002). Whole brain segmentation: automated labeling of neuroanatomical structures in the human brain. *Neuron* 33, 341–355. doi: 10.1016/s0896-6273(02)00569-x
- Fisher, J. R., Wallace, C. E., Tripoli, D. L., Sheline, Y. I., and Cirrito, J. R. (2016). Redundant Gs-coupled serotonin receptors regulate amyloid-beta metabolism *in vivo*. *Mol. Neurodegener.* 11:45. doi: 10.1186/s13024-016-0112-5
- Gandy, S. (2005). The role of cerebral amyloid beta accumulation in common forms of Alzheimer disease. *J. Clin. Invest.* 115, 1121–1129. doi: 10.1172/JCI25100
- Gidicsin, C. M., Maye, J. E., Locascio, J. J., Pepin, L. C., Philiossaint, M., Becker, J. A., et al. (2015). Cognitive activity relates to cognitive performance but not to Alzheimer disease biomarkers. *Neurology* 85, 48–55. doi: 10.1212/WNL.0000000000001704
- Goldberg, L. R. (1992). The development of markers for the big-five factor structure. *Psychol. Assess.* 4, 26–42. doi: 10.1037/1040-3590.4.1.26
- Golden, C. J. (1978). *Stroop Color and Word Test*. Chicago, IL: Stolting.
- Gray, J. R., Burgess, G. C., Schaefer, A., Yarkoni, T., Larsen, R. J., Braver, T. S., et al. (2005). Affective personality differences in neural processing efficiency confirmed using fMRI. *Cogn. Affect. Behav. Neurosci.* 5, 182–190. doi: 10.3758/cabn.5.2.182
- Haas, B. W., Constable, R. T., and Canli, T. (2008). Stop the sadness: neuroticism is associated with sustained medial prefrontal cortex response to emotional facial expressions. *Neuroimage* 42, 385–392. doi: 10.1016/j.neuroimage.2008.04.027
- Haas, B. W., Omura, K., Constable, R. T., and Canli, T. (2007). Emotional conflict and neuroticism: personality-dependent activation in the amygdala and subgenual anterior cingulate. *Behav. Neurosci.* 121, 249–256. doi: 10.1037/0735-7044.121.2.249
- Hardy, J., and Selkoe, D. J. (2002). The amyloid hypothesis of Alzheimer's disease: progress and problems on the road to therapeutics. *Science* 297, 353–356. doi: 10.1126/science.1072994
- Hariri, A. R., Mattay, V. S., Tessitore, A., Kolachana, B., Fera, F., Goldman, D., et al. (2002). Serotonin transporter genetic variation and the response of the human amygdala. *Science* 297, 400–403. doi: 10.1126/science.1071829
- Jack, C. R., Knopman, D. S. Jr., Jagust, W. J., Petersen, R. C., Weiner, M. W., Aisen, P. S., et al. (2013). Tracking pathophysiological processes in Alzheimer's disease: an updated hypothetical model of dynamic biomarkers. *Lancet Neurol.* 12, 207–216. doi: 10.1016/S1474-4422(12)70291-0
- Jagust, W. J., and Mormino, E. C. (2011). Lifespan brain activity, beta-amyloid and Alzheimer's disease. *Trends Cogn. Sci.* 15, 520–526. doi: 10.1016/j.tics.2011.09.004
- Kamenetz, F., Tomita, T., Hsieh, H., Seabrook, G., Borchelt, D., Iwatsubo, T., et al. (2003). APP processing and synaptic function. *Neuron* 37, 925–937. doi: 10.1016/s0896-6273(03)00124-7
- Kapogiannis, D., Sutin, A., Davatzikos, C., Costa, P. Jr., and Resnick, S. (2013). The five factors of personality and regional cortical variability in the Baltimore longitudinal study of aging. *Hum. Brain Mapp.* 34, 2829–2840. doi: 10.1002/hbm.22108
- Koechlin, E., Ody, C., and Kouneiher, F. (2003). The architecture of cognitive control in the human prefrontal cortex. *Science* 302, 1181–1185. doi: 10.1126/science.1088545
- Kumari, V., ffytche, D. H., Williams, S. C., and Gray, J. A. (2004). Personality predicts brain responses to cognitive demands. *J. Neurosci.* 24, 10636–10641. doi: 10.1523/JNEUROSCI.3206-04.2004
- Landau, S. M., Breault, C., Joshi, A. D., Pontecorvo, M., Mathis, C. A., Jagust, W. J., et al. (2013). Amyloid-beta imaging with Pittsburgh compound B and florbetapir: comparing radiotracers and quantification methods. *J. Nucl. Med.* 54, 70–77. doi: 10.2967/jnumed.112.109009
- Landau, S. M., Fero, A., Baker, S. L., Koeppe, R., Mintun, M., Chen, K., et al. (2015). Measurement of longitudinal beta-amyloid change with ¹⁸F-florbetapir PET and standardized uptake value ratios. *J. Nucl. Med.* 56, 567–574. doi: 10.2967/jnumed.114.148981
- Landau, S. M., Harvey, D., Madison, C. M., Koeppe, R. A., Reiman, E. M., Foster, N. L., et al. (2011). Associations between cognitive, functional and FDG-PET measures of decline in AD and MCI. *Neurobiol. Aging* 32, 1207–1218. doi: 10.1016/j.neurobiolaging.2009.07.002
- Low, L. F., Harrison, F., and Lackerstein, S. M. (2013). Does personality affect risk for dementia? A systematic review and meta-analysis. *Am. J. Geriatr. Psychiatry* 21, 713–728. doi: 10.1016/j.jagp.2012.08.004
- McCrae, R. R., and Costa, P. T. Jr. (2008). "The five-factor theory of personality," in *Handbook of Personality: Theory and Research*, eds O. P. John, R. W. Robins, and L. A. Pervin (New York, NY: Guilford Press), 159–181.
- Meng, X., and D'Arcy, C. (2012). Education and dementia in the context of the cognitive reserve hypothesis: a systematic review with meta-analyses and qualitative analyses. *PLoS One* 7:e38268. doi: 10.1371/journal.pone.0038268
- Mormino, E. C. (2014). The relevance of beta-amyloid on markers of Alzheimer's disease in clinically normal individuals and factors that influence these associations. *Neuropsychol. Rev.* 24, 300–312. doi: 10.1007/s11065-014-9267-4
- Nyberg, L., Lovden, M., Riklund, K., Lindenberg, U., and Backman, L. (2012). Memory aging and brain maintenance. *Trends Cogn. Sci.* 16, 292–305. doi: 10.1016/j.tics.2012.04.005
- Oh, H., Madison, C., Baker, S., Rabinovici, G., and Jagust, W. (2016a). Dynamic relationships between age, amyloid-beta deposition and glucose metabolism link to the regional vulnerability to Alzheimer's disease. *Brain* 139, 2275–2289. doi: 10.1093/brain/aww108
- Oh, H., Steffener, J., Razlighi, Q. R., Habeck, C., and Stern, Y. (2016b). beta-Amyloid deposition is associated with decreased right prefrontal activation during task switching among cognitively normal elderly. *J. Neurosci.* 36, 1962–1970. doi: 10.1523/JNEUROSCI.3266-15.2016
- Oh, H., Steffener, J., Razlighi, Q. R., Habeck, C., Liu, D., Gazes, Y., et al. (2015). Abeta-related hyperactivation in frontoparietal control regions in cognitively normal elderly. *Neurobiol. Aging* 36, 3247–3254. doi: 10.1016/j.neurobiolaging.2015.08.016

- Pezawas, L., Meyer-Lindenberg, A., Drabant, E. M., Verchinski, B. A., Munoz, K. E., Kolachana, B. S., et al. (2005). 5-HTTLPR polymorphism impacts human cingulate-amygdala interactions: a genetic susceptibility mechanism for depression. *Nat. Neurosci.* 8, 828–834. doi: 10.1038/nn1463
- Reitan, R. (1978). *Manual for Administration of Neuropsychological Test Batteries for Adults and Children*. Tucson, AZ: Reitan Neuropsychology Laboratories, Inc.
- Rentz, D. M., Locascio, J. J., Becker, J. A., Moran, E. K., Eng, E., Buckner, R. L., et al. (2010). Cognition, reserve and amyloid deposition in normal aging. *Ann. Neurol.* 67, 353–364. doi: 10.1002/ana.21904
- Sinha, R., Lacadie, C. M., Constable, R. T., and Seo, D. (2016). Dynamic neural activity during stress signals resilient coping. *Proc. Natl. Acad. Sci. U S A* 113, 8837–8842. doi: 10.1073/pnas.1600965113
- Snitz, B. E., Weissfeld, L. A., Cohen, A. D., Lopez, O. L., Nebes, R. D., Aizenstein, H. J., et al. (2015). Subjective cognitive complaints, personality and brain amyloid-beta in cognitively normal older adults. *Am. J. Geriatr. Psychiatry* 23, 985–993. doi: 10.1016/j.jagp.2015.01.008
- Stern, Y. (2009). Cognitive reserve. *Neuropsychologia* 47, 2015–2028. doi: 10.1016/j.neuropsychologia.2009.03.004
- Terracciano, A., Iacono, D., O'Brien, R. J., Troncoso, J. C., An, Y., Sutin, A. R., et al. (2013). Personality and resilience to Alzheimer's disease neuropathology: a prospective autopsy study. *Neurobiol. Aging* 34, 1045–1050. doi: 10.1016/j.neurobiolaging.2012.08.008
- Terracciano, A., McCrae, R. R., Brant, L. J., and Costa, P. T. Jr. (2005). Hierarchical linear modeling analyses of the NEO-PI-R scales in the baltimore longitudinal study of aging. *Psychol. Aging* 20, 493–506. doi: 10.1037/0882-7974.20.3.493
- Terracciano, A., Sutin, A. R., An, Y., O'Brien, R. J., Ferrucci, L., Zonderman, A. B., et al. (2014). Personality and risk of Alzheimer's disease: new data and meta-analysis. *Alzheimers Dement.* 10, 179–186. doi: 10.1016/j.jalz.2013.03.002
- Valenzuela, M. J., and Sachdev, P. (2006). Brain reserve and dementia: a systematic review. *Psychol. Med.* 36, 441–454. doi: 10.1017/S0033291705006264
- Vemuri, P., Lesnick, T. G., Przybelski, S. A., Knopman, D. S., Roberts, R. O., Lowe, V. J., et al. (2012). Effect of lifestyle activities on Alzheimer disease biomarkers and cognition. *Ann. Neurol.* 72, 730–738. doi: 10.1002/ana.23665
- Vlassenko, A. G., Vaishnavi, S. N., Couture, L., Sacco, D., Shannon, B. J., Mach, R. H., et al. (2010). Spatial correlation between brain aerobic glycolysis and amyloid-beta (A β) deposition. *Proc. Natl. Acad. Sci. U S A* 107, 17763–17777. doi: 10.1073/pnas.1010461107
- Wang, H. X., Karp, A., Herlitz, A., Crowe, M., Kareholt, I., Winblad, B., et al. (2009). Personality and lifestyle in relation to dementia incidence. *Neurology* 72, 253–259. doi: 10.1212/01.wnl.0000339485.39246.87
- Wechsler, D. (1997). *Wechsler Adult Intelligence Scale - III*. San Antonio, TX: Psychological Corporation.
- Wilson, R. S., Arnold, S. E., Schneider, J. A., Kelly, J. F., Tang, Y., Bennett, D. A., et al. (2006). Chronic psychological distress and risk of Alzheimer's disease in old age. *Neuroepidemiology* 27, 143–153. doi: 10.1159/000095761
- Wilson, R. S., Begnen, C. T., Boyle, P. A., Schneider, J. A., and Bennett, D. A. (2011). Vulnerability to stress, anxiety and development of dementia in old age. *Am. J. Geriatr. Psychiatry* 19, 327–334. doi: 10.1097/JGP.0b013e31820119da
- Wilson, R. S., Boyle, P. A., Yu, L., Barnes, L. L., Schneider, J. A., Bennett, D. A., et al. (2013). Life-span cognitive activity, neuropathologic burden and cognitive aging. *Neurology* 81, 314–321. doi: 10.1212/WNL.0b013e31829c5e8a
- Wilson, R. S., Krueger, K. R., Arnold, S. E., Schneider, J. A., Kelly, J. F., Barnes, L. L., et al. (2007). Loneliness and risk of Alzheimer disease. *Arch. Gen. Psychiatry* 64, 234–240. doi: 10.1001/archpsyc.64.2.234
- Yan, P., Bero, A. W., Cirrito, J. R., Xiao, Q., Hu, X., Wang, Y., et al. (2009). Characterizing the appearance and growth of amyloid plaques in APP/PS1 mice. *J. Neurosci.* 29, 10706–10714. doi: 10.1523/JNEUROSCI.2637-09.2009

Conflict of Interest: The author declares that the research was conducted in the absence of any commercial or financial relationships that could be construed as a potential conflict of interest.

Publisher's Note: All claims expressed in this article are solely those of the authors and do not necessarily represent those of their affiliated organizations, or those of the publisher, the editors and the reviewers. Any product that may be evaluated in this article, or claim that may be made by its manufacturer, is not guaranteed or endorsed by the publisher.

Copyright © 2022 Oh. This is an open-access article distributed under the terms of the Creative Commons Attribution License (CC BY). The use, distribution or reproduction in other forums is permitted, provided the original author(s) and the copyright owner(s) are credited and that the original publication in this journal is cited, in accordance with accepted academic practice. No use, distribution or reproduction is permitted which does not comply with these terms.



Genome Sequencing Variations in the *Octodon degus*, an Unconventional Natural Model of Aging and Alzheimer's Disease

OPEN ACCESS

Edited by:

Allison B. Reiss,
New York University, United States

Reviewed by:

Nobuyuki Kimura,
Okayama University of Science, Japan
Carsten Korth,
Heinrich Heine University of
Düsseldorf, Germany

*Correspondence:

Patricia Cogram
patricia.cogram@gmail.com

†These authors share
senior authorship

Specialty section:

This article was submitted to
Alzheimer's Disease and Related
Dementias,
a section of the journal
Frontiers in Aging Neuroscience

Received: 12 March 2022

Accepted: 31 May 2022

Published: 30 June 2022

Citation:

Hurley MJ, Urrea C, Garduno BM,
Bruno A, Kimbell A, Wilkinson B,
Marino-Buslje C, Ezquer M, Ezquer F,
Aburto PF, Poulin E, Vasquez RA,
Deacon R, Avila A, Altamiras F, Whitney
Vanderklisch P, Zampieri G, Angione C,
Constantino G, Holmes TC, Coda MP,
Xu X and Cogram P (2022) Genome
Sequencing Variations in the *Octodon
degus*, an Unconventional Natural
Model of Aging and Alzheimer's
Disease.
Front. Aging Neurosci. 14:894994.
doi: 10.3389/fnagi.2022.894994

Michael J. Hurley^{1,2}, Claudio Urrea², B. Maximiliano Garduno³, Agostino Bruno⁴,
Allison Kimbell⁵, Brent Wilkinson⁵, Cristina Marino-Buslje⁶, Marcelo Ezquer⁷,
Fernando Ezquer⁷, Pedro F. Aburto², Elie Poulin², Rodrigo A. Vasquez², Robert Deacon²,
Ariel Avila⁸, Francisco Altamiras⁹, Peter Whitney Vanderklisch¹⁰, Guido Zampieri¹¹,
Claudio Angione¹¹, Gabriele Constantino^{4†}, Todd C. Holmes^{12†}, Marcelo P. Coda^{5,13†},
Xiangmin Xu^{3†} and Patricia Cogram^{2,3*†}

¹ Department of Clinical and Movement Neurosciences, UCL Queen Square Institute of Neurology, London, United Kingdom,

² Department of Ecological Sciences, Faculty of Sciences, Institute of Ecology and Biodiversity, Universidad de Chile,

Santiago, Chile, ³ Department of Anatomy and Neurobiology, School of Medicine, University of California, Irvine, Irvine, CA,

United States, ⁴ Department of Food and Drug, University of Parma, Parma, Italy, ⁵ Zilkha Neurogenetic Institute, University of

Southern California, Los Angeles, CA, United States, ⁶ Bioinformatics Unit, Leloir Institute Foundation (FIL), Buenos Aires,

Argentina, ⁷ Centro de Medicina Regenerativa, Facultad de Medicina, Clínica Alemana-Universidad del Desarrollo, Santiago,

Chile, ⁸ Biomedical Sciences Research Laboratory, Faculty of Medicine, Universidad Católica de la Santísima Concepción,

Concepción, Chile, ⁹ Faculty of Engineering and Business, Universidad de las Américas, Santiago, Chile, ¹⁰ Department

Molecular Medicine, Scripps Research, La Jolla, CA, United States, ¹¹ School of Computing, Engineering and Digital

Technologies, Teesside University, Middlesbrough, United Kingdom, ¹² Department Physiology & Biophysics, School of

Medicine, University of California, Irvine, Irvine, CA, United States, ¹³ Department of Psychiatry and Behavioral Sciences,

Keck School of Medicine, University of Southern California, Los Angeles, CA, United States

The degu (*Octodon degus*) is a diurnal long-lived rodent that can spontaneously develop molecular and behavioral changes that mirror those seen in human aging. With age some degu, but not all individuals, develop cognitive decline and brain pathology like that observed in Alzheimer's disease including neuroinflammation, hyperphosphorylated tau and amyloid plaques, together with other co-morbidities associated with aging such as macular degeneration, cataracts, alterations in circadian rhythm, diabetes and atherosclerosis. Here we report the whole-genome sequencing and analysis of the degu genome, which revealed unique features and molecular adaptations consistent with aging and Alzheimer's disease. We identified single nucleotide polymorphisms in genes associated with Alzheimer's disease including a novel apolipoprotein E (*ApoE*) gene variant that correlated with an increase in amyloid plaques in brain and modified the *in silico* predicted degu APOE protein structure and functionality. The reported genome of an unconventional long-lived animal model of aging and Alzheimer's disease offers the opportunity for understanding molecular pathways involved in aging and should help advance biomedical research into treatments for Alzheimer's disease.

Keywords: Alzheimer's disease, aging, genome, APOE, amyloids, lipid droplets, *Octodon degus*, drug development

INTRODUCTION

To understand genetic factors that contribute to aging and with the goal of establishing an unconventional natural (i.e., spontaneous and not through genetic manipulation) animal model that represents the aging process and also the sporadic late-onset form of Alzheimer's disease (AD) we analyzed the whole genome of the long-lived degu (*Octodon degus*) rodent. Degu naturally develop AD-like pathological features like many other mammals such as the guinea pig (Sharman et al., 2013; Bates et al., 2014), marmosets (Ridley et al., 1986; Wenk, 1993), dolphins (Gunn-Moore et al., 2018) and dogs (Jones et al., 2018). Comparative research using non-human non-conventional models of AD helps improve our understanding of dementia.

Degu live in a well-structured social organization, in complex underground burrows. They have a rich vocal repertoire including alarm calls, a diurnal circadian cycle and well-developed prefrontal areas that are sensitive to social deprivation (Vasquez, 1997; Poeggel et al., 2003; Lee, 2004; Jesseau et al., 2008; Ebensperger et al., 2016). In captivity they live ~10 years and adults weigh up to 220 g with an average body length of 12 cm.

More notable is the fact that with age, some, but not all degu, show hallmarks of human age-related diseases such as AD, type 2 diabetes and atherosclerosis (Homan et al., 2010; Ardiles et al., 2012; Hurley et al., 2018; Chang et al., 2021). Wild-caught and wild-type laboratory-outbred (but not laboratory-inbred) degu can spontaneously develop AD-like neuropathology including increased β -amyloid aggregates, tau hyperphosphorylation and neuroinflammation in the brain as part of their natural history (van Groen et al., 2011; Ardiles et al., 2012; Tarragon et al., 2013; Deacon et al., 2015; Salazar et al., 2016; Paushter et al., 2018). Remarkably, the degu and human β -amyloid peptide sequence are 97.5% homologous, with only one amino acid substitution relative to human (Inestrosa et al., 2005).

Degu develop age-dependent cognitive impairments in activities of daily living and by the age of ~3 years, 30% of degu captured from a natural population show impairments in burrowing performance, which was correlated with their expression profiles of AD markers and cytokine and complement component gene expression (Deacon et al., 2015; Altimiras et al., 2017).

Phylogenetically degu and mice are both in the same Rodentia family meaning the degu genome studies we report here in comparison to murine (*Mus musculus*) studies will be particularly valuable for within family comparison of transgenic mouse AD pathways in terms of which AD gene regulatory pathways are common to spontaneous AD-like features in the long-lived degu vs. different transgenic models using short-lived mice (Zhou et al., 2020). It may be the case that different genetic mouse AD models recapitulate some but not all gene regulatory features of spontaneously occurring AD-like features in degu and patients with AD.

Emerging evidence from experimental and epidemiological studies show that both genetic and environmental factors contribute to aging and the onset and progression of late-onset AD. Whole-genome studies provided a much-needed

insight into this unconventional model of AD. Here we show several genes involved in inflammation, DNA repair, lipid metabolism and innate immune regulation as potential critical factors in the AD-like pathology that occurs in the degu. Based on the finding that only a proportion of the degu population spontaneously develop AD-like brain pathology, we hypothesized that there are genetic risk factors that mediate AD susceptibility in degu subpopulations. Single nucleotide polymorphisms (SNP) were identified in 19 AD associated genes in the degu genome [see **Supplementary Table 3** including *ApoE* (Apolipoprotein E)] (Barzilai et al., 2012). As *APOE* status is the dominant driver of late-onset AD risk in humans (Serrano-Pozo et al., 2021), we characterized in detail the functional impact of a novel missense SNP in exon 3 (Mt4) of the degu *ApoE* (*odApoE*) and its association with late-onset AD-like phenotypes in this model. In addition, signaling pathway analysis indicated common pathways in human and degu aging and AD processes. Collectively, our observations showed that the use of unconventional long-lived animals as a model of AD could shed light into human aging and late-onset AD mechanisms and therefore such a model could be of use in drug development for the treatment of AD.

METHODS

Animals

Degu from our outbred wild captive degu colony were housed in standard metal cages (50 × 40 × 35 cm) with a layer of wood shavings as bedding, containing a small metal nesting box (25 × 15 × 10 cm with a single entrance) under a controlled photoperiod (7 a.m. to 7 p.m.) and temperature (23°C). Water and a commercial rodent diet (Prolab RMH 3000, USA) were provided *ad libitum*. All animals used were males aged 4.5 years.

Ethical approval for this project was provided by the Institute of Ecology and Biodiversity Ethics Committee, and the experiments were performed in accordance with the UK Scientific Procedures Act (1986) and the NIH Guide for the Care and Use of Laboratory Animals (1978). All animals were handled consistently in accordance with ARRIVE guidelines.

Behavioral Test of Daily Living: Burrowing

Behavioral assessment of 149 degu was performed to distinguish AD-like from normal degu using the burrowing test as previously described (Deacon et al., 2015).

Whole-Genome Sequencing

The genomes of 11 degu were sequenced on the Illumina NovaSeq 6000 S4 platform at a sequencing depth of 60% by Quick Biology Inc. (Pasadena, CA 91007, USA). A single library was constructed using the TruSeq Nano DNA Kit (Illumina, CA, USA). Library integrity was evaluated by capillary electrophoresis using the Fragment AnalyzerTM Automated CE System (Analytical Advanced Technologies, Iowa, USA) with the DNF-474 High Sensitivity NGS Fragment Analysis Kit (Analytical Advanced Technologies). The NCBI accession number for the whole-genome sequence of the degu was BioProject ID PRJNA623609.

Genome Mapping and *ApoE* Mutation Evaluation

Genome mapping against the degu genome assembly OctDeg1.0 (GCA_000260255.1) was performed using BWA-MEM software v0.7.17-r1188 (Liu et al., 2015; Wong et al., 2017). We evaluated the variants detected previously by Sanger sequencing of exon 3 of *APOE*. We visualized each mutation in the mapped genomes using IGV v2.5.3 software (<https://software.broadinstitute.org/software/igv/>) to identify the presence or absence of each mutation.

Variant Calling and Filtering

The mapped genomes were prepared with Picard-tools v2.16.1 using the AddOrReplaceReadGroups, MarkDuplicates, and CleanSam tools (<https://broadinstitute.github.io/picard/>). The SNP and INDEL variants were identified using the Haplotype Caller tool in GATK v4.0.9.0. Variants were filtered by variant quality $Q > 100$ and by variant depth $DP > 20$.

The last step was the annotation of the unique variant list to the reference genome using the *Octodon degus* GCA_000260255.1 annotation (https://www.ebi.ac.uk/ena/data/view/GCA_000260255) with SnpEff v4.3t tool (Cingolani et al., 2012). The sequences of AD related genes with annotated variants were obtained using the genome annotation deposited in NCBI (https://www.ncbi.nlm.nih.gov/assembly/GCF_000260255.1/). The annotated variants were filtered to keep missense variants. Genes that contain missense variants were obtained using the filtered variant. The OMA browser (<https://omabrowser.org/oma/genomePW/>) was used to obtain mouse (*Mus musculus*) ortholog genes. Then a gene ontology (GO) enrichment analysis by biological process was carried out using the gene ontology web tool (<http://geneontology.org/>). The most significant GO terms were selected filtering by $FDR < 0.05$. To reduce redundancy the resulting GO term list was evaluated with REVIGO tool (<http://revigo.irb.hr/>).

AD-Related Gene Evaluation

The sequences of the genes XBP1 Msh6, IGF1 and *APOE* were extracted from the mapped genomes. The predicted variants found using the GATK pipeline were evaluated *in silico* in the mapped genomes using IGV v2.5.3. The protein sequences were aligned using ClustalOmega software (<https://www.ebi.ac.uk/Tools/msa/clustalo/>) to validate the effects predicted by SnpEff. The amino acid sequences from human and mouse were obtained using Blast (<https://blast.ncbi.nlm.nih.gov/Blast.cgi>) to align the degu amino acid sequences, the best hit of each species was selected.

Degu *ApoE* SNP Validation by Amplicon Sequencing

To validate the SNP detected in *odApoE*, exon 3 was sequenced by nested amplicon sequencing in exon 3 of *odApoE* using an Illumina MiSeq Reagent Nano Kit v2 (500 cycles) at the Universidad Andrés Bello, Santiago, Chile.

The SNP frequency was confirmed *via* Sanger sequencing at 137°C by Quick Biology Inc., Pasadena, CA 91007, US.

Molecular Modeling

The 3-D homology model of *odApoE* was generated using frame 14 of the NMR structure 2L7N. The E213Q and E213K variants were generated starting from the selected 3-D homology model of wild-type *odAPOE* using the wizard mutagenesis tool of PyMol 1.8.2.1 and then refined by applying the same protocol used for the wild-type structure, and the selected structures of wild-type E213E-*odAPOE*, E213Q-*odAPOE*, and E213K-*odAPOE* were prepared for MD simulations (**Supplementary Figure 1**).

β -Amyloid Immunohistochemical Staining and Quantification

Right brain hemispheres of degu were fixed in 4% paraformaldehyde, washed in PBS, and incubated in 30% sucrose overnight before sectioning (30 μ m) with a freezing microtome (Leica SM2010R). The sections were then transferred into two 24-well plates per hemisphere. One well of sections per hemisphere was selected for subsequent β -amyloid immunochemical staining using mouse anti- β -amyloid (BioLegend clone 6E10, 1:500). Five randomly selected regions of interest (1.93 mm \times 1.93 mm each) were assigned to matching coronal sections of the twelve degu of different variant carriers (4 E213K, 3 E213Q, 4 E213E, 1 Q213Q). Plaques were manually counted and plaque counts per cm^2 were subject to the linear mixed-effect model (LME) statistical analysis, which handles correlated data from repeated measurements from multiple single animal tissue samples (Yu et al., 2022). In the graph, data bars represent mean \pm standard error of the mean (SEM), and a statistical significance is considered when $p \leq 0.05$. * indicates $p < 0.05$, ** indicates $p < 0.01$, and *** indicates $p < 0.001$.

ApoE E213K Cell Line Generation

H9 human embryonic stem cells were cultured on Geltrex-coated plates and fed daily with mTeSR-1 medium (Stemcell Technologies). When confluent, human embryonic stem cells were transfected with *APOE-targeting* guide RNA (CCGGCCA GCCGCTACAGGAG) and the HDR repair template (ACAGGGCCGCGTGC GGGGCCGCCACTGTGGGCTCCCTGGCC GGCCAGCCGCTACAGAAGCGTGCCAGGCCTGGGGCG AGCGGCTGCGCGCGCGGATGGAGGAGATGGGCAG CCGGA). Following nucleofection, the cells were plated in three wells of a 6-well plate in mTeSR-1 medium supplemented with 10 μ M Y-27632 2HCl (Selleckchem). The next day, a 48-h selection period was started with 0.6 μ g/ml puromycin. The cells were fed daily with the mTeSR-1 medium until individual colonies became apparent. The colonies were then selected with 0.6 μ g/ml puromycin and genotyped using the following primers: 5'-GATGCCGATGACCTGCAGAA - 3' and 5' - GCTTCGGCGTTTCAGTGATTG - 3' and restriction enzyme-based genotyping.

Neuronal Differentiation

The E213K cell line and the wild-type isogenic control line were then differentiated into neurons as previously described (Zhang et al., 2013; Forrest et al., 2017). After 4 weeks of culture, the neurons were fixed with 4% paraformaldehyde/4% sucrose.

Immunofluorescence Staining and Analysis

Fixed neurons were permeabilized for 15 min with 0.1% PBS-D (Digitonin) and stained with MAP2 and LipidTOX™ Red Neutral Lipid Stain. Coverslips were mounted and imaged using a Zeiss LSM 800 confocal microscope with a 20X objective. At least 50 neurons were imaged per condition. The acquired z-stacks were merged and puncta indicating lipid accumulation were counted using the ImageJ software.

RESULTS

Degu Whole-Genome Sequencing Provides Insights Into Aging and AD-Associated Genes

The whole genome of 11 4.5-year-old male degu was sequenced. A 58-fold sequencing depth resulted in 98.9% mapped reads. The genome was mapped to the degu reference genome (GCF_000260255.1) with 259,905 contigs and 7,135 scaffolds published by the Broad Institute in 2012 (OctDeg1.0 assembly). We identified an average of 11,272,248 variants in all the sequenced individuals; among them, there were 9,501,642 SNP and 1,770,605 insertion-deletions (INDEL) at average frequencies of 3.2 SNP/kip and 0.6 INDEL/kip, respectively (Supplementary Table 1).

The SNP and INDEL variants identified were mainly (39.9%) located in intergenic regions of the degu genome. While the variants located in coding regions represented just 0.46% of the total, however there were still 307,936 variants located in exons (Figure 1A). Within the exonic variants, 103,362 were variants that caused an amino acid change and could therefore influence protein structure and function. The number of genes that contained missense variants and had orthologous genes with *Mus musculus* was 10,870 (Supplementary Table 2). Gene Ontology (GO) biological pathway enrichment analysis revealed that 355 enriched pathways that were associated with immune-regulation, lipid metabolism, DNA repair mechanisms, apoptosis, translation, glucose metabolism, oxidative stress and cell cycle (Figures 1B,C). These biological processes are highly relevant to aging and aging-related diseases (Barzilai et al., 2012; Tower, 2015; Anisimova et al., 2018).

X-Box Binding Protein 1

During aging, there is a reduction in the capacity of the cells to control protein folding and aggregation, and activation of the unfolded protein response (UPR) is compromised. The transcription factors X-box binding protein (XBP1) is a basic leucine-zipper (bZIP) transcription factor, a family of proteins that can lead to disease states including neurodegeneration, diabetes and cancer (Cissé et al., 2017).

The homology between degu and human and mouse XBP1 protein is 78.8 and 79.1% respectively with a similar homology (77.7%) between human and mouse XBP1. The human *XBPI* gene is spliced by the inositol-requiring enzyme 1 (IRE1) that removes a 26-nucleotide intron from XBP1 to shift the coding reading into a XBP1spliced form (XBP1s) that contains a bZIP domain. XBP1s has physiological roles in the brain and the

immune system. In the degu we identified an INDEL of 343bp in *Xbp1*, this INDEL completely deletes exon 1 (Figure 2A) which contains 27 amino acids of the N-terminal bZIP domain (Figure 2B). The lack of exon 1 in the degu carrying this mutation could result in the absence of *Xbp1* unspliced form (*Xbp1u*) isoform due to the high number of amino acids that are removed. Dysregulation of bZIP can lead to neurodegeneration and diabetes. The INDEL we report deletes part of the bZIP domain possibly affecting DNA-binding and dimerization functions in the degu that carry this mutation. Such degu could be an excellent model with which to understand the effect of this mutation in aging, diabetes and AD.

MutS Homolog 6

Among the GO terms found, DNA repair was one of the enriched biological functions that had genes with variants. Deficiency in repair of nuclear and mitochondrial DNA damage has been linked to aging and neurodegeneration. The MSH6 gene provides instructions for making a protein that plays an essential role in repairing DNA (Marsischky et al., 1996).

The homology between degu, human and mouse MSH6 amino acid sequences revealed an 85.5% of identity between degu and human (NP_000170.1) and 80.4% identity between degu and mouse (NP_034960.1) and an identity of 85.3% between human and mouse (Figure 3).

We found a SNP in the degu *Msh6* that caused an amino acid change from tyrosine to histidine in 55% of the degu, this residue is also highly conserved between human, degu and mouse (Figure 3). The SNP was in the DNA mismatch repair protein MutS core domain. Interestingly, mutations in MSH6 result in high rates of accumulation of base substitution mutations in humans (Marsischky et al., 1996). Further studies on the structural characterization of the mutation could help elucidate the effect of this mutation in the degu in comparison to humans and its effect in DNA repair and aging mechanisms.

Insulin-Like Growth Factor 1

The homology between degu and human (XP_016874752.1) IGF1 is 97.9%, whereas, between degu and mouse (AAL34535.1) and human and mouse it is 92.1% and 93.7% respectively. We identified an INDEL of 20 bp in exon 2 of the degu *Igf1*. This INDEL causes a frameshift at residue 76 that changed the amino acid sequence (Figure 3). This change in the amino acid sequence resulted in the complete deletion of E-peptide. This peptide is highly conserved (97.3%) between degu and human.

Apolipoprotein E

The human *APOE* gene has 90.0 % homology with the degu *Apoe* gene. And the degu *APOE* amino acid sequence has 71.3% and 70.2% homology with the human and mouse *APOE* protein, respectively.

We identified seven SNP in the degu *Apoe* gene compared to the reference sequence (NW_004524773.1), one of which was non-synonymous (denoted Mt4) and found in a 631 bp PCR product amplified from genomic DNA (Figure 4).

The degu *Apoe* Mt4 can yield one of three residues at position 213: glutamic acid (E), which is present in Refseq

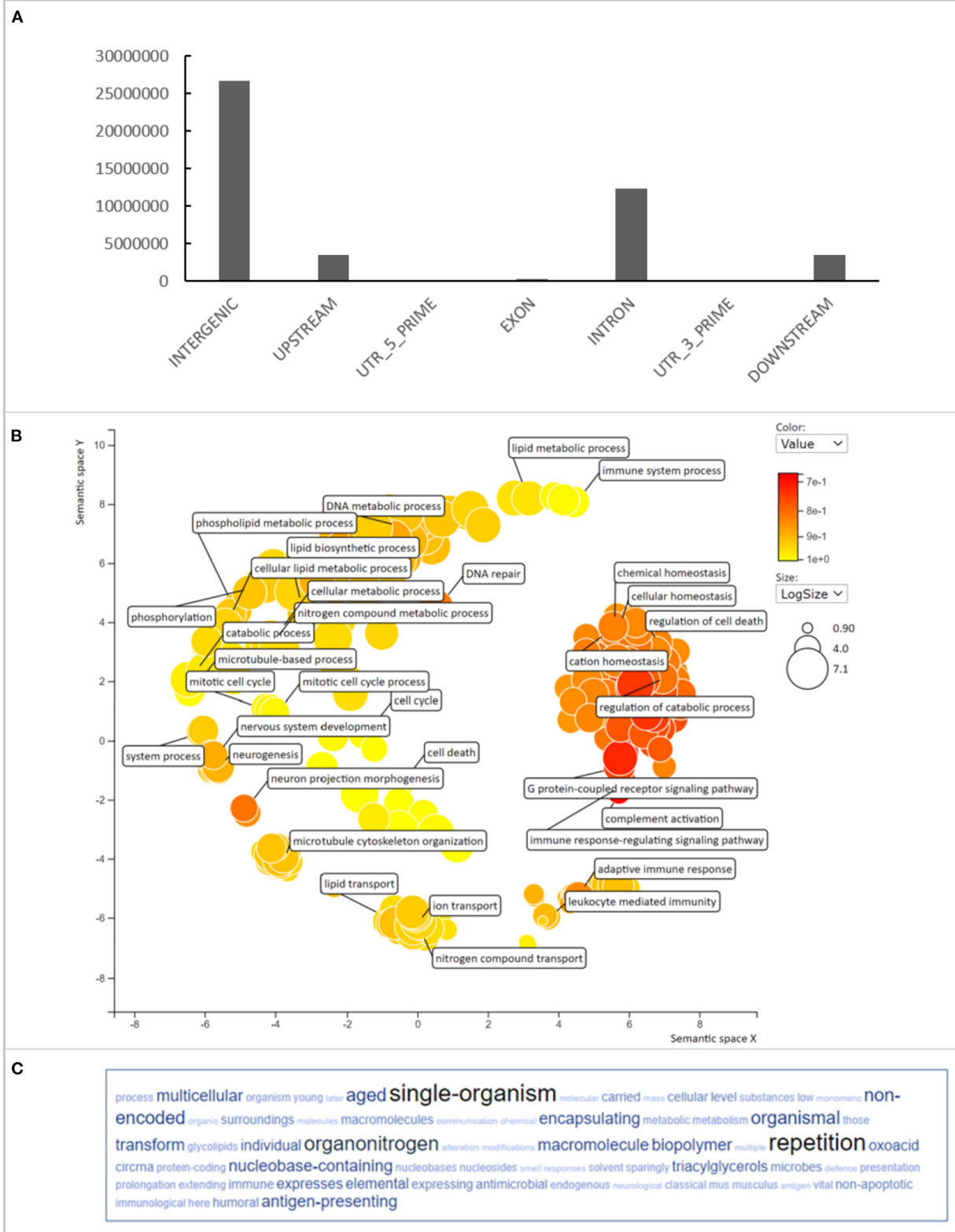


FIGURE 1 | Variant annotation in Degu genomes. **(A)** Represents the variant distribution through the different genomic regions. **(B)** Represents the GO term enrichment of genes that had missense variants found in different Degu genomes. **(C)** Represents the most frequent keywords within the GO terms.

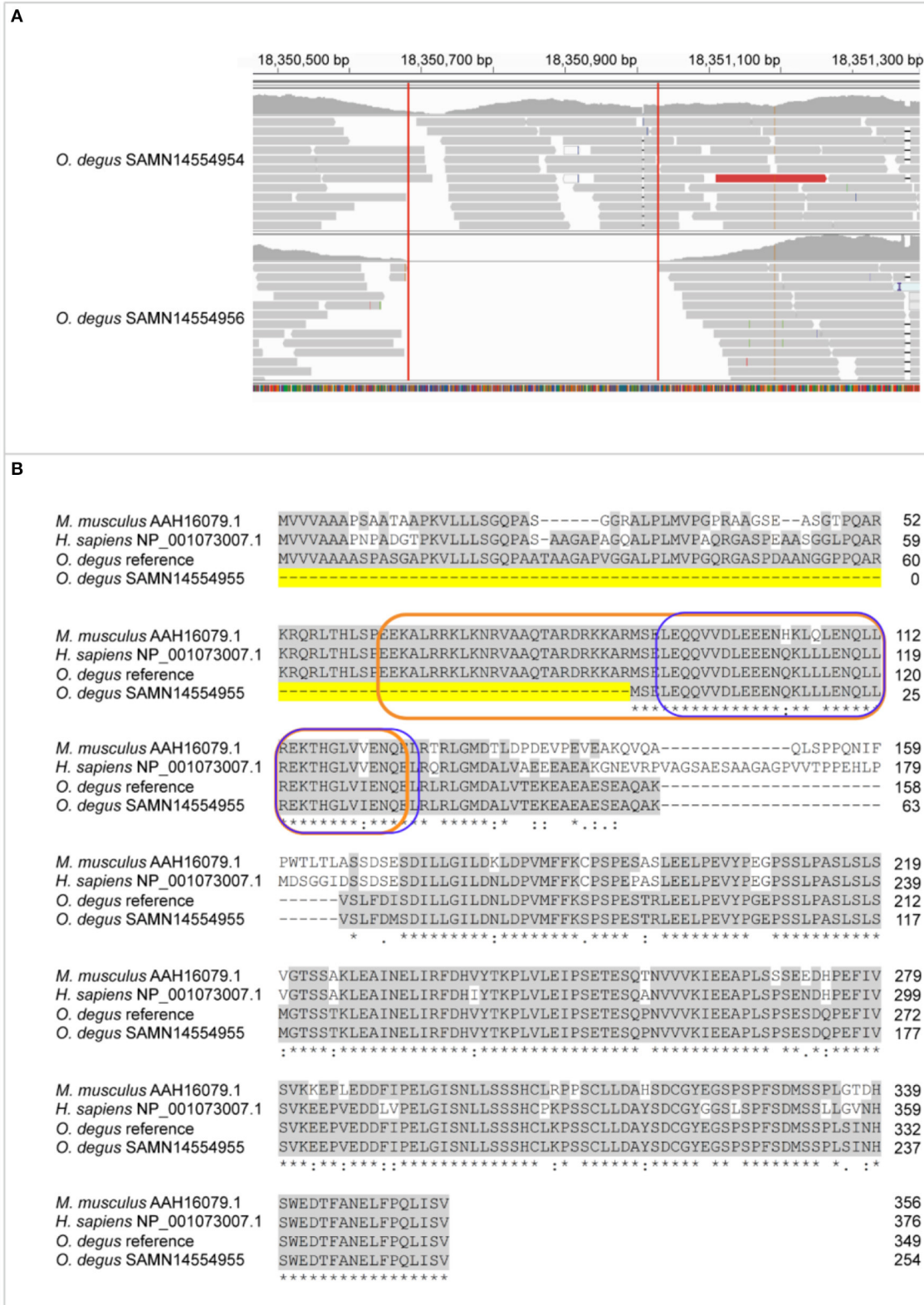


FIGURE 2 | Exon 1 is lost in Xbp1 due to 27bp deletion of bZIP N-terminal. **(A)** Genome mapping of degu SAMN14554954, an animal that had the complete XBP1 sequence and degu SAMN14554956 that carried the exon 1 deletion compared to the degu reference genome GCF000260255 in the XBP1 coding sequence. **(B)** Alignment of amino acid sequence between *M. musculus*, *H. sapiens* XBP1s isoform and degu SAMN14554954 and SAMN14554956. Conserved amino acid sequences among all the aligned organism sequences are greyhighlighted. Dashed line highlighted in yellow represents the amino acid deletion of XBP1 in degu SAMN14554956. The bZIP domain is outlined orange and the leucine zipper outlined in blue.

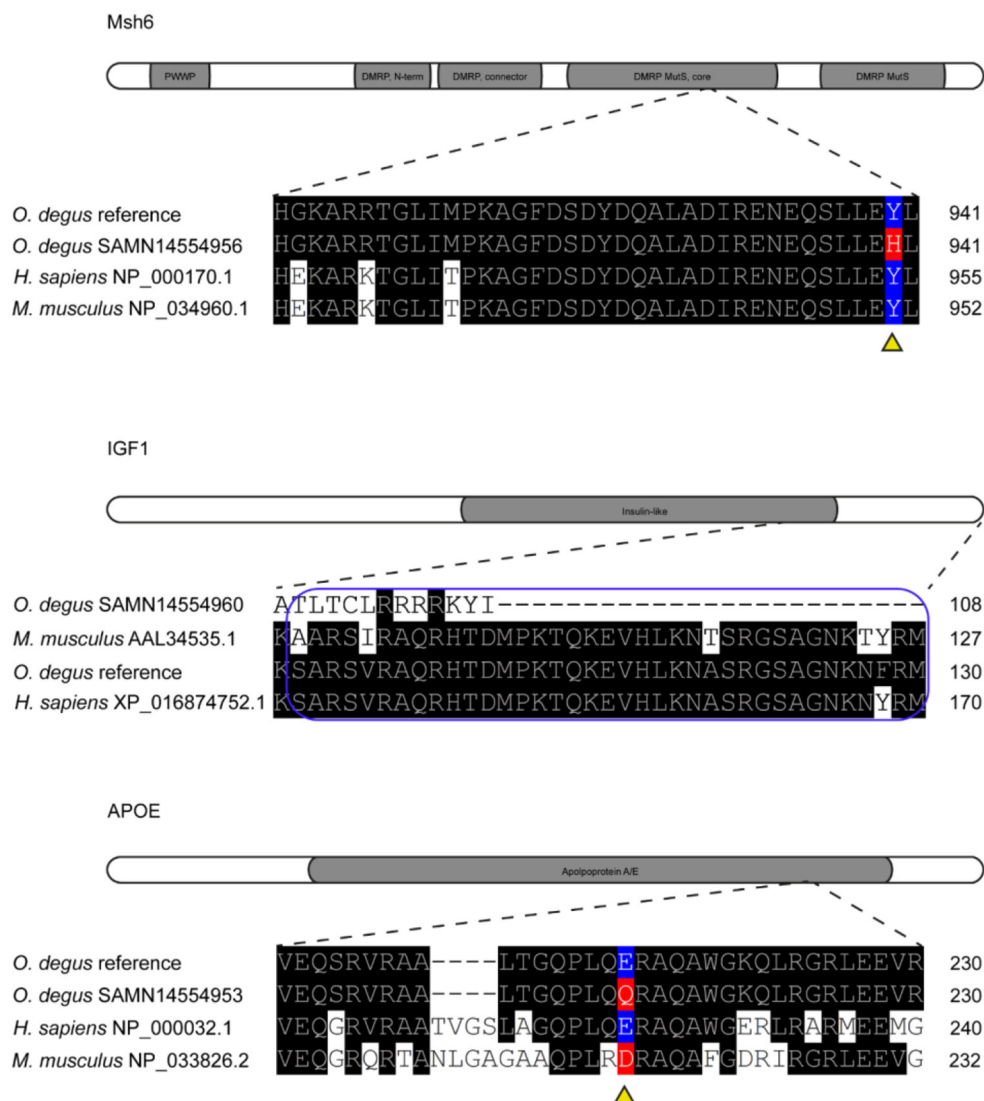


FIGURE 3 | Missense variants in Msh6, IGF1 and APOE genes of degu. Representation of Msh6, IGF1 and APOE genes with missense mutations aligned to degu reference genome annotated gene and human amino acid sequence. Amino acid changes are highlighted in red. Reference amino acids are highlighted in blue. Gray shading shows functional domains of each gene. DMRP correspond to DNA mismatch protein MutS domain. The E-peptide of IGF1 is outlined in blue.

XP_004644379.1, glutamine (Q), or lysine (K) (Figure 4A). The allele E is conserved in human and degu but in mouse corresponds to aspartic acid. The effect of the degu *Apoe* [E213E], *Apoe* [E213Q] and *Apoe* [E213K] variants in protein structure and function were studied in detail.

Degu *Apoe* Mt4 SNP Showed a Genetic Variation Across the Degu Population

The degu *Apoe* Mt4 frequency in 137 degu was confirmed by Sanger sequencing and the allele distribution was E213E = 43%, E213Q = 31%, E213K = 11.0%, Q/Q = 13%, Q213K = 1.0%, and K213K = 1.0% (Figure 4B).

Degu *Apoe* Mt4 SNP Correlated With Deficits in Activities of Daily Living

We evaluated the effect of Mt4 on burrowing, a species-typical task that mirrors “activities of daily living” in patients that decline noticeably in the earliest stages of the AD. The allele E213Q (most frequent) showed a 6-fold correlation with burrowing deficits (OR = 6.46, $P = 0.0005$, Fisher’s exact test) and allele E213K was also significantly associated with burrowing deficits by 5-fold (OR = 5.46, $P = 0.002$) (Figures 4C,D).

Correlation Between the Degu *Apoe* Mt4 SNP and AD-Like Neuropathology

Because *APOE4* is the strongest genetic risk factor for late-onset AD, with a correspondingly high accumulation of amyloid

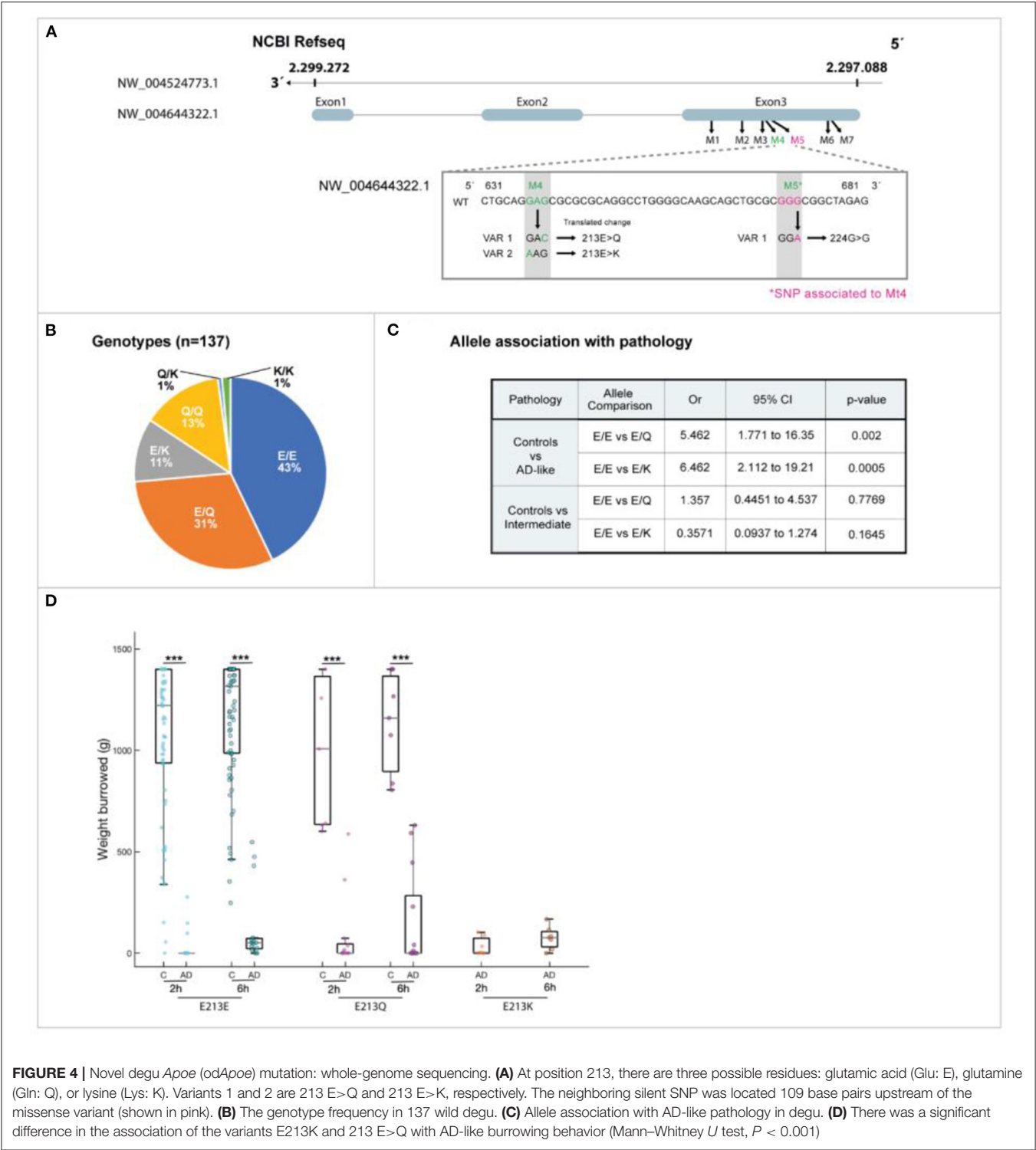


FIGURE 4 | Novel degu *Apoe* (*odApoe*) mutation: whole-genome sequencing. **(A)** At position 213, there are three possible residues: glutamic acid (Glu: E), glutamine (Gln: Q), or lysine (Lys: K). Variants 1 and 2 are 213 E>Q and 213 E>K, respectively. The neighboring silent SNP was located 109 base pairs upstream of the missense variant (shown in pink). **(B)** The genotype frequency in 137 wild degu. **(C)** Allele association with AD-like pathology in degu. **(D)** There was a significant difference in the association of the variants E213K and 213 E>Q with AD-like burrowing behavior (Mann–Whitney *U* test, *P* < 0.001)

plaques (Jansen et al., 2015). We investigated whether degu Mt4 carrier subpopulations have more brain β -amyloid deposition. To examine this association, β -amyloid plaques were assessed in the brains of 12 degu (**Figure 5**). While no significant plaques were observed in the degu with the E213E and Q213Q *Apoe* variants,

β -amyloid plaques were robustly observed throughout the cortical regions in the degu with the E213K and E213Q variants (**Figures 5a–e**). Our quantification of 6E10 immunopositive plaques in the degu brain sections showed that plaque abundance (plaques/cm²) differed significantly between the degu with *Apoe*

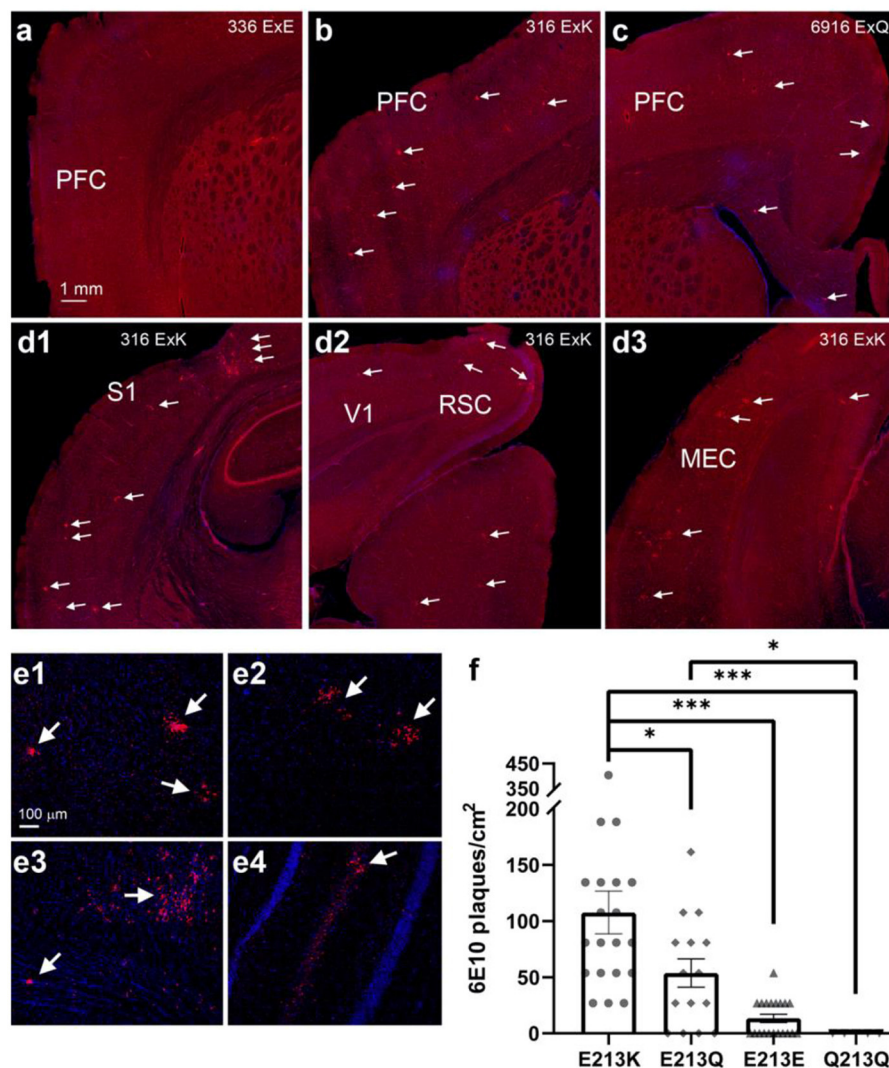


FIGURE 5 | Degu carrying the odAPOE allele E213K presented the highest β -amyloid plaque accumulation in the brain. (a–c) PFC comparison of right brain hemispheres of degu presenting three different residue variants: E213E (a), E213K (b), and E213Q (c). Residue variants E213K and E213Q show brain plaque depositions throughout the PFC, while wild-type E213E shows no perceivable plaques. White arrows denote β -amyloid plaques. (d1–d3) Widespread β -amyloid plaque depositions seen through various posterior brain regions in an E213K variant carrier. White arrows denote β -amyloid plaques. (e1–e4) Confocal micrographs of cortical (e1–e3) and hippocampal plaques (e4). (f) There were among-variant differences in the number of plaques, with the E213K variant carriers showing significant differences compared with carriers of the other variants (4 E213K cases; 8 other cases; Linear mixed-effect model (LME) tests. (* $P < 0.05$, *** $P < 0.001$). PFC, prefrontal cortex; S1, primary somatosensory cortex; V1, primary visual cortex; RSC, retrosplenial cortex; MEC, medial entorhinal cortex.

E213K and other variant types (4 E213K cases; 8 other cases; Linear mixed-effect model (LME) tests, E213K vs. E213Q: $p = 0.0101$, E213K vs. E213E: $p = 7.1919 \times 10^{-6}$, E213K vs. Q213Q: $p = 0.0003$.) (Figure 5f).

Degu *ApoE* Mt4 SNP Alters Protein Structure

In humans APOE binds lipoproteins by opening its four-helix bundle and exposing hydrophobic, amphipathic sequences to the lipid surface. We generated an *in silico* homologous model structure of the degu APOE based on the human APOE protein structure (Frieden et al., 2017) and identified 74% sequence

identity between both proteins, denoting a similar structure, function, and evolutionary origin. The degu *ApoE* contains the equivalent of R112 and Glu255 but lacks the critical R61 equivalent (it contains T61). Despite this difference, Mt4 caused flexibility at the salt bridge dislodging helix C2 allowing the approach of E133 and R148 domains with a similar consequential effect to that observed in human APOE.

Schematic representations of the APOE structure, APOE3, and modeled the degu APOE structures and the alignment of degu, human, and mouse sequences of the relevant structural and functional correlates are shown in Figures 6A–C. Both Q and K variants reduced the local negative electrostatic potential

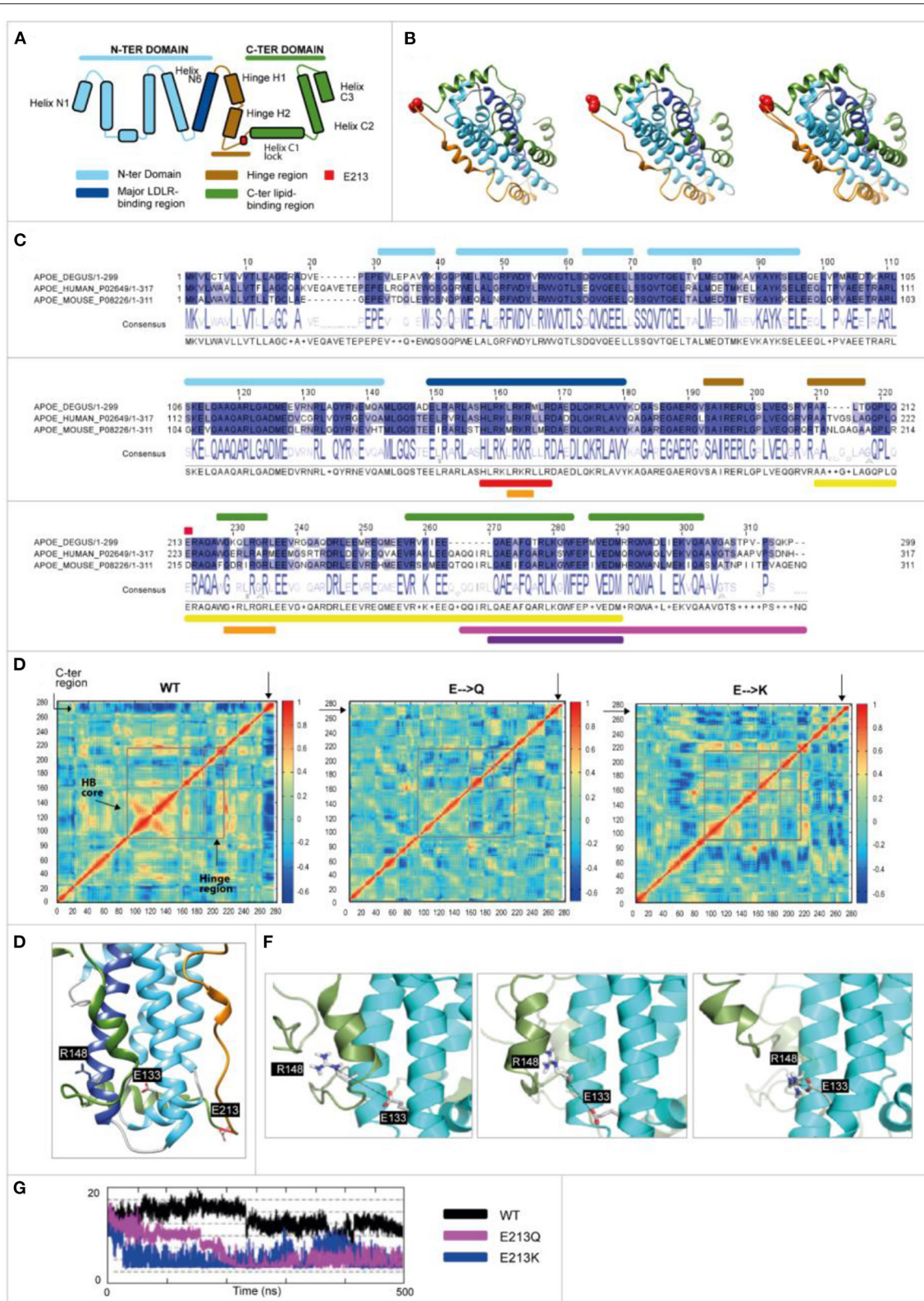


FIGURE 6 | Human and odAPOE isoforms. **(A)** Secondary structural scheme of APOE based on the high-resolution structure of APOE3. **(B)** From left to right: ribbon representation of the APOE3 structure (UniProt code: P02649; PDB code: 2L7B), odApoe wild-type model, and APOE3-degu APOE superposition that are colored as shown in the scheme. Degu E213 and human E223 are shown as red spheres. **(C)** Degu, human, and mouse sequence alignment. Upper bars: secondary structure (Continued)

FIGURE 6 | elements are colored as shown in the scheme. Red circle: Glutamic acid 213 (223 human). Lower bars: *APOE* (UniProt code: P02649) functional domains. Red: LDL and other lipoprotein receptor binding; orange: heparin binding; yellow: lipid-binding and lipoprotein association; pink: homo-oligomerization; violet: specificity for association with VLDL. **(D)** Displacement correlation matrix of the molecular dynamics simulation, with blue and red indicating uncorrelated and highly correlated motions, respectively (X- and Y-axis represent the amino acid number). Regions are indicated by gray boxes. The N-terminal helix bundle (HB) core region showed more correlated motions in the wild-type model while the C-terminal region showed more correlated motions with the rest of the protein in the E213Q and E213K models. Moreover, the hinge region showed differences. **(E)** A 3-D structure of wild-type degu *ApoE* showing the positions of the D133, R148, and E213 residues (represented as sticks). **(F)** Sequential representation of the salt bridge generation observed during the simulations. The N-terminal and C-terminal domains are depicted in cyan and green, respectively. The reference position of helix C2 during the wild-type degu *APOE* simulation is depicted as a cartoon representation in transparent green. **(G)** Distance (Å) between D133 and R148 during the simulations (500 ns). The MD-derived distance between both residues is constant and larger in wild-type (black curve) than in E213K (blue) and E213Q (pink).

(**Supplementary Figure 1**). The displacement correlation matrix was analyzed, and the three model proteins were found to have significantly different conformational properties (**Figure 6D**). The wild-type protein showed highly concerted motions at the helix bundle of the N-terminal domain, while the C-terminal end showed displacements that were completely uncorrelated with the rest of the protein. In contrast, for the E213Q and E213K proteins, the concerted motion at the N-terminal domain was no longer present, increasing the N-terminal domain flexibility. Their C-terminal domain showed motion correlated with the rest of the protein (not present in wild-type degu *APOE*; **Figure 6D**).

A unique salt bridge at Glu 133-Arg 148 (E133-R148) was generated in the E213Q and E213K protein simulations but not in the wild-type protein. The formation of this salt bridge in the wild-type protein was hindered by the presence of helix C2 (**Figure 6E**). In the E213Q and E213K simulations, the increased N-terminal and C-terminal flexibility dislodged helix C2, which in turn allowed the approach of E133 and R148 (**Figures 6F,G**).

Degu *ApoE* Mt4 Isoforms Modulate Lipid Droplet Formation in Degu and Human Neurons

Because of previous reports linking lipid droplets with AD, aging, inflammation and diabetes in the present work we investigated the presence of lipid droplets in skin fibroblasts from AD patients, age-matched controls and old degu to determine whether alterations in lipid droplets occur in degu that may be relevant to AD-like pathology in the degu model of aging and AD.

The skin fibroblasts from AD patients and degu fibroblasts expressing *ApoE* Mt4 (E213K) displayed an evident alteration, namely an anomalous accumulation of lipid droplets in their cytoplasm compared to human control fibroblasts and wild-type (E213E) degu fibroblasts (**Figures 7A–C**).

To examine the cellular functions of Mt4 in fibroblasts we investigated whether the accumulation of lipid droplets observed in degu fibroblasts was also preserved in human fibroblast cells carrying the degu Mt4 mutation. We generated the orthologous degu *ApoE* Mt4 mutation (213E/213K) in human embryonic stem cells using CRISPR/Cas9 genome editing. A heterozygous mutant cell line was confirmed by Sanger sequencing (**Figure 7D**). A significant increase in the number of lipid droplets was found in the degu *ApoE* Mt4 neurons compared to non-mutant wild-type neurons derived from isogenic controls (**Figures 7E,F** $P = 0.0095$, Student's *t*-test, $n = 124$ degu *ApoE* Mt4 neurons and $n = 113$ wild-type neurons derived from two independent cultures).

These data show that the degu *ApoE* Mt4 mutation increases lipid droplet accumulation in both human and degu derived neurons and fibroblasts.

DISCUSSION

The aim of this work was to characterize and validate the unconventional natural degu model of aging and Alzheimer's disease. We use whole-genome sequencing techniques to create a new degu genome annotation that allowed the identification of mutations associated with aging and AD-like pathology in this long-lived animal model. Our research achieved the goal of providing new investigative tools to identify the gaps in current knowledge related to molecular mechanisms of aging and late-onset AD using a long-lived animal model that may assist in the identification of potential therapeutic targets.

We found variants in 14,992 genes (**Supplementary Table 2**) among the 11 degu genomes evaluated and we report novel variants in 19 genes (**Supplementary Table 3**) associated with processes involved in aging and AD such as neuroinflammation, protein misfolding, diabetes and DNA-repair genes. From these we selected 4 genes to report that are involved in DNA repair, glucose metabolism, protein misfolding and lipid homeostasis.

Xbp1 is a very complex protein regulating many physiological functions, including immune system, inflammatory responses, lipid metabolism, neurodegeneration, diabetes and is implicated in AD (Selkoe, 1991; Leuner and Shors, 2004; Piperi et al., 2016; Remondelli and Renna, 2017). We identified an almost identical homology between the degu and humans *Xbp1* (Uniprot code: P17861), conserving the bZIP domain (residues 70 to 133) which suggests that the degu *Xbp1* has the same functions as the human isoform 1. The structure of this protein is unknown for any species. The INDEL we have identified in 80% of the analyzed degu shows that some degu only have the unspliced form of this protein and others the spliced form of this protein which affects the bZIP domain.

The *Octodon degus* naturally develops type-2 diabetes mellitus (T2DM), a known risk factor for AD (Zemva and Schubert, 2011). Based on previous work that insulin and Igf-1 influence Aβ toxicity we examined degu Igf-1 (Westwood et al., 2014). For *Igf-1* we identified the homology between degu and human (XP_016874752.1) IGF1 to be 97.9 %, with only one amino acid substitution relative to human. Although more studies are needed to support these observations, our results indicate that it may be the case that some AD-like degu recapitulate some *Igf1*

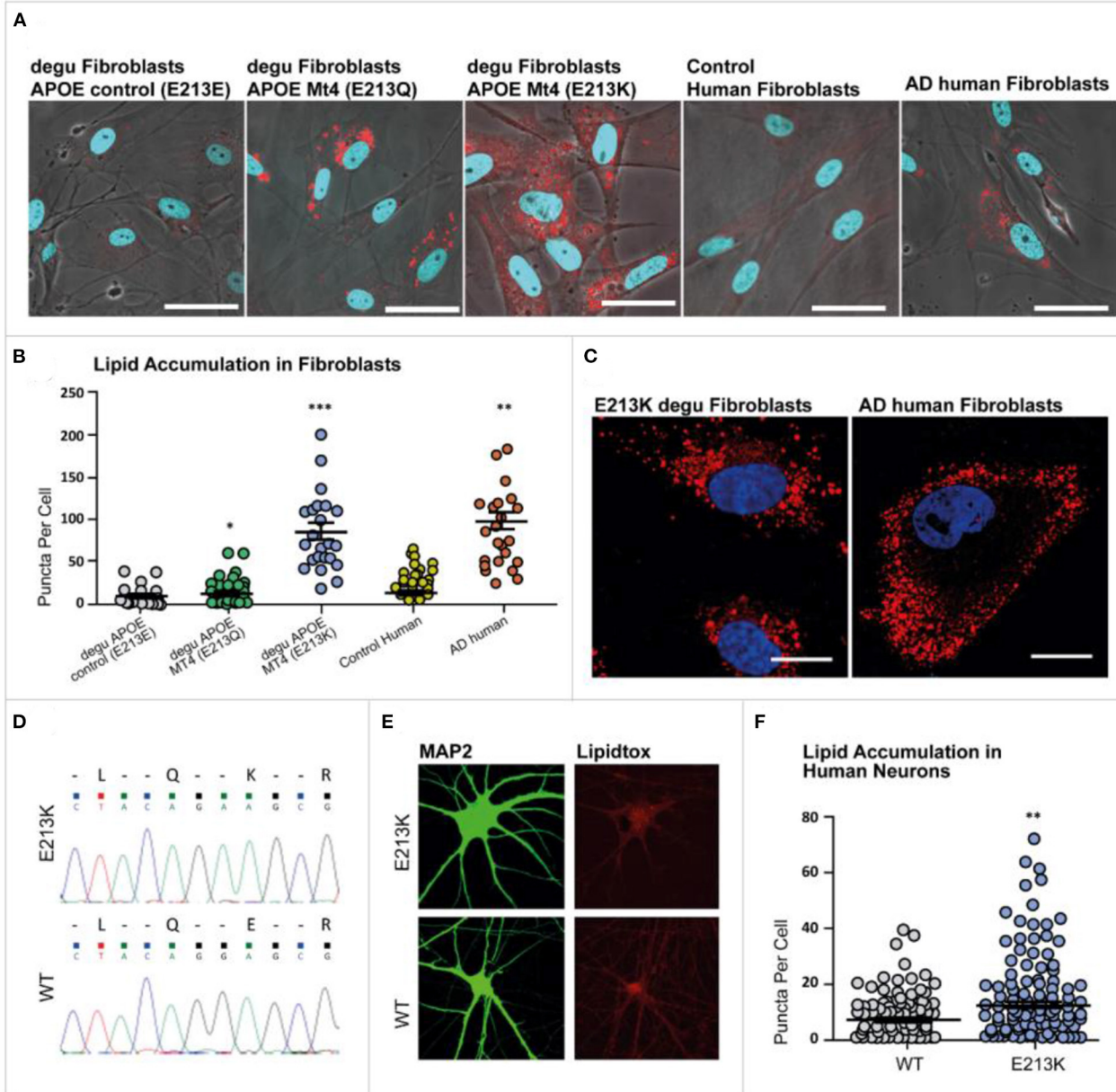


FIGURE 7 | Lipid droplet accumulation in degu and human fibroblasts. Primary cultures of degu and human fibroblasts stained with LipidTOXTM Red Neutral Lipid stain (red), where nuclei were identified through DAPI counterstaining (blue). **(A)** Representative micrographs of E213E, E213Q, and E213K degu fibroblasts, as well as fibroblasts obtained from human controls and patients with AD. **(B)** Lipid droplet quantification in degu and human fibroblasts. **(C)** Representative images of E213K degu fibroblasts and fibroblasts from patients with AD showing prominent lipid droplet accumulation. **(D)** Heterozygous mutant cell line confirmed through Sanger sequencing. **(E)** Neurons were stained using MAP2 and lipid accumulation was visualized with LipidTOXTM. **(F)** Compared with neurons derived from isogenic controls, neurons derived for degu and humans carrying odApoE Mt4 E213Q and E223K, respectively, showed a significant increase in lipid puncta ($P = 0.0095$, Student's t -test, $n = 124$). odApoE Mt4 and wild-type neurons derived from two independent cultures. The scale bar represents 20 μ m.

gene regulatory features seen in aging, insulin resistance and AD pathogenesis (Talbot et al., 2012).

Because in humans *APOE* alleles have a major impact on aging-associated diseases, particularly cardiovascular disease, type 2 diabetes and late-onset AD we focused on the effect of the *ApoE* variants we identified in the degu. The degu *ApoE*

gene (Mt4) was significantly associated with an increase of A β deposition throughout cortical brain regions and correlated with cognitive impairment. Moreover, cell biology analysis suggested that the degu *ApoE* Mt4 was responsible, at least in part, for the excessive accumulation of lipid droplets, in degu fibroblasts and human-derived neurons as reported in *APOE4* human

carriers (Liu et al., 2015; Wong et al., 2017). While altered lipid metabolism is reported here, the degu *Apoe* Mt4 variants may also contribute to AD-like phenotypes *via* other functions of APOE known to be relevant to AD pathogenesis, including brain glucose metabolism and the trafficking of A β , considering that this animal model has been reported as a natural model of atherosclerosis, diabetes and the neuropathogenesis of AD (Homan et al., 2010; Hurley et al., 2018).

Degu were divided according to their performance in activities of daily living (ADL) into two groups, AD-like and normal healthy (control) animals. ADL are defined as the things we normally do such as feeding ourselves, bathing and dressing. Deterioration in the ability to perform ADL is an early sign of cognitive decline. At present, learning and memory tests are widely used in the preclinical search for treatments for AD. However, in most cases these tests do not probe “episodic memory” which is the type most affected in AD. Healthy controls for this task are animals that complete the burrowing test in the expected time. AD-like are the animals that failed to complete the task in time. Burrowing performance also leave a number of intermediate burrowers, animals that in the time of the test, come out as not good or bad burrowers, but with an intermediate outcome. Interestingly, we have observed that with time, as they age, some intermediate individuals tend to become AD-like, although not all. Thus, in **Figure 4C** we compared the allele association with AD pathology and, an intermediate group of degu to analyse the impact of the *Apoe* variants on burrowing speed and variability in AD-like and intermediate degu. Interestingly, the amount of bedding displaced was significantly lower in the E213K group suggesting that this variant could have an impact on burrowing speed and variability.

The human E4 variant contains a single amino acid substitution that strongly influences the compactness and rigidity of APOE and consequent lipid binding capability, which is thought to involve the coordination of N- and C-terminal domains (Frieden et al., 2017). We predicted that the novel degu *Apoe* Mt4 mutation would affect interactions with lipids and/or other relevant macromolecules. The Mt4 forms of the degu *Apoe* change a crucial part of the hinge region immediately before the C-terminal domain, thereby making the hinge region more flexible, which allows conformational changes such as those occurring in APOE4R (with R at position 112) (Mizuguchi et al., 2014). Overall, our analysis of the dynamic properties of wild-type and the different the degu *Apoe* variants revealed how the E213Q and E213K polymorphisms strongly affect proper degu *Apoe* function. Similarities between the E213K and Q mutations and human ApoE4 are shown in **Supplementary Figure 2**.

ApoE3 only differs from ApoE4 by a single amino acid substitution, the human APOE gene has 90.0 % homology with the degu *Apoe* gene. ApoE4 > ApoE3 > ApoE2, lead to increased aggregation and deposition and decreased clearance of A β peptides. In humans APOE ϵ 2 may provide some protection against Alzheimer’s disease, but people with this allele can still develop the disease. APOE ϵ 3, the most common allele plays a neutral role in the disease, people with this isoform can either have or not have the disease. While people with the APOE ϵ 4 are

most at risk of developing AD. It should be noted that the 213 polymorphism is a contributing factor to AD-like risk in the degu and is not exclusive or directly causative of AD-like pathology in all cases.

Lipid droplets are influenced by many variables. Nevertheless, the reasons for exploring lipid droplets in association with the *Apoe* mutation was based on recent publications. Astrocytes expressing E4 accumulate significantly more and smaller lipid droplets compared to E3 astrocytes (Farmer et al., 2019). Moreover, by different mechanisms the over accumulation of lipid droplets has been linked to atherosclerosis, diabetes (Krahmer et al., 2013) and AD (Alzheimer et al., 1995; Hamilton et al., 2015). Furthermore, recent findings suggest that glial cells within the brain form lipid droplets in the fly brain and this process is *Apoe* dependent (Liu et al., 2017; Claes et al., 2021; Yin, 2022). Pani et al. (2009) compared controls and AD patient skin fibroblasts and report elevated lipid droplets in AD fibroblasts.

The work we report here is observational, we do not attempt to identify a mechanism to link the presence of lipid droplets and *Apoe* in *Octodon degus*. We observed an increase of lipid droplets in degu cells carrying the *Apoe* variants. And when we inserted degu *Apoe* mutation by CRISPR into human fibroblasts, we observed a significant increase in lipid droplets. However, numerous genes in addition to *Apoe* are associated with lipid metabolism, transport, and lipid droplet formation and further study is necessary to determine whether there is a direct correlation between lipid droplet formation and the *Apoe* genotype in the degu.

The strengths of our study include the use of an outbred degu population that exhibits the hallmark features of the disease to create a genetic characterization of this model of late-onset AD. Importantly, we found a novel mutation that confers APOE4-like properties to the degu *Apoe* which was correlated with AD-like phenotypes, thereby identifying a genetic AD susceptibility in the degu. Nevertheless, there were limitations to this study. For instance, we did not address the relationship between the degu *Apoe* Mt4 to tau pathology or microglial activation, which are both major mediators of human AD pathogenesis, nor did we test for causal influences of microbiome changes associated with the degu *Apoe* Mt4 and human APOE4. Future studies should be conducted to achieve these observations in degu. Moreover, a population study is necessary to understand the interplay between the degu *Apoe* Mt4 and environmental pressures in the degu population.

In silico modeling revealed that this variant imparted structural and functional changes in the APOE protein that resemble those seen in human APOE4 carriers. *In vitro*, this variant caused an increase in lipid droplet formation. Remarkably, the degu *Apoe* Mt4 variant was highly correlated with the accumulation of β -amyloid in the brain, alterations in neuronal lipid metabolism and a decline in behaviors analogous to activities of daily living in humans.

The whole-genome results suggest that, as in the human population, the *Apoe* gene is a risk factor for AD-like phenotype in a subpopulation of wild type lab-outbred (but not lab inbred) degu that spontaneously develop AD-like neuropathology. Some studies failed to report AD-like pathology in inbred populations

of degu (Steffen et al., 2016). We can only speculate as to whether the inbred colonies that fail to show AD-like pathology also lack the K/Q 213 polymorphisms. However, in order to understand the degu as a model of AD correctly, we maintain our colony as a wild-outbred population because we have found some of these animals to spontaneously develop AD-like behaviors and pathology. The degu colonies in Europe and the USA were imported from Chile in the 1970's primarily to study circadian rhythm. Thus, these colonies have been maintained as inbred since then and have consequently lost genetic diversity. Moreover, when we performed a whole genome study of an inbred Chilean degu colony we identified 2,400,000 variants vs. 11,500,000 variants in our wild outbred colony. Clearly indicating the impact of inbreeding and providing the possible reason for the differences seen between animals from our outbred colony in Chile and inbred European colonies.

In summary, we have produced a genome resource of an unconventional animal model of AD, which is a particularly valuable tool for within family comparison of transgenic mouse AD pathways in terms of which AD gene regulatory pathways are common to spontaneous AD-like features in degu vs. different transgenic mouse models.

DATA AVAILABILITY STATEMENT

The datasets presented in this study can be found in online repositories. The names of the repository/repositories and accession number(s) can be found in the article/**Supplementary Material**.

ETHICS STATEMENT

The animal study was reviewed and approved by Institute of Ecology and Biodiversity Ethics Committee, University of Chile, Santiago, Chile.

AUTHOR CONTRIBUTIONS

PC designed the study and the whole-genome sequencing and data analyses. PC, XX, and MC conceived the strategies. MH, CU, and FA analyzed the genome data. MH and PC wrote and edited the manuscript. XX designed the degu brain amyloid analysis. BG was involved in the amyloid immunohistochemistry experiments on degu brain sections. GC, AB, and CM-B contributed to the protein structure analysis of the degu APOE Mt4. ME and FE contributed to the lipid accumulation experiments on degu and human fibroblasts. MC contributed to the design of experiments involving human fibroblasts and CRISPR, as well as neuron-derived lipid droplet analysis and data interpretation. AK and BW performed the experimental work. PA and RD performed and designed the behavioral studies. EP, RV, TH, AA, PW-V, GZ, and CA worked on the manuscript and data analysis. All authors contributed to writing the final manuscript version and extensively to the work presented in this paper, have approved the submitted version and agreed to be personally accountable

for their contributions, as well as to ensure that questions related to the accuracy and integrity of any part of the work are appropriately investigated, and resolved and that the resolution is documented in the literature.

FUNDING

XX and PC were funded by US National Institutes of Health Grant R24AG073198. PC was funded by ANID-FONDECYT 1200928. RV and EP were funded by AFB-170008-CONICYT-Chile-IEB. BW and MC were funded by grant 3R01MH115005-02S1. AA was funded by ANID EX-CONICYT PAI77180086. GZ and CA are grateful for support from Research England's THYME project. TH is funded by R35 GM127102.

ACKNOWLEDGMENTS

We sincerely thank the Fraunhofer Chile Research and all the Biomedicine division team.

SUPPLEMENTARY MATERIAL

The Supplementary Material for this article can be found online at: <https://www.frontiersin.org/articles/10.3389/fnagi.2022.894994/full#supplementary-material>

Supplementary Figure 1 | Electrostatic potential. (A) Wild-type odAPOE ribbon representation with transparent surface and 90-degree rotation to show the positions of the structures in B; E213 is represented as a red sphere. (B) Coulombic surfaces of wild type odAPOE, K odAPOE and Q odAPOE showing the reduction in electronegative surface potential in the two mutated models. Red indicates more electronegative, and blue indicates more electropositive.

Supplementary Figure 2 | Domain structure of APOE3, APOE 4 and degu odAPOE Mt4. APOE3 and 4 proteins contain two independent domains that are connected by a hinge region. It has been proposed that Arg112 in APOE4 (instead of Cys 112 in APOE3 variant) exposes Arg61, which forms a salt bridge with Glu255 in the C-terminal domain and leads to close contact between the C- and N-terminal domains. The N-terminal domain contains the receptor-binding domain (indicated in green), and the C-terminal domain contains the lipid-binding region (indicated in orange). The odAPOE Mt4 at the E213 residue in the degu sequence is located at the end of the hinge region immediately before the start of the C-terminal domain at the end of the tube before the box representing the C-terminal domain in APOE4 (indicated in blue). The computational analysis suggested that the conformation induced by the mutation is more similar to that reported for APOE4 due to the formation of a salt bridge between Glu133 and Arg148, approaching the C-terminal and N-terminal domains. Similar to APOE4, this unique domain interaction in the degu odAPOE protein may result in lipidation and folding.

Supplementary Table 1 | Variant calling metrics. Variants found in each *O. degus* genome compared to the *O. degus* reference genome (GCA_000260255.1). VQ filter represents the variant quality filter ($Q > 100$). DP filter represents the variant depth filter ($DP > 20$). InDel correspond to Insertions/Deletions.

Supplementary Table 2 | *O. degus* genes containing missense variants. List of genes of *O. degus* that contain missense variants compared to the *O. degus* reference genome (GCA_000260255.1).

Supplementary Table 3 | AD, DNA repair and diabetes related genes with missense variants. Extraction of variant information from vcf file of AD, DNA repair and diabetes related genes that contain missense variants in the evaluated animals compared to the *O. degus* reference genome (GCA_000260255.1).

REFERENCES

- Altimiras, F., Uszczynska-Ratajczak, B., Camara, F., Vlasova, A., Palumbo, E., Newhouse, S., et al. (2017). Brain transcriptome sequencing of a natural model of Alzheimer's disease. *Front. Aging Neurosci.* 9, 64. doi: 10.3389/fnagi.2017.00064
- Alzheimer, A., Stelzmann, R. A., Schnitzlein, H. N., and Murtagh, F. R. (1995). An English translation of Alzheimer's 1907 paper, "Über eine eigenartige Erkrankung der Hirnrinde". *Clin. Anat.* 8, 429–431. doi: 10.1002/ca.980080612
- Anisimova, A. S., Alexandrov, A. I., Makarova, N. E., Gladyshev, V. N., and Dmitriev, S. E. (2018). Protein synthesis and quality control in aging. *Aging* 10, 4269–4288. doi: 10.18632/aging.101721
- Ardiles, A. O., Tapia-Rojas, C. C., Mandal, M., Alexandre, F., Kirkwood, A., Inestrosa, N. C., et al. (2012). Postsynaptic dysfunction is associated with spatial and object recognition memory loss in a natural model of Alzheimer's disease. *Proc. Natl. Acad. Sci. U. S. A.* 109, 13835–13840. doi: 10.1073/pnas.1201209109
- Barzilai, N., Guarente, L., Kirkwood, T. B., Partridge, L., Rando, T. A., and Slagboom, P. E. (2012). The place of genetics in ageing research. *Nat. Rev. Genet.* 13, 589–594. doi: 10.1038/nrg3290
- Bates, K., Vink, R., Martins, R., and Harvey, A. (2014). Aging, cortical injury and Alzheimer's disease-like pathology in the guinea pig brain. *Neurobiol. Aging* 35, 1345–1351. doi: 10.1016/j.neurobiolaging.2013.11.020
- Chang, L. Y., Palanca-Castan, N., Neira, D., Palacios, A. G., and Acosta, M. L. (2021). Ocular health of *octodon degus* as a clinical marker for age-related and age-independent neurodegeneration. *Front. Integr. Neurosci.* 15, 665467. doi: 10.3389/fnint.2021.665467
- Cingolani, P., Platts, A., Wang, L., Coon, M., Nguyen, T., Wang, L., et al. (2012). A program for annotating and predicting the effects of single nucleotide polymorphisms, SnpEff: SNPs in the genome of *Drosophila melanogaster* strain w1118; iso-2; iso-3. *Fly* 6, 80–92. doi: 10.4161/fly.19695
- Cissé, M., Duplan, E., and Checler, F. (2017). The transcription factor XBP1 in memory and cognition: implications in Alzheimer disease. *Mol. Med.* 22, 905–917. doi: 10.2119/molmed.2016.00229
- Claes, C., Danhash, E. P., Hasselmann, J., Chadarevian, J. P., Shabestari, S. K., England, W. E., et al. (2021). Plaque-associated human microglia accumulate lipid droplets in a chimeric model of Alzheimer's disease. *Mol. Neurodegener.* 16, 50. doi: 10.1186/s13024-021-00473-0
- Deacon, R. M., Altimiras, F. J., Bazan-Leon, E. A., Pyrasani, R. D., Nachtigall, F. M., Santos, L. S., et al. (2015). Natural AD-Like neuropathology in *Octodon degus*: impaired burrowing and neuroinflammation. *Curr. Alzheimer Res.* 12, 314–322. doi: 10.2174/1567205012666150324181652
- Ebensperger, L. A., Pérez de Arce, F., Abades, S., and Hayes, L. D. (2016). Limited and fitness-neutral effects of resource heterogeneity on sociality in a communally rearing rodent. *J. Mammal.* 97, 1125–1135. doi: 10.1093/jmammal/gyw056
- Farmer, B. C., Klumper, J., and Johnson, L. A. (2019). Apolipoprotein E4 alters astrocyte fatty acid metabolism and lipid droplet formation. *Cells* 8, 182. doi: 10.3390/cells8020182
- Forrest, M. P., Zhang, H., Moy, W., McGowan, H., Leites, C., Dionisio, L. E., et al. (2017). Open chromatin profiling in hiPSC-derived neurons prioritizes functional noncoding psychiatric risk variants and highlights neurodevelopmental loci. *Cell Stem Cell*, 21, 305–318.e8. doi: 10.1016/j.stem.2017.07.008
- Frieden, C., Wang, H., and Ho, C. (2017). A mechanism for lipid binding to apoE and the role of intrinsically disordered regions coupled to domain-domain interactions. *Proc. Natl. Acad. Sci. U. S. A.* 114, 6292–6297. doi: 10.1073/pnas.1705080114
- Gunn-Moore, D., Kaidanovich-Beilin, O., Gallego Iradi, M. C., Gunn-Moore, F., and Lovestone, S. (2018). Alzheimer's disease in humans and other animals: a consequence of postreproductive life span and longevity rather than aging. *Alzheimers. Dement.* 14, 195–204. doi: 10.1016/j.jalz.2017.08.014
- Hamilton, L. K., Dufresne, M., Joppé S. E., Petryszyn, S., Aumont, A., Calon, F., et al. (2015). Aberrant lipid metabolism in the forebrain niche suppresses adult neural stem cell proliferation in an animal model of Alzheimer's disease. *Cell Stem Cell* 17, 397–411. doi: 10.1016/j.stem.2015.08.001
- Homan, R., Hanselman, J. C., Bak-Mueller, S., Washburn, M., Lester, P., Jensen, H. E., et al. (2010). Atherosclerosis in *Octodon degus* (degu) as a model for human disease. *Atherosclerosis* 212, 48–54. doi: 10.1016/j.atherosclerosis.2010.06.004
- Hurley, M. J., Deacon, R., Beyer, K., Ioannou, E., Ibáñez, A., Teeling, J. L., et al. (2018). The long-lived *Octodon degus* as a rodent drug discovery model for Alzheimer's and other age-related diseases. *Pharmacol. Ther.* 188, 36–44. doi: 10.1016/j.pharmthera.2018.03.001
- Inestrosa, N. C., Reyes, A. E., Chacón, M. A., Cerpa, W., Villalón, A., Montiel, J., et al. (2005). Human-like rodent amyloid-beta-peptide determines Alzheimer pathology in aged wild-type *Octodon degus*. *Neurobiol. Aging* 26, 1023–1028. doi: 10.1016/j.neurobiolaging.2004.09.016
- Jansen, W. J., Ossenkoppele, R., Knol, D. L., Tijms, B. M., Scheltens, P., Verhey, F. R., et al. (2015). Prevalence of cerebral amyloid pathology in persons without dementia: a meta-analysis. *JAMA* 313, 1924–1938. doi: 10.1001/jama.2015.4668
- Jesseau, S. A., Holmes, W. G., and Lee, T. M. (2008). Mother-offspring recognition in communally nesting degus, *Octodon degus*. *Anim. Behav.* 75, 573–582. doi: 10.1016/j.anbehav.2007.06.015
- Jones, A., Head, E., and Greer, K. A. (2018). "The dog as a model for aging research," in *Conn's Handbook of Models for Human Aging, 2nd Edn.*, eds J. Ram and P. Michael (Conn. eBook).
- Krahmer, N., Farese, R. V. Jr, and Walther, T. C. (2013). Balancing the fat: lipid droplets and human disease. *EMBO Mol. Med.* 5, 973–983. doi: 10.1002/emmm.201100671
- Lee, T. M. (2004). *Octodon degus*: a diurnal, social, and long-lived rodent. *ILAR J.* 45, 14–24. doi: 10.1093/ilar.45.1.14
- Leuner, B., and Shors, T. J. (2004). New spines, new memories. *Mol. Neurobiol.* 29, 117–130. doi: 10.1385/MN:29:2:117
- Liu, C. C., Hu, J., Tsai, C. W., Yue, M., Melrose, H. L., Kanekiyo, T., et al. (2015). Neuronal LRP1 regulates glucose metabolism and insulin signaling in the brain. *J. Neurosci.* 35, 5851–5859. doi: 10.1523/JNEUROSCI.5180-14.2015
- Liu, L., MacKenzie, K. R., Putluri, N., Maletić-Savatić M., and Bellen, H. J. (2017). The glia-neuron lactate shuttle and elevated ROS promote lipid synthesis in neurons and lipid droplet accumulation in glia via APOE/D. *Cell Metab.* 26, 719–737.e6. doi: 10.1016/j.cmet.2017.08.024
- Marsischky, G. T., Filosi, N., Kane, M. F., and Kolodner, R. (1996). Redundancy of *Saccharomyces cerevisiae* MSH3 and MSH6 in MSH2-dependent mismatch repair. *Genes Dev.* 10, 407–420. doi: 10.1101/gad.10.4.407
- Mizuguchi, C., Hata, M., Dhanasekaran, P., Nickel, M., Okuhira, K., Phillips, M. C., et al. (2014). Fluorescence study of domain structure and lipid interaction of human apolipoproteins E3 and E4. *Biochim. Biophys. Acta.* 1841, 1716–1724. doi: 10.1016/j.bbailip.2014.09.019
- Pani, A., Dessi S., Diaz, G., La Colla, P., Abete, C., Mulas, C., et al. (2009). Altered cholesterol ester cycle in skin fibroblasts from patients with Alzheimer's disease. *J. Alzheimers. Dis.* 18, 829–841. doi: 10.3233/JAD-2009-1193
- Paushter, D. H., Du, H., Feng, T., and Hu, F. (2018). The lysosomal function of progranulin, a guardian against neurodegeneration. *Acta Neuropathol.* 136, 1–17. doi: 10.1007/s00401-018-1861-8
- Piperi, C., Adamopoulos, C., and Papavassiliou, A. G. (2016). XBP1: a pivotal transcriptional regulator of glucose and lipid metabolism. *Trends Endocrinol. Metab.* 27, 119–122. doi: 10.1016/j.tem.2016.01.001
- Poeggel, G., Nowicki, L., and Braun, K. (2003). Early social deprivation alters monoaminergic afferents in the orbital prefrontal cortex of *Octodon degus*. *Neuroscience* 116, 617–620. doi: 10.1016/S0306-4522(02)00751-0
- Remondelli, P., and Renna, M. (2017). The endoplasmic reticulum unfolded protein response in neurodegenerative disorders and its potential therapeutic significance. *Front. Mol. Neurosci.* 10, 187. doi: 10.3389/fnmol.2017.00187
- Ridley, R. M., Murray, T. K., Johnson, J. A., and Baker, H. F. (1986). Learning impairment following lesion of the basal nucleus of Meynert in the marmoset: modification by cholinergic drugs. *Brain Res.* 376, 108–116. doi: 10.1016/0006-8993(86)90904-2
- Salazar, C., Valdivia, G., Ardiles, Á. O., Ewer, J., and Palacios, A. G. (2016). Genetic variants associated with neurodegenerative Alzheimer disease in natural models. *Biol. Res.* 49, 14. doi: 10.1186/s40659-016-0072-9
- Selkoe, D. J. (1991). The molecular pathology of Alzheimer's disease. *Neuron* 6, 487–498. doi: 10.1016/0896-6273(91)90052-2
- Serrano-Pozo, A., Das, S., and Hyman, B. T. (2021). APOE and Alzheimer's disease: advances in genetics, pathophysiology, and therapeutic approaches. *Lancet Neurol.* 20, 68–80. doi: 10.1016/S1474-4422(20)30412-9

- Sharman, M. J., Moussavi Nik, S. H., Chen, M. M., Ong, D., Wijaya, L., Laws, S. M., et al. (2013). The guinea pig as a model for sporadic Alzheimer's Disease (AD): the impact of cholesterol intake on expression of AD-related genes. *PLoS ONE* 8, e66235. doi: 10.1371/journal.pone.0066235
- Steffen, J., Krohn, M., Paarmann, K., Schwitlick, C., Brüning, T., Marreiros, R., et al. (2016). Revisiting rodent models: *Octodon degus* as Alzheimer's disease model? *Acta Neuropathol. Commun.* 4, 91. doi: 10.1186/s40478-016-0363-y
- Talbot, K., Wang, H. Y., Kazi, H., Han, L. Y., Bakshi, K. P., Stucky, A., et al. (2012). Demonstrated brain insulin resistance in Alzheimer's disease patients is associated with IGF-1 resistance, IRS-1 dysregulation, and cognitive decline. *J. Clin. Invest.* 122, 1316–1338. doi: 10.1172/JCI59903
- Tarragon, E., Lopez, D., Estrada, C., Ana, G. C., Schenker, E., Pifferi, F., et al. (2013). *Octodon degus*: a model for the cognitive impairment associated with Alzheimer's disease. *CNS Neurosci. Ther.* 19, 643–648. doi: 10.1111/cns.12125
- Tower, J. (2015). Programmed cell death in aging. *Ageing Res. Rev.* 23(Pt A), 90–100. doi: 10.1016/j.arr.2015.04.002
- van Groen, T., Kadish, I., Popović, N., Popović, M., Caballero-Bleda, M., Baño-Otálora, B., et al. (2011). Age-related brain pathology in *Octodon degus*: blood vessel, white matter and Alzheimer-like pathology. *Neurobiol. Aging* 32, 1651–1661. doi: 10.1016/j.neurobiolaging.2009.10.008
- Vasquez, R. A. (1997). Vigilance and social foraging in *Octodon degus* (Rodentia: Octodontidae) in central Chile. *Revista Chilena Historia Natural* 70, 557–563
- Wenk, G. L. (1993). A primate model of Alzheimer's disease. *Behav. Brain Res.* 57, 117–122. doi: 10.1016/0166-4328(93)90127-C
- Westwood, A. J., Beiser, A., Decarli, C., Harris, T. B., Chen, T. C., He, X. M., et al. (2014). Insulin-like growth factor-1 and risk of Alzheimer dementia and brain atrophy. *Neurology* 82, 1613–1619. doi: 10.1212/WNL.0000000000000382
- Wong, M. W., Braid, N., Poljak, A., Pickford, R., Thambisetty, M., and Sachdev, P. S. (2017). Dysregulation of lipids in Alzheimer's disease and their role as potential biomarkers. *Alzheimers Dement.* 13, 810–827. doi: 10.1016/j.jalz.2017.01.008
- Yin, F. (2022). Lipid metabolism and Alzheimer's disease: clinical evidence, mechanistic link and therapeutic promise. *FEBS J.* 289, 1858–1875. doi: 10.1111/febs.16344
- Yu, Z., Guindani, M., Grieco, S. F., Chen, L., Holmes, T. C., and Xu, X. (2022). Beyond t test and ANOVA: applications of mixed-effects models for more rigorous statistical analysis in neuroscience research. *Neuron* 110, 21–35. doi: 10.1016/j.neuron.2021.10.030
- Zemva, J., and Schubert, M. (2011). Central insulin and insulin-like growth factor-1 signaling: implications for diabetes associated dementia. *Curr. Diabetes Rev.* 7, 356–366. doi: 10.2174/157339911797415594
- Zhang, Y., Pak, C., Han, Y., Ahlenius, H., Zhang, Z., Chanda, S., et al. (2013). Rapid single-step induction of functional neurons from human pluripotent stem cells. *Neuron* 78, 785–798. doi: 10.1016/j.neuron.2013.05.029
- Zhou, X., Dou, Q., Fan, G., Zhang, Q., Sanderford, M., Kaya, A., et al. (2020). Beaver and naked mole rat genomes reveal common paths to longevity. *Cell Rep.* 32, 107949. doi: 10.1016/j.celrep.2020.107949

Conflict of Interest: The authors declare that the research was conducted in the absence of any commercial or financial relationships that could be construed as a potential conflict of interest.

Publisher's Note: All claims expressed in this article are solely those of the authors and do not necessarily represent those of their affiliated organizations, or those of the publisher, the editors and the reviewers. Any product that may be evaluated in this article, or claim that may be made by its manufacturer, is not guaranteed or endorsed by the publisher.

Copyright © 2022 Hurley, Urra, Garduno, Bruno, Kimbell, Wilkinson, Marino-Buslje, Ezquer, Ezquer, Aburto, Poulin, Vasquez, Deacon, Avila, Altimiras, Whitney Vanderklis, Zampieri, Angione, Constantino, Holmes, Caba, Xu and Cogran. This is an open-access article distributed under the terms of the Creative Commons Attribution License (CC BY). The use, distribution or reproduction in other forums is permitted, provided the original author(s) and the copyright owner(s) are credited and that the original publication in this journal is cited, in accordance with accepted academic practice. No use, distribution or reproduction is permitted which does not comply with these terms.



OPEN ACCESS

Edited by:

Ian M. McDonough,
University of Alabama, United States

Reviewed by:

Samantha Allison,
Intermountain Healthcare,
United States
Denise Head,
Washington University in St. Louis,
United States
Gillian Coughlan,
MGH Institute of Health Professions,
United States

*Correspondence:

Jan Laczó
jan.lacz@lfmotol.cuni.cz

Specialty section:

This article was submitted to
Alzheimer's Disease and Related
Dementias,
a section of the journal
Frontiers in Aging Neuroscience

Received: 28 February 2022

Accepted: 29 April 2022

Published: 02 June 2022

Citation:

Laczó M, Martinkovic L, Lerch O,
Wiener JM, Kalinova J, Matuskova V,
Nedelska Z, Vyhnaek M, Hort J and
Laczó J (2022) Different Profiles of
Spatial Navigation Deficits In
Alzheimer's Disease
Biomarker-Positive Versus
Biomarker-Negative Older Adults
With Amnesic Mild Cognitive
Impairment.
Front. Aging Neurosci. 14:886778.
doi: 10.3389/fnagi.2022.886778

Different Profiles of Spatial Navigation Deficits In Alzheimer's Disease Biomarker-Positive Versus Biomarker-Negative Older Adults With Amnesic Mild Cognitive Impairment

Martina Laczó¹, Lukas Martinkovic¹, Ondrej Lerch^{1,2}, Jan M. Wiener³, Jana Kalinova¹,
Veronika Matuskova^{1,2}, Zuzana Nedelska^{1,2}, Martin Vyhnaek^{1,2}, Jakub Hort^{1,2}
and Jan Laczó^{1,2*}

¹Memory Clinic, Department of Neurology, Charles University, Second Faculty of Medicine and Motol University Hospital, Prague, Czechia, ²International Clinical Research Center, St. Anne's University Hospital Brno, Brno, Czechia, ³Department of Psychology, Ageing and Dementia Research Centre, Bournemouth University, Poole, United Kingdom

Background: Spatial navigation impairment is a promising cognitive marker of Alzheimer's disease (AD) that can reflect the underlying pathology.

Objectives: We assessed spatial navigation performance in AD biomarker positive older adults with amnesic mild cognitive impairment (AD aMCI) vs. those AD biomarker negative (non-AD aMCI), and examined associations between navigation performance, MRI measures of brain atrophy, and cerebrospinal fluid (CSF) biomarkers.

Methods: A total of 122 participants with AD aMCI ($n = 33$), non-AD aMCI ($n = 31$), mild AD dementia ($n = 28$), and 30 cognitively normal older adults (CN) underwent cognitive assessment, brain MRI ($n = 100$ had high-quality images for volumetric analysis) and three virtual navigation tasks focused on route learning (body-centered navigation), wayfinding (world-centered navigation) and perspective taking/wayfinding. Cognitively impaired participants underwent CSF biomarker assessment [amyloid- β_{1-42} , total tau, and phosphorylated tau₁₈₁ (p-tau₁₈₁)] and amyloid PET imaging ($n = 47$ and $n = 45$, respectively), with a subset having both ($n = 19$).

Results: In route learning, AD aMCI performed worse than non-AD aMCI ($p < 0.001$), who performed similarly to CN. In wayfinding, aMCI participants performed worse than CN (both $p \leq 0.009$) and AD aMCI performed worse than non-AD aMCI in the second task session ($p = 0.032$). In perspective taking/wayfinding, aMCI participants performed worse than CN (both $p \leq 0.001$). AD aMCI and non-AD aMCI did not differ

in conventional cognitive tests. Route learning was associated with parietal thickness and amyloid- β_{1-42} , wayfinding was associated with posterior medial temporal lobe (MTL) volume and p-tau₁₈₁ and perspective taking/wayfinding was correlated with MRI measures of several brain regions and all CSF biomarkers.

Conclusion: AD biomarker positive and negative older adults with aMCI had different profiles of spatial navigation deficits that were associated with posterior MTL and parietal atrophy and reflected AD pathology.

Keywords: egocentric navigation, allocentric navigation, hippocampus, entorhinal cortex, precuneus, retrosplenial cortex, neurodegeneration, tauopathies

INTRODUCTION

Alzheimer's disease (AD) is the most common neurodegenerative disease (Barker et al., 2002). AD forms a continuum from the preclinical stage through mild cognitive impairment (MCI) to dementia (Jack et al., 2018). AD is associated with extracellular aggregation of amyloid- β plaques (Thal et al., 2002), intracellular accumulation of abnormally phosphorylated tau protein (Braak and Braak, 1995), progressive neuronal loss (neurodegeneration; Miller et al., 2013) and cognitive impairment (Green et al., 2000). Amyloid- β accumulation first emerges in the neocortical regions, and early affects the posterior-midline regions such as the precuneus and posterior cingulate cortex, including the retrosplenial cortex (RSC; Sojkova et al., 2011; Palmqvist et al., 2017). Tau pathology first emerges in the transentorhinal cortex [the region between the anterolateral entorhinal cortex (aLEC) and the perirhinal cortex] in Braak stage I and spreads to the posteromedial entorhinal cortex (pmEC) and the hippocampus (Braak and Braak, 1995) in Braak stages II and III, respectively. The pathology then spreads to the posterior cortical regions (Braak stage IV) in the early clinical stages (i.e., MCI), and finally to the entire neocortex (Braak stages V and VI) in the dementia stage (Braak and Braak, 1991). Neurodegeneration and brain atrophy essentially parallel the pattern of distribution and propagation of tau pathology (Whitwell et al., 2007) but not amyloid- β deposition (Josephs et al., 2008) in AD. The regions early affected by AD pathology are essential for spatial navigation (Hartley et al., 2003; Blanch et al., 2004; Howett et al., 2019; Schöberl et al., 2020). Spatial navigation is a complex cognitive process of determining and updating one's position and orientation in the environment (Wolbers and Hegarty, 2010). Spatial navigation deficits may thus be one of the earliest cognitive markers of AD, and the assessment of spatial navigation may aid the early diagnosis of AD (Coughlan et al., 2018).

Successful spatial navigation requires a flexible combination of various navigation strategies. When navigating the environment, navigators can remember the traveled route in relation to their own bodies. This navigation strategy is referred to as route learning (i.e., body-centered, egocentric navigation). When learning routes, navigators can encode the sequence of body movements at decision points (e.g., right, left, straight) or form associations between direction changes and specific proximal landmarks (e.g., "Turn left at the shop";

Waller and Lipka, 2007). The posterior parietal cortex (DeIpoli et al., 2007; Ruotolo et al., 2019), precuneus (Weniger et al., 2011; Saj et al., 2014), and the caudate nucleus (Iglói et al., 2010) play an important role in route learning (Hartley et al., 2003; Blanch et al., 2004). Alternatively, navigators can create an internal representation of the environment (i.e., "cognitive map") by encoding positions of distant landmarks relative to each other and relative to specific locations regardless of the navigators' positions. This navigation strategy is referred to as wayfinding (i.e., world-centered, allocentric navigation). The medial temporal lobe (MTL), especially the hippocampus, which is strongly interconnected with the entorhinal cortex (EC; Cholvin et al., 2021), is important for wayfinding (Maguire et al., 1998). The right hippocampus is more strongly associated with wayfinding than the left hippocampus (Maguire et al., 1998; Nedelska et al., 2012; Laczó et al., 2017). The hippocampal and EC subregions show different functional specialization along the anterior-posterior axis, with the posterior regions being more relevant for wayfinding (Doeller et al., 2008). Specifically, the posterior hippocampus (i.e., the body and the tail) is involved in the creation and use of cognitive maps (Schinazi et al., 2013) and in supporting fine-grained spatial representations (Brunec et al., 2018), while the anterior hippocampus (i.e., the head) is involved in responding to novelty (Doeller et al., 2008) and navigational planning (Xu et al., 2010). Within the EC, the pmEC is involved in spatial information processing (Reagh and Yassa, 2014), world-centered direction computations (Chadwick et al., 2015), and fine-grained spatial representations (Evensmoen et al., 2015), while the aLEC is involved in object information processing (Reagh et al., 2018) and encoding of distances between locations related to landmarks (Chen et al., 2019). For successful navigation, it is essential to integrate body-centered and world-centered spatial information (i.e., reference frame translation) and use landmarks for directional orientation, both of which are supported by the RSC (Auger et al., 2012; Clark et al., 2018). Navigators can imagine scenes or parts of the environment from different perspectives during navigation, which is referred to as perspective taking (Marková et al., 2015). The parietal and temporal cortex and the MTL play an important role in this process (Zacks and Michelon, 2005; Lambrey et al., 2008).

Spatial navigation deteriorates as AD progresses along the AD continuum (Hort et al., 2007; Allison et al., 2016;

Levine et al., 2020). Older adults with mild AD dementia are severely impaired in route learning and wayfinding, both in real space (DePolvi et al., 2007; Hort et al., 2007) and in the virtual environment (Cushman et al., 2008; Laczó et al., 2010). They also show deficits in switching between the two spatial strategies (Morganti et al., 2013) and in perspective taking (Marková et al., 2015). Older adults with amnesic MCI (aMCI) frequently show deficits in route learning and wayfinding, both in real space (DePolvi et al., 2007; Laczó et al., 2009) and in the virtual environment (Weniger et al., 2011; Laczó et al., 2012). Perspective taking deficits have also been found in individuals with aMCI (Marková et al., 2015; Laczó et al., 2021a). However, these studies did not use biomarkers to confirm that AD was the cause of aMCI. The recent biomarker studies indicated that aMCI individuals with AD (AD aMCI) compared to cognitively normal (CN) older adults are impaired in wayfinding (Parizkova et al., 2018; Schöberl et al., 2020) and route learning (Schöberl et al., 2020) in real space and in recognition of the environment from a shifted viewpoint (Chan et al., 2016). One study suggested that older adults with preclinical AD [i.e., CN individuals with low cerebrospinal fluid (CSF) amyloid- β_{1-42} levels] have deficits in wayfinding but not route learning in the virtual environment (Allison et al., 2016). A recent study from the same research group replicated the findings of wayfinding deficits in preclinical AD and suggested that lower amyloid- β_{1-42} and higher p-tau₁₈₁ in CSF are associated with worse wayfinding performance in CN older adults (Allison et al., 2019). Together, these studies suggest that wayfinding deficits may already be present in preclinical AD, whereas route learning deficits first occur in the early clinical stages of AD.

In the effort to early diagnose AD, it is important to differentiate AD aMCI from those with other causes of aMCI. However, so far only a few studies addressed this topic. One recent study indicated that individuals with aMCI and amyloid- β positivity on positron emission tomography (PET) and in CSF show worse route learning and wayfinding in a complex real environment than those with negative amyloid- β biomarkers (Schöberl et al., 2020). It is worth noting that in contrast to aMCI individuals with amyloid- β positivity, those with negative amyloid- β biomarkers were impaired only in wayfinding and had similar performance to CN older adults in route learning (Schöberl et al., 2020). Similarly, route learning/body-centered navigation performance as opposed to wayfinding/world-centered navigation performance was shown to reliably discriminate cognitively impaired older adults with AD from those with other neurodegenerative diseases (Tu et al., 2017). Together, these studies suggest that route learning tasks have a greater potential to reveal AD-specific navigational deficits compared to wayfinding tasks. A recent study compared older adults with MCI and positive AD biomarkers in CSF to those with AD negative biomarkers. The former group showed less accurate spatial navigation in an immersive virtual reality task in which participants had to rely on self-motion cues (i.e., the path integration task; Howett et al., 2019). It has also been shown that older adults with aMCI and positive CSF AD

biomarkers were impaired in recognizing environments from a shifted viewpoint compared to those with negative biomarkers (Chan et al., 2016).

The previous studies indicated that spatial navigation may be a promising diagnostic tool to differentiate individuals with AD aMCI from aMCI individuals with negative AD biomarkers (non-AD aMCI; Howett et al., 2019; Schöberl et al., 2020). However, spatial navigation tests in real space and those in virtual environments that require movement in the real world are not optimal for everyday clinical practice because they are difficult to administer given space constraints in clinical settings and requirements of additional equipment. An ideal spatial navigation assessment should be ecologically valid, easy to administer and explain, and one in which participants can move virtually in a realistic-looking complex environment mimicking the real-life navigation (Diersch and Wolbers, 2019). The Navigation Test Suite¹, has been developed to meet these requirements (Wiener et al., 2020). It is performed on a computer screen, takes place in a computer-generated realistic-looking virtual city, provides closely controlled testing conditions, and enables manipulation of navigational parameters, such as landmark availability and navigation complexity. The Test Suite has been designed to evaluate various spatial navigation abilities and consists of three tasks: a Route-repetition task assessing route learning (body-centered navigation), a Route-retracing task assessing wayfinding (world-centered navigation), and a Directional-approach task assessing perspective taking and wayfinding (Wiener et al., 2013; de Condappa and Wiener, 2016). Our previous studies showed that this test is well tolerated by CN (Wiener et al., 2020; Laczó et al., 2021a) and cognitively impaired older adults (Laczó et al., 2021a), and reliably detects spatial navigation deficits in individuals with aMCI and mild AD dementia (Laczó et al., 2021a). However, the potential of this test to differentiate individuals with AD aMCI from those with non-AD aMCI, and associations of navigation performance with magnetic resonance imaging (MRI) measures of brain atrophy and AD biomarkers have not been investigated.

In this study, we built on our previous research using the Navigation Test Suite (Wiener et al., 2020; Laczó et al., 2021a) and aimed to assess: (1) the differences in spatial navigation performance in the specific tasks tested between the participants with AD aMCI, non-AD aMCI, mild AD dementia and CN; (2) the associations of spatial navigation performance with MRI measures of atrophy in the specific MTL, cortical and subcortical regions and; (3) the associations of spatial navigation performance with AD biomarkers in CSF, and the role of regional brain atrophy in these associations.

First, we hypothesized that participants with AD aMCI would show worse spatial navigation performance than those with non-AD aMCI in all three navigation tasks. Based on previous findings (Tu et al., 2017; Schöberl et al., 2020), we assumed that the largest differences between AD aMCI and non-AD aMCI participants would be observed in route learning. AD aMCI participants would perform worse than CN participants and similar to participants with mild AD dementia in all three tasks.

¹<https://osf.io/mx52y/>

Participants with non-AD aMCI would perform similarly to CN participants in route learning and worse than CN participants in wayfinding and perspective taking/wayfinding. Second, we hypothesized that more pronounced regional brain atrophy would be associated with worse spatial navigation performance. Specifically, atrophy of the parietal regions including the precuneus and posterior parietal cortex would be preferentially associated with worse route learning performance. Atrophy of the hippocampus and EC, especially their posterior subregions, would be preferentially associated with worse wayfinding performance. Based on previous findings (Nedelska et al., 2012; Laczó et al., 2017), we assumed that the association with wayfinding would be stronger for the right hippocampus than for the left. Atrophy of the hippocampus and EC, especially their posterior subregions, as well as parietal regions would be associated with worse perspective taking/wayfinding performance. Given that the integration of body-centered and world-centered spatial information is required for this task (Wiener et al., 2020), the association with atrophy of the isthmus cingulate/RSC would also be expected. Third, we hypothesized that lower levels of amyloid- β_{1-42} in CSF would be more strongly associated with worse route learning performance given the early and predominant amyloid- β accumulation in the parietal cortex (Sojkova et al., 2011; Palmqvist et al., 2017), the key region for route learning (DeIpoli et al., 2007; Weniger et al., 2011; Saj et al., 2014; Ruotolo et al., 2019). Higher levels of phosphorylated tau₁₈₁ (p-tau₁₈₁) in CSF would be more strongly associated with worse wayfinding performance given the early and predominant accumulation of tau pathology in the MTL (Braak and Braak, 1991, 1995; i.e., the hippocampus and EC), the key region for wayfinding (Nedelska et al., 2012; Howard et al., 2014; Chen et al., 2019). Levels of amyloid- β_{1-42} and p-tau₁₈₁ in CSF would be associated with perspective taking/wayfinding performance given the early and predominant accumulation of amyloid- β and tau pathology in the parietal cortex and MTL, respectively, the key regions for perspective taking (Zacks and Michelon, 2005; Lambrey et al., 2008). We also hypothesized that the association between CSF amyloid- β_{1-42} levels and performance in the route learning and perspective taking/wayfinding tasks would not be mediated by brain atrophy, as it has been shown that amyloid- β accumulation is not directly linked to regional atrophy (Josephs et al., 2008). Brain atrophy would mediate the association between CSF p-tau₁₈₁ levels and performance in the wayfinding and perspective taking/wayfinding tasks, given that tau pathology was shown to be related to region-specific neurodegeneration (Whitwell et al., 2007).

METHODS

Participants

Recruitment and Inclusion Criteria

A total of 122 participants were included in the study. The participants were recruited from the Czech Brain Aging Study (CBAS) cohort (Sheardova et al., 2019) at the Memory Clinic of the Charles University, Second Faculty of Medicine, and Motol University Hospital in Prague, Czech Republic. All participants

provided informed consent. The study was approved by the institutional ethics committee (no. EK – 701/16 25.5.2016). The participants with cognitive impairment were referred to the Memory Clinic by general practitioners and neurologists for memory complaints reported by participants themselves, their relatives, or health professionals. CN older adults were recruited from the University of the Third Age, senior centers (e.g., the Elpida center) or were relatives of participants and hospital staff (Parizkova et al., 2020).

All participants underwent clinical and laboratory evaluations, comprehensive cognitive assessment, brain MRI and the Navigation Test Suite. The participants with cognitive impairment underwent biomarker assessment including analysis of amyloid- β_{1-42} , total tau, and p-tau₁₈₁ in CSF or amyloid PET imaging or both, CSF biomarker assessment and amyloid PET imaging (Laczó et al., 2021b). They were classified as AD aMCI, non-AD aMCI, and mild AD dementia according to clinical diagnosis, and CSF biomarker and amyloid PET status. The participants with cognitive impairment were assigned to the relevant groups based on all available biomarkers, which had to be in agreement. All data were collected in 3–4 sessions within 60 days for each participant.

(i) Participants with AD aMCI ($n = 33$) met the clinical criteria for aMCI (Albert et al., 2011) including memory complaints, evidence of memory impairment [i.e., score lower than 1.5 standard deviations (SDs) below the age- and education-adjusted norms in any memory test], generally intact instrumental activities of daily living [<6 points on the Functional Activities Questionnaire, Czech Version (FAQ-CZ); Teng et al., 2010; Bezdíček et al., 2011] and absence of dementia. The participants had positive CSF AD biomarkers (reduced amyloid- β_{1-42} and elevated p-tau₁₈₁ (<665 pg/ml and >48 pg/ml, respectively, the internally validated cut-offs; Parizkova et al., 2018; Laczó et al., 2021b; $n = 9$), positive amyloid PET imaging (positive visual read of 18F-flutemetamol PET scan; $n = 16$), or both, positive CSF AD biomarkers and amyloid PET imaging ($n = 8$).

(ii) Participants with non-AD aMCI ($n = 31$) met the clinical criteria for aMCI (Albert et al., 2011) and had negative amyloid- β biomarkers defined as normal CSF amyloid- β_{1-42} (≥ 665 pg/ml; $n = 5$), negative amyloid PET imaging ($n = 19$), or both, normal CSF amyloid- β_{1-42} and negative amyloid PET imaging ($n = 7$). A total of 60% of the participants with CSF biomarkers ($n = 7$) had elevated p-tau₁₈₁ (>48 pg/ml; Parizkova et al., 2018; Laczó et al., 2021b) and about 60% of the participants with elevated p-tau₁₈₁ ($n = 4$) also had elevated total tau (>358 pg/ml; Cerman et al., 2020).

(iii) Participants with mild AD dementia ($n = 28$) met the clinical criteria for dementia (McKhann et al., 2011) with evidence of progressive cognitive impairment in at least two cognitive domains including memory (i.e., score lower than 1.5 SDs below the age- and education adjusted norms in any memory test and in at least one other non-memory cognitive test) and significant impairment in instrumental activities of daily living (≥ 6 points on the FAQ-CZ; Teng et al., 2010; Bezdíček et al., 2011). The participants had positive CSF AD biomarkers [reduced amyloid- β_{1-42} (<665 pg/ml) and elevated

p-tau₁₈₁ (>48 pg/ml; Parizkova et al., 2018; Laczó et al., 2021b) $n = 14$], positive amyloid PET imaging ($n = 10$), or both, positive CSF AD biomarkers and amyloid PET imaging ($n = 4$).

(iv) CN participants ($n = 30$) did not report any cognitive complaints and had cognitive performance within the normal range (i.e., score higher than 1.5 SDs below the age- and education-adjusted norms in all cognitive tests). In addition, they had no evidence of MTL atrophy on MRI. This was confirmed in all participants using the MTA visual scale on coronal T1-weighted (T1w) images, and the previously established age-specific MTA cut-off scores (i.e., score <2 in participants <75 years and score <3 in participants ≥75 years; Scheltens et al., 1992). Further, the participants did not have a family history of AD or other types of dementia in first-degree relatives. These criteria were applied to minimize the risk of including participants at increased risk of AD (i.e., individuals with subjective cognitive decline, hippocampal atrophy, or positive family history of AD).

Exclusion Criteria

Participants with depressive symptoms [≥ 6 points on the 15-item Geriatric Depression Scale (GDS-15)], anxiety [≥ 10 points on the Beck Anxiety Inventory (BAI)], low visual acuity [$< 20/40$ (corrected) on visual acuity tests], moderate to severe white matter vascular lesions on MRI (Fazekas score > 2 points), other primary neurological disorders (multiple sclerosis, epilepsy, Parkinsonian syndromes, and a history of traumatic brain injury or stroke) or psychiatric disorders (psychotic or schizoaffective disorders, major depressive disorder, anxiety disorders, and obsessive compulsive disorder), systemic diseases that can cause cognitive impairment, and a history of alcohol or drug abuse were not included in the study. In total, 131 participants from the CBAS cohort underwent spatial navigation assessment. The participants with cognitive impairment for whom biomarker data were not available at the time of the analysis were excluded ($n = 4$). Also, the participants with mild dementia for whom spatial navigation data were not available because they did not complete training in the Navigation Test Suite were excluded ($n = 5$).

Spatial Navigation Assessment

We used the Navigation Test Suite, which is described in detail in Wiener et al. (2020) and Laczó et al. (2021a). Here we reiterate the description of the test for better comprehension. The Navigation Test Suite consists of three navigation tasks: the Route-repetition task, the Route-retracing task, and the Directional-approach task. The Navigation Test Suite uses a virtual environment that consists of streets with residential houses and four-way intersections. The houses bordering the streets are all identical, except for the unique houses (i.e., distinct landmarks) that are located at each intersection (explained in detail below, **Figures 1A,B**). Participants could always see only one intersection at any time because the other more distant intersections were concealed in white fog. Prior to the testing, all participants completed familiarization training consisting of shorter versions of all three tasks (a three-intersection

path for the Route-repetition and Route-retracing tasks and two separate intersections for the Directional-approach task; Wiener et al., 2020).

(I) Route-Repetition Task

In the encoding phase, the participants were positioned in a street next to a black car. They were then passively transported along a route featuring five intersections with one right turn, three left turns, and one straight movement. The route then stopped at a red phone box. Each intersection featured four identical houses at the four corners. Different intersections featured different houses (i.e., landmarks), such that each intersection had a unique appearance. Participants were instructed to remember the route (**Figure 1A**). In the test phase, the participants were asked to reproduce the same route from the car to the phone box. Participants were passively transported towards each of the intersections where they were stopped 20 m before the center of the intersections and were prompted to verbally indicate the direction in which the route continued. The examiner pressed a corresponding arrow key, and the participants were passively transported to the center of the intersection facing the street, which led to the following intersection. Thus, participants did not receive feedback. The task was composed of three experimental sessions along the same route to assess learning.

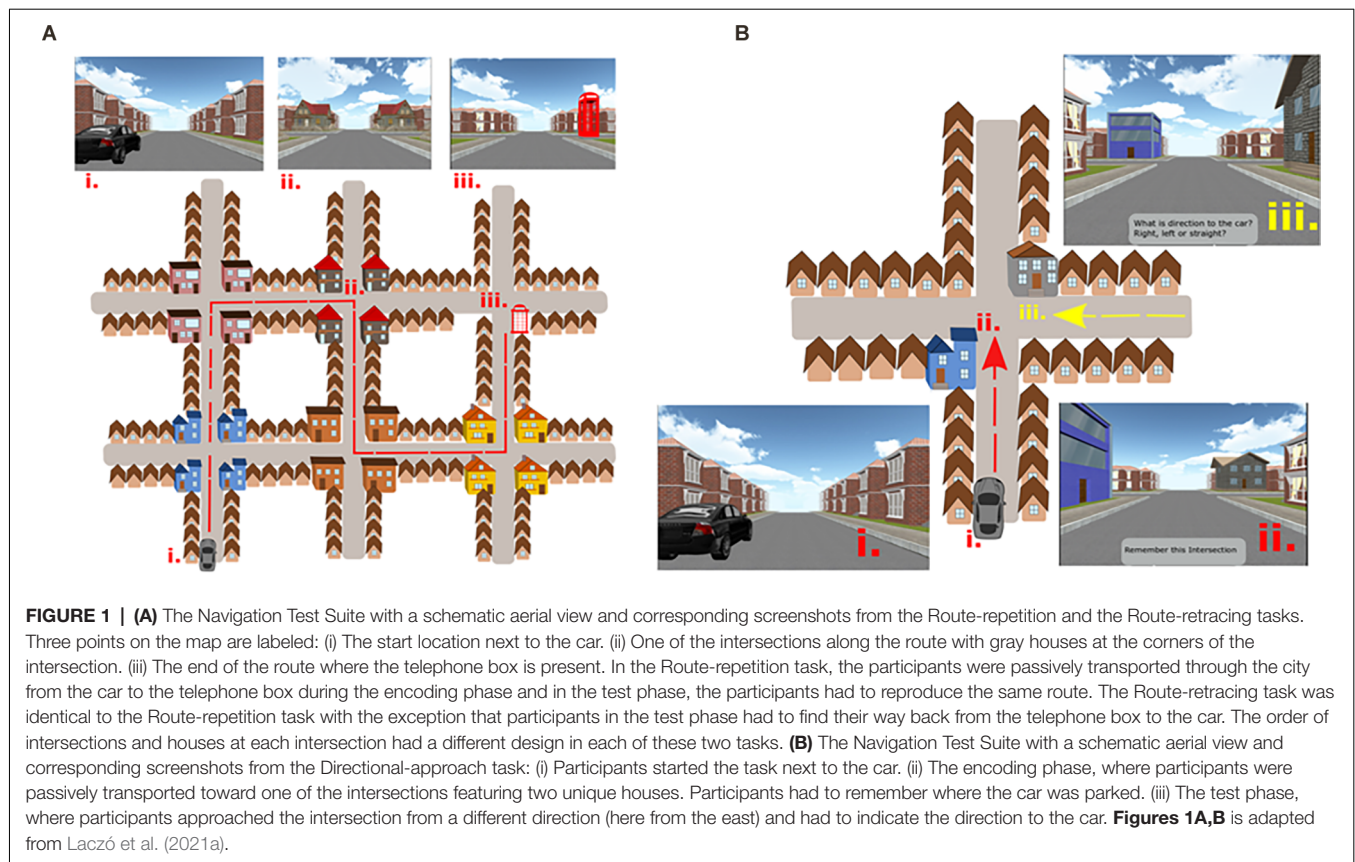
(II) Route-Retracing Task

The encoding phase was similar to the Route-repetition task. The route also comprised five intersections but featured different houses at intersections (**Figure 1A**). In the test phase, the participants had to navigate in the opposite direction compared to the encoding phase, i.e., from the endpoint of the route (the telephone box) back to the start (the black car). The Route-retracing task consisted of three identical consecutive sessions.

(III) Directional-Approach Task

The Directional-approach task assessed participants' ability to encode the configuration of houses (landmarks) at an intersection and assessed perspective taking and wayfinding (Wiener et al., 2013; de Condappa and Wiener, 2016). The task consisted of 15 independent trials. Each trial began with an encoding phase, in which participants were positioned in a street next to a black car from where they were passively transported toward a single intersection, which featured two unique houses (i.e., landmarks) at diagonally opposite corners of the intersection. The movement stopped 20 m before the center of the intersections, such that both unique houses were in view. Two other houses at the corners of the intersection were identical to the other houses along the street. The participants' task was to memorize, in which street the car was parked. Each of the 15 trials featured a different combination of unique houses at the corners of the intersections.

In the test phase, participants were passively transported toward the same intersection, but from one of the other streets. They were then asked to indicate the direction in which the car was parked (i.e., to indicate the street from which they originally approached the intersection). The movement stopped again 20 m before the center of the intersection, such that the unique houses could be seen.



The car was always parked in the street to the south of the intersection (**Figure 1B**). In the test phase, participants approached the intersection from the western, eastern, or northern street. The participants were not aware of these cardinal directions in the experiment, but the information about these cardinal directions was used in the analysis. Participants were required to perform perspective shifts to align the view during the test phase with that during the encoding phase. The perspective shift was 90° when approaching the intersection from the west or east and 180° when approaching from the north. In contrast to the Route-repetition and Route-retracing tasks, the Directional-approach task did not require participants to learn a route with multiple decision points.

Cognitive Assessment

The cognitive assessment included the following tests: (1) verbal memory measured with the Rey Auditory Verbal Learning Test (RAVLT)—trials 1–5 and 30-min Delayed Recall trial (Bezdicsek et al., 2014); (2) non-verbal memory measured with the Rey-Osterrieth Complex Figure Test (ROCFT)—the Recall condition after 3 min (Drozdova et al., 2015); (3) visuospatial function measured with the ROCFT—the Copy condition (Drozdova et al., 2015) and the Clock Drawing Test (Mazancova et al., 2017); (4) executive function measured with the Trail Making Test (TMT) B and Controlled Oral Word Association Test (Czech version with letters N, K, and P; Nikolai et al., 2018); (5) attention and working memory measured with the Forward

and Backward Digit Spans and TMT A (Nikolai et al., 2018); and (6) language measured with the Boston Naming Test (30-item version) and Semantic Verbal Fluency test (Animals; Nikolai et al., 2018). The Mini-Mental State Examination (MMSE; Štěpánková et al., 2015) was administered to measure global cognitive function. The GDS-15 (Yesavage and Sheikh, 1986) and BAI (Beck et al., 1988) were used to assess depressive symptoms and anxiety in the participants. Group-wise neuropsychological characteristics are listed in **Table 1**.

Magnetic Resonance Imaging Image Acquisition

We used the established MRI protocol (Parizkova et al., 2018) performed on a Siemens Avanto 1.5T scanner (Siemens AG, Erlangen, Germany) with a 12-channel head coil. The 3-dimensional T1w (3D T1w) high-resolution magnetization-prepared rapid gradient echo (MPRAGE) sequence was used with the following parameters: TR/TE/TI = 2,000/3.08/1,100 ms, flip angle = 15°, 192 continuous partitions, slice thickness = 1.0 mm and in-plane resolution = 1 mm. Scans were visually inspected to ensure appropriate data quality and to exclude participants with a major brain pathology that could interfere with cognitive functioning. The 3D T1w images of high quality were available for 100 participants, including CN ($n = 29$), non-AD aMCI ($n = 23$), AD aMCI ($n = 26$), and mild AD dementia ($n = 22$). In the remaining participants ($n = 22$), the 3D T1w images were of low quality or unavailable. The

TABLE 1 | Characteristics of study participants.

| | CN (n = 30) | Non-AD aMCI (n = 31) | AD aMCI (n = 33) | Mild AD dementia (n = 28) | P values | Effect sizes |
|--|-------------------------|-----------------------|--------------------|---------------------------|----------|--------------|
| <i>Demographic characteristics</i> | | | | | | |
| Age (years) | 68.73 (5.82)**C | 70.32 (7.67) | 72.27 (6.35) | 74.32 (5.92) | 0.009 | 0.09 |
| Women, n (%) | 21 (70) | 15 (48) | 20 (61) | 18 (64) | 0.361 | 0.16 |
| Education (years) | 16.20 (1.77)**a | 13.87 (2.33) | 14.79 (3.15) | 14.43 (2.70) | 0.005 | 0.10 |
| <i>Spatial navigation assessment</i> | | | | | | |
| Route-repetition task (% correct) | 85.33 (13.33)***b-c | 74.41 (15.41)***b-c | 55.15 (19.31) | 54.52 (17.41) | <0.001 | 0.34 |
| Route-retracing task (% correct) | 71.11 (19.60)**a,***b-c | 54.22 (24.93) | 40.81 (19.42) | 40.00 (16.02) | <0.001 | 0.24 |
| Directional-approach task (% correct) | 71.56 (21.86)**a,***b-c | 54.00 (23.18) | 44.65 (20.51) | 37.62 (17.14) | <0.001 | 0.26 |
| <i>Cognitive assessment</i> | | | | | | |
| MMSE | 29.37 (0.89)***a-c | 27.45 (2.31)***C | 26.27 (1.94)***C | 22.11 (2.32) | <0.001 | 0.65 |
| GDS-15 (score) | 1.20 (2.02)*a,**C | 3.00 (2.73) | 2.25 (2.03) | 3.32 (2.84) | 0.005 | 0.10 |
| BAI (score) | 5.40 (5.56) | 7.58 (6.54) | 8.82 (9.88) | 7.43 (5.12) | 0.304 | 0.03 |
| RAVLT 1–5 (score) | 56.30 (7.72)***a-c | 36.35 (9.57)**C | 34.84 (8.20)*C | 27.31 (4.77) | <0.001 | 0.64 |
| RAVLT 30 (score) | 12.07 (1.82)***a-c | 5.03 (2.94)*C | 3.92 (3.27) | 2.25 (3.19) | <0.001 | 0.66 |
| TMT A (seconds) | 35.72 (10.94)***C | 50.66 (23.41)***C | 53.49 (29.06)**C | 79.97 (41.82) | <0.001 | 0.24 |
| TMT B (seconds) | 79.58 (35.28)***a-c | 160.53 (79.79)***C | 161.40 (87.01)***C | 243.68 (75.69) | <0.001 | 0.39 |
| COWAT (score) | 50.87 (9.26)***a, c,b | 38.32 (11.40) | 42.91 (10.58)***C | 31.57 (13.16) | <0.001 | 0.28 |
| ROCF-C (score) | 32.12 (2.18)**a,***b-c | 27.55 (4.44)*C | 26.62 (5.55) | 23.43 (8.17) | <0.001 | 0.24 |
| ROCF-R (score) | 20.47 (5.29)***a-c | 10.08 (5.32)***C | 7.02 (5.63)*C | 2.87 (3.65) | <0.001 | 0.62 |
| DSF (score) | 10.07 (2.29)**a, c | 8.35 (1.80) | 9.03 (2.04) | 8.07 (1.65) | <0.001 | 0.13 |
| DSB (score) | 6.80 (2.02)*a, b,***C | 5.52 (1.63) | 5.58 (1.80) | 4.64 (1.22) | <0.001 | 0.17 |
| CDT (score) | 15.03 (1.19)*D,***C | 14.42 (1.93)***C | 13.72 (1.97)***C | 11.75 (2.17) | <0.001 | 0.31 |
| SVF Animals (score) | 28.50 (4.47)***a-c | 20.29 (5.78)***C | 20.00 (4.22)***C | 14.00 (4.01) | <0.001 | 0.55 |
| BNT (no. of errors) | 1.13 (1.31)**a, b,***C | 4.39 (3.44)*C | 4.39 (2.82)**C | 7.68 (4.91) | <0.001 | 0.32 |
| <i>CSF analysis^d</i> | | | | | | |
| Amyloid- β_{1-42} (pg/ml) | N/A | 999.80 (338.21)***b-c | 421.96 (83.89) | 445.76 (128.79) | <0.001 | 0.63 |
| Total tau (pg/ml) | N/A | 303.66 (122.29)**C | 607.13 (325.19) | 824.92 (509.72) | 0.004 | 0.24 |
| P-tau ₁₈₁ (pg/ml) | N/A | 54.64 (21.06)*C | 102.49 (72.18) | 111.74 (60.32) | 0.033 | 0.15 |
| <i>MRI brain measures^e</i> | | | | | | |
| Hippocampal head right ^f (volume, cm ³) | 1.65 (0.24)*C | 1.61 (0.25) | 1.53 (0.30) | 1.40 (0.33) | 0.015 | 0.10 |
| Hippocampal head left ^f (volume, cm ³) | 1.50 (0.24)*C | 1.49 (0.26) | 1.41 (0.28) | 1.28 (0.28) | 0.016 | 0.10 |
| Hippocampal body right ^f (volume, cm ³) | 0.93 (0.11)*D,***C | 0.94 (0.16)*b,***C | 0.81 (0.14) | 0.73 (0.14) | <0.001 | 0.27 |
| Hippocampal body left ^f (volume, cm ³) | 0.99 (0.13)**b,***C | 0.93 (0.17)***C | 0.84 (0.16) | 0.76 (0.12) | <0.001 | 0.27 |
| Hippocampal tail right ^f (volume, cm ³) | 0.28 (0.04)***D,***C | 0.27 (0.04)*b,***C | 0.23 (0.05)*C | 0.20 (0.04) | <0.001 | 0.40 |
| Hippocampal tail left ^f (volume, cm ³) | 0.30 (0.04)***b-c | 0.29 (0.05)*b,***C | 0.24 (0.06) | 0.21 (0.04) | <0.001 | 0.36 |
| aIEC right ^f (volume, cm ³) | 0.61 (0.10)*b,***C | 0.61 (0.10)*b,***C | 0.53 (0.08) | 0.49 (0.10) | <0.001 | 0.24 |
| aIEC left ^f (volume, cm ³) | 0.72 (0.10)***C | 0.70 (0.11)**C | 0.65 (0.11) | 0.59 (0.10) | <0.001 | 0.18 |
| pmEC right ^f (volume, cm ³) | 0.34 (0.04)**b-c | 0.35 (0.04)*b-c | 0.30 (0.06) | 0.29 (0.05) | <0.001 | 0.22 |
| pmEC left ^f (volume, cm ³) | 0.38 (0.04)***b-c | 0.37 (0.05)*b,***C | 0.32 (0.07) | 0.30 (0.05) | <0.001 | 0.26 |

(Continued)

TABLE 1 | Continued

| MRI brain measures ^e | CN (n = 30) | Non-AD aMCI (n = 31) | AD aMCI (n = 33) | Mild AD dementia (n = 28) | P values | Effect sizes |
|---|-------------------------------|-------------------------------|------------------|---------------------------|----------|--------------|
| Caudate nucleus right ^f (volume, cm ³) | 3.61 (0.45) | 3.57 (0.46) | 3.50 (0.58) | 3.37 (0.50) | 0.342 | 0.04 |
| Caudate nucleus left ^f (volume, cm ³) | 3.60 (0.38) | 3.50 (0.49) | 3.45 (0.53) | 3.37 (0.43) | 0.348 | 0.03 |
| Precuneus right (thickness, mm) | 2.26 (0.12) ^{***b,c} | 2.19 (0.16) ^{**c} | 2.11 (0.16) | 2.03 (0.18) | <0.001 | 0.23 |
| Precuneus left (thickness, mm) | 2.21 (0.14) ^{***b,c} | 2.18 (0.18) ^{***b,c} | 2.02 (0.18) | 1.99 (0.19) | <0.001 | 0.25 |
| Isthmus cingulate right (thickness, mm) | 2.26 (0.20) ^{***b,c} | 2.18 (0.14) | 2.07 (0.17) | 2.10 (0.19) | <0.001 | 0.16 |
| Isthmus cingulate left (thickness, mm) | 2.32 (0.25) ^{***b,c} | 2.24 (0.19) | 2.07 (0.24) | 2.12 (0.23) | <0.001 | 0.16 |
| Posterior parietal cortex right (thickness, mm) | 2.30 (0.13) ^{***b,c} | 2.26 (0.17) ^{***b,c} | 2.10 (0.16) | 2.06 (0.19) | <0.001 | 0.29 |
| Posterior parietal cortex left (thickness, mm) | 2.29 (0.12) ^{***b,c} | 2.24 (0.15) ^{***b,c} | 2.10 (0.17) | 2.04 (0.19) | <0.001 | 0.29 |

Demographic, cognitive, CSF, and MRI characteristics. Values are mean (SD) except for gender. P values refer to the main effect across all groups; P values indicate the level of significance; * $p < 0.05$; ** $p < 0.01$; *** $p < 0.001$; Effect sizes were calculated as Cramér's V for the χ^2 test (gender) and partial eta-squared for one-way and mixed analyses of variance (all other variables). ^aDifferences compared to the non-AD aMCI group. ^bDifferences compared to the AD aMCI group. ^cDifferences compared to the mild AD dementia group. ^dBased on a sample with CSF data (total $n = 47$) with non-AD aMCI ($n = 12$), AD aMCI ($n = 17$), and mild AD dementia ($n = 18$) participants. ^eBased on a sample with complete brain imaging data (total $n = 100$) with CN ($n = 29$), non-AD aMCI ($n = 23$), AD aMCI ($n = 26$), and mild AD dementia ($n = 22$) participants. ^fVolume normalized to estimated total intracranial volume. Key: CN, cognitively normal; non-AD aMCI, amnesic mild cognitive impairment with negative AD biomarkers; AD aMCI, amnesic mild cognitive impairment with Alzheimer's disease; mild AD dementia, mild dementia with Alzheimer's disease; MMSE, Mini-Mental State Examination; GDS-15, Geriatric Depression Scale 15-item version; BAI, Beck Anxiety Inventory; RAVLT, Rey Auditory Verbal Learning Test; RAVLT 1–5, trials 1–5 total; RAVLT 30, delayed word recall after 30 min; TMT A and B, Trail Making Tests A and B; COWAT, Controlled Oral Word Association Test (Czech version with letters N, K and P); ROCT-R, Rey-Osterrieth Complex Figure Test—the Copy condition; ROCT-F, Rey-Osterrieth Complex Figure Test—the Recall condition after 3 min; DSF, Digit Span Forward total score; DSB, Digit Span Backward total score; CDT, Clock Drawing Test—Cohen's scoring; SVF, Semantic Verbal Fluency; BNT, Boston Naming Test (30-item version); CSF, cerebrospinal fluid; p-tau₁₈₁, phosphorylated tau₁₈₁; MRI, magnetic resonance imaging; aEC, anterolateral entorhinal cortex; pmEC, posteromedial entorhinal cortex.

demographic characteristics of participants with brain imaging data are presented in **Supplementary Table 1**.

Image Processing and Regional Brain Volumetry

We used a processing pipeline based on a population-based template and manual segmentation to measure volumes of the hippocampal head, body, and tail, volumes of the aEC and pmEC, and estimated total intracranial volume (eTIV). The processing pipeline is described in detail in Laczó et al. (2021b). In short, we created a population-based template, using structural 3D T1w images of 26 CN older adults recruited from CBAS (Sheardova et al., 2019). The 3D T1w images were processed using the freely available Advanced Normalization Tools package (ANTs²; Avants et al., 2011). An initial registration template was created first and we then proceeded to create the definite population template by registering 3D T1w images iteratively into the initial template. Manual segmentation of the hippocampus and EC was performed for each of 26 CN participants used for population-based template creation. The hippocampus and the EC were delineated manually in the coronal plane using anatomical landmarks according to the previously published manual segmentation protocol (Berron et al., 2017). The hippocampus was divided into three subregions—the head, the body, and the tail, and EC was divided into the aEC and pmEC subregions according to the previously published segmentation protocols (Berron et al., 2017; Olsen et al., 2017), respectively. The segmentation of the hippocampus and EC is described in detail in Laczó et al. (2021b). Manually delineated ROIs were normalized to MNI space using deformation fields obtained during the template creation. We created a template for each structure (i.e., the hippocampal head, body, and tail, aEC and pmEC) using the same procedure as during the initial template creation (Laczó et al., 2021b). Individual templates were split into the left and right masks using the left and right hemispheric ROIs. The resulting masks were rescaled into values 0–100 to represent probabilistic distribution.

The following steps were implemented to measure the subregional hippocampal and EC volumes of the study participants. We skull-stripped the individual 3D T1w images and performed B1 field intensity inhomogeneity correction using the N4 algorithm and performed three-tissue segmentation using statistical parametric mapping (SPM8, Wellcome Trust Center for Neuroimaging; Ashburner, 2009) and the VBM8-toolbox³ implemented in MatLab R2015b (MathWorks, Natick, MA). We then registered the CBAS template created in the previous step and diffeomorphically warped it into individual participants' space using ANTs, with a cross-correlation method, $100 \times 100 \times 50$ iterations, and symmetric normalization applied on a 0.25 threshold. The resulting warp field was used to transform ROI masks of individual hippocampal and EC subregions into the participants' space. The ROIs masks were subsequently masked with a gray matter ROI and their volumes were extracted. Warps were visually inspected for accuracy, no volumes were removed. FreeSurfer 5.3 suite was used to

²<http://stnava.github.io/ANTs/>

³<http://dbm.neuro.uni-jena.de/vbm/>

calculate volumes of the right and left caudate nucleus and thickness of the right and left precuneus, isthmus cingulate, and composite region of the posterior parietal cortex. The processing details are described elsewhere (Dale et al., 1999; Fischl et al., 2002, 2004; Desikan et al., 2006) and are available online at <http://surfer.nmr.mgh.harvard.edu/>. Individual cortical and subcortical segmentations were projected onto corresponding skull-stripped brain images. Segmentations were visually assessed for accuracy and labeled as acceptable/non-acceptable in a binary fashion. No volumes were removed. Posterior parietal cortical thickness was computed as an area-weighted mean of superior parietal gyrus, inferior parietal gyrus, and supramarginal gyrus thickness obtained from FreeSurfer cortical parcellation using the Desikan-Killiany cortical atlas (Desikan et al., 2006). Volumes were normalized to eTIV using the previously published regression formula (Jack et al., 1992; Laczó et al., 2015).

Cerebrospinal Fluid Analysis of AD Biomarkers

The CSF samples were obtained by lumbar puncture with an atraumatic needle in the lying position. The first 3 ml of CSF were used for routine analysis and the remaining 10 ml of CSF was centrifuged and stored at -80°C 30 min after the puncture. CSF collection, processing, and archiving were performed in accordance with European recommendations (Vanderstichele et al., 2012). CSF amyloid- β_{1-42} , total tau, and p-tau₁₈₁ were analyzed using ELISA (Innogenetics, Ghent, Belgium) in the Cerebrospinal Fluid Laboratory, Institute of Immunology and Department of Neurology, Second Faculty of Medicine, Charles University and Motol University Hospital. Unbiased cut-offs of less than 665 pg/ml and more than 48 pg/ml and 358 pg/ml were used to define amyloid- β_{1-42} , p-tau₁₈₁, and total tau positivity, respectively. These predefined cutoffs (Parizkova et al., 2018; Laczó et al., 2021b) were based on internal receiver operating characteristic (ROC) analyses and were validated against amyloid PET status in the Czech Brain Aging Study with 79% agreement and areas under the ROC curves (AUCs) of 85% (Cerman et al., 2020). The diagnosis of AD was made when both amyloid- β_{1-42} and p-tau₁₈₁ were positive (Laczó et al., 2021b). CSF data were available for 47 of the 92 participants with cognitive impairment, including those with non-AD aMCI ($n = 12$), AD aMCI ($n = 17$), and mild AD dementia ($n = 18$). The demographic characteristics of participants with CSF data are presented in **Supplementary Table 2**.

Amyloid PET Imaging

The PET images were acquired using a Biograph 40 TrueV HD PET/CT scanner (Siemens Healthineers AG, Erlangen, Germany) in the Department of Nuclear Medicine and PET Centre, Na Homolce Hospital. The participants received a single intravenous dose of flutemetamol (18F; Vizamy, GE Healthcare, Chicago, IL) with a gross activity of 206.7 ± 12.7 MBq. Non-contrast low-dose CT brain images were acquired for attenuation correction prior to the PET scans. A PET list-mode acquisition was performed in two phases. The early-phase images were acquired at the time of flutemetamol (18F)

administration for 8 min and rebinned into dynamic datasets of 2×4 min for motion checking. They were iteratively reconstructed to a 168×168 matrices with three iterations, after attenuation, scatter, and point spread function correction. The late-phase images were acquired 90 min after flutemetamol (18F) administration for 10 min and iteratively reconstructed to a 128×128 matrix with other parameters as described above, including rebinning into dynamic sequences for motion checking (Belohlavek et al., 2019). Flutemetamol (18F) PET images were visually read (as positive or negative) by two independent physicians certified in nuclear medicine, who were previously in-person trained and qualified. The late-phase images were evaluated for amyloid- β -specific uptake in the gray matter by the method that visualized the gray-white matter borders derived from the early-phase images (GM-EDGE method; Belohlavek et al., 2019). Eight specific brain regions were assessed, including the frontal lobe, lateral temporal lobe, anterior cingulate, posterior cingulate, precuneus, temporoparietal area, insula, and striatum. If any of these regions was abnormal, the finding was classified as positive for amyloid- β . The GM-EDGE method was shown to have a high inter-rater agreement ($> 90\%$; Belohlavek et al., 2019) and good concordance with amyloid- β_{1-42} levels in CSF ($\approx 80\%$; Cerman et al., 2020). Amyloid PET imaging data were available for 64 of the 92 participants with cognitive impairment, including those with non-AD aMCI ($n = 26$), AD aMCI ($n = 24$), and mild AD dementia ($n = 14$).

Statistical Analysis

A one-way analysis of variance (ANOVA) with *post-hoc* Sidak's test evaluated differences between the groups in continuous demographic variables, cognitive performance, CSF biomarkers, and MRI brain measures. A χ^2 test evaluated differences in gender proportions. A mixed-model analysis of covariance (ANCOVA) with the diagnostic group (CN vs. non-AD aMCI vs. AD aMCI vs. mild AD dementia) as the between-subjects factor and the session (1st vs. 2nd vs. 3rd) or the approach direction (east vs. north vs. west) as the within-subjects factors were used to analyze differences in spatial navigation performance measured as the percentage of correct responses, which was the dependent variable. The analysis was controlled for age (mean-centered), years of education (mean-centered), and gender. The intercept, session/approach direction, and a person identifier were specified as random effects. Based on model fit, the final models used the scaled identity covariance structure. The *post-hoc* Sidak's test was used to assess differences between the individual groups and sessions/approach directions. The *post-hoc* pairwise comparisons with Holm-Bonferroni (H-B) correction for multiple comparisons were used to compare differences in spatial navigation performance between individual groups in each session/approach direction and to interpret significant interactions between variables. A one-sample t-test was used to assess differences from chance performance (i.e., 33.33%) for each diagnostic group in each session/approach direction. The *post-hoc* ROC analysis was used to assess the ability of the spatial navigation tasks to differentiate the CN, non-AD aMCI, AD aMCI, and mild AD dementia groups. Sizes of the AUCs, sensitivity, specificity,

and optimal cut-off values based on the Youden's index were calculated.

Pearson's correlation coefficients were calculated to explore the associations between MRI measures of atrophy in nine specific brain regions for the right and left hemispheres, and performance in three Navigation Test Suite tasks. The H-B correction for multiple comparisons across the 54 pairings was used. Next, the separate linear regression models adjusted for age (mean-centered), years of education (mean-centered), and gender were used to control for the effect of demographic characteristics on the significant associations. To address the specific hypothesis that each CSF biomarker (i.e., amyloid- β_{1-42} , total tau, and p-tau₁₈₁) will be differently associated with performance in each of the Navigation Test Suite tasks (i.e., the Route-repetition, Route-retracing, and Directional-approach tasks), we calculated Pearson's correlation coefficients and if the associations were significant (uncorrected), we used the linear regression model adjusted for age (mean-centered), years of education (mean-centered) and gender. Mediation (path) analyses were conducted to assess the associations between CSF AD biomarkers (the independent variable) and spatial navigation performance in each task (the dependent variable) with MRI brain measures serving as the mediator. Only variables significantly associated with spatial navigation performance in the previous regression analyses were included in the mediation analyses. The analyses were adjusted for age (mean-centered), education (mean-centered), and gender. The bootstrapping method (Hayes, 2013) was used to test for the significance of the indirect effect with a 95% confidence interval (CI). Variable values were converted to z-scores prior to the mediation analyses to present the mediation effects and 95% CI in standardized units. In the mediation analysis (Figure 2), the "c path" (total effect; TE) represents the effect of the independent variable on the dependent variable, the "c' path" (direct effect; DE) represents the effect of the independent variable on the dependent variable while accounting for the mediator, the "a path" represents the relationship between the independent variable and the mediator, and the "b path" represents the relationship between the mediator and the dependent variable. The last two paths form the "a*b path" (indirect effect; IE) that represents the effect of the independent variable on the dependent variable through the mediator.

Statistical significance was set at two-tailed (alpha) of 0.05. Effect sizes are reported using partial eta-squared (η_p^2) for one-way ANOVA and mixed-model ANCOVA. A partial eta-squared of 0.2 corresponds to Cohen's d of 1.0. All analyses were conducted using IBM SPSS 27.0 software.

RESULTS

Demographics and Cognitive Performance

The demographic characteristics are presented in detail in Table 1. The CN group was younger than the mild AD dementia group ($p = 0.008$) and more educated than the non-AD aMCI group ($p = 0.003$). There were no significant differences in gender

between the groups. As expected, the non-AD aMCI, AD aMCI, and mild AD dementia groups had lower MMSE scores (all $p \leq 0.001$) and worse cognitive performance in most of the tests ($p \leq 0.036$) compared to the CN group. The non-AD aMCI and AD aMCI groups did not differ in cognitive performance (all $p \geq 0.100$). The non-AD aMCI ($p = 0.028$) and mild AD dementia ($p = 0.007$) groups reported more depressive symptoms than the CN group. There were no significant differences in anxiety symptoms between the groups.

Spatial Navigation Performance

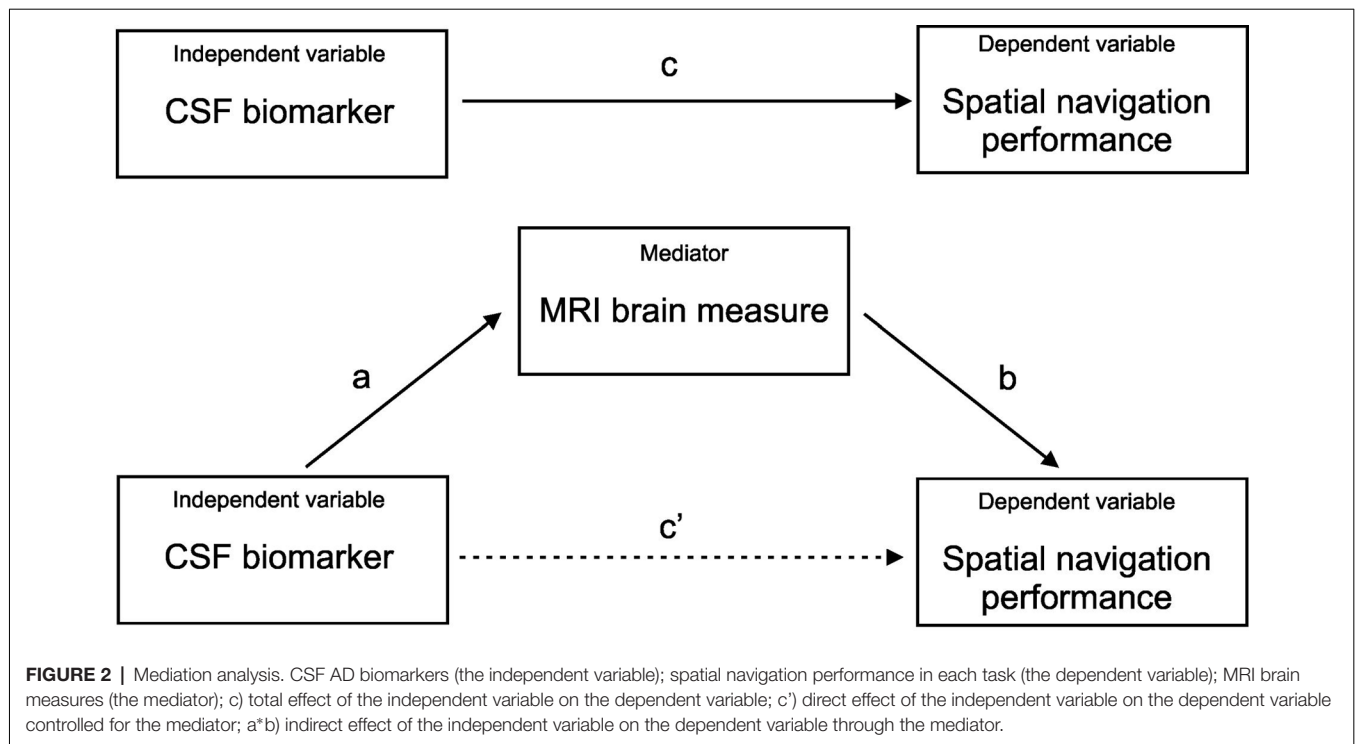
Spatial navigation performance shown as the mean percentage of correct responses in the CN, non-AD aMCI, AD aMCI, and mild AD dementia groups for each Navigation Test Suite task is presented in Figures 3–5.

Route-Repetition Task Performance

In the 4 (diagnostic group) \times 3 (session) mixed-model ANCOVA, there was a significant main effect of diagnostic group ($F_{(3,122)} = 20.67$, $p < 0.001$, $\eta_p^2 = 0.34$) and session ($F_{(2,244)} = 26.96$, $p < 0.001$, $\eta_p^2 = 0.19$; Figure 3). The session-by-diagnostic group interaction was not significant ($F_{[6,244]} = 1.98$, $p = 0.069$, $\eta_p^2 = 0.04$). On average, the AD aMCI group performed worse than the non-AD aMCI group [$p < 0.001$, 95% CI (−29.76, −8.17)] and the CN group [$p < 0.001$, 95% CI (−38.69, −16.44)], and did not differ from the mild AD dementia group [$p = 1.00$, 95% CI (−11.58, 10.27)]. The non-AD aMCI group did not differ from the CN group [$p = 0.272$, 95% CI (−20.29, 3.09)] and performed better than the mild AD dementia group [$p < 0.001$, 95% CI (6.92, 29.71)]. The mild AD dementia group performed worse than the CN group [$p < 0.001$, 95% CI (−38.83, −14.99)]. On average, spatial navigation performance improved across all sessions. Performance in the second session was better than that in the first session [$p < 0.001$, 95% CI (5.35, 17.40)] and performance in the third session was better than that in the first [$p < 0.001$, 95% CI (12.19, 24.24)] and second [$p = 0.020$, 95% CI (0.81, 12.86)] sessions.

The analysis of between-group differences in each session showed that the AD aMCI group performed worse than the non-AD aMCI (all $p_{H-Bcorrected} \leq 0.031$) and CN (all $p_{H-Bcorrected} \leq 0.002$) groups in all three sessions. The mild AD dementia group performed worse than the CN group in all three sessions (all $p_{H-Bcorrected} < 0.050$) and worse than the non-AD aMCI group in the second and the third session (both $p_{H-Bcorrected} \leq 0.011$). Other differences between the diagnostic groups were not significant. All groups performed above the chance level in all sessions [CN group: (all $t_{(29)} \geq 8.60$, $p < 0.001$); non-AD aMCI group: (all $t_{(30)} \geq 7.10$, $p < 0.001$); AD aMCI group: (all $t_{(32)} \geq 3.02$, $p \leq 0.005$); mild AD dementia group: (all $t_{(27)} \geq 3.13$, $p \leq 0.004$)].

In the *post-hoc* ROC analyses, performance in the Route-repetition task differentiated the CN group from the non-AD aMCI, AD aMCI and mild AD dementia groups with AUC values of 0.719 [95% CI (0.59, 0.85), $p = 0.001$], 0.89 [95% CI (0.81, 0.98), $p < 0.001$], and 0.92 [95% CI (0.85, 0.99), $p < 0.001$], respectively, the non-AD aMCI group from the AD aMCI and



mild AD dementia groups with AUC values of 0.78 [95% CI (0.66, 0.89), $p < 0.001$] and 0.80 [95% CI (0.69, 0.91), $p < 0.001$], respectively, and did not differentiate the AD aMCI group from the mild AD dementia group, where the AUC value was 0.63 [95% CI (0.49, 0.77), $p = 0.083$]. The sensitivity and specificity for the relevant cut-off values is listed in **Supplementary Table 3**.

Route-Retracing Task Performance

In the 4 (diagnostic group) \times 3 (session) mixed-model ANCOVA, there was a significant main effect of diagnostic group ($F_{[3,121]} = 12.83$, $p < 0.001$, $\eta_p^2 = 0.24$) and session ($F_{[2,242]} = 7.47$, $p < 0.001$, $\eta_p^2 = 0.06$; **Figure 4**). The session-by-diagnostic group interaction was not significant ($F_{[6,242]} = 1.16$, $p = 0.331$, $\eta_p^2 = 0.03$). On average, the AD aMCI group performed worse than the CN group [$p < 0.001$, 95% CI (−41.88, −15.07)] and did not differ from the non-AD aMCI [$p = 0.128$, 95% CI (−24.48, 1.80)] and mild AD dementia [$p = 1.00$, 95% CI (−14.02, 12.31)] groups. The non-AD aMCI group performed worse than the CN group [$p = 0.009$, 95% CI (−31.30, −2.96)] and did not differ from the mild AD dementia group [$p = 0.244$, 95% CI (−3.40, 24.37)]. The mild AD dementia group performed worse than the CN group [$p < 0.001$, 95% CI (−41.99, −13.25)]. On average, spatial navigation performance improved across the sessions. Performance in the second session was better than that in the first session [$p = 0.021$, 95% CI (0.91, 14.71)]. Performance in the third session was better than that in the first session ($p < 0.001$, 95% CI (3.83, 17.62)) but did not differ from that in the second session [$p = 0.672$, 95% CI (−3.98, 9.81)].

The analysis of between-group differences in each session showed that the AD aMCI group performed worse than the non-AD aMCI group in the second session ($p_{H-Bcorrected} = 0.032$)

and worse than the CN group in all three sessions (all $p_{H-Bcorrected} \leq 0.016$). The non-AD aMCI group performed worse than the CN group in the third session ($p_{H-Bcorrected} = 0.003$). The mild AD dementia group performed worse than the CN group in all three sessions (all $p_{H-Bcorrected} < 0.050$). Other differences between the diagnostic groups were not significant. The CN and non-AD aMCI groups performed above the chance level in each session [CN group: (all $t_{(29)} \geq 5.16$, $p < 0.001$); non-AD aMCI group: (all $t_{(30)} \geq 2.81$, $p \leq 0.009$)]. The AD aMCI group performed above the chance level in the third session ($t_{(32)} = 2.34$, $p = 0.026$) and did not differ from the chance level in the first and the second session (both $t_{(27)} \leq 1.24$, $p \geq 0.223$). The mild AD dementia group did not differ from the chance level in any session (all $t_{(27)} \leq 1.85$, $p \geq 0.075$).

In the *post-hoc* ROC analyses, performance in the Route-retracing task differentiated the CN group from the non-AD aMCI, AD aMCI and mild AD dementia groups with AUC values of 0.68 [95% CI (0.56, 0.83), $p = 0.004$], 0.86 [95% CI (0.77, 0.95), $p < 0.001$], and 0.89 [95% CI (0.81, 0.97), $p < 0.001$], respectively, the non-AD aMCI group from the AD aMCI and mild AD dementia groups with AUC values of 0.64 [95% CI (0.51, 0.78), $p = 0.041$] and 0.65 [95% CI (0.51, 0.80), $p = 0.034$], respectively, and did not differentiate the AD aMCI group from the mild AD dementia group, where the AUC value was 0.50 [95% CI (0.35, 0.65), $p = 0.075$]. The sensitivity and specificity for the relevant cut-off values is listed in **Supplementary Table 3**.

Directional-Approach Task Performance

In the 4 (diagnostic group) \times 3 (approach direction) mixed-model ANCOVA, there was a significant main effect of diagnostic group ($F_{[3,121]} = 14.16$, $p < 0.001$, $\eta_p^2 = 0.26$) and

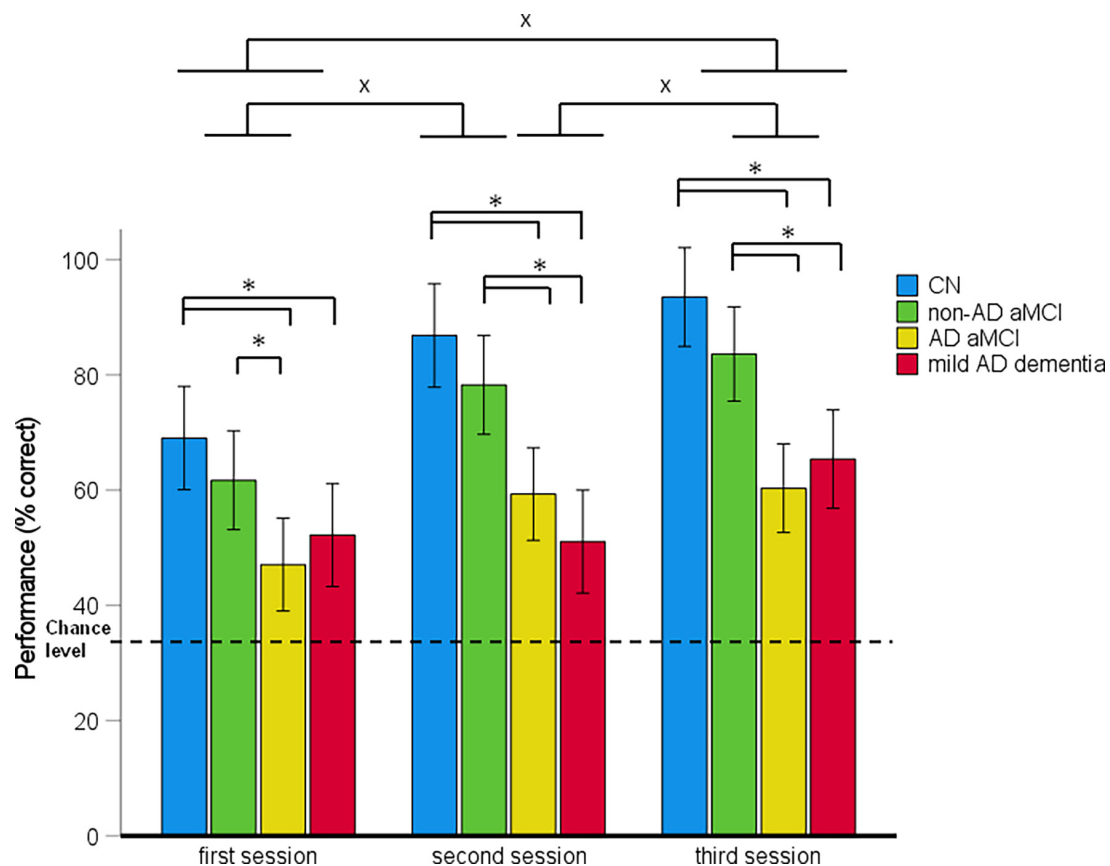


FIGURE 3 | Route-repetition task—spatial navigation performance as mean percentage of correct responses in each session (95% CI). * $p < 0.05$ indicating the differences between the groups; * $p < 0.05$ indicating the differences between the sessions. CN, cognitively normal; non-AD aMCI, amnesic mild cognitive impairment with negative AD biomarkers; AD aMCI, amnesic mild cognitive impairment with Alzheimer's disease; mild AD dementia, mild dementia with Alzheimer's disease; CI, confidence interval.

approach direction ($F_{[2,242]} = 64.19$, $p < 0.001$, $\eta_p^2 = 0.36$; **Figure 5**). The approach direction-by-diagnostic group interaction was not significant ($F_{[6,242]} = 0.26$, $p = 0.955$, $\eta_p^2 = 0.01$). On average, the non-AD aMCI [$p = 0.001$, 95% CI $(-36.14, -6.59)$], AD aMCI [$p < 0.001$, 95% CI $(-41.78, -13.82)$] and mild AD dementia [$p < 0.001$, 95% CI $(-49.03, -19.06)$] groups performed worse than the CN group. Other differences between the diagnostic groups were not significant. On average, spatial navigation performance varied depending on the approach direction. Performance was worse for an approach from the north (180° shift) than for an approach from the west [90° shift; $p < 0.001$, 95% CI $(-38.46, -23.65)$] and the east [90° shift; $p < 0.001$, 95% CI $(-36.69, -21.88)$]. Performance for the west and east approaches did not differ from each other [$p = 0.918$, 95% CI $(-5.63, 9.17)$].

The analysis of between-group differences for each approach direction showed that the non-AD aMCI (all $p_{H-Bcorrected} \leq 0.044$), AD aMCI (all $p_{H-Bcorrected} \leq 0.002$), and mild AD dementia (all $p_{H-Bcorrected} < 0.001$) groups performed worse than the CN group for all three approach directions. Other differences between the diagnostic groups were not significant. The CN group performed above the chance level for all approach

directions (all $t_{(29)} \geq 2.71$, $p \leq 0.011$). The non-AD aMCI, AD aMCI and mild AD dementia groups performed above the chance level for an approach from the west and the east (non-AD aMCI group: [both $t_{(30)} \geq 5.70$, $p < 0.001$]; AD aMCI group: [both $t_{(32)} \geq 4.60$, $p < 0.001$]; mild AD dementia group: [both $t_{(27)} \geq 3.27$, $p \leq 0.003$]). For an approach from the north, performance in the non-AD aMCI ($t_{(30)} = 0.31$, $p = 0.762$) and AD aMCI ($t_{(32)} = -1.71$, $p = 0.098$) groups did not differ from the chance level and the mild AD dementia group performed below the chance level ($t_{(27)} = -4.13$, $p < 0.001$).

In the *post-hoc* ROC analysis, performance in the Directional-approach task differentiated the CN group from the non-AD aMCI, AD aMCI, and mild AD dementia groups with AUC values of 0.717 (95% CI [0.59, 0.85], $p = 0.001$), 0.81 (95% CI [0.69, 0.92], $p < 0.001$), and 0.88 (95% CI [0.79, 0.97], $p < 0.001$), respectively, the non-AD aMCI group from the mild AD dementia group with AUC value of 0.71 (95% CI [0.58, 0.84], $p = 0.002$), and did not differentiate the non-AD aMCI group from the AD aMCI group and the AD aMCI group from the mild AD dementia group, where the AUC values were 0.62 (95% CI [0.47, 0.76], $p = 0.109$), and 0.60 (95% CI [0.46, 0.74], $p = 0.166$),

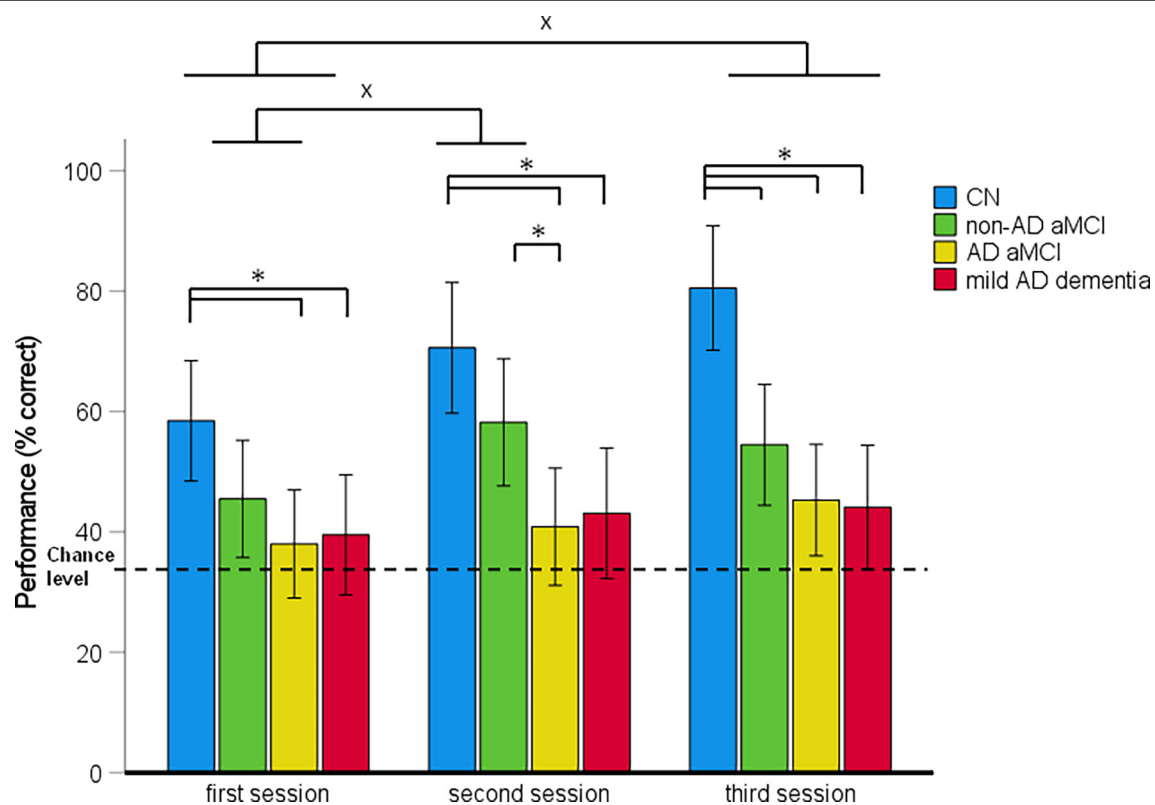


FIGURE 4 | Route-retracing task—spatial navigation performance as mean percentage of correct responses in each session (95% CI). * $p < 0.05$ indicating the differences between the groups; * $p < 0.05$ indicating the differences between the sessions. CN, cognitively normal; non-AD aMCI, amnesic mild cognitive impairment with negative AD biomarkers; AD aMCI, amnesic mild cognitive impairment with Alzheimer's disease; mild AD dementia, mild dementia with Alzheimer's disease; CI, confidence interval.

respectively. The sensitivity and specificity for the relevant cut-off values is listed in **Supplementary Table 3**.

Association Between Regional Brain Atrophy and Spatial Navigation Performance

The MRI brain measures are summarized in **Table 1**. The AD aMCI group had lower volumes of the right and the left hippocampal body, tail and pmEC, the right aLEC, and lower thickness of the right and left isthmus cingulate/RSC, precuneus, and posterior parietal cortex than the CN group (all $p \leq 0.015$). The same was true for the mild AD dementia group, which in addition had lower volumes of the right and left hippocampal head and the left aLEC than the CN group (all $p \leq 0.024$). The AD aMCI group had lower volumes of the right and the left hippocampal tail, the right hippocampal body, and aLEC, the right and left pmEC, and lower thickness of the left precuneus and the right and left posterior parietal cortex than the non-AD aMCI (all $p \leq 0.020$). There were no significant differences in regional brain atrophy between the non-AD aMCI and the CN group (all $p \geq 0.533$).

In the correlational analysis with HB correction (**Table 2**, **Supplementary Figure 1**), volume of the right aLEC and thickness of the right and left precuneus and posterior parietal

cortex were correlated with spatial navigation performance in the Route-repetition task (all $r \geq 0.38$, $p \leq 0.001$), volumes of the right hippocampal body and the right and left pmEC were correlated with spatial navigation performance in the Route-retracing task (all $r \geq 0.34$, $p \leq 0.001$), and volumes of the left hippocampal body, the right hippocampal tail and aLEC, the right and left pmEC, and thickness of the right isthmus cingulate/RSC, the right and left precuneus and posterior parietal cortex were correlated with spatial navigation performance in the Directional-approach task (all $r \geq 0.32$, $p \leq 0.001$). All the associations but the association between volume of the right aLEC and performance in the Directional-approach task remained significant in the regression analyses adjusted for age, education, and gender, where lower volumes and thickness were associated with worse spatial navigation performance (all $\beta \geq 0.24$, $p \leq 0.030$; **Table 3**).

Association Between CSF Biomarkers and Spatial Navigation Performance

The CSF biomarker characteristics are presented in detail in **Table 1**. As expected, the non-AD aMCI group had higher CSF levels of amyloid- β_{1-42} than the AD aMCI and mild AD dementia groups (both $p < 0.001$). There were no significant differences in CSF levels of amyloid- β_{1-42} between the AD aMCI and the mild

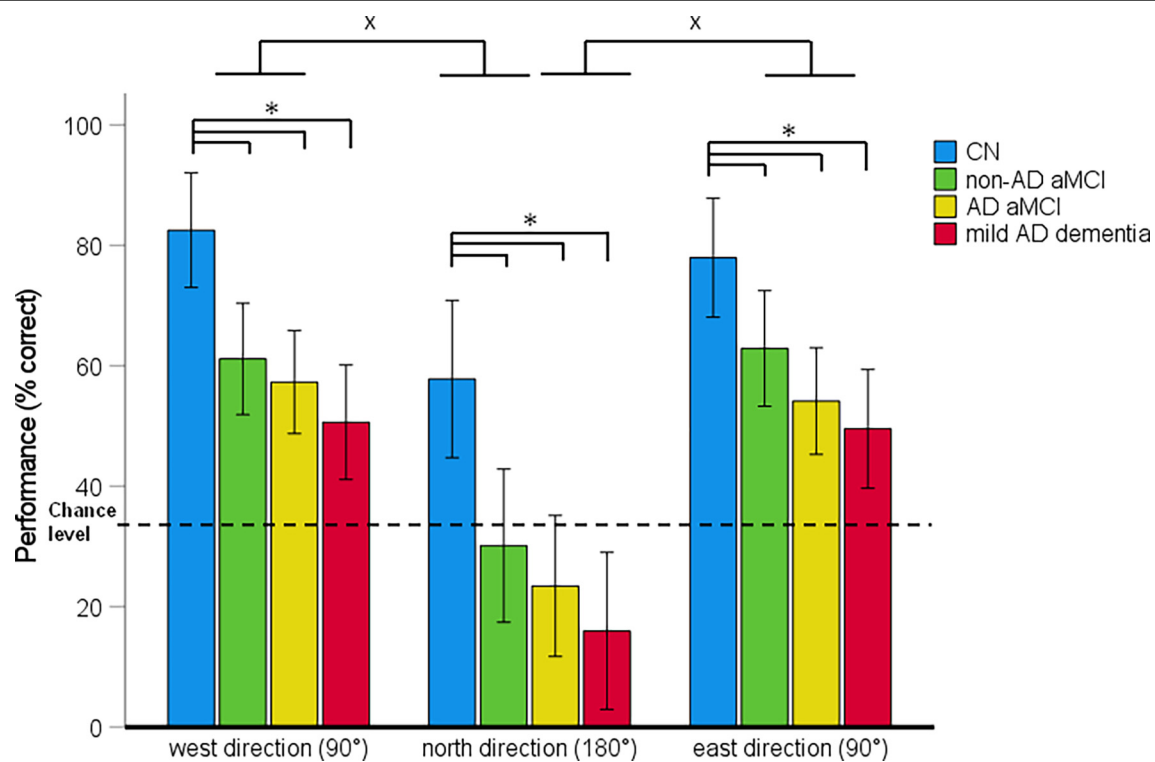


FIGURE 5 | Directional-approach task—spatial navigation performance as mean percentage of correct responses in each approach direction (95% CI).

* $p < 0.05$ indicating the differences between the groups; $X p < 0.05$ indicating the differences between the approach directions. CN, cognitively normal; non-AD aMCI, amnesic mild cognitive impairment with negative AD biomarkers; AD aMCI, amnesic mild cognitive impairment with Alzheimer's disease; mild AD dementia, mild dementia with Alzheimer's disease; CI, confidence interval.

TABLE 2 | Correlation matrix of spatial navigation performance and MRI brain measures.

| | Route-repetition task (% correct) | Route-retracing task (% correct) | Directional-approach task (% correct) |
|--|-----------------------------------|----------------------------------|---------------------------------------|
| Hippocampal head right ^a (volume, cm ³) | 0.279** | 0.237* | 0.160 |
| Hippocampal head left ^a (volume, cm ³) | 0.226* | 0.232* | 0.132 |
| Hippocampal body right ^a (volume, cm ³) | 0.314** | 0.345*** | 0.299** |
| Hippocampal body left ^a (volume, cm ³) | 0.261** | 0.293** | 0.397*** |
| Hippocampal tail right ^a (volume, cm ³) | 0.303** | 0.300** | 0.392*** |
| Hippocampal tail left ^a (volume, cm ³) | 0.220* | 0.239* | 0.300** |
| alEC right ^a (volume, cm ³) | 0.374*** | 0.288** | 0.323** |
| alEC left ^a (volume, cm ³) | 0.250* | 0.265** | 0.256** |
| pmEC right ^a (volume, cm ³) | 0.301** | 0.344*** | 0.345*** |
| pmEC left ^a (volume, cm ³) | 0.277** | 0.340*** | 0.379*** |
| Caudate nucleus right ^a (volume, cm ³) | 0.156 | 0.226* | 0.208* |
| Caudate nucleus left ^a (volume, cm ³) | 0.118 | 0.195 | 0.164 |
| Precuneus right (thickness, mm) | 0.380*** | 0.262** | 0.361*** |
| Precuneus left (thickness, mm) | 0.446*** | 0.286** | 0.359*** |
| Isthmus cingulate right (thickness, mm) | 0.283** | 0.249* | 0.326** |
| Isthmus cingulate left (thickness, mm) | 0.249* | 0.167 | 0.200* |
| Posterior parietal cortex right (thickness, mm) | 0.444*** | 0.254* | 0.339*** |
| Posterior parietal cortex left (thickness, mm) | 0.419*** | 0.254* | 0.342*** |

*Correlation (uncorrected) is significant at the 0.05 level (2-tailed), **Correlation (uncorrected) is significant at the 0.01 level (2-tailed), ***Correlation (uncorrected) is significant at the 0.001 level (2-tailed). Values in bold are significant after Holm-Bonferroni correction for multiple comparisons. ^aVolume normalized to estimated total intracranial volume. Key: MRI, magnetic resonance imaging; alEC, anterolateral entorhinal cortex; pmEC, posteromedial entorhinal cortex.

AD dementia group ($p = 0.978$). The non-AD aMCI group had lower CSF levels of total tau ($p = 0.003$) and p-tau₁₈₁ ($p = 0.038$) than the mild AD dementia group. Other differences in CSF

levels of total tau and p-tau₁₈₁ between the diagnostic groups were not significant. There was a strong correlation between CSF levels of total tau and p-tau₁₈₁ ($r = 0.62$, $p < 0.001$). CSF levels

TABLE 3 | Regression analyses of spatial navigation performance and MRI brain measures controlled for demographic characteristics.

| MRI brain measures | Spatial navigation performance (% correct) | | | |
|--|---|---|----------------------------------|----------|
| | Standardized Regression Coefficient β | Unstandardized Regression Coefficient B | Standard Error of Measurement SE | R Square |
| Route-repetition task | | | | |
| aIEC right ^a (volume, cm ³) | 0.276* | 0.053* | 0.021 | 0.224 |
| Precuneus right (thickness, mm) | 0.278** | 33.077** | 11.147 | 0.272 |
| Precuneus left (thickness, mm) | 0.360*** | 38.799*** | 9.959 | 0.319 |
| Posterior parietal cortex right (thickness, mm) | 0.346*** | 38.666*** | 10.675 | 0.306 |
| Posterior parietal cortex left (thickness, mm) | 0.299** | 33.528** | 11.034 | 0.279 |
| Route-retracing task | | | | |
| Hippocampal body right ^a (volume, cm ³) | 0.243* | 0.037* | 0.016 | 0.173 |
| pmEC right ^a (volume, cm ³) | 0.239* | 0.106* | 0.049 | 0.162 |
| pmEC left ^a (volume, cm ³) | 0.246* | 0.094* | 0.039 | 0.170 |
| Directional-approach task | | | | |
| Hippocampal body left ^a (volume, cm ³) | 0.319** | 0.046** | 0.014 | 0.197 |
| Hippocampal tail right ^a (volume, cm ³) | 0.316** | 0.146** | 0.046 | 0.197 |
| pmEC left ^a (volume, cm ³) | 0.311** | 0.120** | 0.039 | 0.175 |
| pmEC right ^a (volume, cm ³) | 0.261* | 0.118* | 0.050 | 0.144 |
| aIEC right ^a (volume, cm ³) | 0.225 | 0.050 | 0.026 | 0.128 |
| Precuneus left (thickness, mm) | 0.340*** | 44.416*** | 12.740 | 0.245 |
| Precuneus right (thickness, mm) | 0.327*** | 47.143*** | 13.820 | 0.238 |
| Posterior parietal cortex left (thickness, mm) | 0.304** | 40.903** | 13.807 | 0.220 |
| Posterior parietal cortex right (thickness, mm) | 0.308** | 41.174** | 13.541 | 0.223 |
| Isthmus cingulate right (thickness, mm) | 0.258** | 33.406** | 12.535 | 0.203 |

* $p < 0.05$; ** $p < 0.01$; and *** $p < 0.001$. ^aVolume normalized to estimated total intracranial volume. Key: MRI, magnetic resonance imaging; aIEC, anterolateral entorhinal cortex; pmEC, posteromedial entorhinal cortex.

of p-tau₁₈₁ and total tau negatively correlated with CSF levels of amyloid- β_{1-42} (both $r = -0.29$, $p < 0.05$).

In the correlational analysis with spatial navigation tasks (Table 4, Supplementary Figure 2), CSF levels of amyloid- β_{1-42} correlated with performance in the Route-repetition and Directional-approach tasks (both $r \geq 0.31$, $p \leq 0.032$), CSF levels of total tau correlated with performance in the Directional-approach task ($r = -0.31$, $p = 0.041$) and CSF levels of p-tau₁₈₁ correlated with performance in the Route-retracing and Directional-approach tasks (both $r \geq -0.30$, $p \leq 0.043$). In the regression analyses adjusted for age, education and gender (Table 5), lower levels of amyloid- β_{1-42} were associated with worse spatial navigation performance in the Route-repetition task ($\beta = 0.39$, $p = 0.005$) and higher levels of p-tau₁₈₁ were associated with worse spatial navigation performance in the Route-retracing ($\beta = -0.28$, $p = 0.041$) and Directional-approach ($\beta = -0.29$, $p = 0.037$) tasks. Other associations in the regression analyses were not significant.

In the mediation analyses adjusted for age, education, and gender, in the Route-repetition task, lower levels of amyloid- β_{1-42} were directly associated with worse spatial navigation performance when using the thickness of the right and left precuneus and posterior parietal cortex as the mediators [all $DE \geq 0.28$, 95% CI (0.00, 0.55) to (0.02, 0.58), all $p \leq 0.049$]. The direct effect was not significant when using volume of the right aIEC as the mediator [$DE = 0.24$, 95% CI (-0.07, 0.55), $p = 0.119$]. The indirect effect was not significant in any of the analyses with the Route-repetition task performance [all $IE \leq 0.08$, 95% CI (-0.12, 0.34) to (-0.04, 0.11)]. In the Route-retracing task, higher levels of p-tau₁₈₁ were directly associated with worse spatial navigation performance when using volumes of the right and left pmEC as the mediators [both $DE \geq -0.35$,

95% CI (-0.65, -0.05) to (-0.66, -0.07), both $p \leq 0.023$]. The direct effect was not significant when using volume of the right hippocampal body as the mediator [$DE = -0.30$, 95% CI (-0.61, 0.00), $p = 0.052$]. The indirect effect was not significant in any of the analyses with the Route-retracing task performance [all $IE \leq -0.05$, 95% CI (-0.06, 0.05) to (-0.19, 0.01)]. In the Directional-approach task, higher levels of p-tau₁₈₁ were not directly associated with spatial navigation performance when using the thickness of the right and left precuneus and posterior parietal cortex, the thickness of the right isthmus cingulate/RSC and volumes of the right pmEC and hippocampal tail and the left hippocampal body as the mediators [all $DE \leq -0.27$, 95% CI (-0.50, 0.09) to (-0.58, 0.03), all $p \geq 0.074$]. The direct effect was significant when using volume of the left pmEC as the mediator [$DE = -0.29$, 95% CI (-0.58, -0.00), $p = 0.047$]. However, the total effect was not significant in this mediation analysis ($TE = -0.28$ 95% CI [-0.57, 0.22], $p = 0.068$), therefore, the significant direct effect is difficult to interpret. The indirect effect was not significant in any of the analyses with the Directional-approach task performance [all $IE \leq -0.07$, 95% CI (-0.04, 0.05) to (-0.36, 0.03)]. The results of the mediation analyses are described in detail in Supplementary Table 4. Correlations between spatial navigation performance and MRI brain measures in the subsample used for the mediation analyses, and correlations between CSF biomarkers and MRI brain measures are described in Supplementary Tables 5, 6.

DISCUSSION

We examined the differences in spatial navigation performance between the AD biomarker positive and negative aMCI participants in various tasks of the navigation test using a

TABLE 4 | Correlation matrix of spatial navigation performance and CSF biomarkers.

| | Route-repetition task (% correct) | Route-retracing task (% correct) | Directional-approach task (% correct) |
|---------------------------------|-----------------------------------|----------------------------------|---------------------------------------|
| Amyloid- β_{1-42} (pg/ml) | 0.425** | 0.234 | 0.310* |
| Total tau (pg/ml) | -0.212 | -0.290 | -0.307* |
| P-tau ₁₈₁ (pg/ml) | -0.203 | -0.296* | -0.329* |

*Correlation (uncorrected) is significant at the 0.05 level (2-tailed), **Correlation (uncorrected) is significant at the 0.01 level (2-tailed). Key: CSF, cerebrospinal fluid; p-tau₁₈₁, phosphorylated tau₁₈₁.

TABLE 5 | Regression analysis of spatial navigation performance and CSF biomarkers controlled for demographic characteristics.

| CSF biomarkers | Spatial navigation performance (% correct) | | | |
|---------------------------------|---|---|----------------------------------|----------|
| | Standardized Regression Coefficient β | Unstandardized Regression Coefficient B | Standard Error of Measurement SE | R Square |
| Amyloid- β_{1-42} (pg/ml) | 0.394** | Route-repetition task | 0.008 | 0.289 |
| | | 0.024** | | |
| P-tau ₁₈₁ (pg/ml) | -0.283* | Route-retracing task | 0.048 | 0.265 |
| | | -0.100* | | |
| Amyloid- β_{1-42} (pg/ml) | 0.241 | Directional-approach task | 0.009 | 0.243 |
| | | 0.016 | | |
| | | -0.011 | | |
| Total tau (pg/ml) | -0.215 | -0.098* | 0.007 | 0.232 |
| P-tau ₁₈₁ (pg/ml) | -0.298* | | 0.045 | 0.270 |

* $p < 0.05$; ** $p < 0.01$. Key: CSF, cerebrospinal fluid; p-tau₁₈₁, phosphorylated tau₁₈₁.

realistic-looking virtual environment. Next, we explored the relationships between spatial navigation performance and MRI measures of atrophy in the specific MTL, cortical and subcortical regions. Finally, we examined the associations of performance with CSF AD biomarkers and the role of regional brain atrophy in these associations. We found that the AD aMCI participants performed generally worse in route learning (i.e., body-centered navigation) and had a tendency to perform worse in some aspects of wayfinding (i.e., world-centered navigation) than the non-AD aMCI participants. The participants with AD aMCI and non-AD aMCI performed similarly in conventional cognitive tests. The lower thickness of the parietal regions (i.e., the precuneus and the posterior parietal cortex) was associated with worse route learning performance. Lower volume of the MTL, especially the right posterior hippocampus and the pmEC, was associated with worse wayfinding performance. Lower thickness of the parietal regions and the right isthmus cingulate/RSC and lower volume of the MTL, especially the posterior hippocampus and the pmEC, were associated with worse performance in the perspective taking/wayfinding task. Lower levels of amyloid- β_{1-42} were associated with worse route learning performance, whereas higher levels of p-tau₁₈₁ were associated with worse wayfinding performance and worse performance in the perspective taking/wayfinding task. Specifically, lower levels of amyloid- β_{1-42} were directly associated with worse route learning performance and this association was not mediated by the thickness of the parietal regions.

Route-Repetition Task

Route-Repetition Task Performance Is Different in AD aMCI and Non-AD aMCI Participants

Consistent with our hypothesis, this study demonstrated that the aMCI participants with positive AD biomarkers showed worse route learning performance than the aMCI participants with negative AD biomarkers above and beyond demographic

characteristics. The participants with AD aMCI and non-AD aMCI did not significantly differ in any conventional cognitive test. Next, the AD biomarker positive aMCI participants performed similarly to the participants with mild AD dementia, while the AD biomarker negative aMCI participants showed similar performance as the CN participants. These results support and further extend recent findings showing that testing of route learning in a large scale real environment can differentiate amyloid- β positive and negative patients with aMCI, where the latter did not differ from CN older adults (Schöberl et al., 2020). The results are also consistent with previous work indicating that body-centered direction estimation in a virtual reality navigation task can discriminate cognitively impaired older adults with AD from those with other neurodegenerative diseases (Tu et al., 2015, 2017). It should be noted that one study investigating spatial navigation in preclinical AD showed no differences in route learning between CN older adults with and without amyloid- β pathology, as measured by CSF amyloid- β_{1-42} levels (Allison et al., 2016). Together, these findings suggest that route learning deficits may be relatively specific to early clinical stages of AD but do not occur in the earliest, preclinical stage of AD. In accordance with our recent findings (Laczó et al., 2021a), results of the current study showed that all participants performed above the chance level and improved in route learning across all three experimental sessions indicating preserved learning and the absence of a floor effect in our Route-repetition task even in the participants with mild AD dementia.

Route-Repetition Task Performance Is Associated With Amyloid- β Pathology and Parietal Atrophy

Our results further demonstrated that greater amyloid- β pathology measured by amyloid- β_{1-42} levels in CSF was associated with worse route learning performance above and beyond demographic characteristics. This was consistent with

our hypotheses and also with recent data showing that increased cortical amyloid- β accumulation relates to worse scene recognition from a constant first-person viewpoint in CN adults and patients with early AD (Maass et al., 2019). Our data also showed that cortical thinning in the precuneus and the posterior parietal cortex was associated with worse route learning performance above and beyond demographic characteristics. This was in accordance with our hypotheses and with the previously described important role of the parietal regions in route learning/body-centered navigation (Wolbers et al., 2004; Weniger et al., 2011). The finding indicates that impairment of this spatial navigation ability reflects neurodegeneration in the parietal cortex, which is typically found in early AD (Landau et al., 2011). Next, in agreement with our hypotheses, lower amyloid- β_{1-42} in CSF was associated with worse route learning directly and not indirectly through cortical thinning in the parietal regions when controlled for demographic characteristics. This indicates that both amyloid- β deposition and neurodegeneration in the parietal cortex may contribute to route learning deficits in early AD, where neurodegeneration may not be a direct result of amyloid- β accumulation. Amyloid- β accumulation in the parietal cortex that emerges very early in AD (Villain et al., 2012; Palmqvist et al., 2017) was shown to be related to less accurate spatial discrimination (Maass et al., 2019). It should be noted that CSF amyloid- β_{1-42} is a biomarker of amyloid- β pathology that is not specific to regional amyloid- β deposition (Palmqvist et al., 2015). Therefore, based on our data we could not demonstrate whether amyloid- β accumulation in the parietal cortex was associated with worse route learning performance. Future studies with amyloid PET quantifying regional-specific amyloid- β deposition are needed to explore this association.

The Association Between Route-Repetition Task Performance and Atrophy of the Right aLEC

Contrary to our hypothesis, lower volume of the right aLEC was associated with worse route learning, controlling for demographic characteristics. Rodent research showed that the lateral EC, a homolog of the human aLEC, plays a role in processing spatial information in a body-centered frame of reference (Wang et al., 2018; Kuruvilla et al., 2020) and using proximal landmarks for navigation (Kuruvilla and Ainge, 2017). Next, a recent human study found that the aLEC encodes distance information from landmarks (Chen et al., 2019). Our study may suggest that the aLEC could also play a role in computing directional information from proximal landmarks. However, our finding should be interpreted with caution, because no association with the aLEC was found for other tasks. Future studies are needed to investigate this potential association in detail.

Route-Retracing Task

Route-Retracing Task Performance Is Impaired in AD aMCI and Non-AD aMCI Participants

The current study demonstrated that the aMCI participants with positive and negative AD biomarkers showed worse wayfinding performance in a virtual environment than the CN

participants, above and beyond demographic characteristics. This is in agreement with our hypothesis and also with a recent finding showing wayfinding deficits in amyloid- β positive and negative patients with aMCI in real space (Schöberl et al., 2020). Contrary to our hypothesis, our results did not show significant overall differences in wayfinding performance between the aMCI participants with positive and negative AD biomarkers. However, analysis of differences from chance performance suggested that the aMCI participants with positive and negative AD biomarkers may have a different pattern of wayfinding deficits. Specifically, the AD biomarker positive aMCI participants performed at the chance level in the first two of three sessions, whereas the AD biomarker negative aMCI participants performed above the chance level across all sessions. Performance at the chance level in the aMCI participants with positive AD biomarkers also suggested that there may be a floor effect in the Route-retracing task leading to the non-significant differences between AD biomarker positive and negative aMCI participants in the main analysis. Furthermore, the *post-hoc* analysis showed that the aMCI participants with positive AD biomarkers performed worse than the aMCI participants with negative AD biomarkers in the second session of the task. However, this result should be interpreted with caution as there was no significant interaction between group and session. Together, these results indicated that aMCI participants with positive and negative AD biomarkers have wayfinding deficits that tend to be more pronounced in the former group. Wayfinding testing has previously reliably identified individuals with preclinical AD among CN older adults (Allison et al., 2016, 2019). However, previous studies examining wayfinding/world-centered navigation testing as a promising tool to differentiate cognitively impaired individuals with AD and those with other pathologies yielded inconsistent results. A recent study showed that wayfinding performance can reliably discriminate amyloid- β positive and negative aMCI patients in a navigation test in a large scale real environment that required the planning of novel routes including shortcuts (Schöberl et al., 2020). In a virtual reality navigation task, identification of the correct location on a map that required world-centered spatial information did not discriminate between cognitively impaired older adults with AD and those with other neurodegenerative diseases, whose performance was similarly worse than that of age-matched healthy controls (Tu et al., 2017). Overall, studies suggested that preclinical AD is characterized by wayfinding deficits (Allison et al., 2016, 2019) that worsen with disease progression to aMCI and dementia (Hort et al., 2007; Levine et al., 2020). However, wayfinding deficits are also found in cognitively impaired older adults without AD pathology (Tu et al., 2017; Schöberl et al., 2020), reducing the usefulness of wayfinding/world-centered navigation tasks for discriminating aMCI individuals with positive and negative AD biomarkers. The ability of these tasks to differentiate AD biomarker positive and negative older adults with cognitive impairment may also depend on their specific characteristics. These characteristics include the complexity of the task, whether there is a floor effect in the task, whether the task requires planning of new routes, and potentially also whether

the navigation task takes place in real space or in virtual environment.

Route-Retracing Task Performance Is Associated With Atrophy of the Posterior MTL Subregions

Consistent with our hypothesis, lower volumes of the right posterior hippocampus (i.e., the hippocampal body) and the pmEC were associated with worse wayfinding performance above and beyond demographic characteristics. Previous studies showed that the right hippocampus is more strongly associated with wayfinding than the left hippocampus (Maguire et al., 1998; Nedelska et al., 2012; Laczó et al., 2017). In particular, its posterior subregion is involved in the accurate creation and use of cognitive maps (Doeller et al., 2008; Schinazi et al., 2013). The pmEC is important for world-centered direction computations (Chadwick et al., 2015) and spatial information processing (Berron et al., 2018). Our results are consistent with these findings and indicate that wayfinding deficits reflect neurodegeneration in the posterior MTL subregions in older adults. Neurodegeneration in the MTL including the hippocampus and the EC is a common finding in early AD (Scahill et al., 2002; Du et al., 2004; Tapiola et al., 2008) but is also observed in other neurodegenerative diseases (Jack et al., 2002; Nelson et al., 2019). In the current study, smaller MTL volumes were observed predominantly in the posterior (i.e., the hippocampal tail, right hippocampal body, and the pmEC) than in the anterior (i.e., the right aLEC) subregions in the aMCI participants with positive AD biomarkers when compared to those with negative AD biomarkers. This supports previous work showing that in AD, compared to other neurodegenerative diseases, atrophy is more pronounced in the posterior MTL subregions (Lindberg et al., 2017; Lladó et al., 2018).

Route-Retracing Task Performance Is Associated With Tau Pathology

Consistent with our hypothesis, higher p-tau₁₈₁ was associated with worse wayfinding performance, above and beyond demographic characteristics. Thus, our findings suggest that tau pathology may contribute to wayfinding deficits in cognitively impaired older adults. This is consistent with rodent data showing that in older mice, tau pathology is related to world-centered spatial memory deficits (Fu et al., 2017). It may also complement recent findings in CN older adults on the association between higher p-tau₁₈₁ in CSF and worse wayfinding performance in a virtual environment (Allison et al., 2019). However, it is noteworthy that the previous study also found an association between amyloid- β_{1-42} in CSF and wayfinding performance in CN older adults (Allison et al., 2019). Tau pathology in the hippocampus and the EC (Braak and Braak, 1995) together with neocortical amyloid- β deposition (Hyman et al., 2012) is considered a major pathological marker of AD. A similar pattern of regional tau deposition without amyloid- β pathology has been observed in other neurodegenerative diseases including primary age-related tauopathy (Crary et al., 2014) and argyrophilic grain disease (Ferrer et al., 2008). Thus, unlike the association between amyloid- β pathology and route learning, the association between tau pathology and

wayfinding may not be specific to AD. Previous work (Jacobs et al., 2018) showed that the spread of tau pathology to the posterior regions, which is facilitated by amyloid- β deposition, contributes to region-specific neurodegeneration, which in turn leads to cognitive impairment. Based on these findings, one would expect that tau pathology should be related to atrophy of the posterior MTL subregions, which in turn should be associated with wayfinding deficits. However, contrary to our hypothesis, we found that higher p-tau₁₈₁ in CSF was associated with worse wayfinding directly and not indirectly through volume reduction in the posterior MTL (i.e., the pmEC), above and beyond demographic characteristics. This result is most likely driven by a non-significant relationship between p-tau₁₈₁ levels in CSF and region-specific brain atrophy in our sample. However, this finding should be interpreted with caution as our results are based on a subsample of participants with CSF data. Thus, the analyses might not have sufficient power to demonstrate a significant association of p-tau₁₈₁ in CSF with region-specific volume reduction, and the mediation effect of posterior MTL atrophy in the association between p-tau₁₈₁ and wayfinding. It should be noted that CSF p-tau₁₈₁ is a biomarker of tau pathology that is not specific to regional tau deposition (Schöll et al., 2019). Also, tau accumulation, measured by tau PET, was shown to be more strongly associated with neurodegeneration and cognitive decline than p-tau₁₈₁ in CSF (Mattsson et al., 2017). Specifically, tau pathology in the MTL subregions, particularly in the posterior EC, was related to EC atrophy and mirrored its association with memory decline (Maass et al., 2018). Therefore, future studies with tau PET ligands are needed to explore in detail the association between regional-specific tau pathology, neurodegeneration in the posterior MTL subregions, and wayfinding in older adults.

Directional-Approach Task

Directional-Approach Task Performance Is Impaired in AD aMCI and Non-AD aMCI Participants

In the third spatial navigation task, we assessed perspective taking and wayfinding. The task required participants to use the configuration of landmarks at an intersection to interpret a spatial situation from a viewpoint they had not experienced before. Consistent with our hypothesis, we demonstrated that the aMCI participants with positive and negative AD biomarkers and the participants with mild AD dementia performed worse than the CN participants, above and beyond demographic characteristics. These results support and further extend our recent findings indicating that patients with aMCI and mild AD dementia, who were not defined by biomarkers, show spatial navigation impairment in the same task (Laczó et al., 2021a) and perspective taking deficits in a virtual arena task (Marková et al., 2015). The participants' performance in the current task generally decreased when the approach direction in the test phase was misaligned with the encoding phase by 180° compared to 90°, thus when the perspective shift between encoding and retrieval was higher. This finding is consistent with earlier work showing that perspective taking is required to solve the task (de Condappa and Wiener, 2016;

Laczó et al., 2021a). Contrary to our hypothesis, we did not find significant differences between the aMCI participants with positive and negative AD biomarkers. It is worth noting that the aMCI participants with positive and negative AD biomarkers performed at the chance level when the direction in the test phase was misaligned by 180°. This indicates that large misalignment placed great demands on perspective taking. The task could therefore be difficult for most cognitively impaired older adults, as our previous study showed (Laczó et al., 2021a), and may be prone to the floor effect. On the other hand, a recent study indicated that older adults with aMCI and positive CSF AD biomarkers had worse recognition of the topographical layout of four mountains within a computer-generated environment from a shifted point of view than those with negative CSF AD biomarkers (Chan et al., 2016). The discrepant findings in our study and the previous study may be due to the different nature and difficulty of both tasks. Specifically, the degree of misalignment between the encoding and the test perspective differed greatly between these studies. In the previous study (Chan et al., 2016), the degree of misalignment ranged between 15° and 90°, and in our current study, the perspective was misaligned by 90° and 180°. Therefore, the demands on perspective taking were considerably higher in our task, which could result in non-significant differences between the cognitively impaired participants.

Directional-Approach Task Performance Is Associated With Atrophy of the Posterior MTL Subregions and Parietal Cortex

Consistent with our hypothesis, lower volumes of the posterior MTL subregions, especially the posterior hippocampus (i.e., the right hippocampal tail and the left hippocampal body) and the pmEC, together with cortical thinning in the precuneus, the posterior parietal cortex, and the right isthmus cingulate/RSC were associated with worse performance in the perspective taking/wayfinding task, above and beyond demographic characteristics. Our findings, therefore, indicated that multiple specific brain regions are involved in perspective taking and wayfinding. This is in accordance with the previously reported important role of the MTL (Lambrey et al., 2008) and the parietal regions (Zacks and Michelon, 2005) in perspective taking, and the role of the posterior hippocampus (Schinazi et al., 2013) and the pmEC (Chadwick et al., 2015) in world-centered navigation. Our findings are also consistent with the notion that the RSC plays a key role in the use of landmarks for directional orientation (Auger et al., 2012) and the integration of body-centered and world-centered spatial information (Clark et al., 2018), both of which can be important for successful task performance. Our results further indicate that perspective taking/wayfinding deficits reflect neurodegeneration in the posterior MTL subregions, parietal cortex, and the isthmus cingulate/RSC in older adults. This supports and further extends recent findings showing that atrophy of the hippocampus and precuneus is associated with worse recognition of the computer-generated environment from a shifted viewpoint in cognitively impaired and CN older adults (Chan et al., 2016).

Directional-Approach Task Performance Is Predominantly Associated With Tau Pathology

In accordance with our hypothesis, higher levels of p-tau₁₈₁ in CSF were associated with worse task performance, above and beyond demographic characteristics. Also consistent with our hypothesis, higher levels of total tau and lower levels of amyloid- β_{1-42} in CSF correlated with worse performance. However, these findings should be interpreted with caution as the associations of amyloid- β_{1-42} and total tau in CSF with task performance were not significant after controlling for demographic characteristics. Previous research showed that lower amyloid- β_{1-42} (of borderline significance) and higher total tau in CSF are associated with worse recognition of the computer-generated environment from a shifted viewpoint in patients with aMCI (Wood et al., 2016). Next, the recent study indicated that higher p-tau₁₈₁ and lower amyloid- β_{1-42} in CSF are associated with worse wayfinding performance in a virtual environment in CN older adults (Allison et al., 2019). Overall, these findings, including ours, suggested that tau and amyloid- β pathologies may contribute to perspective taking/wayfinding deficits in older adults with and without cognitive impairment. In addition, they suggest that neurodegeneration (as measured by total tau in CSF) may contribute to perspective taking deficits in cognitively impaired older adults. It should be noted that the association between p-tau₁₈₁ levels and task performance was not significant in the mediation analyses with MRI brain measures. Next, the association between amyloid- β_{1-42} levels and task performance was not significant in the regression analyses, controlling for demographic characteristics. Therefore, we were unable to support our hypotheses about the different mediation effects of regional brain atrophy in these associations. It is plausible that the analyses based on a subsample of participants with CSF data might not have sufficient power to demonstrate significant associations with perspective taking/wayfinding performance. Our preliminary findings should therefore be interpreted with caution and verified by future studies. Future studies with larger cohorts of participants are needed to explore in detail the interrelations between tau and amyloid- β pathologies (measured by CSF biomarkers and PET), regional brain atrophy, and perspective taking in cognitively impaired older adults.

Characteristics of the Participants With Non-AD aMCI

The participants with non-AD aMCI were defined by negative amyloid- β biomarkers including normal CSF amyloid- β_{1-42} and negative amyloid PET imaging. However, the underlying disease causing their cognitive impairment was mostly unknown. It is worth noting that 60% of these participants with available CSF biomarkers had abnormal p-tau₁₈₁ levels indicating that tau pathology was the underlying condition. About 60% of the participants with underlying tau pathology also had abnormal total tau levels indicative of neurodegeneration. This may at least partially explain non-significant differences between the participants with non-AD aMCI and AD aMCI in p-tau₁₈₁ and total tau levels. However, it should be noted that the participants with non-AD aMCI had almost twice as low

levels of p-tau181 and total tau compared to those with AD aMCI. As only 45% of the aMCI participants underwent CSF biomarker assessment, the non-significant differences between the non-AD aMCI and AD aMCI participants may have been due to the insufficient power of the analyses. The participants with non-AD aMCI did not show significant brain atrophy on MRI compared to the CN participants. However, we cannot rule out ongoing neurodegenerative diseases because FDG-PET, a sensitive marker of regional neurodegeneration, was not performed. The general uncertainty regarding the etiology of the non-AD aMCI participants is consistent with previous studies showing that this group may consist of various entities, including the neurodegenerative ones (i.e., tauopathy, synucleinopathy, and TDP-43 pathology), that may fully manifest several years later (Villemagne et al., 2011; Ye et al., 2018). Longitudinal follow-up is therefore essential to detect the underlying disease.

Strengths and Limitations of the Study

One of the strengths of the current study is the fact that this is the first study to date to comprehensively examine the differences between AD biomarker positive and negative older adults with aMCI in various navigational abilities (i.e., route learning, wayfinding, and perspective taking) using an established and ecologically valid spatial navigation test in a realistic-looking virtual environment that mimics real-life navigation. In addition, we investigated the complex interrelations between structural measures of the specific MTL subregions, cortical and subcortical brain regions, CSF AD biomarkers, and spatial navigation that have not been thoroughly studied. Finally, we used well-defined homogeneous cohorts of CN participants and cognitively impaired older adults, where the diagnosis of AD and non-AD was supported by biomarker assessment including amyloid PET imaging and CSF biomarkers. There are also several limitations to this study. First, assessment of CSF biomarkers and amyloid PET imaging were not performed in the CN participants to rule out preclinical AD, which may limit the generalizability of our findings. However, it should be noted that we used several inclusion criteria to minimize the possibility of recruiting individuals at increased risk of AD. Second, CSF AD biomarkers were available in a subset of the participants (i.e., 47 of the 92 participants with cognitive impairment), which may reduce the statistical power of the observed associations with spatial navigation performance in the regression and mediation analyses. Therefore, these findings should be interpreted with caution and replicated in larger study cohorts. Third, the statistical power to detect significant differences with medium effect sizes for the interactions in the main analyses of spatial navigation performance was less than 0.80. Therefore, the results of the interactions, especially the non-significant ones, should be interpreted with caution. Fourth, amyloid- β_{1-40} was not available and therefore we could not use amyloid- β_{1-42} /amyloid- β_{1-40} ratio as a more reliable marker of amyloid- β pathology. Fifth, the dichotomous visual read of amyloid PET did not allow quantifying amyloid- β accumulation in specific brain regions of interest and examining its association with spatial navigation performance, which should be the focus of future studies. Sixth, the underlying disease of the non-AD aMCI participants

was mostly unknown, which may limit the interpretation and generalizability of our findings. Seventh, segmentation of the hippocampus and EC was performed on 3D T1w images, whereas the use of T2-weighted images would be more preferable as it could provide better resolution. Eighth, because of the lack of an anatomical mask for measurement of the RSC, we used a proximal anatomical measure, the thickness of the isthmus cingulate, which may limit the specificity of our results and their interpretation regarding the role of the RSC in spatial navigation. Ninth, given that previous studies considered the subregions of the posterior hippocampus (i.e., body and tail) as a single region, and given the lack of specific hypotheses regarding their equal or different associations with spatial navigation performance, our results should be considered exploratory and these associations should be examined in more detail in future studies. Finally, the cross-sectional design did not allow evaluating changes in spatial navigation performance over time, but longitudinal follow-up is ongoing.

CONCLUSIONS

Using the Navigation Test Suite, the current study demonstrated that older adults with aMCI and positive AD biomarkers showed worse spatial navigation performance compared to those with negative AD biomarkers although both groups performed similarly in conventional cognitive tests. The profile and severity of spatial navigation deficits in the AD aMCI and non-AD aMCI participants varied between the tasks. Specifically, route learning (i.e., body-centered navigation) was worse in the AD aMCI participants than in the non-AD aMCI participants who were similar to the CN older adults. Wayfinding (i.e., world-centered navigation) deficits were found in the AD aMCI and non-AD aMCI participants and tended to be more pronounced in those with AD aMCI. Spatial navigation deficits in the perspective-taking/wayfinding task were observed in aMCI participants regardless of the biomarker status. The Navigation Test Suite thus provides complex information about spatial navigation abilities in cognitively impaired older adults and may complement cognitive assessment with conventional neuropsychological tests. This test may also help distinguish cognitive deficits in early AD from those in other diseases. Further, we demonstrated that deficits in various spatial navigation abilities were differently associated with neurodegeneration in the MTL and posterior cortical regions, the areas that atrophy early during the AD progression. Route learning deficits were associated with parietal cortical atrophy and wayfinding deficits were associated with posterior MTL atrophy. Navigation deficits in the perspective taking/wayfinding task were associated with atrophy in several brain regions. Finally, we demonstrated that various spatial navigation abilities reflected different aspects of AD pathology as measured by CSF biomarkers. Specifically, route learning deficits were directly associated with amyloid- β pathology regardless of parietal atrophy and wayfinding deficits were associated with tau pathology. Navigation deficits in the perspective taking/wayfinding task were associated with tau pathology and also correlated with amyloid- β pathology and neurodegeneration

measured by CSF total tau (without adjustment for demographic characteristics). In conclusion, the Navigation Test Suite has the potential to improve the early detection of AD-related cognitive deficits and could be used as a screening tool for the diagnosis of early AD in clinical settings. It should be noted that this test may have some limitations due to the floor effect in the wayfinding and perspective taking/wayfinding tasks that deserve further attention. The search for new reliable cognitive screening tools is of great importance as PET imaging, CSF, and blood-based biomarkers are currently limited to research settings and expert clinics. This is also particularly important as therapeutic interventions targeting the AD pathology are now becoming available.

DATA AVAILABILITY STATEMENT

The datasets presented in this article are not readily available because of the policy of the Czech Brain Aging Study (CBAS), which allows sharing of the data only after previous approval. Requests to access the datasets should be directed to JL, jan.laczo@lfmotol.cuni.cz.

ETHICS STATEMENT

The studies involving human participants were reviewed and approved by EK - 701/16 25.5.2016. The participants provided their written informed consent to participate in this study.

AUTHOR CONTRIBUTIONS

ML and JL participated in the design of the study, data interpretation, and wrote the draft of the manuscript. JW

participated in the design of the study. LM, OL, and ZN were involved in MRI data acquisition and processing. JK, VM, MV, and JH were involved in data acquisition and interpretation. All authors contributed to the article and approved the submitted version.

FUNDING

This study was supported by the European Regional Development Fund—Project ENOCH no. CZ.02.1.01/0.0/0.0/16_019/0000868; the Ministry of Health, Czech Republic—conceptual development of research organization, University Hospital Motol, Prague, Czech Republic grant no. 00064203; the Institutional Support of Excellence 2. LF UK grant no. 6990332; Alzheimer's Foundation; Czech Science Foundation (GACR) registration number 22-33968S; and the Grant Agency of Charles University grant no. 327821.

ACKNOWLEDGMENTS

We would like to thank Ms. M. Dokoupilova, Dr. K. Kopecka, Dr. J. Korb, Ms. S. Krejcova, Dr. H. Horakova, Dr. K. Veverova, and Dr. T. Nikolai for help with data collection; Dr. J. Cerman, Dr. I. Trubacik Mokrisova, and Dr. I. Wolfova for help with participant recruitment; and Mr. M. Uller for help with MRI data processing.

SUPPLEMENTARY MATERIAL

The Supplementary Material for this article can be found online at: <https://www.frontiersin.org/articles/10.3389/fnagi.2022.886778/full#supplementary-material>.

REFERENCES

- Albert, M. S., DeKosky, S. T., Dickson, D., Dubois, B., Feldman, H. H., Fox, N. C., et al. (2011). The diagnosis of mild cognitive impairment due to Alzheimer's disease: recommendations from the national institute on aging-Alzheimer's association workgroups on diagnostic guidelines for Alzheimer's disease. *Alzheimers Dement.* 7, 270–279. doi: 10.1016/j.jalz.2011.03.008
- Allison, S. L., Fagan, A. M., Morris, J. C., and Head, D. (2016). Spatial navigation in preclinical Alzheimer's disease. *J. Alzheimers Dis.* 52, 77–90. doi: 10.3233/JAD-150855
- Allison, S. L., Rodebaugh, T. L., Johnston, C., Fagan, A. M., Morris, J. C., and Head, D. (2019). Developing a spatial navigation screening tool sensitive to the preclinical Alzheimer disease continuum. *Arch. Clin. Neuropsychol.* 34, 1138–1155. doi: 10.1093/arclin/acz019
- Ashburner, J. (2009). Computational anatomy with the SPM software. *Magn. Reson. Imaging* 27, 1163–1174. doi: 10.1016/j.mri.2009.01.006
- Auger, S. D., Mullally, S. L., and Maguire, E. A. (2012). Retrosplenial cortex codes for permanent landmarks. *PLoS One* 7:e43620. doi: 10.1371/journal.pone.0043620
- Avants, B. B., Tustison, N. J., Song, G., Cook, P. A., Klein, A., and Gee, J. C. (2011). A reproducible evaluation of ANTs similarity metric performance in brain image registration. *Neuroimage* 54, 2033–2044. doi: 10.1016/j.neuroimage.2010.09.025
- Barker, W. W., Luis, C. A., Kashuba, A., Luis, M., Harwood, D. G., Loewenstein, D., et al. (2002). Relative frequencies of Alzheimer disease, lewy body, vascular and frontotemporal dementia and hippocampal sclerosis in the state of florida brain bank. *Alzheimer Dis. Assoc. Disord.* 16, 203–212. doi: 10.1097/00002093-200210000-00001
- Beck, A. T., Epstein, N., Brown, G., and Steer, R. A. (1988). An inventory for measuring clinical anxiety: psychometric properties. *J. Consult. Clin. Psychol.* 56, 893–897. doi: 10.1037//0022-006x.56.6.893
- Belohlavek, O., Jaruskova, M., Skopalova, M., Szarazova, G., and Simonova, K. (2019). Improved beta-amyloid PET reproducibility using two-phase acquisition and grey matter delineation. *Eur. J. Nucl. Med. Mol. Imaging* 46, 297–303. doi: 10.1007/s00259-018-4140-y
- Berron, D., Neumann, K., Maass, A., Schütze, H., Fliessbach, K., Kiven, V., et al. (2018). Age-related functional changes in domain-specific medial temporal lobe pathways. *Neurobiol. Aging* 65, 86–97. doi: 10.1016/j.neurobiolaging.2017.12.030
- Berron, D., Vieweg, P., Hochkeppeler, A., Pluta, J. B., Ding, S. L., Maass, A., et al. (2017). A protocol for manual segmentation of medial temporal lobe subregions in 7 Tesla MRI. *Neuroimage Clin.* 15, 466–482. doi: 10.1016/j.nicl.2017.05.022
- Bezdiček, O., Lukavský, J., and Preiss, M. (2011). Functional activities questionnaire, Czech Version—a validation study. *Ces. Slov. Neurol. N* 74/107, 36–42.
- Bezdiček, O., Stepankova, H., Moták, L., Axelrod, B. N., Woodard, J. L., Preiss, M., et al. (2014). Czech version of rey auditory verbal learning test: normative data. *Neuropsychol. Dev. Cogn. B. Aging. Neuropsychol. Cogn.* 21, 693–721. doi: 10.1080/13825585.2013.865699
- Blanch, R. J., Brennan, D., Condon, B., Santosh, C., and Hadley, D. (2004). Are there gender-specific neural substrates of route learning from different perspectives? *Cereb. Cortex* 14, 1207–1213. doi: 10.1093/cercor/bhh081

- Braak, H., and Braak, E. (1991). Neuropathological staging of Alzheimer-related changes. *Acta Neuropathol.* 82, 239–259. doi: 10.1007/BF00308809
- Braak, H., and Braak, E. (1995). Staging of Alzheimer's disease-related neurofibrillary changes. *Neurobiol. Aging* 16, 271–284. doi: 10.1016/0197-4580(95)00021-6
- Brunec, I. K., Bellana, B., Ozubko, J. D., Man, V., Robin, J., Liu, Z. X., et al. (2018). Multiple scales of representation along the hippocampal anteroposterior axis in humans. *Curr. Biol.* 28, 2129–2135.e6. doi: 10.1016/j.cub.2018.05.016
- Cerman, J., Laczó, J., Vyhánek, M., Malinová, J., Hanzalová, J., and Hort, J. (2020). Cerebrospinal fluid ratio of phosphorylated tau protein and beta amyloid predicts amyloid PET positivity. *Czech Slov. Neurol. Neurosurg.* 83, 173–179. doi: 10.14735/amcsnn2020173
- Chadwick, M. J., Jolly, A. E. J., Amos, D. P., Hassabis, D., and Spiers, H. J. (2015). A goal direction signal in the human entorhinal/subicular region. *Curr. Biol.* 25, 87–92. doi: 10.1016/j.cub.2014.11.001
- Chan, D., Gallaher, L. M., Moodley, K., Minati, L., Burgess, N., and Hartley, T. (2016). The 4 mountains test: a short test of spatial memory with high sensitivity for the diagnosis of pre-dementia Alzheimer's disease. *J. Vis. Exp.* 116:54454. doi: 10.3791/54454
- Chen, X., Vieweg, P., and Wolbers, T. (2019). Computing distance information from landmarks and self-motion cues - differential contributions of anterior-lateral vs. posterior-medial entorhinal cortex in humans. *Neuroimage* 202:116074. doi: 10.1016/j.neuroimage.2019.116074
- Cholvin, T., Hainmueller, T., and Bartos, M. (2021). The hippocampus converts dynamic entorhinal inputs into stable spatial maps. *Neuron* 109, 3135–3148.e7. doi: 10.1016/j.neuron.2021.09.019
- Clark, B. J., Simmons, C. M., Berkowitz, L. E., and Wilber, A. A. (2018). The retrosplenial-parietal network and reference frame coordination for spatial navigation. *Behav. Neurosci.* 132, 416–429. doi: 10.1037/bne0000260
- Coughlan, G., Laczó, J., Hort, J., Minihane, A. M., and Hornberger, M. (2018). Spatial navigation deficits — overlooked cognitive marker for preclinical Alzheimer disease? *Nat. Rev. Neurol.* 14, 496–506. doi: 10.1038/s41582-018-0031-x
- Crary, J. F., Trojanowski, J. Q., Schneider, J. A., Abisambra, J. F., Abner, E. L., Alafuzoff, I., et al. (2014). Primary age-related tauopathy (PART): a common pathology associated with human aging. *Acta Neuropathol.* 128, 755–766. doi: 10.1007/s00401-014-1349-0
- Cushman, L. A., Stein, K., and Duffy, C. J. (2008). Detecting navigational deficits in cognitive aging and Alzheimer disease using virtual reality. *Neurology* 71, 888–895. doi: 10.1212/01.wnl.0000326262.67613.fe
- Dale, A. M., Fischl, B., and Sereno, M. I. (1999). Cortical surface-based analysis. I. Segmentation and surface reconstruction. *Neuroimage* 9, 179–194. doi: 10.1006/nimg.1998.0395
- de Condappa, O., and Wiener, J. M. (2016). Human place and response learning: navigation strategy selection, pupil size and gaze behavior. *Psychol. Res.* 80, 82–93. doi: 10.1007/s00426-014-0642-9
- DeIpoli, A., Rankin, K., Mucke, L., Miller, B., and Gorno-Tempini, M. (2007). Spatial cognition and the human navigation network in AD and MCI. *Neurology* 69, 986–987. doi: 10.1212/01.wnl.0000271376.19515.c6
- Desikan, R. S., Ségonne, F., Fischl, B., Quinn, B. T., Dickerson, B. C., Blacker, D., et al. (2006). An automated labeling system for subdividing the human cerebral cortex on MRI scans into gyral based regions of interest. *Neuroimage* 31, 968–980. doi: 10.1016/j.neuroimage.2006.01.021
- Diersch, N., and Wolbers, T. (2019). The potential of virtual reality for spatial navigation research across the adult lifespan. *J. Exp. Biol.* 222:jeb187252. doi: 10.1242/jeb.187252
- Doeller, C. F., King, J. A., and Burgess, N. (2008). Parallel striatal and hippocampal systems for landmarks and boundaries in spatial memory. *Proc. Natl. Acad. Sci. U S A* 105, 5915–5920. doi: 10.1073/pnas.0801489105
- Drozdzova, K., Štěpánková, H., Lukavský, J., Bezdiček, M., and Kopeček, M. (2015). Normativní studie testu Reyovy-Osterriethovy komplexní figury v populaci českých seniorů. *Ces. Slov. Neurol. N.* 78/111, 542–549.
- Du, A. T., Schuff, N., Kramer, J. H., Ganzler, S., Zhu, X. P., Jagust, W. J., et al. (2004). Higher atrophy rate of entorhinal cortex than hippocampus in AD. *Neurology* 62, 422–427. doi: 10.1212/01.wnl.0000106462.72282.90
- Evensmoen, H. R., Ladstein, J., Hansen, T. I., Møller, J. A., Witter, M. P., Nadel, L., et al. (2015). From details to large scale: the representation of environmental positions follows a granularity gradient along the human hippocampal and entorhinal anterior-posterior axis. *Hippocampus* 25, 119–135. doi: 10.1002/hipo.22357
- Ferrer, I., Santpere, G., and van Leeuwen, F. W. (2008). Argyrophilic grain disease. *Brain* 131, 1416–1432. doi: 10.1093/brain/awn305
- Fischl, B., Salat, D. H., Busa, E., Albert, M., Dieterich, M., Haselgrove, C., et al. (2002). Whole brain segmentation: automated labeling of neuroanatomical structures in the human brain. *Neuron* 33, 341–355. doi: 10.1016/s0896-6273(02)00569-x
- Fischl, B., van der Kouwe, A., Destrieux, C., Halgren, E., Ségonne, F., Salat, D. H., et al. (2004). Automatically parcellating the human cerebral cortex. *Cereb. Cortex* 14, 11–22. doi: 10.1093/cercor/bhg087
- Fu, H., Rodriguez, G. A., Herman, M., Emrani, S., Nahmani, E., Barrett, G., et al. (2017). Tau pathology induces excitatory neuron loss, grid cell dysfunction and spatial memory deficits reminiscent of early Alzheimer's disease. *Neuron* 93, 533–541.e5. doi: 10.1016/j.neuron.2016.12.023
- Green, M. S., Kaye, J. A., and Ball, M. J. (2000). The Oregon brain aging study: neuropathology accompanying healthy aging in the oldest old. *Neurology* 54, 105–113. doi: 10.1212/wnl.54.1.105
- Hartley, T., Maguire, E. A., Spiers, H. J., and Burgess, N. (2003). The well-worn route and the path less traveled: distinct neural bases of route following and wayfinding in humans. *Neuron* 37, 877–888. doi: 10.1016/s0896-6273(03)00095-3
- Hayes, A. (2013). *Introduction to Mediation, Moderation and Conditional Process Analysis: A Regression-Based Approach*. New York, NY: The Guilford Press.
- Hort, J., Laczó, J., Vyhánek, M., Bojar, M., Bureš, J., and Vlček, K. (2007). Spatial navigation deficit in amnesic mild cognitive impairment. *Proc. Natl. Acad. Sci. U S A* 104, 4042–4047. doi: 10.1073/pnas.0611314104
- Howard, L. R., Javadi, A. H., Yu, Y., Mill, R. D., Morrison, L. C., Knight, R., et al. (2014). The hippocampus and entorhinal cortex encode the path and euclidean distances to goals during navigation. *Curr. Biol.* 24, 1331–1340. doi: 10.1016/j.cub.2014.05.001
- Howett, D., Castegnaro, A., Krzywicka, K., Hagman, J., Marchment, D., Henson, R., et al. (2019). Differentiation of mild cognitive impairment using an entorhinal cortex-based test of virtual reality navigation. *Brain* 142, 1751–1766. doi: 10.1093/brain/awz116
- Hyman, B. T., Phelps, C., Beach, T. G., Bigio, E. H., Cairns, N. J., Carrillo, M. C., et al. (2012). National institute on aging-Alzheimer's association guidelines for the neuropathologic assessment of Alzheimer's disease. *Alzheimers Dement.* 8, 1–13. doi: 10.1016/j.jalz.2011.10.007
- Iglói, K., Doeller, C. F., Berthoz, A., Rondi-Reig, L., and Burgess, N. (2010). Lateralized human hippocampal activity predicts navigation based on sequence or place memory. *Proc. Natl. Acad. Sci. U S A* 107, 14466–14471. doi: 10.1002/jdn.10189
- Jack, C. R., Bennett, D. A., Blennow, K., Carrillo, M. C., Dunn, B., Haeberlein, S. B., et al. (2018). NIA-AA research framework: toward a biological definition of Alzheimer's disease. *Alzheimer's Dement.* 14, 535–562. doi: 10.1016/j.jalz.2018.02.018
- Jack, C. R., Dickson, D. W., Parisi, J. E., Xu, Y. C., Cha, R. H., O'Brien, P. C., et al. (2002). Antemortem MRI findings correlate with hippocampal neuropathology in typical aging and dementia. *Neurology* 58, 750–757. doi: 10.1212/wnl.58.5.750
- Jack, C. R., Jr., Petersen, R. C., O'Brien, P. C., and Tangalos, E. G. (1992). MR-based hippocampal volumetry in the diagnosis of Alzheimer's disease. *Neurology* 42, 183–188. doi: 10.1212/wnl.42.1.183
- Jacobs, H. I. L., Hedden, T., Schultz, A. P., Sepulcre, J., Perea, R. D., Amariglio, R. E., et al. (2018). Structural tract alterations predict downstream tau accumulation in amyloid-positive older individuals. *Nat. Neurosci.* 21, 424–431. doi: 10.1038/s41593-018-0070-z
- Josephs, K. A., Whitwell, J. L., Ahmed, Z., Shiung, M. M., Weigand, S. D., Knopman, D. S., et al. (2008). Beta-amyloid burden is not associated with rates of brain atrophy. *Ann. Neurol.* 63, 204–212. doi: 10.1002/ana.21223
- Kuruvilla, M. V., and Ainge, J. A. (2017). Lateral entorhinal cortex lesions impair local spatial frameworks. *Front. Syst. Neurosci.* 11:30. doi: 10.3389/fnsys.2017.00030
- Kuruvilla, M. V., Wilson, D. I. G., and Ainge, J. A. (2020). Lateral entorhinal cortex lesions impair both egocentric and allocentric object-place associations. *Brain Neurosci. Adv.* 4:2398212820939463. doi: 10.1177/2398212820939463

- Laczó, J., Andel, R., Nedelska, Z., Vyhnaek, M., Vlcek, K., Crutch, S., et al. (2017). Exploring the contribution of spatial navigation to cognitive functioning in older adults. *Neurobiol. Aging* 51, 67–70. doi: 10.1016/j.neurobiolaging.2016.12.003
- Laczó, J., Andel, R., Vyhnaek, M., Matoska, V., Kaplan, V., Nedelska, Z., et al. (2015). The effect of TOMM40 on spatial navigation in amnesic mild cognitive impairment. *Neurobiol. Aging* 36, 2024–2033. doi: 10.1016/j.neurobiolaging.2015.03.004
- Laczó, J., Andel, R., Vyhnaek, M., Vlcek, K., Magerova, H., Varjassyova, A., et al. (2010). Human analogue of the morris water maze for testing subjects at risk of Alzheimer's disease. *Neurodegener. Dis.* 7, 148–152. doi: 10.1159/000289226
- Laczó, J., Andel, R., Vyhnaek, M., Vlcek, K., Magerova, H., Varjassyova, A., et al. (2012). From morris water maze to computer tests in the prediction of Alzheimer's disease. *Neurodegener. Dis.* 10, 153–157. doi: 10.1159/00033121
- Laczó, M., Wiener, J. M., Kalinova, J., Matuskova, V., Vyhnaek, M., Hort, J., et al. (2021a). Spatial navigation and visuospatial strategies in typical and atypical aging. *Brain Sci.* 11:1421. doi: 10.3390/brainsci11111421
- Laczó, M., Lerch, O., Martinkovic, L., Kalinova, J., Markova, H., Vyhnaek, M., et al. (2021b). Spatial pattern separation testing differentiates Alzheimer's disease biomarker-positive and biomarker-negative older adults with amnesic mild cognitive impairment. *Front. Aging Neurosci.* 13:774600. doi: 10.3389/fnagi.2021.774600
- Laczó, J., Vlcek, K., Vyhnaek, M., Vajnerová, O., Ort, M., Holmerová, I., et al. (2009). Spatial navigation testing discriminates two types of amnesic mild cognitive impairment. *Behav. Brain Res.* 202, 252–259. doi: 10.1016/j.bbr.2009.03.041
- Lambrey, S., Amorim, M. A., Samson, S., Noulhiane, M., Hasboun, D., Dupont, S., et al. (2008). Distinct visual perspective-taking strategies involve the left and right medial temporal lobe structures differently. *Brain* 131, 523–534. doi: 10.1093/brain/awm317
- Landau, S. M., Harvey, D., Madison, C. M., Koeppe, R. A., Reiman, E. M., Foster, N. L., et al. (2011). Associations between cognitive, functional and FDG-PET measures of decline in AD and MCI. *Neurobiol. Aging* 32, 1207–1218. doi: 10.1016/j.neurobiolaging.2009.07.002
- Levine, T. F., Allison, S. L., Stojanovic, M., Fagan, A. M., Morris, J. C., and Head, D. (2020). Spatial navigation ability predicts progression of dementia symptomatology. *Alzheimers. Dement.* 16, 491–500. doi: 10.1002/alz.12031
- Lindberg, O., Mårtensson, G., Stomrud, E., Palmqvist, S., Wahlund, L. O., Westman, E., et al. (2017). Atrophy of the posterior subiculum is associated with memory impairment, tau- and A β pathology in non-demented individuals. *Front. Aging Neurosci.* 9:306. doi: 10.3389/fnagi.2017.00306
- Lladó, A., Tort-Merino, A., Sánchez-Valle, R., Falgàs, N., Balasa, M., Bosch, B., et al. (2018). The hippocampal longitudinal axis-relevance for underlying tau and TDP-43 pathology. *Neurobiol. Aging* 70, 1–9. doi: 10.1016/j.neurobiolaging.2018.05.035
- Maass, A., Berron, D., Harrison, T. M., Adams, J. N., La Joie, R., Baker, S., et al. (2019). Alzheimer's pathology targets distinct memory networks in the ageing brain. *Brain* 142, 2492–2509. doi: 10.1093/brain/awz154
- Maass, A., Lockhart, S. N., Harrison, T. M., Bell, R. K., Mellinger, T., Swinnerton, K., et al. (2018). Entorhinal tau pathology, episodic memory decline and neurodegeneration in aging. *J. Neurosci.* 38, 530–543. doi: 10.1523/JNEUROSCI.2028-17.2017
- Maguire, E. A., Burgess, N., Donnett, J. G., Frackowiak, R. S., Frith, C. D., and O'Keefe, J. (1998). Knowing where and getting there: a human navigation network. *Science* 280, 921–924. doi: 10.1126/science.280.5365.921
- Marková, H., Laczó, J., Andel, R., Hort, J., and Vlcek, K. (2015). Perspective taking abilities in amnesic mild cognitive impairment and Alzheimer's disease. *Behav. Brain Res.* 281, 229–238. doi: 10.1016/j.bbr.2014.12.033
- Mattsson, N., Schöll, M., Strandberg, O., Smith, R., Palmqvist, S., Insel, P. S., et al. (2017). 18F-AV-1451 and CSF T-tau and P-tau as biomarkers in Alzheimer's disease. *EMBO Mol. Med.* 9, 1212–1223. doi: 10.15252/emmm.201707809
- Mazancova, A. F., Nikolai, T., Stepankova, H., Kopecek, M., and Bezdicek, O. (2017). The reliability of clock drawing test scoring systems modeled on the normative data in healthy aging and nonamnesic mild cognitive impairment. *Assessment* 24, 945–957. doi: 10.1177/1073191116632586
- Mckhann, G. M., Knopman, D. S., Chertkow, H., Hyman, B. T., Jack Jr, C. R., Kawas, C. H., et al. (2011). The diagnosis of dementia due to Alzheimer's disease: recommendations from the national institute on aging and the Alzheimer's association workgroup. *Alzheimers. Dement.* 7, 263–269. doi: 10.1016/j.jalz.2011.03.005
- Miller, M. I., Younes, L., Ratnanather, J. T., Brown, T., Trinh, H., Postell, E., et al. (2013). The diffeomorphometry of temporal lobe structures in preclinical Alzheimer's disease. *Neuroimage Clin.* 3, 352–360. doi: 10.1016/j.nicl.2013.09.001
- Morganti, F., Stefanini, S., and Riva, G. (2013). From allo- to egocentric spatial ability in early Alzheimer's disease: a study with virtual reality spatial tasks. *Cogn. Neurosci.* 4, 171–180. doi: 10.1080/17588928.2013.854762
- Nedelska, Z., Andel, R., Laczó, J., Vlcek, K., Horinek, D., Lisy, J., et al. (2012). Spatial navigation impairment is proportional to right hippocampal volume. *Proc. Natl. Acad. Sci. U S A* 109, 2590–2594. doi: 10.1073/pnas.1121588109
- Nelson, P. T., Dickson, D. W., Trojanowski, J. Q., Jack, C. R., Boyle, P. A., Arfanakis, K., et al. (2019). Limbic-predominant age-related TDP-43 encephalopathy (LATE): consensus working group report. *Brain* 142, 1503–1527. doi: 10.1093/brain/awz099
- Nikolai, T., Stepankova, H., Kopecek, M., Sulc, Z., Vyhnaek, M., and Bezdicek, O. (2018). The uniform data set, czech version: normative data in older adults from an international perspective. *J. Alzheimers. Dis.* 61, 1233–1240. doi: 10.3233/JAD-170595
- Olsen, R. K., Yeung, L. K., Noly-Gandon, A., D'Angelo, M. C., Kacollja, A., Smith, V. M., et al. (2017). Human anterolateral entorhinal cortex volumes are associated with cognitive decline in aging prior to clinical diagnosis. *Neurobiol. Aging* 57, 195–205. doi: 10.1016/j.neurobiolaging.2017.04.025
- Palmqvist, S., Schöll, M., Strandberg, O., Mattsson, N., Stomrud, E., Zetterberg, H., et al. (2017). Earliest accumulation of β -amyloid occurs within the default-mode network and concurrently affects brain connectivity. *Nat. Commun.* 8:1214. doi: 10.1038/s41467-017-01150-x
- Palmqvist, S., Zetterberg, H., Mattsson, N., Johansson, P., Minthon, L., Blennow, K., et al. (2015). Detailed comparison of amyloid PET and CSF biomarkers for identifying early Alzheimer disease. *Neurology* 85, 1240–1249. doi: 10.1212/WNL.0000000000001991
- Parizkova, M., Lerch, O., Andel, R., Kalinova, J., Markova, H., Vyhnaek, M., et al. (2020). Spatial pattern separation in early Alzheimer's disease. *J. Alzheimers. Dis.* 76, 121–138. doi: 10.3233/JAD-200093
- Parizkova, M., Lerch, O., Moffat, S. D., Andel, R., Mazancova, A. F., Nedelska, Z., et al. (2018). The effect of Alzheimer's disease on spatial navigation strategies. *Neurobiol. Aging* 64, 107–115. doi: 10.1016/j.neurobiolaging.2017.12.019
- Reagh, Z. M., and Yassa, M. A. (2014). Object and spatial mnemonic interference differentially engage lateral and medial entorhinal cortex in humans. *Proc. Natl. Acad. Sci. U S A* 111, E4264–E4273. doi: 10.1073/pnas.1411250111
- Reagh, Z. M., Noche, J. A., Tustison, N. J., Delisle, D., Murray, E. A., and Yassa, M. A. (2018). Functional imbalance of anterolateral entorhinal cortex and hippocampal dentate/CA3 underlies age-related object pattern separation deficits. *Neuron* 97, 1187–1198.e4. doi: 10.1016/j.neuron.2018.01.039
- Ruotolo, F., Ruggiero, G., Raemaekers, M., Iachini, T., van der Ham, I. J. M., Fracasso, A., et al. (2019). Neural correlates of egocentric and allocentric frames of reference combined with metric and non-metric spatial relations. *Neuroscience* 409, 235–252. doi: 10.1016/j.neuroscience.2019.04.021
- Saj, A., Cojan, Y., Musel, B., Honoré, J., Borel, L., and Vuilleumier, P. (2014). Functional neuro-anatomy of egocentric versus allocentric space representation. *Neurophysiol. Clin.* 44, 33–40. doi: 10.1016/j.neucli.2013.10.135
- Scahill, R. I., Schott, J. M., Stevens, J. M., Rossor, M. N., and Fox, N. C. (2002). Mapping the evolution of regional atrophy in Alzheimer's disease: unbiased analysis of fluid-registered serial MRI. *Proc. Natl. Acad. Sci. U S A* 99, 4703–4707. doi: 10.1073/pnas.052587399
- Scheltens, P., Leys, D., Barkhof, F., Huglo, D., Weinstein, H. C., Vermersch, P., et al. (1992). Atrophy of medial temporal lobes on MRI in "probable" Alzheimer's disease and normal ageing: diagnostic value and neuropsychological correlates. *J. Neurol. Neurosurg. Psychiatry* 55, 967–972. doi: 10.1136/jnnp.55.10.967
- Schinazi, V. R., Nardi, D., Newcombe, N. S., Shipley, T. F., and Epstein, R. A. (2013). Hippocampal size predicts rapid learning of a cognitive map in humans. *Hippocampus* 23, 515–528. doi: 10.1002/hipo.22111
- Schöberl, F., Pradhan, C., Irving, S., Buerger, K., Xiong, G., Kugler, G., et al. (2020). Real-space navigation testing differentiates between amyloid-

- positive and -negative aMCI. *Neurology* 94, e861–e873. doi: 10.1212/WNL.00000000000008758
- Schöll, M., Maass, A., Mattsson, N., Ashton, N. J., Blennow, K., Zetterberg, H., et al. (2019). Biomarkers for tau pathology. *Mol. Cell. Neurosci.* 97, 18–33. doi: 10.1016/j.mcn.2018.12.001
- Sheardova, K., Vyhnalek, M., Nedelska, Z., Laczó, J., Andel, R., Marciniak, R., et al. (2019). Czech brain aging study (CBAS): prospective multicentre cohort study on risk and protective factors for dementia in the Czech republic. *BMJ Open* 9:e030379. doi: 10.1136/bmjopen-2019-030379
- Sojkova, J., Zhou, Y., An, Y., Kraut, M. A., Ferrucci, L., Wong, D. F., et al. (2011). Longitudinal patterns of β -amyloid deposition in nondemented older adults. *Arch. Neurol.* 68, 644–649. doi: 10.1001/archneurol.2011.77
- Štěpánková, H., Nikolai, T., Lukavský, J., Bezdiček, M., Vraňová, M., and Kopeček, M. (2015). Mini-mental state examination - Czech normative study. *Ces. Slov. Neurol. N* 78/111, 57–63.
- Tapiola, T., Pennanen, C., Tapiola, M., Tervo, S., Kivipelto, M., Hänninen, T., et al. (2008). MRI of hippocampus and entorhinal cortex in mild cognitive impairment: a follow-up study. *Neurobiol. Aging* 29, 31–38. doi: 10.1016/j.neurobiolaging.2006.09.007
- Teng, E., Becker, B. W., Woo, E., Knopman, D. S., Cummings, J. L., and Lu, P. H. (2010). Utility of the functional activities questionnaire for distinguishing mild cognitive impairment from very mild Alzheimer's disease. *Alzheimer Dis. Assoc. Disord.* 24, 348–353. doi: 10.1097/WAD.0b013e3181e2fc84
- Thal, D. R., Rüb, U., Orantes, M., and Braak, H. (2002). Phases of A beta-deposition in the human brain and its relevance for the development of AD. *Neurology* 58, 1791–1800. doi: 10.1212/wnl.58.12.1791
- Tu, S., Spiers, H. J., Hodges, J. R., Piguet, O., and Hornberger, M. (2017). Egocentric versus allocentric spatial memory in behavioral variant frontotemporal dementia and Alzheimer's disease. *J. Alzheimers Dis.* 59, 883–892. doi: 10.3233/JAD-160592
- Tu, S., Wong, S., Hodges, J. R., Irish, M., Piguet, O., and Hornberger, M. (2015). Lost in spatial translation – A novel tool to objectively assess spatial disorientation in Alzheimer's disease and frontotemporal dementia. *Cortex* 67, 83–94. doi: 10.1016/j.cortex.2015.03.016
- Vanderstichele, H., Bibl, M., Engelborghs, S., Le Bastard, N., Lewczuk, P., Molinuevo, J. L., et al. (2012). Standardization of preanalytical aspects of cerebrospinal fluid biomarker testing for Alzheimer's disease diagnosis: a consensus paper from the Alzheimer's biomarkers standardization initiative. *Alzheimers Dement.* 8, 65–73. doi: 10.1016/j.jalz.2011.07.004
- Villain, N., Chételat, G., Grassiot, B., Bourgeat, P., Jones, G., Ellis, K. A., et al. (2012). Regional dynamics of amyloid- β deposition in healthy elderly, mild cognitive impairment and Alzheimer's disease: a voxelwise PiB-PET longitudinal study. *Brain* 135, 2126–2139. doi: 10.1093/brain/aww125
- Villemagne, V. L., Pike, K. E., Chételat, G., Ellis, K. A., Mulligan, R. S., Bourgeat, P., et al. (2011). Longitudinal assessment of A β and cognition in aging and Alzheimer disease. *Ann. Neurol.* 69, 181–192. doi: 10.1002/ana.22248
- Waller, D., and Lippa, Y. (2007). Landmarks as beacons and associative cues: their role in route learning. *Mem. Cognit.* 35, 910–924. doi: 10.3758/bf03193465
- Wang, C., Chen, X., Lee, H., Deshmukh, S. S., Yoganarasimha, D., Savelli, F., et al. (2018). Egocentric coding of external items in the lateral entorhinal cortex. *Science* 362, 945–949. doi: 10.1126/science.aau4940
- Weniger, G., Ruhleder, M., Lange, C., Wolf, S., and Irle, E. (2011). Egocentric and allocentric memory as assessed by virtual reality in individuals with amnesic mild cognitive impairment. *Neuropsychologia* 49, 518–527. doi: 10.1016/j.neuropsychologia.2010.12.031
- Whitwell, J. L., Przybelski, S. A., Weigand, S. D., Knopman, D. S., Boeve, B. F., Petersen, R. C., et al. (2007). 3D maps from multiple MRI illustrate changing atrophy patterns as subjects progress from mild cognitive impairment to Alzheimer's disease. *Brain* 130, 1777–1786. doi: 10.1093/brain/awm112
- Wiener, J. M., Carroll, D., Moeller, S., Bibi, I., Ivanova, D., Allen, P., et al. (2020). A novel virtual-reality-based route-learning test suite: assessing the effects of cognitive aging on navigation. *Behav. Res. Methods* 52, 630–640. doi: 10.3758/s13428-019-01264-8
- Wiener, J. M., de Condappa, O., Harris, M. A., and Wolbers, T. (2013). Maladaptive bias for extrahippocampal navigation strategies in aging humans. *J. Neurosci.* 33, 6012–6017. doi: 10.1523/JNEUROSCI.0717-12.2013
- Wolbers, T., and Hegarty, M. (2010). What determines our navigational abilities? *Trends Cogn. Sci.* 14, 138–146. doi: 10.1016/j.tics.2010.01.001
- Wolbers, T., Weiller, C., and Büchel, C. (2004). Neural foundations of emerging route knowledge in complex spatial environments. *Brain Res. Cogn. Brain Res.* 21, 401–411. doi: 10.1016/j.cogbrainres.2004.06.013
- Wood, R. A., Moodley, K. K., Lever, C., Minati, L., and Chan, D. (2016). Allocentric spatial memory testing predicts conversion from mild cognitive impairment to dementia: an initial proof-of-concept study. *Front. Neurol.* 7:215. doi: 10.3389/fneur.2016.00215
- Xu, J., Evensmoen, H. R., Lehn, H., Pintzka, C. W. S., and Häberg, A. K. (2010). Persistent posterior and transient anterior medial temporal lobe activity during navigation. *Neuroimage* 52, 1654–1666. doi: 10.1016/j.neuroimage.2010.05.074
- Ye, B. S., Kim, H. J., Kim, Y. J., Jung, N. Y., Lee, J. S., Lee, J., et al. (2018). Longitudinal outcomes of amyloid positive versus negative amnesic mild cognitive impairments: a three-year longitudinal study. *Sci. Rep.* 8:5557. doi: 10.1038/s41598-018-23676-w
- Yesavage, J. A., and Sheikh, J. I. (1986). Geriatric depression scale (GDS). *Clin. Gerontol.* 5, 165–173. doi: 10.1300/J018v05n01_09
- Zacks, J. M., and Michelon, P. (2005). Transformations of visuospatial images. *Behav. Cogn. Neurosci. Rev.* 4, 96–118. doi: 10.1177/1534582305281085

Conflict of Interest: The authors declare that the research was conducted in the absence of any commercial or financial relationships that could be construed as a potential conflict of interest.

Publisher's Note: All claims expressed in this article are solely those of the authors and do not necessarily represent those of their affiliated organizations, or those of the publisher, the editors and the reviewers. Any product that may be evaluated in this article, or claim that may be made by its manufacturer, is not guaranteed or endorsed by the publisher.

Copyright © 2022 Laczó, Martinkovic, Lerch, Wiener, Kalinova, Matuskova, Nedelska, Vyhnalek, Hort and Laczó. This is an open-access article distributed under the terms of the Creative Commons Attribution License (CC BY). The use, distribution or reproduction in other forums is permitted, provided the original author(s) and the copyright owner(s) are credited and that the original publication in this journal is cited, in accordance with accepted academic practice. No use, distribution or reproduction is permitted which does not comply with these terms.



OPEN ACCESS

EDITED BY

Agustin Ibanez,
Latin American Brain Health Institute
(BrainLat), Chile

REVIEWED BY

Claudia Duran-Aniotz,
Adolfo Ibáñez University, Chile
Diego Albani,
Mario Negri Pharmacological Research
Institute (IRCCS), Italy

*CORRESPONDENCE

Jong-Ling Fuh
jlfuh@vghtpe.gov.tw

SPECIALTY SECTION

This article was submitted to
Alzheimer's Disease and Related
Dementias,
a section of the journal
Frontiers in Aging Neuroscience

RECEIVED 27 February 2022

ACCEPTED 12 July 2022

PUBLISHED 05 August 2022

CITATION

Chen C-Y, Lin Y-S, Lee W-J, Liao Y-C,
Kuo Y-S, Yang AC and Fuh J-L
(2022) Endophenotypic effects of the
SORL1 variant rs2298813 on regional
brain volume in patients with
late-onset Alzheimer's disease.
Front. Aging Neurosci. 14:885090.
doi: 10.3389/fnagi.2022.885090

COPYRIGHT

© 2022 Chen, Lin, Lee, Liao, Kuo, Yang
and Fuh. This is an open-access article
distributed under the terms of the
Creative Commons Attribution License
(CC BY). The use, distribution or
reproduction in other forums is
permitted, provided the original
author(s) and the copyright owner(s)
are credited and that the original
publication in this journal is cited, in
accordance with accepted academic
practice. No use, distribution or
reproduction is permitted which does
not comply with these terms.

Endophenotypic effects of the *SORL1* variant rs2298813 on regional brain volume in patients with late-onset Alzheimer's disease

Chun-Yu Chen^{1,2,3}, Yung-Shuan Lin^{2,3,4,5}, Wei-Ju Lee^{3,4,6,7,8},
Yi-Chu Liao^{3,4,9}, Yu-Shan Kuo², Albert C. Yang^{3,5}
and Jong-Ling Fuh^{2,3,4*}

¹Department of Medicine, Taipei Veterans General Hospital Yuli Branch, Hualien, Taiwan, ²Division of General Neurology, Neurological Institute, Taipei Veterans General Hospital, Taipei, Taiwan, ³Faculty of Medicine, National Yang Ming Chiao Tung University, Taipei, Taiwan, ⁴Brain Research Center, National Yang-Ming Chiao Tung University, Taipei, Taiwan, ⁵Institute of Brain Science, National Yang Ming Chiao Tung University, Taipei, Taiwan, ⁶Neurological Institute, Taichung Veterans General Hospital, Taichung, Taiwan, ⁷Dementia Center and Center for Geriatrics and Gerontology, Taichung Veterans General Hospital, Taichung, Taiwan, ⁸Department of Post-Baccalaureate Medicine, College of Medicine, National Chung Hsing University, Taichung, Taiwan, ⁹Division of Peripheral Neurology, Neurological Institute, Taipei Veterans General Hospital, Taipei, Taiwan

Introduction: Two common variants of sortilin-related receptor 1 gene (*SORL1*), rs2298813 and rs1784933, have been associated with late-onset Alzheimer's disease (AD) in the Han Chinese population in Taiwan. However, neuroimaging correlates of these two *SORL1* variants remain unknown. We aimed to determine whether the two *SORL1* polymorphisms were associated with any volumetric differences in brain regions in late-onset AD patients.

Methods: We recruited 200 patients with late-onset AD from Taipei Veterans General Hospital. All patients received a structural magnetic resonance (MR) imaging brain scan and completed a battery of neurocognitive tests at enrollment. We followed up to assess changes in Mini-Mental State Examination (MMSE) scores in 155 patients (77.5%) at an interval of 2 years. Volumetric measures and cortical thickness of various brain regions were performed using FreeSurfer. Regression analysis controlled for apolipoprotein E status. Multiple comparisons were corrected for using the false discovery rate.

Results: The homozygous major allele of rs2298813 was associated with larger volumes in the right putamen ($p = 0.0442$) and right pallidum ($p = 0.0346$). There was no link between the rs1784933 genotypes with any regional volume or thickness of the brain. In the rs2298813 homozygous major allele carriers, the right putamen volume was associated with verbal

Abbreviations: Aβ, amyloid-beta; AD, Alzheimer's disease; APOE, apolipoprotein E; APP, amyloid beta precursor protein (APP); MCI, mild cognitive impairment; MMSE, Mini-Mental State Examination; MR, magnetic resonance; SNP, single-nucleotide polymorphism; *SORL1*, sortilin-related receptor 1; *SORL1A*, sorting-related receptor with type-A repeats; VPS10P, vacuolar protein sorting 10 protein.

fluency ($p = 0.008$), and both the right putaminal and pallidal volumes were predictive of clinical progression at follow-up ($p = 0.020$). In the minor allele carriers, neither of the nuclei was related to cognitive test performance or clinical progression.

Conclusion: The major and minor alleles of rs2298813 had differential effects on the right lentiform nucleus volume and distinctively modulated the association between the regional volume and cognitive function in patients with AD.

KEYWORDS

Alzheimer's disease, dementia, sortilin-related receptor 1 gene, SORL1, MRI

Introduction

Accumulation of the neurotoxic proteolytic derivative of amyloid beta precursor protein (APP), amyloid-beta ($A\beta$) peptide, is proposed to be key to the pathogenesis of Alzheimer's disease (AD) (Hardy and Selkoe, 2002). Sortilin-related receptor 1 (SORL1) encodes a mosaic protein (SORLA) consisting of several distinct domains, including the vacuolar protein sorting 10 protein (VPS10P) domain for $A\beta$ binding and the low-density lipoprotein receptor domain for APP binding and lipoprotein binding (Barthelson et al., 2020). SORLA acts as a sorting receptor for retrograde trafficking of APP to the trans-Golgi-network to prevent APP processing to $A\beta$ and anterograde movement of $A\beta$ for lysosomal degradation (Andersen et al., 2016). SORL1 mutations in human neurons lead to reduced levels of SORLA, resulting in defects of the neuronal endolysosome function and autophagy (Hung et al., 2021). In addition, being a low-density lipoprotein receptor, SORLA mediates neuronal uptake of apolipoprotein E (ApoE)-rich lipoproteins (Yajima et al., 2015), the misfolding of which contributes significantly to AD pathogenesis (Barthelson et al., 2020). Ablation of SORLA expression increases $A\beta$ in the brain of knockout mice (Andersen et al., 2005), and SORLA-overexpressing cells have remarkably reduced levels of extracellular $A\beta$ and lower levels of intracellular APP (Offe et al., 2006). In the brains of AD patients, SORL1 expression is reduced (Scherzer et al., 2004). Moreover, both common and rare variants of SORL1 have been associated with late-onset and early-onset AD, respectively (Campion et al., 2019).

SORL1 variants were first identified, among several genes belonging to endocytic pathways, to be associated with sporadic AD by a pioneering study in Caucasians (Rogaeva et al., 2007). Targeted single-nucleotide polymorphism (SNP) analyses and genome-wide association studies have validated the association not only in populations of Caucasian origin but also in Asian populations (Reitz et al., 2011; Lambert et al., 2013; Miyashita et al., 2013). A number of studies have shown

significant associations between specific SORL1 polymorphisms and various phenotypes in AD patients, including lower $A\beta$ levels in cerebrospinal fluid (Alexopoulos et al., 2011) and serum (Chou et al., 2016), increased tau protein in cerebrospinal fluid (Louwersheimer et al., 2015), hippocampal atrophy (Cuenco et al., 2008; Louwersheimer et al., 2015; Xiomerisiou et al., 2021), white matter hyperintensity (Cuenco et al., 2008), frontal symptoms (Huang et al., 2020), rate of cognitive decline (Hsieh et al., 2021), and Parkinsonian features (Cuccaro et al., 2016; Xiomerisiou et al., 2021).

We have previously reported that in the Han Chinese population in Taiwan, two common variants of SORL1, rs2298813, and rs1784933, were associated with late-onset AD (Chou et al., 2016). In the elderly population in Australia and the United States, rs2298813 has also been identified in individuals with late-onset AD (Assareh et al., 2014; Cuccaro et al., 2016). The association of rs1784933 with the risk of late-onset AD has also been reported in the Han Chinese population in China (Feng et al., 2015; Zhang et al., 2017) and Mexicans (Toral-Rios et al., 2022). The SNPrs2298813 is located at the VPS10P domain, and the nonsynonymous substitution of alanine to threonine at the 528th residue (A528T) of SORLA has been shown to increase the secretion of $A\beta_{42}$, soluble APP α , and APP β *in vitro* (Vardarajan et al., 2015). The SNPrs1784933 is located in the 3' region of SORL1, and minor allele carriers with late-onset AD had lower plasma concentrations of $A\beta_{42}$ (Chou et al., 2016). The endophenotypic effects of various SORL1 polymorphisms on the brain have been revealed in nondemented individuals (Liang et al., 2015; Huang et al., 2016; Yin et al., 2016; Li et al., 2017). For example, among the non-demented elders, rs1699102 was associated with gray matter volume of the right middle temporal pole (Li et al., 2017), and rs1784933 and rs753780 was associated with right parahippocampal volume (Yin et al., 2016). However, the neuroimaging correlates of rs2298813 and rs1784933 have not been established in AD patients. We, therefore, aimed to examine the associations between the two SORL1 SNPs and gray matter

volume and cortical thickness of different brain regions in late-onset AD patients.

Materials and methods

Subjects

A total of 200 patients with late-onset AD were enrolled from Taipei Veterans General Hospital, Taiwan. All participants were of Han Chinese descent in Taiwan. Probable AD was diagnosed based on the criteria of the National Institute of Neurological and Communicative Disorders and Stroke/Alzheimer's Disease and Related Disorders Association (Mckhann et al., 2011). The diagnostic survey included history queries (including confirmation of ethnicity by family history), neurological examinations, laboratory tests (including thyroid function, vitamin B12, folate, treponemal tests, renal function, liver enzymes, electrolytes, cell counts, glucose, etc.), and magnetic resonance (MR) imaging of the brain. A subset of patients ($n = 92$) was screened for cognitive fluctuation using the Mayo fluctuation scale (Ferman et al., 2004). The study was approved by the institutional review boards of Taipei Veterans General Hospital. Informed consent was obtained from all patients in accordance with our institutional guidelines and the recommendations of the Declaration of Helsinki.

Genotyping

Whole blood genomic DNA was extracted with a commercial kit in accordance with the manufacturer's instructions (QIAGEN, Hilden, Germany). The alleles of APOE ($\epsilon 2$, $\epsilon 3$, and $\epsilon 4$) were determined by rs429358 and rs7412 (Chen et al., 2012). Genotyping of the two *SORL1* SNPs (rs2298813 and rs1784933) and APOE alleles was performed using the TaqMan genotyping assay (Applied Biosystems, Foster City, CA, USA). Polymerase chain reactions were carried out in 96-well microplates using an ABI 7500 real-time polymerase chain reaction system (Applied Biosystems International, Framingham, MA). For allele discrimination, the fluorescence signal from the TaqMan polymerase chain reaction was analyzed using SDS software version 1.2.3 (Applied Biosystems International, Framingham, MA). Duplicate confirmation was performed if the initial genotyping result was undetermined. The failure rate for rs1784933 and rs2298813 was 0.59% and 1.19% respectively.

Cognitive testing

Global cognitive performance was assessed in each patient using the Mini-Mental State Examination (MMSE; Folstein et al.,

1975). Cognitive domain-specific tests were performed on all patients. Attention was tested by the forward and backward digit span tests from the Wechsler Memory Scale-IV (Wechsler, 2009), memory by the 12-item word recall test (Vanderploeg et al., 2000), language and executive function by the verbal fluency category test (Harrison et al., 2000), processing speed by the Trail Making Test A (Lu and Bigler, 2002), and naming by the Boston naming test (Mack et al., 1992). We followed up to assess changes in MMSE scores over a mean interval of approximately 2 years in these patients. Rapid clinical progression was defined as a decrease in follow-up MMSE by at least 3 points per year (Schmidt et al., 2011).

Imaging analysis

MR images were scanned at Taipei Veterans General Hospital, Taipei, Taiwan, on a 3.0-T GE Signa MRI scanner (GE Medical Systems, Milwaukee, WI, USA). High-resolution anatomic MR images were acquired through a 3D inversion-recovery fast spoiled gradient-echo (BRAVO) sequence. The high-resolution structural T1 images were processed using FreeSurfer version 5.3¹ based on the 2010 Desikan-Killiany atlas. Cortical reconstruction using FreeSurfer involved automated and manual processing. The automated processing included motion correction, nonbrain tissue removal (Fischl et al., 2002), Talairach transformation, segmentation of the subcortical white matter and deep gray matter structures, intensity normalization, tessellation of the boundary between gray and white matter (Segonne et al., 2007), automated topology correction, and surface deformation. When necessary, manual editing was undertaken to correct the pial surface error, skull strip error, or intensity normalization error following the FreeSurfer tutorial. Cortical thickness was calculated as the distance between the white and gray matter surfaces at each point across the regional cortex. There were 68 regions of cortical thickness and 21 regions of gray matter volume included in the statistical analysis. AD-related brain regions included volumes in the hippocampus and thickness of the parahippocampal gyrus, posterior cingulate cortex, middle temporal gyrus, and entorhinal cortex (Yin et al., 2016). Other regions (other than AD-related regions) included all regions except the AD-related brain regions (19 regions of gray matter volume and 60 regions of cortical thickness).

Statistical analysis

Hardy-Weinberg equilibrium tests were conducted for each SNP. A dominant model of inheritance of the minor allele was presumed to test the associations between *SORL1* SNPs and

¹ <http://surfer.nmr.mgh.harvard.edu/>

imaging parameters. The analyses were executed with PASW Statistics software (version 25.0; SPSS, Chicago, IL, USA). Data are expressed as the mean \pm standard deviation or number of patients (%), as appropriate. The χ^2 test was performed for categorical variables, and the t-test was performed for the comparison of two means. Multivariate linear regression analyses were used to assess the relationships between regional cortical thickness or gray matter volume and the *SORL1* SNPs or cognitive test results. The covariates included age, gender, education level, and APOE status. A logistic regression model was conducted to investigate the associations between rapid clinical progression or MMSE changes (points/year) at follow-up and features of selected brain regions with covariates that included age, gender, education level, and APOE status. For regression analysis involving gray matter volume, the estimated intracranial volume was additionally included as a covariate. Multiple comparisons were corrected with the false discovery rate (Benjamini–Hochberg procedure) respectively for gray matter volume (21 regions) and cortical thickness (70 regions). Statistical significance was taken at $P < 0.05$ or Benjamini–Hochberg corrected $P_c < 0.05$.

Results

Demographic data

The demographic data for those with rs2298813 and rs1784933 are shown in **Table 1**. Regarding rs2298813, there were 147 patients carrying the wild homozygote (GG), and 51 patients carrying the minor allele (51 AG and 3 AA). Regarding rs1784933, there were 92 patients carrying the wild homozygote (AA), and 109 patients carrying the minor allele (93 AG and 16 GG). Age, gender, MMSE score, years of education, disease duration, and APOE status did not differ between the homozygous major allele carriers and the minor allele carriers of both SNPs. The Mayo fluctuation scale scores tended to be higher in minor allele carriers than in homozygous major allele carriers of rs2298813 ($p = 0.052$) but were similar between minor allele carriers and non carriers of rs1784933 ($p = 0.935$). For both SNPs, the minor allele carriers performed similarly in all the neuropsychiatric tests as did the homozygous major allele carriers (**Table 1**). A total of 155 patients (77.5%) had a follow-up MMSE

TABLE 1 The demographic data and cognitive test performance of the homozygous major allele carriers and minor allele carriers.

| | Homozygous major allele (<i>n</i> = 146) | Minor allele (<i>n</i> = 54) | <i>P</i> |
|----------------------------|--|----------------------------------|----------|
| rs2298813 | | | |
| <i>Demographic</i> | | | |
| Age, years | 77.5 \pm 7.9 | 78.2 \pm 6.7 | 0.590 |
| Gender (male) | 67 (45.9%) | 23 (42.6%) | 0.677 |
| Education level, years | 10.0 \pm 4.2 | 9.1 \pm 5.0 | 0.240 |
| Disease duration, months | 31.8 \pm 42.5 | 32.9 \pm 29.4 | 0.860 |
| Mayo fluctuations scale | 1.2 \pm 1.3 | 1.8 \pm 1.1 | 0.052 |
| Clinical progression | 26/118 (22.0%) | 10/38 (26.3) | 0.586 |
| <i>Genetic test</i> | | | |
| APOE ϵ 4 | 41 (28.1%) | 24 (44.4%) | 0.074 |
| ϵ 4/ ϵ 4 | 4 (2.7%) | 2 (3.7%) | |
| <i>Cognitive test</i> | | | |
| MMSE score | 19.9 \pm 5.1 | 20.9 \pm 5.2 | 0.197 |
| 12-item word recall | 1.5 \pm 2.0 | 2.1 \pm 2.5 | 0.127 |
| Forward digit span | 8.7 \pm 2.9 | 8.8 \pm 2.7 | 0.900 |
| Backward digit span | 4.2 \pm 1.8 | 4.6 \pm 2.4 | 0.290 |
| Verbal fluency | 7.1 \pm 2.9 | 7.9 \pm 2.9 | 0.079 |
| Boston Naming | 11.1 \pm 2.5 | 11.2 \pm 2.6 | 0.808 |
| Trail Making, seconds | 146.4 \pm 97.4 | 128.9 \pm 81.0 | 0.261 |
| rs1784933 | | | |
| <i>Demographic</i> | | | |
| Age (years) | 77.7 \pm 8.2 | 77.55 \pm 7.38 | 0.870 |
| Gender (male) | 45 (48.9%) | 45 (41.7%) | 0.305 |
| Education (years) | 9.4 \pm 4.2 | 10.0 \pm 4.5 | 0.341 |
| Disease duration (months) | 27.6 \pm 25.0 | 36.1 \pm 48.0 | 0.111 |
| Mayo fluctuations scale | 1.4 \pm 1.3 | 1.4 \pm 1.2 | 0.935 |
| Clinical progression | 19/67 (28.4%) | 18/88 (20.5%) | 0.253 |
| <i>Genetic test</i> | | | |
| APOE ϵ 4 | 29 (31.5%) | 36 (33.3%) | 0.770 |
| ϵ 4/ ϵ 4 | 2 (2.2%) | 4 (3.7%) | |
| <i>Cognitive test</i> | | | |
| MMSE | 19.8 \pm 5.4 | 20.5 \pm 4.7 | 0.313 |
| 12-item word recall | 1.7 \pm 2.1 | 1.7 \pm 2.3 | 0.983 |
| Forward digit span | 8.5 \pm 2.9 | 8.9 \pm 2.8 | 0.253 |
| Backward digit span | 4.2 \pm 1.9 | 4.4 \pm 2.0 | 0.415 |
| Verbal fluency | 7.2 \pm 3.1 | 7.4 \pm 2.8 | 0.696 |
| Boston Naming | 11.0 \pm 2.7 | 11.3 \pm 2.4 | 0.367 |
| Trail Making, seconds | 145.7 \pm 96.1 | 140.7 \pm 93.7 | 0.715 |

APOE, apolipoprotein E; MMSE, Mini-Mental State Examination.

TABLE 2 Associations of homozygous major allele carriers of rs2298813 and rs1784933 with regional cortical thickness/gray matter volume in Alzheimer’s disease (AD)-related brain regions.

| AD-related brain regions | rs2298813 | | | rs1784933 | | |
|---------------------------------|-----------|----------|----------------------|-----------|----------|----------------------|
| | <i>r</i> | <i>p</i> | <i>p_c</i> | <i>r</i> | <i>p</i> | <i>p_c</i> |
| Gray matter volume | | | | | | |
| Right hippocampus | 0.062 | 0.392 | 0.784 | 0.096 | 0.181 | 0.362 |
| Left hippocampus | 0.056 | 0.441 | 0.441 | 0.069 | 0.338 | 0.676 |
| Cortical thickness | | | | | | |
| Right parahippocampal gyrus | 0.122 | 0.0874 | 0.350 | −0.007 | 0.921 | 0.921 |
| Left parahippocampal gyrus | 0.162 | 0.0231 | 0.185 | −0.040 | 0.574 | 0.765 |
| Right posterior cingulate gyrus | 0.047 | 0.517 | 1.000 | 0.087 | 0.224 | 0.896 |
| Left posterior cingulate gyrus | −0.040 | 0.582 | 0.931 | −0.051 | 0.478 | 0.765 |
| Right middle temporal gyrus | −0.080 | 0.263 | 0.701 | −0.121 | 0.0898 | 0.718 |
| Left middle temporal gyrus | −0.032 | 0.652 | 0.869 | −0.073 | 0.311 | 0.622 |
| Right entorhinal cortex | 0.017 | 0.810 | 0.926 | −0.074 | 0.301 | 0.803 |
| Left entorhinal cortex | 0.016 | 0.820 | 0.820 | −0.030 | 0.681 | 0.778 |

r, partial correlation coefficient.

assessment after a mean interval of 2.1 ± 0.8 years, and 37 patients had clinical progression. At follow-up, the minor allele carriers of both SNPs showed no differences in the risk of clinical progression vs. the homozygous major allele carriers.

Associations of rs2298813 and rs1784933 with regional cortical thickness and gray matter volume

The correlations of the genotype of rs2298813 and rs1784933 with regional gray matter volumes or regional cortical thickness in AD-related brain regions and other brain regions are shown in **Tables 2, 3**, respectively. The genotype of rs2298813 was not associated with any of the AD-related brain regions (**Table 2**). Among other brain regions, there were significant partial correlations of volumes in the right putamen and right pallidum with the genotype of rs2298813; the homozygous major allele was associated with larger volumes in the two regions (**Figure 1, Table 3**). With respect to rs1784933, there was no association with any of the brain regions.

Associations of the right lentiform nucleus with cognitive test performance in the homozygous major allele carriers and minor allele carriers of rs2298813

The associations between the right lentiform nucleus and cognitive test performance for the homozygous major allele carriers and minor allele carriers of rs2298813 are shown in **Table 4**. Among the homozygous major allele carriers, the right putaminal volume was significantly related to verbal fluency ($p = 0.008$). At follow-up, the volumes in the right putamen and right pallidum at baseline were positively related to the change in

TABLE 3 Associations of homozygous major allele carriers of rs2298813 and rs1784933 with regional cortical thickness/gray matter volume in other brain regions.

| rs2298813 | <i>r</i> | <i>p</i> | <i>p_c</i> |
|-------------------------------|----------|----------|----------------------|
| | | | |
| Gray matter volume | | | |
| Right putamen | 0.217 | 0.00233 | 0.0442 |
| Right pallidum | 0.207 | 0.00364 | 0.0346 |
| rs1784933 | <i>r</i> | <i>p</i> | <i>p_c</i> |
| Cortical thickness | | | |
| Right superior temporal gyrus | −0.171 | 0.0163 | 0.978 |
| Right postcentral gyrus | −0.154 | 0.0307 | 0.921 |
| Right pars triangularis | −0.149 | 0.0370 | 0.740 |
| Left precentral gyrus | −0.144 | 0.0444 | 0.666 |

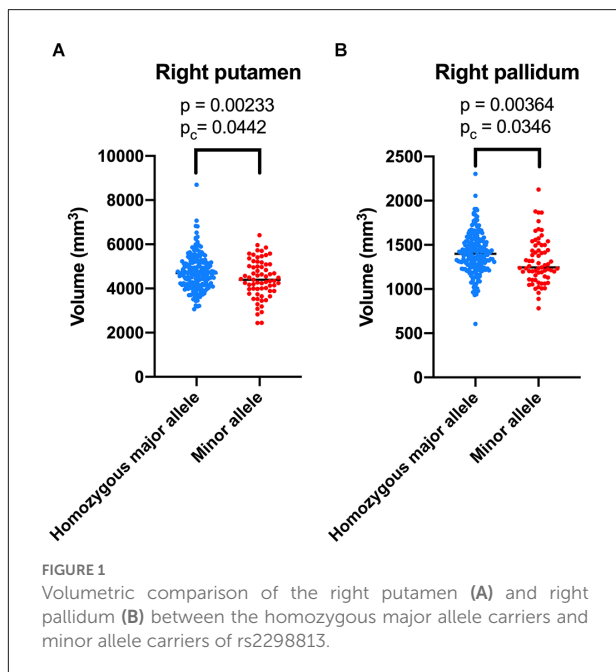
r, partial correlation coefficient.

MMSE scores (partial $r = 0.181$, $p = 0.056$ for the right putamen; partial $r = 0.192$, $p = 0.042$ for the right pallidum, **Table 5**). Logistic regression revealed that lower volumes in both the right putamen ($p = 0.020$) and the right pallidum ($p = 0.013$) were predictive of clinical progression at follow-up (**Table 5**).

Among the minor allele carriers, the volumes of the right putamen and the right pallidum were not associated with any of the cognitive test performance (**Table 4**). At follow-up, neither the right putaminal volume nor the right pallidal volume was associated with the change in MMSE scores (partial $r = 0.043$, $p = 0.814$ for the right putamen; partial $r = -0.138$, $p = 0.444$ for the right pallidum) or clinical progression ($p = 0.791$ for the right putamen, $p = 0.191$ for the right pallidum, **Table 5**).

Discussion

We found that the volume of the right lentiform nucleus differed between the homozygous major allele carriers of rs2298813 and the minor allele carriers in late-onset AD patients. With respect to rs1784933, there were no neuroimaging correlates of the genotype. Among the homozygous major allele carriers



of rs2298813, there was an association between right putamen volume and verbal fluency performance, and the right putamen and right pallidal volumes were predictive of clinical progression. On the contrary, the minor allele carriers of rs2298813 had a smaller volume of the right lentiform nucleus and a higher cognitive fluctuation score. However, the right putamen and right pallidal volumes were not related to neurocognitive test performance nor predictive of clinical progression among these patients. It appeared that the major and minor alleles of rs2298813 had differential effects on the volume of the right lentiform nucleus and differentially modulated the association between the right lentiform nucleus and cognitive function.

The earliest associations between rs2298813 and rs1784933 and brain atrophy were delineated in a collection of autopsied AD brains (Cuenco et al., 2008). The 3-SNP

haplotypes containing the rs1784933 region were related to pathological scoring and MRI traits of hippocampal atrophy in white AD patients, whereas no significant associations were identified for rs2298813 (Cuenco et al., 2008). In an Australian cohort, a 3-SNP haplotype containing rs2298813 was associated with whole brain atrophy in both males and females, but rs2298813 was not individually associated with brain atrophy (Assareh et al., 2014). A study using the Alzheimer's Disease Neuroimaging Initiative database investigated the effect of eight *SORL1* SNPs, including rs2298813 and rs1784933, on AD-related brain atrophy in subjects with normal cognition or mild cognitive impairment (MCI) (Yin et al., 2016). The A allele of rs2298813 tended to be associated with a lower volume in the right parahippocampal gyrus, and the G allele of rs1784933 was found to be associated with a higher rate of atrophy in the right parahippocampal gyrus across a 2-year span (Yin et al., 2016). In a young healthy Caucasian population, 117 SNPs in and surrounding *SORL1* were examined to determine any association with hippocampal volume, and the majority of significant associations occurred at the 3' region, where rs1784933 is located (Bralten et al., 2011). The discrepancy in the relationship between rs2298813/rs1784933 and brain atrophy may lie in ethnic differences (Jin et al., 2013) and the small effect of a single SNP that may be better demonstrated in quantitative measurement of brain volume or in haplotype analysis.

The putamen and pallidum (forming the lentiform nucleus) are essential elements of the extrapyramidal system and are usually involved in motor disturbances, such as Parkinsonism or Huntington's disease (Albin et al., 1989). Although not included among the typical AD-related brain structures, numerous studies have disclosed an association of these regions with AD. The volume of the putamen has been shown to be reduced in AD brains relative to subjects with MCI or normal aging (De Jong et al., 2008; Roh et al., 2011; Cho et al., 2014; Tang et al., 2014; Eustache et al., 2016; Pini et al., 2016). Such reductions can occur as early as in the prodromal stage (Eustache et al., 2016). Atrophy in the pallidum has not been consistently observed in

TABLE 4 Associations of the volume of the right lentiform nucleus with cognitive test performance in homozygous major allele carriers ($n = 146$) and minor allele carriers ($n = 54$) of rs2298813.

| | Homozygous major allele | | | | Minor allele | | | |
|---------------------|-------------------------|-------|----------------|-------|---------------|-------|----------------|-------|
| | Right putamen | | Right pallidum | | Right putamen | | Right pallidum | |
| | r | p | r | p | r | p | r | p |
| MMSE | 0.161 | 0.056 | 0.061 | 0.473 | 0.151 | 0.302 | 0.131 | 0.371 |
| 12-item word recall | 0.088 | 0.299 | 0.020 | 0.815 | -0.149 | 0.311 | -0.093 | 0.529 |
| Forward digit span | 0.121 | 0.152 | -0.030 | 0.723 | 0.239 | 0.098 | 0.223 | 0.123 |
| Backward digit span | 0.013 | 0.878 | 0.016 | 0.847 | 0.098 | 0.501 | 0.186 | 0.201 |
| Verbal fluency | 0.224 | 0.008 | 0.058 | 0.494 | 0.037 | 0.802 | 0.057 | 0.696 |
| Boston Naming | 0.100 | 0.238 | 0.092 | 0.276 | 0.159 | 0.276 | 0.209 | 0.149 |
| Trail Making | -0.146 | 0.090 | 0.009 | 0.916 | -0.121 | 0.435 | -0.086 | 0.578 |

MMSE, Mini-Mental State Examination; r, partial correlation coefficient.

TABLE 5 Associations of the volumes of the right lentiform nucleus at baseline with clinical progression and MMSE changes at follow-up in homozygous major allele carriers ($n = 118$) and minor allele carriers ($n = 38$) of rs2298813.

| Clinical progression | Homozygous major allele | | Minor allele | |
|---|-------------------------|----------|----------------------|----------|
| | OR (95% CI) | <i>p</i> | OR (95% CI) | <i>p</i> |
| Right putaminal volume (mm ³) | 0.999 (0.998–1.000) | 0.020 | 1.000 (0.999–1.001) | 0.791 |
| Right pallidal volume (mm ³) | 0.997 (0.994–0.999) | 0.013 | 1.003 (0.998–1.009) | 0.191 |
| MMSE changes at follow-up | Standardized β | | Standardized β | |
| | | <i>p</i> | | <i>p</i> |
| Right putaminal volume (mm ³) | 0.188 | 0.056 | 0.041 | 0.814 |
| Right pallidal volume (mm ³) | 0.211 | 0.042 | −0.179 | 0.444 |

CI, confidence interval; MMSE, Mini-Mental State Examination; OR, odds ratio.

previous studies (Cho et al., 2014; Pini et al., 2016). The pallidum is relatively resistant to degeneration even in moderate stages of the disease (Roh et al., 2011) although mild atrophy may be observed (Li et al., 2013; Tang et al., 2014; Wang et al., 2018). AD pathology has been demonstrated to deposit heavily in the putamen and less in the pallidum (Braak and Braak, 1990). Similarly, iron detection using MR techniques (quantitative susceptibility mapping or phase imaging) has revealed iron accumulation in the putamen and pallidum (Bartzikis et al., 2000; Cogswell et al., 2021), which was associated with higher amyloid PET standardized uptake value ratios (Cogswell et al., 2021). The association of putaminal or pallidal atrophy with common variants of *SORL1* has not been previously specified in AD patients. The most relevant study was conducted by Huang et al. investigating the effect of rs3824968 on gray matter volume in a nondemented Chinese population across a wide age span (Huang et al., 2016). Participants carrying the A allele had accelerated atrophy with age in the right putamen (Huang et al., 2016). Thus, we are the first to identify a link between putaminal/pallidal atrophy and *SORL1* polymorphisms in AD.

The putamen and pallidum also have functions related to cognition. In patients with Parkinson's disease, deep brain stimulation of the pallidum has been shown to improve verbal fluency. (Lee et al., 2018) In human immunodeficiency virus-associated neurocognitive impairment, there was an association between cognitive impairment and putaminal volume (Qi et al., 2021). Among patients with behavioral variant frontotemporal dementia, there is a relationship between atrophy in the putamen and the theory of mind impairment (Baez et al., 2019). In support of this, in our study, relationships between both verbal fluency and the annual rate of changes in MMSE scores and right putaminal volume were observed in the homozygous major allele carriers of rs2298813. In contrast, there were no significant associations between right putaminal/right pallidal volumes and cognitive test performance or clinical progression in the minor allele carriers even though the right lentiform nucleus was smaller in these patients. This may suggest that in this subgroup of patients, atrophy in the right lentiform nucleus did not have a deleterious impact on cognitive function. The

atrophy may, for example, have more effect on motor function. Further study is needed to elucidate the phenotypic effect of regional atrophy in the right lentiform nucleus in the minor allele carriers of rs2298813.

The link between rs2298813 and the lentiform nucleus volume may provide a pathophysiological basis for the association between AD and parkinsonism. Indeed, Parkinsonism is not uncommon in AD. Extrapyramidal signs can be detected in one-third of AD patients during the course of the disease (Scarmeas et al., 2004), and Parkinsonian features are related to neuronal loss in the substantia nigra and putamen (Horvath et al., 2014). A previous study reported that three out of four patients with late-onset AD with Parkinsonism carried the A allele of rs2298813 (Cuccaro et al., 2016). In a case report, 4 AD patients with Parkinsonism and psychiatric symptoms were found to have novel mutations in *SORL1*, with two mutations at the VPS10P region, where rs2298813 is located (Qiu et al., 2021). Our minor allele carriers also had higher scores on the Mayo fluctuation scale, implying a link with features of Lewy body dementia. Moreover, the minor allele of rs2298813 has been found to increase the risk of developing dementia in patients with Parkinson's disease (Maple-Groden et al., 2018). In the northern Chinese population, rs2298813 was associated with an increased risk of Parkinson's disease (Wang et al., 2022). In addition to its involvement in the APP pathway, *SORL1* also mediates the trophic pathway involving glial cell line-derived neurotrophic factor (Glerup et al., 2013), the absence of which could lead to the loss of dopaminergic neurons (Lin et al., 1993).

There were several limitations of the current study. First, we did not systemically qualify and quantify the motor symptoms in these patients. Therefore, the postulated relationship between atrophy in the putamen and pallidum and pyramidal/extrapyramidal symptoms warrants further study. Second, these patients were followed up for an average of 2 years, so a longer follow-up duration may better confirm the cognitive or motor effects of the volumetric changes in the putamen and pallidum. Third, the sample size is much smaller in the minor allele carrier of rs2298813, so the absence of an association with

cognitive test performance may be a consequence of low power. The inclusion of more patients with this genotype would help to confirm our findings.

Conclusion

The volume of the right lentiform nucleus was associated with cognitive function and clinical progression in late-onset AD patients with the homozygous major allele of rs2298813. Whereas, among the minor allele carriers, the volume of the right lentiform nucleus was smaller, and was not associated with cognitive function or clinical progression.

Data availability statement

The original contributions presented in the study are included in the article, further inquiries can be directed to the corresponding author.

Ethics statement

The studies involving human participants were reviewed and approved by the institutional review boards of Taipei Veterans General Hospital (IRB number 2012-05-033B). The patients/participants provided their written informed consent to participate in this study.

Author contributions

C-YC wrote the manuscript. J-LF, C-YC, Y-CL, and W-JL contributed to the study concept and design. C-YC, Y-SL, W-JL, AY, and J-LF contributed to analysis and interpretation of data. Y-SL, W-JL, Y-SK, and J-LF contributed to acquisition of data. W-JL, Y-CL, and J-LF revised the manuscript. All authors contributed to the article and approved the submitted version.

References

- Albin, R. L., Young, A. B., and Penney, J. B. (1989). The functional anatomy of basal ganglia disorders. *Trends Neurosci.* 12, 366–375. doi: 10.1016/0166-2236(89)90074-x
- Alexopoulos, P., Guo, L. H., Kratzer, M., Westerteicher, C., Kurz, A., and Perneczky, R. (2011). Impact of SORL1 single nucleotide polymorphisms on Alzheimer's disease cerebrospinal fluid markers. *Dement. Geriatr. Cogn. Disord.* 32, 164–170. doi: 10.1159/000332017
- Andersen, O. M., Reiche, J., Schmidt, V., Gotthardt, M., Spoelgen, R., Behlke, J., et al. (2005). Neuronal sorting protein-related receptor sorLA/LR11 regulates processing of the amyloid precursor protein. *Proc. Natl. Acad. Sci. U S A* 102, 13461–13466. doi: 10.1073/pnas.0503689102
- Andersen, O. M., Rudolph, I. M., and Willnow, T. E. (2016). Risk factor SORL1: from genetic association to functional validation in Alzheimer's disease. *Acta Neuropathol.* 132, 653–665. doi: 10.1007/s00401-016-1615-4
- Assareh, A. A., Piguet, O., Lye, T. C., Mather, K. A., Broe, G. A., Schofield, P. R., et al. (2014). Association of SORL1 gene variants with hippocampal and cerebral atrophy and Alzheimer's disease. *Curr. Alzheimer Res.* 11, 558–563. doi: 10.2174/1567205011666140618101408
- Baez, S., Pinasco, C., Roca, M., Ferrari, J., Couto, B., Garcia-Cordero, I., et al. (2019). Brain structural correlates of executive and social cognition profiles in behavioral variant frontotemporal dementia and elderly bipolar disorder. *Neuropsychologia* 126, 159–169. doi: 10.1016/j.neuropsychologia.2017.02.012
- Barthelson, K., Newman, M., and Lardelli, M. (2020). Sorting out the role of the sortilin-related receptor 1 in Alzheimer's disease. *J. Alzheimers Dis. Rep.* 4, 123–140. doi: 10.3233/ADR-200177
- Bartzokis, G., Sultzer, D., Cummings, J., Holt, L. E., Hance, D. B., Henderson, V. W., et al. (2000). *in vivo* evaluation of brain iron in Alzheimer disease using magnetic resonance imaging. *Arch. Gen. Psychiatry* 57, 47–53. doi: 10.1001/archpsyc.57.1.47

Funding

This study was supported by grants from the National Health Research Institutes, Taiwan (NHRI-11A1-CG-CO-05-2225-1), the Ministry of Science and Technology, Taiwan (MOST 109-2314-B-075-052-MY2, 110-2321-B-001-011-, 110-2321-B-A49A-502-, 110-2634-F-A49-005-), Taipei Veterans General Hospital (V110C-057, VGHUST110-G1-5-1, V111C-216) and the Brain Research Center, National Yang Ming Chiao Tung University from the Featured Areas Research Center Program within the framework of the Higher Education Sprout Project by the Ministry of Education (MOE) in Taiwan.

Acknowledgments

We thank Dr. Judy Pa and Vahan Aslanyan for their suggestions regarding the imaging preprocessing and acknowledge all neuropsychological assessors and patients for their cooperation.

Conflict of interest

The authors declare that the research was conducted in the absence of any commercial or financial relationships that could be construed as a potential conflict of interest.

Publisher's note

All claims expressed in this article are solely those of the authors and do not necessarily represent those of their affiliated organizations, or those of the publisher, the editors and the reviewers. Any product that may be evaluated in this article, or claim that may be made by its manufacturer, is not guaranteed or endorsed by the publisher.

- Braak, H., and Braak, E. (1990). Alzheimer's disease: striatal amyloid deposits and neurofibrillary changes. *J. Neuropathol. Exp. Neurol.* 49, 215–224.
- Bralten, J., Arias-Vasquez, A., Makkinje, R., Veltman, J. A., Brunner, H. G., Fernandez, G., et al. (2011). Association of the Alzheimer's gene SORL1 with hippocampal volume in young, healthy adults. *Am. J. Psychiatry* 168, 1083–1089. doi: 10.1176/appi.ajp.2011.10101509
- Campion, D., Charbonnier, C., and Nicolas, G. (2019). SORL1 genetic variants and Alzheimer disease risk: a literature review and meta-analysis of sequencing data. *Acta Neuropathol.* 138, 173–186. doi: 10.1007/s00401-019-01991-4
- Chen, C. S., Ouyang, P., Yeh, Y. C., Lai, C. L., Liu, C. K., Yen, C. F., et al. (2012). Apolipoprotein E polymorphism and behavioral and psychological symptoms of dementia in patients with Alzheimer disease. *Alzheimer Dis. Assoc. Disord.* 26, 135–139. doi: 10.1097/WAD.0b013e31821f5787
- Cho, H., Kim, J. H., Kim, C., Ye, B. S., Kim, H. J., Yoon, C. W., et al. (2014). Shape changes of the basal ganglia and thalamus in Alzheimer's disease: a three-year longitudinal study. *J. Alzheimers Dis.* 40, 285–295. doi: 10.3233/JAD-132072
- Chou, C. T., Liao, Y. C., Lee, W. J., Wang, S. J., and Fuh, J. L. (2016). SORL1 gene, plasma biomarkers and the risk of Alzheimer's disease for the Han Chinese population in Taiwan. *Alzheimers Res. Ther.* 8:53. doi: 10.1186/s13195-016-0222-x
- Cogswell, P. M., Wiste, H. J., Senjem, M. L., Gunter, J. L., Weigand, S. D., Schwarz, C. G., et al. (2021). Associations of quantitative susceptibility mapping with Alzheimer's disease clinical and imaging markers. *Neuroimage* 224:117433. doi: 10.1016/j.neuroimage.2020.117433
- Cuccaro, M. L., Carney, R. M., Zhang, Y., Bohm, C., Kunkle, B. W., Vardarajan, B. N., et al. (2016). SORL1 mutations in early- and late-onset Alzheimer disease. *Neurol. Genet.* 2:e116. doi: 10.1212/NXG.0000000000000116
- Cuenca, K. T., Lunetta, K. L., Baldwin, C. T., McKee, A. C., Guo, J., Cupples, L. A., et al. (2008). Association of distinct variants in SORL1 with cerebrovascular and neurodegenerative changes related to Alzheimer disease. *Arch. Neurol.* 65, 1640–1648. doi: 10.1001/archneur.65.12.1640
- De Jong, L. W., Van Der Hiele, K., Veer, I. M., Houwing, J. J., Westendorp, R. G., Bollen, E. L., et al. (2008). Strongly reduced volumes of putamen and thalamus in Alzheimer's disease: an MRI study. *Brain* 131, 3277–3285. doi: 10.1093/brain/awn278
- Eustache, P., Nemmi, F., Saint-Aubert, L., Pariente, J., and Peran, P. (2016). Multimodal magnetic resonance imaging in Alzheimer's disease patients at prodromal stage. *J. Alzheimers Dis.* 50, 1035–1050. doi: 10.3233/JAD-150353
- Feng, X., Hou, D., Deng, Y., Li, W., Tian, M., and Yu, Z. (2015). SORL1 gene polymorphism association with late-onset Alzheimer's disease. *Neurosci. Lett.* 584, 382–389. doi: 10.1016/j.neulet.2014.10.055
- Ferman, T. J., Smith, G. E., Boeve, B. F., Ivnik, R. J., Petersen, R. C., Knopman, D., et al. (2004). DLB fluctuations: specific features that reliably differentiate DLB from AD and normal aging. *Neurology* 62, 181–187. doi: 10.1212/wnl.62.2.181
- Fischl, B., Salat, D. H., Busa, E., Albert, M., Dieterich, M., Haselgrove, C., et al. (2002). Whole brain segmentation: automated labeling of neuroanatomical structures in the human brain. *Neuron* 33, 341–355. doi: 10.1016/s0896-6273(02)00569-x
- Folstein, M. F., Folstein, S. E., and McHugh, P. R. (1975). "Mini-mental state". A practical method for grading the cognitive state of patients for the clinician. *J. Psychiatr. Res.* 12, 189–198. doi: 10.1016/0022-3956(75)90026-6
- Glerup, S., Lume, M., Olsen, D., Nyengaard, J. R., Vaegter, C. B., Gustafsen, C., et al. (2013). SorLA controls neurotrophic activity by sorting of GDNF and its receptors GFR α 1 and RET. *Cell Rep.* 3, 186–199. doi: 10.1016/j.celrep.2012.12.011
- Hardy, J., and Selkoe, D. J. (2002). The amyloid hypothesis of Alzheimer's disease: progress and problems on the road to therapeutics. *Science* 297, 353–356. doi: 10.1126/science.1072994
- Harrison, J. E., Buxton, P., Husain, M., and Wise, R. (2000). Short test of semantic and phonological fluency: normal performance, validity and test-retest reliability. *Br. J. Clin. Psychol.* 39, 181–191. doi: 10.1348/014466500163202
- Horvath, J., Burkhard, P. R., Herrmann, F. R., Bouras, C., and Kovari, E. (2014). Neuropathology of parkinsonism in patients with pure Alzheimer's disease. *J. Alzheimers Dis.* 39, 115–120. doi: 10.3233/JAD-131289
- Hsieh, T. J., Lee, W. J., Liao, Y. C., Hsu, C. C., Fang, Y. H., Chen, T. Y., et al. (2021). Association between Alzheimer's disease genes and trajectories of cognitive function decline in Han Chinese in Taiwan. *Aging (Albany NY)* 13, 17237–17252. doi: 10.18632/aging.203204
- Huang, M. F., Lee, W. J., Yeh, Y. C., Liao, Y. C., Wang, S. J., Yang, Y. H., et al. (2020). Genetics of neuropsychiatric symptoms in patients with Alzheimer's disease: a 1-year follow-up study. *Psychiatry Clin. Neurosci.* 74, 645–651. doi: 10.1111/pcn.13150
- Huang, C. C., Liu, M. E., Kao, H. W., Chou, K. H., Yang, A. C., Wang, Y. H., et al. (2016). Effect of Alzheimer's disease risk variant rs3824968 at SORL1 on regional gray matter volume and age-related interaction in adult lifespan. *Sci. Rep.* 6:23362. doi: 10.1038/srep23362
- Hung, C., Tuck, E., Stubbs, V., Van Der Lee, S. J., Aalfs, C., Van Spaendonk, R., et al. (2021). SORL1 deficiency in human excitatory neurons causes APP-dependent defects in the endolysosome-autophagy network. *Cell Rep.* 35:109259. doi: 10.1016/j.celrep.2021.109259
- Jin, C., Liu, X., Zhang, F., Wu, Y., Yuan, J., Zhu, J., et al. (2013). An updated meta-analysis of the association between SORL1 variants and the risk for sporadic Alzheimer's disease. *J. Alzheimers Dis.* 37, 429–437. doi: 10.3233/JAD-130533
- Lambert, J. C., Ibrahim-Verbaas, C. A., Harold, D., Naj, A. C., Sims, R., Bellenguez, C., et al. (2013). Meta-analysis of 74,046 individuals identifies 11 new susceptibility loci for Alzheimer's disease. *Nat. Genet.* 45, 1452–1458. doi: 10.1038/ng.2802
- Lee, P. S., Crammond, D. J., and Richardson, R. M. (2018). Deep brain stimulation of the subthalamic nucleus and globus pallidus for Parkinson's disease. *Prog. Neurol. Surg.* 33, 207–221. doi: 10.1159/000481105
- Li, Y. D., He, H. J., Dong, H. B., Feng, X. Y., Xie, G. M., and Zhang, L. J. (2013). Discriminative analysis of early-stage Alzheimer's disease and normal aging with automatic segmentation technique in subcortical gray matter structures: a multicenter in vivo MRI volumetric and DTI study. *Acta Radiol.* 54, 1191–1200. doi: 10.1177/0284185113492971
- Li, H., Lv, C., Yang, C., Wei, D., Chen, K., Li, S., et al. (2017). SORL1 rs1699102 polymorphism modulates age-related cognitive decline and gray matter volume reduction in non-demented individuals. *Eur. J. Neurol.* 24, 187–194. doi: 10.1111/ene.13182
- Liang, Y., Li, H., Lv, C., Shu, N., Chen, K., Li, X., et al. (2015). Sex moderates the effects of the Sorl1 gene rs2070045 polymorphism on cognitive impairment and disruption of the cingulum integrity in healthy elderly. *Neuropsychopharmacology* 40, 1519–1527. doi: 10.1038/npp.2015.1
- Lin, L. F., Doherty, D. H., Lile, J. D., Bektess, S., and Collins, F. (1993). GDNF: a glial cell line-derived neurotrophic factor for midbrain dopaminergic neurons. *Science* 260, 1130–1132. doi: 10.1126/science.8493557
- Louwensheimer, E., Ramirez, A., Cruchaga, C., Becker, T., Kornhuber, J., Peters, O., et al. (2015). Influence of genetic variants in SORL1 gene on the manifestation of Alzheimer's disease. *Neurobiol. Aging* 36, 1605.e13–1620.e13. doi: 10.1016/j.neurobiolaging.2014.12.007
- Lu, L., and Bigler, E. D. (2002). Normative data on trail making test for neurologically normal, Chinese-speaking adults. *Appl. Neuropsychol.* 9, 219–225. doi: 10.1207/S15324826AN0904_4
- Mack, W. J., Freed, D. M., Williams, B. W., and Henderson, V. W. (1992). Boston naming test: shortened versions for use in Alzheimer's disease. *J. Gerontol.* 47, P154–P158. doi: 10.1093/geronj/47.3.p154
- Maple-Groden, J., Chung, J., Lund, K. A., Tzoulis, C., Tysnes, O. B., Pedersen, K. F., et al. (2018). Alzheimer disease associated variants in SORL1 accelerate dementia development in Parkinson disease. *Neurosci. Lett.* 674, 123–126. doi: 10.1016/j.neulet.2018.03.036
- Mckhann, G. M., Knopman, D. S., Chertkow, H., Hyman, B. T., Jack, C. R., Jr., Kawas, C. H., et al. (2011). The diagnosis of dementia due to Alzheimer's disease: recommendations from the National Institute on Aging-Alzheimer's Association workgroups on diagnostic guidelines for Alzheimer's disease. *Alzheimers Dement.* 7, 263–269. doi: 10.1016/j.jalz.2011.03.005
- Miyashita, A., Koike, A., Jun, G., Wang, L. S., Takahashi, S., Matsubara, E., et al. (2013). SORL1 is genetically associated with late-onset Alzheimer's disease in Japanese, Koreans and Caucasians. *PLoS One* 8:e58618. doi: 10.1371/journal.pone.0058618
- Offe, K., Dodson, S. E., Shoemaker, J. T., Fritz, J. J., Gearing, M., Levey, A. I., et al. (2006). The lipoprotein receptor LR11 regulates amyloid β production and amyloid precursor protein traffic in endosomal compartments. *J. Neurosci.* 26, 1596–1603. doi: 10.1523/JNEUROSCI.4946-05.2006
- Pini, L., Pievani, M., Bocchetta, M., Altomare, D., Bosco, P., Cavado, E., et al. (2016). Brain atrophy in Alzheimer's Disease and aging. *Ageing Res. Rev.* 30, 25–48. doi: 10.1016/j.arr.2016.01.002
- Qi, Y., Xu, M., Wang, W., Wang, Y. Y., Liu, J. J., Ren, H. X., et al. (2021). Early prediction of putamen imaging features in HIV-associated neurocognitive impairment syndrome. *BMC Neurol.* 21:106. doi: 10.1186/s12883-021-02114-x
- Qiu, G., Xu, C., Guo, Q., and Zhu, F. Q. (2021). SORL1 mutations are associated with parkinsonian and psychiatric features in Alzheimer disease: Case reports. *Medicine (Baltimore)* 100:e25585. doi: 10.1097/MD.00000000000025585

- Reitz, C., Cheng, R., Rogaeva, E., Lee, J. H., Tokuhira, S., Zou, F., et al. (2011). Meta-analysis of the association between variants in SORL1 and Alzheimer disease. *Arch. Neurol.* 68, 99–106. doi: 10.1001/archneurol.2010.346
- Rogaeva, E., Meng, Y., Lee, J. H., Gu, Y., Kawarai, T., Zou, F., et al. (2007). The neuronal sortilin-related receptor SORL1 is genetically associated with Alzheimer disease. *Nat. Genet.* 39, 168–177. doi: 10.1038/ng1943
- Roh, J. H., Qiu, A., Seo, S. W., Soon, H. W., Kim, J. H., Kim, G. H., et al. (2011). Volume reduction in subcortical regions according to severity of Alzheimer's disease. *J. Neurol.* 258, 1013–1020. doi: 10.1007/s00415-010-5872-1
- Scarmeas, N., Hadjigeorgiou, G. M., Papadimitriou, A., Dubois, B., Sarazin, M., Brandt, J., et al. (2004). Motor signs during the course of Alzheimer disease. *Neurology* 63, 975–982. doi: 10.1212/01.wnl.0000138440.39918.0c
- Scherzer, C. R., Offe, K., Gearing, M., Rees, H. D., Fang, G., Heilman, C. J., et al. (2004). Loss of apolipoprotein E receptor LR11 in Alzheimer disease. *Arch. Neurol.* 61, 1200–1205. doi: 10.1001/archneur.61.8.1200
- Schmidt, C., Wolff, M., Weitz, M., Bartlau, T., Korth, C., and Zerr, I. (2011). Rapidly progressive Alzheimer disease. *Arch. Neurol.* 68, 1124–1130. doi: 10.1001/archneurol.2011.189
- Segonne, F., Pacheco, J., and Fischl, B. (2007). Geometrically accurate topology-correction of cortical surfaces using nonseparating loops. *IEEE Trans. Med. Imaging* 26, 518–529. doi: 10.1109/TMI.2006.887364
- Tang, X., Holland, D., Dale, A. M., Younes, L., Miller, M. I., and Alzheimer's Disease Neuroimaging Initiative (2014). Shape abnormalities of subcortical and ventricular structures in mild cognitive impairment and Alzheimer's disease: detecting, quantifying and predicting. *Hum. Brain Mapp.* 35, 3701–3725. doi: 10.1002/hbm.22431
- Toral-Rios, D., Ruiz-Sánchez, E., Rodríguez, N. L. M., Maury-Rosillo, M., Rosas-Carrasco, Ó., Becerril-Pérez, F., et al. (2022). SORL1 polymorphisms in Mexican patients with Alzheimer's disease. *Genes (Basel)* 13:587. doi: 10.3390/genes13040587
- Vanderploeg, R. D., Schinka, J. A., Jones, T., Small, B. J., Graves, A. B., and Mortimer, J. A. (2000). Elderly norms for the Hopkins Verbal Learning Test-Revised. *Clin. Neuropsychol.* 14, 318–324. doi: 10.1076/1385-4046(200008)14:3;1-P;FT318
- Vardarajan, B. N., Zhang, Y., Lee, J. H., Cheng, R., Bohm, C., Ghani, M., et al. (2015). Coding mutations in SORL1 and Alzheimer disease. *Ann. Neurol.* 77, 215–227. doi: 10.1002/ana.24305
- Wang, Y., Luan, M., Xue, L., Jin, J., and Xie, A. (2022). Evaluation of the relationship between SORL1 gene polymorphism and Parkinson's disease in the Chinese population. *Neurosci. Lett.* 778:136602. doi: 10.1016/j.neulet.2022.136602
- Wang, M. L., Wei, X. E., Fu, J. L., Li, W., Yu, M. M., Li, P. Y., et al. (2018). Subcortical nuclei in Alzheimer's disease: a volumetric and diffusion kurtosis imaging study. *Acta Radiol.* 59, 1365–1371. doi: 10.1177/0284185118758122
- Wechsler, D. (2009). *WMS-IV: Wechsler Memory Scale 4th Edition*. New York, NY: The Psychological Corporation.
- Xiromerisiou, G., Bourinaris, T., Houlden, H., Lewis, P. A., Senkevich, K., Hammer, M., et al. (2021). SORL1 mutation in a Greek family with Parkinson's disease and dementia. *Ann. Clin. Transl. Neurol.* 8, 1961–1969. doi: 10.1002/acn3.51433
- Yajima, R., Tokutake, T., Koyama, A., Kasuga, K., Tezuka, T., Nishizawa, M., et al. (2015). ApoE-isoform-dependent cellular uptake of amyloid- β is mediated by lipoprotein receptor LR11/SorLA. *Biochem. Biophys. Res. Commun.* 456, 482–488. doi: 10.1016/j.bbrc.2014.11.111
- Yin, R. H., Li, J., Tan, L., Wang, H. F., Tan, M. S., Yu, W. J., et al. (2016). Impact of SORL1 genetic variations on MRI markers in non-demented elders. *Oncotarget* 7, 31689–31698. doi: 10.18632/oncotarget.9300
- Zhang, H., Zheng, W., Hua, L., Wang, Y., Li, J., Bai, H., et al. (2017). Interaction between PPAR gamma and SORL1 gene with Late-Onset Alzheimer's disease in Chinese Han Population. *Oncotarget* 8, 48313–48320. doi: 10.18632/oncotarget.15691



Differential Abnormality in Functional Connectivity Density in Preclinical and Early-Stage Alzheimer's Disease

Yu Song^{1†}, Huimin Wu^{1†}, Shanshan Chen^{1†}, Honglin Ge^{2,3}, Zheng Yan^{2,3}, Chen Xue⁴, Wenzhang Qi⁴, Qianqian Yuan⁴, Xuhong Liang⁴, Xingjian Lin^{1*} and Jiu Chen^{2,3*}

¹ Department of Neurology, The Affiliated Brain Hospital of Nanjing Medical University, Nanjing, China, ² Institute of Neuropsychiatry, The Affiliated Brain Hospital of Nanjing Medical University, Nanjing, China, ³ Institute of Brain Functional Imaging, Nanjing Medical University, Nanjing, China, ⁴ Department of Radiology, The Affiliated Brain Hospital of Nanjing Medical University, Nanjing, China

OPEN ACCESS

Edited by:

Yang Jiang,
University of Kentucky, United States

Reviewed by:

Meng Zhang,
Xinxiang Medical University, China
Qiang Wei,
First Affiliated Hospital of Anhui
Medical University, China
Jiaojian Wang,
University of Electronic Science and
Technology of China, China

*Correspondence:

Xingjian Lin
linxingjian@njmu.edu.cn
Jiu Chen
ericcst@aliyun.com

[†]These authors have contributed
equally to this work and share first
authorship

Specialty section:

This article was submitted to
Alzheimer's Disease and Related
Dementias,
a section of the journal
Frontiers in Aging Neuroscience

Received: 20 February 2022

Accepted: 27 April 2022

Published: 25 May 2022

Citation:

Song Y, Wu H, Chen S, Ge H, Yan Z,
Xue C, Qi W, Yuan Q, Liang X, Lin X
and Chen J (2022) Differential
Abnormality in Functional Connectivity
Density in Preclinical and Early-Stage
Alzheimer's Disease.
Front. Aging Neurosci. 14:879836.
doi: 10.3389/fnagi.2022.879836

Background: Both subjective cognitive decline (SCD) and amnesic mild cognitive impairment (aMCI) have a high risk of progression to Alzheimer's disease (AD). While most of the available evidence described changes in functional connectivity (FC) in SCD and aMCI, there was no confirmation of changes in functional connectivity density (FCD) that have not been confirmed. Therefore, the purpose of this study was to investigate the specific alterations in resting-state FCD in SCD and aMCI and further assess the extent to which these changes can distinguish the preclinical and early-stage AD.

Methods: A total of 57 patients with SCD, 59 patients with aMCI, and 78 healthy controls (HC) were included. The global FCD, local FCD, and long-range FCD were calculated for each voxel to identify brain regions with significant FCD alterations. The brain regions with abnormal FCD were then used as regions of interest for FC analysis. In addition, we calculated correlations between neuroimaging alterations and cognitive function and performed receiver-operating characteristic analyses to assess the diagnostic effect of the FCD and FC alterations on SCD and aMCI.

Results: FCD mapping revealed significantly increased global FCD in the left parahippocampal gyrus (PHG.L) and increased long-range FCD in the left hippocampus for patients with SCD when compared to HCs. However, when compared to SCD, patients with aMCI showed significantly decreased global FCD and long-range FCD in the PHG.L. The follow-up FC analysis further revealed significant variations between the PHG.L and the occipital lobe in patients with SCD and aMCI. In addition, patients with SCD also presented significant changes in FC between the left hippocampus, the left cerebellum anterior lobe, and the inferior temporal gyrus. Moreover, changes in abnormal indicators in the SCD and aMCI groups were significantly associated with cognitive function. Finally, combining FCD and FC abnormalities allowed for a more precise differentiation of the clinical stages.

Conclusion: To our knowledge, this study is the first to investigate specific alterations in FCD and FC for both patients with SCD and aMCI and confirms differential abnormalities that can serve as potential imaging markers for preclinical and early-stage Alzheimer's

disease (AD). Also, it adds a new dimension of understanding to the diagnosis of SCD and aMCI as well as the evaluation of disease progression.

Keywords: subjective cognitive decline, amnesic mild cognitive impairment, functional connectivity density, functional connectivity, functional magnetic resonance imaging

INTRODUCTION

Subjective cognitive decline (SCD) and amnesic mild cognitive impairment (aMCI) have been recognized as the preclinical and prodromal stages of Alzheimer's disease (AD), respectively (Rabin and Smart, 2017; Hadjichrysanthou et al., 2020). SCD is used to describe the condition of elderly people who perceive their cognitive function to be impaired despite the absence of verifiable neuropsychological dysfunction, whereas aMCI refers to individuals who experience memory loss with or without a decline in other cognitive abilities (Xue et al., 2021). Accumulating evidence has suggested that both of them have a high probability of progressing to AD (Rabin and Smart, 2017; Hadjichrysanthou et al., 2020). As for the lack of effective treatment for AD, sensitive diagnostic procedures and prompt interventions are critical.

Resting-state fMRI (rs-fMRI), known as a non-invasive technique, is extensively applied in the AD-related spectrum for detecting functional activity in the brain by measuring various indicators such as functional connectivity (FC) and others (Xu et al., 2020; Song et al., 2021). Functional abnormalities of cortical or subcortical hubs are closely associated with cognitive dysfunction (Yu et al., 2017). Wang et al. discovered altered intrinsic FC patterns with insular subnetworks in patients with SCD and aMCI, as opposed to healthy controls (HCs), and those specific changes were correlated with episodic memory (EM; Wang et al., 2021). Furthermore, using graph analysis, patients with AD or mild cognitive impairment (MCI) had global and local FC disruptions (Zhao et al., 2012; Wang et al., 2013). Abnormal FC between regions with a greater physical distance should also be attenuated. Studies confirmed that long-distance connectivity loss was linked to brain network dysfunction (Liu et al., 2014; Tao et al., 2020). In this investigation, we chose functional connectivity density (FCD) mapping, an ultrafast data-driven method, to identify functional hubs in patients with SCD and aMCI, as it performs multi-perspective assessments of the whole brain, short- and long-range aspects.

FCD mapping quantifies the importance of a voxel by comparing it to all other voxels in the whole brain. The higher a voxel's FCD value, the greater the number of effective FCs it possesses in comparison to other voxels, implying that it is essential for function maintenance (Tomasi, 2010; Tomasi and Shokri-Kojori, 2016). FCD can be further subdivided into global FCD (gFCD), local FCD (lFCD), and long-range FCD (lrFCD) based on neighbor relationships between voxels (Li et al., 2018a). The gFCD of a voxel reflects functional coupling throughout the brain, whereas the lFCD presents local changes, and the lrFCD presents functional integration between voxels that are not adjacent to each other (Tomasi, 2010). Different metrics can describe different characteristics of a functional hub

(Tomasi, 2010), and multiscale assessment can be more accurate in disease identification (Liu et al., 2018; Xue et al., 2021). Previous studies have shown dramatic changes in FCD in patients with neuropsychological diseases (Zhuo et al., 2014; Zhang et al., 2015, 2016). Mao et al., while analyzing FCD in patients with AD and MCI, found a disrupted balance of the lFCD and lrFCD in both of them (Mao et al., 2021). However, to the best of our knowledge, no study exploring the alterations of FCD in patients with SCD or aMCI has been conducted.

The purpose of this study was to comprehensively characterize abnormalities of functional coupling in SCD, aMCI, and HC by combining FCD analyses and seed-based FC analyses, as the FCD analysis does not reveal specific regions abnormally connected to the region with altered FCD (Hu et al., 2017). Besides, correlation analyses and receiver-operating characteristic (ROC) analyses were simultaneously performed. We hypothesized that different altered patterns of FCD and FC were shown in patients with SCD and aMCI. These changes may contribute to cognitive deterioration and can help distinguish different phases of preclinical and early-stage AD.

MATERIALS AND METHODS

NBH-ADsnp Database

The data for the applied research were obtained from our domestic database, the Nanjing Brain Hospital Alzheimer's Disease Spectrum Neuroimaging Project (NBH-ADsnp) (Nanjing, China; Chen et al., 2020; Wang et al., 2021; Xu et al., 2021), which is regularly updated. Detailed information about NBH-ADsnp is available in the **Supplementary Material**. This study has been approved by the Association for Responsible Human Participant Ethics Committee of the Affiliated Brain Hospital of Nanjing Medical University School (2018-KY010-01, 2020-KY010-42). All volunteers provided informed consent.

Participants

Patients with SCD and healthy seniors were recruited from local communities through advertisements and broadcasts, while patients with aMCI were recruited from both the hospital and local communities. Initially, 234 individuals from the baseline period of the NBH-ADsnp database were enrolled. Among them, eight participants were excluded due to excessive head motion (cumulative translation or rotation of > 3.0 mm or 3.0°). According to previous studies (Wang et al., 2021; Xue et al., 2021), a total of 194 participants, including 59 aMCI, 57 SCD, and 78 HC, were eventually included after strict exclusion. Detailed information about inclusive and exclusive criteria is summarized in the **Supplementary Material**.

Neuropsychological Assessment

A comprehensive neuropsychological assessment covering general cognitive function and four cognitive domains, including episodic memory (EM), executive function (EF), visuospatial function (VF), and information processing speed (IPS), was conducted among the participants (Chen et al., 2020; Wang et al., 2021; Xue et al., 2021; Xu et al., 2021). All evaluations were performed by two experienced neuropsychologists (Dr. Chen and Song). Details regarding the assessment can be obtained in the **Supplementary Material**.

MRI Data Acquisition

The detailed parameters of image acquisition, including resting-state fMRI images and structural MRI images, are provided in the **Supplementary Material**. Scanning technologists and preprocessors were unaware of the clinical status of the participants.

Preprocessing of Resting-State fMRI

All fMRI images were preprocessed by DPABI software and implemented in MATLAB2014a (Yan et al., 2016). First, 10 initial volumes were discarded to equilibrate brain signals, and the remaining voxels were subjected to slice time correction and realignment. Subsequently, structural images were segmented into gray matter, white matter, and cerebrospinal fluid partitions using the DARTEL technique (The gray matter would be used as a covariate in the subsequent statistical analysis; Ashburner, 2009). Then, all images were normalized to the Montreal Neurological Institute (MNI) EPI template and resampled at $3 \times 3 \times 3$ mm voxels. After normalization, the Friston 24-parameter model, cerebrospinal fluid, white matter, and linear drift signals were all regressed. At the same time, head motion scrubbing regressors were also used with a threshold at $FD_Jenkinson > 0.2$ for bad time (Chao-Gan, 2010). Finally, the fMRI data were temporal band-pass filtered (0.01–0.08 Hz; Li et al., 2018a). Subjects who moved more than 3° of rotations or 3 mm of translation were excluded. For FCD calculation, we did not adopt spatial smoothing (Tomasí, 2012; Cheng et al., 2021). To analyze resting-state FC, all fMRI images were smoothed with a $6 \times 6 \times 6$ mm FWHM Gaussian kernel (Chen et al., 2020).

FCD Mapping

The voxel-wise FCD map for each participant was analyzed using the Neuroscience Information Toolbox (NIT, version 1.3, <http://www.neuro.uestc.edu.cn/NIT.html>; Dong et al., 2018), based on the protocol introduced by Tomasí and Volkow (Tomasí, 2010). FCD maps, mainly gFCD, lFCD, and lrFCD, are defined as the number of voxels with an FC strength (correlation coefficient) greater than 0.6, as determined by previous studies (Tomasí, 2010; Tomasí and Shokri-Kojori, 2016). The gFCD value was calculated by counting the total number of FC between a voxel and other voxels. A growing algorithm was used to obtain the lFCD. In this algorithm, given a voxel χ_0 , the FC between χ_0 and the voxel χ_i adjacent to χ_0 was calculated. If the FC strength was > 0.6 , χ_i could be a neighbor of χ_0 . Additionally, the voxel χ_j , adjacent to χ_i , could also add to

the list of χ_0 neighbors if it is functionally connected to χ_0 via a correlation coefficient > 0.6 . This formula was repeated until no voxel could be added. The lFCD represented the number of all neighbors of χ_0 . In addition, the lrFCD map of each participant was obtained by removing lFCD from gFCD. Finally, for standardization, FCD maps were divided by the mean FCD value.

Seed-Based Functional Connectivity Analysis

A resting-state FC analysis was performed to show direct functional couplings between brain areas with altered FCD maps. Specifically, we used each region showing significant alteration of FCD as a spherical region of interest (ROI), with the center corresponding to the peak voxel (radius = 6 mm), and then conducted a Pearson correlation analysis between the average time courses of ROI and whole-brain voxel under the gray matter mask of the whole brain. Finally, Fisher's $r - z$ transformation was performed on all FC maps for normality (Chen et al., 2021a).

Statistical Analyses

Statistical Package for Social Sciences (SPSS) software, version 22.0 (IBM, Armonk, NY, USA), was used to perform statistical analyses that were not related to voxel computations. The χ^2 -test and the analysis of variance ANOVA were used to compare the differences in demographic and neuropsychological data among the CN, SCD, and aMCI groups. *Post-hoc* comparisons were further conducted with the Bonferroni correction ($p < 0.05$).

Using DPABI software, a one-way ANOVA was applied to compare the differences in gFCD, lFCD, and lrFCD across three groups with age, gender, years of education, and gray matter volumes as covariates. The nonparametric permutation test (1000 permutations) was applied, and the significance level was set to $p < 0.01$ with a cluster size > 150 voxels. *Post-hoc* comparisons, using the two-sample t-test with the results of ANOVA analyses as the mask, were conducted with age, gender, education level, and gray matter volumes as covariates. To strictly correct the results, a TFCE and the familywise error (FWE) were applied with a threshold of $p < 0.05$ and a cluster size > 50 voxels.

For the resting-state FC analysis, it is important to note that we only performed further FC analysis between groups with significantly different FCD values. That is, if the FCD value of a seed point differed between all three groups, we would apply ANOVA and a two-sample t-test to determine the FC changes between groups. However, if the FCD value of the seed point differed between two groups, we would perform a two-sample t-test to analyze the FC changes between only these two groups. All statistical analyses included age, gender, years of education, and gray matter volume as covariates.

The Pearson correlation analysis was performed to examine the correlation between the altered FCD, FCs, and cognitive domains after controlling age, gender, and education level using SPSS software. Additionally, also in SPSS software, ROC curves were analyzed based on substantially changed indicators

TABLE 1 | Demographics and clinical characteristics of HC, SCD, and aMCI groups.

| | HC (n = 78) | SCD (n = 57) | aMCI (n = 59) | F-values (χ^2) | P-values |
|--|---------------|---------------|----------------|-----------------------|--------------------------|
| Age (years) | 63.51 (6.79) | 65.09 (7.66) | 65.10 (7.81) | 1.074 | 0.3435 |
| Gender (F/M) | 48/30 | 47/10 | 38/21 | 7.362 | 0.0252* |
| Education level (years) | 12.31 (2.51) | 11.74 (2.73) | 11.09 (3.07) | 3.267 | 0.0402b* |
| MMSE | 28.59 (1.22) | 28.05 (1.49) | 27.10 (2.09) | 7.166 | 0.0000b*** / c** |
| MoCA | 25.47 (2.41) | 24.91 (2.07) | 23.03 (3.11) | 7.918 | 0.0000b*** / c*** |
| SCD-Q | 3.64 (1.43) | 6.31 (0.82) | 5.03 (1.87) | 23.907 | 0.0000a*** / b*** / c*** |
| Composite Z-scores of each cognitive domain | | | | | |
| Episodic memory | 0.240 (0.502) | 0.286 (0.482) | -0.593 (0.641) | 23.756 | 0.0000b*** / c*** |
| Executive function | 0.212 (0.528) | 0.167 (0.539) | -0.442 (0.600) | 23.138 | 0.0000b*** / c*** |
| Information processing speed | 0.197 (0.750) | 0.107 (0.692) | -0.364 (0.702) | 24.969 | 0.0000b*** / c** |
| Visuospatial function | 0.165 (0.649) | 0.084 (0.658) | -0.299 (0.975) | 6.750 | 0.0000b* / c* |

Data are presented as mean (standard deviation). Values for age and education level derived from ANOVA; gender from χ -square test; all clinical characteristics from ANOVA with age, gender, and education level as covariates.

HC, healthy control; SCD, subjective cognitive decline; aMCI, amnesic mild cognitive impairment; MMSE, Mini-Mental State Examination; MoCA, the Montreal Cognitive Assessment test; SCD-Q, Subjective Cognitive Decline Questionnaire.

^aPost-hoc analyses showed a significant group difference between SCD and HC.

^bPost-hoc analyses showed a significant group difference between aMCI and HC.

^cPost-hoc analyses showed a significant group difference between aMCI and SCD; Bonferroni correction was applied for multiple comparisons.

* $p < 0.05$; ** $P < 0.01$; *** $P < 0.001$.

TABLE 2 | Global, local, and long-range FCD alterations across three groups.

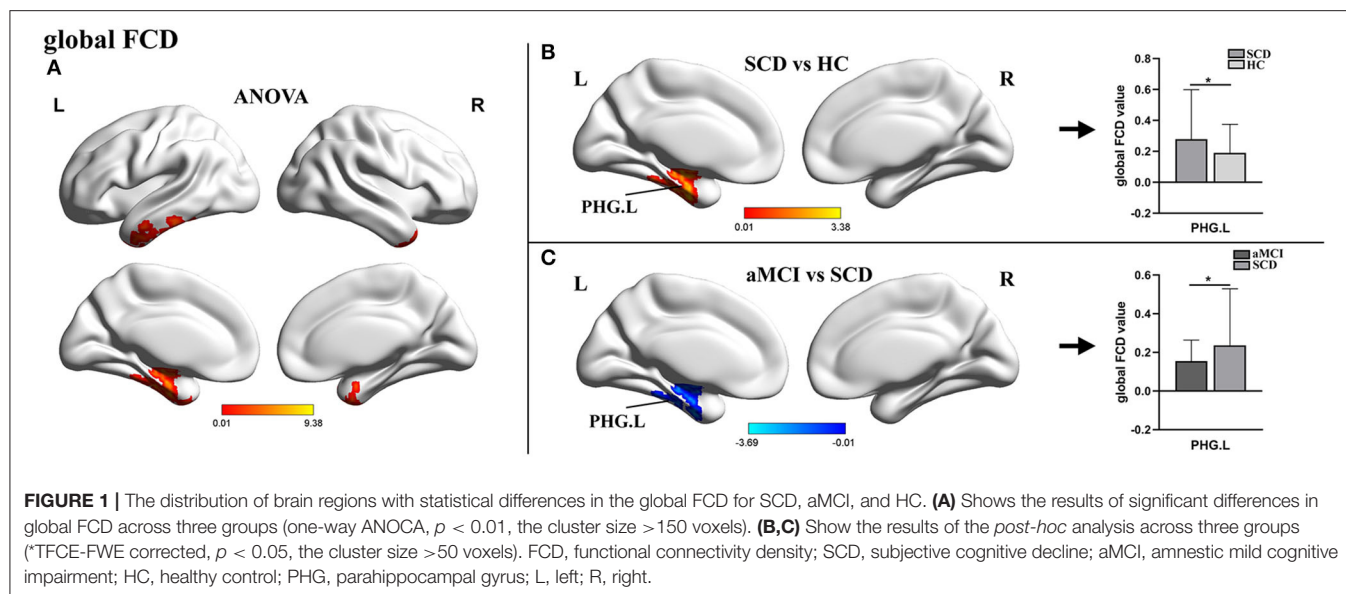
| FCD | Cluster index | Cluster size (voxels) | Brain regions | Peak MNI coordinate (x, y, z) | Peak intensity (t-value) |
|----------------|---------------|-----------------------|---|-------------------------------|--------------------------|
| Global FCD | ANOVA | | | | |
| | 1 | 436 | Left Parahippocampal Gyrus | -27, -27, -24 | 9.3845 |
| | 2 | 101 | Right Temporal_Pole_Mid | 45, 15, -42 | 7.7385 |
| | SCD>HC | | | | |
| Local FCD | 1 | 196 | Left Parahippocampal Gyrus | -27, -27, -24 | 3.3817 |
| | aMCI<SCD | | | | |
| | 1 | 121 | Left Parahippocampal Gyrus | -27, -27, -24 | -3.6892 |
| | NA | | | | |
| Long-range FCD | ANOVA | | | | |
| | 1 | 686 | Left Inferior Temporal Gyrus / Middle Frontal Gyrus / Hippocampus | -9, -6, -45 | 10.8675 |
| | 2 | 242 | Right Temporal_Pole_Mid | 18, 46, 12 | 7.8173 |
| | SCD>HC | | | | |
| | 1 | 355 | Left Hippocampus | -27, -18, -18 | 3.5523 |
| | aMCI<SCD | | | | |
| | 1 | 301 | Left Parahippocampal Gyrus | -27, -27, -24 | -3.1684 |

Cluster size > 150 voxels in ANOVA analysis, $p < 0.01$; Cluster size > 50 voxels in post hoc test, $p < 0.05$, TFCE-FWE corrected; All results had controlled the effects of age, gender, education level, and gray matter volumes.

FCD, functional connectivity density; aMCI, amnesic mild cognitive impairment; SCD, subjective cognitive decline; HC, healthy control.

between the patient and HC groups, such as FCD and FC, to assess their value in the distinction of pre-Alzheimer's spectrum. Each index's discriminating performance was assessed independently. Moreover, significantly altered indexes were

combined using a binary logistic regression model, and the model's performance was also evaluated. Finally, we assessed the sensitivity and specificity of each biomarker individually and in combination.



RESULTS

Demographic and Clinical Characteristics of Participants

We found no statistical discrepancy in age ($P = 0.3435$) between the three groups but found significant differences in gender ($P = 0.0252$) and education level ($P = 0.0402$). To avoid the impact of demographic differences on subsequent analyses, all statistical analyses included gender, age, and education level as covariates. As expected, general cognitive function scores (the Mini-Mental State Examination and the Montreal Cognitive Assessment test) of patients with aMCI showed significant decreases as compared to those of patients with SCD ($p < 0.01$) and HCs ($p < 0.001$). In terms of every cognitive domain, including EM, EF, IPS, and VF, patients with aMCI also had statistical deficits in comparison with HC ($p < 0.05$) and SCD ($p < 0.05$). Moreover, for the Subjective Cognitive Decline Questionnaire (SCD-Q), there were significant alterations between the three groups ($p < 0.001$). Details can be obtained in **Table 1**.

Functional Connectivity Density Analyses

The analyses of FCD showed that gFCD and lrFCD values were statistically different between the SCD and HC groups or between the SCD and aMCI groups, but lfFCD values were not found to be significantly altered between the three groups. Details are available in **Table 2**.

For gFCD, the ANOVA analysis revealed significant differences between the left parahippocampal gyrus (PHG.L) and the right temporal pole: the middle temporal gyrus. In comparison to HC, the value of gFCD of the PHG.L was significantly different between groups, with significantly higher values in patients with SCD and significantly lower values in patients with aMCI (**Table 2, Figure 1**).

For lrFCD, the ANOVA analysis revealed statistical differences in the left inferior temporal gyrus, the middle frontal gyrus

(ITG.L/MFG.L), and the left hippocampus. In the *post-hoc* test, patients with SCD exhibited significantly higher lrFCD in the left hippocampus than HCs and significantly higher lrFCD in the PHG.L than patients with aMCI (**Table 2, Figure 2**).

Functional Connectivity Analyses Based on Regions With Altered FCD

For the PHG.L seed (ROI 1, $x = -27$ $y = -27$ $z = -24$), the statistical differences in FCD values of this brain area involved three groups. An ANOVA analysis and a *post-hoc* test were carried out. Compared with HCs, patients with SCD showed markedly increased FC in bilateral superior occipital gyrus/middle occipital gyrus (SOG/MFG) and bilateral cuneus with the peak coordinate ($x = -15$, $y = -87$, $z = 18$) located in the left SOG (SOG.L). In addition, in comparison with SCD, the aMCI group presented significantly decreased FC in bilateral SOG/MFG and right calcarine with the peak coordinated ($x = 6$, $y = -78$, $z = 9$) located in the right calcarine. No statistical significance was found between aMCI and HC groups (**Table 3, Figure 3**).

For the left hippocampus seed (ROI 2, $X = -27$, $Y = -18$, $Z = -18$), a two-sample t-test was applied between SCD and HC groups. In this comparison, the SCD group exhibited increased FC in the left cerebellum anterior lobe (CAL.L) and the ITG.L (**Table 3, Figure 4**).

Correlation Analyses

Pearson correlation analysis showed that, in the groups consisting of aMCI and SCD, the abnormal gFCD value in the PHG.L was prominently positively correlated with EM and EF. Besides, the altered FC between the PHG.L and right calcarine was also correlated with EM positively (**Figure 5**).

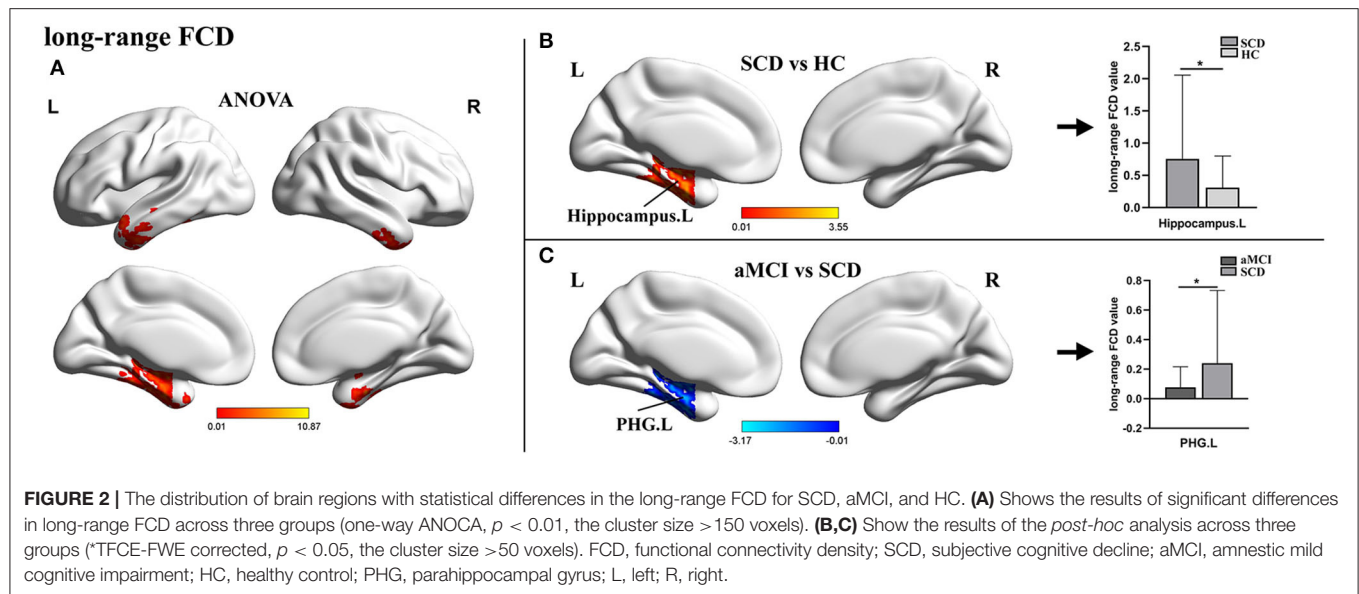


TABLE 3 | Regions with changed resting-state FC based on seed-based analyses across three groups.

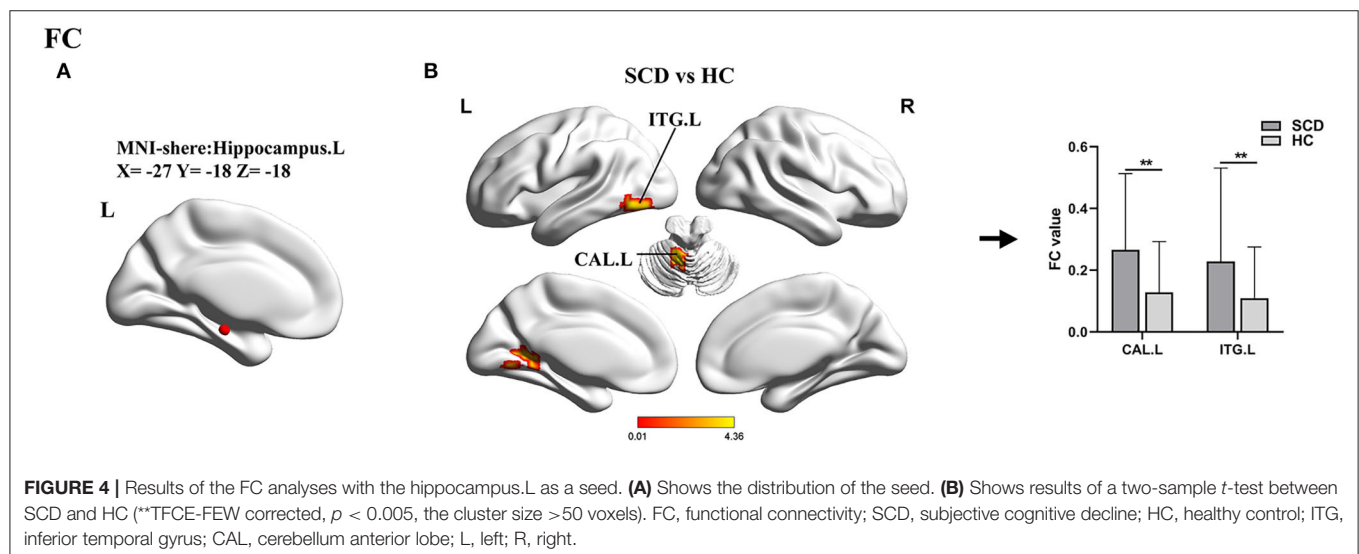
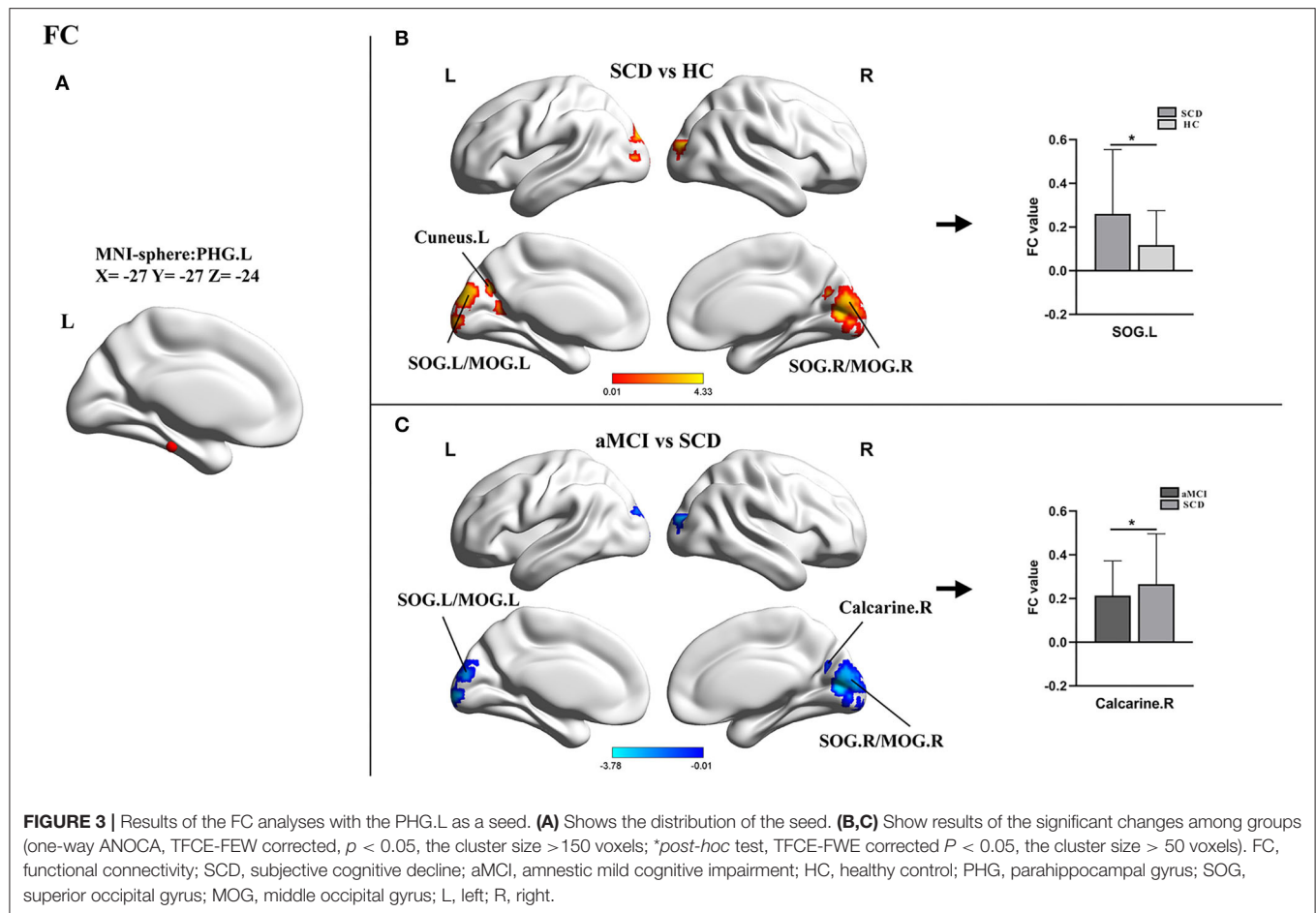
| Seed (MNI-sphere) | Cluster index | Cluster size (voxels) | Brain regions | Peak MNI coordinate (x, y, z) | Peak intensity (t-value) |
|----------------------------------|---------------|-----------------------|---|-------------------------------|--------------------------|
| ROI1 (x = -27, y = -27, z = -24) | ANOVA | | | | |
| | 1 | 799 | Bilateral Superior Occipital Gyrus / Middle Occipital Gyrus / Cuneus | -15, -87, 18 | 10.3461 |
| | SCD > HC* | 799 | Bilateral Superior Occipital Gyrus / Middle Occipital Gyrus / Cuneus | -15, -87, 18 | 4.3291 |
| ROI2 (x = -27, y = -18, z = -18) | aMCI < SCD* | 492 | Bilateral Superior Occipital Gyrus / Middle Occipital Gyrus / Right Calcarine | 6, -78, 9 | -3.7846 |
| | SCD > HC** | 174 | Left Cerebellum Anterior Lobe | -9, -51, -6 | 4.3587 |
| | | 128 | Left Inferior Temporal Gyrus | -48, -63, -6 | 4.3412 |

When analyzing FC with ROI1 as the seed, the ANOVA analysis was carried out with TFCE-FWE corrected $P < 0.05$ and a cluster size > 150 voxels; in the *post-hoc* test, TFCE-FWE corrected $*P < 0.05$ and a cluster size > 50 voxels were set. A voxel-wise two-sample *t*-test was applied when analyzing FC with ROI2 as the seed with TFCE-FWE corrected $**P < 0.005$ and a cluster size > 50 voxels. All results had controlled the effects of age, gender, education level, and gray matter volumes. FC, functional connectivity; ROI, region of interest; SCD, subjective cognitive decline; HC, healthy control.

Receiver-Operating Characteristic Analyses

Within the group containing SCD and HC, the area under the curve (AUC) values of gFCD of the PHG.L and lrFCD of the left hippocampus were 0.678 with $p < 0.001$ and 0.652 with $p = 0.003$. FC between PHG.L and SOG.L, FC between the left

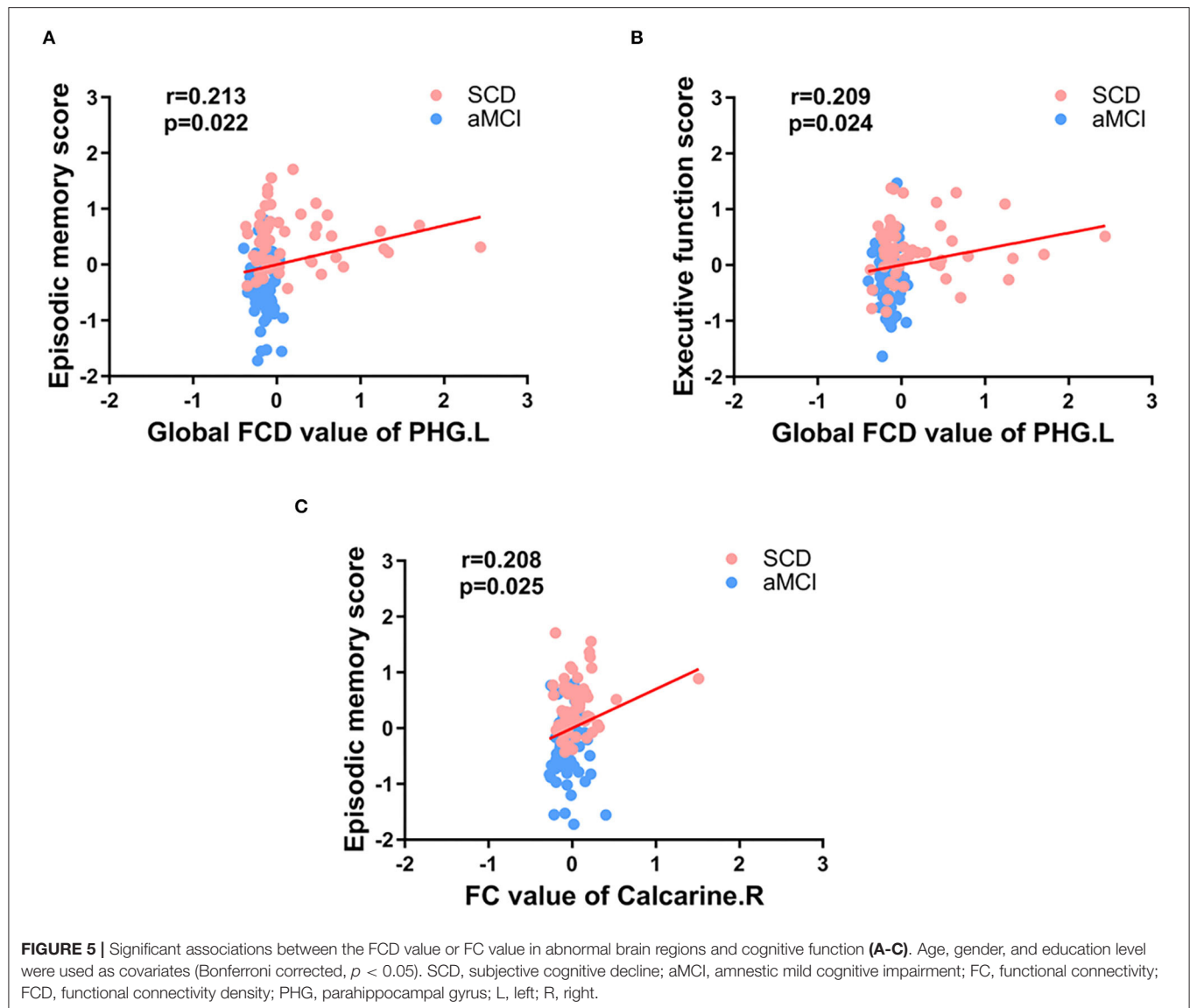
hippocampus and CAL.L, and FC between the left hippocampus and ITG.L had AUC values of 0.684 with $p < 0.001$, 0.722 with $p < 0.001$, and 0.661 with $p = 0.001$, respectively. In addition, using a binary logistic regression model, we obtained individual predictors of the combination of multiple indexes. The AUC value of the combination of multiple indexes was



0.827 with $p < 0.001$, sensitivity = 87.7%, specificity = 66.7% (Figure 6).

Within the group containing aMCI and SCD, the AUC values of the EM and EF were 0.870 with $p < 0.001$ and

0.771 with $p < 0.001$. The AUC values of gFCD of the PHG.L and lrFCD of the PHG.L were 0.741 with $p < 0.001$ and 0.643 with $p < 0.08$. The AUC value of FC between the PHG.L and right calcarine was 0.635 with $p < 0.012$. In



addition, the AUC value of the combined index was 0.941 with $p < 0.001$, sensitivity = 93.2%, specificity = 80.7% (Figure 6).

DISCUSSION

This was the first study to examine the alterations in FCD maps and relevant functional connectivity in preclinical and early-stage AD and their clinical implications. According to our findings, in patients with SCD and aMCI, abnormalities in FCD emerged largely in the hippocampus and PHG. Based on FCD analyses, further FC analyses revealed that altered FC is mainly located in the occipital lobe, including the SOG, MOG, cuneus, and calcarine. Notably, the differences between MCI and SCD were linked to damages in cognitive domains. In addition, patients with

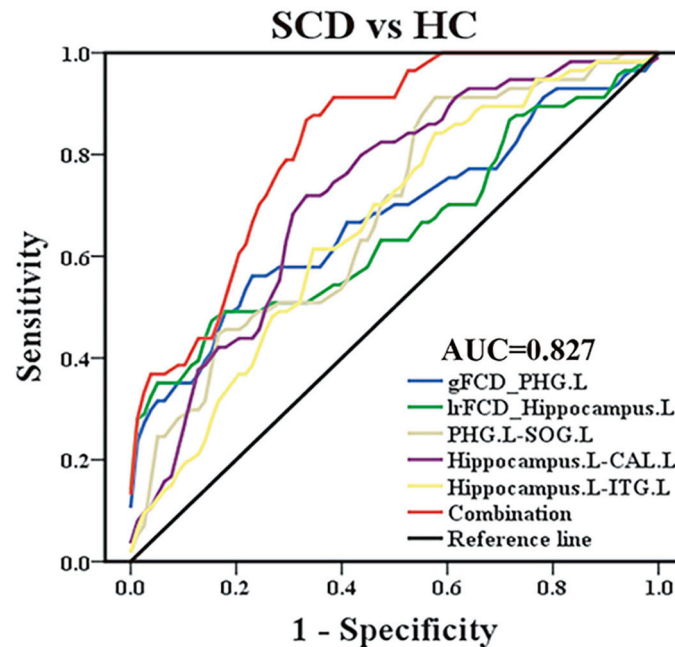
SCD also had altered FC of the hippocampus with the cerebellum and the temporal lobe compared with HCs. In general, these findings have crucial implications for understanding the neural mechanisms that underpin these disparate manifestations of different stages of the preclinical AD spectrum.

Altered FCD in SCD and aMCI

The significant changes in the gFCD between the three groups were exhibited in PHG. The PHG, bordering the subiculum and lying adjacent to the hippocampus, is the prime cortical input of the hippocampus and a crucial part involved in episodic memory encoding and recognition (van Strien and Cappaert, 2009; Mégevand et al., 2014). Although it is generally accepted that patients with SCD suffer from mild neuronal damage, sufficient functional compensation allows for

ROC curve

A



B

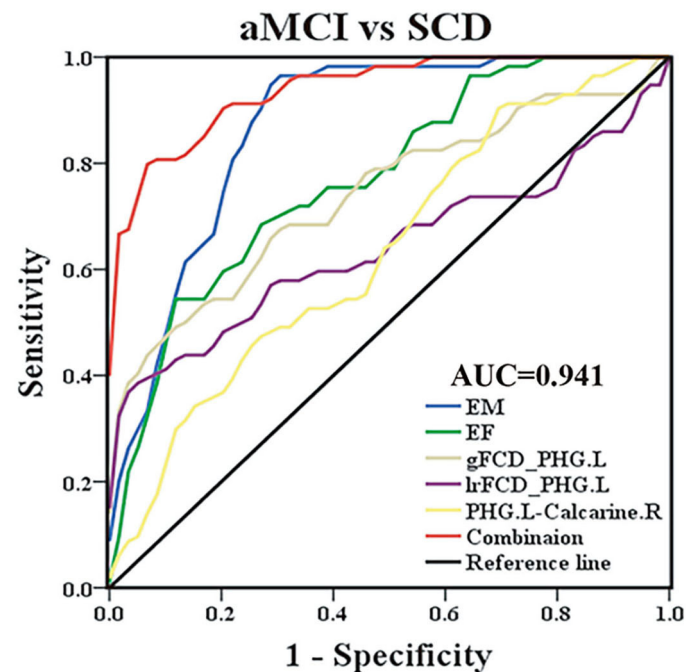


FIGURE 6 | Classification of individuals as SCD vs. HC and aMCI vs. SCD based on the ROC analysis. **(A)** The ROC curve presenting the classification of SCD and HC; **(B)** ROC curve showcasing the classification of aMCI and SCD. ROC, receiver operating characteristic; AUC, area under the ROC curve (of the combination of multiple indexes); SCD, subjective cognitive decline; aMCI, amnesic mild cognitive impairment; HC, healthy control; gFCD, global functional connectivity density; lrFCD, long-range functional connectivity density; EM, episodic memory; EF, executive function; PHG, parahippocampal gyrus; SOG, superior occipital gyrus; ITG, inferior temporal gyrus; CAL, cerebellum anterior lobe; L, left; R, right.

regular clinical and cognitive performance. Here, we found that the gFCD of the PHG in SCD was much higher in HCs, which indicated that PHG established more efficient functional connections with other regions. This finding was consistent with previous research on topological changes in the functional connectome, which revealed that increased nodal properties such as global nodal efficiency and nodal strength in the SCD were primarily found in the default mode network (DMN), including the medial temporal and PHG (Li et al., 2018b; Chen et al., 2020a). However, in patients with aMCI, the gFCD of the PHG was markedly decreased compared with patients with SCD, a trend consistent with the previous studies (Liu et al., 2016; Mao et al., 2021; Yuan et al., 2021). This result suggested that, as the disease progressed, functional compensations became insufficient to compensate for further neurological damage, resulting in objective impairment in cognitive domains. Moreover, it has been confirmed that the presence of neurofibrillary tangles started in this brain area (Braak, 1991). Thus, we hypothesized that the absence of compensatory mechanisms was a manifestation of further impairment of neural functions in individuals.

In terms of the lrFCD, patients with aMCI also showed a decreased change in the PHG when compared with patients with SCD. Given that lrFCDs were derived from gFCD scores and that there were no significant changes in lfCDs, it was no surprise that analyses of the lrFCD and gFCD could obtain consistent results. However, compared with HCs, the abnormal lrFCD of patients with SCD was located in the hippocampus. The hippocampus, one of the most studied regions, plays an essential role in the creation of new memories, pattern separation, and cognitive flexibility (Virley et al., 1999; Sekeres et al., 2021). A mediation analysis revealed that indirect FCs between the hippocampus and other brain areas were mediated by the PHG (Ward et al., 2014), which may be one of the reasons for the different results of the two indicators. Existing rs-fMRI studies on patients with SCD have been more concerned with exploring the significance of general functional connectivity alterations (Liang et al., 2020; Xue et al., 2021), and this is the first report of specific alterations of the lrFCD in the hippocampus of patients with SCD. We hypothesized that this specific elevation was also a manifestation of functional compensation and could become a specific biomarker that distinguishes SCD from normal aging.

Reviewing the results of the FCD analyses, we found that FCD abnormalities (increased or decreased) were first found in the left hemisphere. It is well-known that directional hemispheric dominance has been established for a variety of cognitive functions and that lateralization is particularly important for cognitive functions (Banks et al., 2018; Vingerhoets, 2019). Available studies suggested that left functional lateralization of the DMN was influenced by aging and/or AD progression (Banks et al., 2018). Furthermore, in terms of structure, in patients with MCI and AD, brain atrophy was also left lateralized (Chen et al., 2020b). Therefore, we hypothesized that left functional lateralization in FCD of patients with SCD might have a more compensatory role, whereas a decrease in functional lateralization suggested further disease progression.

Altered FC in SCD and aMCI

Using the left PHG as the seed, we found significantly altered FC in the occipital lobe, including SOG, MOG, cuneus, and calcarine in patients with SCD and aMCI and the changing trends were consistent with the results of FCD analyses. According to the processing theory of the memory system, the occipital-temporal visual object processing pathway is important for memory formation (Ren et al., 2019). Studies on scene perception revealed that the occipital place area, as well as the parahippocampal place area, played a key role in scene recognition and spatial perception (Julian et al., 2016; Epstein, 2019). Previous investigations also determined statistically increased spontaneous functional activity in the occipital lobe in SCD when compared with HCs (Sun et al., 2016). The SOG, MOG, and calcarine were considered to belong to the visual network (VN). Our results confirmed again that patients with SCD had increased connectivity in VN (Lista et al., 2015; Liang et al., 2021). However, there were some studies that reported disrupted FC of the PHG to other brain areas such as the posterior cingulate cortex when comparing patients with SCD and HCs (Chen et al., 2020; Sharma et al., 2021). In actuality, the PHG is a region consisting of five sub-regions, including the parasubiculum, the presubiculum, the perirhinal cortex, the entorhinal cortex, and the post rhinal cortex. Each subregion may develop different functions during cognitive impairment, and our results were only for a small part of the PHG (van Strien and Cappaert, 2009).

In addition, one study about functional brain networks reported internetwork connectivities between the DMN (PHG et al.) and the VN (Cai et al., 2017) when comparing patients with aMCI to HCs. The cuneus gradually becomes hypoperfused and develops amyloid deposits earlier in patients with prodromal AD due to pathological downregulation (Cho et al., 2013; Ding et al., 2014). Furthermore, acetylcholinesterase activity in the occipital lobe was found to be reduced in patients with MCI and positive AD biomarkers (Richter et al., 2019). Therefore, we hypothesized that the increased FC of the PHG to the occipital lobe was a compensatory response to mild cognitive decline, and this compensation gradually dissipated as neuronal damage increased.

Furthermore, using the left hippocampus as a seed, we found significantly increased FC in the CAL and ITG of patients with SCD when compared to healthy elders. Although motor coordination has traditionally been considered the cerebellum's core function, it is now well-understood that the cerebellum is also involved in learning and sensory processing, and the CAL was proved to be associated with visual-spatial and executive function (Schmahmann, 1998; Salman, 2016). The ITG is identified as a tertiary visual association cortex and is involved in the learning of cognitive tasks (Scheff et al., 2011). Experiments in mice have demonstrated that the senescence in the cerebellum was present earlier than that in the hippocampus (Woodruff-Pak et al., 2010). Previous studies reported that patients with SCD had increased cerebral blood flow in the hippocampus and ITG relative to HCs and patients with MCI (Thomas

et al., 2021). All these results further confirmed that, despite the absence of objective cognitive impairment in SCD, reactive changes in brain function, especially functional compensation, had occurred.

Behavioral and Clinical Significance of FCD and FC Abnormalities in SCD and aMCI

Correlation analyses showed that reduced gFCD values in the PHG were accompanied by decreased EM and EF in patients with aMCI and SCD, and FC values in the occipital lobe were also positively correlated with EM. These results further confirmed that the PHG, as well as the occipital lobe, were closely related to cognitive function, which was consistent with previous studies (Li et al., 2018b; Chen et al., 2020a). In contrast, in the SCD and HC groups, the results of the assessment of each cognitive domain were not significantly correlated with functional changes. Such a result was not unexpected, as there were no abnormalities in patients with SCD on the neuropsychological scales (Liang et al., 2020; Chen et al., 2021b). Because there are no effective and objective methods for diagnosing SCD or determining whether patients with SCD have been exacerbated, existing studies have attempted to improve disease differentiation accuracy by combining multiple indicators (Hadjichrysanthou et al., 2020; Parker et al., 2020; Mao et al., 2021). By ROC analysis, Xue et al. (2021) combined abnormal FC of the abnormal salience network, ALFF, and gray matter volume with the AUC value up to 0.852 in the SCD and HC groups and combined scale assessment results, cortical thickness of abnormal brain regions, and FC changes with the AUC value up to 0.931 in the SCD and aMCI groups. However, our study found that, in the SCD and HC groups, by virtue of changes in the FCD in the PHG and the hippocampus and altered FC, the AUC value was 0.827. Although the accuracy was not very high, the differentiation method was simpler. In addition, in the SCD and aMCI groups, the combination of scales, the FCD and FC changes in the PHG resulted in an AUC value of 0.941, which was more accurate. All results showed the advantages of FCD and FC analyses in studying preclinical and early-stage AD and provided a new vantage point for the diagnosis and differentiation of preclinical and early-stage AD, especially the conversion of SCD to aMCI.

Reviewing the study results, we did not find statistical differences between the aMCI and HC groups, which contradicted the general perception (Wang et al., 2013). In fact, previous studies based on FCD analyses were more centered on patients with AD and patients with MCI (Mao et al., 2021; Liu et al., 2022), whereas the current study was the first to include patients with aMCI and SCD, resulting in a dearth of comparable research. Second, FCD maps of patients with aMCI at different stages of aMCI may yield inconsistent results (Song et al., 2021; Liu et al., 2022). We hypothesized that, because most of the volunteers with aMCI in this study were in the early stage of the disease, the neurological damage was not very severe, and the decreased and compensatory elevation of FC among brain regions caused no significant changes in their FCD maps compared to HCs.

Limitations

It is important to note that this study has several limitations. First, the relatively small sample size limited the conclusions that could be drawn. However, because our NBA-ADsnp database is constantly being updated, more participants will be included in future studies. Second, the gender and education levels of the three groups were not exactly matched, which might have affected our results. To avoid this effect, we included age, gender, and education as covariates in all statistical analyses. Third, in FCD analyses, we set a single threshold based on prior knowledge, and this fixed value could also lead to false positives or false negatives; thus, further studies will assess the between-group differences in FCD for different thresholds to better examine the stability of the results. Finally, this study was a cross-sectional study, and further analytical studies of longitudinal data are needed to help fully assess the neuroimaging changes in preclinical and early-stage AD.

CONCLUSION

Our study investigated changes in FCD maps in the brain in SCD and aMCI. We found that the abnormalities of the FCD maps were predominantly localized in the PHG and the hippocampus, whereas FC alterations were mainly located in the occipital lobes, the cerebellum, and the ITG. In comparison to HCs, the changes in patients with SCD showed a specific increase, which may suggest the presence of compensatory mechanisms; in comparison to SCD, the changes in patients with aMCI showed a specific decrease, which was indicative of increasing impairment and closely related to cognitive decline. Furthermore, these abnormalities could be used to identify patients at different stages of the preclinical AD spectrum and may serve as potential biomarkers for diagnosis.

DATA AVAILABILITY STATEMENT

The raw data supporting the conclusions of this article will be made available by the authors, without undue reservation.

ETHICS STATEMENT

The studies involving human participants were reviewed and approved by the Ethics Committees of the Affiliated Brain Hospital of Nanjing Medical University. The patients/participants provided their written informed consent to participate in this study. Written informed consent was obtained from the individual(s) for the publication of any potentially identifiable images or data included in this article.

AUTHOR CONTRIBUTIONS

XLin, JC, and YS designed the study. HW, SC, CX, YS, QY, HG, WQ, XLia, and ZY collected the data. YS, HW,

and SC analyzed the data and prepared the manuscript. All authors contributed to the article and approved the submitted version.

FUNDING

This study was supported by the National Natural Science Foundation of China (No. 81701675); the Key Project supported by Medical Science and the Technology Development

Foundation, Nanjing Department of Health (No. JQX18005); and the Key Research and Development Plan (Social Development) Project of Jiangsu Province (No. BE2018608).

SUPPLEMENTARY MATERIAL

The Supplementary Material for this article can be found online at: <https://www.frontiersin.org/articles/10.3389/fnagi.2022.879836/full#supplementary-material>

REFERENCES

- Ashburner, J. (2009). Computing average shaped tissue probability templates. *NeuroImage* 45, 333–341. doi: 10.1016/j.neuroimage.2008.12.008
- Banks, S. J., Zhuang, X., Bayram, E., Bird, C., Cordes, D., and Caldwell, J. Z. K. (2018). Default mode network lateralization and memory in healthy aging and Alzheimer's disease. *J. Alzheimer's Dis.* 66, 1223–1234. doi: 10.3233/JAD-180541
- Braak, H. (1991). Neuropathological staging of Alzheimer-related changes. *Acta Neuropathol.* 82, 239–259. doi: 10.1007/BF00308809
- Cai, S., Chong, T., Peng, Y., Shen, W., Li, J., and von Deneen, K. M. (2017). Altered functional brain networks in amnesic mild cognitive impairment: a resting-state fMRI study. *Brain Imag. Behav.* 11, 619–631. doi: 10.1007/s11682-016-9539-0
- Chao-Gan, Y. (2010). DPARSF: a MATLAB toolbox for “pipeline” data analysis of resting-state fMRI. *Front. Syst. Neurosci.* 4:13. doi: 10.3389/fnsys.2010.00013
- Chen, H., Sheng, X., Luo, C., Qin, R., Ye, Q., and Zhao, H. (2020a). The compensatory phenomenon of the functional connectome related to pathological biomarkers in individuals with subjective cognitive decline. *Transl. Neurodegener.* 9:21. doi: 10.1186/s40035-020-00201-6
- Chen, J., Ma, N., Hu, G., Nousayhah, A., Xue, C., and Qi, W. (2020). rTMS modulates precuneus-hippocampal subregion circuit in patients with subjective cognitive decline. *Aging* 13, 1314–1331. doi: 10.18632/aging.202313
- Chen, S., Song, Y., Wu, H., Ge, H., Qi, W., and Xi, Y. (2021a). Hyperconnectivity associated with anosognosia accelerating clinical progression in amnesic mild cognitive impairment. *ACS Chem. Neurosci.* 2021:1c00595. doi: 10.1021/acschemneuro.1c00595
- Chen, S., Song, Y., Xu, W., Hu, G., Ge, H., and Xue, C. (2021b). Impaired memory awareness and loss integration in self-referential network across the progression of Alzheimer's disease spectrum. *J. Alzheimer's Dis.* 83, 111–126. doi: 10.3233/JAD-210541
- Chen, S., Xu, W., Xue, C., Hu, G., Ma, W., and Qi, W. (2020b). Voxelwise meta-analysis of gray matter abnormalities in mild cognitive impairment and subjective cognitive decline using activation likelihood estimation. *J. Alzheimer's Dis.* 77, 1495–1512. doi: 10.3233/JAD-200659
- Cheng, B., Zhou, Y., Kwok, V. P. Y., Li, Y., Wang, S., and Zhao, Y. (2021). Altered functional connectivity density and couplings in postpartum depression with and without anxiety. *Soc. Cogn. Affect. Neurosci.* 2021:nsab127. doi: 10.1093/scan/nsab127
- Cho, H., Seo, S. W., Kim, J. H., Suh, M. K., Lee, J. H., and Choe, Y. S. (2013). Amyloid deposition in early onset versus late onset Alzheimer's disease. *J. Alzheimer's Dis.* 35, 813–821. doi: 10.3233/JAD-121927
- Ding, B., Ling, H. W., Zhang, Y., Huang, J., Zhang, H., and Wang, T. (2014). Pattern of cerebral hyperperfusion in Alzheimer's disease and amnesic mild cognitive impairment using voxel-based analysis of 3D arterial spin-labeling imaging: initial experience. *Clin. Interv. Aging* 9, 493–500. doi: 10.2147/CIA.S58879
- Dong, L., Luo, C., Liu, X., Jiang, S., Li, F., and Feng, H. (2018). Neuroscience information toolbox: an open source toolbox for EEG-fMRI multimodal fusion analysis. *Front. Neuroinform.* 12:56. doi: 10.3389/fninf.2018.00056
- Epstein, R. A. (2019). Scene perception in the human brain. *Ann. Rev. Vis. Sci.* 5, 373–397. doi: 10.1146/annurev-vision-091718-014809
- Hadjichrysanthou, C., Evans, S., Bajaj, S., Siakallis, L. C., McRae-McKee, K., de Wolf, F., et al. (2020). The dynamics of biomarkers across the clinical spectrum of Alzheimer's disease. *Alzheimer's Res. Ther.* 12:74. doi: 10.1186/s13195-020-00636-z
- Hu, X., Jiang, Y., Jiang, X., Zhang, J., Liang, M., and Li, J. (2017). Altered functional connectivity density in subtypes of Parkinson's disease. *Front. Hum. Neurosci.* 11:458. doi: 10.3389/fnhum.2017.00458
- Julian, J. B., Ryan, J., and Hamilton, R. H. (2016). The occipital place area is causally involved in representing environmental boundaries during navigation. *Curr. Biol.* 26, 1104–1109. doi: 10.1016/j.cub.2016.02.066
- Li, K., Luo, X., Zeng, Q., Jiaerken, Y., Xu, X., and Huang, P. (2018b). Aberrant functional connectivity network in subjective memory complaint individuals relates to pathological biomarkers. *Transl. Neurodegener.* 7:27. doi: 10.1186/s40035-018-0130-z
- Li, W., Zhang, J., Zhou, C., Hou, W., Hu, J., and Feng, H. (2018a). Abnormal functional connectivity density in amyotrophic lateral sclerosis. *Front. Aging Neurosci.* 10:215. doi: 10.3389/fnagi.2018.00215
- Liang, L., Chen, Z., Wei, Y., Tang, F., Nong, X., and Li, C. (2021). Fusion analysis of gray matter and white matter in subjective cognitive decline and mild cognitive impairment by multimodal CCA-joint ICA. *NeuroImage Clin.* 32:102874. doi: 10.1016/j.nicl.2021.102874
- Liang, L., Zhao, L., Wei, Y., Mai, W., Duan, G., and Su, J. (2020). Structural and functional hippocampal changes in subjective cognitive decline from the community. *Front. Aging Neurosci.* 12:64. doi: 10.3389/fnagi.2020.00064
- Lista, S., Molinuevo, J. L., Cavado, E., Rami, L., Amouyel, P., and Teipel, S. J. (2015). Evolving evidence for the value of neuroimaging methods and biological markers in subjects categorized with subjective cognitive decline. *J. Alzheimer's Dis.* 48(Suppl.1), S171–191. doi: 10.3233/JAD-150202
- Liu, C., Zhao, L., Xu, K., Wei, Y., Mai, W., and Liang, L. (2022). Altered functional connectivity density in mild cognitive impairment with moxibustion treatment: a resting-state fMRI study. *Brain Res.* 1775:147732. doi: 10.1016/j.brainres.2021.147732
- Liu, J., Zhang, X., Yu, C., Duan, Y., Zhuo, J., and Cui, Y. (2016). Impaired parahippocampus connectivity in mild cognitive impairment and Alzheimer's disease. *J. Alzheimer's Dis.* 49, 1051–1064. doi: 10.3233/JAD-150727
- Liu, X., Chen, J., Shen, B., Wang, G., Li, J., and Hou, H. (2018). Altered intrinsic coupling between functional connectivity density and amplitude of low-frequency fluctuation in mild cognitive impairment with depressive symptoms. *Neural Plast.* 2018:1672708. doi: 10.1155/2018/1672708
- Liu, Y., Yu, C., Zhang, X., Liu, J., Duan, Y., and Alexander-Bloch, A. F. (2014). Impaired long distance functional connectivity and weighted network architecture in Alzheimer's disease. *Cereb. Cortex* 24, 1422–1435. doi: 10.1093/cercor/bhs410
- Mao, Y., Liao, Z., Liu, X., Li, T., Hu, J., and Le, D. (2021). Disrupted balance of long and short-range functional connectivity density in Alzheimer's disease (AD) and mild cognitive impairment (MCI) patients: a resting-state fMRI study. *Ann. Transl. Med.* 9:65. doi: 10.21037/atm-20-7019
- Mégevand, P., Groppe, D. M., Goldfinger, M. S., Hwang, S. T., Kingsley, P. B., and Davidesco, I. (2014). Seeing scenes: topographic visual hallucinations evoked by direct electrical stimulation of the parahippocampal place area. *J. Neurosci.* 34, 5399–5405. doi: 10.1523/JNEUROSCI.5202-13.2014
- Parker, A. F., Smart, C. M., and Scarapicchia, V. (2020). Identification of earlier biomarkers for Alzheimer's disease: a multimodal neuroimaging study of individuals with subjective cognitive decline. *J. Alzheimer's Dis.* 77, 1067–1076. doi: 10.3233/JAD-200299

- Rabin, L. A., and Smart, C. M. (2017). Subjective cognitive decline in preclinical Alzheimer's disease. *Ann. Rev. Clin. Psychol.* 13, 369–396. doi: 10.1146/annurev-clinpsy-032816-045136
- Ren, Z., Zhang, Y., He, H., Feng, Q., and Bi, T. (2019). The different brain mechanisms of object and spatial working memory: voxel-based morphometry and resting-state functional connectivity. *Front. Hum. Neurosci.* 13:248. doi: 10.3389/fnhum.2019.00248
- Richter, N., Nellesen, N., Dronse, J., Dillen, K., Jacobs, H. I. L., and Langen, K. J. (2019). Spatial distributions of cholinergic impairment and neuronal hypometabolism differ in MCI due to AD. *NeuroImage Clin.* 24:101978. doi: 10.1016/j.nicl.2019.101978
- Salman, M. S. (2016). The role of the pediatric cerebellum in motor functions, cognition, and behavior: a clinical perspective. *Neuroimag. Clin. North America* 26, 317–329. doi: 10.1016/j.nic.2016.03.003
- Scheff, S. W., Price, D. A., Schmitt, F. A., and Scheff, M. A. (2011). Synaptic loss in the inferior temporal gyrus in mild cognitive impairment and Alzheimer's disease. *J. Alzheimer's Dis.* 24, 547–557. doi: 10.3233/JAD-2011-101782
- Schmahmann, J. D. (1998). The cerebellar cognitive affective syndrome. *Brain* 121, 561–579. doi: 10.1093/brain/121.4.561
- Sekeres, M. J., Bradley-Garcia, M., and Martinez-Canabal, A. (2021). Chemotherapy-induced cognitive impairment and hippocampal neurogenesis: a review of physiological mechanisms and interventions. *Int. J. Mol. Sci.* 22:2312697. doi: 10.3390/ijms222312697
- Sharma, N., Murari, G., Vandermorris, S., Verhoeff, N., Herrmann, N., and Chen, J. J. (2021). Functional connectivity between the posterior default mode network and parahippocampal gyrus is disrupted in older adults with subjective cognitive decline and correlates with subjective memory ability. *J. Alzheimer's Dis.* 82, 435–445. doi: 10.3233/JAD-201579
- Song, Y., Xu, W., Chen, S., Hu, G., Ge, H., and Xue, C. (2021). Functional MRI-specific alterations in salience network in mild cognitive impairment: an ALE meta-analysis. *Front. Aging Neurosci.* 13:695210. doi: 10.3389/fnagi.2021.695210
- Sun, Y., Dai, Z., Li, Y., Sheng, C., Li, H., and Wang, X. (2016). Subjective cognitive decline: mapping functional and structural brain changes—a combined resting-state functional and structural MR imaging study. *Radiology* 281, 185–192. doi: 10.1148/radiol.2016151771
- Tao, W., Sun, J., Li, X., Shao, W., Pei, J., and Yang, C. (2020). The anterior-posterior functional connectivity disconnection in the elderly with subjective memory impairment and amnesic mild cognitive impairment. *Curr. Alzheimer's Res.* 17, 373–381. doi: 10.2174/1567205017666200525015017
- Thomas, K. R., Osuna, J. R., Weigand, A. J., Edmonds, E. C., Clark, A. L., and Holmqvist, S. (2021). Regional hyperperfusion in older adults with objectively-defined subtle cognitive decline. *J. Cerebr. Blood Flow Metabol.* 41, 1001–1012. doi: 10.1177/0271678X20935171
- Tomasi, D. (2010). Functional connectivity density mapping. *Proc. Natl. Acad. Sci. U. S. A.* 107, 9885–9890. doi: 10.1073/pnas.1001414107
- Tomasi, D. (2012). Resting functional connectivity of language networks: characterization and reproducibility. *Mol. Psychiatry* 17, 841–854. doi: 10.1038/mp.2011.177
- Tomasi, D., and Shokri-Kojori, E. (2016). High-resolution functional connectivity density: hub locations, sensitivity, specificity, reproducibility, and reliability. *Cerebr. Cortex* 26, 3249–3259. doi: 10.1093/cercor/bhv171
- van Strien, N. M., and Cappaert, N. L. (2009). The anatomy of memory: an interactive overview of the parahippocampal-hippocampal network. *Nat. Rev. Neurosci.* 10, 272–282. doi: 10.1038/nrn2614
- Vingerhoets, G. (2019). Phenotypes in hemispheric functional segregation? Perspectives and challenges. *Phys. Life Rev.* 30, 1–18. doi: 10.1016/j.plrev.2019.06.002
- Virley, D., Ridley, R. M., Sinden, J. D., Kershaw, T. R., Harland, S., and Rashid, T. (1999). Primary CA1 and conditionally immortal MHP36 cell grafts restore conditional discrimination learning and recall in marmosets after excitotoxic lesions of the hippocampal CA1 field. *Brain* 122, 2321–2335. doi: 10.1093/brain/122.12.2321
- Wang, J., Zuo, X., Dai, Z., Xia, M., Zhao, Z., and Zhao, X. (2013). Disrupted functional brain connectome in individuals at risk for Alzheimer's disease. *Biol. Psychiatry* 73, 472–481. doi: 10.1016/j.biopsych.2012.03.026
- Wang, S., Sun, H., Hu, G., Xue, C., Qi, W., and Rao, J. (2021). Altered insular subregional connectivity associated with cognitions for distinguishing the spectrum of pre-clinical Alzheimer's disease. *Front. Aging Neurosci.* 13:597455. doi: 10.3389/fnagi.2021.597455
- Ward, A. M., Schultz, A. P., Huijbers, W., Van Dijk, K. R., and Hedden, T. (2014). The parahippocampal gyrus links the default-mode cortical network with the medial temporal lobe memory system. *Hum. Brain Map.* 35, 1061–1073. doi: 10.1002/hbm.22234
- Woodruff-Pak, D. S., Foy, M. R., Akopian, G. G., Lee, K. H., Zach, J., and Nguyen, K. P. (2010). Differential effects and rates of normal aging in cerebellum and hippocampus. *Proc. Natl. Acad. Sci. U. S. A.* 107, 1624–1629. doi: 10.1073/pnas.0914207107
- Xu, W., Chen, S., Xue, C., Hu, G., Ma, W., and Qi, W. (2020). Functional MRI-specific alterations in executive control network in mild cognitive impairment: an ALE meta-analysis. *Front. Aging Neurosci.* 12:578863. doi: 10.3389/fnagi.2020.578863
- Xu, W., Rao, J., Song, Y., Chen, S., Xue, C., and Hu, G. (2021). Altered functional connectivity of the basal nucleus of meynert in subjective cognitive impairment, early mild cognitive impairment, and late mild cognitive impairment. *Front. Aging Neurosci.* 13:671351. doi: 10.3389/fnagi.2021.671351
- Xue, C., Sun, H., Yue, Y., Wang, S., Qi, W., and Hu, G. (2021). Structural and functional disruption of salience network in distinguishing subjective cognitive decline and amnesic mild cognitive impairment. *ACS Chem. Neurosci.* 12, 1384–1394. doi: 10.1021/acscchemneuro.1c00051
- Yan, C. G., Wang, X. D., and Zuo, X. N. (2016). DPABI: data processing & analysis for (resting-state) brain imaging. *Neuroinformatics* 14, 339–351. doi: 10.1007/s12021-016-9299-4
- Yu, M., Engels, M. M. A., Hillebrand, A., van Straaten, E. C. W., Gouw, A. A., and Teunissen, C. (2017). Selective impairment of hippocampus and posterior hub areas in Alzheimer's disease: an MEG-based multiplex network study. *Brain* 140, 1466–1485. doi: 10.1093/brain/awx050
- Yuan, Q., Qi, W., Xue, C., Ge, H., Hu, G., and Chen, S. (2021). Convergent functional changes of default mode network in mild cognitive impairment using activation likelihood estimation. *Front. Aging Neurosci.* 13:708687. doi: 10.3389/fnagi.2021.708687
- Zhang, B., Li, M., Qin, W., Demenescu, L. R., Metzger, C. D., and Bogerts, B. (2016). Altered functional connectivity density in major depressive disorder at rest. *Eur. Archiv. Psychiatry Clin. Neurosci.* 266, 239–248. doi: 10.1007/s00406-015-0614-0
- Zhang, J., Bi, W., Zhang, Y., Zhu, M., and Feng, H. (2015). Abnormal functional connectivity density in Parkinson's disease. *Behav. Brain Res.* 280, 113–118. doi: 10.1016/j.bbr.2014.12.007
- Zhao, X., Liu, Y., Wang, X., Liu, B., Xi, Q., and Guo, Q. (2012). Disrupted small-world brain networks in moderate Alzheimer's disease: a resting-state FMRI study. *PLoS ONE* 7:e33540. doi: 10.1371/journal.pone.0033540
- Zhuo, C., Zhu, J., Qin, W., Qu, H., Ma, X., and Tian, H. (2014). Functional connectivity density alterations in schizophrenia. *Front. Behav. Neurosci.* 8:404. doi: 10.3389/fnbeh.2014.00404

Conflict of Interest: The authors declare that the research was conducted in the absence of any commercial or financial relationships that could be construed as a potential conflict of interest.

Publisher's Note: All claims expressed in this article are solely those of the authors and do not necessarily represent those of their affiliated organizations, or those of the publisher, the editors and the reviewers. Any product that may be evaluated in this article, or claim that may be made by its manufacturer, is not guaranteed or endorsed by the publisher.

Copyright © 2022 Song, Wu, Chen, Ge, Yan, Xue, Qi, Yuan, Liang, Lin and Chen. This is an open-access article distributed under the terms of the Creative Commons Attribution License (CC BY). The use, distribution or reproduction in other forums is permitted, provided the original author(s) and the copyright owner(s) are credited and that the original publication in this journal is cited, in accordance with accepted academic practice. No use, distribution or reproduction is permitted which does not comply with these terms.



OPEN ACCESS

EDITED BY

Agustin Ibanez,
Latin American Brain Health Institute
(BrainLat), Chile

REVIEWED BY

Kirk R. Daffner,
Brigham and Women's Hospital
and Harvard Medical School,
United States
Jeffrey Maneval
Brigham and Women's Hospital and
Harvard Medical School, United States,
contributed to the review of KD
Aaron Meyer,
Georgetown University, United States
Jin San Lee,
Kyung Hee University, South Korea
Yeo Jin Kim,
Hallym University, South Korea

*CORRESPONDENCE

Mee Kyung Suh
mk.suh@samsung.com
Sang Won Seo
sw72.seo@samsung.com;
sw72.seo@gmail.com

†These authors have contributed
equally to this work

SPECIALTY SECTION

This article was submitted to
Alzheimer's Disease and Related
Dementias,
a section of the journal
Frontiers in Aging Neuroscience

RECEIVED 18 February 2022

ACCEPTED 01 August 2022

PUBLISHED 25 August 2022

CITATION

Kang SH, Park YH, Shin J, Kim H-R,
Yun J, Jang H, Kim HJ, Koh S-B, Na DL,
Suh MK and Seo SW (2022) Cortical
neuroanatomical changes related
to specific language impairments
in primary progressive aphasia.
Front. Aging Neurosci. 14:878758.
doi: 10.3389/fnagi.2022.878758

Cortical neuroanatomical changes related to specific language impairments in primary progressive aphasia

Sung Hoon Kang^{1,2†}, Yu Hyun Park^{1,3†}, Jiho Shin¹,
Hang-Rai Kim^{1,4}, Jihwan Yun¹, Hyemin Jang¹, Hee Jin Kim¹,
Seong-Beom Koh², Duk L. Na¹, Mee Kyung Suh^{1*} and
Sang Won Seo^{1,3,5,6,7*}

¹Department of Neurology, Samsung Medical Center, Sungkyunkwan University School of Medicine, Seoul, South Korea, ²Department of Neurology, Korea University Guro Hospital, Korea University College of Medicine, Seoul, South Korea, ³Department of Health Sciences and Technology, SAIHST, Sungkyunkwan University, Seoul, South Korea, ⁴Department of Neurology, Dongguk University Ilsan Hospital, Dongguk University College of Medicine, Goyang, South Korea, ⁵Department of Digital Health, SAIHST, Sungkyunkwan University, Seoul, South Korea, ⁶Alzheimer's Disease Convergence Research Center, Samsung Medical Center, Seoul, South Korea, ⁷Department of Intelligent Precision Healthcare Convergence, Sungkyunkwan University, Suwon, South Korea

Objective: Language function test-specific neural substrates in Korean patients with primary progressive aphasia (PPA) might differ from those in other causes of dementia and English-speaking PPA patients. We investigated the correlation between language performance tests and cortical thickness to determine neural substrates in Korean patients with PPA.

Materials and methods: Ninety-six patients with PPA were recruited from the memory clinic. To acquire neural substrates, we performed linear regression using the scores of each language test as a predictor, cortical thickness as an outcome and age, sex, years of education, and intracranial volume as confounders.

Results: Poor performance in each language function test was associated with lower cortical thickness in specific cortical regions: (1) object naming and the bilateral anterior to mid-portion of the lateral temporal and basal temporal regions; (2) semantic generative naming and the bilateral anterior to mid-portion of the lateral temporal and basal temporal regions; (3) phonemic generative naming and the left prefrontal and inferior parietal regions; and (4) comprehension and the left posterior portion of the superior and middle temporal regions. In particular, the neural substrates of the semantic generative naming test in PPA patients, left anterior to mid-portion of the lateral and basal temporal regions, quite differed from those in patients with other causes of dementia.

Conclusion: Our findings provide a better understanding of the different pathomechanisms for language impairments among PPA patients from those with other causes of dementia.

KEYWORDS

neural substrate, language function test, primary progressive aphasia, object naming, generative naming, comprehension, cortical atrophy

Introduction

Primary progressive aphasia (PPA) is a clinical syndrome characterized by focal neurodegeneration in the language-dominant cerebral hemisphere that leads to language impairment in the absence of other salient cognitive impairments. There are three PPA subtypes: non-fluent/agrammatic variant PPA (nfvPPA), semantic variant PPA (svPPA), and logopenic variant PPA (lvPPA), which are based on the nature of language impairment (Gorno-Tempini et al., 2011). Specifically, nfvPPA shows an abnormality of syntax/grammar or effortful/halting speech with apraxia of speech, svPPA has poor performance in single-word comprehension and confrontational naming, and lvPPA has word-finding hesitation and impaired repetition of sentences and phrases (Gorno-Tempini et al., 2011). During the course of the PPA diagnosis, patients undergo a series of language assessments using normalized language evaluation tools (ex. Western Aphasia Battery [WAB], Boston Naming Test [BNT]) and supporting tasks/tests to determine whether the patient has disrupted grammatical abilities, semantics, phonological processing, or other language-related processes.

The development of neuroimaging methods has enabled the detection of subtle cortical atrophy in neurodegenerative diseases. Specifically, three PPA subtypes showed distinct cortical atrophy patterns that correlated with language impairment patterns: left prefrontal atrophy in nfvPPA, left anterior temporal atrophy in svPPA, and left superior temporal and inferior parietal atrophy in lvPPA (Sapolsky et al., 2010; Gorno-Tempini et al., 2011). Especially, given that cortical atrophy precedes the onset of language impairment in patients with PPA (Rogalski and Mesulam, 2009), the language impairment-cortical atrophy correlation, called neural substrates of language impairment, is important in clinical practice, not only to understand a patient's current language impairment but also to predict the progression of symptoms. Previous studies based on patients with PPA showed that performances in language fluency, comprehension, repetition, and object naming tests were mainly associated with cortical atrophy in specific regions (Rogalski et al., 2011a; Mesulam et al., 2014, 2019; Forkel et al., 2020).

However, the neural substrates of each language component differed slightly among the research groups (Amici et al., 2007; Rogalski et al., 2011a). The differences may have come from the different tasks the researchers used to detect the associated brain areas of a certain language function. Furthermore, there is a paucity of information about the atrophy patterns of the three PPA subtypes in the Korean population, although growing evidence reveals distinct cortical atrophy patterns based on PPA subtypes in the Western population. Given that the Korean language is quite different from English in, for example, grammar and generative syntax, the neural substrates of language tests may show different patterns between the Korean and English-speaking populations. Regarding grammar and generative syntax, the main differences between the two languages are word order, usage of postpositions/particles, and verb conjugations. Thus, these differences may reflect different neural substrates of fluency and atrophy patterns of nfvPPA in the Korean, compared to those in the English-speaking populations. Hence, it is necessary to reduce the knowledge gaps in the current understanding of cortical atrophy patterns of PPA subtypes and neural substrates of language impairments in different racial/ethnic populations, such as the Korean population. Previously, our group revealed the neural substrates of language impairment in Korean Alzheimer's continuum (Albert et al., 2011; McKhann et al., 2011; Sperling et al., 2011) including preclinical Alzheimer's disease (AD), mild cognitive impairment due to AD and AD dementia (Ahn et al., 2011; Kang et al., 2019) and subcortical vascular cognitive impairment (SVCI) (Kang et al., 2021). However, given that neural substrates are affected by cortical atrophy patterns in specific diseases, it might be noteworthy to examine the neural substrates of language tests in PPA and find a pattern which differs from previously reported results of patients with other causes of dementia.

Therefore, our study aimed to investigate language function test-specific neural substrates in a relatively large sample of Korean patients with PPA. First, we identified distinct cortical atrophy patterns in the three Korean PPA subtypes. Second, we explored the correlation between language performance across six domains of language, namely, language fluency,

comprehension, sentence repetition, object naming, semantic generative naming, and phonemic generative naming, and cortical thickness in Korean patients with PPA.

Materials and methods

Study participants

We recruited 109 patients with PPA (35 patients with svPPA, 51 patients with nvPPA, and 23 patients with lvPPA) from the dementia clinic in the Department of Neurology at Samsung Medical Center in Seoul, Korea, between October 2014 and December 2019. All patients met the core criteria for PPA (Gorno-Tempini et al., 2011) as follows: (1) language impairment being the earliest and most prominent clinical feature and (2) the principal cause of impaired activities of daily living, at initial phases of the disease. Based on the PPA consensus criteria (Gorno-Tempini et al., 2011), we classified the patients as having nvPPA, svPPA, and lvPPA.

All participants underwent comprehensive dementia evaluation including a clinical interview, neurological examination, standardized neuropsychological test, standardized language function test, blood tests, and high-resolution T1-weighted magnetic resonance imaging (MRI) scans. The time interval between the language function tests and MRI scans was less than 1 year.

All participants were determined for handedness using a questionnaire “measurement of handedness in Koreans” (Kang, 1994), which included five questions in such as “Which hand do you use most when. . .?” There were five questions concerning writing, using chopsticks, throwing a ball, using a knife, and using scissors. Further, to exclude the forced right-handedness linked with cultural aspects, we defined individuals who wrote and/or used chopsticks with their right hand and did the rest of the items with their left hand as left-handedness.

We excluded patients with secondary causes of cognitive deficits confirmed with laboratory tests, including vitamin B12 test, syphilis serology, and thyroid/renal/hepatic function tests, and those with structural lesions on conventional brain MRI, such as territorial infarction, intracranial hemorrhage, brain tumor, hydrocephalus, or severe white matter hyperintensities (D3P3), according to the modified Fazekas ischemic scale (Noh et al., 2014). Patients clinically diagnosed with other types of degenerative diseases, such as AD, progressive supranuclear palsy, cortico-basal syndrome, behavioral variant frontotemporal dementia, or Lewy body/Parkinson’s disease dementia, were also excluded at baseline evaluation.

We also recruited 308 participants with normal controls (NC) as previously described (Kang et al., 2021). All participants with NC met the following criteria: (1) no medical history, which is likely to affect cognitive function based on Christensen’s health screening criteria (Christensen et al., 1991); (2)

no objective cognitive impairment from comprehensive neuropsychological test battery on any cognitive domains (≥ -1.0 SD of age- and education-matched norms on any cognitive tests); (3) independence in activities of daily living; (4) neither structural lesions nor severe white matter hyperintensity on brain MRI; and (5) negative amyloid deposition on positron emission tomography, by using visual assessment.

This study was approved by the institutional review board of the Samsung Medical Center. Written informed consent was obtained from all the patients or their caregivers.

Language assessment

A total of 109 patients with PPA underwent the Korean version of the Western Aphasia Battery (K-WAB), a standardized language function test (Kim and Na, 2004). All patients were evaluated by certified linguistic pathologists, and the scoring system of most tests in the K-WAB remained the same as that of the original Western Aphasia Battery. However, some aspects of the rating scale have been changed, as previously described (Lee et al., 2020). Among the many language function tests evaluated in the K-WAB, we used tests that provided numeric scores and represented the six domains of language function: language fluency, comprehension, sentence repetition, object naming, semantic generative naming, and phonemic generative naming. For language fluency, spontaneous speech was scored using the 10-point fluency scale and 10 points for information content. The comprehension task (200-point) consisted of yes/no questions (60-point), auditory word recognition (60-point), and sequential command (80-point). Yes/no question and sequential commands tasks include a few syntactically-complex sentences. The repetition task consisted of single syllable word to sentences of six groupings in length with combinations of words and word + postpositions (10-point). For object naming (60-point), we used the 20 objects provided in the K-WAB battery. Object naming task is performed by asking the subjects/patients to name the objects shown to them, thus the task does not require overt responses of object knowledge. However, when patients are unable to respond or make errors spontaneously, after the semantic and phonemic cues are given, respectively, and the patient’s responses all marked, the patients are asked to describe what the object is for or how it is used, either verbally or through gestures. This was to check to see whether the patient’s object knowledge functions were preserved or not. For semantic generative naming, animal category was used, and phonemic generative naming consisted of Korean letters categories. Furthermore, we calculated aphasia quotient (AQ) to assess the overall severity of language impairment as a following formula: scores for information content and fluency in the subtest of spontaneous speech and the converted scores of comprehension, repetition

and naming tasks all of which are 10 points, respectively, are added and then multiplied by 2 to make 100.

Acquisition of three-dimensional magnetic resonance images

We acquired three-dimensional T1 Turbo Field Echo MRI scans of 109 patients with PPA using a 3.0 T MRI scanner (Philips 3.0T Achieva) with the following imaging parameters: sagittal slice thickness, 1.0 mm with 50% overlap; no gap; repetition time of 9.9 ms; echo time of 4.6 ms; flip angle of 8°; and matrix size of 240 × 240 pixels reconstructed to 480 × 480 over a field view of 240 mm.

Magnetic resonance imaging data processing for cortical thickness measurements

The images were processed using the CIVET anatomical pipeline (version 2.1.0) (Zijdenbos et al., 2002). The native MRI images were registered to the Montreal Neurological Institute—152 templates by linear transformation (Collins et al., 1994) and corrected for intensity non-uniformities using the N3 algorithm (Sled et al., 1998). The registered and corrected images were divided into white matter, gray matter, cerebrospinal fluid, and background. The constrained Laplacian-based automated segmentation with proximity algorithm (Kim et al., 2005) automatically extracts the surfaces of the inner and outer cortices. The inner and outer surfaces had the same number of vertices, and there were close correspondences between the vertices of the inner and outer cortical surfaces. Cortical thickness, defined as the Euclidean distance between the linked vertices of the inner and outer surfaces (Lerch and Evans, 2005), was not calculated in Talairach spaces but in native brain spaces because of the limit of linear stereotaxic normalization. As expected, there was a significant positive correlation between cortical thickness and intracranial volume (ICV) in the native space (Im et al., 2008). Controlling for ICV, which reflects the brain size effect, is necessary to compare cortical thickness among participants. In a previous study (Im et al., 2008), the measurement of native space cortical thickness, followed by analyses that include brain size as a covariate, is an efficient method that explains the relationship between cortical thickness and brain size in depth. The ICV is defined as the total volume of gray matter, white matter, and cerebrospinal fluid. It was calculated by measuring the total volumes of the voxels within the brain mask, which were obtained *via* functional MRI of the brain software library bet algorithm (Smith, 2002). Cortical surface models were extracted from MRI volumes transformed into stereotaxic space, and cortical thickness was measured in the native space by applying an inverse transformation matrix to

the cortical surfaces and reconstructing them in the native space (Im et al., 2006).

We applied surface-based two-dimensional registration with a sphere-to-sphere warping algorithm and spatially normalized the cortical thickness values to compare the thickness of corresponding regions among subjects. We used an improved surface registration algorithm and an unbiased iterative group template showing enhanced anatomic detail (Lyttelton et al., 2007) to transform the thickness information of the vertices into an unbiased iterative group template.

Surface-based diffusion smoothing with a full-width at half-maximum of 20 mm was used to blur each cortical thickness map, which increased the signal-to-noise ratio and statistical power (Chung et al., 2003; Im et al., 2006).

Thirteen patients with PPA were excluded due to errors in the analyses of cortical thickness, including CIVET pipeline errors ($n = 6$) and gray-white matter segmentation errors due to severe atrophy ($n = 7$). Therefore, a total of 96 patients with PPA were included in the main analyses.

Magnetic resonance imaging data processing for cortical thickness measurement

As described in a previous study (Kang et al., 2019) to measure asymmetric degrees of neural substrates for language function tests, we acquired an asymmetric index (AI), which was calculated using the following formula: $(R - L/R + L)$, where R indicates the number of vertices with significant correlations in the right hemisphere and L indicates the number of vertices with significant correlations in the left hemisphere. After acquiring the AI, we divided the extent of asymmetry into three groups according to the absolute AI value. When the absolute value of AI was ≤ 0.1 , > 0.1 , and ≤ 0.5 , or > 0.5 , we classified the cases as no hemispheric dominance, weak hemispheric dominance, or strong hemispheric dominance, respectively.

Statistical analyses

We used analysis of variance and chi-square tests to compare the clinical demographic data and the results of the language function tests between the PPA subtype groups. SPSS version 25.0 (SPSS Inc., Chicago, IL, United States) was used to analyze the statistical data. Statistical significance was set at $p < 0.05$.

For cortical thickness analyses of MRI data from patients with PPA, we used a MATLAB-based toolbox (freely available online at the University of Chicago website: <http://galton.uchicago.edu/faculty/InMemoriam/worsley/research/surfstat/>). To identify the cortical atrophy pattern in the three PPA subtypes, we analyzed localized differences in cortical thickness between the NC and PPA subtype groups using

a general linear model after controlling for age, sex, years of education, AQ, and ICV.

In order to investigate the correlation between each language function test score and cortical thickness in patients with PPA, we entered cortical thickness data into the dependent variable and language scores into the independent variable due to the high dimensionality of cortical thickness data (about 80,000 vertices). To check the consistency in the neural substrate depending on the ratio of PPA subtypes, we further performed a sensitivity analysis after excluding the 26 patients with nvPPA to change the ratio of PPA subtypes (20 nvPPA, 30 svPPA, and 20 lvPPA). Linear regression was performed after controlling for age, sex, years of education, and ICV as covariates. The statistical maps were thresholded using random field theory (RFT) at $p < 0.05$.

Results

Clinical characteristics of the patients

Table 1 shows the baseline demographics of the patients with PPA. The mean baseline age was 67.1 ± 8.9 years and 46 out of 96 (47.9%) were women. The mean years

of education were 11.6 ± 4.4 and the mean AQ score was 65.9 ± 21.4 . All patients were right-handed. In terms of each PPA subtype, patients with svPPA had higher years of education (13.8 ± 2.7 years) than those with nvPPA (11.5 ± 4.8 years) and lvPPA (10.2 ± 4.4 years). There was no difference in age ($p = 0.089$), sex ratio ($p = 0.920$), disease duration ($p = 0.558$), AQ score ($p = 0.853$), and CDR ($p = 0.950$) between the three groups.

Topography of cortical thinning in patients with subtypes of primary progressive aphasia

Figure 1 shows the topography of cortical thinning in patients with PPA subtypes. Compared to participants with NC, patients with nvPPA mainly exhibited cortical thinning in the bilateral prefrontal (superior, middle, inferior, and medial frontal), left superior and middle temporal, right superior temporal, bilateral parietal, and right occipital regions. Patients with svPPA mainly exhibited cortical thinning in the bilateral temporal (superior, middle, inferior, and anterior temporal) and inferior frontal regions. Patients with lvPPA exhibited significant cortical thinning in the left superior/inferior/anterior

TABLE 1 Demographic variables and AQ of the patients with primary progressive aphasia.

| | Total (n = 96) | nvPPA (n = 46) | svPPA (n = 30) | lvPPA (n = 20) | p-value | NC (n = 308) |
|---------------|-----------------|-----------------|-----------------|-----------------|---------|------------------|
| Age | 67.1 ± 8.9 | 69.0 ± 9.2 | 66.8 ± 9.9 | 64.5 ± 7.0 | 0.089 | $69.5 \pm 8.4^*$ |
| Sex (M:W) | 46:50 | 23:23 | 14:16 | 9:11 | 0.920 | 189:119* |
| Duration (m) | 29.0 ± 16.9 | 29.2 ± 19.6 | 30.9 ± 15.0 | 25.7 ± 12.2 | 0.558 | |
| Education (y) | 11.6 ± 4.4 | 11.5 ± 4.8 | 13.8 ± 2.7 | 10.2 ± 4.4 | 0.019 | 11.9 ± 4.7 |
| AQ | 65.9 ± 21.4 | 65.5 ± 22.3 | 68.3 ± 21.3 | 65.0 ± 20.7 | 0.853 | |
| CDR | | | | | 0.794 | |
| 0/0.5 | 56 (58.3%) | 26 (56.5%) | 17 (56.7%) | 13 (65.0%) | | |
| 1/2/3 | 40 (41.7%) | 20 (43.5%) | 13 (43.3%) | 7 (35.0%) | | |

Values are presented as the mean \pm standard deviation. The p -values were obtained using analysis of variance, chi-square tests between three PPA subtypes.

*Normal control had older age and higher men ratio than patients with PPA. AQ, aphasia quotient; CDR, clinical dementia rating; lvPPA, logopenic variant primary progressive aphasia; M, men; m, month; n, number of patients whose data were available for analysis; NC, normal control; nvPPA, non-fluent variant primary progressive aphasia; svPPA, semantic variant primary progressive aphasia; W, women; y, year.

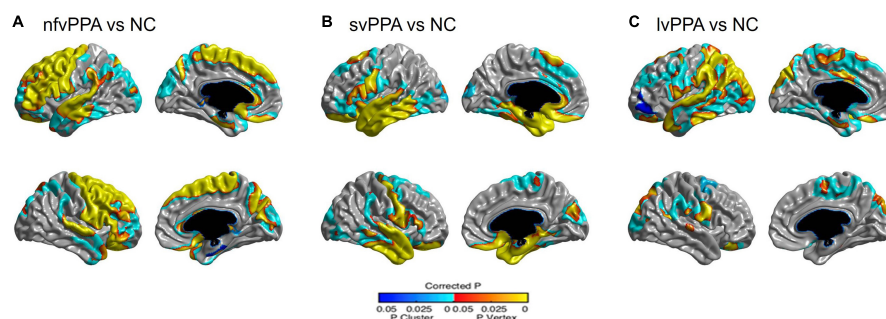


FIGURE 1

Statistical representation of cortical thickness in (A) nvPPA compared to NC, (B) svPPA compared to NC, and (C) lvPPA compared to NC. nvPPA, non-fluent variant primary progressive aphasia; svPPA, semantic variant primary progressive aphasia; lvPPA, logopenic variant primary progressive aphasia; NC, normal controls.

temporal, superior/inferior parietal, and occipital regions and right inferior parietal regions.

Correlation between language function tests and cortical thickness

The statistical map showed that lower cortical thickness in specific brain regions was associated with raw scores on language function tests, including comprehension, object naming, semantic generative naming, and phonemic generative naming, whereas the scores for language fluency and sentence repetition were not (Figure 2). Specifically, the score on the comprehension test was positively associated with cortical thickness in the left posterior portion of the superior and middle temporal regions. The score on the object naming test was positively associated with cortical thickness in the bilateral anterior to mid-portion of the lateral temporal and basal temporal regions. The score on the semantic generative naming test was positively associated with cortical thickness in the left anterior to mid-portion of the lateral and basal temporal regions. The score on the phonemic generative naming test was positively associated with cortical thickness in the left prefrontal and inferior parietal regions. After the threshold of the statistical map was changed from RFT correction at a p -value of 0.05 to an uncorrected p -value of 0.01, the score in sentence repetition was positively associated with the posterior portion of the left superior temporal, temporo-parietal junction, and inferior parietal regions (Supplementary Figure 1).

We explored the hemispheric dominance of neural substrates using the AI value. Neural substrates for comprehension, semantic generative naming, and phonemic generative naming have a strong left hemispheric dominance.

Sensitivity analysis

Among 70 patients with PPA (20 nvfPPA, 30 svPPA, and 20 lvPPA), the neural substrate of object naming tests was similar to those in main results, while the correlations between the other language function tests (comprehension, semantic generative naming, and phonemic generative naming) and cortical thickness were not significant, because the sample size was small (Supplementary Figure 2). However, after the threshold of the statistical map was changed from RFT correction to an uncorrected p -value of 0.05, the patterns in neural substrates of semantic and phonemic generative naming test were similar to those in main results. The neural substrate of comprehension tests were bilateral inferior temporal and inferior parietal regions, which was partially consistent with those in main results.

Discussion

In this study, we investigated the neural substrates of language function tests in a relatively large cohort of Korean

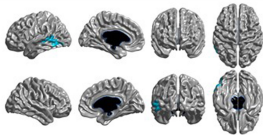
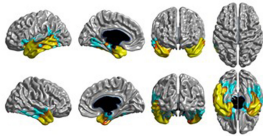
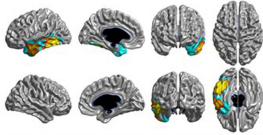
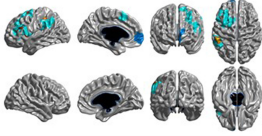
| Subtests | Correlation Maps | Correlation Areas | AI = R-L/R+L |
|----------------------------|---|---|--------------|
| Comprehension |  | Lt: posterior portion of superior and middle temporal regions | -0.51 |
| | | Rt: none | |
| Object naming |  | Lt: lateral and basal temporal regions | -0.29 |
| | | Rt: anterior to mid-portion of lateral temporal, and basal temporal regions | |
| Semantic generative naming |  | Lt: lateral and basal temporal regions | -0.54 |
| | | Rt: none | |
| Phonemic generative naming |  | Lt: prefrontal and inferior parietal regions | -0.60 |
| | | Rt: none | |

FIGURE 2

Correlation maps demonstrating the association between cortical thickness and language function tests in patients with PPA (AI > 0 means right-sided correlated areas > left-sided correlated areas, and vice versa for AI < 0). AI, asymmetric index; Rt, right; Lt, left.

patients with PPA. Our major findings are as follows: First, the three PPA subtypes showed distinct cortical atrophy patterns, which are consistent with previous studies from Western countries. Second, poor performance on each language function test was associated with lower cortical thickness in specific cortical regions. Specifically, object naming and semantic generative naming had similar neural substrates, whereas, different neural substrates were manifested in each of the generative naming tests: semantic and phonemic: the bilateral anterior to mid-portion of the lateral temporal and basal temporal regions in the object naming test, left anterior to mid-portion of the lateral and basal temporal regions in the semantic generative naming test, and left prefrontal and inferior parietal regions in the phonemic generative naming test. In particular, the neural substrates related to the semantic generative naming test in patients with PPA quite differ from previously reported results of patients with other causes of dementia. Taken together, our findings suggest that the neural substrates of language performance in Korean patients with PPA are specific to each language domain. Furthermore, a better understanding of the neural substrates specific to PPA might help clinicians understand the neural network of each language component and predict cortical atrophy patterns from the results of language function tests in Korean patients with PPA.

In the present study, the PPA subtypes showed distinct patterns of cortical atrophy. Specifically, we identified prefrontal and temporal atrophy in the nfvPPA, inferior frontal and anterior to mid-portion of temporal atrophy in the svPPA, and superior temporal and inferior parietal atrophy in the lvPPA. Our findings are consistent with those of previous studies conducted in Western countries (Sapolsky et al., 2010; Mesulam et al., 2014). However, there were several overlaps in atrophy across the PPA subtypes: left temporal atrophy in all three PPA subtypes and left inferior frontal atrophy in nfvPPA and svPPA. This finding may be due to higher proportion of middle-stage PPA in the present study compared to the previous studies (Sapolsky et al., 2010). Therefore, our findings suggest that the patterns of cortical atrophy in the three PPA subtypes lead to the development of corresponding clinical syndromes, regardless of differences in language.

Our major finding was that poor performance on each language function test was associated with lower cortical thickness in specific regions. Each naming test yielded different neural substrates. Specifically, poor performance in the object naming test was associated with lower cortical thickness in the bilateral (left predominant) anterior to the mid-portion of the lateral temporal and basal temporal regions. Our findings were consistent with those of previous studies investigating neural substrates for object naming in patients with PPA (Patterson et al., 2007; Hurley et al., 2012; Mesulam et al., 2013, 2019). The studies consistently suggested that anterior temporal atrophy was responsible for impaired object naming function observed in PPA patients. The basal temporal regions, which are one of

the neural substrates of object naming in the present study, are reported to be vital to object naming. Previous MRI studies with patients with AD or SVCI revealed consistent findings that poor performance in BNT, which is a different evaluation tool for object naming, was associated with basal temporal regions (Ahn et al., 2011; Baldo et al., 2013; Kang et al., 2019). However, our study revealed that the mid-portion of temporal atrophy was associated with impaired object naming as well. According to the progression patterns of cortical atrophy in PPA, mid-portion temporal atrophy was accompanied by anterior temporal atrophy (Rogalski et al., 2011b); therefore, it might be reasonable to expect a result related to the mid-portion of temporal atrophy.

Unlike object naming tests, word fluency tasks rely on frontal executive control processes, such as initiation, self-monitoring, cognitive flexibility, and inhibition of dominant responses (Miyake and Friedman, 2012), as well as language-related functions, such as accessing semantic and lexical knowledge to identify related items (Henry and Crawford, 2004), lexical access ability (Shao et al., 2014), and language processing abilities (Whiteside et al., 2016). However, in the present study, poor performance in the semantic generative naming test was mainly associated with lower cortical thickness in the left anterior to mid-portion of the lateral and basal temporal regions. Our findings are inconsistent with those of previous studies on other causes of dementia (Kang et al., 2019, 2021). The previous studies showed that the neural substrates for semantic generative naming turned out to be frontal regions as well as anterior and inferior temporal regions in AD patients (Kang et al., 2019) and only superior and inferior frontal regions (but not temporal regions) in SVCI patients (Kang et al., 2019, 2021).

It is important to know the reason for the different patterns of the neural substrates related to the semantic generative naming test between our results and previous reported results of patients with other causes of dementia because it might provide a better understanding of the different pathomechanisms for semantic generative naming dysfunction among these patients. The ability to access semantic and lexical knowledge is required to perform semantic word fluency tasks (Gordon et al., 2018). One of the PPA subtypes (i.e., svPPA) manifests with severe deficits in semantic processing associated with temporal regions (Wilson et al., 2014). Severe semantic processing dysfunction in patients with PPA causes them to struggle to come up with a word within a category, which may leave no room for frontal executive functions to play a role in performing the task (Riello et al., 2021). In contrast, the previous results shown in patients with AD may reflect the fact that both temporal and frontal functions affect their performance on this task (Ahn et al., 2011; Kang et al., 2019). In addition, in patients with SVCI, because their semantic system is somewhat intact, frontal dysfunction may be the main function influencing their performance on this task (Kang et al., 2021). In fact, our findings were consistent

with those of a recent study based on patients with PPA, which showed that poor performance in the semantic generative naming test was associated with lower cortical thickness in left lateral temporal region (Riello et al., 2021).

Moreover, we found that poor performance on the phonemic generative naming test was associated with lower cortical thickness in the left prefrontal and inferior parietal regions. These findings are in line with those of previous studies in patients with AD and SVCI (Keilp et al., 1999; Kitabayashi et al., 2001; Kang et al., 2021). A recent study based on PPA patients revealed that poor performances in the phonemic generative naming test were associated with prefrontal atrophy (Riello et al., 2021). Phonemic word fluency tasks may require access to a certain phoneme and active frontal executive functions that include self-monitoring, set shifting, and applying different strategies to come up with words that satisfy the target phoneme (Dilkina et al., 2010; Biesbroek et al., 2021). The inferior parietal region has previously been reported to be related to phonologic errors, which might indicate partial difficulty in appropriate phoneme access (Petroi et al., 2020). lvPPA manifests difficulties in phonological processing, involving atrophy in the inferior parietal region. Additionally, nvPPA is characterized by frontal executive dysfunction and atrophy of the frontal region. Therefore, our neuroimaging findings of the frontal and inferior parietal atrophies related to the phonemic generative naming test may reflect the phoneme access functions and frontal executive functions required to perform this task. Meta-analysis also revealed that the phonemic generative naming test mainly relies on frontal executive function, which supports our finding (Henry and Crawford, 2004).

We found that impairment of overall comprehension was associated with lower cortical thickness in the left posterior portion of the superior and middle temporal regions. Meta-analyses investigating the neural substrates of comprehension have reported that the temporal lobe plays an important role in various comprehension tasks (Ferstl et al., 2008; Binder et al., 2009). Recent studies with PPA suggested that the anterior portion of the temporal region was associated with comprehension (Rogalski et al., 2011a; Mesulam et al., 2015, 2019), which was different from classic aphasiology. Prior anatomical studies of stroke lesions have shown that Wernicke's area plays an important role in comprehension (Robson et al., 2013; Hillis et al., 2017). Given that the neural substrates in our study included Wernicke's area, our results support the findings of stroke studies. An explanation for these discrepant results between our study and previous studies using PPA patients is the difference in the components of comprehension. Previous studies have explored the neural substrates of only word comprehension rather than overall comprehension. However, comprehension tests on the K-WAB include word comprehension, sentence comprehension, and command comprehension.

Poor sentence repetition performance was not associated with lower cortical thickness in any of the regions. However,

before RFT correction, there was a trend of positive correlation between the score on sentence repetition and cortical thickness in the posterior portion of the superior temporal, temporo-parietal junction, and inferior parietal regions, which was significant at an uncorrected p -value of 0.01. These regions include Wernicke's area associated with comprehension rather than repetition by classic aphasiology. However, these regions were consistent with known neural substrates of repetition in patients with PPA (Amici et al., 2007; Mesulam et al., 2019; Forkel et al., 2020). Furthermore, previous studies have revealed that the temporoparietal junction is vital for the integrity of phonological encoding and auditory working memory necessary for repetition (Gorno-Tempini et al., 2008; Binder, 2015, 2017).

In the present study, no specific cortical atrophy regions were identified in the language fluency task, although previous studies with English-speaking patients with PPA showed that the inferior and middle frontal regions were mainly correlated with language fluency (Sapolsky et al., 2010; Rogalski et al., 2011a). We have used the 10-point fluency scores (fluency, grammatical competence, and paraphasia in K-WAB) to see the associated cortical areas with language fluency, which showed null results. Since the Korean language is somewhat less strict in grammar compared to English, there is no adequate evaluation tool that can be used to detect grammatical processing in Korean. Further research using detailed utterance analysis based on the transcription of spontaneous speech performances may enable us to detect areas specific to fluency characteristics in Korean.

According to our expectations, poor performance in most language function tests was more likely to be associated with lower cortical thickness in the left hemisphere, and left hemispheric dominance were strong. The neural substrates of overall comprehension, sentence repetition, semantic generative naming, and phonemic generative naming were strongly lateralized in the left hemisphere. This may also be explained by the left-dominant cerebral atrophy pattern in patients with PPA. Contrary to expectations, however, the neural substrate of object naming had weak left hemispheric dominance. The absence of lateralization in object naming has been reported previously (Teipel et al., 2006; Apostolova et al., 2008). Another study showed that right anterior temporal area was responsible for making semantic decision, although the significance of the right hemisphere for naming is not fully understood. Some researchers have suggested that the neural substrate of naming is primarily lateralized to the left hemisphere and becomes bilateral during the aging process (Cabeza, 2002). Actually, one study comparing naming performance between younger and older adults showed that older participants were more likely to have bilateral activation than younger participants (Wierenga et al., 2008). The other MRI study observed a positive correlation between naming ability and bilateral gray matter volume in older participants (Obler et al., 2010). Increasing involvement of the right hemisphere might be explained by the compensation for brain atrophy with aging. Given that the patients in our study were elderly, our findings are in line with those of previous studies.

In the present study, we investigated the neural substrates of language function tests in a relatively large sample of Korean patients with PPA. However, this study has several limitations. First, although we showed that specific cortical regions were associated with poor performance on language function tests, it is doubtful that all cortical regions that we found represent test-specific cortical areas. Rather, some neural substrates for each language function test may be relevant to basic language or cognitive processes shared by a variety of cognitive functions. Second, we used the measure of cortical thickness representing the gray matter structure to explore neural substrates. Thus, we did not include changes in white matter structure. However, this argument has been mitigated to some degree by the fact that PPA is a neurodegenerative disease that primarily affects the cerebral cortex. Third, we did not assess the cerebral dysfunction which precedes the cortical atrophy. Finally, we could not perform a direct comparison of neural substrates between patients with Korean-speaking PPA and those with AD or between those with Korean-speaking PPA and those with English-speaking PPA. Nevertheless, our study is noteworthy because it was based on Korean patients who had a different language and culture from English-speaking PPA patients. Furthermore, our findings may help clinicians diagnose PPA and predict disease progression through a better understanding of the neural substrates of language impairment in patients with PPA.

In conclusion, Korean patients with PPA showed that poor performance in each language function test was associated with atrophy in specific cortical regions. In particular, the neural substrates of the semantic generative naming test in patients with PPA quite differ from those in patients with other causes of dementia. This might provide a better understanding of the different pathomechanisms of language impairment among these patients.

Data availability statement

The raw data supporting the conclusions of this article will be made available by the authors, without undue reservation.

Ethics statement

This study was approved by the Institutional Review Board of the Samsung Medical Center. Written informed consent was obtained from all the patients or their caregivers. The patients/participants provided their written informed consent to participate in this study.

Author contributions

SK, MS, and SS: concept and design. JS, JY, H-RK, HJ, HK, S-BK, DN, MS, and SS: acquisition of data. SK, YP, MS,

and SS: analysis or interpretation of data. SK: drafting of the manuscript. SK, S-BK, MS, and SS: intellectual content. SK and YP: statistical analysis. MS and SS: administrative, technical, or material support and supervision. All authors contributed to the article and approved the submitted version.

Funding

This research was supported by a grant from the Korean Health Technology R&D Project, Ministry of Health & Welfare, South Korea (HI19C1132); a grant from the Korea Health Technology R&D Project through the Korea Health Industry Development Institute (KHIDI), funded by the Ministry of Health & Welfare and Ministry of science and ICT, South Korea (Grant Nos. HU20C0111, HU22C0170, and HR21C0885); the National Research Foundation of Korea (NRF) grant funded by the Korea government (MSIT) (NRF-2019R1A5A2027340); Institute of Information & Communications Technology Planning & Evaluation (IITP) grant funded by the Korea government (MSIT) (No. 2021-0-02068, Artificial Intelligence Innovation Hub); Future Medicine 20*30 Project of the Samsung Medical Center (#SMX1220021); the “National Institute of Health” research project (2021-ER1006-01); Korea University Guro Hospital (KOREA RESEARCH-DRIVEN HOSPITAL) and grant funded by Korea University Medicine (K2210201); and Basic Science Research Program through the National Research Foundation of Korea (NRF) funded by the Ministry of Education (Grant No. 2022R1I1A1A01056956).

Conflict of interest

The authors declare that the research was conducted in the absence of any commercial or financial relationships that could be construed as a potential conflict of interest.

Publisher's note

All claims expressed in this article are solely those of the authors and do not necessarily represent those of their affiliated organizations, or those of the publisher, the editors and the reviewers. Any product that may be evaluated in this article, or claim that may be made by its manufacturer, is not guaranteed or endorsed by the publisher.

Supplementary material

The Supplementary Material for this article can be found online at: <https://www.frontiersin.org/articles/10.3389/fnagi.2022.878758/full#supplementary-material>

References

- Ahn, H. J., Seo, S. W., Chin, J., Suh, M. K., Lee, B. H., Kim, S. T., et al. (2011). The cortical neuroanatomy of neuropsychological deficits in mild cognitive impairment and Alzheimer's disease: a surface-based morphometric analysis. *Neuropsychologia* 49, 3931–3945. doi: 10.1016/j.neuropsychologia.2011.10.010
- Albert, M. S., DeKosky, S. T., Dickson, D., Dubois, B., Feldman, H. H., Fox, N. C., et al. (2011). The diagnosis of mild cognitive impairment due to Alzheimer's disease: recommendations from the National Institute on Aging-Alzheimer's Association workgroups on diagnostic guidelines for Alzheimer's disease. *Alzheimers Dement.* 7, 270–279. doi: 10.1016/j.jalz.2011.03.008
- Amici, S., Ogar, J., Brambati, S. M., Miller, B. L., Neuhaus, J., Dronkers, N. L., et al. (2007). Performance in specific language tasks correlates with regional volume changes in progressive aphasia. *Cogn. Behav. Neurol.* 20, 203–211. doi: 10.1097/WNN.0b013e31815e6265
- Apostolova, L. G., Lu, P., Rogers, S., Dutton, R. A., Hayashi, K. M., Toga, A. W., et al. (2008). 3D mapping of language networks in clinical and pre-clinical Alzheimer's disease. *Brain Lang.* 104, 33–41. doi: 10.1016/j.bandl.2007.03.008
- Baldo, J. V., Arévalo, A., Patterson, J. P., and Dronkers, N. F. (2013). Grey and white matter correlates of picture naming: evidence from a voxel-based lesion analysis of the Boston Naming Test. *Cortex* 49, 658–667. doi: 10.1016/j.cortex.2012.03.001
- Biesbroek, J. M., Lim, J. S., Weaver, N. A., Arikian, G., Kang, Y., Kim, B. J., et al. (2021). Anatomy of phonemic and semantic fluency: a lesion and disconnectome study in 1231 stroke patients. *Cortex* 143, 148–163. doi: 10.1016/j.cortex.2021.06.019
- Binder, J. R. (2015). The Wernicke area: modern evidence and a reinterpretation. *Neurology* 85, 2170–2175. doi: 10.1212/wnl.0000000000002219
- Binder, J. R. (2017). Current controversies on wernicke's area and its role in language. *Curr. Neurol. Neurosci. Rep.* 17:58. doi: 10.1007/s11910-017-0764-8
- Binder, J. R., Desai, R. H., Graves, W. W., and Conant, L. L. (2009). Where is the semantic system? A critical review and meta-analysis of 120 functional neuroimaging studies. *Cereb. Cortex* 19, 2767–2796. doi: 10.1093/cercor/bhp055
- Cabeza, R. (2002). Hemispheric asymmetry reduction in older adults: the HAROLD model. *Psychol. Aging* 17, 85–100. doi: 10.1037/0882-7974.17.1.85
- Christensen, K. J., Multhaup, K. S., Nordstrom, S., and Voss, K. (1991). A cognitive battery for dementia: development and measurement characteristics. *Psychol. Assess.* 3, 168–174. doi: 10.1037/1040-3590.3.2.168
- Chung, M. K., Worsley, K. J., Robbins, S., Paus, T., Taylor, J., Giedd, J. N., et al. (2003). Deformation-based surface morphometry applied to gray matter deformation. *Neuroimage* 18, 198–213. doi: 10.1016/s1053-8119(02)00017-4
- Collins, D. L., Neelin, P., Peters, T. M., and Evans, A. C. (1994). Automatic 3D intersubject registration of MR volumetric data in standardized Talairach space. *J. Comput. Assist. Tomogr.* 18, 192–205.
- Dilkina, K., McClelland, J. L., and Plaut, D. C. (2010). Are there mental lexicons? The role of semantics in lexical decision. *Brain Res.* 1365, 66–81. doi: 10.1016/j.brainres.2010.09.057
- Ferstl, E. C., Neumann, J., Bogler, C., and von Cramon, D. Y. (2008). The extended language network: a meta-analysis of neuroimaging studies on text comprehension. *Human Brain Mapp.* 29, 581–593. doi: 10.1002/hbm.20422
- Forkel, S. J., Rogalski, E., Drossinos Sancho, N., D'Anna, L., Luque Laguna, P., Sridhar, J., et al. (2020). Anatomical evidence of an indirect pathway for word repetition. *Neurology* 94, e594–e606. doi: 10.1212/wnl.00000000000008746
- Gordon, J. K., Young, M., and Garcia, C. (2018). Why do older adults have difficulty with semantic fluency? *Neuropsychol. Dev. Cogn. B Aging Neuropsychol. Cogn.* 25, 803–828. doi: 10.1080/13825585.2017.1374328
- Gorno-Tempini, M. L., Brambati, S. M., Ginex, V., Ogar, J., Dronkers, N. F., Marcone, A., et al. (2008). The logopenic/phonological variant of primary progressive aphasia. *Neurology* 71, 1227–1234. doi: 10.1212/01.wnl.0000320506.79811.da
- Gorno-Tempini, M. L., Hillis, A. E., Weintraub, S., Kertesz, A., Mendez, M., Cappa, S. F., et al. (2011). Classification of primary progressive aphasia and its variants. *Neurology* 76, 1006–1014. doi: 10.1212/WNL.0b013e31821103e6
- Henry, J. D., and Crawford, J. R. (2004). A meta-analytic review of verbal fluency performance following focal cortical lesions. *Neuropsychology* 18, 284–295. doi: 10.1037/0894-4105.18.2.284
- Hillis, A. E., Rorden, C., and Fridriksson, J. (2017). Brain regions essential for word comprehension: drawing inferences from patients. *Ann. Neurol.* 81, 759–768. doi: 10.1002/ana.24941
- Hurley, R. S., Paller, K. A., Rogalski, E. J., and Mesulam, M. M. (2012). Neural mechanisms of object naming and word comprehension in primary progressive aphasia. *J. Neurosci.* 32, 4848–4855. doi: 10.1523/jneurosci.5984-11.2012
- Im, K., Lee, J. M., Lee, J., Shin, Y. W., Kim, I. Y., Kwon, J. S., et al. (2006). Gender difference analysis of cortical thickness in healthy young adults with surface-based methods. *Neuroimage* 31, 31–38. doi: 10.1016/j.neuroimage.2005.11.042
- Im, K., Lee, J. M., Lyttelton, O., Kim, S. H., Evans, A. C., and Kim, S. I. (2008). Brain size and cortical structure in the adult human brain. *Cereb. Cortex* 18, 2181–2191. doi: 10.1093/cercor/bhm244
- Kang, S. H., Park, Y. H., Kim, J. P., Kim, C. H., Jang, H., et al. (2021). Cortical neuroanatomical changes related to specific neuropsychological deficits in subcortical vascular cognitive impairment. *Neuroimage Clin.* 30:102685. doi: 10.1016/j.nicl.2021.102685
- Kang, S. H., Park, Y. H., Lee, D., Kim, J. P., Chin, J., Ahn, Y., et al. (2019). The cortical neuroanatomy related to specific neuropsychological deficits in alzheimer's continuum. *Dement. Neurocogn. Disord.* 18, 77–95. doi: 10.12779/dnd.2019.18.3.77
- Kang, Y. W. (1994). Who is left-handed?: Measurement of handedness in Koreans. *Korean J. Clin. Psychol.* 13, 91–113.
- Keilp, J. G., Gorlyn, M., Alexander, G. E., Stern, Y., and Prohovnik, I. (1999). Cerebral blood flow patterns underlying the differential impairment in category vs letter fluency in Alzheimer's disease. *Neuropsychologia* 37, 1251–1261. doi: 10.1016/s0028-3932(99)00032-9
- Kim, H., and Na, D. L. (2004). Normative data on the Korean version of the Western Aphasia Battery. *J. Clin. Exp. Neuropsychol.* 26, 1011–1020. doi: 10.1080/1380390490515397
- Kim, J. S., Singh, V., Lee, J. K., Lerch, J., Ad-Dab'bagh, Y., MacDonald, D., et al. (2005). Automated 3-D extraction and evaluation of the inner and outer cortical surfaces using a Laplacian map and partial volume effect classification. *Neuroimage* 27, 210–221. doi: 10.1016/j.neuroimage.2005.03.036
- Kitabayashi, Y., Ueda, H., Tsuchida, H., Izumi, H., Narumoto, J., Nakamura, K., et al. (2001). Relationship between regional cerebral blood flow and verbal fluency in Alzheimer's disease. *Psychiatry Clin. Neurosci.* 55, 459–463. doi: 10.1046/j.1440-1819.2001.00890.x
- Lee, J. S., Yoo, S., Park, S., Kim, H. J., Park, K. C., Seong, J. K., et al. (2020). Differences in neuroimaging features of early- versus late-onset nonfluent/agrammatic primary progressive aphasia. *Neurobiol. Aging* 86, 92–101. doi: 10.1016/j.neurobiolaging.2019.10.011
- Lerch, J. P., and Evans, A. C. (2005). Cortical thickness analysis examined through power analysis and a population simulation. *Neuroimage* 24, 163–173. doi: 10.1016/j.neuroimage.2004.07.045
- Lyttelton, O., Boucher, M., Robbins, S., and Evans, A. (2007). An unbiased iterative group registration template for cortical surface analysis. *Neuroimage* 34, 1535–1544. doi: 10.1016/j.neuroimage.2006.10.041
- McKhann, G. M., Knopman, D. S., Chertkow, H., Hyman, B. T., Jack, C. R. Jr., Kawas, C. H., et al. (2011). The diagnosis of dementia due to Alzheimer's disease: recommendations from the National Institute on Aging-Alzheimer's Association workgroups on diagnostic guidelines for Alzheimer's disease. *Alzheimers Dement.* 7, 263–269. doi: 10.1016/j.jalz.2011.03.005
- Mesulam, M. M., Rader, B. M., Sridhar, J., Nelson, M. J., Hyun, J., Rademaker, A., et al. (2019). Word comprehension in temporal cortex and Wernicke area: a PPA perspective. *Neurology* 92, e224–e233. doi: 10.1212/wnl.0000000000006788
- Mesulam, M. M., Rogalski, E. J., Wieneke, C., Hurley, R. S., Geula, C., Bigio, E. H., et al. (2014). Primary progressive aphasia and the evolving neurology of the language network. *Nat. Rev. Neurol.* 10, 554–569. doi: 10.1038/nrneurol.2014.159
- Mesulam, M. M., Thompson, C. K., Weintraub, S., and Rogalski, E. J. (2015). The Wernicke conundrum and the anatomy of language comprehension in primary progressive aphasia. *Brain* 138, 2423–2437. doi: 10.1093/brain/awv154
- Mesulam, M. M., Wieneke, C., Hurley, R., Rademaker, A., Thompson, C. K., Weintraub, S., et al. (2013). Words and objects at the tip of the left temporal lobe in primary progressive aphasia. *Brain* 136, 601–618. doi: 10.1093/brain/awv336
- Miyake, A., and Friedman, N. P. (2012). The nature and organization of individual differences in executive functions: four general conclusions. *Curr. Dir. Psychol. Sci.* 21, 8–14. doi: 10.1177/0963721411429458

- Noh, Y., Lee, Y., Seo, S. W., Jeong, J. H., Choi, S. H., Back, J. H., et al. (2014). A new classification system for ischemia using a combination of deep and periventricular white matter hyperintensities. *J. Stroke Cerebrovasc. Dis.* 23, 636–642. doi: 10.1016/j.jstrokecerebrovasdis.2013.06.002
- Obler, L. K., Rykhlevskaia, E., Schnyer, D., Clark-Cotton, M. R., Spiro, A. III, Hyun, J., et al. (2010). Bilateral brain regions associated with naming in older adults. *Brain Lang.* 113, 113–123. doi: 10.1016/j.bandl.2010.03.001
- Patterson, K., Nestor, P. J., and Rogers, T. T. (2007). Where do you know what you know? The representation of semantic knowledge in the human brain. *Nat. Rev. Neurosci.* 8, 976–987. doi: 10.1038/nrn2277
- Petroi, D., Duffy, J. R., Borgert, A., Strand, E. A., Machulda, M. M., Senjem, M. L., et al. (2020). Neuroanatomical correlates of phonologic errors in logopenic progressive aphasia. *Brain Lang.* 204:104773. doi: 10.1016/j.bandl.2020.10.4773
- Riello, M., Frangakis, C. E., Ficek, B., Webster, K. T., Desmond, J. E., Faria, A. V., et al. (2021). Neural Correlates of Letter and Semantic Fluency in Primary Progressive Aphasia. *Brain Sci.* 12:1. doi: 10.3390/brainsci12010001
- Robson, H., Grube, M., Lambon Ralph, M. A., Griffiths, T. D., and Sage, K. (2013). Fundamental deficits of auditory perception in Wernicke's aphasia. *Cortex* 49, 1808–1822. doi: 10.1016/j.cortex.2012.11.012
- Rogalski, E., Cobia, D., Harrison, T. M., Wieneke, C., Thompson, C. K., Weintraub, S., et al. (2011a). Anatomy of language impairments in primary progressive aphasia. *J. Neurosci.* 31, 3344–3350. doi: 10.1523/jneurosci.5544-10.2011
- Rogalski, E., Cobia, D., Harrison, T. M., Wieneke, C., Weintraub, S., and Mesulam, M. M. (2011b). Progression of language decline and cortical atrophy in subtypes of primary progressive aphasia. *Neurology* 76, 1804–1810. doi: 10.1212/WNL.0b013e31821ccd3c
- Rogalski, E. J., and Mesulam, M. M. (2009). Clinical trajectories and biological features of primary progressive aphasia (PPA). *Curr. Alzheimer Res.* 6, 331–336. doi: 10.2174/156720509788929264
- Sapolsky, D., Bakkour, A., Negreira, A., Nalipinski, P., Weintraub, S., Mesulam, M. M., et al. (2010). Cortical neuroanatomic correlates of symptom severity in primary progressive aphasia. *Neurology* 75, 358–366. doi: 10.1212/WNL.0b013e3181ea15e8
- Shao, Z., Janse, E., Visser, K., and Meyer, A. S. (2014). What do verbal fluency tasks measure? Predictors of verbal fluency performance in older adults. *Front. Psychol.* 5:772. doi: 10.3389/fpsyg.2014.00772
- Sled, J. G., Zijdenbos, A. P., and Evans, A. C. (1998). A nonparametric method for automatic correction of intensity nonuniformity in MRI data. *IEEE Trans. Med. Imaging* 17, 87–97. doi: 10.1109/42.668698
- Smith, S. M. (2002). Fast robust automated brain extraction. *Hum. Brain Mapp.* 17, 143–155. doi: 10.1002/hbm.10062
- Sperling, R. A., Aisen, P. S., Beckett, L. A., Bennett, D. A., Craft, S., Fagan, A. M., et al. (2011). Toward defining the preclinical stages of Alzheimer's disease: recommendations from the National Institute on Aging-Alzheimer's Association workgroups on diagnostic guidelines for Alzheimer's disease. *Alzheimers Dement.* 7, 280–292. doi: 10.1016/j.jalz.2011.03.003
- Teipel, S. J., Willech, F., Ishii, K., Bürger, K., Drzezga, A., Engel, R., et al. (2006). Resting state glucose utilization and the CERAD cognitive battery in patients with Alzheimer's disease. *Neurobiol. Aging* 27, 681–690. doi: 10.1016/j.neurobiolaging.2005.03.015
- Whiteside, D. M., Kealey, T., Semla, M., Luu, H., Rice, L., Basso, M. R., et al. (2016). Verbal fluency: language or executive function measure? *Appl. Neuropsychol. Adult* 23, 29–34. doi: 10.1080/23279095.2015.1004574
- Wierenga, C. E., Benjamin, M., Gopinath, K., Perlstein, W. M., Leonard, C. M., Roth, L. J., et al. (2008). Age-related changes in word retrieval: role of bilateral frontal and subcortical networks. *Neurobiol. Aging* 29, 436–451. doi: 10.1016/j.neurobiolaging.2006.10.024
- Wilson, S. M., DeMarco, A. T., Henry, M. L., Gesierich, B., Babiak, M., Mandelli, M. L., et al. (2014). What role does the anterior temporal lobe play in sentence-level processing? Neural correlates of syntactic processing in semantic variant primary progressive aphasia. *J. Cogn. Neurosci.* 26, 970–985. doi: 10.1162/jocn_a_00550
- Zijdenbos, A. P., Forghani, R., and Evans, A. C. (2002). Automatic "pipeline" analysis of 3-D MRI data for clinical trials: application to multiple sclerosis. *IEEE Trans. Med. Imaging* 21, 1280–1291. doi: 10.1109/tmi.2002.806283

COPYRIGHT

© 2022 Kang, Park, Shin, Kim, Yun, Jang, Kim, Koh, Na, Suh and Seo. This is an open-access article distributed under the terms of the [Creative Commons Attribution License \(CC BY\)](https://creativecommons.org/licenses/by/4.0/). The use, distribution or reproduction in other forums is permitted, provided the original author(s) and the copyright owner(s) are credited and that the original publication in this journal is cited, in accordance with accepted academic practice. No use, distribution or reproduction is permitted which does not comply with these terms.



Autophagy Impairment in *App* Knock-in Alzheimer's Model Mice

Richeng Jiang^{1,2}, Makoto Shimozawa¹, Johanna Mayer¹, Simone Tambaro¹, Rakesh Kumar³, Axel Abelein³, Bengt Winblad^{1,4}, Nenad Bogdanovic⁵ and Per Nilsson^{1*}

¹ Division of Neurogeriatrics, Department of Neurobiology, Care Sciences and Society, Center for Alzheimer Research, Karolinska Institutet, Solna, Sweden, ² Department of Otolaryngology Head and Neck Surgery, The First Hospital of Jilin University, Changchun, China, ³ Department of Biosciences and Nutrition, Karolinska Institutet, Huddinge, Sweden, ⁴ Theme Inflammation and Aging, Karolinska University Hospital, Huddinge, Sweden, ⁵ Division of Clinical Geriatrics, Department of Neurobiology, Care Sciences and Society, Center for Alzheimer Research, Karolinska Institutet, Huddinge, Sweden

OPEN ACCESS

Edited by:

Ruben Vidal,
Indiana University, Purdue University
Indianapolis, United States

Reviewed by:

Bradlee Heckmann,
University of South Florida Health,
United States
Ravi Manjithaya,
Jawaharlal Nehru Centre
for Advanced Scientific Research,
India

Dun-Sheng Yang,
Nathan Kline Institute for Psychiatric
Research, United States

*Correspondence:

Per Nilsson
Per.et.Nilsson@ki.se

Specialty section:

This article was submitted to
Alzheimer's Disease and Related
Dementias,
a section of the journal
Frontiers in Aging Neuroscience

Received: 17 February 2022

Accepted: 29 March 2022

Published: 19 May 2022

Citation:

Jiang R, Shimozawa M, Mayer J, Tambaro S, Kumar R, Abelein A, Winblad B, Bogdanovic N and Nilsson P (2022) Autophagy Impairment in *App* Knock-in Alzheimer's Model Mice. *Front. Aging Neurosci.* 14:878303. doi: 10.3389/fnagi.2022.878303

Alzheimer's disease (AD) is characterized by impaired protein homeostasis leading to amyloid- β peptide ($A\beta$) amyloidosis. Amyloid precursor protein (APP) knock-in mice exhibit robust $A\beta$ pathology, providing possibilities to determine its effect on protein homeostasis including autophagy. Here we compared human AD postmortem brain tissue with brains from two different types of *App* knock-in mice, *App*^{NL-F} and *App*^{NL-G-F} mice, exhibiting AD-like pathology. In AD postmortem brains, p62 levels are increased and p62-positive staining is detected in neurons, including potential axonal beadings, as well as in the vasculature and in corpora amylacea. Interestingly, p62 is also increased in the neurons in 12-month-old *App*^{NL-G-F} mice. In brain homogenates from 12-month-old *App*^{NL-G-F} mice, both p62 and light chain 3 (LC3)-II levels are increased as compared to wildtype (WT) mice, indicating inhibited autophagy. Double immunostaining for LC3 and $A\beta$ revealed LC3-positive puncta in hippocampus of 24-month-old *App*^{NL-F} mice around the $A\beta$ plaques which was subsequently identified by electron microscopy imaging as an accumulation of autophagic vacuoles in dystrophic neurites around the $A\beta$ plaques. Taken together, autophagy is impaired in *App* knock-in mice upon increased $A\beta$ pathology, indicating that *App* knock-in mouse models provide a platform for understanding the correlation between $A\beta$ and autophagy.

Keywords: Alzheimer's disease, APP knock-in mice, autophagy, amyloid beta, protein homeostasis, p62, LC3, electron microscopy

INTRODUCTION

Alzheimer's disease (AD) is the major form of dementia, leading to cognitive impairment. Extracellular amyloid- β ($A\beta$) peptide depositions and intracellular tau aggregation are the two pathological hallmarks found in the AD brain parenchyma. $A\beta$ may also accumulate in the vasculature and lead to cerebral amyloid angiopathy (Lendahl et al., 2019). In addition to $A\beta$ and tau pathologies, autophagy is impaired in AD (Nixon et al., 2005). Macroautophagy (herein referred to as autophagy) is a major intracellular degradative pathway and plays a crucial role in the metabolism of $A\beta$ (Yu et al., 2005; Nilsson et al., 2013; Nilsson and Saido, 2014). In AD brains, an accumulation of autophagosomes accompanied by increased levels of lysosomal proteases is observed (Boland et al., 2008). Furthermore, previous studies have shown an increase in autophagy-related genes in the early stage of AD, indicating an activation of autophagy (Lipinski, 2010; Lipinski et al., 2010), whereas it becomes impaired in the

late stage of the disease (Nixon et al., 2005; Yu et al., 2005; Lee et al., 2011; Wolfe et al., 2013). A compromised autophagy in AD is further supported by downregulation of key autophagy proteins including FIP200, Rubicon, Atg5, and Atg16 (Heckmann et al., 2020).

Autophagy is initiated from the phagophore that is induced by cargo receptors like sequestosome 1/p62 and NBR1 (Johansen and Lamark, 2011). In the p62-dependent autophagy pathway, p62 binds to microtubule-associated protein 1 light chain 3 (LC3) and participates in the formation of autophagosomes which have double membrane structures. p62 delivers cargos to be degraded by autophagy and is degraded by the lysosome (Pankiv et al., 2007). During autophagosome formation, LC3-I is conjugated with phosphatidylethanolamine to form LC3-II (Hemelaar et al., 2003; Tanida et al., 2004). LC3-II is therefore a specific autophagosome associated marker (Kabeya et al., 2000) and both p62 and LC3-II are commonly used for measuring autophagic flux (Tanida et al., 2008).

App knock-in mice exhibit robust A β pathology whereas *App* expression is at physiological levels because gene expression of the mouse *App* gene is under the control of the endogenous mouse *App* promoter. In these mice, two clinical mutations found in familial AD (FAD) have been inserted to the mouse *App* gene, the Swedish (NL) and the Beyreuther/Iberian (F) mutations. This leads to an increased generation of A β 42 in the *App*^{NL-F} line, inducing an onset of A β amyloidosis at nine months of age and cognitive impairment at 18 months of age (Saito et al., 2014). In *App*^{NL-G-F} mice, the Arctic mutation (G) was additionally introduced, which leads to a more aggressive A β pathology starting at two months of age and memory impairment at six months of age (Saito et al., 2014). This aggressive A β pathology of *App*^{NL-G-F} mice drives earlier and more severe neuroinflammation and synaptic alteration as compared to *App*^{NL-F} mice (Saito et al., 2014).

In the current study, we analyzed two key autophagy markers p62 and LC3 in the two *App* knock-in mice, and the data indicate that *App*^{NL-G-F} mice are, at least to some extent, similar to the late stage of AD in terms of autophagy alterations. Moreover, electron microscopy (EM) analysis shows a significant autophagic vacuole accumulation, specifically around the A β plaques in 24-month-old *App*^{NL-F} mice.

METHODS

Human Brain Samples

Human brain slides were provided by the brain bank of Karolinska Institutet (approval nr 2013/1301-31/2) (Supplementary Table 1). p62 immunoblotting was performed in brain homogenates from the Netherlands Brain Bank under ethical permit Dnr EPN 2011/962-31/1 and 2018/1993-32.

Animals

App^{NL-F} and *App*^{NL-G-F} knock-in mice have been described previously (Saito et al., 2014). *App*^{NL-F} mice contain the Swedish (KM670/671NL) and the Beyreuther/Iberian (I716F) mutations whereas *App*^{NL-G-F} mice have additionally the Arctic

(E693G) mutation inserted into the mouse *App* gene (Saito et al., 2014). *App* knock-in mouse experiments were performed under ethical permit ID 407 approved by Linköping animal ethical board and 12570-2021 approved by Stockholm animal ethical board. Mice were kept on 12:12 light-dark cycle and with *ad libitum* access to food.

Mouse Brain Dissection

The mice were anesthetized by isoflurane. Thereafter, the mice were perfused with phosphate buffered saline (PBS) through cardiac perfusion and the mouse brains were collected. One hemisphere of the brain tissue was fixed in 10% formalin solution (Merck Millipore, MA, United States, Cat. HT501128) for immunohistochemistry, and the other hemisphere was dissected into hippocampus and cortex for biochemical analysis.

Primary Neuron Culture

Six-well plates were coated by poly-D-lysine (Sigma-Aldrich, MO, United States, cat. P6407) for 1 h at room temperature and washed three times with Milli-Q water. Mouse brains from E17 embryos from WT and *App*^{NL-G-F} female mice were separated in Hanks' balanced salt solution (HBSS) (Thermo Fisher Scientific, MA, United States, Cat. 14175095) and cortex/hippocampus were dissected under the dissection microscope. Cortex/hippocampus were transferred to a falcon tube and HBSS was removed. Mixture of 97% Neurobasal Medium (Thermo Fisher Scientific, MA, United States, Cat. 21103049), 1% Glutamax (Thermo Fisher Scientific, MA, United States, Cat. 35050038), and 2% B-27 (Thermo Fisher Scientific, MA, United States, Cat. 17504044) were added and tissues were separated by pipetting 20–30 times. Cells were counted by using a hemacytometer after trypan blue staining and 4.5×10^5 cells were seeded. After 18 DIV, cells were treated with 100 nM bafilomycin A1 (Sigma-Aldrich, MO, United States, Cat. B1793) for 6 h and then the cells were collected and lysed in radioimmunoprecipitation assay (RIPA) buffer (Thermo Fisher Scientific, MA, United States, Cat. 89901) containing protease and phosphatase inhibitors for 10 min. Cell lysate was sonicated for 1 min and centrifuged at 15,000 rpm at 4°C for 20 min. Supernatant was transferred to the new tubes for western blot analysis.

Immunohistochemistry

For human brain samples, 3,3'-Diaminobenzidine (DAB) staining was performed with Dako EnVision Systems/HRP (Agilent Technologies, CA, United States, Cat. K401011-2). Slides were deparaffinized by xylene and ethanol and blocked by peroxidase (Dako kit) for 5 min and with 10% normal goat serum for 20 min at room temperature. The slides were incubated with anti-p62 antibody (Cell Signaling Technology, MA, United States, Cat. 5114) (1:500) in 3% normal goat serum overnight. After washing with 0.05% PBS-T buffer, slides were incubated with an anti-rabbit secondary antibody (Dako kit) for 30 min at room temperature, followed by incubating with chromogen solution, which was diluted in DAB substrate buffer (Dako kit), for 5 min at room temperature. Before mounting, slides were counterstained with Mayer's Hematoxylin for 30 s

and processed by dehydration. Images were acquired by the Nikon Eclipse E800 microscope with Nikon DS-Ri2 camera (acquisition parameters: 64 analog gain, 15-ms exposure time, and $4,908 \times 3,264$ pixel resolution) and were quantified by ImageJ software.

For mouse brain samples, paraffin-embedded brain tissues were sectioned into 4- μ m thick sections. Antigen retrieval was performed, and after blocking, slides were incubated with anti-A β antibody (82E1) (Immuno-Biological Laboratories, Hokkaido, Japan, Cat.10323) (1:1,000), anti-LC3B (Novus Biologicals, CO, United States, Cat. NB100-2220) (1:2,000), and anti-p62 antibody (1:100). The following day, slides were incubated with secondary antibodies: alexa 546 goat anti-mouse (Invitrogen, MA, United States, Cat. A11030) (1:200), biotinylated goat anti-mouse IgG (Vector Laboratories, CA, United States, Cat. BA-9200) (1:200), and biotinylated goat anti-rabbit IgG (Vector Laboratories, CA, United States, Cat. BA-1000) (1:200). The biotinylated secondary antibodies were amplified with TSA Fluorescein System (PerkinElmer, MA, United States, Cat. NEL701001KT). Images were acquired by the Nikon Eclipse E800 microscope with Nikon DS-Qi2 camera (acquisition parameters: 64 analog gain, 500 ms or 1 s exposure time and $4,908 \times 3,264$ pixel resolution) and were quantified by ImageJ software.

Western Blot

Fresh frozen mouse brain samples were homogenized in RIPA buffer supplemented with phosphatases inhibitors (Sigma-Aldrich, MO, United States, Cat. P0044) and proteases inhibitors (G-Biosciences, MO, United States, Cat. 786-433) or separated into cytosolic and membrane fractions. For cytosolic fraction, tissues were homogenized in 10 mM Tris (pH: 8.0) and 0.25 M sucrose and centrifuged at 4,000 rpm for 15 min at 4°C. Supernatant was centrifuged at 53,000 rpm for 1 h at 4°C. The supernatant was kept as a cytosolic fraction. Tissue homogenates and cell lysates were boiled at 95°C for 3 min except for analysis of Atg9A and Atg16L. A 20 μ g portion of protein was loaded onto 4–20% SDS-PAGE for separation and transferred to polyvinylidene difluoride (PVDF) or nitrocellulose membranes. The membranes were blocked by 5% skim milk and were probed by primary antibodies, anti-p62 (1:500), anti-LC3 (Novus Biologicals, CO, United States, Cat. NB100-2331) (1:1,000), anti-p-Ulk1 S555 (Cell Signaling Technology, MA, United States, Cat. 5869) (1:500), anti-p-Ulk1 S757 (Cell Signaling Technology, MA, United States, Cat. 14202) (1:500), anti-Ulk1 (Cell Signaling Technology, MA, United States, Cat. 8054) (1:500), anti-Atg5 (Novus Biologicals, CO, United States, Cat. NB110-53818) (1:500), anti-Atg7 (Santa Cruz Biotechnology, CA, United States, Cat. sc-376212) (1:200), anti-Atg9A (Abcam, United Kingdom, Cat. ab108338) (1:500), anti-Atg16L (MBL Life Science, Tokyo, Japan Cat. PM040) (1:500), and anti- β -actin (Sigma-Aldrich, MO, United States, Cat. A2228) (1:10,000) overnight at 4°C. The next day, the PVDF or nitrocellulose membranes were incubated with fluorescently labeled secondary antibodies (LI-COR Biosciences, NE, United States), IRDye 800CW donkey anti-rabbit (Cat. 926-32213) (1:10,000), IRDye 680RD goat anti-rabbit (Cat. 926-68071) (1:10,000), IRDye 800CW donkey anti-mouse (Cat. 926-32212) (1:10,000), or IRDye 680RD goat anti-mouse (Cat. 926-68070) (1:10,000) for 1 h at room temperature.

Images were acquired by a fluorescence imaging system (LI-COR Biosciences, NE, United States, Odyssey CLx) and were analyzed by Image Studio Lite (LI-COR Biosciences, NE, United States) software.

Ribonucleic Acid Extraction, Complementary Deoxyribonucleic Acid Synthesis, and Real-Time Polymerase Chain Reaction

Fresh mouse brain tissue was kept in RNAlater Tissue Reagent (Qiagen, Venlo, Netherlands, Cat. 76104) and Ribonucleic acid (RNA) was extracted according to the manufacturer's instruction of RNeasy Lipid Tissue Mini Kit (Qiagen, Venlo, Netherlands, Cat. 74804). After measuring RNA concentration, 200 ng of RNA was used for complementary deoxyribonucleic acid (cDNA) synthesis according to manufacturer's instructions of the High-Capacity cDNA Reverse Transcription Kit (Thermo Fisher Scientific, MA, United States, Cat. 4374966). The TaqMan Fast Advanced Master Mix (Thermo Fisher Scientific, MA, United States, Cat. 4444557) was used to perform the real-time polymerase chain reaction (RT-PCR) using TaqMan mouse gene expression assays (FAM) (Thermo Fisher Scientific, MA, United States, Cat. 4331182), Mm00448091_m1 for Sqstm1 (Gene aliases: p62). The gene expression level was normalized to TaqMan mouse gene expression assays (VIC) (Thermo Fisher Scientific, MA, United States, Cat. 4448489), Mm02619580_g1 for Atcb. Each sample was triplicated and run in the 7500 Fast Real-Time PCR System (Applied Biosystems, MA, United States).

Transmission Electron Microscopy

Mice, 24-month-old, were anesthetized by isoflurane and perfused with 2.5% glutaraldehyde and 1% paraformaldehyde in 0.1 M phosphate buffer by cardiac perfusion. Thereafter, the mouse brains were collected and fixed in the same solution as used in perfusion process. Brain tissues were sectioned coronally into 1-mm thickness on the brain slicer matrix. The coronal brain slices were further dissected under the dissection microscope to separate the hippocampus. The hippocampal tissues were rinsed in 0.1 M phosphate buffer prior to the post fixation in 2% osmium tetroxide in 0.1 M phosphate buffer at 4°C for 2 h. Tissues were dehydrated stepwise in ethanol and acetone and eventually embedded in LX-112. Prior to the ultrathin sections, the tissue slices were mounted on the glass slides and stained with a toluidine blue solution to visualize the hippocampal area. Ultrathin sections were prepared using an EM UC7 (Leica, Wetzlar, Germany) and the grids contrasted with uranyl acetate and lead citrate. A β 42 was expressed and purified from *Escherichia coli* (Abelein et al., 2020). A β 42 fibril was prepared by incubating 3 μ M A β 42 monomer at 37°C for 24 h. After fibril formation, 10 μ l of A β 42 fibril was spotted on copper grid coated with formvar/carbon. Excess sample was wiped with Whatman filter paper and then grid was washed two times with 10 μ l of Milli-Q water. It was then stained with 1% uranyl formate and then air dried. The sample was then imaged using TEM. Imaging was performed under the Hitachi HT7700 transmission electron microscope (Hitachi High-Technologies, Tokyo, Japan) operated at 80 kV equipped with a $2k \times 2k$

Veleta CCD camera (Olympus Soft Imaging Solutions, Münster, Germany).

Statistical Analysis

For the analysis of biochemical data, one-way ANOVA followed by Dunnett's multiple comparisons test was performed for the three-group comparisons while two-tailed Student's *t*-test was performed for the two-group comparisons in GraphPad Prism 8.

RESULTS

Autophagy Alterations in Alzheimer's Disease Postmortem Brain

To investigate autophagy alteration in AD postmortem brain, we stained for p62. p62 is normally degraded along with the cargo during functional autophagy and therefore p62 accumulation and aggregation indicate impaired autophagy. We immunostained brains from healthy controls (**Figures 1A–D**) and AD subjects (**Figures 1E–H**) and quantified the p62-positive signals. In AD brains, p62 accumulation occurs in pyramidal neurons as previously shown (Kuusisto et al., 2002) in both cortex (**Figure 1E**) and hippocampus including dentate gyrus (DG) (**Figure 1F**) and CA1 (**Figure 1G**) of AD brains (semi-quantified in **Figures 1I,J**), whereas no p62 accumulation was found in brains of non-demented individuals (**Figures 1A–C**). p62 accumulated inside the neurons (**Figures 1E,G** arrow in depicted area and **Figure 1F** arrow in depicted area 1) and was also identified as small round puncta (**Figure 1F** arrows in depicted area 2). The puncta may represent axonal beadings, which are a series of swellings along the axons located in the molecular layer of DG. Interestingly, tunica intima of the vessels and corpora amylacea also contains substantial amount of p62 whereas no staining was observed in healthy controls (**Figures 1D,H**). Western blot analysis of brain homogenates from AD subjects with Braak stages 5–6 revealed significantly increased p62 levels as compared to healthy subjects (**Figures 1K,L**). In summary, p62 accumulation was frequently observed in AD brains, which indicates a disturbed autophagy-lysosomal system potentially caused by an inhibition of autophagy in both neurons and cells in the tunica intima of vessels.

Autophagy Alterations in *App* Knock-in Mice

To investigate the effect of the increasing A β amyloidosis in the *App* knock-in mice (**Figure 2A**) on autophagy, we analyzed markers of autophagic flux. The *App* knock-in mice exhibited alterations in autophagy as shown by western blot analysis for autophagy markers LC3 and p62 using 12-month-old WT, *App*^{NL-F}, and *App*^{NL-G-F} mouse brains. *App*^{NL-F} mice started to accumulate A β plaques at 12 months of age whereas *App*^{NL-G-F} mice exhibited a very pronounced A β pathology at this age (**Figure 2A**). We found that p62, LC3-II, and LC3-II/LC3-I ratio were significantly increased in the cortex of *App*^{NL-G-F} mice (**Figures 2B,D** and full blot of p62 in **Supplementary Figure 1A**, higher exposure of LC3 blots in **Supplementary Figure 1B**, and LC3-II/LC3-I

in **Supplementary Figure 1C**) whereas p62 mRNA level was unaltered (**Supplementary Figure 1E**), indicating that autophagy was inhibited in the cortex of *App*^{NL-G-F} mice. The LC3-II levels were also similarly increased in the hippocampus of *App*^{NL-G-F} mice, although the ratio of LC3-II/LC3-I did not change significantly (**Figures 2C,E** and higher exposure time of LC3 blots in **Supplementary Figure 1B**, and LC3-II/LC3-I in **Supplementary Figure 1D**). In agreement with the p62 western blot data, immunostaining showed a significant accumulation of p62 in the cortex of *App*^{NL-G-F} mice as compared to WT mice (**Figures 2F,G**) whereas both p62 and LC3-II levels are unaltered in mouse primary neurons from *App*^{NL-G-F} mice as compared to WT (**Supplementary Figures 1F–J**). In contrast to *App*^{NL-G-F} mice, the LC3-II levels were significantly decreased in the hippocampus of *App*^{NL-F} mice whereas no changes of p62 levels in cortex and hippocampus were detected (**Figures 2B–G**).

Previous studies have identified alterations in several key autophagy proteins in AD brains (Heckmann et al., 2020). We therefore next analyzed the brains of the *App* knock-in mice for these proteins. The data interestingly showed a significant increase of p-Ulk1 S555 specifically in *App*^{NL-G-F} mouse cortex, which is involved in activating initiation of autophagy; whereas no change of p-Ulk1 S757, which is involved in inhibition of autophagy initiation, was observed (**Figures 3A–E**). In addition, a significant increase of both Atg7 and Atg9A was detected in the brains of *App*^{NL-G-F} mice whereas Atg5–Atg12 and Atg16L were unaltered (**Figures 3F–J**).

To further investigate the autophagy alterations upon aging of the *App*^{NL-F} mice, we next performed western blot analysis of LC3 and p62 using 18- and 24-month-old *App*^{NL-F} mice and no significant differences were observed, which was also confirmed with p62 immunostaining (**Supplementary Figures 2A–J**). However, EM analysis of 24-month-old *App*^{NL-F} mice exhibiting robust A β pathology (**Figure 4A**), including the region of striatum lacunosum-moleculare layer (**Figures 4B,C**), revealed a significant accumulation of autophagic vacuoles in the dystrophic neurites, around the A β plaques consisting of A β fibrils (**Figures 4D–I**) whereas no A β plaques or dystrophic neurites containing autophagic vacuoles were found in 24-month-old WT mouse hippocampus (**Figures 4J,K**). In agreement with the EM data, double immunostaining of A β and LC3 further confirmed the presence of LC3-positive puncta in association with the A β plaques in the 24-month-old *App*^{NL-F} mice (**Figure 4L**). Taken these data together indicate that the autophagic system of *App*^{NL-G-F} mice is characterized by an increase of both p62 and LC3-II, indicating that the autophagic system is inhibited, whereas the *App*^{NL-F} mice exhibited a region-specific alteration around the A β plaques. Hence, the degree of A β pathology correlates with the extent of autophagy alterations in the *App* knock-in mice.

DISCUSSION

In this study, we aimed at investigating autophagy status in *App* knock-in mice and compare the pathology to human AD postmortem samples. Autophagy is altered in most

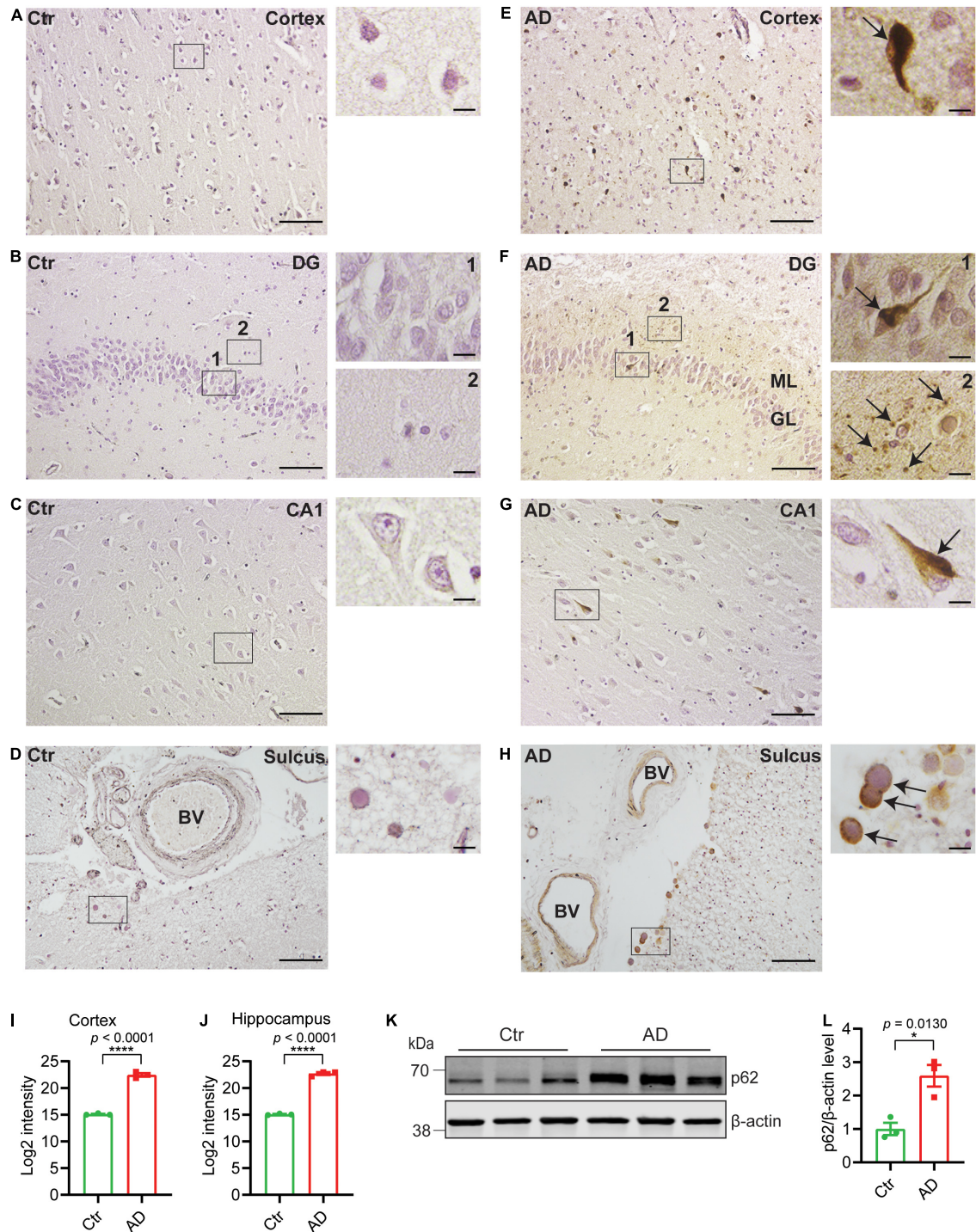


FIGURE 1 | p62 accumulates in AD brains. Immunohistochemistry of p62 in entorhinal cortex, DG, and CA1 of hippocampus and sulcus as indicated from healthy control (Ctr) (A–D) and AD brains (E–H). Scale bars represent 100 μ m. Higher magnification images of depicted areas (black boxes) are shown to the right. Scale bars represent 10 μ m. Arrows in (E,F1,G) indicate p62 accumulation in neurons of entorhinal cortex and hippocampus; (F2) indicates potential axonal beading in ML of DG; (H) indicates corpora amylacea. (H) p62 is accumulated in tunica intima of the blood vessels in AD. (I) Semiquantitative density measurement was performed for quantification; 20 \times magnification images of six different and separate regions of cortex were chosen from each individual and the intensities were quantified and presented as log2-transformed data. (J) 20 \times magnification images of DG, CA1, and CA3 (two for each region) were chosen for hippocampus and the intensities were quantified and presented as log2-transformed data ($n = 3$ patients/group, **** $p < 0.0001$). (K) Western blot analysis of p62 in human postmortem prefrontal cortex from AD and healthy control subjects and (L) quantified by densitometry ($n = 3$ patients/group, * $p < 0.05$). Data were analyzed by Student's *t*-test. Data are represented as mean \pm SEM. DG, dentate gyrus; BV, blood vessel; ML, molecular layer; GL, granular layer.

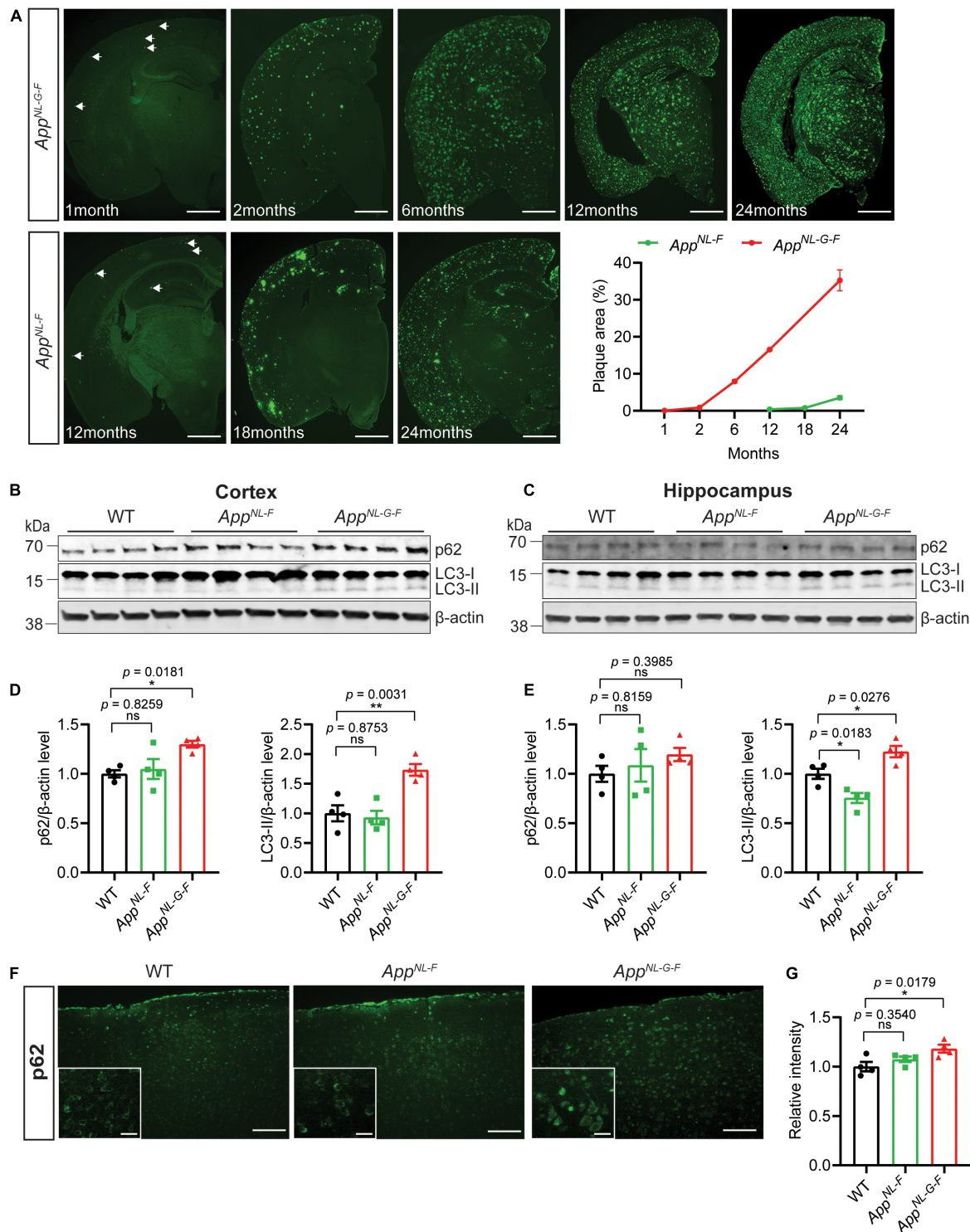


FIGURE 2 | Autophagy alterations in *App* knock-in mice. **(A)** Immunostaining for A β plaque deposition in the brains of *App^{NL-F}* and *App^{NL-G-F}* mice of indicated ages. The percentage of A β plaque area in the whole brain was quantified. Scale bars represent 1,000 μ m. **(B)** Cytosolic fraction of cortical and **(C)** hippocampal brain homogenates from 12-month-old WT, *App^{NL-F}*, and *App^{NL-G-F}* mice were immunoblotted with autophagic markers p62 and LC3. **(D)** The levels of p62 and LC3-II in cortex and **(E)** hippocampus were quantified by densitometry ($n = 4$, * $p < 0.05$, ** $p < 0.01$). **(F)** Immunostaining of p62 in 12-month-old WT, *App^{NL-F}*, and *App^{NL-G-F}* mouse cortex. Scale bars represent 100 μ m. The zoom in images of p62 positive neurons were inserted in white box. Scale bars represent 20 μ m. **(G)** The relative intensities were quantified ($n = 4$, * $p < 0.05$). Data were analyzed by one-way ANOVA followed by Dunnett's multiple comparisons test. Data are represented as mean \pm SEM. ns, not significant.

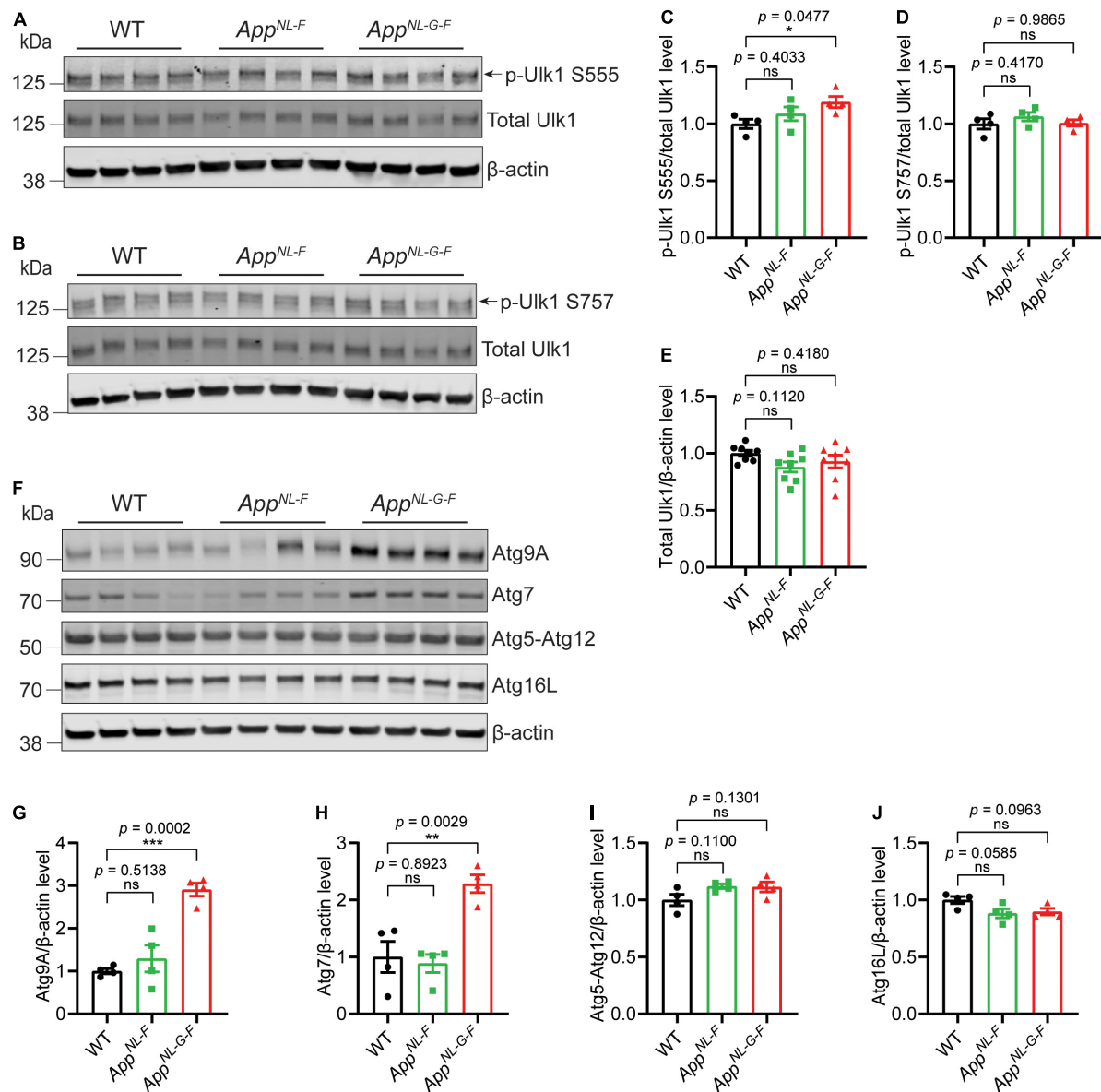


FIGURE 3 | Increased levels of key autophagy proteins in *App^{NL-G-F}* mice. Western blot analysis of cytosolic fraction of cortical brain homogenates from 12-month-old *App^{NL-F}* and *App^{NL-G-F}* mice were analyzed for Ulk1, p-Ulk1 S555 and p-Ulk1 S757 (A–E), Atg9A, Atg7, Atg5-Atg12, Atg16L (F–J), and the levels were quantified by densitometry ($n = 4$, * $p < 0.05$, ** $p < 0.01$, *** $p < 0.001$). Data are represented as mean \pm SEM. Ns, not significant.

neurodegenerative diseases, which share the common feature of dysfunctional protein homeostasis leading to aberrant protein aggregation. Both genetic and biochemical evidence for a dysfunctional autophagy-lysosomal system in AD is compelling (Kabeya et al., 2000; Wong and Cuervo, 2010). An accumulation of autophagosomes paralleled with increased levels of lysosomal proteases in brain tissues indicates that the autophagic activity is upregulated early in the disease while it at later stages is impaired (Nixon et al., 2005; Yu et al., 2005; Boland et al., 2008; Lee et al., 2011; Wolfe et al., 2013). FAD-linked mutation in presenilin 1 also leads to impaired acidification due to reduced vATPase activity

(Lee et al., 2010). Accumulation of autophagy adaptor protein p62 is an indicator of impaired autophagy which colocalizes with phosphorylated tau in AD postmortem brains (Kuusisto et al., 2002). Here we further substantiate these findings by showing that p62 also accumulates in tunica intima of vessels, indicating autophagy alteration in the vasculature in the AD brain. In addition, p62 accumulates in corpora amylacea. Though of largely unknown function, they could be related to debris clearance, for instance, from degenerating neurons. To further investigate the relationship between A β amyloidosis and autophagy, taking into account that autophagy plays a key role in A β metabolism (Yu et al., 2005; Nilsson et al., 2013), we

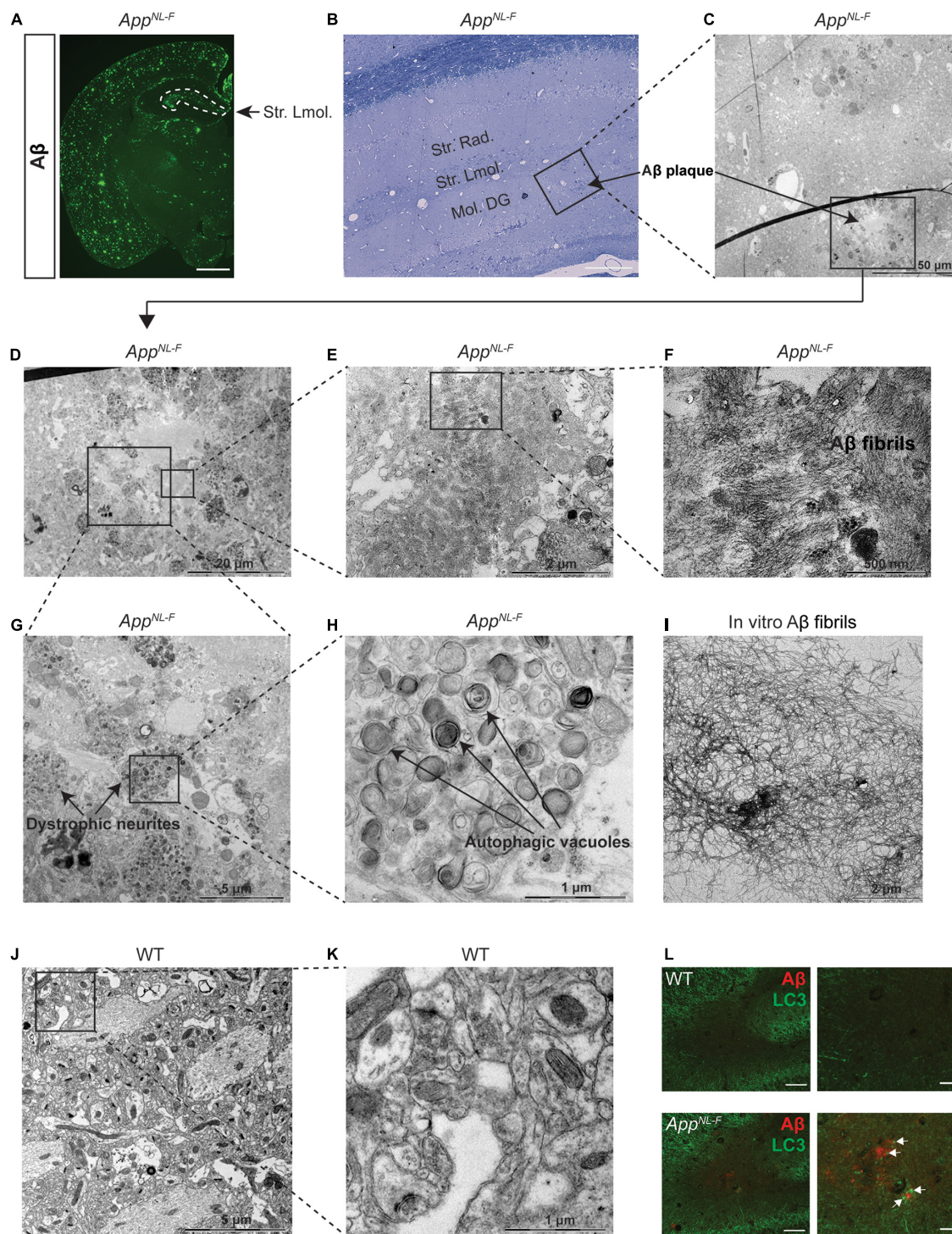


FIGURE 4 | Autophagic vacuole accumulation in dystrophic neurites in aged *App*^{NL-F} mice. **(A)** Immunostaining of Aβ plaques in 24-month-old *App*^{NL-F} mouse brains. Scale bars represent 1,000 μm. **(B)** Toluidine blue staining of 24-month-old *App*^{NL-F} mouse hippocampus. Scale bars represent 100 μm. The area labeled in black box was imaged under electron microscopy (EM) and shown in **(C)**. The area in black box in **(C)** showing Aβ plaques was zoomed in **(D)**. The area in black boxes in **(D)** were further zoomed in and shown in **(E,G)**, showing Aβ plaques and dystrophic neurites, respectively. Aβ plaques and fibrils were shown in **(F)** and the autophagic vacuoles were shown by higher magnification in **(H)**. **(I)** Aβ fibrils formed *in vitro* and imaged by EM. **(J)** The EM image from 24-month-old WT mouse hippocampus and the area in the black box was zoomed in **(K)**. Scale bars for EM images were presented in the images. **(L)** Double immunostaining of Aβ and LC3 in the hippocampus in 24-month-old WT and *App*^{NL-F} mice. Scale bars represent 100 μm. Str. Lmol., stratum lacunosum-moleculare; Str. Rad., stratum radiatum; Mol. DG, molecular dentate gyrus.

analyzed the brains of *App* knock-in mice. These mouse models exhibit robust A β 42 pathology, neuroinflammation, and synaptic alterations with physiological levels of amyloid precursor protein (APP) due to the knock-in strategy of FAD mutations. Thereby, potential artifacts caused by APP overexpression employed in APP transgenic mice can be circumvented. Interestingly, we observed, similar to AD brains, an inhibition of autophagy as indicated by an increase of p62 and LC3-II in the *App*^{NL-G-F} mice, especially in the cortex wherein the A β pathology starts at an earlier age as compared to hippocampus. Interestingly, we also found an increase in p-Ulk1 S555 and in Atg7 and Atg9A, indicating that an increase in autophagy initiation is also present in *App*^{NL-G-F} mouse brain potentially as a compensatory effect of the heavy A β burden and impaired end-stage clearance present in the 12-month-old *App*^{NL-G-F} mice. However, it remains to be established if this effect is present in the neurons or in other cell types of the brain such as astrocytes or microglia. In contrast, the brains of *App*^{NL-F} mice are characterized by a slight decrease in LC3-II levels. Since no activation of autophagy as measured by p-Ulk1/Ulk1 nor any increase in key autophagy proteins was observed, the decrease in LC3-II could be linked to increased lysosomal clearance which needs further analysis. Even though the two *App* knock-in models share the Swedish and the Beyreuther mutations leading to increase A β 42 generation, the *App*^{NL-G-F} mice additionally exhibit the Arctic mutation that induces a fast oligomerization of the A β peptide and an early and robust A β plaque deposition. It is tempting to speculate that the autophagy inhibition observed in the 12-month-old *App*^{NL-G-F} mice is due to the much-pronounced A β pathology; however, it cannot be excluded that the difference in autophagy status is a direct effect of the Arctic mutation on the autophagy-lysosomal system. In support of an effect on autophagy by an increased A β burden is the very pronounced accumulation of autophagic vacuoles specifically located around the A β plaques in the 24-month-old *App*^{NL-F} mice. The impaired autophagy may in turn induce aggregation of intracellular A β and potentially cause a vicious cycle and further contribute to the increased A β pathology.

DATA AVAILABILITY STATEMENT

The original contributions presented in the study are included in the article/**Supplementary Material**, further inquiries can be directed to the corresponding author/s.

REFERENCES

- Abelein, A., Chen, G., Kitoka, K., Aleksis, R., Oleskovs, F., Sarr, M., et al. (2020). High-yield production of Amyloid- β peptide enabled by a customized spider silk domain. *Sci. Rep.* 10:235. doi: 10.1038/s41598-019-57143-x
- Boland, B., Kumar, A., Lee, S., Platt, F. M., Wegiel, J., Yu, W. H., et al. (2008). Autophagy induction and autophagosome clearance in neurons: relationship to autophagic pathology in Alzheimer's disease. *J. Neurosci.* 28, 6926–6937. doi: 10.1523/JNEUROSCI.0800-08.2008
- Heckmann, B. L., Teubner, B. J. W., Boada-Romero, E., Tummers, B., Guy, C., Fitzgerald, P., et al. (2020). Noncanonical function of an autophagy protein

ETHICS STATEMENT

The studies involving human participants were reviewed and approved by approval nr 2013/1301-31/2 and EPN 2011/962-31/1 and 2018/1993-32. The patients/participants provided their written informed consent to participate in this study. The animal study was reviewed and approved by ethical permit ID 407 approved by Linköping animal ethical board and 12570-2021 approved by Stockholm animal ethical board.

AUTHOR CONTRIBUTIONS

RJ and PN initiated the project and designed the study. RJ, MS, JM, and ST conducted the biochemical experiments related to autophagy. RK and AA performed EM analysis of A β fibrils formed *in vitro*. RJ, NB, and BW analyzed human postmortem immunohistology. RJ, PN, and BW wrote the first draft of manuscript. NB advised on the study and commented on the manuscript. All authors reviewed and revised the manuscript.

ACKNOWLEDGMENTS

We thank Takashi Saito and Takaomi C. Saido at RIKEN Center for Brain Science for providing *App* knock-in mice. We are most grateful for the technical support for EM data acquisition at the EM unit EMil at Huddinge University Hospital. We thank the following financial support: Hållsten Research Foundation (PN), Swedish Research Council (PN), Swedish Brain foundation (PN), Torsten Söderberg Foundation (PN), Sonja Leikrans donation (PN), The Erling-Persson Family Foundation (PN), China Scholarship Council (RJ), Gun and Bertil Stohne's Foundation (RJ and PN), Gamla Tjänarinnor grant (RJ and PN), Margaretha af Ugglas Stiftelse (BW), and Alzheimerfonden (PN and BW).

SUPPLEMENTARY MATERIAL

The Supplementary Material for this article can be found online at: <https://www.frontiersin.org/articles/10.3389/fnagi.2022.878303/full#supplementary-material>

prevents spontaneous Alzheimer's disease. *Sci. Adv.* 6:eabb9036. doi: 10.1126/sciadv.abb9036

- Hemelaar, J., Lelyveld, V. S., Kessler, B. M., and Ploegh, H. L. (2003). A single protease, Apg4B, is specific for the autophagy-related ubiquitin-like proteins GATE-16, MAP1-LC3, GABARAP, and Apg8L. *J. Biol. Chem.* 278, 51841–51850. doi: 10.1074/jbc.M308762200
- Johansen, T., and Lamark, T. (2011). Selective autophagy mediated by autophagic adapter proteins. *Autophagy* 7, 279–296. doi: 10.4161/auto.7.3.14487
- Kabeya, Y., Mizushima, N., Ueno, T., Yamamoto, A., Kirisako, T., Noda, T., et al. (2000). LC3, a mammalian homologue of yeast Apg8p, is localized in autophagosome membranes after processing. *EMBO J.* 19, 5720–5728. doi: 10.1093/emboj/19.21.5720

- Kuusisto, E., Salminen, A., and Alafuzoff, I. (2002). Early accumulation of p62 in neurofibrillary tangles in Alzheimer's disease: possible role in tangle formation. *Neuropathol. Appl. Neurobiol.* 28, 228–237. doi: 10.1046/j.1365-2990.2002.00394.x
- Lee, J.-H., Yu, W. H., Kumar, A., Lee, S., Mohan, P. S., Peterhoff, C. M., et al. (2010). Lysosomal proteolysis and autophagy require presenilin 1 and are disrupted by Alzheimer-Related PS1 mutations. *Cell* 141, 1146–1158. doi: 10.1016/j.cell.2010.05.008
- Lee, S., Sato, Y., and Nixon, R. A. (2011). Lysosomal proteolysis inhibition selectively disrupts axonal transport of degradative organelles and causes an alzheimer's-like axonal dystrophy. *J. Neurosci.* 31, 7817–7830. doi: 10.1523/JNEUROSCI.6412-10.2011
- Lendahl, U., Nilsson, P., and Betsholtz, C. (2019). Emerging links between cerebrovascular and neurodegenerative diseases—a special role for pericytes. *EMBO Rep.* 20:e48070. doi: 10.15252/embr.201948070
- Lipinski, M. M. (2010). Towards the global understanding of the autophagy regulatory network. *Autophagy* 6, 1218–1220. doi: 10.4161/auto.6.8.13772
- Lipinski, M. M., Zheng, B., Lu, T., Yan, Z., Py, B. F., Ng, A., et al. (2010). Genome-wide analysis reveals mechanisms modulating autophagy in normal brain aging and in Alzheimer's disease. *Proc. Natl. Acad. Sci. U S A.* 107, 14164–14169. doi: 10.1073/pnas.1009485107
- Nilsson, P., and Saido, T. C. (2014). Dual roles for autophagy: degradation and secretion of Alzheimer's disease Aβ peptide. *Bioessays* 36, 570–578. doi: 10.1002/bies.201400002
- Nilsson, P., Loganathan, K., Sekiguchi, M., Matsuba, Y., Hui, K., Tsubuki, S., et al. (2013). Aβ secretion and plaque formation depend on autophagy. *Cell Rep.* 5, 61–69. doi: 10.1016/j.celrep.2013.08.042
- Nixon, R. A., Wegiel, J., Kumar, A., Yu, W. H., Peterhoff, C., Cataldo, A., et al. (2005). Extensive involvement of autophagy in Alzheimer disease: an immunoelectron microscopy study. *J. Neuropathol. Exp. Neurol.* 64, 113–122. doi: 10.1093/jnen/64.2.113
- Pankiv, S., Clausen, T. H., Lamark, T., Brech, A., Bruun, J. A., Outzen, H., et al. (2007). p62/SQSTM1 binds directly to Atg8/LC3 to facilitate degradation of ubiquitinated protein aggregates by autophagy. *J. Biol. Chem.* 282, 24131–24145. doi: 10.1074/jbc.M702824200
- Saito, T., Matsuba, Y., Mihira, N., Takano, J., Nilsson, P., Itohara, S., et al. (2014). Single App knock-in mouse models of Alzheimer's disease. *Nat. Neurosci.* 17, 661–663. doi: 10.1038/nn.3697
- Tanida, I., Ueno, T., and Kominami, E. (2004). LC3 conjugation system in mammalian autophagy. *Int. J. Biochem. Cell Biol.* 36, 2503–2518. doi: 10.1016/j.biocel.2004.05.009
- Tanida, I., Ueno, T., and Kominami, E. (2008). LC3 and Autophagy. *Methods Mol. Biol.* 445, 77–88.
- Wolfe, D. M., Lee, J. H., Kumar, A., Lee, S., Orenstein, S. J., and Nixon, R. A. (2013). Autophagy failure in Alzheimer's disease and the role of defective lysosomal acidification. *Eur. J. Neurosci.* 37, 1949–1961. doi: 10.1111/ejn.12169
- Wong, E., and Cuervo, A. M. (2010). Autophagy gone awry in neurodegenerative diseases. *Nat. Neurosci.* 13, 805–811. doi: 10.1038/nn.2575
- Yu, W. H., Cuervo, A. M., Kumar, A., Peterhoff, C. M., Schmidt, S. D., Lee, J. H., et al. (2005). Macroautophagy – a novel beta-amyloid peptide-generating pathway activated in Alzheimer's disease. *J. Cell Biol.* 171, 87–98. doi: 10.1083/jcb.200505082

Conflict of Interest: The authors declare that the research was conducted in the absence of any commercial or financial relationships that could be construed as a potential conflict of interest.

Publisher's Note: All claims expressed in this article are solely those of the authors and do not necessarily represent those of their affiliated organizations, or those of the publisher, the editors and the reviewers. Any product that may be evaluated in this article, or claim that may be made by its manufacturer, is not guaranteed or endorsed by the publisher.

Copyright © 2022 Jiang, Shimozawa, Mayer, Tambaro, Kumar, Abelein, Winblad, Bogdanovic and Nilsson. This is an open-access article distributed under the terms of the Creative Commons Attribution License (CC BY). The use, distribution or reproduction in other forums is permitted, provided the original author(s) and the copyright owner(s) are credited and that the original publication in this journal is cited, in accordance with accepted academic practice. No use, distribution or reproduction is permitted which does not comply with these terms.



Phenotypic Displays of Cholinergic Enzymes Associate With Markers of Inflammation, Neurofibrillary Tangles, and Neurodegeneration in Pre- and Early Symptomatic Dementia Subjects

OPEN ACCESS

Edited by:

Margaret Fahnestock,
McMaster University, Canada

Reviewed by:

Elena Rodriguez-Vieitez,
Karolinska Institutet (KI), Sweden
Changiz Geula,
Northwestern University,
United States
Sumera Zaib,
University of Central Punjab, Pakistan
Hermona Soreq,
Hebrew University of Jerusalem,
Israel
Vikneswaran Murugaiyah,
Universiti Sains Malaysia (USM),
Malaysia

*Correspondence:

Unnur D. Teitsdottir
udt1@hi.is

Specialty section:

This article was submitted to
Alzheimer's Disease and Related
Dementias,
a section of the journal
Frontiers in Aging Neuroscience

Received: 14 February 2022

Accepted: 02 May 2022

Published: 26 May 2022

Citation:

Teitsdottir UD, Darreh-Shori T,
Lund SH, Jonsdottir MK, Snaedal J
and Petersen PH (2022) Phenotypic
Displays of Cholinergic Enzymes
Associate With Markers of
Inflammation, Neurofibrillary Tangles,
and Neurodegeneration in Pre- and
Early Symptomatic Dementia
Subjects.
Front. Aging Neurosci. 14:876019.
doi: 10.3389/fnagi.2022.876019

Unnur D. Teitsdottir^{1*}, Taher Darreh-Shori², Sigrun H. Lund³, Maria K. Jonsdottir^{4,5},
Jon Snaedal⁶ and Petur H. Petersen¹

¹Faculty of Medicine, Department of Anatomy, Biomedical Center, University of Iceland, Reykjavik, Iceland, ²Division of Clinical Geriatrics, Department of Neurobiology, Care Sciences and Society, Center for Alzheimer Research, Karolinska Institutet, Campus Flemingsberg, Stockholm, Sweden, ³deCODE genetics/Amgen, Inc., Reykjavik, Iceland, ⁴Department of Psychology, Reykjavik University, Reykjavik, Iceland, ⁵Department of Psychiatry, Landspítali-National University Hospital, Reykjavik, Iceland, ⁶Memory Clinic, Department of Geriatric Medicine, Landspítali-National University Hospital, Reykjavik, Iceland

Background: Cholinergic drugs are the most commonly used drugs for the treatment of Alzheimer's disease (AD). Therefore, a better understanding of the cholinergic system and its relation to both AD-related biomarkers and cognitive functions is of high importance.

Objectives: To evaluate the relationships of cerebrospinal fluid (CSF) cholinergic enzymes with markers of amyloidosis, neurodegeneration, neurofibrillary tangles, inflammation and performance on verbal episodic memory in a memory clinic cohort.

Methods: In this cross-sectional study, 46 cholinergic drug-free subjects (median age = 71, 54% female, median MMSE = 28) were recruited from an Icelandic memory clinic cohort targeting early stages of cognitive impairment. Enzyme activity of acetylcholinesterase (AChE) and butyrylcholinesterase (BuChE) was measured in CSF as well as levels of amyloid- β_{1-42} ($A\beta_{42}$), phosphorylated tau (P-tau), total-tau (T-tau), neurofilament light (NFL), YKL-40, S100 calcium-binding protein B (S100B), and glial fibrillary acidic protein (GFAP). Verbal episodic memory was assessed with the Rey Auditory Verbal Learning (RAVLT) and Story tests.

Results: No significant relationships were found between CSF $A\beta_{42}$ levels and AChE or BuChE activity ($p > 0.05$). In contrast, T-tau ($r = 0.46$, $p = 0.001$) and P-tau ($r = 0.45$, $p = 0.002$) levels correlated significantly with AChE activity. Although neurodegeneration markers T-tau and NFL did correlate with each other ($r = 0.59$, $p < 0.001$), NFL did not correlate with AChE ($r = 0.25$, $p = 0.09$) or BuChE ($r = 0.27$, $p = 0.06$). Inflammation markers S100B and YKL-40 both correlated significantly with AChE (S100B: $r = 0.43$,

$p = 0.003$; YKL-40: $r = 0.32$, $p = 0.03$) and BuChE (S100B: $r = 0.47$, $p < 0.001$; YKL-40: $r = 0.38$, $p = 0.009$) activity. A weak correlation was detected between AChE activity and the composite score reflecting verbal episodic memory ($r = -0.34$, $p = 0.02$). LASSO regression analyses with a stability approach were performed for the selection of a set of measures best predicting cholinergic activity and verbal episodic memory score. S100B was the predictor with the highest model selection frequency for both AChE (68%) and BuChE (73%) activity. Age (91%) was the most reliable predictor for verbal episodic memory, with selection frequency of both cholinergic enzymes below 10%.

Conclusions: Results indicate a relationship between higher activity of the ACh-degrading cholinergic enzymes with increased neurodegeneration, neurofibrillary tangles and inflammation in the stages of pre- and early symptomatic dementia, independent of CSF A β_{42} levels.

Keywords: Alzheimer's disease, cerebrospinal fluid, acetylcholinesterase, butyrylcholinesterase, cholinergic system, inflammation, neurodegeneration, biomarkers

INTRODUCTION

The neuropathological changes in AD include the accumulation of beta-amyloid (A β) in plaques and hyper-phosphorylated tau protein in neurofibrillary tangles (NFT), leading to loss of synapses, dendrites, and eventually neurons. The most consistent neuronal loss through the progression of AD is found within the cholinergic system of the basal forebrain (Mufson et al., 2003; Giacobini et al., 2022). The cholinergic neurons of this region are the major source of cholinergic innervation to the cerebral cortex and hippocampus, playing a pivotal role in cognitive functions including memory, learning and attention (Ballinger et al., 2016). Due to the critical role of the neurotransmitter acetylcholine (ACh) in cognitive functions, most of the approved pharmacological treatments for AD are cholinesterase inhibitors (ChEIs). ChEIs increase the availability of ACh at synapses in the brain and are among the few drugs that have been proven clinically useful in the treatment of AD, thus validating the cholinergic system as an important therapeutic target in the disease (Hampel et al., 2018).

According to the classical view of cholinergic signaling (Adem, 1992), the neurotransmitter ACh is synthesized in the cytoplasm of cholinergic neurons by the enzyme choline acetyltransferase (ChAT). ACh molecules are released into the synaptic clefts for initiating or propagating neurotransmission. The transmission is subsequently terminated by the cleavage of ACh by cholinesterases, acetylcholinesterase (AChE) and butyrylcholinesterase (BuChE). Notably, ACh is not restricted to neurons and synapses. The cholinergic signaling system has also been associated with inflammation, both generally and in neurodegenerative diseases like AD. ACh is hypothesized to act as a suppressor on non-excitable cholinergic cells, including astrocytes and microglia, inhibiting cytokine release through activation of nicotinic $\alpha 7$ -ACh receptors (Van Westerloo et al., 2005; Pavlov et al., 2009; Benfante et al., 2021). Recent research demonstrated that astrocytes secrete the ACh synthesizing enzyme ChAT, suggesting that the physiological function of extracellular ChAT is to maintain a

steady-state equilibrium of hydrolysis and synthesis of ACh (Vijayaraghavan et al., 2013).

Extracellular accumulation of A β in AD may cause imbalances in cholinergic signaling, which facilitates increased degradation of ACh and enhanced cytokine expression and release. Such an exaggerated inflammatory microenvironment could, in turn, have consequential neurodegenerative effects (Malmsten et al., 2014). BuChE may also have a particularly critical role in the dynamic control of levels of extracellular ACh, *via* its ACh hydrolyzing activity, as the primary source of it in the CNS is attributed to non-excitable cells such as astrocytes and microglia (Mesulam et al., 2002; Revathikumar et al., 2016). In plasma, increased AChE activity has been associated with AD, although results have been inconsistent (García-Ayllón et al., 2010).

In recent years, a paradigm shift has occurred from clinical to biological definition of AD based on *in vivo* biomarkers measured in cerebrospinal fluid (CSF) or with positron emission tomography (PET) imaging. In 2018, the National Institute on Aging and Alzheimer's Association (NIA-AA) (Jack et al., 2018) created a research framework for AD diagnosis, defining AD based on biomarker evidence of pathology. Understanding how biomarkers reflecting different biological processes could influence AD pathogenesis and severity is critical for the improvement of diagnosis and development of effective pharmacologic treatments. It is essential for the evaluation of novel biomarkers to examine their relationship with signature AD pathology, independent of diagnosis. Such an approach could both enhance understanding of the underlying pathology of AD and the sequence of events leading to cognitive impairment. The aim of this study was to examine the association between the activity of cholinergic enzymes and CSF markers reflecting the state of brain amyloidosis (A β_{42}), neurodegeneration (T-tau, NFL), neurofibrillary tangles (P-tau) and inflammation (YKL-40, S100B, GFAP) among subjects at the pre-and early symptomatic stages of dementia. The second aim was to explore the relationships of the same enzymes with the loss of verbal episodic memory.

MATERIALS AND METHODS

Subjects

The current study cohort and the selection criteria have been described earlier (Teitsdottir et al., 2020, 2021). Subjects were recruited from the Icelandic MCI study cohort ($n = 165$). The cohort was comprised of individuals who had been referred to Landspítali University Hospital (LUH) Memory Clinic over a four-year period. The inclusion criteria for joining the cohort study were: (i) a score between 24 and 30 on the Mini-Mental State Examination (MMSE) (Folstein et al., 1975); and (ii) a score of 4.0 or less on the Informant Questionnaire on Cognitive Decline in the Elderly (IQCODE) (Jorm, 1994). The exclusion criteria were the following: (i) cognitive impairment caused by a pre-existing condition; (ii) difficulties participating due to health or social issues; and (iii) residency outside the Reykjavík Capital Area. Each subject underwent various measurements at baseline, which included a medical assessment and a detailed neuropsychological assessment as well as brain magnetic resonance imaging (MRI) for the evaluation of medial temporal lobe atrophy (MTA), global cortical atrophy (GCA) and white matter lesions (Fazekas). Lumbar puncture was carried out for the collection of CSF, but the intervention was optional by the requirement of the National Bioethics Committee. For this cross-sectional study, the final sample included 46 subjects (**Figure 1**). Only those who underwent lumbar puncture were selected from the Icelandic MCI study cohort, excluding 113 subjects. In addition, six other subjects were removed due to excessively high CSF P-tau ($n = 1$), GFAP ($n = 1$), AChE and BuChE ($n = 1$) values or blood-contamination in CSF samples ($n = 3$). Clinical diagnosis of AD was based on the criteria for probable AD dementia defined by the National Institute on Aging-

Alzheimer's Association (NIA-AA) (McKhann et al., 2011), with evidence of AD pathophysiological processes (based on MTA score or/and analysis of core CSF markers). Patients with Lewy body dementia (LBD) were diagnosed based on the consensus criteria of McKeith (McKeith et al., 2017). The diagnosis of MCI required the fulfillment of the Winblad criteria (Winblad et al., 2004). Those without cognitive impairment were considered to have subjective mild cognitive impairment (SCI), as they had been referred to the Memory Clinic due to concerns of cognitive decline. Of the 46 subjects in this study, 15 were diagnosed with SCI or MCI and remained stable after a two-year follow-up. One subject converted from a diagnosis of MCI to AD after a two-year follow-up and another one from MCI to cortico-basilar degeneration (CBD) after a one-year follow-up. A total of 18 subjects were diagnosed with AD, three with LBD and one with Parkinson's disease (PD) at baseline. Seven of the subjects were diagnosed with SCI and MCI at baseline but left the study before one year or two-year follow-up. None of the subjects had been prescribed cholinergic drugs before entering or were prescribed them during the study.

CSF Collection and Analysis

The collection of CSF and the measurements of protein concentrations have previously been described (Teitsdottir et al., 2020, 2021). Collection of CSF was done via lumbar puncture with a 22-gauge spinal needle at the L3/4 or L4/5 interspace. Samples, uncentrifuged, were frozen in 2 ml polypropylene tubes and stored at -80°C . Levels of all proteins were determined using commercially available sandwich enzyme-linked immunosorbent assays (ELISAs) and performed according to manufacturer's instructions.

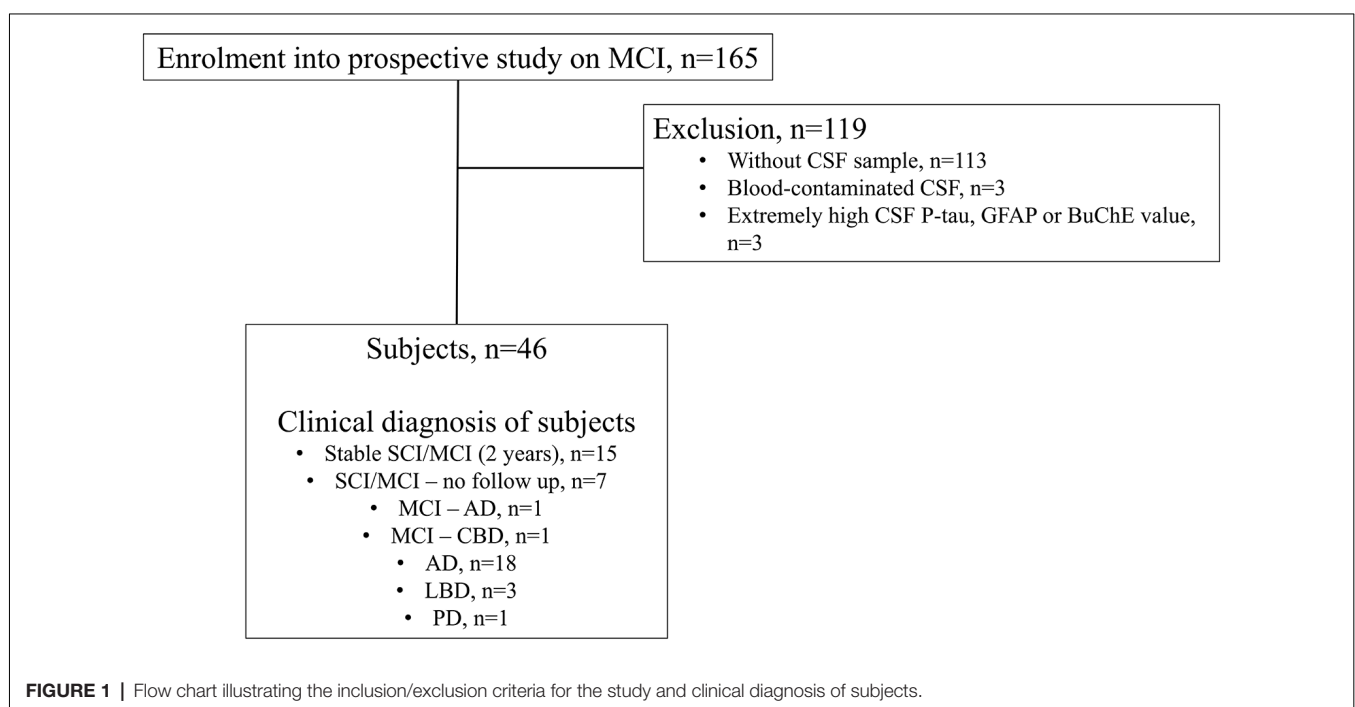


FIGURE 1 | Flow chart illustrating the inclusion/exclusion criteria for the study and clinical diagnosis of subjects.

Levels of T-tau (IBL International, Hamburg, Germany), P-tau181 (INNOTEST, Gent, Belgium), and $A\beta_{42}$ (IBL International, Hamburg, Germany), were measured in the ISO 15189 accredited medical laboratory MVZ Labor P.D. Dr. Volkmann und Kollegen GbR (Karlsruhe, Germany). Levels of NFL (Uman Diagnostics, Umeå, Sweden), YKL-40 (Quantikine ELISA Human Chitinase-3-like 1; R&D systems, MN, USA), S100B (BioVendor GmbH, Heidelberg, Germany) and GFAP (BioVendor GmbH, Heidelberg, Germany) were measured in a laboratory at the University of Iceland. All assays had mean Intra-assay CV <10% and Inter-assay CV <15%. The activity of BuChE and AChE in CSF was measured as described in Darreh-Shori et al. (2006, 2008).

Subject Grouping Based on CSF Measures

Three different CSF biomarker profiles were created, each based on the levels of one core CSF biomarker ($A\beta_{42}$ T-tau and P-tau). The CSF profile was divided into two categories, abnormal (positive) or normal (negative). The specific cut-off points were established by MVZ Labor P.D. Dr. Volkmann und Kollegen GbR, the laboratory performing the ELISAs. Abnormal values were defined as $A\beta_{42}$ < 375 pg/ml, T-tau > 445 pg/ml and P-tau > 61 pg/ml.

Neuropsychological Tests

A detailed neuropsychological assessment was carried out by licensed psychologists under the guidance of a clinical neuropsychologist. Two tests were used for the evaluation of verbal episodic memory, The Rey Auditory Verbal Learning Test (RAVLT) (Lezak et al., 2012), and a Story test based on the Logical Memory test of the Wechsler Memory Scale-Revised (Wechsler, 1987). RAVLT requires the subject to learn 15 nouns presented across five consecutive trials. Each trial is followed by a free-recall test (immediate recall). The sum of the number of words recalled from trials 1 through 5 (0–75 points) is calculated for the score of RAVLT immediate recall. After a 30 min delay, the subject is asked to recall as many words as possible without hearing them again (delayed recall). The score is a sum of correctly recalled words (0–15 points). Lastly, a list containing the previous 15 nouns as well as 30 new ones, is read to the subject whose task is to recognize the nouns from the list, with number of false positives subtracted from the score (–30–15 points). The second test is composed of a brief story, presented orally by the examiner. The story includes 25 story ideas, where the subject is required to repeat it immediately after presentation without any clues given. A point is given for the number of story ideas correctly recalled (0–25 points). After a 30-min delay, the subject is asked to recall the story again without it being orally repeated again.

Statistical Analysis

Descriptive group comparisons were performed using Mann-Whitney U tests or Kruskal-Wallis H tests for continuous variables and chi-square tests for categorical variables. The composite score for verbal episodic memory was calculated by averaging the z-scores of each neuropsychological test and subsequently converting those scores into z-scores. Raw

values of CSF proteins ($A\beta_{42}$, P-tau, T-tau, NFL, YKL-40, S100B, GFAP) were naturally log-transformed to account for a non-normal distribution. Pearson's correlations and scatter plots were used for estimation and visualization of relationships between continuous variables. Least absolute shrinkage and selection operator (LASSO) regression combined with stability selection was applied for the identification of stable predictors in multivariable models (Tibshirani, 1996). The function `stabsel` from the package `stabs` in R was implemented for the performance of stability selection, which utilized the package `glmnet` for LASSO model fitting on each subsample (Meinshausen and Bühlmann, 2010; Hofner et al., 2015). A total of 100 subsamples were drawn, with each being half the size of the original sample. The cut-off value of 75% was chosen as a criterion for stable selection (calculated as the percentage frequency of a variable being selected into a model) and per-family error rate (PFER) was set to 1. All statistical analyses were performed using R (version 3.6.1, The R Foundation for Statistical Computing).

RESULTS

Study Cohort Characteristics

Table 1 shows the demographic, pathophysiological and clinical characteristics of the cohort by CSF $A\beta_{42}$ and T-tau profiles. No statistical difference ($p > 0.05$) was found in characteristics between subjects with abnormally low CSF $A\beta_{42}$ levels (positive profile; +) and those with normal $A\beta_{42}$ levels (negative profile; -). In contrast, statistical difference was found between the CSF T-tau profile groups. Subjects with abnormally high CSF T-tau levels (+) were statistically higher in age ($p = 0.02$), CSF NFL levels ($p < 0.001$) and CSF YKL-40 levels ($p = 0.02$) compared to those with normal T-tau levels (-). The T-tau+ group did also score significantly lower on all neuropsychological subtests reflecting verbal episodic memory ($p < 0.01$).

Distributions in cholinergic activity (AChE and BuChE) between CSF profiles ($A\beta_{42}$, T-tau and P-tau) and clinical diagnosis are visualized with boxplots in **Figure 2**. No significant differences were detected in AChE (**Figure 2A**, $p = 0.35$) or BuChE activity (**Figure 2B**, $p = 0.92$) between the $A\beta$ + and $A\beta$ -profile groups. In contrast, AChE activity was significantly higher among subjects with T-tau+ profile compared to those with a T-tau- profile (**Figure 2C**, $p = 0.008$). No differences were detected between BuChE activity between the same groups (**Figure 2D**, $p = 0.11$). The same pattern was observed as well for P-tau, with higher AChE activity found among the positive group compared to the negative one (**Figure 2E**, $p = 0.02$), and no difference between groups in regard to BuChE activity (**Figure 2F**, $p > 0.05$). No significant difference was observed in AChE (**Figure 2G**, $p > 0.05$) or BuChE activity (**Figure 2H**, $p > 0.05$) between different diagnostic groups.

Correlation Matrix Between CSF Markers, Age, and Education

Pearson's correlations between the CSF markers, age, and education are presented in **Figure 3**. Inflammatory markers

TABLE 1 | Subject demographics, CSF marker levels, and cognitive scores by CSF A β_{42} and T-tau profiles.

| | CSF A β_{42} profile | | | CSF T-tau profile | | |
|--|--|--|------------------|---|---|------------------|
| | A β_{42} -, A β_{42} > 375 pg/ml (n = 33) | A β_{42} +, A β_{42} < 375 pg/ml (n = 13) | p value a | T-tau-, T-tau < 445 pg/ml (n = 29) | T-tau+, T-tau > 445 pg/ml (n = 17) | p value a |
| Demographics | | | | | | |
| Gender (M/F) | 13/20 | 8/5 | 0.18 | 14/15 | 7/10 | 0.64 |
| Age, years | 71 (46–85) | 70 (51–84) | 0.75 | 70 (46–85) | 77 (51–84) | 0.02 |
| Education, years | 13 (6–19) | 13 (6–20) | 0.77 | 13 (6–19) | 13 (6–20) | 0.75 |
| Clinical diagnosis | | | | | | |
| Stable SCI or MCI/AD ^b / | | | | | | |
| OD ^c /SCI or MCI—no follow-up | 12/11/5/5 | 3/8/0/2 | N/A ^d | 15/4/3/7 | 0/15/2/0 | N/A ^d |
| CSF measures | | | | | | |
| A β_{42} (pg/ml) | 671 (404–1434) | 254 (140–335) | N/A | 594 (167–1434) | 490 (140–977) | 0.27 |
| T-tau (pg/ml) | 294 (106–1886) | 397 (132–916) | 0.09 | 253 (106–438) | 643 (475–1086) | N/A |
| P-tau (pg/ml) | 57 (33–144) | 83 (30–125) | 0.40 | 49 (30–87) | 106 (70–144) | N/A |
| AChE activity (nmol/min/ml) | 12.2 (4.4–16.3) | 10.5 (8.0–16.0) | 0.35 | 11.1 (4.4–15.5) | 13.5 (8.0–16.3) | 0.008 |
| BuChE activity (nmol/min/ml) | 6.3 (4.2–10.9) | 6.4 (4.7–11.5) | 0.92 | 6.2 (4.2–9.4) | 7.0 (4.7–11.5) | 0.11 |
| NFL (ng/ml) | 2.1 (1.0–5.0) | 2.3 (1.2–5.3) | 0.60 | 2.0 (1.0–3.6) | 3.0 (1.6–5.3) | <0.001 |
| YKL-40 (ng/ml) | 194 (83–367) | 177 (124–351) | 0.87 | 160 (83–365) | 235 (124–367) | 0.02 |
| S100B (pg/ml) | 233 (143–458) | 240 (175–509) | 0.89 | 228 (143–382) | 243 (175–509) | 0.15 |
| GFAP (ng/ml) | 1.2 (0.2–21.3) | 1.4 (0.8–5.8) | 0.14 | 1.3 (0.2–6.3) | 1.1 (0.5–21.3) | 0.59 |
| Global cognition | | | | | | |
| MMSE, score | 28 (24–30) | 27 (24–30) | 0.32 | 28 (24–30) | 27 (24–30) | 0.25 |
| Verbal episodic memory | | | | | | |
| RAVLT immediate recall, score ^e | 30 (13–65) | 26 (15–51) | 0.27 | 31 (16–65) | 25 (13–39) | 0.009 |
| RAVLT delayed recall, score ^e | 3 (0–15) | 2 (0–12) | 0.13 | 4 (0–15) | 1 (0–8) | 0.003 |
| RAVLT recognition-fp, score ^f | 7 (–3–15) | 6 (0–15) | 0.61 | 7 (2–15) | 4 (–3–9) | 0.001 |
| Story immediate recall, score | 9 (1–21) | 6 (2–18) | 0.21 | 11 (2–21) | 6 (1–14) | 0.003 |
| Story delayed recall, score | 7 (0–19) | 6 (0–16) | 0.30 | 8 (0–19) | 3 (0–12) | 0.002 |
| Composite z-score ^f | –0.1 (–1.5–2.3) | –0.5 (–1.2–1.9) | 0.13 | 0.1 (–1.0–2.3) | –0.7 (–1.5–0.2) | <0.001 |

AD, Alzheimer's disease; CSF, Cerebrospinal fluid; MCI, Mild Cognitive Impairment; MMSE, Mini-Mental State—Examination; N/A, Not applicable; OD, Other dementia; RAVLT, Rey Auditory-Verbal Learning Test; SCI, Subjective Cognitive Impairment. Values are shown as median (range) or as numbers per group. ^aMann-Whitney U non-parametric tests used for continuous variables and Chi-Square tests for categorical variables. ^bThe AD category included one subject who converted from MCI to AD. ^cThe OD category included one subject who converted from MCI to OD. P-values not applicable for ^dclinical diagnosis due to CSF A β_{42} and Tau values being a part of the diagnostic criteria for AD. Analysis based on 45^e or 44^f subjects.

YKL-40 and S100B and neurodegeneration markers NFL, P-tau and T-tau all correlated positively and significantly ($p < 0.05$) with each other. GFAP did only significantly correlate with the CSF markers S100B ($r = 0.69$, $p < 0.001$) and NFL ($r = 0.36$, $p = 0.01$). No CSF marker correlated significantly with A β_{42} ($p > 0.05$). All the CSF markers, except for A β_{42} and the cholinergic enzymes, correlated positively with age ($p < 0.05$). AChE activity correlated significantly with levels of P-tau, T-tau, YKL-40, and S100B ($p < 0.05$), but not with levels of NFL ($r = 0.25$, $p = 0.09$). BuChE activity correlated significantly with levels of YKL-40 and S100B ($p < 0.01$), but not with P-tau ($r = 0.27$, $p = 0.07$), T-tau ($r = 0.20$, $p = 0.18$) or NFL ($r = 0.27$, $p = 0.06$).

Significant relationships of CSF AChE and BuChE activities with CSF markers from **Figure 3** are visualized by scatter plots in **Figure 4**. Moderately strong, positive correlations were detected between AChE activity and levels of: (A) T-tau ($r = 0.46$, $p = 0.001$), (B) P-tau ($r = 0.45$, $p = 0.002$), and (C) S100B ($r = 0.43$, $p = 0.003$). Weak correlation was found between AChE activity and (D) YKL-40 levels ($r = 0.32$, $p = 0.03$). As with AChE, BuChE also showed moderately strong, positive correlation with levels of (E) S100B ($r = 0.47$, $p < 0.001$) and (F) YKL-40 ($r = 0.38$, $p = 0.009$).

Selection of Best Predictors for Cholinergic Enzyme Activity

LASSO linear regression with a stability selection was performed for the identification of a set of variables predicting cholinergic enzyme activity with the highest consistency (**Figure 5**). Variables with stability selection above 75% were considered reliable predictors. Two analyses were performed, one for each enzyme (AChE and BuChE) as a dependent variable. Ten possible predictors could be selected for each analysis, five CSF markers (A β_{42} , T-tau, P-tau, NFL, YKL-40, S100B, GFAP) and three demographic measures (gender, age, and length of education).

No variables reached the selection criteria for prediction of AChE activity (**Figure 5A**). S100B was the predictor with the highest selection frequency (68%), by far the highest compared to other measures. The next predictors in order of selection frequency were education (49%), T-tau (45%), and P-tau (44%). All other possible predictors had much lower selection frequency ($\leq 25\%$).

S100B was also the measure most often selected into a model (73%) for the best prediction of BuChE activity (**Figure 5B**). The CSF marker almost reached the selection criteria of 75%. Gender (64%) and YKL-40 (61%) both had selection frequency over 60%.

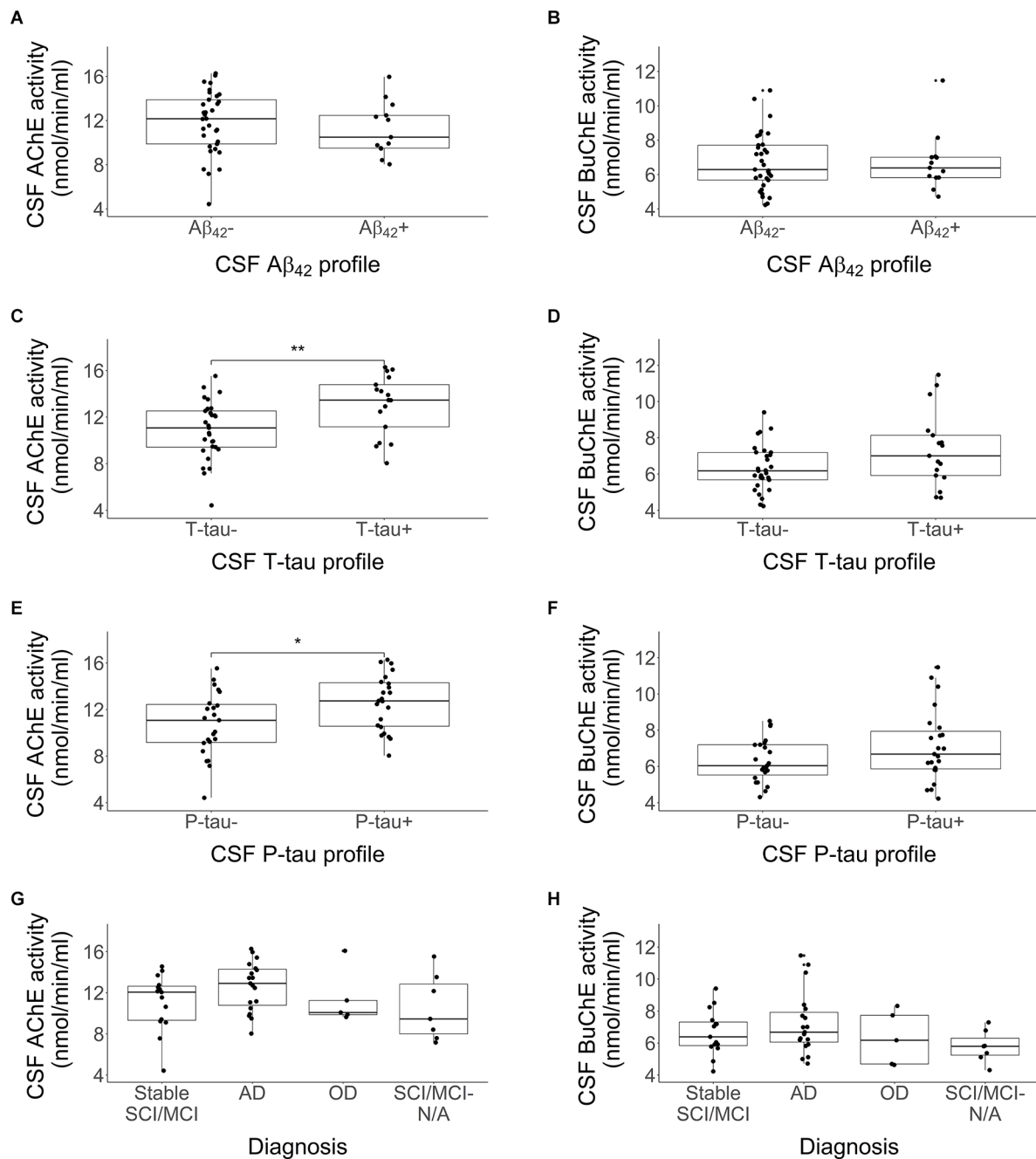


FIGURE 2 | Comparison in activity of CSF AChE and BuChE enzymes by CSF Aβ₄₂ profile (A,B), T-tau profile (C,D), P-tau profile (E,F), and clinical diagnosis (G,H), * $p < 0.05$, ** $p < 0.01$. Each profile was divided into two categories, abnormal (+) and normal (-) values. Abnormal values were defined as Aβ₄₂ < 375 pg/ml, T-tau > 445 pg/ml and P-tau > 61 pg/ml. The lower and upper horizontal lines of the boxplot correspond to the 25th centile and 75th centile and the middle line to the median. CSF AChE activity was significantly higher among subjects with a CSF T-tau+ or P-tau+ profiles compared to those without.

Education had the fourth highest frequency (38%). All other possible predictors had far lower selection frequency ($\leq 15\%$).

Association Between CSF Markers and Verbal Episodic Memory

CSF activity of AChE (Figure 6A) showed a weak, negative correlation with the composite z-score reflecting verbal episodic

memory ($r = -0.34$, $p = 0.02$), while BuChE (Figure 6B) did not reach significance ($r = -0.19$, $p = 0.21$). The analysis was based on 44 subjects as two subjects did not take the RAVLT test.

LASSO linear regression with a stability selection was also applied for identifying a set of variables (CSF markers and demographic variables) predicting verbal episodic memory composite score (Figure 7). Only age was selected

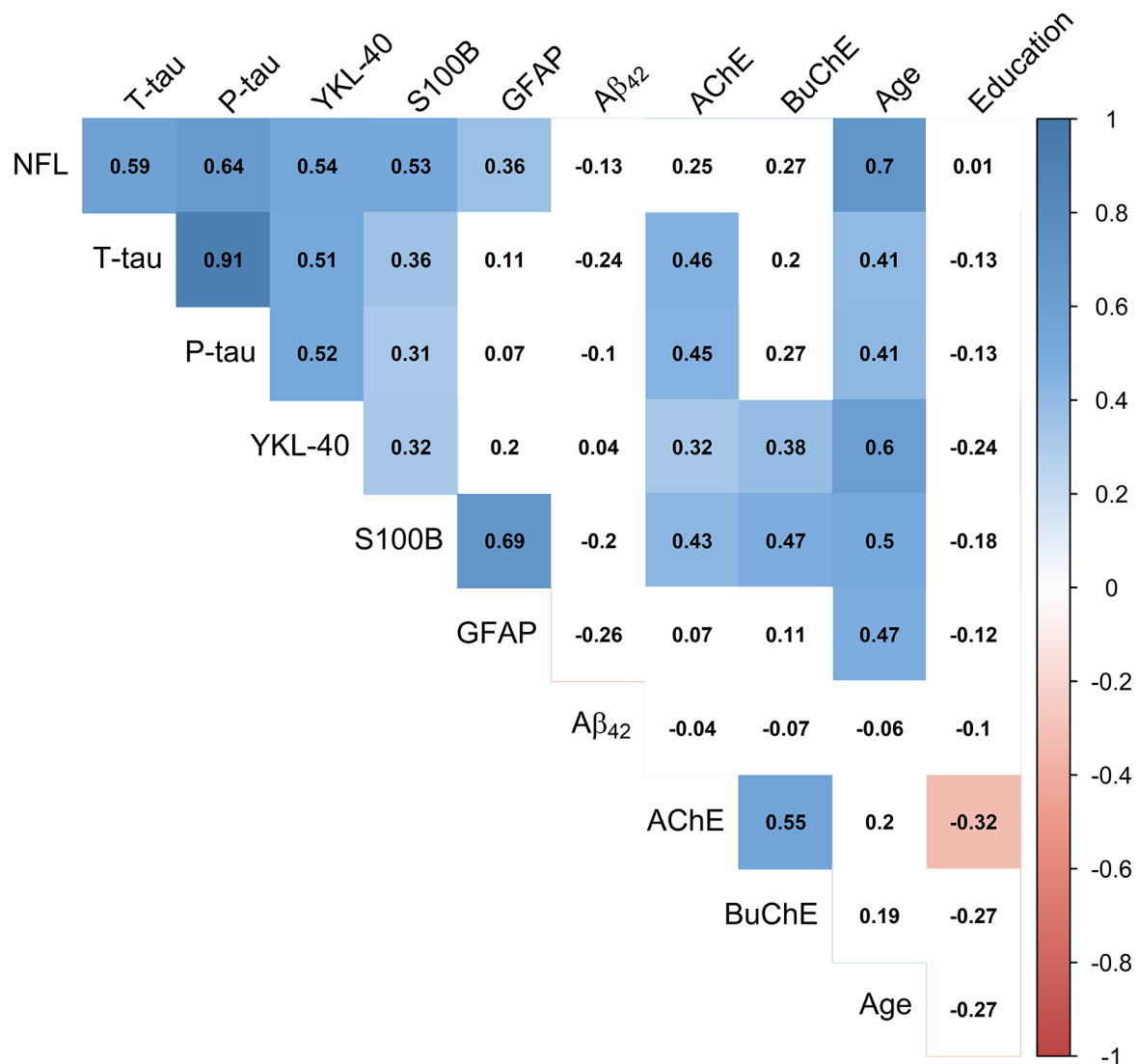


FIGURE 3 | Correlation matrix depicting Pearson's coefficients between CSF activity of cholinergic enzymes, CSF protein levels, age and education. Colored squares indicate statistical significance ($p < 0.05$). Blue and red colors present positive and negative coefficients, respectively. Values of CSF proteins (Aβ₄₂, T-tau, P-tau, NFL, YKL-40, S100B, and GFAP) were natural log-transformed.

as a reliable predictor, with a selection frequency of 91%. CSF markers NFL (61%) and P-tau (55%) both had a selection frequency above 50%. All other measurements had selection frequencies below 30%, including AChE (8%) and BuChE (0%).

DISCUSSION

We explored the association of cholinergic enzyme activity with CSF markers reflecting amyloidosis, neurodegeneration, neurofibrillary tangles and inflammation as well as with loss of verbal episodic memory among subjects in a memory clinic cohort. Our results indicated no difference in AChE and BuChE activity between individuals with abnormal and normal Aβ₄₂

levels. In contrast, individuals with abnormally high T-tau or P-tau levels had increased AChE activity compared to those with normal levels. Higher levels of inflammatory markers S100B and YKL-40 associated with higher activity of AChE and BuChE. Interestingly, S100B was also the most reliable predictor of both AChE and BuChE activity in comparison to other CSF markers and demographic measures. Weak association was detected between AChE activity and verbal episodic memory performance, although the enzyme did not prove to be a reliable predictor when other measures had also been accounted for. Overall, these results indicate a relationship between higher activity of the ACh-degrading cholinergic enzymes and increased inflammation, accumulation of neurofibrillary tangles and neurodegeneration in the stages of pre- and early symptomatic dementia, independent of CSF Aβ₄₂ levels.

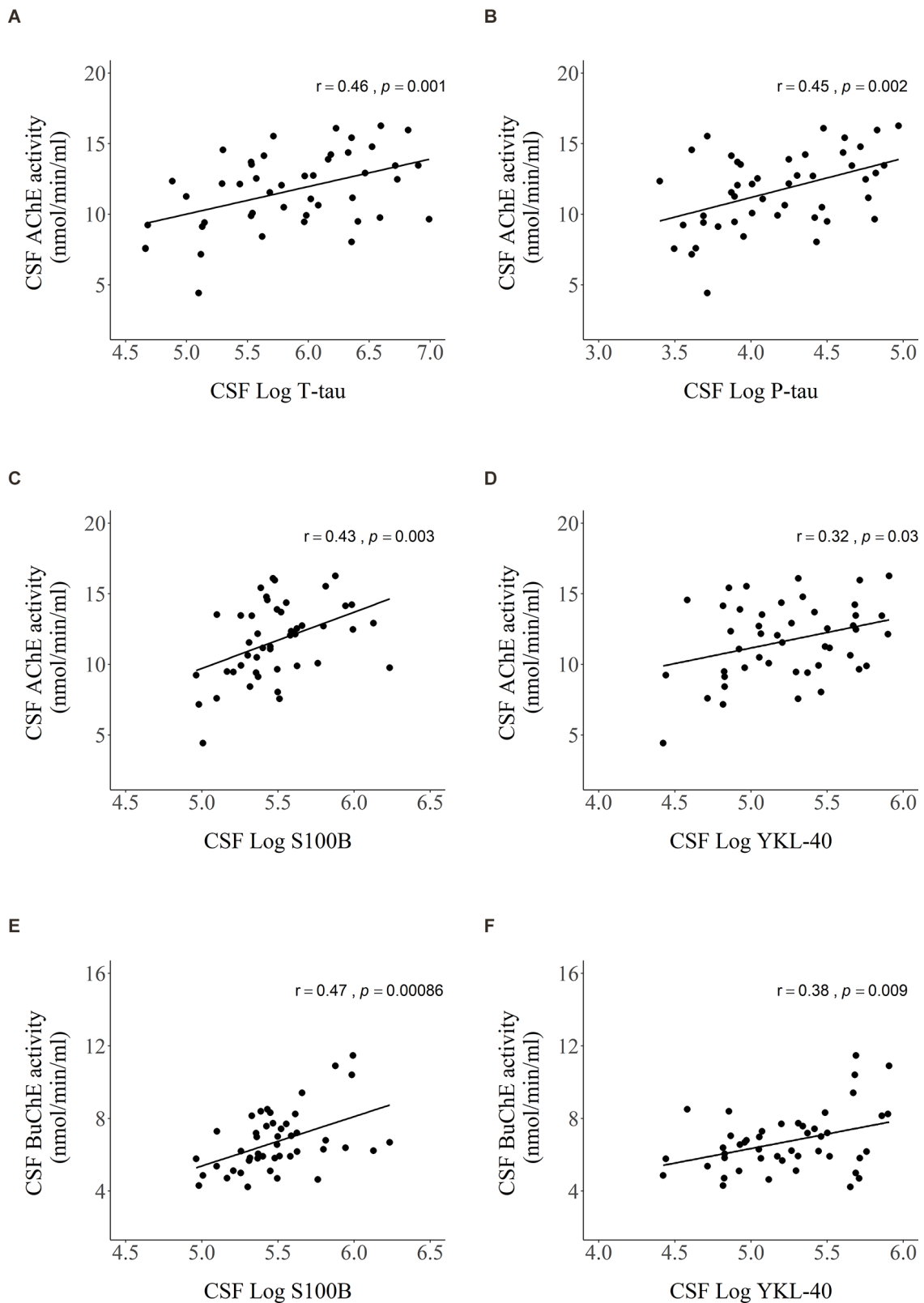
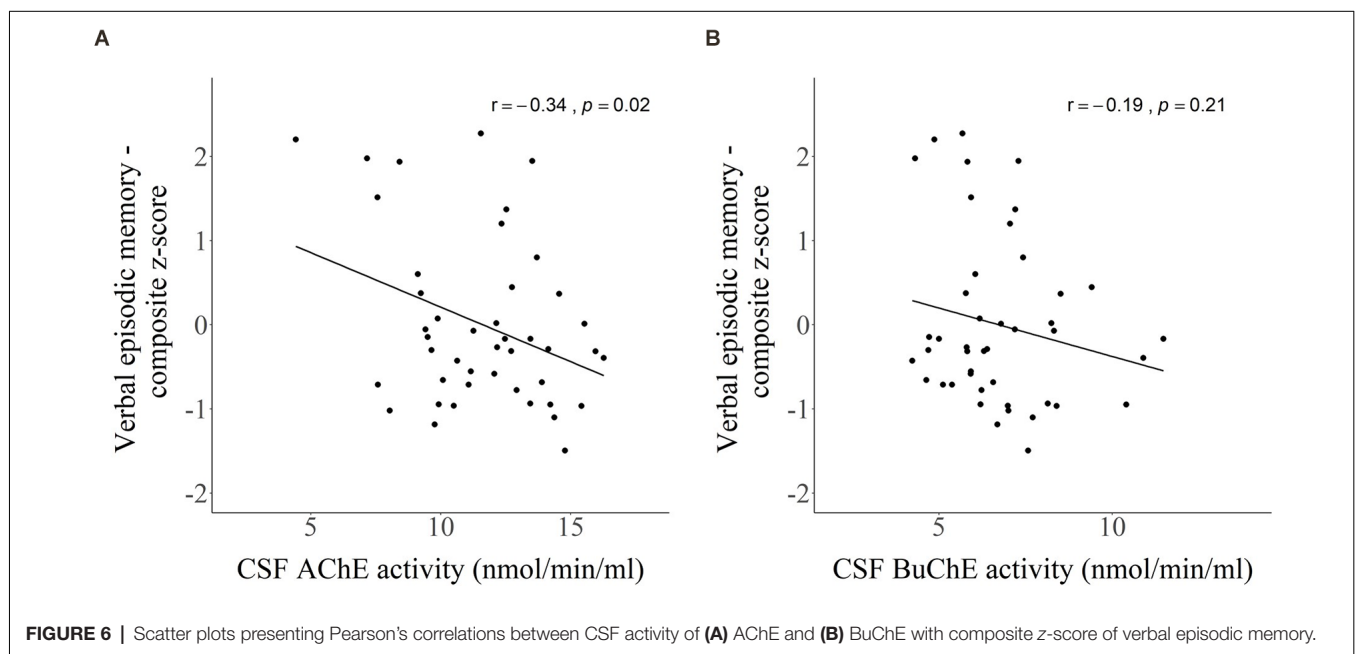
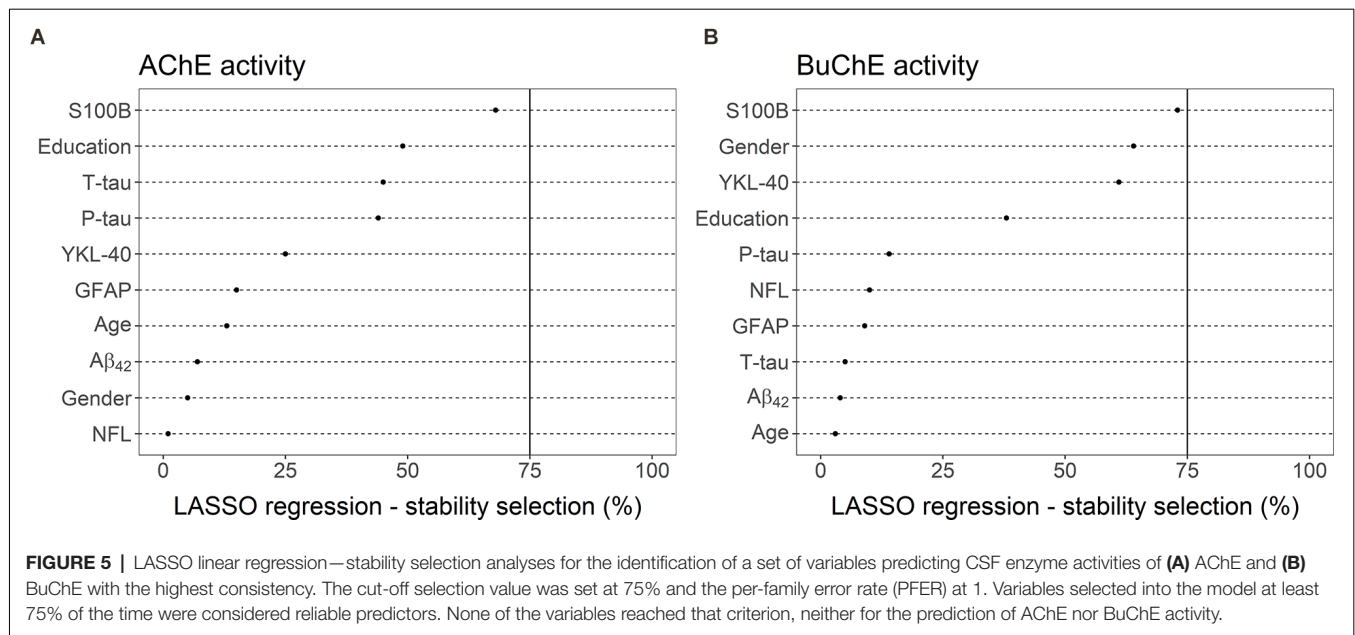
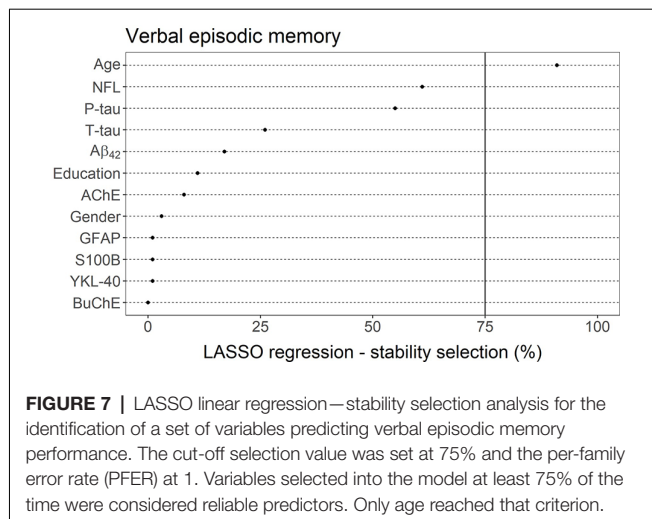


FIGURE 4 | Scatter plots presenting Pearson's correlations between AChE activity and levels of **(A)** T-tau, **(B)** P-tau, **(C)** S100B, **(D)** YKL-40, and BuChE activity and levels of **(E)** S100B and **(F)** YKL-40 in CSF. Values of CSF proteins (T-tau, P-tau, YKL-40, and S100B) were natural log-transformed.



The relationship between A β protein and cholinergic dysfunction has long been established through *in vitro* and post-mortem studies. AChE activity is consistently increased in regions around A β plaques and NFTs at all stages of the disease, although overall AChE activity decreases in the AD brain (Perry et al., 1980; Mesulam and Asuncion Morán, 1987; Ulrich et al., 1990). Studies have also reported about 40%–50% reduction in ACh synthesis in cultured cholinergic neurons upon exposure to a high nanomolar concentration of A β_{42} (Pedersen et al., 1996; Hoshi et al., 1997; Kar et al., 1998; Nunes-Tavares et al., 2012). More recent research indicate that A β peptides act directly as allosteric modulators of cholinergic signaling by

forming highly stable and soluble complexes with apolipoprotein E (ApoE) and cholinesterases (Darreh-Shori et al., 2011a,b; Vijayaraghavan et al., 2013; Kumar et al., 2016). A better understanding of the functional relationship between A β and the cholinergic system is though needed, as the biochemical environment *in vivo* is complex. Results regarding association between A β_{42} levels and AChE activity in CSF have, for example, been inconsistent (Darreh-Shori et al., 2006; García-Ayllón et al., 2008; Johansson et al., 2013). Darreh-Shori et al. (2006) did not detect a relationship between A β_{42} levels and AChE activity among patients with mild AD. Similarly, Johansson et al. (2013) did not detect an association between same measures among AD



patients. In contrast, García-Ayllón et al. (2008) did observe an association between Aβ₄₂ levels and AChE activity within same patient group. Johansson et al. (2013) also did find a positive relationship between the proteins, but only within the whole study population (AD, other dementias, stable MCI and healthy controls). Neither Darreh-Shori et al. (2006) nor Gabriel et al. (2017) detected relationship between BuChE activity and Aβ₄₂ levels among AD patients. Gabriel et al. (2017) did, however, detect a positive association among those patients carrying the ApoE-ε4 allele. In this current study, relationships between the activities of the cholinergic enzymes and Aβ₄₂ levels were not detected.

Previous post-mortem studies have shown that the loss of cortical cholinergic innervation is associated with, and potentially caused by, NFT in the nucleus basalis of Meynert (NBM) of the basal forebrain (Geula and Mesulam, 1995; Braak and Del Tredici, 2013; Mesulam, 2013), with degeneration already present at the very early stages of AD (Mesulam et al., 2004; Mufson et al., 2008). Silveyra et al. (2012) reported that P-tau could be an important regulator of AChE expression. Over-expression of P-tau in transgenic mice (Tg-VLW) led to an increase in the activity of AChE, suggesting that increase in AChE expression around NFTs could be a consequence of disturbed tau phosphorylation. Very few studies have, however, examined the relations between CSF tau levels and cholinesterase activity in CSF. Our study found a correlation between T-tau and P-tau with AChE activity. This is in accordance with a study by Johansson et al. (2013), where a positive association between T-tau and P-tau levels with AChE activity was detected in CSF among cases of AD, other dementias, stable MCI and healthy controls. We did not find a correlation between T-tau or P-tau levels and BuChE activity. The results are in line with results from a study by Gabriel et al. (2017), which did not find correlations between CSF T-tau and P-tau with BuChE activity among AD patients. One possible explanation for the difference in results between the enzymes in regard to the neurodegeneration markers, could be due to localization. BuChE activity is mainly localized to glial cells while AChE is predominantly located within neurons and axons

(Wright et al., 1993; Giacobini, 2003; Picciotto et al., 2012). Interestingly, we did not find a relationship between NFL, a marker of both neurodegeneration and white matter changes, and the activity of the cholinergic enzymes. NFL is considered a more general marker for neurodegeneration compared to T-tau, which has been associated with Aβ pathology (Mattsson et al., 2016). To the best of our knowledge, NFL has not been researched in regard to AChE and BuChE activity in CSF samples from a dementia cohort. A study by Aeinehband et al. (2015) among patients with multiple sclerosis (MS) found a positive correlation between NFL levels and BuChE activity, but not AChE activity.

The neurotransmitter ACh is not only restricted to neurons but can also act on regions distal from synaptic sites (Nizri et al., 2006). It has anti-inflammatory effects, inhibiting pro-inflammatory responses by acting on α7 nicotinic ACh receptors expressed on non-excitable cholinergic cells like astrocytes and microglia (Benfante et al., 2021). Extracellular ACh is therefore hypothesized to play a key role in homeostatic functions that include neuronal support, the maintenance of myelin, synaptic function and plasticity, Aβ clearance, and maintenance of the blood-brain barrier (Lane and He, 2013). Both AChE and BuChE enzymes play a major dynamic role in this homeostasis as they degrade ACh, with BuChE being specifically important for the function of glial cells as they serve as the enzyme's primary source and location (Lane and He, 2013). S100B and GFAP are two commonly used CSF markers of astroglial reactivity. A study by Darreh-Shori et al. (2013) found that BuChE activity positively associated with S100B and GFAP in CSF among AD patients. A possible explanation could be that lower levels of extracellular ACh associate with higher BuChE activity, enhancing the reactivity of glia. This heightened function can be protective, but prolonged glial activation may gradually lead to degeneration and eventually loss of neurons, further triggering inflammatory responses (Lane and Darreh-Shori, 2015). No relationship was detected between AChE activity and levels of S100B and GFAP in the same study. Our study found a positive relationship between S100B, and to lesser extent YKL-40, with activity of both enzymes. To the best of our knowledge, YKL-40 has not been explored before in association with cholinergic enzymes. YKL-40 is widely used as a glial activation marker, although the cellular source of expression in brain remains uncertain. A variable pattern of YKL-40 expression that includes astrocytes, microglia or, on rare occasions, neurons have been associated with AD in studies (Querol-Vilaseca et al., 2017). Interestingly, we did not find association between GFAP levels with either enzyme. Different patterns of association between the enzymes with different inflammatory markers could possibly be explained by different cellular functions. Both YKL-40 (Bonneh-Barkay et al., 2012) and S100B (Donato et al., 2009) have extracellular functions while GFAP (Yang and Wang, 2015) is an intracellular protein. Increased GFAP levels in CSF may therefore be a later event in the pathogenic cascade.

Although all ChEs enhance synaptic transmission, they exert their effects on cholinesterases differently. The drugs

donepezil and galantamine are reversible inhibitors of AChE while rivastigmine is a pseudo-irreversible inhibitor of both AChE and BuChE. The difference in pharmacological properties affects both the ability of breaking down extrasynaptic ACh as well as the expression of extracellular AChE (Nordberg et al., 2009; Darreh-Shori and Soininen, 2010; Marucci et al., 2021). Therefore, different ChEIs could alter glial-neuronal interactions in different ways (Lane and Darreh-Shori, 2015). A larger, longitudinal study might be able to detect the effect of each ChEI on CSF markers reflecting cholinergic activity, inflammation, and neurodegeneration. Measures of those markers, in combination with factors including age, gender, and genotype, could potentially be of use in predicting which patients could benefit from a treatment with a specific ChEI.

It is unclear to what extent episodic memory dysfunction relates to structural and functional changes in the cholinergic system at the symptomatic pre-dementia stages (SCI or MCI; Peter et al., 2016). The basal forebrain undergoes severe neurofibrillary degeneration and neuronal loss in patients with moderate to severe AD, most prominent in the NBM. In comparison, changes at the MCI stage are thought to be characterized by alterations in cholinergic functions rather than by cholinergic neuronal loss (Schliebs and Arendt, 2011). In accordance with this, histological studies have revealed that cognitive deficits are not evident before at least 30% of the basal forebrain cholinergic neurons have degenerated (Schliebs and Arendt, 2006) and individuals with MCI show only around 15% volume loss compared to healthy controls (Peter et al., 2016). Our results are in line with those findings as only a weak association was found between AChE activity and verbal episodic memory performance. When other factors (e.g., age) were simultaneously considered, neither of the cholinergic enzymes proved to be a good predictor for verbal episodic memory. Previous studies have revealed NFL to be a promising progression marker, associating with cognitive impairment in both AD and LBD (Zetterberg et al., 2016; Olsson et al., 2019). In our study, the cholinergic enzymes did not correlate with levels of NFL, emphasizing further the lack of contribution of the cholinergic system to episodic memory dysfunction at the very early stages of dementia.

This study has several limitations. First, the results need to be validated in a larger study due to the sample being relatively small. Second, the association between variables could also possibly be underestimated as no healthy controls were included in the sample. Third, no genetic data was available for this study. It would have been of importance to explore the associations between different measures by genotype, especially BChE. The BChE-K variant has been linked to increased risk of developing AD, although results have been conflicting. In addition, a reduction of the BuChE activity in CSF of AD patients carrying both the K variant and the ApoE-ε4 allele has previously been reported (Darreh-Shori et al., 2012; Jasiecki and Wasąg, 2019; Jasiecki et al., 2019). However, the influence of the BChE-K variant on the levels of Aβ₄₂, T-tau or P-tau in CSF is still unknown. Finally, a list of prescribed anticholinergic drugs was not available for the subjects of this

study. This class of drugs binds to ACh receptors and blocks ACh neurotransmission. Anticholinergic burden refers to their cumulative effect and has been linked to adverse effects such as decline in cognitive function (Salahudeen et al., 2015; Lozano-Ortega et al., 2020). Therefore, the study could have benefited from including an anticholinergic burden score in the statistical analyses.

Our findings suggest that the activity of ACh-degrading cholinergic enzymes at the pre- and early symptomatic stages of dementia relate to inflammatory and neurodegenerative processes, but not to loss in verbal episodic memory as measured in this study. A better understanding of the cholinergic system and its relations to both pathology and cognitive functions are critical, given that it is the main target of current symptomatic treatment of AD. Further studies are needed for validation of these results, preferably with larger samples and access to genotype information.

DATA AVAILABILITY STATEMENT

The raw data supporting the conclusions of this article will be made available by the authors, without undue reservation.

ETHICS STATEMENT

The studies involving human participants were reviewed and approved by the National Research Ethics Committee of Iceland (VSN-14-028). The study was conducted in accordance with the Helsinki Declaration latest revision of 2013. The patients/participants provided their written informed consent to participate in this study.

AUTHOR CONTRIBUTIONS

UT, TD-S, JS, and PP contributed to the conception and design of the study. UT and MJ contributed to the collection of data. UT wrote the first draft, performed the statistical analysis, and prepared figures and tables. SL provided guidance on statistical analysis. TD-S, SL, MJ, JS, and PP revised the manuscript. All authors contributed to the article and approved the submitted version.

FUNDING

This study was supported by the St. Josef's Hospital Fund, Reykjavik, Iceland, the Landspítali University Hospital Research Fund, and the Icelandic Research Fund of the Icelandic Centre for Research (163172-051).

ACKNOWLEDGMENTS

We thank all the subjects of The Icelandic MCI study for their participation. We also wish to thank Kristin H. Hannesdottir for managing participant administration and the staff of the LUH Memory Clinic.

REFERENCES

- Adem, A. (1992). Putative mechanisms of action of tacrine in Alzheimer's disease. *Acta Neurol. Scand. Suppl.* 139, 69–74. doi: 10.1111/j.1600-0404.1992.tb04458.x
- Aeinehband, S., Lindblom, R. P. F., Al Nimer, F., Vijayaraghavan, S., Sandholm, K., Khademi, M., et al. (2015). Complement component C3 and butyrylcholinesterase activity are associated with neurodegeneration and clinical disability in multiple sclerosis. *PLoS One* 10:e0122048. doi: 10.1371/journal.pone.0122048
- Ballinger, E. C., Ananth, M., Talmage, D. A., and Role, L. W. (2016). Basal forebrain cholinergic circuits and signaling in cognition and cognitive decline. *Neuron* 91, 1199–1218. doi: 10.1016/j.neuron.2016.09.006
- Benfante, R., Di Lascio, S., Cardani, S., and Fornasari, D. (2021). Acetylcholinesterase inhibitors targeting the cholinergic anti-inflammatory pathway: a new therapeutic perspective in aging-related disorders. *Aging Clin. Exp. Res.* 33, 823–834. doi: 10.1007/s40520-019-01359-4
- Bonneh-Barkay, D., Bissel, S. J., Kofler, J., Starkey, A., Wang, G., and Wiley, C. A. (2012). Astrocyte and macrophage regulation of YKL-40 expression and cellular response in neuroinflammation. *Brain Pathol.* 22, 530–546. doi: 10.1111/j.1750-3639.2011.00550.x
- Braak, H., and Del Tredici, K. (2013). Reply: the early pathological process in sporadic Alzheimer's disease. *Acta Neuropathol.* 126, 615–618. doi: 10.1007/s00401-013-1170-1
- Darreh-Shori, T., Brimijoin, S., Kadir, A., Almkvist, O., and Nordberg, A. (2006). Differential CSF butyrylcholinesterase levels in Alzheimer's disease patients with the ApoE epsilon4 allele, in relation to cognitive function and cerebral glucose metabolism. *Neurobiol. Dis.* 24, 326–333. doi: 10.1016/j.nbd.2006.07.013
- Darreh-Shori, T., Forsberg, A., Modiri, N., Andreassen, N., Blennow, K., Kamil, C., et al. (2011a). Differential levels of apolipoprotein E and butyrylcholinesterase show strong association with pathological signs of Alzheimer's disease in the brain *in vivo*. *Neurobiol. Aging* 32, 2320.e2315–2332. doi: 10.1016/j.neurobiolaging.2010.04.028
- Darreh-Shori, T., Modiri, N., Blennow, K., Baza, S., Kamil, C., Ahmed, H., et al. (2011b). The apolipoprotein E ϵ 4 allele plays pathological roles in AD through high protein expression and interaction with butyrylcholinesterase. *Neurobiol. Aging* 32, 1236–1248. doi: 10.1016/j.neurobiolaging.2009.07.015
- Darreh-Shori, T., Kadir, A., Almkvist, O., Grut, M., Wall, A., Blomquist, G., et al. (2008). Inhibition of acetylcholinesterase in CSF versus brain assessed by ^{11}C -PMP PET in AD patients treated with galantamine. *Neurobiol. Aging* 29, 168–184. doi: 10.1016/j.neurobiolaging.2006.09.020
- Darreh-Shori, T., Siawesh, M., Mousavi, M., Andreassen, N., and Nordberg, A. (2012). Apolipoprotein ϵ 4 modulates phenotype of butyrylcholinesterase in CSF of patients with Alzheimer's disease. *J. Alzheimers Dis.* 28, 443–458. doi: 10.3233/JAD-2011-111088
- Darreh-Shori, T., and Soininen, H. (2010). Effects of cholinesterase inhibitors on the activities and protein levels of cholinesterases in the cerebrospinal fluid of patients with Alzheimer's disease: a review of recent clinical studies. *Curr. Alzheimer Res.* 7, 67–73. doi: 10.2174/156720510790274455
- Darreh-Shori, T., Vijayaraghavan, S., Aeinehband, S., Pehl, F., Lindblom, R. P., Nilsson, B., et al. (2013). Functional variability in butyrylcholinesterase activity regulates intrathecal cytokine and astroglial biomarker profiles in patients with Alzheimer's disease. *Neurobiol. Aging* 34, 2465–2481. doi: 10.1016/j.neurobiolaging.2013.04.027
- Donato, R., Sorci, G., Riuizi, F., Arcuri, C., Bianchi, R., Brozzi, F., et al. (2009). S100B's double life: intracellular regulator and extracellular signal. *Biochim. Biophys. Acta* 1793, 1008–1022. doi: 10.1016/j.bbamer.2008.11.009
- Folstein, M. F., Folstein, S. E., and Mchugh, P. R. (1975). "Mini-mental state". A practical method for grading the cognitive state of patients for the clinician. *J. Psychiatr. Res.* 12, 189–198. doi: 10.1016/0022-3956(75)90026-6
- Gabriel, A. J., Almeida, M. R., Ribeiro, M. H., Durães, J., Tábuas-Pereira, M., Pinheiro, A. C., et al. (2017). Association between butyrylcholinesterase and cerebrospinal fluid biomarkers in Alzheimer's disease patients. *Neurosci. Lett.* 641, 101–106. doi: 10.1016/j.neulet.2017.01.036
- García-Ayllón, M. S., Riba-Llena, I., Serra-Basante, C., Alom, J., Boopathy, R., and Sáez-Valero, J. (2010). Altered levels of acetylcholinesterase in Alzheimer plasma. *PLoS One* 5:e8701. doi: 10.1016/j.onehlt.2021.100325
- García-Ayllón, M. S., Silveyra, M. X., and Sáez-Valero, J. (2008). Association between acetylcholinesterase and beta-amyloid peptide in Alzheimer's cerebrospinal fluid. *Chem. Biol. Interact.* 175, 209–215. doi: 10.1016/j.cbi.2008.04.047
- Geula, C., and Mesulam, M. M. (1995). Cholinesterases and the pathology of Alzheimer disease. *Alzheimer Dis. Assoc. Disord.* 9, 23–28. doi: 10.1097/00002093-199501002-00005
- Giacobini, E. (2003). Cholinesterases: new roles in brain function and in Alzheimer's disease. *Neurochem. Res.* 28, 515–522. doi: 10.1023/a:1022869222652
- Giacobini, E., Cuello, A. C., and Fisher, A. (2022). Reimagining cholinergic therapy for Alzheimer's disease. *Brain*. doi: 10.1093/brain/awac096. [Online ahead of print].
- Hampel, H., Mesulam, M. M., Cuello, A. C., Farlow, M. R., Giacobini, E., Grossberg, G. T., et al. (2018). The cholinergic system in the pathophysiology and treatment of Alzheimer's disease. *Brain* 141, 1917–1933. doi: 10.1093/brain/awy132
- Hofner, B., Boccuto, L., and Göker, M. (2015). Controlling false discoveries in high-dimensional situations: boosting with stability selection. *BMC Bioinform.* 16:144. doi: 10.1186/s12859-015-0575-3
- Hoshi, M., Takashima, A., Murayama, M., Yasutake, K., Yoshida, N., Ishiguro, K., et al. (1997). Nontoxic amyloid beta peptide 1–42 suppresses acetylcholine synthesis. Possible role in cholinergic dysfunction in Alzheimer's disease. *J. Biol. Chem.* 272, 2038–2041. doi: 10.1074/jbc.272.4.2038
- Jack, C. R., Jr., Bennett, D. A., Blennow, K., Carrillo, M. C., Dunn, B., Haeberlein, S. B., et al. (2018). NIA-AA research framework: toward a biological definition of Alzheimer's disease. *Alzheimers Dement.* 14, 535–562. doi: 10.1016/j.jalz.2018.02.018
- Jasiecki, J., Limon-Sztencel, A., Zuk, M., Chmara, M., Cysewski, D., Limon, J., et al. (2019). Synergy between the alteration in the N-terminal region of butyrylcholinesterase K variant and apolipoprotein E4 in late-onset Alzheimer's disease. *Sci. Rep.* 9:5223. doi: 10.1038/s41598-019-41578-3
- Jasiecki, J., and Wasąg, B. (2019). Butyrylcholinesterase protein ends in the pathogenesis of Alzheimer's disease—could BCHE genotyping be helpful in Alzheimer's therapy? *Biomolecules* 9:592. doi: 10.3390/biom9100592
- Johansson, P., Almqvist, E. G., Johansson, J. O., Mattsson, N., Andreasson, U., Hansson, O., et al. (2013). Cerebrospinal fluid (CSF) 25-hydroxyvitamin D concentration and CSF acetylcholinesterase activity are reduced in patients with Alzheimer's disease. *PLoS One* 8:e81989. doi: 10.1371/journal.pone.0081989
- Jorm, A. F. (1994). A short form of the informant questionnaire on cognitive decline in the elderly (IQCODE): development and cross-validation. *Psychol. Med.* 24, 145–153. doi: 10.1017/s003329170002691x
- Kar, S., Issa, A. M., Seto, D., Auld, D. S., Collier, B., and Quirion, R. (1998). Amyloid beta-peptide inhibits high-affinity choline uptake and acetylcholine release in rat hippocampal slices. *J. Neurochem.* 70, 2179–2187. doi: 10.1046/j.1471-4159.1998.70052179.x
- Kumar, R., Nordberg, A., and Darreh-Shori, T. (2016). Amyloid- β peptides act as allosteric modulators of cholinergic signalling through formation of soluble BA β ACs. *Brain* 139, 174–192. doi: 10.1093/brain/awv318
- Lane, R. M., and Darreh-Shori, T. (2015). Understanding the beneficial and detrimental effects of donepezil and rivastigmine to improve their therapeutic value. *J. Alzheimers Dis.* 44, 1039–1062. doi: 10.3233/JAD-142268
- Lane, R. M., and He, Y. (2013). Butyrylcholinesterase genotype and gender influence Alzheimer's disease phenotype. *Alzheimers Dement.* 9, e17–e73. doi: 10.1016/j.jalz.2010.12.005
- Lezak, M. D., Howieson, D. B., Bigler, E. D., and Tranel, D. (2012). *Neuropsychological Assessment*. New York: Oxford University Press.
- Lozano-Ortega, G., Johnston, K. M., Cheung, A., Wagg, A., Campbell, N. L., Dmochowski, R. R., et al. (2020). A review of published anticholinergic scales and measures and their applicability in database analyses. *Arch. Gerontol. Geriatr.* 87:103885. doi: 10.1016/j.archger.2019.05.010
- Malmsten, L., Vijayaraghavan, S., Hovatta, O., Marutle, A., and Darreh-Shori, T. (2014). Fibrillar β -amyloid 1–42 alters cytokine secretion, cholinergic signalling and neuronal differentiation. *J. Cell. Mol. Med.* 18, 1874–1888. doi: 10.1111/jcmm.12343

- Marucci, G., Buccioni, M., Ben, D. D., Lambertucci, C., Volpini, R., and Amenta, F. (2021). Efficacy of acetylcholinesterase inhibitors in Alzheimer's disease. *Neuropharmacology* 190:108352. doi: 10.1016/j.neuropharm.2020.108352
- Mattsson, N., Insel, P. S., Palmqvist, S., Portelius, E., Zetterberg, H., Weiner, M., et al. (2016). Cerebrospinal fluid tau, neurogranin and neurofilament light in Alzheimer's disease. *EMBO Mol. Med.* 8, 1184–1196. doi: 10.15252/emmm.201606540
- McKeith, I. G., Boeve, B. F., Dickson, D. W., Halliday, G., Taylor, J. P., Weintraub, D., et al. (2017). Diagnosis and management of dementia with Lewy bodies: fourth consensus report of the DLB consortium. *Neurology* 89, 88–100. doi: 10.1212/WNL.0000000000004058
- Mckhann, G. M., Knopman, D. S., Chertkow, H., Hyman, B. T., Jack, C. R., Jr., Kawas, C. H., et al. (2011). The diagnosis of dementia due to Alzheimer's disease: recommendations from the National Institute on Aging-Alzheimer's association workgroups on diagnostic guidelines for Alzheimer's disease. *Alzheimers Dement.* 7, 263–269. doi: 10.1016/j.jalz.2011.03.005
- Meinshausen, N., and Bühlmann, P. (2010). Stability selection. *J. R. Stat. Soc. Series B* 72, 417–473. doi: 10.1111/j.1467-9868.2010.00740.x
- Mesulam, M. M. (2013). Cholinergic circuitry of the human nucleus basalis and its fate in Alzheimer's disease. *J. Comp. Neurol.* 521, 4124–4144. doi: 10.1002/cne.23415
- Mesulam, M. M., and Asuncion Morán, M. (1987). Cholinesterases within neurofibrillary tangles related to age and Alzheimer's disease. *Ann. Neurol.* 22, 223–228. doi: 10.1002/ana.410220206
- Mesulam, M., Guillozet, A., Shaw, P., and Quinn, B. (2002). Widely spread butyrylcholinesterase can hydrolyze acetylcholine in the normal and Alzheimer brain. *Neurobiol. Dis.* 9, 88–93. doi: 10.1006/nbdi.2001.0462
- Mesulam, M., Shaw, P., Mash, D., and Weintraub, S. (2004). Cholinergic nucleus basalis tauopathy emerges early in the aging-MCI-AD continuum. *Ann. Neurol.* 55, 815–828. doi: 10.1002/ana.20100
- Mufson, E. J., Counts, S. E., Perez, S. E., and Ginsberg, S. D. (2008). Cholinergic system during the progression of Alzheimer's disease: therapeutic implications. *Exp. Rev. Neurother.* 8, 1703–1718. doi: 10.1586/14737175.8.11.1703
- Mufson, E. J., Ginsberg, S. D., Ikonomic, M. D., and Dekosky, S. T. (2003). Human cholinergic basal forebrain: chemoanatomy and neurologic dysfunction. *J. Chem. Neuroanat.* 26, 233–242. doi: 10.1016/s0891-0618(03)00068-1
- Nizri, E., Hamra-Amitay, Y., Sicsic, C., Lavon, I., and Brenner, T. (2006). Anti-inflammatory properties of cholinergic up-regulation: a new role for acetylcholinesterase inhibitors. *Neuropharmacology* 50, 540–547. doi: 10.1016/j.neuropharm.2005.10.013
- Nordberg, A., Darreh-Shori, T., Peskind, E., Soininen, H., Mousavi, M., Eagle, G., et al. (2009). Different cholinesterase inhibitor effects on CSF cholinesterases in Alzheimer patients. *Curr. Alzheimer Res.* 6, 4–14. doi: 10.2174/156720509787313961
- Nunes-Tavares, N., Santos, L. E., Stutz, B., Brito-Moreira, J., Klein, W. L., Ferreira, S. T., et al. (2012). Inhibition of choline acetyltransferase as a mechanism for cholinergic dysfunction induced by amyloid- β peptide oligomers. *J. Biol. Chem.* 287, 19377–19385. doi: 10.1074/jbc.M111.321448
- Olsson, B., Portelius, E., Cullen, N. C., Sandelius, Å., Zetterberg, H., Andreasson, U., et al. (2019). Association of cerebrospinal fluid neurofilament light protein levels with cognition in patients with dementia, motor neuron disease and movement disorders. *JAMA Neurol.* 76, 318–325. doi: 10.1001/jamaneurol.2018.3746
- Pavlov, V. A., Parrish, W. R., Rosas-Ballina, M., Ochani, M., Puerta, M., Ochani, K., et al. (2009). Brain acetylcholinesterase activity controls systemic cytokine levels through the cholinergic anti-inflammatory pathway. *Brain Behav. Immun.* 23, 41–45. doi: 10.1016/j.bbi.2008.06.011
- Pedersen, W. A., Kloczewiak, M. A., and Blusztajn, J. K. (1996). Amyloid beta-protein reduces acetylcholine synthesis in a cell line derived from cholinergic neurons of the basal forebrain. *Proc. Natl. Acad. Sci. U S A* 93, 8068–8071. doi: 10.1073/pnas.93.15.8068
- Perry, R. H., Blessed, G., Perry, E. K., and Tomlinson, B. E. (1980). Histochemical observations on cholinesterase activities in the brains of elderly normal and demented (Alzheimer-type) patients. *Age Ageing* 9, 9–16. doi: 10.1093/ageing/9.1.9
- Peter, J., Lahr, J., Minkova, L., Lauer, E., Grothe, M. J., Teipel, S., et al. (2016). Contribution of the cholinergic system to verbal memory performance in mild cognitive impairment. *J. Alzheimers Dis.* 53, 991–1001. doi: 10.3233/JAD-160273
- Picciotto, M. R., Higley, M. J., and Mineur, Y. S. (2012). Acetylcholine as a neuromodulator: cholinergic signaling shapes nervous system function and behavior. *Neuron* 76, 116–129. doi: 10.1016/j.neuron.2012.08.036
- Querol-Vilaseca, M., Colom-Cadena, M., Peguerols, J., San Martín-Paniello, C., Clarimon, J., Belbin, O., et al. (2017). YKL-40 (Chitinase 3-like I) is expressed in a subset of astrocytes in Alzheimer's disease and other tauopathies. *J. Neuroinflammation* 14:118. doi: 10.1186/s12974-017-0893-7
- Revathikumar, P., Bergqvist, F., Gopalakrishnan, S., Korotkova, M., Jakobsson, P. J., Lampa, J., et al. (2016). Immunomodulatory effects of nicotine on interleukin 1 β activated human astrocytes and the role of cyclooxygenase 2 in the underlying mechanism. *J. Neuroinflammation* 13:256. doi: 10.1186/s12974-016-0725-1
- Salahudeen, M. S., Duffull, S. B., and Nishtala, P. S. (2015). Anticholinergic burden quantified by anticholinergic risk scales and adverse outcomes in older people: a systematic review. *BMC Geriatr.* 15:31. doi: 10.1186/s12877-015-0029-9
- Schliebs, R., and Arendt, T. (2006). The significance of the cholinergic system in the brain during aging and in Alzheimer's disease. *J. Neural Transm. (Vienna)* 113, 1625–1644. doi: 10.1007/s00702-006-0579-2
- Schliebs, R., and Arendt, T. (2011). The cholinergic system in aging and neuronal degeneration. *Behav. Brain Res.* 221, 555–563. doi: 10.1016/j.bbr.2010.11.058
- Silveyra, M. X., García-Ayllón, M. S., De Barreda, E. G., Small, D. H., Martínez, S., Avila, J., et al. (2012). Altered expression of brain acetylcholinesterase in FTDP-17 human tau transgenic mice. *Neurobiol. Aging* 33, 624.e623–634. doi: 10.1016/j.neurobiolaging.2011.03.006
- Teitsdottir, U. D., Halldorsson, S., Rolfsson, O., Lund, S. H., Jonsdottir, M. K., Snaedal, J., et al. (2021). Cerebrospinal fluid C18 ceramide associates with markers of Alzheimer's disease and inflammation at the pre- and early stages of dementia. *J. Alzheimers Dis.* 81, 231–244. doi: 10.3233/JAD-200964
- Teitsdottir, U. D., Jonsdottir, M. K., Lund, S. H., Darreh-Shori, T., Snaedal, J., and Petersen, P. H. (2020). Association of glial and neuronal degeneration markers with Alzheimer's disease cerebrospinal fluid profile and cognitive functions. *Alzheimers Res. Ther.* 12:92. doi: 10.1186/s13195-020-00657-8
- Tibshirani, R. (1996). Regression shrinkage and selection via the lasso. *J. R. Stat. Soc. Series B* 58, 267–288. doi: 10.1111/j.2517-6161.1996.tb02080.x
- Ulrich, J., Meier-Ruge, W., Probst, A., Meier, E., and Ipsen, S. (1990). Senile plaques: staining for acetylcholinesterase and A4 protein: a comparative study in the hippocampus and entorhinal cortex. *Acta Neuropathol.* 80, 624–628. doi: 10.1007/BF00307630
- Van Westerloo, D. J., Giebelen, I. A., Florquin, S., Daalhuisen, J., Bruno, M. J., De Vos, A. F., et al. (2005). The cholinergic anti-inflammatory pathway regulates the host response during septic peritonitis. *J. Infect. Dis.* 191, 2138–2148. doi: 10.1086/430323
- Vijayaraghavan, S., Karami, A., Aeinehband, S., Behbahani, H., Grandien, A., Nilsson, B., et al. (2013). Regulated extracellular choline acetyltransferase activity- the plausible missing link of the distant action of acetylcholine in the cholinergic anti-inflammatory pathway. *PLoS One* 8:e65936. doi: 10.1371/journal.pone.0065936
- Wechsler, D. (1987). *WMS-R : Wechsler Memory Scale--Revised: Manual*. San Antonio, CA: Psychological Corp: Harcourt Brace Jovanovich.
- Winblad, B., Palmer, K., Kivipelto, M., Jelic, V., Fratiglioni, L., Wahlund, L. O., et al. (2004). Mild cognitive impairment--beyond controversies, towards a consensus: report of the international working group on mild cognitive impairment. *J. Intern. Med.* 256, 240–246. doi: 10.1111/j.1365-2796.2004.01380.x
- Wright, C. I., Geula, C., and Mesulam, M. M. (1993). Neurological cholinesterases in the normal brain and in Alzheimer's disease: relationship to plaques, tangles and patterns of selective vulnerability. *Ann. Neurol.* 34, 373–384. doi: 10.1002/ana.410340312
- Yang, Z., and Wang, K. K. (2015). Glial fibrillary acidic protein: from intermediate filament assembly and gliosis to neurobiomarker. *Trends Neurosci.* 38, 364–374. doi: 10.1016/j.tins.2015.04.003

Zetterberg, H., Skillbäck, T., Mattsson, N., Trojanowski, J. Q., Portelius, E., Shaw, L. M., et al. (2016). Association of cerebrospinal fluid neurofilament light concentration with Alzheimer disease progression. *JAMA Neurol.* 73, 60–67. doi: 10.1001/jamaneurol.2015.3037

Conflict of Interest: SL is employed by deCODE genetics/Amgen, Inc.

The remaining authors declare that the research was conducted in the absence of any commercial or financial relationships that could be construed as a potential conflict of interest.

The reviewer ER-V declared a shared affiliation with the author TD-S to the handling editor at the time of review.

Publisher's Note: All claims expressed in this article are solely those of the authors and do not necessarily represent those of their affiliated organizations, or those of the publisher, the editors and the reviewers. Any product that may be evaluated in this article, or claim that may be made by its manufacturer, is not guaranteed or endorsed by the publisher.

Copyright © 2022 Teitsdottir, Darreh-Shori, Lund, Jonsdottir, Snaedal and Petersen. This is an open-access article distributed under the terms of the Creative Commons Attribution License (CC BY). The use, distribution or reproduction in other forums is permitted, provided the original author(s) and the copyright owner(s) are credited and that the original publication in this journal is cited, in accordance with accepted academic practice. No use, distribution or reproduction is permitted which does not comply with these terms.



The Effects of Brain Magnetic Resonance Imaging Indices in the Association of Olfactory Identification and Cognition in Chinese Older Adults

Ziyi Tan^{1,2†}, Yingzhe Wang^{1,2†}, Heyang Lu³, Weizhong Tian⁴, Kelin Xu^{2,5}, Min Fan⁶, Xiaolan Zhao⁷, Li Jin^{1,2}, Mei Cui^{2,3}, Yanfeng Jiang^{1,2,8*} and Xingdong Chen^{1,2,3,9*}

¹ State Key Laboratory of Genetic Engineering, Zhangjiang Fudan International Innovation Center, School of Life Sciences, Human Phenome Institute, Fudan University, Shanghai, China, ² Fudan University Taizhou Institute of Health Sciences, Taizhou, China, ³ Department of Neurology, Huashan Hospital, Fudan University, Shanghai, China, ⁴ Department of Medical Imaging, Taizhou People's Hospital Affiliated to Nantong University, Taizhou, China, ⁵ The Key Laboratory of Public Health Safety of Ministry of Education, Department of Biostatistics, School of Public Health, Fudan University, Shanghai, China, ⁶ Taixing Disease Control and Prevention Center, Taizhou, China, ⁷ Taizhou Disease Control and Prevention Center, Taizhou, China, ⁸ International Human Phenome Institute (Shanghai), Shanghai, China, ⁹ Yiwu Research Institute of Fudan University, Yiwu, China

OPEN ACCESS

Edited by:

Allison B. Reiss,
New York University, United States

Reviewed by:

Kai Wang,
Anhui Medical University, China
Xiaoliu Liang,
Fudan University, China
Qing Shen,
Karolinska Institutet (KI), Sweden

*Correspondence:

Yanfeng Jiang
yanfengjiang@fudan.edu.cn
Xingdong Chen
xingdongchen@fudan.edu.cn

[†] These authors have contributed
equally to this work and share first
authorship

Specialty section:

This article was submitted to
Alzheimer's Disease and Related
Dementias,
a section of the journal
Frontiers in Aging Neuroscience

Received: 10 February 2022

Accepted: 15 June 2022

Published: 05 July 2022

Citation:

Tan Z, Wang Y, Lu H, Tian W,
Xu K, Fan M, Zhao X, Jin L, Cui M,
Jiang Y and Chen X (2022) The
Effects of Brain Magnetic Resonance
Imaging Indices in the Association
of Olfactory Identification and
Cognition in Chinese Older Adults.
Front. Aging Neurosci. 14:873032.
doi: 10.3389/fnagi.2022.873032

Background: Olfactory identification dysfunction frequently occurs in individuals with cognitive decline; however, a pathological mechanism linking the two has not been discovered. We aimed to study the association between olfactory identification and cognitive function, and determine the effects of brain regions atrophy therein.

Methods: A total of 645 individuals (57.5% were female) from the Taizhou Imaging Study, who underwent cognitive and olfactory identification measurements, were included. A subsample of participants underwent brain magnetic resonance imaging ($n = 622$). Cognition was assessed with a neuropsychological battery. Olfactory identification was measured using a 12-item Sniffin' Sticks test. Beta and logistic regressions were used to elucidate the association between olfactory identification and cognition, and the effects of brain regions atrophy in this association.

Results: Dementia was diagnosed in 41 (6.4%) individuals (mean age = 64.8 years), and mild cognitive impairment (MCI) in 157 (24.3%) individuals (mean age = 64.4 years). Olfactory identification was associated with MMSE and MoCA (both $P < 0.001$) and specific cognitive domains (memory, executive function, visuospatial function, and language; all $P < 0.05$). Higher olfactory identification was associated with lower likelihood of MCI and dementia ($P < 0.05$). The amygdala volume was significantly related to olfactory identification, MMSE, MoCA, and language, and could attenuate the association between olfactory identification and cognitive function.

Conclusion: The association between olfactory identification and cognition can be partly attributable to differences in amygdala volume, suggesting that the amygdala could be a shared neural substrate that links olfactory identification and cognitive function. Limitations of this study include that all these results were based on a cross-sectional study.

Keywords: olfactory identification, cognitive function, dementia, mild cognitive impairment, brain atrophy

INTRODUCTION

Dementia is being a great challenge for health and social care in China. It occurs mainly in residents older than 65 years and the prevalence increases with age (Jia et al., 2020). Nowadays, disease-modifying treatment is still not available, however, it is possible to predict the progression of dementia with biomarkers (Livingston et al., 2017). Olfactory identification is associated with cognitive function, including global and domain-specific cognitive function (Liang et al., 2016; Vassilaki et al., 2017; Dahmani et al., 2018; Palta et al., 2018; Yahiaoui-Doktor et al., 2019). Olfactory identification dysfunction is frequently observed in populations with cognitive decline and cognitive dysfunction (Devanand, 2016; Fullard et al., 2016; Roberts et al., 2016; Roalf et al., 2017; Walker et al., 2021). For example, it was reported previously that olfactory identification dysfunction appears in early Alzheimer's disease (AD) stages and shows accelerated progression over the course of dementia (Serby et al., 1991; Djordjevic et al., 2008). Thus, olfactory identification is considered a non-invasive marker for identifying preclinical stages of mild cognitive impairment (MCI) or dementia and predicting disease progression (Devanand et al., 2015; Vassilaki et al., 2017). However, the mechanisms that explain the association between olfactory identification and cognitive dysfunction remain unclear and the pathway underlying requires more investigation.

Disruption of brain structure is associated with cognitive decline and dementia in elderly adults (Apostolova et al., 2010; Wang et al., 2018). Atrophy of brain regions like hippocampus and amygdala is associated with diminished performance in olfactory function test both in healthy individuals and those with dementia (Smitka et al., 2012; Lian et al., 2019). Brain atrophy occurred in people with olfactory dysfunction and people with cognitive dysfunction (Dintica et al., 2019). In dementia population, the hippocampus and amygdala are smaller in those with olfactory dysfunction than those with normal olfactory function, suggesting that hippocampus and amygdala atrophy may be shared by olfactory function and cognitive function changes (Lian et al., 2019). It seems that brain atrophy both correlates with these two clinical manifestations. Therefore, exploring the effects of brain structure in the association of olfactory identification and cognition may help to understand the underlying mechanisms. However, till now, how the structural damage of brain regions relate to cognitive dysfunction in olfactory dysfunctions has remained to be studied. Thus, we hypothesized that impaired olfactory identification is associated with cognitive dysfunction, and such association might be partly attributable to brain atrophy. In this study, we aimed to replicate previous findings on the associations between olfactory identification and cognitive function, including scores of global and domain-specific cognitive function, as well as cognitive dysfunction (MCI and dementia); elucidate the associations between olfactory identification, cognitive function, and brain magnetic resonance imaging (MRI) indices; and determine whether differences in brain MRI indices might explain the association between olfactory identification and cognitive function, by using data from a community-based study of rural Chinese older adults.

MATERIALS AND METHODS

Study Design and Participants

Participants in this study were chosen from the Taizhou Imaging Study (TIS), an ongoing well-characterized community-based neuroimaging cohort nested in the Taizhou Longitudinal Study (TZL) that aims to monitor the risk factors and progression of dementia and cerebrovascular disease in a rural Chinese population. The study design of TIS has been described previously (Jiang et al., 2021). Briefly, 904 individuals aged 55–65 years without a history of physician-diagnosed stroke, dementia, cancer, and other severe diseases were enrolled and received baseline examinations including epidemiological questionnaire survey, physical and clinical examination (e.g., multimodal brain MRI), and neuropsychological and olfactory identification assessment from 2013 to 2018. In annual cognitive follow-ups, the TIS conducted more comprehensive cognitive function assessments, and olfactory identification tests (Jiang et al., 2021). In the present study, we performed a cross-sectional analysis using data from the first round of follow-ups of the TIS. As shown in **Supplementary Figure 1**, 904 individuals were included in TIS at baseline. After the exclusion of individuals without taking olfaction or cognitive function test due to various reasons, including death, refusal, not able to cooperate, etc. ($N = 219$) and data missing ($N = 2$), 683 individuals left. Among them, two individuals had history of nasal surgery, 12 individuals had nasal disease, one individual got cold and 22 individuals had unqualified data due to poor cooperation, leaving 645 individuals (622 individuals had MRI data) with full of cognition assessment and involved in final analysis. The TIS was approved by the Ethics Committee of the School of Life Sciences, Fudan University, and Fudan University Taizhou Institute of Health Sciences (institutional review board approval number: 496 and B017, respectively). Written informed consent was obtained from each participant before data and biospecimen collection.

Neuropsychological Measurements and Diagnosis of Mild Cognitive Impairment and Dementia

A neuropsychological test battery was used to assess participants' cognitive function, as described previously (Jiang et al., 2021). Briefly, several neuropsychological tests generated from developed countries, which covered global cognition, memory, executive function and attention, visuospatial function, and language, were adapted, normalized, and validated to suit Chinese culture (Jiang et al., 2021). The neuropsychological tests used in this study have been validated in Chinese population and normative data has been published previously (Ding et al., 2015). The test battery included (1) Mini-Mental State Examination (MMSE); (2) Beijing version Montreal Cognitive Assessment (MoCA); (3) Chinese version of Auditory Verbal Learning Test (AVLT); (4) Modified Fuld Object Memory Evaluation (FOME); (5) Clock Drawing Test (CDT); (6) Conflicting Instructions Task (Go/No Go task); (7) Trail-Making Test A & B; and (8) Animal Fluency Test (AFT). According to the education levels of the participants, two versions of tests were assessed separately: (1) to (3) and (5)–(8) were used for participants with ≥ 6

years of formal education (participants who completed primary education), while (1), (2), and (4)–(8) were used for participants with <6 years of education (Cui et al., 2020; Jiang et al., 2021). Among them, The Auditory Verbal Learning Test was adapted from California Verbal Learning Test and The Modified Fuld Object Memory Evaluation was adapted from the Fuld Object Memory Evaluation (Ding et al., 2015). All the assessments were conducted by neurologists, neuropsychologists, and trained technicians with over 3 years' experience independently. Dementia and MCI were diagnosed by a committee consisting of expert neurologists and neuropsychologists, according to the Diagnostic and Statistical Manual of Mental Disorders, 4th edition (DSM-IV) (Blashfield et al., 2014) and Petersen RC's criteria (Petersen, 2004), respectively, depending on each participant's cognitive measurements, clinical manifestations, and specific neuroimaging features (Ding et al., 2015; Cui et al., 2020; Jiang et al., 2021).

Measurement of Olfactory Identification

Olfactory identification was measured using the 12-item Sniffin' Sticks screening test (Palta et al., 2018; Jiang et al., 2021). Each participant was asked to smell 12 common odorants (orange, leather, cinnamon, peppermint, banana, lemon, licorice, coffee, cloves, pineapple, rose, and fish) one at a time, in different orders, for longer than 3–4 s, and then asked to identify the odor from four answer choices. Three rounds of separate tests were performed for the left nostril, right nostril, and nostrils on both sides. When the nostril on one side was under test, participants were asked to block the other nostril. To accommodate the differences in education levels of the participants, the list of odors was represented as pictures. The administrators of the test were blind for the cognitive status of each participant. Before the tests, the participants were asked about olfactory history, previous diseases, and occupations that could have an influence on olfactory identification. People who have these problems were excluded. One point was given for each correctly identified odor, and the possible score ranged from 0 to 12. Score on both sides was calculated for olfactory identification. A higher test score indicated better olfactory identification.

Magnetic Resonance Imaging Acquisition and Measurements

All the participants of the TIS were scanned on a 3.0-T multi-modality brain MRI scanner (Magnetom Verio Tim scanner; Siemens, Erlangen, Germany) at baseline. The protocol and MRI sequence parameters have been reported previously (Wang et al., 2019; Cui et al., 2020; Jiang et al., 2021). FreeSurfer software (v6.0.0) was used to estimate the volume of brain regions on T1-weighted images (Desikan et al., 2006). We measured the volumes of the hippocampus, thalamus, amygdala, cerebral cortex, and other subcortical structures correlated to cognitive function. Total intracranial volume (TIV) and volumes of cerebrospinal fluid (CSF), ventricle, white matter, and gray matter were used to determine global atrophy. All the brain region volumes were standardized by z-score. Further, we obtained and log-transformed volume of white matter hyperintensity (WMH) by using SPM8 (Schmidt et al., 2012).

Covariates

Demographics (age, sex, and years of education) and lifestyle characteristics (smoking and alcohol consumption) data were collected using a detailed epidemiological questionnaire. Medical history of hypertension, diabetes, and hyperlipidemia were obtained from diagnoses by physicians, and physical examination (Jiang et al., 2021).

Statistical Analyses

Statistical Analyses for Association of Olfactory Identification and Cognition

Continuous variables were presented as mean (standard deviation, *SD*) or median (interquartile range, *IQR*) and categorical variables were presented as frequencies (%). The normality of continuous variables was evaluated using Shapiro-Wilk test. Kruskal-Wallis test and Pearson chi-square test were used to compare differences among groups of different cognitive status when appropriate. For bounded continuous variables with skewed distribution (MMSE, MoCA, AVLT, FOME, and Conflicting Instructions Task), we transformed the scores into beta distribution (0–1) and then used beta regression to assess the association between olfactory identification with global cognition, memory and executive function (Zou et al., 2010; Martinelli-Boneschi et al., 2013; Jiang et al., 2019). For ordinal categorical variable (CDT), we conducted ordinal logistic regression to evaluate the associations of olfactory identification and visuospatial function (Paula et al., 2013). For continuous variable (AFT), generalized liner regression was used (Caldwell et al., 2019). The regression analyses were conducted in all participants. We used multinomial logistic regression to estimate the association of olfactory identification score and cognitive dysfunction, using cognitively normal as a reference.

Statistical Analyses for Association Between Olfactory Identification, Cognitive Function, and Brain Volume

For the reasons mentioned above, the associations between brain region volumes and olfactory identification, global cognition, and domain-specific cognitive function were assessed using beta regression, ordinal logistic regression and generalized liner regression, respectively. Since we did the analyses between 14 brain regions with olfactory identification and cognitive function, to account for multiple comparison correction to reduce false positivity, we used a false discovery rate (FDR) correction and interpreted FDR-corrected *P*-values < 0.05 as significance levels for the associations among olfactory identification, cognition, and brain region volumes. Finally, to determine whether differences in brain MRI indices might explain the association between olfactory identification and cognition in all participants, brain region volumes associated with both olfactory identification and cognitive function were included in beta regression or generalized liner regression models to assess whether they could attenuate the association between olfactory identification and cognition (Rosso et al., 2017). The attenuation of the association was evaluated using R package (mediation) with 10,000 repetitions. We also stratify the association between

TABLE 1 | Characteristics of the study participants.

| Characteristics | Cognitively normal N = 447 | MCI N = 157 | Dementia N = 41 | P-value |
|---|-------------------------------|----------------|--------------------|---------|
| Demographics | | | | |
| Age, mean (SD), years | 63.7 (3.2) | 64.4 (3.0) | 64.8 (3.1) | 0.033 |
| Female | 237 (53.0) | 100 (63.7) | 34 (82.9) | <0.001 |
| Years of education | 6 (2, 9) | 2 (0, 8) | 0 (0, 3) | <0.001 |
| Pre-existing comorbidity and lifestyle | | | | |
| Hypertension | 231 (51.7) | 101 (64.3) | 23 (56.1) | 0.421 |
| Diabetes | 63 (14.1) | 15 (9.6) | 5 (12.2) | 0.024 |
| Hyperlipidemia | 250 (55.9) | 79 (50.3) | 24 (58.5) | 0.037 |
| Smoker | 136 (30.4) | 38 (24.2) | 5 (12.2) | 0.341 |
| Alcohol drinker | 149 (33.3) | 41 (26.1) | 7 (17.1) | 0.023 |
| Olfactory function | | | | |
| Olfactory identification | 6 (5, 8) | 6 (4, 7) | 5 (3, 6) | <0.001 |
| Cognitive function | | | | |
| MMSE | 26 (23, 28) | 21 (16, 25) | 13 (9, 15) | <0.001 |
| MoCA | 18 (14, 22) | 12 (9, 17) | 7 (4, 8) | <0.001 |
| Short delay recall | 8 (6, 10) | 7 (4, 8) | 7 (5, 8) | <0.001 |
| Long delay recall | 8 (6, 10) | 7 (4, 8) | 6 (5, 8) | <0.001 |
| Executive function | 2.5 (2, 3) | 2 (1.5, 2.5) | 1 (1, 1.5) | <0.001 |
| Visuospatial function | 2 (1, 3) | 1 (0, 2) | 0 (0, 1) | <0.001 |
| Language | 12 (10.50, 15) | 10 (8, 12) | 7 (4, 10) | <0.001 |

Values are median (interquartile range) or N (%), except for indicated.

SD, Standard deviation; MMSE, Mini-Mental State Examination; MoCA, Montreal Cognitive Assessment; MCI, Mild cognitive impairment.

olfactory identification and cognition according to the median of amygdala volume. All regression analyses were fitted in two models: Model 1 was adjusted for age, sex, and years of education; Model 2 was further adjusted for hypertension, diabetes, hyperlipidemia, smoking, and alcohol consumption (time interval and standardized TIV was added in both models when brain region volumes were included). Age, sex, and education were reported to be associated with cognitive function previously. Hypertension, diabetes and hyperlipidemia were also reported as risk factors for cognitive dysfunction (Livingston et al., 2017; Barthold et al., 2020). Time interval between brain MRI and cognitive assessment and standardized TIV were also adjusted in the model to eliminate the effects due to individual differences. Differences were considered statistically significant at $P < 0.05$. All statistical analyses were performed using R program (R core team, Version 3.6.1).

RESULTS

Characteristics of the Study Population

The demographic and olfactory and cognitive performance characteristics of the study population ($n = 645$) are presented according to cognitive status in **Table 1**. Among the 645 followed-up TIS participants, dementia was diagnosed in 41 (6.4%) individuals, and MCI in 157 (24.3%) individuals at the first round of cognitive follow-up (Jiang et al., 2021). The individuals with dementia and MCI tended to be female and older. Participants

TABLE 2 | Association of olfactory identification with cognitive function.

| Cognitive function | Model 1 | P-value | Model 2 | P-value |
|-----------------------|---------------|---------|---------------|---------|
| MMSE | 0.075 (0.016) | <0.001 | 0.073 (0.016) | <0.001 |
| MoCA | 0.107 (0.013) | <0.001 | 0.106 (0.013) | <0.001 |
| Short delay recall | 0.045 (0.020) | 0.022 | 0.046 (0.019) | 0.018 |
| Long delay recall | 0.066 (0.020) | 0.001 | 0.065 (0.020) | 0.001 |
| Executive function | 0.068 (0.026) | 0.008 | 0.066 (0.026) | 0.011 |
| Visuospatial function | 0.160 (0.038) | <0.001 | 0.159 (0.038) | <0.001 |
| Language | 0.033 (0.006) | <0.001 | 0.032 (0.006) | <0.001 |

Values are estimated coefficients (standard error). Model 1 was adjusted for age, sex, and years of education; Model 2 was further adjusted for hypertension, diabetes, hyperlipidemia, smoking and alcohol consumption.

MMSE, Mini-Mental State Examination; MoCA, Montreal Cognitive Assessment.

with cognitive dysfunction were likely to have obtained less education years and have higher rate of hypertension. As expected, participants with MCI and dementia had significant lower neuropsychological scores, including global cognitive function (MMSE and MoCA) and domain-specific cognitive function (all $P < 0.001$). Moreover, in olfactory identification tests, cognitively normal individuals (median: 6, IQR: 5, 8) had a higher median score and showed better performance than individuals with dementia (median: 5, IQR: 3, 6).

Association of Olfactory Identification and Cognitive Function

We first assessed the association between olfactory identification and cognitive function (**Table 2**). Olfactory identification score was associated with MMSE and MoCA (Beta = 0.075 and 0.107, respectively; both $P < 0.001$). Results were robust to further adjustment for smoking, alcohol consumption, and comorbidities (Model 2, both $P < 0.001$). In the fully adjusted Model 2, olfactory identification score was also associated with specific cognitive domain (short delay recall: Beta = 0.046, $P = 0.018$; long delay recall: Beta = 0.065, $P = 0.001$; executive function: Beta = 0.066, $P = 0.011$; visuospatial function: Beta = 0.159, $P < 0.001$; language: Beta = 0.032, $P < 0.001$).

Association Between Olfactory Identification, Cognitive Function, and Brain Volume

As is shown in **Figure 1** and **Supplementary Table 2**, olfactory identification score was associated with the volume of amygdala (of the 14 brain structures tested), in Model 1. Hypertension, diabetes, hyperlipidemia, smoking, and alcohol consumption, did not modify the association between olfactory identification and the volume of amygdala (Beta = 0.134, FDR = 0.028). After full adjustment (Model 2), MMSE results were significantly associated with the volumes of the amygdala (Beta = 0.121, FDR = 0.019), CSF (Beta = -0.122, FDR = 0.013), hippocampus (Beta = 0.196, FDR < 0.001), ventricle (Beta = -0.112, FDR = 0.013), and WMH (Beta = -0.221, FDR = 0.023), as shown in the middle column in **Figure 1** and **Supplementary Table 2**. In addition, MoCA was associated with the volumes of the amygdala (Beta = 0.149, FDR < 0.001), hippocampus (Beta =

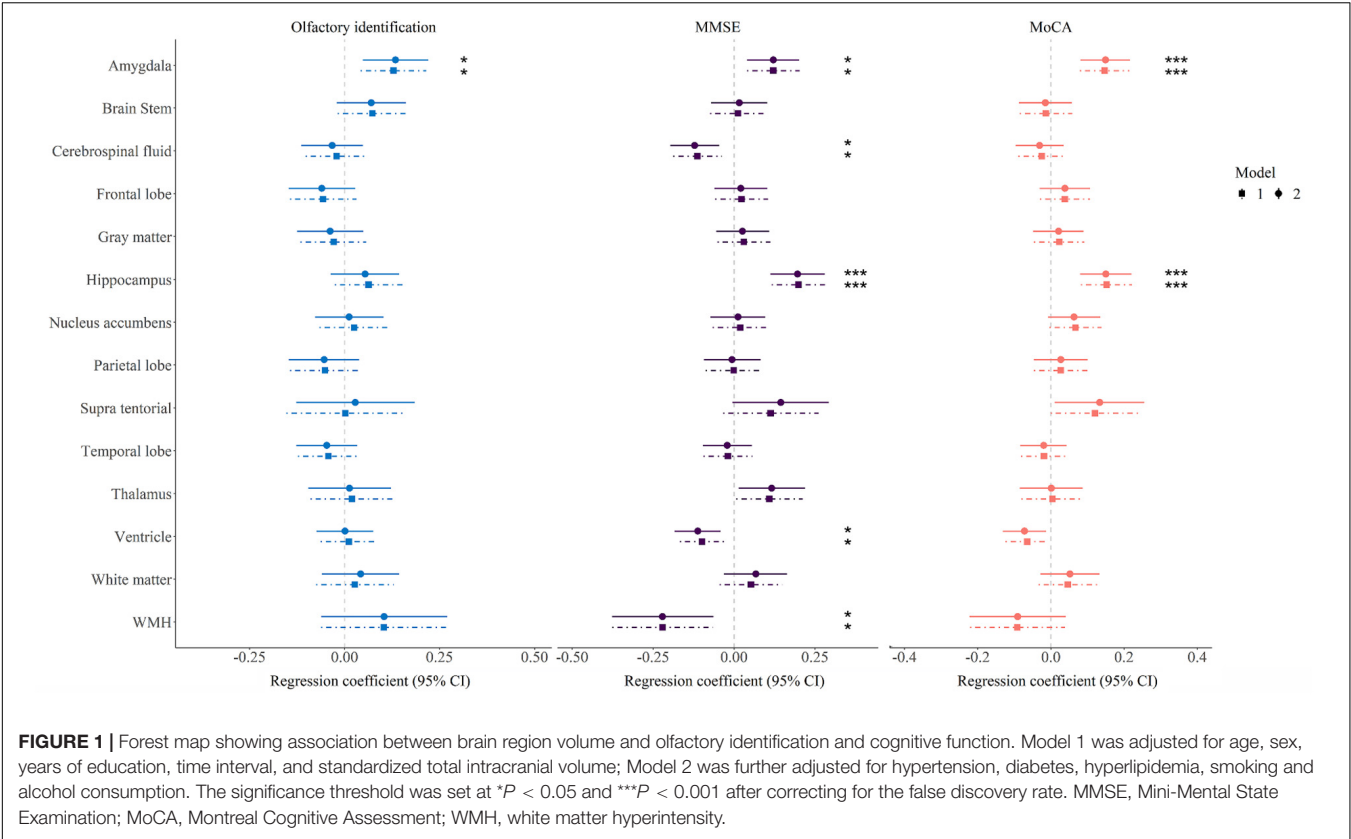


TABLE 3 | Association of olfactory identification with cognitive function before and after adjustment for amygdala.

| | MMSE | | | MoCA | | | Language | | |
|---|---------------|---------|-------------|---------------|---------|-------------|---------------|---------|-------------|
| | Beta (SE) | P-value | Attenuation | Beta (SE) | P-value | Attenuation | Beta (SE) | P-value | Attenuation |
| Olfactory identification | 0.068 (0.017) | <0.001 | | 0.098 (0.014) | <0.001 | | 0.332 (0.070) | <0.001 | |
| Olfactory identification, adjusted for amygdala | 0.066 (0.017) | <0.001 | 9.5% | 0.095 (0.014) | <0.001 | 5.7% | 0.322 (0.070) | <0.001 | 5.9% |

Values are estimated coefficients (standard error). All models were adjusted for age, sex, years of education, hypertension, diabetes, hyperlipidemia, smoking and alcohol consumption (time interval and standardized total intracranial volume and was added when amygdala volume was included). MMSE, Mini-Mental State Examination; MoCA, Montreal Cognitive Assessment.

0.150, FDR < 0.001) in Model 2 (right column in **Figure 1** and **Supplementary Table 2**). For domain-specific cognitive function, the ventricle and WMH volumes were related to long delay recall, and hippocampal volume was correlated with executive function with nominal $P < 0.05$ in Model 2, however, only the amygdala volume (Beta = 0.046, FDR = 0.028) was significantly associated with language after multiple comparison correction (**Supplementary Table 3**).

Association of Olfactory Identification With Cognitive Function Before and After Adjustment for Brain Magnetic Resonance Imaging Markers

As shown in **Table 3**, olfactory identification was associated with MMSE (Beta = 0.068, $P < 0.001$), MoCA (Beta = 0.098, $P < 0.001$), and language (Beta = 0.332, $P < 0.001$). When amygdala volume was introduced into the model, the associations

were attenuated but remained significant between olfactory identification and MMSE (Beta = 0.066, $P < 0.001$, 9.5% attenuation), MoCA (Beta = 0.095, $P < 0.001$, 5.7% attenuation), and language (Beta = 0.322, $P < 0.001$, 5.9% attenuation), which indicated that these associations were attributable, at least in part, to differences in amygdala volume.

DISCUSSION

The main findings from this community-based study in rural older Chinese adults can be summarized as follows: (1) a higher olfactory identification score was associated with better global and domain-specific cognitive function; (2) brain atrophy (especially of the amygdala) impaired olfactory identification and global cognition; and (3) the association between olfactory identification and cognition can be partly attributable to differences in amygdala volume. These findings suggest that

poor olfactory identification could indicate cognitive dysfunction associated with brain neurodegeneration. Moreover, the olfactory identification score was negatively associated with the presence of MCI [odds ratio (OR): 0.89, 95% confidence interval (CI): 0.81, 0.97] and dementia (OR: 0.79, 95% CI: 0.66, 0.93) in Model 2 (**Supplementary Table 1**). After stratification according to the median of amygdala volume, in participants with amygdala volume both in the top 50% and the last 50%, the associations between olfactory identification with MMSE, MoCA and language were found significant (**Supplementary Table 5**). There is an increase in studies focusing on the association between olfaction dysfunctions and cognitive decline in older people. Previous studies have indicated that olfactory identification is associated with global cognitive function and specific cognitive domains, including memory, language, and executive function (Palta et al., 2018; Yahiaoui-Doktor et al., 2019), which was corroborated by our results. Additionally, poor olfactory identification performance was associated with higher risks of MCI and dementia in older people, as reported previously (Liang et al., 2016; Roberts et al., 2016).

Global cognition and specific cognitive domains were associated with several structural brain features/markers, such as volume of the hippocampus, amygdala, thalamus, caudate, gray matter, white matter, and WMH (Apostolova et al., 2010; Wang et al., 2018; Novellino et al., 2019; Oswald et al., 2019). We also found that hippocampal and amygdala volumes were associated with MMSE and MoCA. The association between the hippocampal volume and cognitive function has been well established. The hippocampus likely plays a crucial part in the cognitive neural circuit, including learning, decision making, declarative, episodic memory (Wikenheiser and Schoenbaum, 2016; Yang and Wang, 2017), and particularly memory formation (Bellmund et al., 2018). Similarly, amygdala atrophy was closely associated with MMSE, and the symptoms increased in severity when the amygdala volume declined in individuals with early AD (Poulin et al., 2011).

Olfactory dysfunctions have recently been linked with brain lesions such as atrophy (Lee et al., 2014; Takeda et al., 2014). Olfactory dysfunction was associated with smaller volumes of the hippocampus, amygdala, entorhinal cortex, fusiform gyrus, temporal pole, and inferior temporal cortex (Dintica et al., 2019; Lian et al., 2019; Wu et al., 2019). The amygdala is involved in the primary and secondary olfactory cortex, which links several structural pathways that modulate olfactory dysfunction (Han et al., 2019). In this study, we found that amygdala atrophy is associated with declining olfactory identification.

Several pathophysiological pathways could affect the association between olfactory identification dysfunction and cognitive decline in aging. In this study, we aimed to elucidate the effect of specific brain MRI indices on the correlation between olfactory identification and cognitive function. Our results suggest that the amygdala volume is associated with cognitive function, and could attenuate the association between olfactory identification and cognitive function, indicating that the amygdala could be a neural substrate that links olfactory identification to cognitive function. In patients with AD, Baek et al. (2020) found that atrophy in brain regions related

to olfactory process may have a direct effect on olfactory identification. As an important component of the cognitive and olfactory neural circuits (Devanand, 2016; Herrington et al., 2017), the volume of the amygdala decreased along with cognitive decline (Poulin et al., 2011). The amygdala is associated with emotion and motivation (Janak and Tye, 2015), and in the progression of learning and consolidation with memory structures such as the hippocampus (Herrington et al., 2017). On the other hand, the amygdala also receives neuronal projections directly from the olfactory bulb (Devanand, 2016), making it a crucial part of the olfactory neural circuit. There has been little research on the effects of brain structure in associations between olfactory identification and cognitive function. Our results suggest that the association between olfactory identification and cognitive function is at least partly attributable to amygdala volume, providing a basis for the elucidation of a possible underlying neurological mechanism.

We studied the relationship between olfactory identification and cognitive function by linking olfactory identification to MRI data, and investigated the probable underlying mechanism. The major strength of our study includes the unique sample of rural Chinese older adults as well as the use of the 3.0-T multi-modality brain MRI scanner. However, this study has several limitations. All these results were based on a cross-sectional study so the order in which cognitive dysfunction and olfactory dysfunction occurred cannot be determined, and more community-based longitudinal data are warranted. Continuous follow-ups will be performed as part of the TIS, in which the associations and effects observed could be further evaluated in the future. Further, we only used odor identification to assess olfactory function in this study. However, due to its sensitivity and specificity, the olfactory identification test has been widely used in olfactory function evaluation and cognition-related research (Boesveldt et al., 2008). Finally, our study indicated that the amygdala could be one of the neural links underlying the association between olfaction and cognition, which is a preliminary result for mechanistic studies. Pathological analysis or longitudinal changes in brain properties and network analysis could be measured in future research to assess the level or percentage of brain atrophy and its contribution to get more evidence for mechanisms that explain this association.

CONCLUSION

The results of our community-based study indicate that higher olfactory identification is associated with better global cognition and specific cognitive domains, and lower olfactory identification is positively associated with occurrence of cognitive dysfunction, including MCI and dementia. The association between olfactory identification and cognitive function is attenuated by the volume of amygdala, indicating that the amygdala could be one of the neural links underlying this association. These findings should be further validated in larger populations and in longitudinal studies, and could form the basis for the development of a non-invasive and cost-effective screening tool to identify cognitive dysfunction and monitor the progression of dementia.

DATA AVAILABILITY STATEMENT

The raw data supporting the conclusions of this article will be made available by the authors, without undue reservation.

ETHICS STATEMENT

The studies involving human participants were reviewed and approved by the Ethics Committee of the School of Life Sciences, Fudan University, and Fudan University Taizhou Institute of Health Sciences (institutional review board approval number: 496 and B017, respectively). The patients/participants provided their written informed consent to participate in this study.

AUTHOR CONTRIBUTIONS

YJ and XC: concept and design. YW, WT, MF, and XZ: data collection. ZT and YJ: data analyses and manuscript writing. All authors: manuscript proofing and results interpretations.

FUNDING

This study was supported by the National Key Research and Development program of China (Award No. 2021YFC2500100),

the National Natural Science Foundation of China (Award No. 82001142), the Natural Science Foundation of Shanghai, China (Award No. 22ZR1405300), the Shanghai Rising-Star Program (Award No. 22QA1404000), the Shanghai Municipal Science and Technology Major Project (Award No. 2017SHZDZX01), the Key Research and Development Plans of Jiangsu Province, China (Award No. BE2021696), and the China Postdoctoral Science Foundation (Award No. 2020M681184).

ACKNOWLEDGMENTS

We appreciate all the participants and staff of TIS for their crucial contributions. We thank the staff of Fudan University Taizhou Institute of Health Science, Taizhou People's Hospital, and Taizhou and Taixing Center for Disease Control and Prevention (CDC) for their timely help, and graduate students from Fudan University for their assistance in data collection.

SUPPLEMENTARY MATERIAL

The Supplementary Material for this article can be found online at: <https://www.frontiersin.org/articles/10.3389/fnagi.2022.873032/full#supplementary-material>

REFERENCES

- Apostolova, L. G., Beyer, M., Green, A. E., Hwang, K. S., Morra, J. H., Chou, Y. Y., et al. (2010). Hippocampal, caudate, and ventricular changes in Parkinson's disease with and without dementia. *Mov. Disord.* 25, 687–695. doi: 10.1002/mds.22799
- Baek, M. S., Cho, H., Lee, H. S., Lee, J. H., Ryu, Y. H., and Lyoo, C. H. (2020). Effect of A/T/N imaging biomarkers on impaired odor identification in Alzheimer's disease. *Sci. Rep.* 10:11556. doi: 10.1038/s41598-020-68504-2
- Barthold, D., Joyce, G., Diaz Brinton, R., Wharton, W., Kehoe, P. G., and Zissimopoulos, J. (2020). Association of combination statin and antihypertensive therapy with reduced Alzheimer's disease and related dementia risk. *PLoS One* 15:e0229541. doi: 10.1371/journal.pone.0229541
- Bellmund, J. L. S., Gärdenfors, P., Moser, E. I., and Doeller, C. F. (2018). Navigating cognition: Spatial codes for human thinking. *Science* 362:eaat6766. doi: 10.1126/science.aat6766
- Blashfield, R. K., Keeley, J. W., Flanagan, E. H., and Miles, S. R. (2014). The cycle of classification: DSM-I through DSM-5. *Annu. Rev. Clin. Psychol.* 10, 25–51. doi: 10.1146/annurev-clinpsy-032813-153639
- Boesveldt, S., Verbaan, D., Knol, D. L., Visser, M., van Rooden, S. M., van Hilten, J. J., et al. (2008). A comparative study of odor identification and odor discrimination deficits in Parkinson's disease. *Mov. Disord.* 23, 1984–1990. doi: 10.1002/mds.22155
- Caldwell, J. Z. K., Cummings, J. L., Banks, S. J., Palmqvist, S., and Hansson, O. (2019). Cognitively normal women with Alzheimer's disease proteinopathy show relative preservation of memory but not of hippocampal volume. *Alzheimers Res. Ther.* 11:109. doi: 10.1186/s13195-019-0565-1
- Cui, M., Jiang, Y., Zhao, Q., Zhu, Z., Liang, X., Zhang, K., et al. (2020). Metabolomics and incident dementia in older Chinese adults: The Shanghai Aging Study. *Alzheimers Dement.* 16, 779–788. doi: 10.1002/alz.12074
- Dahmani, L., Patel, R. M., Yang, Y., Chakravarty, M. M., Fellows, L. K., and Bohbot, V. D. (2018). An intrinsic association between olfactory identification and spatial memory in humans. *Nat. Commun.* 9:4162. doi: 10.1038/s41467-018-06569-4
- Desikan, R. S., Ségonne, F., Fischl, B., Quinn, B. T., Dickerson, B. C., Blacker, D., et al. (2006). An automated labeling system for subdividing the human cerebral cortex on MRI scans into gyral based regions of interest. *Neuroimage* 31, 968–980. doi: 10.1016/j.neuroimage.2006.01.021
- Devanand, D. P. (2016). Olfactory Identification Deficits, Cognitive Decline, and Dementia in Older Adults. *Am. J. Geriatr. Psychiatry* 24, 1151–1157. doi: 10.1016/j.jagp.2016.08.010
- Devanand, D. P., Lee, S., Manly, J., Andrews, H., Schupf, N., Doty, R. L., et al. (2015). Olfactory deficits predict cognitive decline and Alzheimer dementia in an urban community. *Neurology* 84, 182–189. doi: 10.1212/wnl.0000000000001132
- Ding, D., Zhao, Q., Guo, Q., Meng, H., Wang, B., Luo, J., et al. (2015). Prevalence of mild cognitive impairment in an urban community in China: a cross-sectional analysis of the Shanghai Aging Study. *Alzheimers Dement.* 11, 300–309.e2. doi: 10.1016/j.jalz.2013.11.002
- Dintica, C. S., Marseglia, A., Rizzuto, D., Wang, R., Seubert, J., Arfanakis, K., et al. (2019). Impaired olfaction is associated with cognitive decline and neurodegeneration in the brain. *Neurology* 92:e700–e709. doi: 10.1212/wnl.0000000000006919
- Djordjevic, J., Jones-Gotman, M., De Sousa, K., and Chertkow, H. (2008). Olfaction in patients with mild cognitive impairment and Alzheimer's disease. *Neurobiol. Aging* 29, 693–706. doi: 10.1016/j.neurobiolaging.2006.11.014
- Fullard, M. E., Tran, B., Xie, S. X., Toledo, J. B., Scordia, C., Linder, C., et al. (2016). Olfactory impairment predicts cognitive decline in early Parkinson's disease. *Parkinsonism Relat. Disord.* 25, 45–51. doi: 10.1016/j.parkreldis.2016.02.013
- Han, P., Zang, Y., Akshita, J., and Hummel, T. (2019). Magnetic Resonance Imaging of Human Olfactory Dysfunction. *Brain Topogr.* 32, 987–997. doi: 10.1007/s10548-019-00729-5
- Herrington, J. D., Parma, V., and Miller, J. S. (2017). "Chapter 4 - Neurobiological Mechanisms of Anxiety in ASD," in *Anxiety in Children and Adolescents with Autism Spectrum Disorder*, eds C. M. Kerns, P. Renno, E. A. Storch, P. C. Kendall, and J. J. Wood (Cambridge: Academic Press), 55–77.
- Janak, P. H., and Tye, K. M. (2015). From circuits to behaviour in the amygdala. *Nature* 517, 284–292. doi: 10.1038/nature14188

- Jia, L., Quan, M., Fu, Y., Zhao, T., Li, Y., Wei, C., et al. (2020). Dementia in China: epidemiology, clinical management, and research advances. *Lancet Neurol.* 19, 81–92. doi: 10.1016/s1474-4422(19)30290-x
- Jiang, Y., Cui, M., Tian, W., Zhu, S., Chen, J., Suo, C., et al. (2021). Lifestyle, multi-omics features, and preclinical dementia among Chinese: The Taizhou Imaging Study. *Alzheimers Dement.* 17, 18–28. doi: 10.1002/alz.12171
- Jiang, Y., Wang, Y., Yuan, Z., Xu, K., Zhang, K., Zhu, Z., et al. (2019). Total Cerebral Small Vessel Disease Burden Is Related to Worse Performance on the Mini-Mental State Examination and Incident Dementia: A Prospective 5-Year Follow-Up. *J. Alzheimers Dis.* 69, 253–262. doi: 10.3233/jad-181135
- Lee, E. Y., Eslinger, P. J., Du, G., Kong, L., Lewis, M. M., and Huang, X. (2014). Olfactory-related cortical atrophy is associated with olfactory dysfunction in Parkinson's disease. *Mov. Disord.* 29, 1205–1208. doi: 10.1002/mds.25829
- Lian, T. H., Zhu, W. L., Li, S. W., Liu, Y. O., Guo, P., Zuo, L. J., et al. (2019). Clinical, Structural, and Neuropathological Features of Olfactory Dysfunction in Patients with Alzheimer's Disease. *J. Alzheimers Dis.* 70, 413–423. doi: 10.3233/jad-181217
- Liang, X., Ding, D., Zhao, Q., Guo, Q., Luo, J., and Hong, Z. (2016). Association between olfactory identification and cognitive function in community-dwelling elderly: the Shanghai aging study. *BMC Neurol.* 16:199. doi: 10.1186/s12883-016-0725-x
- Livingston, G., Sommerlad, A., Orgeta, V., Costafreda, S. G., Huntley, J., Ames, D., et al. (2017). Dementia prevention, intervention, and care. *Lancet* 390, 2673–2734. doi: 10.1016/s0140-6736(17)31363-6
- Martinelli-Boneschi, F., Giacalone, G., Magnani, G., Biella, G., Coppi, E., Santangelo, R., et al. (2013). Pharmacogenomics in Alzheimer's disease: a genome-wide association study of response to cholinesterase inhibitors. *Neurobiol. Aging* 34:1711.e7–13. doi: 10.1016/j.neurobiolaging.2012.12.008
- Novellino, F., López, M. E., Vaccaro, M. G., Miguel, Y., Delgado, M. L., and Maestu, F. (2019). Association Between Hippocampus, Thalamus, and Caudate in Mild Cognitive Impairment APOEε4 Carriers: A Structural Covariance MRI Study. *Front. Neurol.* 10:1303. doi: 10.3389/fneur.2019.01303
- Oschwald, J., Guye, S., Liem, F., Rast, P., Willis, S., Röcke, C., et al. (2019). Brain structure and cognitive ability in healthy aging: a review on longitudinal correlated change. *Rev. Neurosci.* 31, 1–57. doi: 10.1515/revneuro-2018-0096
- Palta, P., Chen, H., Deal, J. A., Sharrett, A. R., Gross, A., Knopman, D., et al. (2018). Olfactory function and neurocognitive outcomes in old age: The Atherosclerosis Risk in Communities Neurocognitive Study. *Alzheimers Dement.* 14, 1015–1021. doi: 10.1016/j.jalz.2018.02.019
- Paula, J. J., Miranda, D. M., Moraes, E. N., and Malloy-Diniz, L. F. (2013). Mapping the clockworks: what does the Clock Drawing Test assess in normal and pathological aging? *Arq. Neuropsiquiatr.* 71, 763–768. doi: 10.1590/0004-282x20130118
- Petersen, R. C. (2004). Mild cognitive impairment as a diagnostic entity. *J. Intern. Med.* 256, 183–194. doi: 10.1111/j.1365-2796.2004.01388.x
- Poulin, S. P., Dautoff, R., Morris, J. C., Barrett, L. F., and Dickerson, B. C. (2011). Amygdala atrophy is prominent in early Alzheimer's disease and relates to symptom severity. *Psychiatry Res.* 194, 7–13. doi: 10.1016/j.psychres.2011.06.014
- Roalf, D. R., Moberg, M. J., Turetsky, B. I., Brennan, L., Kabadi, S., Wolk, D. A., et al. (2017). A quantitative meta-analysis of olfactory dysfunction in mild cognitive impairment. *J. Neurol. Neurosurg. Psychiatry* 88, 226–232. doi: 10.1136/jnnp-2016-314638
- Roberts, R. O., Christianson, T. J., Kremers, W. K., Mielke, M. M., Machulda, M. M., Vassilaki, M., et al. (2016). Association Between Olfactory Dysfunction and Amnesic Mild Cognitive Impairment and Alzheimer Disease Dementia. *JAMA Neurol.* 73, 93–101. doi: 10.1001/jamaneurol.2015.2952
- Rosso, A. L., Verghese, J., Metti, A. L., Boudreau, R. M., Aizenstein, H. J., Kritchevsky, S., et al. (2017). Slowing gait and risk for cognitive impairment: The hippocampus as a shared neural substrate. *Neurology* 89, 336–342. doi: 10.1212/wnl.0000000000004153
- Schmidt, P., Gaser, C., Arsic, M., Buck, D., Förstner, A., Berthele, A., et al. (2012). An automated tool for detection of FLAIR-hyperintense white-matter lesions in Multiple Sclerosis. *Neuroimage* 59, 3774–3783. doi: 10.1016/j.neuroimage.2011.11.032
- Serby, M., Larson, P., and Kalkstein, D. (1991). The nature and course of olfactory deficits in Alzheimer's disease. *Am. J. Psychiatry* 148, 357–360. doi: 10.1176/ajp.148.3.357
- Smitka, M., Puschmann, S., Buschhuetter, D., Gerber, J. C., Witt, M., Honeycutt, N., et al. (2012). Is there a correlation between hippocampus and amygdala volume and olfactory function in healthy subjects? *Neuroimage* 59, 1052–1057. doi: 10.1016/j.neuroimage.2011.09.024
- Takeda, A., Baba, T., Kikuchi, A., Hasegawa, T., Sugeno, N., Konno, M., et al. (2014). Olfactory dysfunction and dementia in Parkinson's disease. *J. Parkinsons Dis.* 4, 181–187. doi: 10.3233/jpd-130277
- Vassilaki, M., Christianson, T. J., Mielke, M. M., Geda, Y. E., Kremers, W. K., Machulda, M. M., et al. (2017). Neuroimaging biomarkers and impaired olfaction in cognitively normal individuals. *Ann. Neurol.* 81, 871–882. doi: 10.1002/ana.24960
- Walker, I. M., Fullard, M. E., Morley, J. F., and Duda, J. E. (2021). Olfaction as an early marker of Parkinson's disease and Alzheimer's disease. *Handb. Clin. Neurol.* 182, 317–329. doi: 10.1016/b978-0-12-819973-2.00030-7
- Wang, R., Laveskog, A., Laukka, E. J., Kalpouzos, G., Bäckman, L., Fratiglioni, L., et al. (2018). MRI load of cerebral microvascular lesions and neurodegeneration, cognitive decline, and dementia. *Neurology* 91:e1487–e1497. doi: 10.1212/wnl.0000000000006355
- Wang, Y., Jiang, Y., Suo, C., Yuan, Z., Xu, K., Yang, Q., et al. (2019). Deep/mixed cerebral microbleeds are associated with cognitive dysfunction through thalamocortical connectivity disruption: The Taizhou Imaging Study. *Neuroimage Clin.* 22:101749. doi: 10.1016/j.nicl.2019.101749
- Wikenheiser, A. M., and Schoenbaum, G. (2016). Over the river, through the woods: cognitive maps in the hippocampus and orbitofrontal cortex. *Nat. Rev. Neurosci.* 17, 513–523. doi: 10.1038/nnrn.2016.56
- Wu, X., Geng, Z., Zhou, S., Bai, T., Wei, L., Ji, G. J., et al. (2019). Brain Structural Correlates of Odor Identification in Mild Cognitive Impairment and Alzheimer's Disease Revealed by Magnetic Resonance Imaging and a Chinese Olfactory Identification Test. *Front. Neurosci.* 13:842. doi: 10.3389/fnins.2019.00842
- Yahiaoui-Doktor, M., Luck, T., Riedel-Heller, S. G., Loeffler, M., Wirkner, K., and Engel, C. (2019). Olfactory function is associated with cognitive performance: results from the population-based LIFE-Adult-Study. *Alzheimers Res. Ther.* 11:43. doi: 10.1186/s13195-019-0494-z
- Yang, Y., and Wang, J. Z. (2017). From Structure to Behavior in Basolateral Amygdala-Hippocampus Circuits. *Front. Neural Circuits* 11:86. doi: 10.3389/fncir.2017.00086
- Zou, K. H., Carlsson, M. O., and Quinn, S. A. (2010). Beta-mapping and beta-regression for changes of ordinal-rating measurements on Likert scales: a comparison of the change scores among multiple treatment groups. *Stat. Med.* 29, 2486–2500. doi: 10.1002/sim.4012

Conflict of Interest: The authors declare that the research was conducted in the absence of any commercial or financial relationships that could be construed as a potential conflict of interest.

The reviewer XL declared a shared affiliation with the authors ZT, YW, HL, KX, LJ, MC, YJ and XC to the handling editor at the time of review.

Publisher's Note: All claims expressed in this article are solely those of the authors and do not necessarily represent those of their affiliated organizations, or those of the publisher, the editors and the reviewers. Any product that may be evaluated in this article, or claim that may be made by its manufacturer, is not guaranteed or endorsed by the publisher.

Copyright © 2022 Tan, Wang, Lu, Tian, Xu, Fan, Zhao, Jin, Cui, Jiang and Chen. This is an open-access article distributed under the terms of the Creative Commons Attribution License (CC BY). The use, distribution or reproduction in other forums is permitted, provided the original author(s) and the copyright owner(s) are credited and that the original publication in this journal is cited, in accordance with accepted academic practice. No use, distribution or reproduction is permitted which does not comply with these terms.



Characterizing Differences in Functional Connectivity Between Posterior Cortical Atrophy and Semantic Dementia by Seed-Based Approach

Yi Chen^{1,3†}, Qingze Zeng^{2†}, Yunyun Wang^{1,4}, Xiao Luo², Yan Sun¹, Lumi Zhang¹, Xiaoyan Liu¹, Kaicheng Li², Minming Zhang^{2*} and Guoping Peng^{1*}

¹ Department of Neurology, The First Affiliated Hospital, Zhejiang University School of Medicine, Hangzhou, China,

² Department of Radiology, The Second Affiliated Hospital, Zhejiang University School of Medicine, Hangzhou, China,

³ Department of Neurology, The Affiliated Hospital of Hangzhou Normal University, Hangzhou, China, ⁴ Department of Neurology, Shengzhou People's Hospital, Shengzhou, China

OPEN ACCESS

Edited by:

Allison B. Reiss,
New York University, United States

Reviewed by:

Jiu Chen,
Nanjing Medical University, China
Junhua Ding,
University of Edinburgh,
United Kingdom

*Correspondence:

Minming Zhang
zhangminming@zju.edu.cn
Guoping Peng
guopingpeng@zju.edu.cn

[†]These authors have contributed
equally to this work

Specialty section:

This article was submitted to
Alzheimer's Disease and Related
Dementias,
a section of the journal
Frontiers in Aging Neuroscience

Received: 08 January 2022

Accepted: 31 March 2022

Published: 29 April 2022

Citation:

Chen Y, Zeng Q, Wang Y, Luo X,
Sun Y, Zhang L, Liu X, Li K, Zhang M
and Peng G (2022) Characterizing
Differences in Functional Connectivity
Between Posterior Cortical Atrophy
and Semantic Dementia by
Seed-Based Approach.
Front. Aging Neurosci. 14:850977.
doi: 10.3389/fnagi.2022.850977

Background: Posterior cortical atrophy (PCA) and semantic dementia (SD) are focal syndromes involving different cerebral regions. This study aimed to demonstrate the existence of abnormal functional connectivity (FC) with an affected network in PCA and SD.

Methods: A total of 10 patients with PCA, 12 patients with SD, and 11 controls were recruited to undergo a detailed clinical history interview and physical examination, neuropsychological assessments, and PET/MRI scan. Seed-based FC analyses were conducted to construct FC in language network, visual network, and salience network. The two-sample *t*-test was performed to reveal distinct FC patterns in PCA and SD, and we further related the FC difference to cognition. Meanwhile, the uptake value of fluorodeoxyglucose in regions with FC alteration was also extracted for comparison.

Results: We found a global cognitive impairment in patients with PCA and SD. The results of FC analyses showed that patients with PCA present decreased FC in left precentral gyrus to left V1 and increased FC in right inferior frontal gyrus to right V1 in the visual network, right medial frontal gyrus and left fusiform to left anterior temporal lobe and post-superior temporal gyrus in the language network, and left superior temporal gyrus to left anterior insula in the salience network, which were related to cognitive function. Patients with SD had decreased FC from right superior frontal gyrus, right middle frontal gyrus and right superior frontal gyrus to left anterior temporal lobe, or post-superior temporal gyrus in the language network, as well as left superior frontal gyrus to right anterior insula in the salience network, positively relating to cognitive function, but increased FC in the right superior temporal gyrus to left anterior temporal lobe in the language network, and right insula and left anterior cingulum to right anterior insula in the salience network, negatively relating to cognitive function. Most of the regions with FC change in patients with PCA and SD had abnormal metabolism simultaneously.

Conclusion: Abnormal connectivity spread over the cortex involving language and salience networks was common in patients with PCA and SD, whereas FC change involving the visual network was unique to patients with PCA. The FC changes were matched for cognitive deficits.

Keywords: posterior cortical atrophy, semantic dementia, language deficits, functional connectivity, network

INTRODUCTION

Alzheimer's disease (AD) is well known as the most common cause of dementia worldwide; however, there are increasingly other degenerative pathological brain processes that may cause dementia. Based on neuroradiology, focal degenerative dementia syndromes are classified by a lobar approach, which was associated with a characteristic clinical picture (Lam et al., 2013). For example, behavioral-variant frontotemporal dementia was localized in the frontal lobe, semantic dementia (SD) in the anterior temporal lobe (ATL), and posterior cortical atrophy (PCA) in the occipital-parietal-temporal lobe (Ossenkoppele et al., 2015; Pasquini et al., 2020). AD is the most common pathology of PCA, whereas Lewy body disease, corticobasal degeneration, and prion disease are pathologically less frequently associated (Holden et al., 2020); however, most cases of SD have TDP-43 pathology at post mortem, and a small minority are accounted for tauopathies and AD (Marshall et al., 2018). Reviewing the previous literature, the overlapping could be found in presentation and even the underlying dysfunction between these focal syndromes, such as PCA and SD.

Posterior cortical atrophy is characterized by predominant visuospatial and visuoperceptual dysfunction, which are selectively associated with primary visual (caudal), occipitoparietal (dorsal), occipitotemporal (ventral), and dominant parietal cerebral pathways bilaterally, with varying degrees of lateralization (Crutch et al., 2017; Miller et al., 2018; Firth et al., 2019). Regarding the category specificity in patients with PCA, their visual deficits received far more attention than their less obvious language, attention, and memory deficits (Shebani et al., 2017), whereas non-visual presentations can also be seen in PCA. However, there indeed existed language deficits in PCA compared to healthy. For example, Crutch et al. (2013) found that all the domains of language examined were impaired in PCA, especially naming and fluency. Simultaneously, Rik Ossenkoppele et al. showed that naming was significantly damaged in PCA compared with healthy while fluency was not. Both these studies have not been related to regions, which have already presented neuroimaging dysfunction. PCA also had difficulty in semantic categories with impairment in processing

function words, number words, and prepositions, and the region of primary hypometabolism and atrophy in PCA might be the fundamental factors (Shebani et al., 2017). Although it has been concluded that the language functions have been, to some degree, damaged, there was no research reflecting the language network change in PCA.

The progressive loss of language abilities is the predominant neurobehavior of primary progressive aphasia with three main phenotypic clinical presentations, including semantic variants (SD), logopenic variants (lvPPA), and non-fluent/agrammatic variants (nfvPPA) (Ranasinghe et al., 2017). Each PPA variant has a unique anatomical pattern of neuronal loss, namely, asymmetric bilateral ATL atrophy in SD, left posterior temporoparietal atrophy in lvPPA, and left posterior frontoinsula and subcortical atrophy in nfvPPA (Mandelli et al., 2014; Leyton et al., 2016). Meanwhile, each PPA variant revealed a distinct deficit in language function with anomia, loss of word comprehension, object concepts and semantic representations in SD; prominent phonological impairments in lvPPA; and motor speech and/or grammatical processing in nfvPPA (Gorno-Tempini et al., 2011). Consistent with PCA, one of the primary language deficits was naming in patients with SD, and both had semantic word-processing problems. Anatomically, the regional lesions of SD encompassed a large portion of the temporal lobes and extended to posterior temporal, parietal cortex, frontal, anterior insular, and anterior cingulate (Collins et al., 2017). Previous neuroimaging studies have shown specific impacts within language networks in SD—taking the ATL as the hub region, distributing to nodes in frontal, posterior temporal, and even parietal areas. Based on this hub with distributed node framework, intrinsic functional connectivity (FC) integrity was disrupted in a wide array of selective regions. Salience network might be involved in this framework, which was linked to clinical anxiety and lack of self-regulation (Day et al., 2013), and this pattern seemed to be presented in PCA (Fredericks et al., 2019). In addition, patients with SD were not only confused by face recognition and emotional processing implemented by posterior cortices (Ding et al., 2020), and they are also expected to be more impaired in words carrying visual semantic information about how an object looks (e.g., its color and form) (Shebani et al., 2017). However, the node in the abnormal region of SD has not reported the relevance of the visual network.

Posterior cortical atrophy and SD were selected because they have well-defined focal lesions in the cortex. Areas affected in each condition are proposed to make a region-specific contribution to language and visual processing (Shebani et al., 2017). Resting-state functional magnetic resonance imaging (rs-fMRI) is one of the neuroimaging

Abbreviations: AD, Alzheimer's disease; SD, semantic dementia; PCA, posterior cortical atrophy; lvPPA, logopenic variants primary progressive aphasia; nfvPPA, non-fluent/agrammatic variants primary progressive aphasia; ATL, anterior temporal lobe; MRI, magnetic resonance imaging; FDG, 2-fluoro-2-deoxy-D-glucose; PET, positron emission tomography; CSF, cerebrospinal fluid; SUVR, standard uptake value ratio; SPECT, single-photon emission computed tomography; HC, healthy control; MMSE, Mini-Mental State Exam; MoCA, Montreal Cognitive Assessment; CDR, clinical dementia rate; CDT, Clock Drawing Test; BNT, Boston Naming Test; TE, echo time; TR, repetition time; TI, inversion time; rsfMRI, resting-state functional MRI; GM, gray matter; WM, white matter; FC, functional connectivity.

techniques that allows the investigation of functional brain networks (Montembeault et al., 2019). A growing body of rs-fMRI research suggests that abnormalities of these networks are associated with presentations of neurological disorders belonging to proteinopathies, such as AD (including PCA) and frontotemporal dementia (including SD) (Pini et al., 2021). With advances in neuroimaging models, it is now clear that the network is distributed (Ghosh, 2020). Pathogenic proteins spreading through large-scale networks produce macroscopic signatures of network dysfunction that might differentiate neurodegenerative diseases (Warren et al., 2013). Brain network FC is considered sensitive and may be a useful non-invasive marker for dementia (Spina et al., 2019).

The main hypotheses in this study are based on factors such as (1) specific regional brain lesions in the two patient groups and relevance of these regions to clinical manifestations; (2) previous studies demonstrating similar language deficits, visual semantic processing, and emotional disorder in the two patient groups; (3) the fact that PCA lacks language network research when SD lacks visual network research; and (4) the necessity of making comparisons about the pattern of network dysfunction on account of different pathology but similar symptoms. Therefore, we showed how FC changes in PCA and SD related to three networks, a “visual network” (atrophied in PCA), a “language network” (atrophied in SD), and a “salience network” (atrophied in SD and both have shown to be altered previously). Then, to explore the role of connectivity from seed to specific regions, we correlated connectivity intensity and neuropsychological features. Finally, we further compared the value of standard uptake value ratio (SUVR) in the specific regions with connectivity altering.

MATERIALS AND METHODS

Participants

A total of 11 patients with PCA, 14 patients with SD, and 11 matched controls were recruited from the Memory Clinic and Neurology Unit, First Affiliated Hospital of Zhejiang University School of Medicine, Hangzhou, China. All participants underwent a detailed clinical history interview and physical examination, neuropsychological assessment, and a (positron emission tomography) PET/MRI scan. All participants were native Chinese speakers, right-handed, and provided written informed consent. This study was approved by the Institutional Ethics Board of the First Affiliated Hospital, Zhejiang University School of Medicine.

Patients With PCA

Participants with PCA fulfilled previously proposed clinical diagnostic criteria (Crutch et al., 2017). Core features included clinical features (insidious onset, gradual progression, and prominent early disturbance of visual functions); cognitive features [space perception deficit, simultanagnosia, object perception deficit, constructional dyspraxia, environmental agnosia, oculomotor apraxia, dressing apraxia, optic ataxia,

alexia, left/right disorientation, acalculia, limb apraxia (not limb-kinetic), apperceptive prosopagnosia, agraphia, homonymous visual field defect, and finger agnosia]—at least three of the following must be present as early or presenting features, with evidences of their impact on activities of daily living, and relatively spared anterograde memory function, speech and non-visual language functions, executive functions and behavior and personality must be evident; neuroimaging features [predominant occipitoparietal or occipitotemporal atrophy/hypometabolism MRI/FDG-PET (2-fluoro-2-deoxy-D-glucose FDG)]; exclusion criteria—evidence of a brain tumor or other mass lesion sufficient to explain the symptoms, significant vascular diseases, including focal stroke sufficient to explain the symptoms, afferent visual cause (e.g., optic nerve, chiasm, or tract), and other identifiable causes for cognitive impairment (e.g., renal failure). All the patients with PCA were fulfilled with pure-PCA.

Patients With SD

Patients with SD had normal or corrected-to-normal hearing and vision, and no history of alcoholism, head trauma, and psychiatric or other neurological illness. The neuropsychological performance and predominant ATL atrophy of each patient met the diagnostic criteria for SD (Gorno-Tempini et al., 2011). For clinical diagnosis of SD, both of the following core features must be present, namely, (1) impaired confrontation naming and (2) impaired single-word comprehension. In addition, at least three of the following other diagnostic features must be present, namely, (1) impaired object knowledge, particular for low-frequency or low-familiarity items, (2) surface dyslexia or dysgraphia, (3) spared repetition, and (4) spared speech production (grammar and motor speech). Imaging-supported SD, including both of the following criteria, must be present, namely, (1) clinical diagnosis of SD and (2) imaging must show one or more of the following results (a, predominant ATL atrophy; b, predominant ATL hypoperfusion or hypometabolism on SPECT or PET).

Healthy Control Subjects

Healthy control subjects also had normal or corrected-to-normal hearing and vision, and no history of alcoholism, head trauma, and psychiatric or neurological illness.

Neuropsychological Assessment

All participants underwent a standardized neuropsychological battery within 7 days of imaging to evaluate cognitive functioning, consisting of assessments of global functioning and language functioning. Patients (PCA or SD groups) and HC groups were compared in each of these domains. Global functioning was measured using the Mini-Mental State Exam (MMSE), Montreal Cognitive Assessment (MoCA), clinical dementia rate (CDR), and Clock Drawing Test (CDT). Language function was evaluated by the Boston Naming Test (BNT) scores.

Imaging Data Collection

All images were performed on a hybrid 3.0-Tesla TOF PET/MRI system (Signa, GE Healthcare), with PET and MR images

simultaneously acquired in 19-channel head and neck union coil. Each patient was required to fast for at least 6 h and then received a manual intravenous injection of ^{18}F -FDG (0.08–0.12 mCi/kg). Then, 45 min after this injection, the patients were placed in the PET/MR scanner, instructed to remain calm in a supine position, and with their eyes closed. All images were completed after 30 min. For 3D BRAVO T1-weighted sequence, the following parameters were applied, namely, echo time (TE) = 3.2 ms; repetition time (TR) = 8.5 ms; 170 sagittal slices; inversion time (TI) = 400 ms; within-plane field of view (FOV) = 256 mm \times 256 mm; flip angle = 15°; voxel size = 1 mm \times 1 mm \times 1 mm; and bandwidth = 240 Hz/pix. For blood oxygenation level-dependent resting-state functional MRI, the following parameters were applied, namely, time point = 200; TR = 2,000 ms; TE = 35 ms; flip angle = 90°; 32 sagittal slices; FOV = 220 mm \times 220 mm; and matrices = 64 \times 64.

Imaging Data Preprocessing

Functional MRI

The resting-state functional MRI (rsfMRI) data preprocessing was performed using the resting-state fMRI toolbox (DPARF) (Yan et al., 2016) based on the Statistical Parametric Mapping 12 (SPM12) on the MATLAB platform (MathWorks, Natick, MA, United States). One patient with PCA was excluded because of incomplete images. The first 10 rsfMRI scans were discarded for the signal equilibrium and subject's adaptation to the scanning noise. The remaining 190 images were corrected for timing differences in slice acquisition. Then, head motion correction was performed. Subjects with more than 3 mm maximum displacement in any of the x, y, or z directions or 3° of any angular motion were discarded. Two participants (SD) did not meet these criteria and were excluded from the initial sample. Then, the rsfMRI data based on rigid-body transformation were subsequently normalized to a Montreal Neurological Institute space using the echo-planar images template (Calhoun et al., 2017) and then resampled into 3 mm \times 3 mm \times 3 mm cubic voxel. Functional images were spatially smoothed with a 6 mm \times 6 mm \times 6 mm Gaussian kernel of full width at half maximum to decrease spatial noise. Linear trends estimation was finally performed.

Structural MRI

The T1 images were preprocessed by using the CAT12 toolbox¹ in SPM12 (Wellcome Trust Centre for Neuroimaging²) (Friston et al., 1995) and was performed on MATLAB software (MathWorks, Natick, MA, United States). Images preprocessing was performed by the CAT12 toolbox under the default setting. First, all 3D T1-weighted MRI scans were normalized using an affine followed by non-linear registration, corrected for bias field inhomogeneities, and then segmented into gray matter (GM), white matter (WM), and cerebrospinal fluid (CSF) components (Ashburner and Friston, 2005). Next, the segmented scans were normalized into a standard MNI space by using the Diffeomorphic Anatomic Registration Through Exponentiated

Lie algebra algorithm (Ashburner, 2007), which can provide more precise spatial normalization to the template.

FDG-PET Data Preprocessing

The PETPVE12 toolbox (PETPVE12: an SPM toolbox for PVE correction in brain PET, application to amyloid imaging with FDG-PET) was used to analyze PET data. First, the structural MRI (T1-weighted) data were segmented into GM, WM, CSF, and skull-stripped image based on the segmentation function of the VBM8 toolbox. Second, the structural MRI (without skull stripping) was used as “reference” images, and FDG-PET images were used as “source image.” Third, a voxel-based method was performed using the three-compartmental algorithm, including GM, WM, and CSF, which is described as Muller-Gartner et al. (1992) (MG) (Muller-Gartner et al., 1992) or “modified Müller-Gärtner” (mMG) (Rousset et al., 1998) to correct the PVE of the PET images.

Seed-Based FC

Seed regions of interest (ROIs) were based on previous studies using the DynamicBC toolbox (Liao et al., 2014). On account of the changing mode of connectivity that was reported in the two diseases, seeds were selected based on previous studies for primary visual network [left V1 (−11, −81, 7) and right V1 (11, −78, 9)] (Glick-Shames et al., 2019), language network [left ATL (39, 15, −33) and left posterior superior temporal gyrus (−49, −9, 6)] (Migliaccio et al., 2016; Montembeault et al., 2019), and salience network [left anterior insula (−32, 24, −6) and right anterior insula (37, 25, −4)] (Fredericks et al., 2019). The seed regions were 4-mm radius centered at the peak. For each seed, correlations were calculated between the averaged signal from the seed and each individual ROI across the brain to configure a statistical map.

Statistical Analysis

Quantitative variables are expressed as the mean and standard deviation except gender. The categorical variables are given as absolute and relative frequencies. All statistical analyses were performed using the IBM SPSS26.0 statistical software for Windows. Regarding the demographics, the chi-square test was used for gender distribution difference assessment ($p < 0.05$). We then used the analysis of two-sample t -test to compare the education, age, and neuropsychological scales among all groups.

Voxel-wise statistical analyses of FC, GM, and FDG-PET SUVR were conducted by DPABI toolbox. The effect of group on FC was assessed using the two-sample t -test, controlled for age, gender, and years of education. Comparison of FC maps was restricted to the GM areas, and the Gaussian random field (GRF) method was applied to multiple-comparison correction. The statistical threshold was set at $p < 0.005$ with a cluster-level $p < 0.05$ (two-tailed). To test the clinical significance, we also correlated mean FC values from the clusters with neuropsychological scales by partial correlation analysis, controlled for age, gender, years of education, and FC values in seed ROIs. The relationship between FC values and cognitive test scores is presented as a scatter diagram drawn using GraphPad Prism 8.0. The ROI with FC discrepancy was used as template to

¹<http://dbm.neuro.uni-jena.de/cat/>

²<http://www.fil.ion.ucl.ac.uk/spm/>

extract the SUVR of FDG-PET and then compared between the two groups using two-sample *t*-test.

RESULTS

Demographic and Clinical Characteristics

There were no statistically significant differences in gender, age, or education between patients (PCA or SD) and controls ($p > 0.05$), except that patients with SD were older than controls ($p = 0.017$). The age comparison between PCA and SD was also significant ($p = 0.019$). There were substantial differences in neuropsychological scores between patients (PCA or SD) and controls ($p < 0.001$). Detailed information can be found in **Table 1**. Patients with PCA and SD performed worse across global cognitive function, BST, and CDT tests. Patients with PCA performed significantly worse than SD in neuropsychological CDT scores ($p = 0.001$), whereas other neuropsychological tests had no significant differences between the two groups.

Seed-Based FC

First, to compare with controls, taking the left V1 region in visual network as seed, PCA showed decreased FC between this region and left precentral gyrus (**Figure 1A**). Meanwhile, the FC was significantly increased between the right V1 seed and the right inferior frontal gyrus (**Figure 1B**). Taking the left ATL in language network as seed, patients with PCA showed increased FC to right medial frontal gyrus (**Figure 1D**). Left post superior temporal gyrus, as another seed in the language network, showed increased FC from this region to left fusiform in patients with PCA (**Figure 1E**). Increased FC was also significant between left anterior insula SN seed to left superior temporal gyrus (**Figure 1C**).

Second, compared with controls, changes in the SD group are more focused on the temporal lobe. Decreased FC has been showed from the left ATL seed in the language network to the right superior frontal gyrus (**Figure 1G2**), as well as another

language seed post-superior temporal gyrus to right middle frontal gyrus and right superior temporal gyrus (**Figure 1H**), whereas increased FC was showed from left ATL to the right superior temporal gyrus (**Figure 1G1**). Interestingly, taking the anterior insula in the salience network as the seed, patients with SD showed increased FC from right side to right insula and left anterior cingulum, and decreased FC from right seed to left superior frontal gyrus. However, the left seed did not have significant change (**Figure 1F**). Besides, left and right V1 regions in visual network did not have significant FC change in patients with SD either. Detailed information can be found in **Tables 2, 3**.

The comparisons between PCA and SD have found that PCA showed decreased FC from left ATL to bilateral middle occipital gyrus, as well as from right V1 to bilateral anterior cingulum (**Supplementary Figure 1**).

Relationship Between FC and Neuropsychological Performance

The global two groups (one patient group and controls) showed significant and strong correlations between neuropsychological measures and regional mean FC intensity. All the regional mean FCs were significant in the relative two groups. Positive correlations were found with regions showing diminished FC from seed, and negative correlations were found with regions showing increased FC from seed. However, the patient group alone was hardly seen significant correlations between neuropsychological measures and regional mean FC intensity both in PCA and SD, and the significant relations were only in PCA. Detailed information can be found in **Figures 2, 3**, **Supplementary Figure 2**, **Table 4**, and **Supplementary Table 1**.

The Patterns of Atrophy and FDG-PET in Patients With PCA and SD

The patients with PCA shared a large region of brain atrophy mainly including bilateral associative parietooccipital, temporal regions, precuneus, and posterior cingulate, extending to frontal regions (**Supplementary Figure 3**). Patients with SD showed

TABLE 1 | Demographic and neuropsychological data.

| Demographic characteristics | NC N = 11 | PCA N = 10 | SD N = 12 | PCA vs NC P value | SD vs NC P value | PCA vs SD P value |
|-----------------------------|----------------|----------------|----------------|----------------------|---------------------|----------------------|
| Sex | 3:8 | 6:4 | 4:8 | 0.291 | 0.100 | 0.391 |
| M:F | | | | | | |
| Age (years) | 60.00 ± 6.387 | 59.70 ± 6.865 | 66.67 ± 5.944 | 0.918 | 0.017 | 0.019 |
| Education (years) | 8.82 ± 1.991 | 10.20 ± 4.756 | 6.50 ± 3.826 | 0.588 | 0.094 | 0.057 |
| MMSE | 25.64 ± 2.541 | 15.30 ± 5.376 | 14.33 ± 6.329 | < 0.001 | <0.001 | 0.707 |
| MoCA | 23.45 ± 2.252 | 9.90 ± 5.216 | 10.08 ± 4.833 | < 0.001 | <0.001 | 0.933 |
| CDR | 0.045 ± 0.1508 | 1.800 ± 0.6325 | 1.333 ± 0.6155 | < 0.001 | <0.001 | 0.096 |
| BNT | 22.82 ± 1.662 | 13.50 ± 4.927 | 10.42 ± 5.178 | < 0.001 | <0.001 | 0.171 |
| CDT | 4.00 ± 0.000 | 0.80 ± 0.632 | 2.25 ± 1.215 | < 0.001 | <0.001 | 0.003 |

Data are presented as means ± standard deviations except for sex (male to female ratio).

NC, normal control; PCA, posterior cortical atrophy; SD, semantic dementia; MMSE, Mini-Mental State Examination; MoCA, Montreal Cognitive Assessment; CDR, clinical dementia rating; BNT, Boston Naming Test; CDT, Clock Drawing Test.

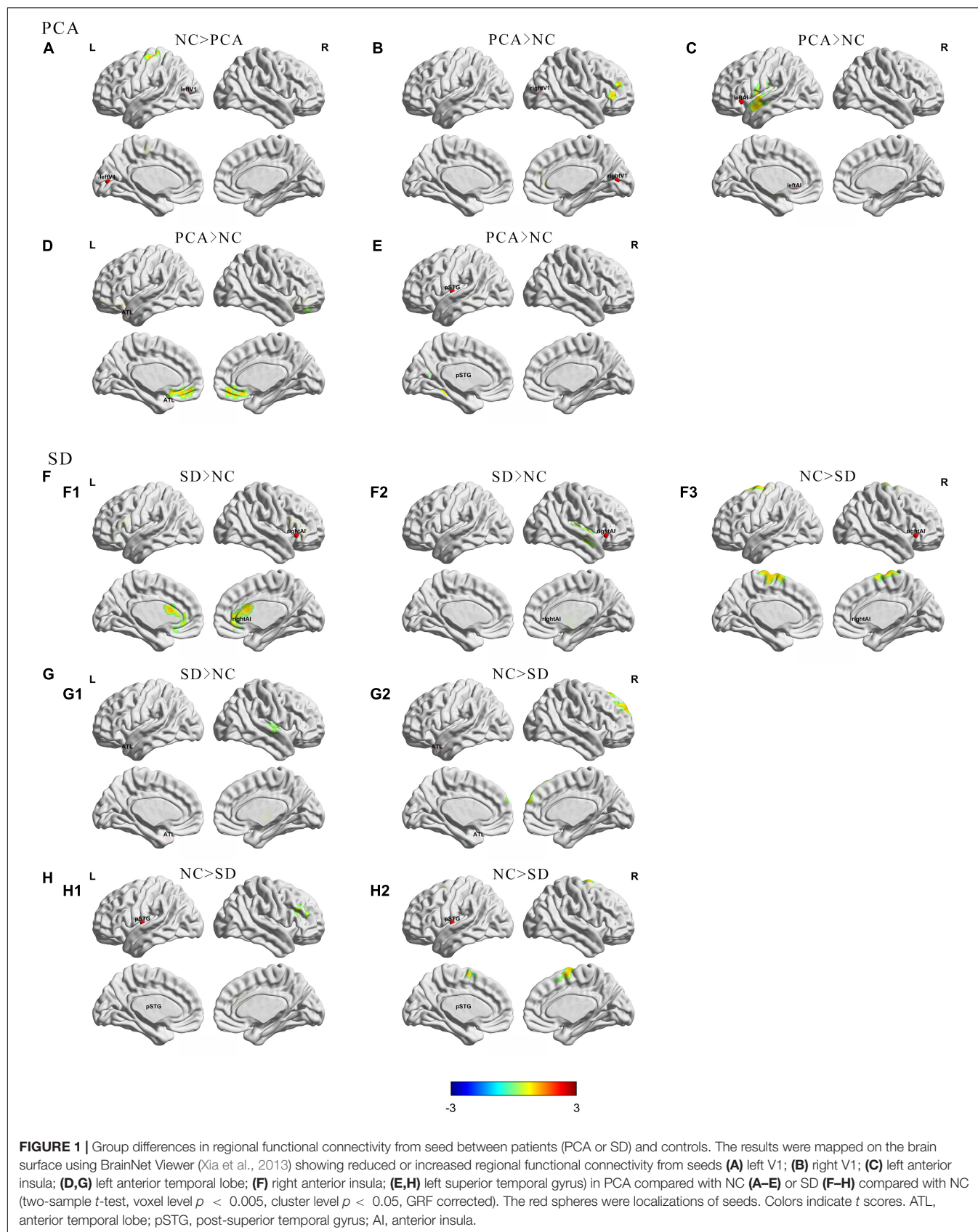


TABLE 2 | Regions of changed resting state functional connectivity in patients with PCA compared with healthy controls.

| Seeds | Clusters | | | | | |
|------------------------------|------------------------------|-----|-----|-----|------------------|----------------|
| | Peak regions | x | y | z | Number of voxels | Peak intensity |
| Left anterior temporal lobe | Right medial frontal gyrus | 9 | 45 | -15 | 131/232 | 5.3305 |
| Left anterior insula | Left superior temporal gyrus | -57 | -3 | 0 | 111/231 | 5.7633 |
| Left superior temporal gyrus | Left fusiform | -33 | -19 | -15 | 74/188 | 5.318 |
| Left V1 | Left precentral areas | -36 | -24 | 60 | 71/169 | -6.5434 |
| Right V1 | Right inferior frontal gyrus | 57 | 39 | 15 | 93/174 | 5.0356 |

Coordinates (x, y, z) are in Montreal Neurological Institute space. Results are shown at $p < 0.05$ GRF corrected.

TABLE 3 | Regions of changed resting state functional connectivity in patients with SD compared with healthy controls.

| Seeds | Clusters | | | | | |
|------------------------------|-------------------------------|----|-----|----|------------------|----------------|
| | Peak regions | x | Y | z | Number of voxels | Peak intensity |
| Left anterior temporal lobe | Right superior frontal gyrus | -2 | 63 | 36 | 158/225 | -6.0639 |
| | Right superior temporal gyrus | 39 | -21 | -3 | 60/138 | 6.3062 |
| right anterior insula | Right insula | 45 | -3 | -9 | 59/158 | 4.9877 |
| | Left superior frontal gyrus | -3 | -15 | 72 | 141/382 | -6.44 |
| | Left anterior cingulum | 0 | 18 | 21 | 70/186 | 7.176 |
| left superior temporal gyrus | Left middle frontal gyrus | 27 | 30 | 33 | 70/105 | -5.6875 |
| | Right superior frontal gyrus | 9 | -3 | 72 | 91/145 | -5.7519 |

Coordinates (x, y, z) are in Montreal Neurological Institute space. Results are shown at $p < 0.05$ GRF corrected.

brain atrophy mainly in bilateral temporal, insula, and frontal regions (**Supplementary Figure 3**). Compared to patients with SD, the atrophy of PCA was more severe in left temporal regions (**Supplementary Figure 3**).

Similarly, patients with PCA showed hypometabolism mainly in bilateral parietal, occipital, temporal regions and precuneus, with extension to a part of frontal regions; hypometabolism in SD was primarily distributed in bilateral temporal and frontal areas (**Supplementary Figure 4**). To compare PCA with SD, patients with PCA showed that hypometabolism was in bilateral parietal, occipital, and left temporal lobe, and hypermetabolism was in the right temporal and bilateral frontal lobe (**Supplementary Figure 4**). In contrast to controls, based on regions with FC abnormality, patients with PCA showed hypometabolism in the left superior temporal gyrus, fusiform, superior frontal gyrus, middle frontal gyrus, and precentral areas, as well as right inferior

frontal gyrus, superior temporal gyrus, and insula ($p < 0.05$). Meanwhile, patients with SD showed hypometabolism in the left temporal superior gyrus, superior frontal gyrus, and right frontal superior gyrus, right insula ($p < 0.05$). Detailed information can be found in **Table 5**.

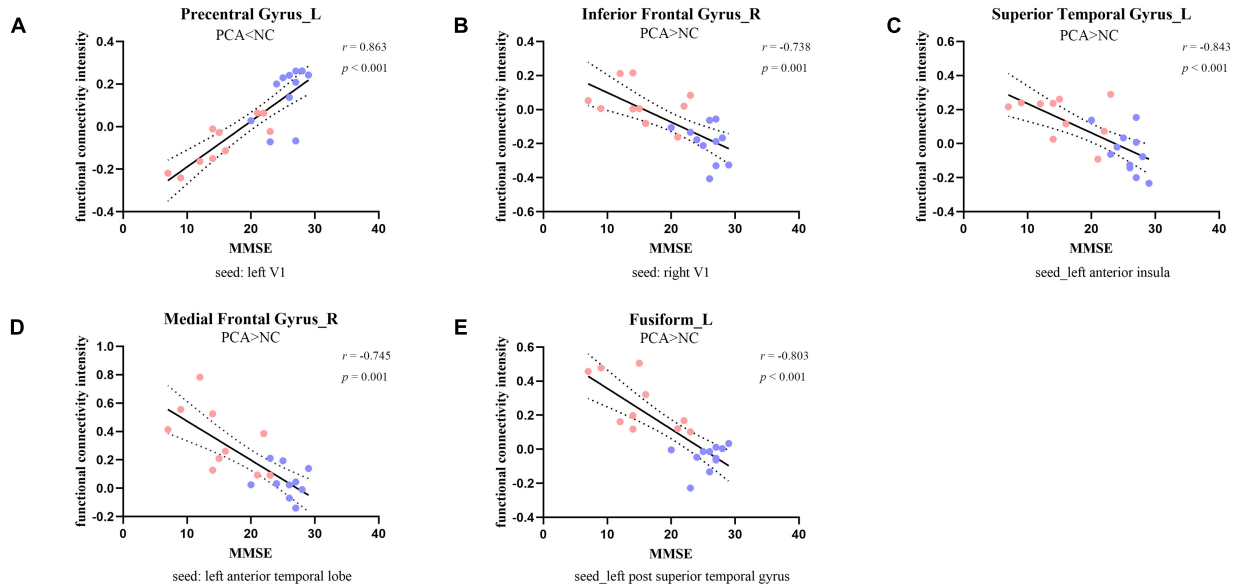
DISCUSSION

We examined the characteristics involving the visual, language, and salience network in patients with SD or PCA. The major findings of this study are (1) patients with PCA would be impaired in language functions, such as naming; (2) patients with PCA have performed functional impairment involving visual network, while patients with SD have not; (3) patients with PCA and SD showed FC change from seed in language network and salience network to other regions, and the patterns of SD were more diffused than PCA; (4) hyperconnectivity, in general, was the main pattern in patients with PCA, whereas the hypo- and hyperconnectivity were level pegging in patients with SD; and (5) the hypometabolism and atrophy were disease-specific patterns in patients with PCA and SD widespread in posterior area of PCA but restricted in the temporal-frontal area of SD.

We found that PCA had language declining alike SD. Although the consensus required relatively spared speech and non-visual language functions, it emphasized the contrast between the posterior cortical dysfunction and the relative sparing of other cognitive domains, aiming to distinguish PCA from lvPPA (Crutch et al., 2017). Crutch et al. (2013) concluded that PCA was characterized by a progressive oral language dysfunction such as degradation of vision, literacy, and numeracy, and had prominent difficulties in word retrieval. Additionally, previous studies verified that patients with PCA would be impaired in semantic word processing, and spatial preposition disposing was even worse than SD, which could be due to the dysfunction of posterior regions in PCA (Shebani et al., 2017). It indicated that the specific regions of PCA are critical for word processing. A case-control study showed that most patients with PCA had non-language domain learning disabilities, whereas 27.8% presented with language-only learning disabilities (Miller et al., 2018). Therefore, despite the prominent deficits in visual domain, language damage exists in PCA. Characterizing and quantifying the aphasia associated with PCA is vital for clarifying differential diagnoses for clinical and research studies.

Consistent with the study that used bilateral V1 region as seeds (Glick-Shames et al., 2019), FC deficits in our PCA cohort were also observed compared to healthy controls. The previous study has seen reduced connections between V1 and higher visual areas, as well as between V1 and the frontal eye field (precentral gyrus) (Glick-Shames et al., 2019). Likewise, our study also showed reduced connections between left V1 and left precentral areas, known to be involved in control of eye movement and visual attention, which might account for the attentional/frontal deficits of this clinical syndrome. It seems that our FC results in the PCA suggest more localized damage. It is important to note that the seeds used in our study are based on a previous study

PCA



SD

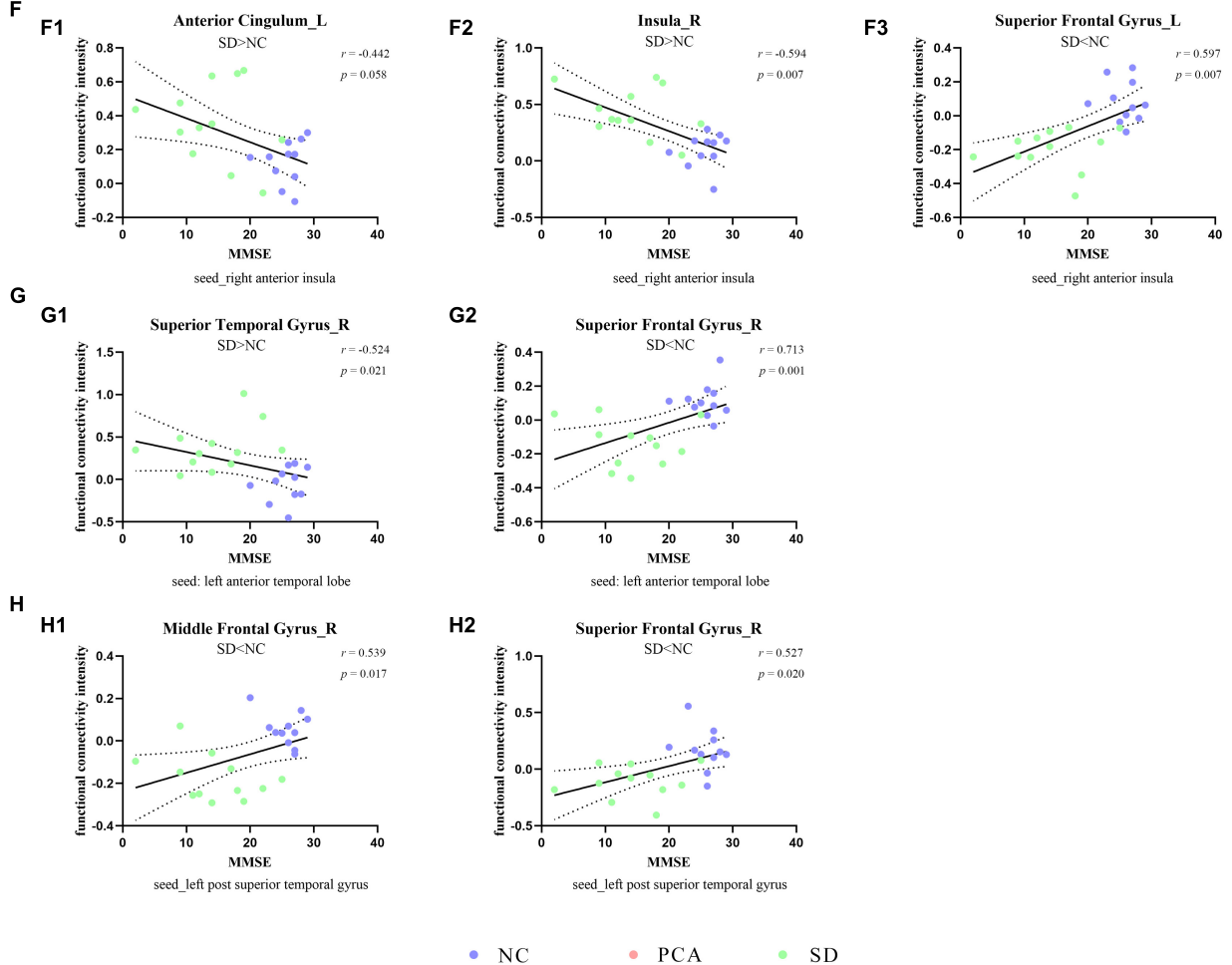


FIGURE 2 | Correlation between functional connectivity and global cognition. The scatterplots illustrate the associations between MMSE scores and intensity of functional connectivity in patients [PCA (A–E) or SD (F–H)] and controls based on different seeds [(A) left V1, (B) right V1, (C) left anterior insula, (D,G) left anterior temporal lobe, (F) right anterior insula, and (E,H) left superior temporal gyrus].

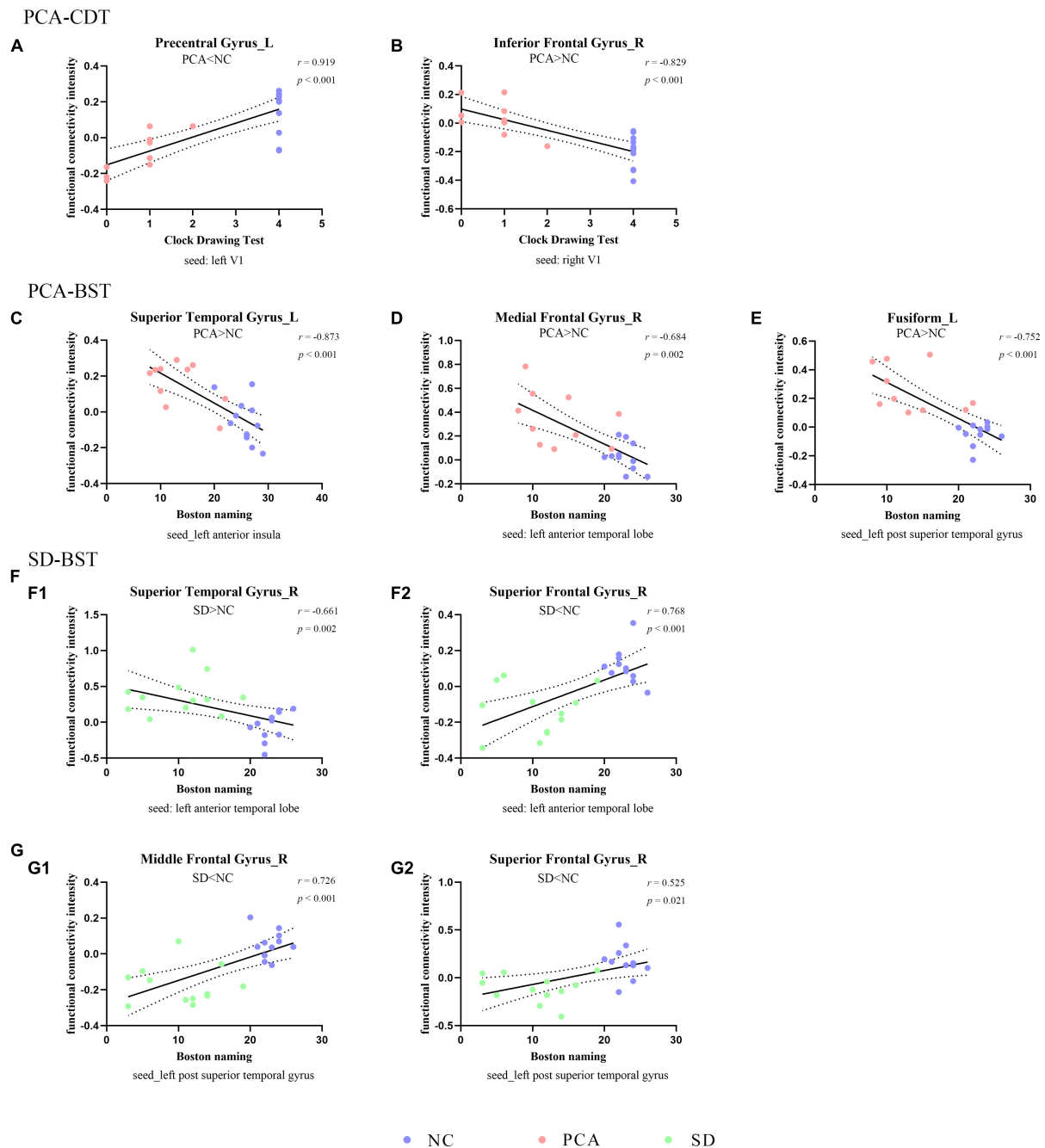


FIGURE 3 | Correlation between functional connectivity and subdomain of cognition. The scatterplots illustrate the associations between CDT (A,B) or BST (C–G) and intensity of functional connectivity in patients (PCA: A–E or SD: F–G) and controls based on different seeds [(A) left V1, (B) right V1, (C) left anterior insula, (D,F) left anterior temporal lobe, and (E,G) left superior temporal gyrus].

(Glick-Shames et al., 2019). However, the patient cohort differed between our study and previous study in various aspects. The aberrant communication in response to brain damage and neural resilience during the disease stage is heterogeneity in diverse patient groups (Agosta et al., 2018). Then, possibly, the central regions, either within or between networks, are interconnected flexibly and the change may not synchronize (Pini et al., 2021).

Further studies using longitudinal data are required to better understand the origin and spread of FC changes in PCA.

Besides, relative to controls, increased connectivity was apparent in our seed-voxel analysis showing intra- or inter-hemisphere of patients with PCA. Apart from right V1 and right inferior frontal gyrus, left ATL and right medial frontal gyrus, left superior temporal gyrus and left fusiform, as well as

TABLE 4 | Partial correlation analysis between functional connectivity intensity and neuropsychological scales.

| Functional connectivity changing groups | Clusters (seeds) | Neuropsychological scales | | | |
|---|---|-------------------------------|-------------------------------|-------------------------------|-------------------------------|
| | | MMSE | MoCA | BST | CDT |
| PCA compared to NC | Right medial frontal gyrus (left anterior temporal lobe) | $r = -0.745$, $p = 0.001$ | $r = -0.826$, $p < 0.001$ | $r = -0.684$, $p = 0.002$ | $r = -0.824$, $p < 0.001$ |
| | PCA > NC | | | | |
| | Left superior temporal gyrus (left anterior insula) | $r = -0.843$, $p < 0.001$ | $r = -0.867$, $p < 0.001$ | $r = -0.873$, $p < 0.001$ | $r = -0.890$, $p < 0.001$ |
| | PCA > NC | | | | |
| | Left fusiform (left superior temporal gyrus) | $r = -0.803$, $p < 0.001$ | $r = -0.794$, $p < 0.001$ | $r = -0.752$, $p < 0.001$ | $r = -0.831$, $p < 0.001$ |
| | PCA > NC | | | | |
| | Left precentral areas (left V1) | $r = 0.863$, $p < 0.001$ | $r = 0.922$, $p < 0.001$ | $r = 0.892$, $p < 0.001$ | $r = 0.919$, $p < 0.001$ |
| | PCA < NC | | | | |
| SD compared to NC | Right inferior frontal gyrus (right V1) | $r = -0.738$, $p = 0.001$ | $r = -0.824$, $p < 0.001$ | $r = -0.780$, $p < 0.001$ | $r = -0.829$, $p < 0.001$ |
| | PCA > NC | | | | |
| | Right superior frontal gyrus (left anterior temporal lobe) | $r = 0.713$, $p = 0.001$ | $r = 0.771$, $p < 0.001$ | $r = 0.768$, $p < 0.001$ | $r = 0.648$, $p = 0.003$ |
| | SD < NC | | | | |
| | Right superior temporal gyrus (left anterior temporal lobe) | $r = -0.524$, $p = 0.021$ | $r = -0.642$, $p = 0.003$ | $r = -0.661$, $p = 0.002$ | $r = -0.518$, $p = 0.023$ |
| | SD > NC | | | | |
| | Right insula (right anterior insula) | $r = -0.594$, $p = 0.007$ | $r = -0.661$, $p = 0.002$ | $r = -0.651$, $p = 0.003$ | $r = -0.627$, $p = 0.004$ |
| | SD > NC | | | | |
| | Left superior frontal gyrus (right anterior insula) | $r = 0.597$, $p = 0.007$ | $r = 0.659$, $p = 0.002$ | $r = 0.699$, $p = 0.001$ | $r = 0.590$, $p = 0.008$ |
| | SD < NC | | | | |
| | Left anterior cingulum (right anterior insula) | $r = -0.442$, $p = 0.058$ | $r = -0.525$, $p = 0.021$ | $r = -0.492$, $p = 0.032$ | $r = -0.483$, $p = 0.036$ |
| | SD > NC | | | | |
| | Right middle frontal gyrus (left superior temporal gyrus) | $r = 0.539$, $p = 0.017$ | $r = 0.611$, $p = 0.005$ | $r = 0.726$, $p < 0.001$ | $r = 0.535$, $p = 0.018$ |
| | SD < NC | | | | |
| | Right superior frontal gyrus (left superior temporal gyrus) | $r = 0.527$, $p = 0.020$ | $r = 0.544$, $p = 0.016$ | $r = 0.525$, $p = 0.021$ | $r = 0.541$, $p = 0.017$ |
| | SD < NC | | | | |

NC, normal control; PCA, posterior cortical atrophy; SD, semantic dementia; MMSE, Mini-Mental State Examination; MoCA, Montreal Cognitive Assessment; BNT, Boston Naming Test; CDT, Clock Drawing Test.

anterior insula and left superior temporal region have all seen FC increasing, and these increased FC intensities were negatively correlated to cognition. Although the anterior regions have not atrophied, the brain FC involves language and salience network. It has been reported that patients with PCA showed increased connectivity between key nodes of SN than controls, which is thought to play a role in social-emotional functioning (Fredericks et al., 2019). We first used seeds in language network to explore the brain FC change in patients with PCA, and its negative correlations to global cognitive scores and Boston Naming scores could explain the language deficits in PCA.

As expected, there were no significant differences in patients with SD compared to controls when using bilateral V1 region as seeds. However, seeds in language and salience networks have shown more regions that had FC change. It is worth emphasizing that ATL is the semantic “hub” and principle of semantic topography, which employs structure and connectivity of frontotemporal cortex (Pulvermuller et al., 2010). Hence, a series of studies used ATL as the seed to do the connectivity research (Guo et al., 2013; Wilson et al., 2014; Montembeault et al., 2019); one of these studies presented decreased FC between the left ATL and the cluster, including left post middle temporal gyrus, right medial orbitofrontal cortex and right medial superior frontal gyrus (Montembeault et al., 2019). In accordance with the study, our SD cohorts showed reduced connectivity between the left ATL and right superior frontal gyrus. Although it is not a critical language region, this region has been consistently

reported as functionally connected to key regions of the language network (Hurley et al., 2015). Additionally, our study also observed decreased FC between the left superior temporal gyrus and right superior frontal gyrus. It indicated that right superior frontal gyrus might be essential to SD.

Few studies focused on salience network in patients with SD. Day et al. (2013) found that low-frequency fluctuations in the insula could predict behavioral changes in patients with frontotemporal dementia, including SD. We initially used anterior insula in the salience network as the seed, finding that connection from seed to right insula showed increased FC. It reminded that the intrinsic connectivity was increased within salience network in SD. Moreover, salience network FC is a critical neurological mechanism underlying interpersonal warmth (Toller et al., 2019). How the specific circuit of network works in patients with SD requires further research.

Except for diminished FC, there were increased brain FC in patients with PCA and SD, inversely correlated to cognition. The FC seeded by brain regions was vulnerable to any distinct neurodegenerative diseases, and the regions with higher connectional flow revealed greater disease-related vulnerability (Zhou et al., 2012). Neuroimmune may be a potential etiopathogenesis of dementia as the cascade of immune responses can occur as long as there is a neuronal injury or a potent immune stimulation (Cacabelos et al., 2016). A recent study showed how to link the FC with neuroinflammation with the combination of [^{11}C]PK11195 PET and resting-state functional MRI. The

TABLE 5 | Averaged ^{18}F -FDG SUVR in cluster with abnormal connectivity to seed in normal controls and patients with PCA and SD.

| Functional connectivity changing groups | Clusters (seeds) | SUVR value | | | P value | | |
|---|---|-------------|-------------|-------------|-----------|----------|-----------|
| | | NC | PCA | SD | PCA vs NC | SD vs NC | PCA vs SD |
| PCA compared to NC | Right medial frontal gyrus (left anterior temporal lobe) PCA > NC | 0.66 ± 0.09 | 0.67 ± 0.07 | 0.49 ± 0.05 | 0.757 | 0.971 | < 0.001 |
| | Left superior temporal gyrus (left anterior insula) PCA > NC | 0.56 ± 0.08 | 0.43 ± 0.10 | 0.45 ± 0.11 | 0.003 | 0.009 | 0.726 |
| | Left fusiform (left superior temporal gyrus) PCA > NC | 0.12 ± 0.06 | 0.01 ± 0.05 | 0.05 ± 0.09 | < 0.001 | 0.029 | 0.199 |
| | Left precentral areas (left V1) PCA < NC | 0.59 ± 0.08 | 0.44 ± 0.12 | 0.59 ± 0.12 | 0.004 | 0.999 | 0.011 |
| | Right inferior frontal gyrus (right V1) PCA > NC | 0.49 ± 0.09 | 0.39 ± 0.06 | 0.40 ± 0.16 | 0.010 | 0.105 | 0.944 |
| SD compared to NC | Right superior frontal gyrus (left anterior temporal lobe) SD < NC | 0.61 ± 0.09 | 0.53 ± 0.13 | 0.46 ± 0.12 | 0.148 | 0.005 | 0.234 |
| | Right superior temporal gyrus (left anterior temporal lobe) SD > NC | 0.53 ± 0.10 | 0.45 ± 0.09 | 0.40 ± 0.11 | 0.08 | 0.01 | 0.279 |
| | Right insula (right anterior insula) SD > NC | 0.40 ± 0.10 | 0.22 ± 0.08 | 0.94 ± 0.18 | 0.091 | < 0.001 | 0.003 |
| | Left superior frontal gyrus (right anterior insula) SD < NC | 0.60 ± 0.09 | 0.48 ± 0.13 | 0.37 ± 0.14 | 0.023 | < 0.001 | 0.059 |
| | Left anterior cingulum (right anterior insula) SD > NC | 0.45 ± 0.15 | 0.39 ± 0.15 | 0.46 ± 0.17 | 0.345 | 0.920 | 0.316 |
| | Left middle frontal gyrus (left superior temporal gyrus) SD < NC | 0.66 ± 0.10 | 0.49 ± 0.10 | 0.61 ± 0.17 | 0.001 | 0.414 | 0.083 |
| | Right superior frontal gyrus (left superior temporal gyrus) SD < NC | 0.57 ± 0.15 | 0.48 ± 0.16 | 0.55 ± 0.18 | 0.203 | 0.777 | 0.353 |

SUVR values are presented as means ± standard deviations.

NC, normal control; PCA, posterior cortical atrophy; SD, semantic dementia.

results showed that the region with higher ^{11}C PK11195 binding values in individuals also showed increased connectivity between the default mode network, hippocampus, and other subcortical regions, mediating cognitive deficits in AD cohorts (Passamonti et al., 2019). Therefore, the change in increased FC may become a strong risk factor for PCA and SD.

^{18}F -FDG-PET, as a potential sensitive molecular imaging marker indicating neuronal damage, is useful in subtyping dementia and helpful in managing patients, especially patients with early-onset dementia (Mukku et al., 2019). Both PCA and SD belong to early-onset dementia. With these two dementias characterized by the presence of disease-specific protein aggregates in and around neuronal cells, the neuroimaging-derived indexes may potentially reveal distinct neuropathological processes. Increasing evidence supports that before protein aggregates spread in preexisting networks they developed in topographic patterns (Seeley et al., 2009; Hodges et al., 2010; Bejanin et al., 2019). These neuropathological lesions were partly reflected in GM atrophy and hypometabolism (Bejanin et al., 2019). We compared the topographic discrepancies based on FC change regions in PCA and SD, showing that PCA has a more extended pattern of hypometabolism while SD is restricted in regions of temporal-frontal area. The results were consistent with the pattern of atrophy in our findings and previous studies (Montembeault et al., 2018; Duignan et al., 2021). Altogether, the disease-specific pattern might be suggested, whereas

region-specific pattern might also be reflected as an obvious overlapping area in temporal lobe (e.g., language modality).

There are some limitations to this study. The size of our PCA and SD groups was relatively small, which limited the statistical power of our analyses. Consequently, the significant effects of these two groups might have been overestimated and need replication by an independent, ideally larger sample of PCA and SD. Second, the consistency between the connectivity results and the symptomatology suggested that the results are valuable for further studies. More specific language and semantic abilities (visual or non-visual) were not investigated. Future studies are required with more fine-grained tasks. One methodological limitation was that we just used FC to measure the topological attributes of the network.

CONCLUSION

Based on global cognition degeneration, language deficits existed in both PCA and SD groups. The finding that patients with PCA had abnormal connectivity spreading over the cortex involving visual, language, and salience network also matched the observation that they showed several cognitive deficits. In contrast, the aberrant connectivity in patients with SD was restricted to frontal and temporal lobes, relating to the symptomatology. This study demonstrates that the progression of

PCA and SD is determined not only by GM atrophy localization and distinct symptomatology, but also by the connectivity of the functional network. In general, regarding focal syndrome, the FC change involving visual network was specific to PCA, whereas SD was restricted to temporal and frontal areas.

DATA AVAILABILITY STATEMENT

The original contributions presented in the study are included in the article/**Supplementary Material**, further inquiries can be directed to the corresponding author/s.

ETHICS STATEMENT

The studies involving human participants were reviewed and approved by the First Affiliated Hospital, Zhejiang University School of Medicine. The patients/participants provided their written informed consent to participate in this study.

AUTHOR CONTRIBUTIONS

YC collected the data, designed the study, and wrote the first draft of the article. QZ analyzed the MRI data and wrote the

protocol. XL and KL assisted with study design and interpretation of findings. YW, YS, LZ, and XL collected clinical and MRI data. GP and MZ revised the manuscript for content, analysis and interpretation of data, and accept responsibility for conduct of research and final approval. All authors have contributed to and approved the final article.

FUNDING

This study was funded by the National Natural Science Foundation (82071182) and Zhejiang Provincial Natural Science Foundation (LY20H090014).

ACKNOWLEDGMENTS

We thank the patients and subjects for participating in this study.

SUPPLEMENTARY MATERIAL

The Supplementary Material for this article can be found online at: <https://www.frontiersin.org/articles/10.3389/fnagi.2022.850977/full#supplementary-material>

REFERENCES

- Agosta, F., Mandic-Stojmenovic, G., Canu, E., Stojkovic, T., Imperiale, F., Caso, F., et al. (2018). Functional and structural brain networks in posterior cortical atrophy: a two-centre multiparametric MRI study. *Neuroimage Clin.* 19, 901–910. doi: 10.1016/j.nicl.2018.06.013
- Ashburner, J. (2007). A fast diffeomorphic image registration algorithm. *Neuroimage* 38, 95–113. doi: 10.1016/j.neuroimage.2007.07.007
- Ashburner, J., and Friston, K. J. (2005). Unified segmentation. *Neuroimage* 26, 839–851. doi: 10.1016/j.neuroimage.2005.02.018
- Bejanin, A., La Joie, R., Landeau, B., Belliard, S., de La Sayette, V., Eustache, F., et al. (2019). Distinct interplay between atrophy and hypometabolism in alzheimer's versus semantic dementia. *Cereb. Cortex* 29, 1889–1899. doi: 10.1093/cercor/bhy069
- Cacabelos, R., Torrellas, C., Fernandez-Novoa, L., and Aliev, G. (2016). Neuroimmune crosstalk in CNS disorders: the histamine connection. *Curr. Pharm. Des.* 22, 819–848. doi: 10.2174/1381612822666151209150954
- Calhoun, V. D., Wager, T. D., Krishnan, A., Rosch, K. S., Seymour, K. E., Nebel, M. B., et al. (2017). The impact of T1 versus EPI spatial normalization templates for fMRI data analyses. *Hum. Brain Mapp.* 38, 5331–5342. doi: 10.1002/hbm.23737
- Collins, J. A., Montal, V., Hochberg, D., Quimby, M., Mandelli, M. L., Makris, N., et al. (2017). Focal temporal pole atrophy and network degeneration in semantic variant primary progressive aphasia. *Brain* 140, 457–471. doi: 10.1093/brain/aww313
- Crutch, S. J., Lehmann, M., Warren, J. D., and Rohrer, J. D. (2013). The language profile of posterior cortical atrophy. *J. Neurol. Neurosurg. Psychiatry* 84, 460–466. doi: 10.1136/jnnp-2012-303309
- Crutch, S. J., Schott, J. M., Rabinovici, G. D., Murray, M., Snowden, J. S., van der Flier, W. M., et al. (2017). Consensus classification of posterior cortical atrophy. *Alzheimer's Dementia* 13, 870–884. doi: 10.1016/j.jalz.2017.01.014
- Day, G. S., Farb, N. A. S., Tang-Wai, D. F., Masellis, M., Black, S. E., Freedman, M., et al. (2013). Salience network resting-state activity: Prediction of frontotemporal dementia progression. *JAMA Neurol.* 70, 1249.
- Ding, J., Chen, K., Liu, H., Huang, L., Chen, Y., Lv, Y., et al. (2020). A unified neurocognitive model of semantics language social behaviour and face recognition in semantic dementia. *Nat. Commun.* 11:2595. doi: 10.1038/s41467-020-16089-9
- Duignan, J. A., Haughey, A., Kinsella, J. A., and Killeen, R. P. (2021). Molecular and anatomical imaging of dementia with lewy bodies and frontotemporal lobar degeneration. *Semin. Nucl. Med.* 51, 264–274. doi: 10.1053/j.semnuclmed.2020.12.002
- Firth, N. C., Primativo, S., Marinescu, R., Shakespeare, T. J., Suarez-Gonzalez, A., Lehmann, M., et al. (2019). Longitudinal neuroanatomical and cognitive progression of posterior cortical atrophy. *Brain* 142, 2082–2095. doi: 10.1093/brain/awz136
- Fredericks, C. A., Brown, J. A., Deng, J., Kramer, A., Ossenkoppele, R., Rankin, K., et al. (2019). Intrinsic connectivity networks in posterior cortical atrophy: a role for the pulvinar? *Neuroimage. Clinical* 21:101628. doi: 10.1016/j.nicl.2018.101628
- Friston, K. J., Ashburner, J., Frith, C. D., Poline, J. B., Heather, J. D., and Frackowiak, R. S. J. (1995). Spatial registration and normalization of images. *Hum. Brain Mapp.* 3, 165–189. doi: 10.1002/hbm.460030303
- Ghosh, A. (2020). Language breakdown in primary progressive aphasia. *Ann. Indian Acad. Neurol.* 23(Suppl. 2), S67–S72. doi: 10.4103/aian.AIAN_715_20
- Glick-Shames, H., Backner, Y., Bick, A., Raz, N., and Levin, N. (2019). The impact of localized grey matter damage on neighboring connectivity: posterior cortical atrophy and the visual network. *Brain Imaging Behav.* 13, 1292–1301. doi: 10.1007/s11682-018-9952-7
- Gorno-Tempini, M. L., Hillis, A. E., Weintraub, S., Kertesz, A., Mendez, M., Cappa, S. F., et al. (2011). Classification of primary progressive aphasia and its variants. *Neurology* 76, 1006–1014. doi: 10.1212/WNL.0b013e31821103e6
- Guo, C. C., Gorno-Tempini, M. L., Gesierich, B., Henry, M., Trujillo, A., Shany-Ur, T., et al. (2013). Anterior temporal lobe degeneration produces widespread network-driven dysfunction. *Brain* 136, 2979–2991. doi: 10.1093/brain/awt222
- Hodges, J. R., Mitchell, J., Dawson, K., Spillantini, M. G., Xuereb, J. H., McMonagle, P., et al. (2010). Semantic dementia: demography, familial factors and survival in a consecutive series of 100 cases. *Brain* 133(Pt 1), 300–306. doi: 10.1093/brain/awp248
- Holden, S. K., Bettcher, B. M., and Pelak, V. S. (2020). Update on posterior cortical atrophy. *Curr. Opin. Neurol.* 33, 68–73. doi: 10.1097/WCO.0000000000000767

- Hurley, R. S., Bonakdarpour, B., Wang, X., and Mesulam, M. M. (2015). Asymmetric connectivity between the anterior temporal lobe and the language network. *J. Cogn. Neurosci.* 27, 464–473. doi: 10.1162/jocn_a.00722
- Lam, B., Masellis, M., Freedman, M., Stuss, D. T., and Black, S. E. (2013). Clinical, imaging, and pathological heterogeneity of the alzheimer's disease syndrome. *Alzheimers Res. Ther.* 5:1. doi: 10.1186/alzrt155
- Leyton, C. E., Britton, A. K., Hodges, J. R., Halliday, G. M., and Kril, J. J. (2016). Distinctive pathological mechanisms involved in primary progressive aphasia. *Neurobiol. Aging* 38, 82–92. doi: 10.1016/j.neurobiolaging.2015.10.017
- Liao, W., Wu, G., Xu, Q., Ji, G., Zhang, Z., Zang, Y., et al. (2014). DynamicBC : a matlab toolbox for dynamic brain connectome analysis. *Brain Connect.* 4, 780–790. doi: 10.1089/brain.2014.0253
- Mandelli, M. L., Caverzasi, E., Binney, R. J., Henry, M. L., Lobach, I., Block, N., et al. (2014). Frontal white matter tracts sustaining speech production in primary progressive aphasia. *J. Neurosci.* 34, 9754–9767. doi: 10.1523/JNEUROSCI.3464-13.2014
- Marshall, C. R., Hardy, C. J. D., Volkmer, A., Russell, L. L., Bond, R. L., Fletcher, P. D., et al. (2018). Primary progressive aphasia: a clinical approach. *J. Neurol.* 265, 1474–1490. doi: 10.1007/s00415-018-8762-6
- Migliaccio, R., Gallea, C., Kas, A., Perlberg, V., Samri, D., Trotta, L., et al. (2016). Functional connectivity of ventral and dorsal visual streams in posterior cortical atrophy. *J. Alzheimers Dis.* 51, 1119–1130. doi: 10.3233/JAD-150934
- Miller, Z. A., Rosenberg, L., Santos-Santos, M. A., Stephens, M., Allen, I. E., Hubbard, H. I., et al. (2018). Prevalence of mathematical and visuospatial learning disabilities in patients with posterior cortical atrophy. *JAMA Neurol.* 75, 728–737. doi: 10.1001/jamaneurol.2018.0395
- Montembeault, M., Brambati, S. M., Lamari, F., Michon, A., Samri, D., Epelbaum, S., et al. (2018). Atrophy, metabolism and cognition in the posterior cortical atrophy spectrum based on alzheimer's disease cerebrospinal fluid biomarkers. *NeuroImage Clin.* 20, 1018–1025. doi: 10.1016/j.nicl.2018.10.010
- Montembeault, M., Chapleau, M., Jarret, J., Boukadi, M., Laforce, R. J., Wilson, M. A., et al. (2019). Differential language network functional connectivity alterations in alzheimer's disease and the semantic variant of primary progressive aphasia. *Cortex* 117, 284–298. doi: 10.1016/j.cortex.2019.03.018
- Mukku, S. S. R., Sivakumar, P. T., Nagaraj, C., Mangalore, S., Harbisethtar, V., and Varghese, M. (2019). Clinical utility of 18F-FDG-PET/MRI brain in dementia: Preliminary experience from a geriatric clinic in South India. *Asian J. Psychiat.* 44, 99–105. doi: 10.1016/j.ajp.2019.07.001
- Muller-Gartner, H. W., Links, J. M., Prince, J. L., Bryan, R. N., McVeigh, E., Leal, J. P., et al. (1992). Measurement of radiotracer concentration in brain gray matter using positron emission tomography: MRI-based correction for partial volume effects. *J. Cereb. Blood Flow Metab.* 12, 571–583. doi: 10.1038/jcbfm.1992.81
- Ossenkopp, R., Cohn-Sheehy, B. I., La Joie, R., Vogel, J. W., Moller, C., Lehmann, M., et al. (2015). Atrophy patterns in early clinical stages across distinct phenotypes of alzheimer's disease. *Hum. Brain Mapp.* 36, 4421–4437. doi: 10.1002/hbm.22927
- Pasquini, L., Nana, A. L., Toller, G., Brown, J. A., Deng, J., Staffaroni, A., et al. (2020). Salience network atrophy links neuron type-specific pathobiology to loss of empathy in frontotemporal dementia. *Cereb. Cortex* 30, 5387–5399. doi: 10.1093/cercor/bhaa119
- Passamonti, L., Tsvetanov, K. A., Jones, P. S., Bevan-Jones, W. R., Arnold, R., Borchert, R. J., et al. (2019). Neuroinflammation and functional connectivity in alzheimer's disease: Interactive influences on cognitive performance. *J. Neurosci.* 39, 7218–7226. doi: 10.1523/JNEUROSCI.2574-18.2019
- Pini, L., Wennberg, A. M., Salvalaggio, A., Vallesi, A., Pievani, M., and Corbetta, M. (2021). Breakdown of specific functional brain networks in clinical variants of alzheimer's disease. *Ageing Res. Rev.* 72:101482. doi: 10.1016/j.arr.2021.101482
- Pulvermuller, F., Cooper-Pye, E., Dine, C., Hauk, O., Nestor, P. J., and Patterson, K. (2010). The word processing deficit in semantic dementia: all categories are equal, but some categories are more equal than others. *J. Cogn. Neurosci.* 22, 2027–2041. doi: 10.1162/jocn.2009.21339
- Ranasinghe, K. G., Hinkley, L. B., Beagle, A. J., Mizuiri, D., Honma, S. M., Welch, A. E., et al. (2017). Distinct spatiotemporal patterns of neuronal functional connectivity in primary progressive aphasia variants. *Brain* 140, 2737–2751. doi: 10.1093/brain/awx217
- Rousset, O. G., Ma, Y., and Evans, A. C. (1998). Correction for partial volume effects in PET: Principle and validation. *J. Nucl. Med.* 39, 904–911.
- Seeley, W. W., Crawford, R. K., Zhou, J., Miller, B. L., and Greicius, M. D. (2009). Neurodegenerative diseases target large-scale human brain networks. *Neuron* 62, 42–52. doi: 10.1016/j.neuron.2009.03.024
- Shebani, Z., Patterson, K., Nestor, P. J., Diaz-de-Grenu, L. Z., Dawson, K., and Pulvermüller, F. (2017). Semantic word category processing in semantic dementia and posterior cortical atrophy. *Cortex* 93, 92–106. doi: 10.1016/j.cortex.2017.04.016
- Spina, S., Brown, J. A., Deng, J., Gardner, R. C., Nana, A. L., Hwang, J. L., et al. (2019). Neuropathological correlates of structural and functional imaging biomarkers in 4-repeat tauopathies. *Brain* 142, 2068–2081. doi: 10.1093/brain/awz122
- Toller, G., Yang, W., Brown, J. A., Ranasinghe, K. G., Shdo, S. M., Kramer, J. H., et al. (2019). Divergent patterns of loss of interpersonal warmth in frontotemporal dementia syndromes are predicted by altered intrinsic network connectivity. *Neuroimage Clin.* 22:101729. doi: 10.1016/j.nicl.2019.10.1729
- Warren, J. D., Rohrer, J. D., Schott, J. M., Fox, N. C., Hardy, J., and Rossor, M. N. (2013). Molecular nexopathies: a new paradigm of neurodegenerative disease. *Trends Neurosci.* 36, 561–569. doi: 10.1016/j.tins.2013.06.007
- Wilson, S. M., DeMarco, A. T., Henry, M. L., Gesierich, B., Babiak, M., Mandelli, M. L., et al. (2014). What role does the anterior temporal lobe play in sentence-level processing? Neural correlates of syntactic processing in semantic variant primary progressive aphasia. *J. Cogn. Neurosci.* 26, 970–985. doi: 10.1162/jocn_a.00550
- Xia, M., Wang, J., and He, Y. (2013). BrainNet Viewer: A network visualization tool for human brain connectomics. *PLoS One* 8:e68910. doi: 10.1371/journal.pone.0068910
- Yan, C. G., Wang, X. D., Zuo, X. N., and Zang, Y. F. (2016). DPABI: Data processing & analysis for (Resting-State) brain imaging. *Neuroinformatics* 14, 339–351. doi: 10.1007/s12021-016-9299-4
- Zhou, J., Gennatas, E. D., Kramer, J. H., Miller, B. L., and Seeley, W. W. (2012). Predicting regional neurodegeneration from the healthy brain functional connectome. *Neuron* 73, 1216–1227. doi: 10.1016/j.neuron.2012.03.004

Conflict of Interest: The authors declare that the research was conducted in the absence of any commercial or financial relationships that could be construed as a potential conflict of interest.

Publisher's Note: All claims expressed in this article are solely those of the authors and do not necessarily represent those of their affiliated organizations, or those of the publisher, the editors and the reviewers. Any product that may be evaluated in this article, or claim that may be made by its manufacturer, is not guaranteed or endorsed by the publisher.

Copyright © 2022 Chen, Zeng, Wang, Luo, Sun, Zhang, Liu, Li, Zhang and Peng. This is an open-access article distributed under the terms of the Creative Commons Attribution License (CC BY). The use, distribution or reproduction in other forums is permitted, provided the original author(s) and the copyright owner(s) are credited and that the original publication in this journal is cited, in accordance with accepted academic practice. No use, distribution or reproduction is permitted which does not comply with these terms.



OPEN ACCESS

Edited by:

Nilton Custodio,
Peruvian Institute of Neurosciences
(IPN), Peru

Reviewed by:

Mary Jo LaDu,
University of Illinois at Chicago,
United States
Deebika Balu,
University of Illinois at Chicago, United
States, contributed to the
review of ML
Davneet S. Minhas,
University of Pittsburgh, United States

***Correspondence:**

Sang Won Seo
sangwonseo@empas.com

†ORCID:

Jun Pyo Kim
orcid.org/0000-0003-4376-3107
Min Young Chun
orcid.org/0000-0003-3731-6132
Soo-Jong Kim
orcid.org/0000-0003-1798-3982
Hyemin Jang
orcid.org/0000-0003-3152-1274
Hee Jin Kim
orcid.org/0000-0002-3186-9441
Jee Hyang Jeong
orcid.org/0000-0001-7945-6956
Duk L. Na
orcid.org/0000-0002-0098-7592
Sang Won Seo
orcid.org/0000-0002-8747-0122

†These authors have contributed
equally to this work and share first
authorship

Specialty section:

This article was submitted to
Alzheimer's Disease and Related
Dementias,
a section of the journal
Frontiers in Aging Neuroscience

Received: 05 December 2021

Accepted: 14 January 2022

Published: 07 February 2022

Distinctive Temporal Trajectories of Alzheimer's Disease Biomarkers According to Sex and *APOE* Genotype: Importance of Striatal Amyloid

Jun Pyo Kim^{1,2†}, Min Young Chun^{1†}, Soo-Jong Kim^{1,3,4†}, Hyemin Jang^{1,5†},
Hee Jin Kim^{1,3,5,6†}, Jee Hyang Jeong^{7†}, Duk L. Na^{1,3,5,8†} and
Sang Won Seo^{1,3,4,5,6*†} for the Alzheimer's Disease Neuroimaging Initiative

¹ Department of Neurology, Samsung Medical Center, Sungkyunkwan University School of Medicine, Seoul, South Korea,

² Center for Neuroimaging, Radiology and Imaging Sciences, Indiana University School of Medicine, Indianapolis, IN,

United States, ³ Department of Health Sciences and Technology, SAIHST, Sungkyunkwan University, Seoul, South Korea,

⁴ Department of Intelligent Precision Healthcare Convergence, Sungkyunkwan University, Suwon, South Korea, ⁵ Alzheimer's Disease Convergence Research Center, Samsung Medical Center, Seoul, South Korea, ⁶ Department of Digital Health, SAIHST, Sungkyunkwan University, Seoul, South Korea, ⁷ Departments of Neurology, Ewha Womans University Seoul Hospital, Ewha Womans University College of Medicine, Seoul, South Korea, ⁸ Stem Cell & Regenerative Medicine Institute, Samsung Medical Center, Seoul, South Korea

Purpose: Previously, sex and apolipoprotein E (*APOE*) genotype had distinct effects on the cognitive trajectory across the Alzheimer's disease (AD) continuum. We therefore aimed to investigate whether these trajectory curves including β -amyloid ($A\beta$) accumulation in the cortex and striatum, and tau accumulation would differ according to sex and *APOE* genotype.

Methods: We obtained 534 subjects for ¹⁸F-florbetapir (AV45) PET analysis and 163 subjects for ¹⁸F-flortaucipir (AV1451) PET analysis from the Alzheimer's Disease Neuroimaging Initiative database. For cortical $A\beta$, striatal $A\beta$, and tau SUVR, we fitted penalized splines to model the slopes of SUVR value as a non-linear function of baseline SUVR value. By integrating the fitted splines, we obtained the predicted SUVR curves as a function of time.

Results: The time from initial SUVR to the cutoff values were 14.9 years for cortical $A\beta$, 18.2 years for striatal $A\beta$, and 22.7 years for tau. Although there was no difference in cortical $A\beta$ accumulation rate between women and men, striatal $A\beta$ accumulation was found to be faster in women than in men, and this temporal difference according to sex was more pronounced in tau accumulation. However, *APOE* $\epsilon 4$ carriers showed faster progression than non-carriers regardless of kinds of AD biomarkers' trajectories.

Conclusion: Our temporal trajectory models illustrate that there is a distinct progression pattern of AD biomarkers depending on sex and *APOE* genotype. In this regard, our models will be able to contribute to designing personalized treatment and prevention strategies for AD in clinical practice.

Keywords: Alzheimer's disease, trajectory curve, sex, apolipoprotein E, positron emission tomography

INTRODUCTION

Alzheimer's disease (AD) is the most common cause of dementia, characterized by the accumulation of amyloid- β (A β) plaques and neurofibrillary tangles formed by high levels of phosphorylated tau (Sperling et al., 2011). According to the amyloid cascade hypothesis, the deposition of A β plaques leads to the development of neurofibrillary tangles, cortical atrophy, and cognitive impairment (Price and Morris, 1999; Jack et al., 2018). Clarifying temporal trajectories of AD biomarkers would be crucial to better understand the disease. In this regard, accumulation of longitudinal positron emission tomography (PET) scans or cerebrospinal fluid (CSF) data has made it possible to model temporal changes in A β and tau biomarkers (Mattsson et al., 2012; Hanseeuw et al., 2019). It is a challenging task to clearly demonstrate the general pattern of pathological progression over decades, as the durations of follow-ups of individual subjects are relatively limited. However, modeling of AD biomarker trajectories remains an important goal, as future treatments targeting A β and tau are expected to be developed.

One way to overcome the limited individual follow-up period is to group subjects who share similar properties, such as initial clinical diagnosis (Hadjichrysanthou et al., 2020; Cho et al., 2021) or the shape of their longitudinal trajectory (Koscik et al., 2020). Alternatively, an integration-based method (Hahn, 1991) can be used to obtain the calculated time curves of the biomarkers (Jack et al., 2013; Villemagne et al., 2013; Baek et al., 2020a). This method does not require subjects to be grouped, which makes the process of analysis more straightforward. Using this method, Jack et al. proposed a temporal trajectory model of A β accumulation using serial amyloid PET scans, showing that A β accumulation exhibits a sigmoidal shape across time (Jack et al., 2013). In fact, a recent study showed that this model of A β and tau accumulation matches the hypothetical model that shows the orderly appearance of AD biomarkers (Baek et al., 2020a).

According to recent studies using amyloid PET data, A β accumulation occurs first in the neocortex and then in the striatum, suggesting a downward spreading pattern consistent with Thal A β pathology staging (Thal et al., 2002; Cho et al., 2018; Hanseeuw et al., 2018). Furthermore, the striatal A β is associated with worse AD biomarkers and cognitive function (Cho et al., 2018; Hanseeuw et al., 2018). Therefore, we propose that it would be worthwhile to investigate A β accumulation in the striatum as well. It is especially important to investigate how the striatal A β trajectory is positioned relative to the cortical A β and tau trajectories, as it may provide us with more insight regarding AD pathobiology.

In addition, the trajectory of pathological tau accumulation is studied with tau PET data. The transition from normal aging to preclinical AD can be characterized by tau tangles that spread from the medial temporal lobe to limbic areas (Braak stages III and IV) (Petersen et al., 2006). Especially, increased tau uptakes in the Braak stages III and IV regions may reflect pathological tau accumulation. Tau accumulation in Braak stages I and II may occur before the evidence of A β accumulation. Also, tau accumulation in Braak stages I and II may be found even in people at a young age or in normal cognitive function or primary

age-related tauopathy (Braak and Del Tredici, 2015; Zhu et al., 2019). In fact, many studies calculated the cut-off values of tau positivity using the tau uptakes in the Braak stages III and IV (Maass et al., 2017).

Several factors may affect the cognitive trajectory. Specifically, a previous study from our group showed that sex and apolipoprotein E (*APOE*) genotype had distinct effects on the cognitive trajectory across the AD continuum (Cho et al., 2021). However, in previous studies, *APOE* ϵ 4 carriers with normal cognition showed more A β uptake in the cerebral cortex than that by non-carriers (Oveisgharan et al., 2018; Buckley et al., 2019), but these studies did not show women with normal cognition to have more A β uptake in the cerebral cortex than men. Therefore, this raised the question as to whether AD biomarkers begin to show different trajectories, including uptakes of cortical A β , striatal A β , and tau, according to sex or *APOE* ϵ 4 genotype.

In the present study, we aimed to model the temporal trajectories of pathological tau accumulation as well as A β accumulation in the cortex and striatum. We also investigated whether these trajectory curves would differ according to sex and *APOE* genotype. We hypothesized that women would show faster progression of AD biomarker accumulation than men in case of striatal A β and tau, but not in case of cortical A β . We also hypothesized that *APOE* ϵ 4 carriers would show faster progression in accumulation than non-carriers, regardless of the AD biomarker type.

MATERIALS AND METHODS

Data Acquisition

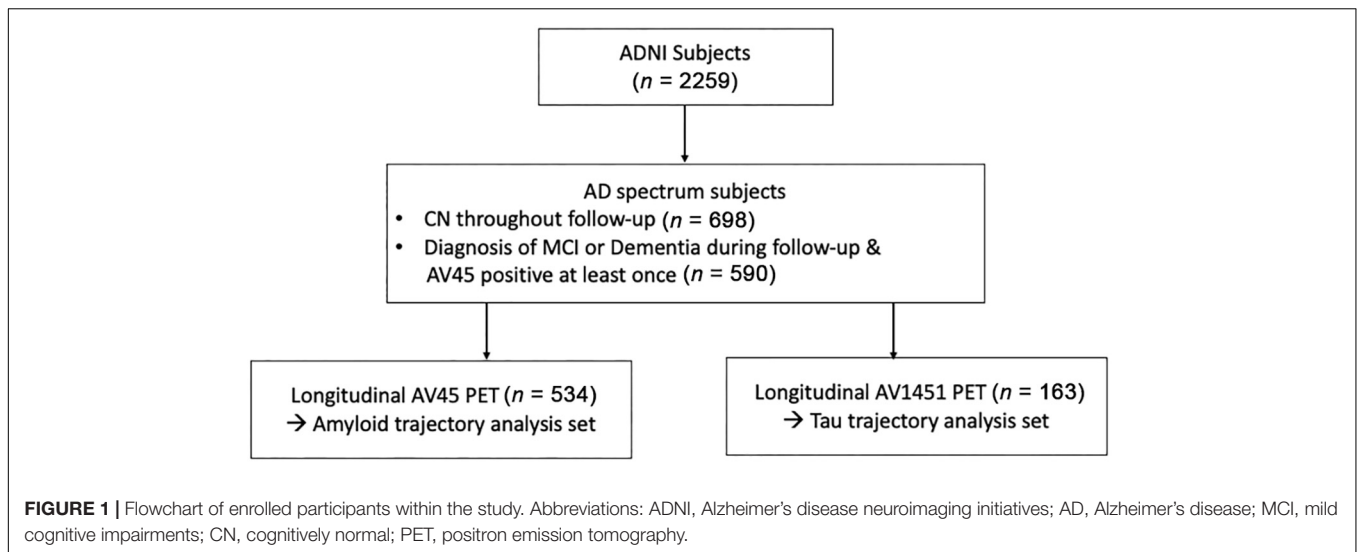
Data used in the present study were obtained from the Alzheimer's Disease Neuroimaging Initiative (ADNI) database led by Principal Investigator Michael W. Weiner, MD. ADNI is the outcome of a public-private partnership started in 2003. Its main goal is to test whether clinical and cognitive assessment, PET, CSF, serial magnetic resonance imaging (MRI), and other biological markers can be combined to evaluate the progression of mild cognitive impairment (MCI) and early AD dementia (ADD).

Study Participants

The present study included subjects from the ADNI dataset. Detailed inclusion and exclusion criteria for the ADNI data are provided on the ADNI website¹. Cognitive function of the participants was evaluated using the Alzheimer's Disease Assessment Scale Cognitive subscale 13. For trajectory analysis of cortical and subcortical A β , subjects who underwent ¹⁸F-florbetapir (AV45) PET tests were selected. Similarly, subjects who underwent ¹⁸F-flortaucipir (AV1451) PET were included in the tau trajectory analysis. Information on *APOE* genotype was also investigated.

Among the subjects who underwent corresponding PET for each biomarker, we included subjects within the AD continuum from "amyloid-negative, cognitively normal subjects"

¹<http://www.adni-info.org>



to “amyloid-positive, demented subjects.” To this end, we included subjects who showed A β positivity at least once, regardless of cognitive function. In addition, subjects who remained cognitively normal throughout the follow-up period were included, regardless of A β positivity. Subjects with cognitive impairment who did not show A β positivity within the follow-up period were excluded (**Figure 1**).

All participants provided written informed consent and underwent protocols approved by the institutional review board of each participating site. The data use and publication by authors were approved by the ADNI Data Sharing and Publications Committee.

Image Data Acquisition and ^{18}F -Florbetapir Positron Emission Tomography Preprocessing

The ADNI PET acquisition protocols are described on www.adni-info.org. In terms of ^{18}F -florbetapir PET, we obtained standardized uptake value ratios (SUVRs) for Braak stages III and IV from the UCBERKELEYAV1451_PVC table as part of the ADNIMERGE R package. For the analysis of amyloid PET scans, we downloaded the ^{18}F -florbetapir PET and corresponding MRI image files from the LONI website and processed them. ^{18}F -florbetapir images consisted of 4×5 min frames acquired 50–70 min post-injection; these were realigned, averaged, resliced to a common voxel size ($1.5 \text{ mm} \times 1.5 \text{ mm} \times 1.5 \text{ mm}$), and smoothed to a common resolution of 8 mm^3 . All T1 images were preprocessed using CIVET pipeline. Segmentation was performed by ANIMAL segmentation in the implemented pipeline (Collins et al., 1994; Collins et al., 1995). The region-based voxel-wise correction method was used for partial volume correction (PVC) and performed using the PETPVC toolbox into total ^{18}F -florbetapir PET images (Thomas et al., 2011; Thomas et al., 2016). The ^{18}F -florbetapir PET images were co-registered onto corresponding T1 images, and SUVRs were calculated for partial

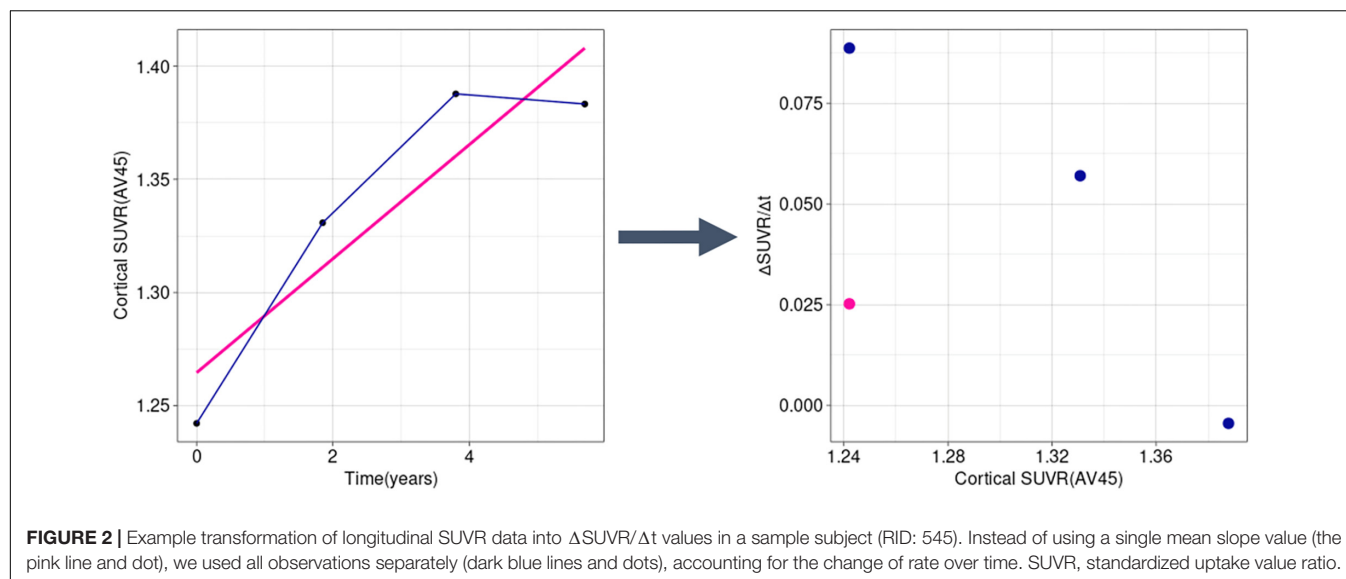
volume-corrected PET images. The whole cerebellum was used as the reference region.

Trajectory Analysis

We used an in-house program implemented in R for trajectory analysis using a modified method of the previously used method to determine the temporal trajectory of AD-related biomarkers (Jack et al., 2013; Villemagne et al., 2013; Baek et al., 2020a). We calculated the rates of change for each biomarker, using longitudinally observed values. Instead of obtaining a single rate value ($\Delta\text{SUVR}/\Delta t$) per subject, we calculated the slope for every interval, thus obtaining at $n-1$ rate values for a subject with n observations (**Figure 2**). Using this method, we were able to capture the change in rate within a subject throughout the follow-up period.

Thereafter, for each biomarker, we fitted a penalized spline to model the slope of the SUVR as a non-linear function of the baseline SUVR. Penalized splines can be an efficient tool to describe complex non-linear relationships because researchers do not have to determine the amount and placement of the knots. Instead, penalized splines use a large number of knots and allow the fit to be controlled by a penalty (Perperoglou et al., 2019). We used the *gam* function in the *mgcv* R package to fit the penalized splines with the extended Feller Schall optimization method (Wood and Fasiolo, 2017), and other parameters were set to default settings. The default basis for smoothing by the *gam* function is the thin plate regression spline, which uses knots as many as the number of unique values of the data up to 2,000, placed on every unique value (Wood, 2003).

Using the fitted splines, we obtained predicted SUVR curves as a function of time by using the *ode* function in the *deSolve* R package to solve the first-order differential equation. For each variable, the initial SUVR for time = 0 was anchored to the mean SUVR of amyloid-negative, cognitively normal subjects who underwent the test. The number of subjects and the mean (standard deviation) values of the normative groups are shown in **Table 1**. The FreeSurfer-based SUVR cortical cutoff of 1.11,



calculated based on the same ADNI data (Landau and Jagust, 2015), was found to be 1.043 for the CIVET-based cortical SUVR by regression analysis. The cortical A β cutoff of 1.043 corresponded to a z-score of -2.0 , so the cutoff values of striatal A β and tau were set to z-score -2.0 . We indicated the abnormal cutoff (z-score -2.0) values, the mean SUVRs of MCI subjects, and the mean SUVRs of ADD subjects for each trajectory model.

RESULTS

Study Participants

We included a different number of subjects for each biomarker's final analysis because we included all AD continuum subjects with longitudinal data for the given biomarker. For example, while a total of 534 subjects were included in the trajectory analysis of amyloid PET, 163 subjects were available for tau PET trajectory analysis. Demographic data are summarized in **Table 2**.

Rate of Change of Biomarkers According to Baseline SUVRs

The rates of changes in the SUVRs for the biomarkers are shown in **Figure 3**. The cortical and striatal A β accumulation rates showed different patterns. While the accumulation rate of cortical A β increased until the SUVR reached 1.26 and decreased subsequently (**Figure 3A**), $\Delta\text{SUVR}/\Delta t$ for the striatal

A β remained constant throughout the entire range of SUVRs (**Figure 3B**). The worsening rate of tau PET also remained substantially constant (**Figure 3C**), although tau accumulation showed a slightly increasing pattern.

Temporal Trajectories of Alzheimer's Disease Related Markers

For each variable, we obtained the curve of the expected SUVRs as a function of time (**Figure 4**). The time from initial SUVR to the cutoff values (z-score -2.0) was the longest for tau PET (22.7 years) and shortest for cortical A β (14.9 years). For the cortical A β , striatal A β , and tau trajectories, after reaching the cutoff, the mean SUVR of MCI subjects and the mean SUVR of ADD subjects appeared.

For comparison between men and women, trajectory curves were generated separately, according to sex (**Figure 5**). There was no significant difference in the cortical A β accumulation rate between women and men (**Figure 5A**). However, for striatal A β accumulation, women reached the cutoff values 2.7 years earlier

TABLE 1 | Normative values used for z-transformation.

| | N | Mean | SD |
|--------------------|-----|-------|-------|
| Amyloid (cortex) | 204 | 0.863 | 0.091 |
| Amyloid (striatum) | 204 | 1.58 | 0.159 |
| Tau (Braak 3,4) | 177 | 1.69 | 0.144 |

N, number of amyloid-negative, cognitively normal subjects used to derive normative values; SD, standard deviation.

TABLE 2 | Characteristics of analyzed subjects by test modality and biomarker.

| | ¹⁸ F-florbetapir (AV45) PET | ¹⁸ F-flortaucipir (AV1451) PET |
|-------------------------------|--|---|
| No. | 534 | 163 |
| Diagnosis (%) | | |
| CN | 297 (55.6) | 107 (65.6) |
| –Dementia | 42 (7.9) | 18 (11.0) |
| –MCI | 195 (36.5) | 38 (23.3) |
| Age, mean (SD), y | 74.0 (6.9) | 75.2 (7.5) |
| Men (%) | 282 (52.8) | 81 (49.7) |
| Education, mean (SD), y | 16.22 (2.72) | 16.39 (2.48) |
| APOE ϵ 4 carrier (%) | 253 (47.4) | 82 (50.6) |

PET, positron emission tomography; N, number; CN, cognitively normal; MCI, mild cognitive impairment; SD, standard deviation.

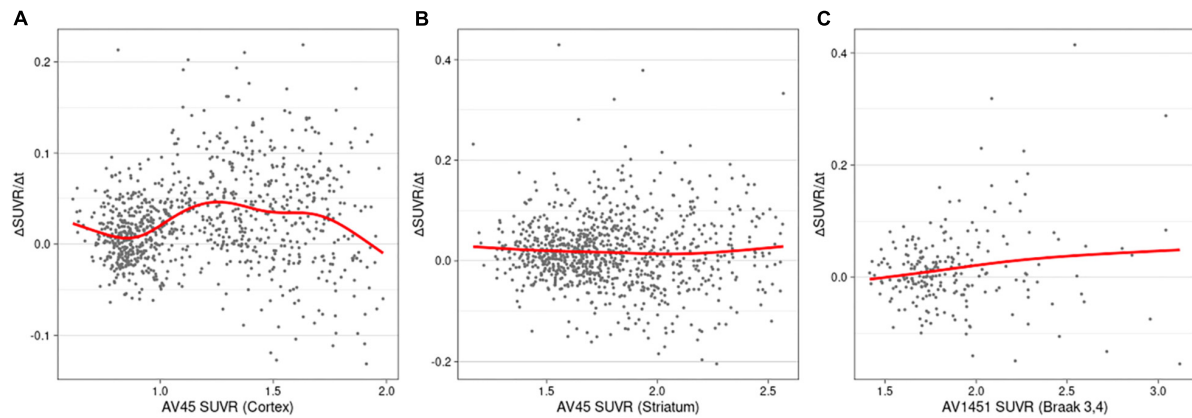


FIGURE 3 | Rates of change (worsening) as a function of SUVRs in cortical amyloid (A), striatal amyloid (B), and pathological tau (C). AV45, ^{18}F -florbetapir; SUVR, standardized uptake value ratio; AV1451, ^{18}F -flortaucipir.

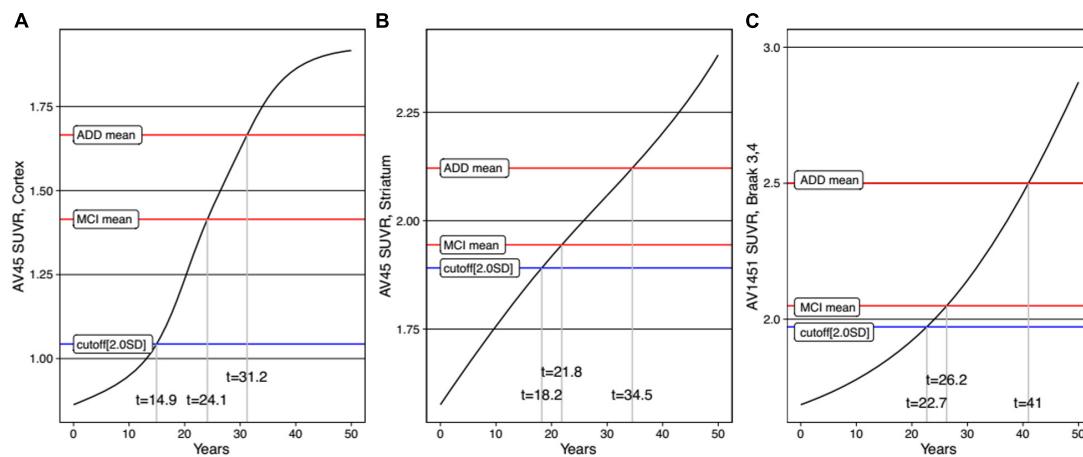


FIGURE 4 | Trajectories of AD biomarkers as a function of time in cortical amyloid (A), striatal amyloid (B), and pathological tau (C). AV45, ^{18}F -florbetapir; SUVR, standardized uptake value ratio; AV1451, ^{18}F -flortaucipir.

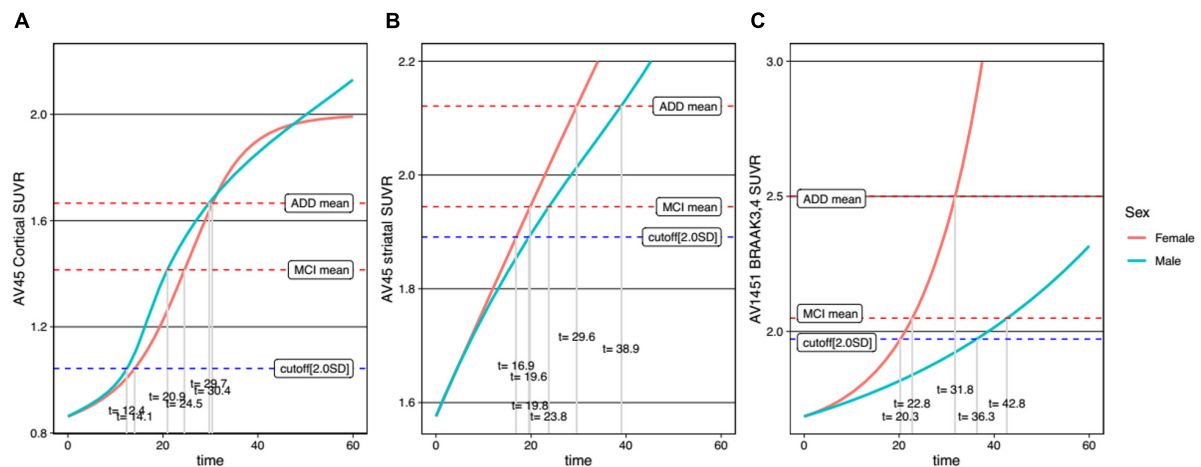
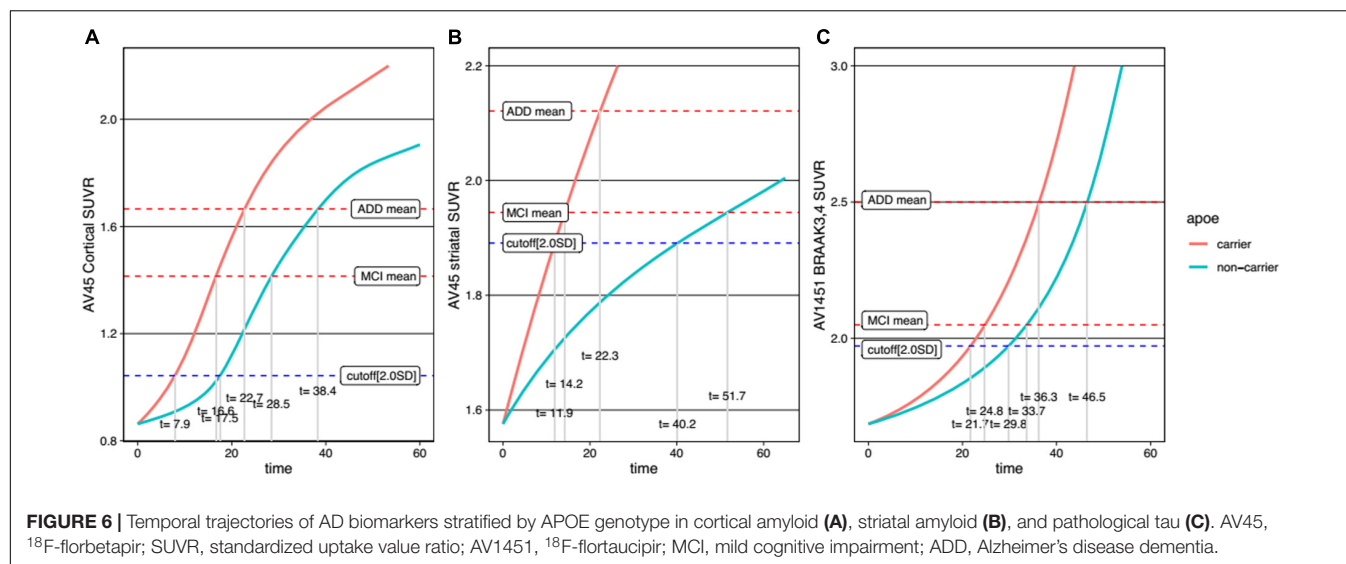


FIGURE 5 | Temporal trajectories of AD biomarkers stratified by sex in cortical amyloid (A), striatal amyloid (B), and pathological tau (C). AV45, ^{18}F -florbetapir; SUVR, standardized uptake value ratio; AV1451, ^{18}F -flortaucipir; MCI, mild cognitive impairment; ADD, Alzheimer's disease dementia.



than men (Figure 5B). The temporal difference according to sex was more pronounced for tau accumulation, as women reached the cutoff 16.0 years earlier than men (Figure 5C). In terms of APOE $\epsilon 4$ carrier status, carriers showed faster progression for all biomarkers (Figure 6).

DISCUSSION

In the present study, we developed a model that allows for the mapping of the temporal trajectories of cortical A β , striatal A β , and tau protein deposition according to sex and APOE genotype from a large sample of ADNI subjects. Our major findings are as follows: First, A β was found to accumulate in the cortex and then in the striatum, followed by pathological tau accumulation in the limbic regions, which correspond to the Braak stages III and IV. Second, while there was no difference in cortical A β accumulation rate between women and men, striatal A β accumulation was found to be faster in women than in men, and this temporal difference according to sex was more pronounced in tau accumulation. Finally, APOE $\epsilon 4$ carriers showed faster accumulation of cortical A β , striatal A β , and tau than non-carriers. Taken together, our findings suggest that our temporal trajectory models can reveal a distinctive progression pattern of AD biomarkers depending on sex and APOE genotype. Therefore, our trajectory models can contribute to the design of personalized treatment and prevention strategies for AD in clinical practice.

Our finding that A β accumulates in the cortex and striatum sequentially is in line with Thal A β pathology staging, with A β deposits found initially in the cortex, and subsequently in the striatum (Thal et al., 2002), as also shown in a previous imaging study (Cho et al., 2018). Our other finding regarding the order of striatal A β and tau accumulation is also consistent with previous pathological studies showing that striatal A β plaques predicted the possible development of higher Braak stages (Braak and Braak, 1990; Beach et al., 2012). Therefore, our findings

are consistent with the A β pathological cascade hypothesis. Regarding cortical A β , the time to reach the abnormal SUVR cutoff was 14.9 years in the present study, but 6.4 years in the previous study (Jagust et al., 2021). This discrepancy might be explained by the differences in the subjects. In the previous study, subjects with A β -negative normal cognition at baseline with increasing ¹⁸F-florbetapir slopes were used as a control group (Jagust et al., 2021). By contrast, in the present study, subjects who were consistently A β -negative cognitively normal during the follow-up period were included as a control group. However, the time to reach the abnormal cortical A β SUVR cutoff of the present study (14.9 years) is closer to that of previous studies (12–16 years) (Villemagne et al., 2013; Baek et al., 2020a). For the tau trajectory curve, the Baek et al. (2020a) estimate of the time interval to reach the z-score 2.0 for tau (30.6 years) was similar to our findings (22.7 years for the cutoff, z-score -2.0). Since striatal A β plaques are regarded as a predictor of higher Braak stages (Braak and Braak, 1990; Beach et al., 2012) and worse cognitive impairment (Beach et al., 2016; Grothe et al., 2017; Cho et al., 2018), it is important to take the striatal A β trajectory into account during clinical practice. Notably, our trajectory curve for striatal A β also calculated that it took 18.2 years to reach the abnormal SUVR cutoff. Thus, our study elucidating the temporal order in the accumulation of cortical A β , striatal A β , and pathological tau protein, along with their estimated time intervals, may support Thal A β pathology staging and the A β pathological cascade (Jack et al., 2010).

Several previous studies, including our group, showed that women had faster cognitive decline than men (Buckley et al., 2018; Cho et al., 2021), but that there was no such difference in terms of cortical A β accumulation, cross-sectionally (Hanseeuw et al., 2019) or longitudinally (Buckley et al., 2018). However, we found that this was different for striatal A β and tau accumulation. In particular, it was found that women took 2.7 years faster than men to reach the abnormal cut-off value of striatal A β trajectory. For tau accumulation, a previous longitudinal tau-PET study showed that tau protein accumulation is faster in women

(Smith et al., 2020). We also found this to be the case in our study, where the temporal difference between the sexes was more pronounced in the tau trajectory than in the striatal A β trajectory. Specifically, tau accumulation was found to be 16.0 years faster in women than in men to reach the abnormal tau cut-off. Thus, our trajectory model showed that the rate of accumulation between sexes was different for each AD biomarker. Therefore, this faster accumulation of striatal A β and tau in women may explain the worse cognitive decline and greater frequency and prevalence of AD dementia in women.

Our final major finding was that, unlike the differences between sexes, the differences between *APOE* ϵ 4 carriers and non-carriers showed a different pattern. In particular, for the *APOE* ϵ 4 carriers, there was a faster decline in all three AD biomarker trajectories. Our findings are supported by previous studies showing that *APOE* ϵ 4 carriers accumulate A β faster than non-carriers (Liu et al., 2013), as shown in amyloid PET (Ossenkoppele et al., 2015) and CSF studies (Resnick et al., 2015). Also, *APOE* ϵ 4 carriers accumulated tau faster than non-carriers, as previously described (Sepulcre et al., 2018; Baek et al., 2020b). Since there were differences in AD biomarker trajectories depending on sex and *APOE* genotype, our findings will help to design individualized therapeutic and preventive strategies to ameliorate AD biomarkers, resulting in cognitive decline.

The ADNI is a well-organized, longitudinal cohort that serves as an excellent resource for investigating the disease course of AD with multimodal imaging markers, including A β and tau PET. However, this study had several limitations. First, the number of subjects who underwent tau PET was small compared to the number of subjects who underwent amyloid PET. Second, we defined the time 0 for a specific biomarker as the point when the SUVR value of that biomarker was in the mean level of A β -negative CN subjects. We were able to estimate the durations for each biomarker to reach certain values, but we need to synchronize the time axes between biomarkers in future studies. Also, further studies with long-term longitudinal follow-up are needed to validate our findings. Since statistical comparison was difficult, we explained the time comparison of each graph descriptively, as in other trajectories studies (Baek et al., 2020a; Jagust et al., 2021). Third, we did not investigate the interactive effects of gender and *APOE* genotype on the biomarkers' trajectories because of a small sized sample. Further studies with a larger sized sample are needed to evaluate this issue. Nevertheless, our study is noteworthy in that we demonstrated that trajectory curves of AD biomarkers differ according to striatal A β involvement, sex, and *APOE* genotype.

In conclusion, the temporal trajectory in this study reflects the Thal A β pathology staging and the amyloid cascade hypothesis, showing that pathological tau protein accumulation occurred only when striatal A β accumulation emerged. Furthermore, trajectory curves differed according to sex and *APOE* genotype. In particular, a similar or higher rate of cortical A β accumulation in men compared to women was reversed with respect to striatal A β and tau accumulation. In clinical practice, the prognoses for AD patients should be approached differently in relation to striatal A β involvement, sex, and *APOE* genotype.

DATA AVAILABILITY STATEMENT

The original contributions presented in the study are included in the article/supplementary material, further inquiries can be directed to the corresponding author/s. The datasets generated during the study are available in the <http://adni.loni.usc.edu/data-samples/access-data/>.

ETHICS STATEMENT

The Ethics committees/institutional review boards that approved the ADNI study are: Albany Medical Center Committee on Research Involving Human Subjects Institutional Review Board, Boston University Medical Campus and Boston Medical Center Institutional Review Board, Butler Hospital Institutional Review Board, Cleveland Clinic Institutional Review Board, Columbia University Medical Center Institutional Review Board, Duke University Health System Institutional Review Board, Emory Institutional Review Board, Georgetown University Institutional Review Board, Health Sciences Institutional Review Board, Houston Methodist Institutional Review Board, Howard University Office of Regulatory Research Compliance, Icahn School of Medicine at Mount Sinai Program for the Protection of Human Subjects, Indiana University Institutional Review Board, Institutional Review Board of Baylor College of Medicine, Jewish General Hospital Research Ethics Board, Johns Hopkins Medicine Institutional Review Board, Lifespan - Rhode Island Hospital Institutional Review Board, Mayo Clinic Institutional Review Board, Mount Sinai Medical Center Institutional Review Board, Nathan Kline Institute for Psychiatric Research & Rockland Psychiatric Center Institutional Review Board, New York University Langone Medical Center School of Medicine Institutional Review Board, Northwestern University Institutional Review Board, Oregon Health and Science University Institutional Review Board, Partners Human Research Committee Research Ethics, Board Sunnybrook Health Sciences Centre, Roper St. Francis Healthcare Institutional Review Board, Rush University Medical Center Institutional Review Board, St. Joseph's Phoenix Institutional Review Board, Stanford Institutional Review Board, The Ohio State University Institutional Review Board, University Hospitals Cleveland Medical Center Institutional Review Board, University of Alabama Office of the IRB, University of British Columbia Research Ethics Board, University of California Davis Institutional Review Board Administration, University of California Los Angeles Office of the Human Research Protection Program, University of California San Diego Human Research Protections Program, University of California San Francisco Human Research Protection Program, University of Iowa Institutional Review Board, University of Kansas Medical Center Human Subjects Committee, University of Kentucky Medical Institutional Review Board, University of Michigan Medical School Institutional Review Board, University of Pennsylvania Institutional Review Board, University of Pittsburgh Institutional Review Board, University of Rochester

Research Subjects Review Board, University of South Florida Institutional Review Board, University of Southern California Institutional Review Board, UT Southwestern Institutional Review Board, VA Long Beach Healthcare System Institutional Review Board, Vanderbilt University Medical Center Institutional Review Board, Wake Forest School of Medicine Institutional Review Board, Washington University School of Medicine Institutional Review Board, Western Institutional Review Board, Western University Health Sciences Research Ethics Board, and Yale University Institutional Review Board. The patients/participants provided their written informed consent to participate in this study.

AUTHOR CONTRIBUTIONS

JK, MC, and SS: conceptualization and methodology. JK and SK: formal analysis and investigation. JK and MC: writing –

original draft preparation. HJ, HK, JJ, and SS: writing – review and editing. SS: funding acquisition. DN and SS: supervision. All authors contributed to manuscript revision, read, and approved the submitted version.

FUNDING

This research was supported by a grant of the Korea Health Technology R&D Project through the Korea Health Industry Development Institute (KHIDI), funded by the Ministry of Health & Welfare and Ministry of Science and ICT, Republic of Korea (Grant Nos. HU20C0111 and HI19C1088), the National Research Foundation of Korea (NRF) grant funded by the Korea government (MSIT) (NRF-2019R1A5A2027340), Future Medicine 20*30 Project of the Samsung Medical Center (#SMX1220021), and a fund (2021-ER1006-00) by the Research of Korea Disease Control and Prevention Agency.

REFERENCES

- Baek, M. S., Cho, H., Lee, H. S., Choi, J. Y., Lee, J. H., Ryu, Y. H., et al. (2020a). Temporal trajectories of in vivo tau and amyloid-beta accumulation in Alzheimer's disease. *Eur. J. Nucl. Med. Mol. Imaging* 47, 2879–2886. doi: 10.1007/s00259-020-04773-3
- Baek, M. S., Cho, H., Lee, H. S., Lee, J. H., Ryu, Y. H., and Lyoo, C. H. (2020b). Effect of APOE epsilon4 genotype on amyloid-beta and tau accumulation in Alzheimer's disease. *Alzheimers Res. Ther.* 12:140. doi: 10.1186/s13195-020-00710-6
- Beach, T. G., Sue, L. I., Walker, D. G., Sabbagh, M. N., Serrano, G., Dugger, B. N., et al. (2012). Striatal amyloid plaque density predicts Braak neurofibrillary stage and clinicopathological Alzheimer's disease: implications for amyloid imaging. *J. Alzheimers Dis.* 28, 869–876. doi: 10.3233/JAD-2011-111340
- Beach, T. G., Thal, D. R., Zante, M., Smith, A., and Buckley, C. (2016). Detection of Striatal Amyloid Plaques with [18F]flutemetamol: validation with Postmortem Histopathology. *J. Alzheimers Dis.* 52, 863–873. doi: 10.3233/JAD-150732
- Braak, H., and Braak, E. (1990). Alzheimer's disease: striatal amyloid deposits and neurofibrillary changes. *J. Neuropathol. Exp. Neurol.* 49, 215–224. doi: 10.1097/00005072-199005000-00003
- Braak, H., and Del Tredici, K. J. B. (2015). The preclinical phase of the pathological process underlying sporadic Alzheimer's disease. *Brain* 138, 2814–2833. doi: 10.1093/brain/awv236
- Buckley, R. F., Mormino, E. C., Amariglio, R. E., Properzi, M. J., Rabin, J. S., Lim, Y. Y., et al. (2018). Sex, amyloid, and APOE epsilon4 and risk of cognitive decline in preclinical Alzheimer's disease: findings from three well-characterized cohorts. *Alzheimers Dement.* 14, 1193–1203. doi: 10.1016/j.jalz.2018.04.010
- Buckley, R. F., Mormino, E. C., Rabin, J. S., Hohman, T. J., Landau, S., Hanseeuw, B. J., et al. (2019). Sex Differences in the Association of Global Amyloid and Regional Tau Deposition Measured by Positron Emission Tomography in Clinically Normal Older Adults. *JAMA Neurol.* 76, 542–551. doi: 10.1001/jamaneurol.2018.4693
- Cho, S. H., Shin, J. H., Jang, H., Park, S., Kim, H. J., Kim, S. E., et al. (2018). Amyloid involvement in subcortical regions predicts cognitive decline. *Eur. J. Nucl. Med. Mol. Imaging* 45, 2368–2376. doi: 10.1007/s00259-018-4081-5
- Cho, S. H., Woo, S., Kim, C., Kim, H. J., Jang, H., Kim, B. C., et al. (2021). Disease progression modelling from preclinical Alzheimer's disease (AD) to AD dementia. *Sci. Rep.* 11:4168. doi: 10.1038/s41598-021-83585-3
- Collins, D. L., Holmes, C. J., Peters, T. M., and Evans, A. C. (1995). Automatic 3-D model-based neuroanatomical segmentation. *Hum. Brain Mapp.* 3, 190–208.
- Collins, D. L., Neelin, P., Peters, T. M., and Evans, A. C. (1994). Automatic 3D intersubject registration of MR volumetric data in standardized Talairach space. *J. Comput. Assist. Tomogr.* 18, 192–205.
- Grothe, M. J., Barthel, H., Sepulcre, J., Dyrba, M., Sabri, O., Teipel, S. J., et al. (2017). In vivo staging of regional amyloid deposition. *Neurology* 89, 2031–2038. doi: 10.1212/WNL.0000000000004643
- Hadjichrysanthou, C., Evans, S., Bajaj, S., Siakallis, L. C., McRae-McKee, K., de Wolf, F., et al. (2020). The dynamics of biomarkers across the clinical spectrum of Alzheimer's disease. *Alzheimers Res. Ther.* 12:74. doi: 10.1186/s13195-020-00636-z
- Hahn, G. D. (1991). A modified Euler method for dynamic analyses. *Int. J. Numer. Method Eng.* 32, 943–955. doi: 10.1002/nme.1620320502
- Hanseeuw, B. J., Betensky, R. A., Jacobs, H. I. L., Schultz, A. P., Sepulcre, J., Becker, J. A., et al. (2019). Association of Amyloid and Tau With Cognition in Preclinical Alzheimer Disease: a Longitudinal Study. *JAMA Neurol.* 76, 915–924. doi: 10.1001/jamaneurol.2019.1424
- Hanseeuw, B. J., Betensky, R. A., Mormino, E. C., Schultz, A. P., Sepulcre, J., Becker, J. A., et al. (2018). PET staging of amyloidosis using striatum. *Alzheimers Dement.* 14, 1281–1292. doi: 10.1016/j.jalz.2018.04.011
- Jack, C. R. Jr., Bennett, D. A., Blennow, K., Carrillo, M. C., Dunn, B., Haeberlein, S. B., et al. (2018). NIA-AA Research Framework: toward a biological definition of Alzheimer's disease. *Alzheimers Dement.* 14, 535–562. doi: 10.1016/j.jalz.2018.02.018
- Jack, C. R. Jr., Knopman, D. S., Jagust, W. J., Shaw, L. M., Aisen, P. S., Weiner, M. W., et al. (2010). Hypothetical model of dynamic biomarkers of the Alzheimer's pathological cascade. *Lancet Neurol.* 9, 119–128. doi: 10.1016/S1474-4422(09)70299-6
- Jack, C. R. Jr., Wiste, H. J., Lesnick, T. G., Weigand, S. D., Knopman, D. S., Vemuri, P., et al. (2013). Brain beta-amyloid load approaches a plateau. *Neurology* 80, 890–896. doi: 10.1212/WNL.0b013e3182840bbe
- Jagust, W. J., Landau, S. M., and Alzheimer's Disease Neuroimaging Initiative (2021). Temporal Dynamics of beta-Amyloid Accumulation in Aging and Alzheimer Disease. *Neurology* 96, e1347–e1357. doi: 10.1212/WNL.00000000000011524
- Koscik, R. L., Betthausen, T. J., Jonaitis, E. M., Allison, S. L., Clark, L. R., Hermann, B. P., et al. (2020). Amyloid duration is associated with preclinical cognitive decline and tau PET. *Alzheimers Dement.* 12:e12007. doi: 10.1002/dad2.12007
- Landau, S., and Jagust, W. (2015). *Florbetapir processing methods. Alzheimer's Disease Neuroimaging Initiative*. Available online at: https://adni.bitbucket.io/reference/docs/UCBERKELEYAV45/ADNI_AV45_Methods_JagustLab_06.25.15.pdf/ (Accessed January 12, 2022).
- Liu, C. C., Liu, C. C., Kanekiyo, T., Xu, H., and Bu, G. (2013). Apolipoprotein E and Alzheimer disease: risk, mechanisms and therapy. *Nat. Rev. Neurol.* 9, 106–118. doi: 10.1038/nrneurol.2012.263

- Maass, A., Landau, S., Baker, S. L., Horng, A., Lockhart, S. N., La Joie, R., et al. (2017). Comparison of multiple tau-PET measures as biomarkers in aging and Alzheimer's disease. *Neuroimage* 157, 448–463. doi: 10.1016/j.neuroimage.2017.05.058
- Mattsson, N., Portelius, E., Rolstad, S., Gustavsson, M., Andreasson, U., Stridsberg, M., et al. (2012). Longitudinal cerebrospinal fluid biomarkers over four years in mild cognitive impairment. *J. Alzheimers Dis.* 30, 767–778. doi: 10.3233/JAD-2012-120019
- Ossenkoppe, R., Jansen, W. J., Rabinovici, G. D., Knol, D. L., van der Flier, W. M., van Berckel, B. N., et al. (2015). Prevalence of amyloid PET positivity in dementia syndromes: a meta-analysis. *JAMA* 313, 1939–1949. doi: 10.1001/jama.2015.4669
- Oveisgharan, S., Arvanitakis, Z., Yu, L., Farfel, J., Schneider, J. A., and Bennett, D. A. (2018). Sex differences in Alzheimer's disease and common neuropathologies of aging. *Acta Neuropathol.* 136, 887–900. doi: 10.1007/s00401-018-1920-1
- Perperoglou, A., Sauerbrei, W., Abrahamowicz, M., and Schmid, M. (2019). A review of spline function procedures in R. *BMC Med. Res. Methodol.* 19:46. doi: 10.1186/s12874-019-0666-3
- Petersen, R. C., Parisi, J. E., Dickson, D. W., Johnson, K. A., Knopman, D. S., Boeve, B. F., et al. (2006). Neuropathologic features of amnesic mild cognitive impairment. *Arch. Neurol.* 63, 665–672. doi: 10.1001/archneur.63.5.665
- Price, J. L., and Morris, J. C. (1999). Tangles and plaques in nondemented aging and “preclinical” Alzheimer's disease. *Ann. Neurol.* 45, 358–368. doi: 10.1002/1531-8249(199903)45:3<358::aid-ana12<3.0.co;2-x
- Resnick, S. M., Bilgel, M., Moghekar, A., An, Y., Cai, Q., Wang, M. C., et al. (2015). Changes in Abeta biomarkers and associations with APOE genotype in 2 longitudinal cohorts. *Neurobiol. Aging* 36, 2333–2339. doi: 10.1016/j.neurobiolaging.2015.04.001
- Sepulcre, J., Grothe, M. J., d'Oleire Uquillas, F., Ortiz-Teran, L., Diez, I., Yang, H. S., et al. (2018). Neurogenetic contributions to amyloid beta and tau spreading in the human cortex. *Nat. Med.* 24, 1910–1918. doi: 10.1038/s41591-018-0206-4
- Smith, R., Strandberg, O., Mattsson-Carlgrén, N., Leuzy, A., Palmqvist, S., Pontecorvo, M. J., et al. (2020). The accumulation rate of tau aggregates is higher in females and younger amyloid-positive subjects. *Brain* 143, 3805–3815. doi: 10.1093/brain/awaa327
- Sperling, R. A., Aisen, P. S., Beckett, L. A., Bennett, D. A., Craft, S., Fagan, A. M., et al. (2011). Toward defining the preclinical stages of Alzheimer's disease: recommendations from the National Institute on Aging-Alzheimer's Association workgroups on diagnostic guidelines for Alzheimer's disease. *Alzheimers Dement.* 7, 280–292. doi: 10.1016/j.jalz.2011.03.003
- Thal, D. R., Rub, U., Orantes, M., and Braak, H. (2002). Phases of A beta-deposition in the human brain and its relevance for the development of AD. *Neurology* 58, 1791–1800. doi: 10.1212/wnl.58.12.1791
- Thomas, B. A., Cuplov, V., Bousse, A., Mendes, A., Thielemans, K., Hutton, B. F., et al. (2016). PETPVC: a toolbox for performing partial volume correction techniques in positron emission tomography. *Phys. Med. Biol.* 61, 7975–7993. doi: 10.1088/0031-9155/61/22/7975
- Thomas, B. A., Erlandsson, K., Modat, M., Thurfjell, L., Vandenberghe, R., Ourselin, S., et al. (2011). The importance of appropriate partial volume correction for PET quantification in Alzheimer's disease. *Eur. J. Nucl. Med. Mol. Imaging* 38, 1104–1119. doi: 10.1007/s00259-011-1745-9
- Villemagne, V. L., Burnham, S., Bourgeat, P., Brown, B., Ellis, K. A., Salvado, O., et al. (2013). Amyloid beta deposition, neurodegeneration, and cognitive decline in sporadic Alzheimer's disease: a prospective cohort study. *Lancet Neurol.* 12, 357–367. doi: 10.1016/S1474-4422(13)70044-9
- Wood, S. N. (2003). Thin plate regression splines. *J. R. Stat. Soc. Ser. B Stat. Methodol.* 65, 95–114.
- Wood, S. N., and Fasiolo, M. (2017). A generalized Feller-Schall method for smoothing parameter optimization with application to Tweedie location, scale and shape models. *Biometrics* 73, 1071–1081. doi: 10.1111/biom.12666
- Zhu, K., Wang, X., Sun, B., Wu, J., Lu, H., Zhang, X., et al. (2019). Primary age-related tauopathy in human subcortical nuclei. *Front. Neurosci.* 13:529. doi: 10.3389/fnins.2019.00529

Conflict of Interest: The authors declare that the research was conducted in the absence of any commercial or financial relationships that could be construed as a potential conflict of interest.

Publisher's Note: All claims expressed in this article are solely those of the authors and do not necessarily represent those of their affiliated organizations, or those of the publisher, the editors and the reviewers. Any product that may be evaluated in this article, or claim that may be made by its manufacturer, is not guaranteed or endorsed by the publisher.

Citation: Kim JP, Chun MY, Kim SJ, Jang H, Kim HJ, Jeong JH, Na DL and Seo SW (2022) Distinctive Temporal Trajectories of Alzheimer's Disease Biomarkers According to Sex and APOE Genotype: Importance of Striatal Amyloid. *Front. Aging Neurosci.* 14:829202. doi: 10.3389/fnagi.2022.829202

Copyright © 2022 Kim, Chun, Kim, Jang, Kim, Jeong, Na and Seo. This is an open-access article distributed under the terms of the Creative Commons Attribution License (CC BY). The use, distribution or reproduction in other forums is permitted, provided the original author(s) and the copyright owner(s) are credited and that the original publication in this journal is cited, in accordance with accepted academic practice. No use, distribution or reproduction is permitted which does not comply with these terms.



Aged Cattle Brain Displays Alzheimer's Disease-Like Pathology and Promotes Brain Amyloidosis in a Transgenic Animal Model

Ines Moreno-Gonzalez^{1,2,3,4*}, George Edwards III¹, Rodrigo Morales^{1,4}, Claudia Duran-Aniotz^{1,5,6}, Gabriel Escobedo Jr.¹, Mercedes Marquez⁷, Marti Pumarola^{7,8} and Claudio Soto^{1*}

¹ Department of Neurology, Mitchell Center for Alzheimer's Disease and Related Brain Disorders, University of Texas Health Science Center at Houston, Houston, TX, United States, ² Departamento Biología Celular, Genética y Fisiología, Instituto de Investigación Biomedica de Málaga-IBIMA, Universidad de Málaga, Málaga, Spain, ³ Center for Biomedical Research on Neurodegenerative Diseases (CIBERNED), Madrid, Spain, ⁴ Centro Integrativo de Biología y Química Aplicada (CIBQA), Universidad Bernardo O'Higgins, Santiago, Chile, ⁵ Center for Social and Cognitive Neuroscience (CSCN), School of Psychology, Universidad Adolfo Ibáñez, Santiago, Chile, ⁶ Latin American Institute for Brain Health (BrainLat), Universidad Adolfo Ibáñez, Santiago, Chile, ⁷ Department of Animal Medicine and Surgery, Veterinary Faculty, Animal Tissue Bank of Catalunya (BTAC), Universitat Autònoma de Barcelona, Bellaterra (Cerdanyola del Valles), Barcelona, Spain, ⁸ Networking Research Center on Bioengineering, Biomaterials and Nanomedicine (CIBER-BBN), Universitat Autònoma de Barcelona, Bellaterra (Cerdanyola del Valles), Barcelona, Spain

OPEN ACCESS

Edited by:

Nilton Custodio,
Peruvian Institute of Neurosciences
(IPN), Peru

Reviewed by:

Diana Laura Castillo-Carranza,
University of Monterrey, Mexico
M. Heather West Greenlee,
Iowa State University, United States

*Correspondence:

Ines Moreno-Gonzalez
inesmoreno@uma.es
Claudio Soto
Claudio.Soto@uth.tmc.edu

Specialty section:

This article was submitted to
Alzheimer's Disease and Related
Dementias,
a section of the journal
Frontiers in Aging Neuroscience

Received: 15 November 2021

Accepted: 17 December 2021

Published: 31 January 2022

Citation:

Moreno-Gonzalez I, Edwards G III, Morales R, Duran-Aniotz C, Escobedo G Jr, Marquez M, Pumarola M and Soto C (2022) Aged Cattle Brain Displays Alzheimer's Disease-Like Pathology and Promotes Brain Amyloidosis in a Transgenic Animal Model.
Front. Aging Neurosci. 13:815361.
doi: 10.3389/fnagi.2021.815361

Alzheimer's disease (AD) is one of the leading causes of dementia in late life. Although the cause of AD neurodegenerative changes is not fully understood, extensive evidence suggests that the misfolding, aggregation and cerebral accumulation of amyloid beta (A β) and tau proteins are hallmark events. Recent reports have shown that protein misfolding and aggregation can be induced by administration of small quantities of preformed aggregates, following a similar principle by which prion diseases can be transmitted by infection. In the past few years, many of the typical properties that characterize prions as infectious agents were also shown in A β aggregates. Interestingly, prion diseases affect not only humans, but also various species of mammals, and it has been demonstrated that infectious prions present in animal tissues, particularly cattle affected by bovine spongiform encephalopathy (BSE), can infect humans. It has been reported that protein deposits resembling A β amyloid plaques are present in the brain of several aged non-human mammals, including monkeys, bears, dogs, and cheetahs. In this study, we investigated the presence of A β aggregates in the brain of aged cattle, their similarities with the protein deposits observed in AD patients, and their capability to promote AD pathological features when intracerebrally inoculated into transgenic animal models of AD. Our data show that aged cattle can develop AD-like neuropathological abnormalities, including amyloid plaques, as studied histologically. Importantly, cow-derived aggregates accelerate A β amyloid deposition in the brain of AD transgenic animals. Surprisingly, the rate of induction produced by administration of the cattle material was substantially higher than induction produced by injection of similar amounts of human AD material. Our findings demonstrate that cows develop seeding-competent A β aggregates, similarly as observed in AD patients.

Keywords: amyloid, prions, Alzheimer's disease, spreading, protein misfolding, seeding, cattle

INTRODUCTION

Alzheimer's disease (AD) is the most common form of dementia among elderly people and one of leading public health problems in developed countries. AD involves progressive brain atrophy, neuronal death, synaptic dysfunction, astrogliosis and the accumulation of protein aggregates in the form of amyloid-beta ($A\beta$) deposits, and tau neurofibrillary tangles. Although the etiology of AD is not yet clear, extensive evidence suggests that the central pathological event is the misfolding, aggregation and brain deposition of $A\beta$ and tau (Soto, 2003; Huang and Mucke, 2012; Masters and Selkoe, 2012). Amyloid accumulates as senile plaques and diffuse deposits in the brain parenchyma and around cerebral blood vessels walls termed cerebral amyloid angiopathy (CAA) (Gomez-Isla et al., 2008).

In addition to AD, various other protein misfolding diseases (PMDs) are thought to be caused by accumulation of misfolded aggregated proteins in various tissues, including highly prevalent illnesses such as Parkinson's disease (PD), type 2 diabetes and more than 20 other diseases (Chiti et al., 2006; Soto, 2012). Among the latter, prion diseases are quite intriguing because they are transmissible by infection through a proteinaceous infectious agent known as prion (Prusiner, 1998). The molecular mechanism responsible for prion infectivity depends on the ability of the misfolded prion protein aggregates to act as seeds, inducing the templated conversion of natively folded prion protein into the developing aggregates (Soto, 2012). In this manner, the pathological protein progressively grows by recruiting more and more of the normal protein. This process is often referred as seeding/nucleation polymerization. Importantly, protein aggregation of all proteins involved in PMDs follows the seeding-nucleation mechanism (Caughey and Lansbury, 2003; Soto, 2012). The similarities between prion replication and amyloid formation, and the intrinsic ability of aggregated seeds to self-propagate the polymerization process led us and others to hypothesize over 10 years ago that misfolded aggregates associated to other PMDs can spread by the prion principle (Soto et al., 2006; Walker et al., 2006). Remarkably, a series of exciting recent reports have demonstrated that several PMDs can be experimentally transmitted by a prion-like mechanism in various cellular and animal models of diverse diseases (Prusiner, 2012; Walker and Jucker, 2015). Over the past decade, many of the hallmark properties of prions as infectious agents have been shown to be shared by several of the prion-like misfolded proteins. For the specific case of $A\beta$, studies from us and other groups have shown that inoculation of transgenic mouse models of amyloidosis with tissue homogenates from patients affected by AD results in induction or acceleration of amyloid pathology in the recipient animals (Kane et al., 2000; Meyer-Luehmann et al., 2006; Morales et al., 2011; Watts et al., 2011). Moreover, in animals not genetically programmed to develop the disease spontaneously, inoculation with AD brain homogenates leads to a completely *de novo* disease, more akin to infectious prions (Morales et al., 2011; Rosen et al., 2011). Importantly, pathological induction can be reduced by depleting the inoculum of $A\beta$ aggregates (Meyer-Luehmann et al., 2006; Duran-Aniotz et al., 2014). Even more strikingly, efficient

induction has been observed by the addition of misfolded protein aggregates prepared *in vitro* using synthetic $A\beta$ (Stöhr et al., 2012). Accumulation of $A\beta$ aggregates can be promoted by inoculation of very small amounts of aggregated seeds (Fritsch et al., 2014; Morales et al., 2015a) and titration experiments have shown that the rate of induction is proportional to the amount of seeds inoculated. Finally, disease transmission has been observed even when seeds were administered systemically (Eisele et al., 2010).

The findings described above suggest that $A\beta$ and other misfolded protein aggregates can indeed behave as prions. Still, the main controversy is whether other misfolded proteins can act as infectious agents to transmit the disease among individuals under natural conditions (Fernández-Borges et al., 2013; Irwin et al., 2013; Beekes et al., 2014; Collinge, 2016). Aside from this important point, another aspect that has not been explored is the possibility that protein aggregates accumulating in animals may initiate the disease in humans. Indeed, prion diseases affect not only humans, but also various species of mammals. The accumulation of $A\beta$ aggregates has not been extensively analyzed in animals, however, it has been reported that AD aggregates are present in the brain of several aged non-human mammals, including monkeys, bears, dogs, and cheetahs (Moreno-Gonzalez and Soto, 2018). In bovine brains, $A\beta$ has been as previously observed as granular aggregates, but not depositing in plaques (Costassa et al., 2016). In this study, we investigated the presence of AD-like pathology in aged cow brains and whether, in analogy to prion diseases, $A\beta$ aggregates derived from cattle brain can induce $A\beta$ misfolding and aggregation in a transgenic mice model of AD amyloidosis.

MATERIALS AND METHODS

Cattle Samples

Cattle samples were obtained from the Animal Tissue Bank of Catalunya (BTAC), Department of Animal Medicine and Surgery, Veterinary Faculty, Universitat Autònoma de Barcelona, Bellaterra (Cerdanyola del Valles), Barcelona, Spain. Brain samples were obtained from slaughterhouses after the animals were sacrificed. Samples with a *post-mortem* time lower than 10 h were immersed in formol, processed and embedded in paraffin. As shown in **Supplementary Figure 1**, we received 63 samples from female cattle that were 13 to 23 years old. These animals were from 10 different breeds, including Charolais, Bruna of Pirineus, Pirinenca, Limousin, Montbeliard, Simmental, and crossbreeds. We also obtained ten samples of 10 month-old young crossbreed calves that were used as controls. Samples were obtained from the temporal area and contained the hippocampal area, entorhinal cortex, and part of the thalamus.

Human Samples

AD brain hippocampal samples were acquired from the National Disease Research Interchange (USA). Informed consent was obtained for experimentation with human subjects. The Code of Ethics of the World Medical Association (Declaration of Helsinki) was followed to perform research on human samples and they were manipulated following the universal precautions

for working with human samples and as directed by the Institutional Review Board of McGovern Medical School at The University of Texas Health Science Center at Houston.

Brain Homogenate

Cattle and human brain tissue were homogenized at 10% w/v in PBS containing a cocktail of protease inhibitors for western blot and ELISA quantifications. For intracerebral inoculations, samples were homogenized at 40% w/v in the same solution and sterilized by the addition of 1% of antibiotic/antimycotic solution (Gibco) and γ -irradiated for 1 h.

Western Blot

10% cattle brain homogenates were mixed with denaturing loading buffer (Invitrogen), heated for 10 min at 95 °C and fractionated in 4–12% NuPAGE gels (Invitrogen). Proteins were transferred to a nitrocellulose membrane (GE Healthcare), blocked with 10% milk, and incubated with rabbit anti-A β 42 polyclonal antibody (Covance). After incubation with secondary antibody, A β 42 was visualized by chemoluminescence using ECL plus (GE Healthcare) in a dark chamber (BioRad).

ELISA

Mouse brain hemispheres were homogenized at 10% w/v in PBS containing a cocktail of protease inhibitors. Brain extracts were centrifuged at 32,600 rpm for 1 h at 4°C in an ultracentrifuge (Beckman-Coulter). The pellets were resuspended in 200 μ L of 70% formic acid followed by sonication. Samples were centrifuged for 30 min in the same conditions and the supernatant was collected. This insoluble fraction was neutralized in 1M Tris buffer, pH 11. Brain levels of A β 42 were measured using a human A β ELISA kit (Invitrogen) on an ELISA plate reader (EL800 BIO-TEK).

Histology

Serial 10- μ m-thick sections from all cattle, human, and mouse groups were processed for immunostaining. After blocking the endogenous peroxidase activity with 3% H₂O₂–10% methanol for 20 min, sections were incubated overnight at room temperature in mouse anti-A β 4G8 (1:1,000 Covance). Sections stained for A β were pretreated with 85% formic acid. Primary antibody was detected by incubating 1 h with goat anti-mouse HRP-linked secondary antibody and the peroxidase reaction was visualized using a DAB Kit (Vector) following the manufacturer's instructions. For counterstaining, sections were incubated in Harris hematoxylin for 1 min (Fisher). For Thioflavin-S (ThS) staining, tissue slices were incubated in ThS solution (0.025% in 50% ethanol) for 8 min. Finally, all sections were dehydrated in graded ethanol, cleared in xylene, cover-slipped with DPX mounting medium, and examined under a bright field/epifluorescent microscope (DMI6000B, Leica).

Animals

Hemizygous APP/PS1 (B6C3-Tg APP^{swe}, PSEN1^{dE9} 85Dbo/J, The Jackson Laboratory) mice express human amyloid precursor protein (APP^{695swe}) and a mutant human presenilin 1 (PS1-^{dE9}) in a B6C3 background. These animals develop amyloid plaques and other AD-like features starting around 6 months of

age (Jankowsky et al., 2004). Animals were housed in groups of up to five in individually ventilated cages under standard conditions (22°C, 12 h light–dark cycle) receiving food and water *ad libitum*. All animal experiments were carried out in accordance with the NIH regulations and approved by the committee of animal use for research at The University of Texas Health Science Center at Houston. Mice were sacrificed by CO₂ inhalation and perfused transcardially with PBS. Brains were removed, post-fixed into fixative solution (10% neutral buffered formalin) and embedded in paraffin.

Animal Inoculation

For intracerebral inoculation, 30–40 days-old APP/PS1 mice were injected with 10 μ L of 40% (w/v) cattle or human brain homogenate in each hemisphere ($n = 8$ to 11 per group), without any purification or isolation. Briefly, mice were anesthetized using isoflurane. Skin was incised and a small hole was drilled in the skull and samples were injected into both hippocampi. At the end of the treatment, skin was closed using surgical suture. Animals were placed on a thermal pad until recovery and monitored daily for several days.

Histological Quantification

Burden quantification was done through the lateromedial extent of the cortical and hippocampal areas in the sagittal plane, being the first section of each animal randomly collected. Quantification was assessed in every tenth section (with a distance of 100 μ m among them), and four to six 10 μ m sections were measured for each animal ($n = 8$ –11 per group). Photomicrographs were taken by using a DFC310 FX Leica digital camera, imported into ImageJ 1.45s software (NIH) and converted to black and white images. Threshold intensity was manually set and kept constant, and the number of pixels was determined for 4G8 immunostained sections to quantify amyloid load in the hippocampal formation (CA1, CA2, CA3, and dentate gyrus) and several cortical areas (including motor, somatosensory, visual, frontal, parietal and retrosplenial cortex). Analysis for each was done by a single examiner blinded to sample identities.

Statistical Analysis

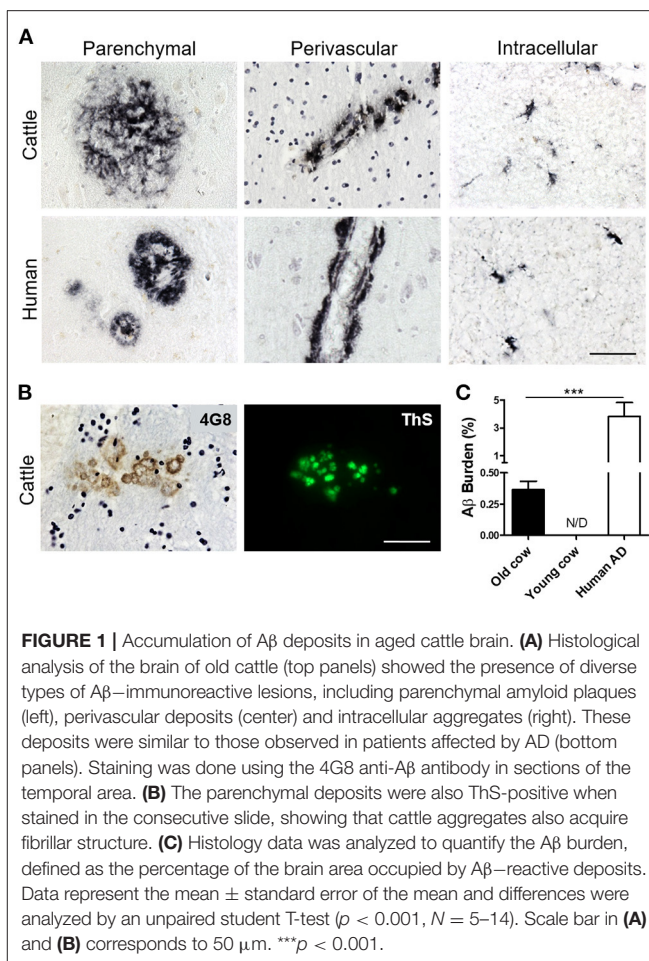
Graphs are expressed as means \pm standard error (s.e.m.). After confirming normal distribution with Skewness and Kurtosis statistic test, *T*-test or one way analysis of variance (ANOVA) followed by a *post-hoc* Tukey's multiple comparisons test were used to analyze differences among groups. Statistical analyses were performed using GraphPad Prism 5.0 software (GraphPad Software Inc). Statistical differences for all tests were considered significant at the $p < 0.05$ level.

RESULTS

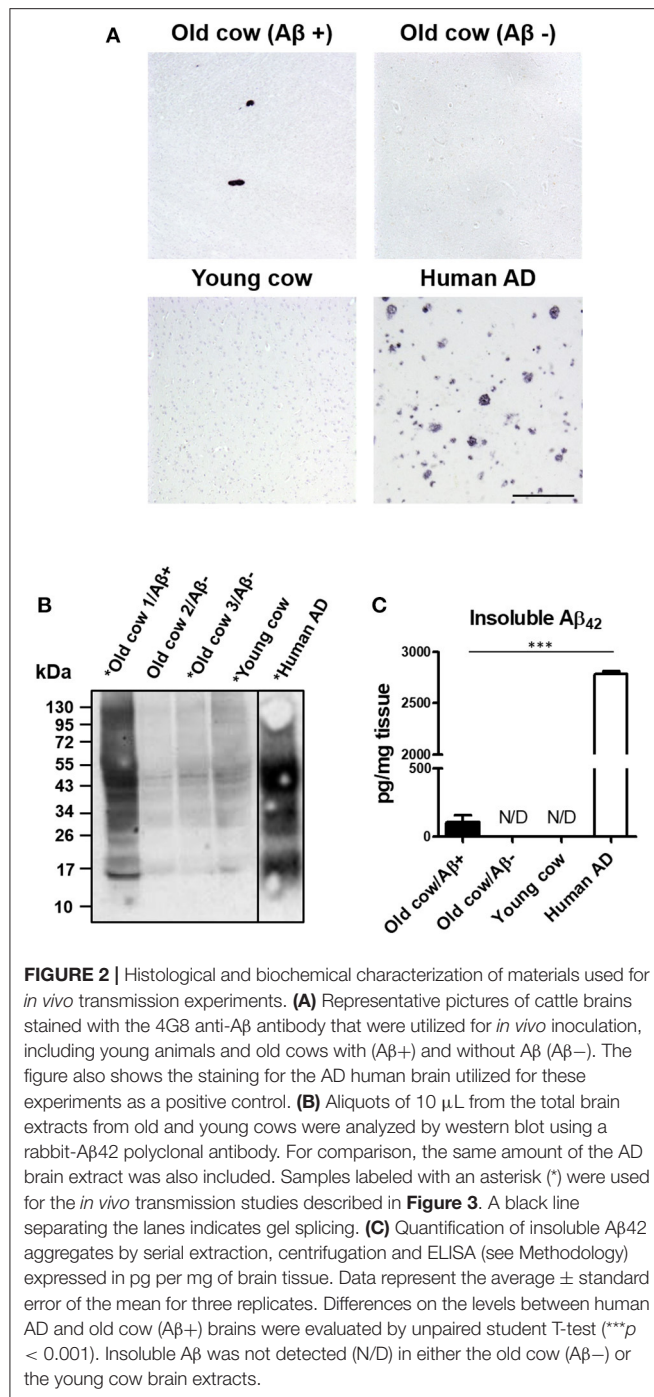
To investigate whether cattle develops AD-related abnormalities, we performed a detailed histological study for the presence of amyloid-like deposits in the brain of cows of different ages. The majority of the samples were from female cattle of the Bruna of Pirineus and various crossbreed

(**Supplementary Figure 1A**). Old animal ages ranged from 13 to 23 years old (**Supplementary Figure 1B**). For this study, we analyzed the hippocampus, temporal cortex, and thalamus of more than 60 cows (**Supplementary Figure 1C**). For most of the specimens analyzed, we had access to both snap-frozen and formalin-fixed material. Positive and negative controls included human AD brains and 10 month-old calf brains, respectively. Paraffin embedded fixed tissue from all the specimens (cattle and human samples) were processed and stained for A β . The amino acid sequence of A β in both humans and cattle is exactly the same (Johnstone et al., 1991); therefore, we were able to use the same antibodies. After a complete histopathological analysis, we observed a scattered appearance of A β deposits in many slices of some aged cow brains (**Figure 1A**). A β deposits were detected in the cortex and hippocampus of various cows >13 years old, but not in any young animals. Cow amyloid deposits were reactive against human anti-A β antibody (4G8), depositing as mature plaques similar to those seen in human AD patients' brains (**Figure 1A**, left panels). We also observed perivascular deposits, which are highly reminiscent of cerebral amyloid angiopathy lesions commonly seen in human AD brains (**Figure 1A**, center panels). In addition, intracellular A β staining was observed in both cattle and human brains (**Figure 1A**, right panels). Most of the deposits observed in cattle brain corresponded to fibrillar amyloid aggregates, as confirmed by the positive staining of the plaques using thioflavin-S (ThS) in the consecutive slice (**Figure 1B**). In total, 14 out of 63 brains from cows older than 13 years of age displayed A β aggregates in the brain areas studied, although just nine of them presented A β plaques similar to those observed in humans (14.3%). To examine the relative amount of amyloid deposits observed in cattle brain and compare it with that present in patients affected by AD, we performed image analysis of the temporal area from 14 old cows exhibiting amyloid pathology and five patients with AD (**Figure 1C**). The results show that the brains of old cows have a substantial amount of amyloid deposits. Indeed, in the hippocampal region, the animals analyzed showed an amyloid burden of $0.37 \pm 0.07\%$, which means that 0.37% of the brain area analyzed was occupied by amyloid. Nevertheless, this burden is significantly smaller (>10-fold lower) than the one estimated on the AD patients ($3.82 \pm 1.0\%$) analyzed (**Figure 1C**). We could not detect any A β aggregates in young cattle brain samples.

We and others have shown that inoculation of A β -rich brain homogenate from AD patients or transgenic mice is able to induce an early AD-like pathology in recipient transgenic animals (Meyer-Luehmann et al., 2006; Eisele et al., 2010; Morales et al., 2011). Knowing that the sequence of cattle A β peptide is identical to the human one, we wanted to test whether cattle brain harboring amyloid aggregates exacerbate AD pathology in susceptible mice. To that end, we intracerebrally (i.c.) injected amyloid-containing cow brain tissue extracts into a double transgenic (APP/PS1) mouse model of brain amyloidosis (Jankowsky et al., 2004) and analyzed the possible acceleration of the pathology. For the experiment, the following five groups ($n = 8$ –11 per group) of animals were used: (i) the experimental group injected with 40% brain homogenate from an old cow containing amyloid deposits (Old cow/A β +); (ii) a group injected with the



same amount of old cow brain homogenate in which amyloid deposition was not detected by histological or biochemical analysis (old cow/A β -); (iii) a control group injected with 40% brain extract from a young cow; (iv) a negative control consisting of untreated animals; and (v) a positive control in animals injected with human AD brain homogenate. Before treatment, the inocula for the different groups were thoroughly analyzed by histological and biochemical techniques to measure the presence and quantity of A β aggregates. **Figure 2A** shows the comparative histological staining of representative brain sections from the different subjects used for inoculation. No amyloid staining was seen in any of the slices analyzed from the young cow or the old cow/A β -. In contrast, the old cow/A β + exhibited scattered appearance of 4G8 positive deposits reminiscent of amyloid plaques, similar in morphology to human AD brains (**Figure 2A**). Biochemical analysis of cattle brain homogenate by western blot demonstrated that the specimen selected for the experimental group (old cow1/A β +) presented a wide range of high molecular weight species reactive with an antibody that recognizes specifically human A β 42 (**Figure 2B**). Only some of these bands were detectable and at a much lesser intensity in 10-month-old young cow or the old cows/A β -, used as age-matched controls. The samples indicated with an asterisk in **Figure 2B**

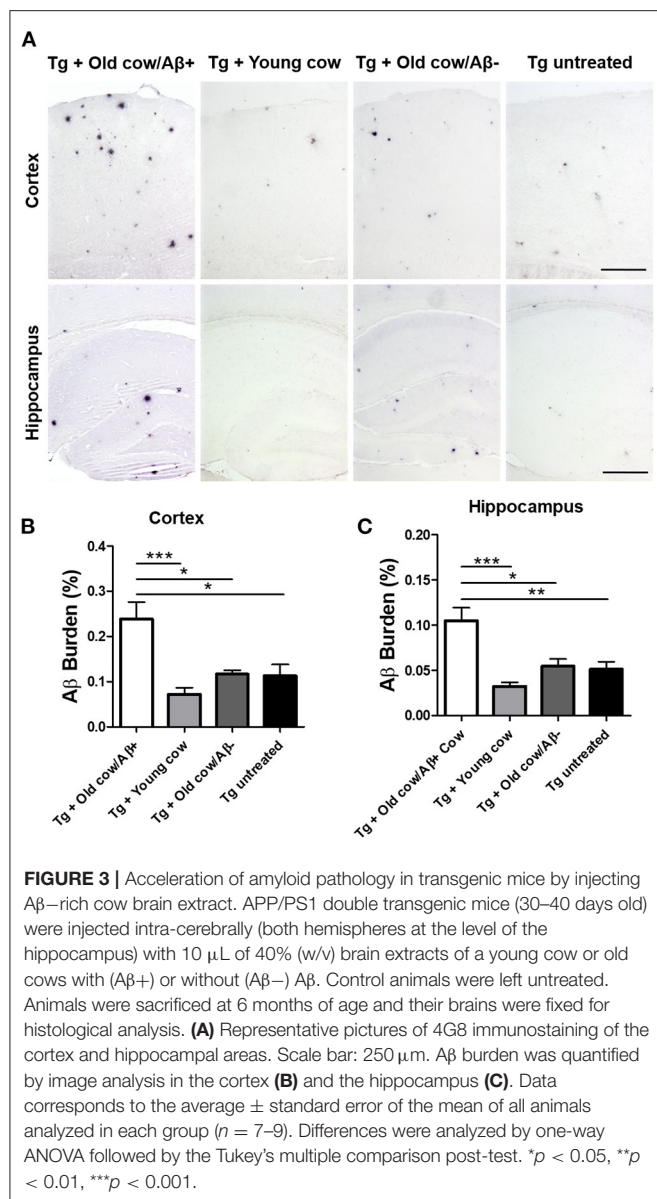


were used for the transmissibility experiments described below. Finally, we measured the amount of $A\beta_{42}$ in the insoluble fraction after extraction with formic acid in each of the inocula (**Figure 2C**). The results showed a concentration of insoluble $A\beta_{42}$ of 31.72 pg/mg of tissue in the old cow/ $A\beta+$. In contrast, no detectable insoluble $A\beta_{42}$ was observed in the young cow or the old cow/ $A\beta-$. It is important to highlight that even though the levels of insoluble $A\beta_{42}$ in the old cow/ $A\beta+$ brain

were significantly higher than in young animals, they represent only around 1% of the levels detectable in human AD brain homogenate (2,788.78 pg/mg) (**Figure 2C**).

To evaluate the ability of $A\beta$ aggregates deposited in cattle brain to seed amyloid formation *in vivo*, double transgenic animals were injected i.c. at 30–40 days old with 10 μ L of 40% amyloid-containing old cow brain homogenate into both hippocampal hemispheres through stereotactic surgery (Tg + Old cow/ $A\beta+$). In addition, various groups of control animals were treated with the diverse inocula described above. Animals were sacrificed at 6 months-old, when they normally start developing plaques due to the transgenic expression of the mutant genes. 4G8 immunostaining showed that animals injected with amyloid-containing cattle brain homogenate displayed more amyloid plaques in the cortical area than the control groups (**Figure 3A**, top panels). When $A\beta$ load was measured by image analysis, we could observe that there was a statistically significant increase in $A\beta$ burden (stained area/total area analyzed) in the group injected with old cow/ $A\beta+$. The increase was as much as 2-fold (0.24 ± 0.04 vs. 0.11 ± 0.03 %) compared to non-treated animals (**Figure 3B**). Analysis of $A\beta$ deposition in the hippocampus, where the inoculation occurred, showed similar results (**Figure 3A**, bottom panels). Quantification of the hippocampal amyloid burden in experimental and control groups also showed that animals injected with $A\beta$ -containing cattle brain homogenate doubled the regular amount of $A\beta$ (0.11 ± 0.02 vs. $0.05 \pm 0.01\%$) found in the hippocampus of APP/PS1 at this age (**Figure 3C**). Moreover, staining of fibrillar aggregates by ThS also showed that animals injected with $A\beta$ -containing cow brain tissue displayed more ThS-positive plaques in both cortex and hippocampus than control groups (**Figure 4**). These results indicate that amyloid deposits present in cattle brain homogenate contain seeding-competent $A\beta$ aggregates that are able to accelerate $A\beta$ deposition when inoculated into a transgenic animal model of AD.

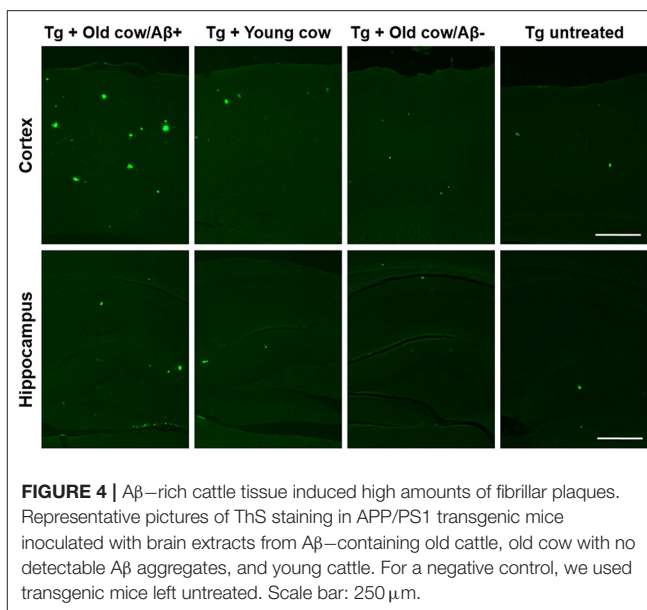
To compare the seeding capability of cattle and human $A\beta$ aggregates to induce amyloid deposition, APP/PS1 transgenic animals were also inoculated with human brain extracts from a patient affected by AD. The amyloid deposition pattern and burden was analyzed by immunohistochemistry in both groups. As shown in **Figure 5A**, the human inoculum was able to induce amyloid deposition to a substantially higher extent than the cattle inoculum in both cortex and hippocampus. In the cortical area, the human brain injection increases amyloid burden 4-fold more than the cattle inoculum (0.92 ± 0.22 vs. $0.24 \pm 0.04\%$) (**Figure 5B**, $p = 0.003$ T-test), whereas in the hippocampus the increase was ~ 10 -fold (1.59 ± 0.30 vs. $0.15 \pm 0.2\%$) (**Figure 5C**, $p < 0.0001$ T-test). However, when the induction ratio (amyloid burden/concentration of insoluble $A\beta_{42}$ injected) was calculated, the data indicates that cattle material promotes amyloid deposition > 10 -fold better than an equivalent quantity of human $A\beta$ aggregates (**Figures 5D,E**). This surprising data suggests that although the cattle sample contains less concentration of aggregated $A\beta$, these structures appear to be more competent to seed amyloid deposition than human samples. In addition, the human aggregates produced a higher proportion of smaller



parenchymal and perivascular amyloid aggregates and in areas where plaques are not generally found in the non-treated animal, such as in the corpus callosum (Figure 5A), whereas cow seeds seem to trigger the formation of larger plaques. The differences in the seeding competency and the profile of aggregates induced suggest that Aβ aggregates present in human and cattle brain may represent different arrangements or “conformational strains” of Aβ seeds.

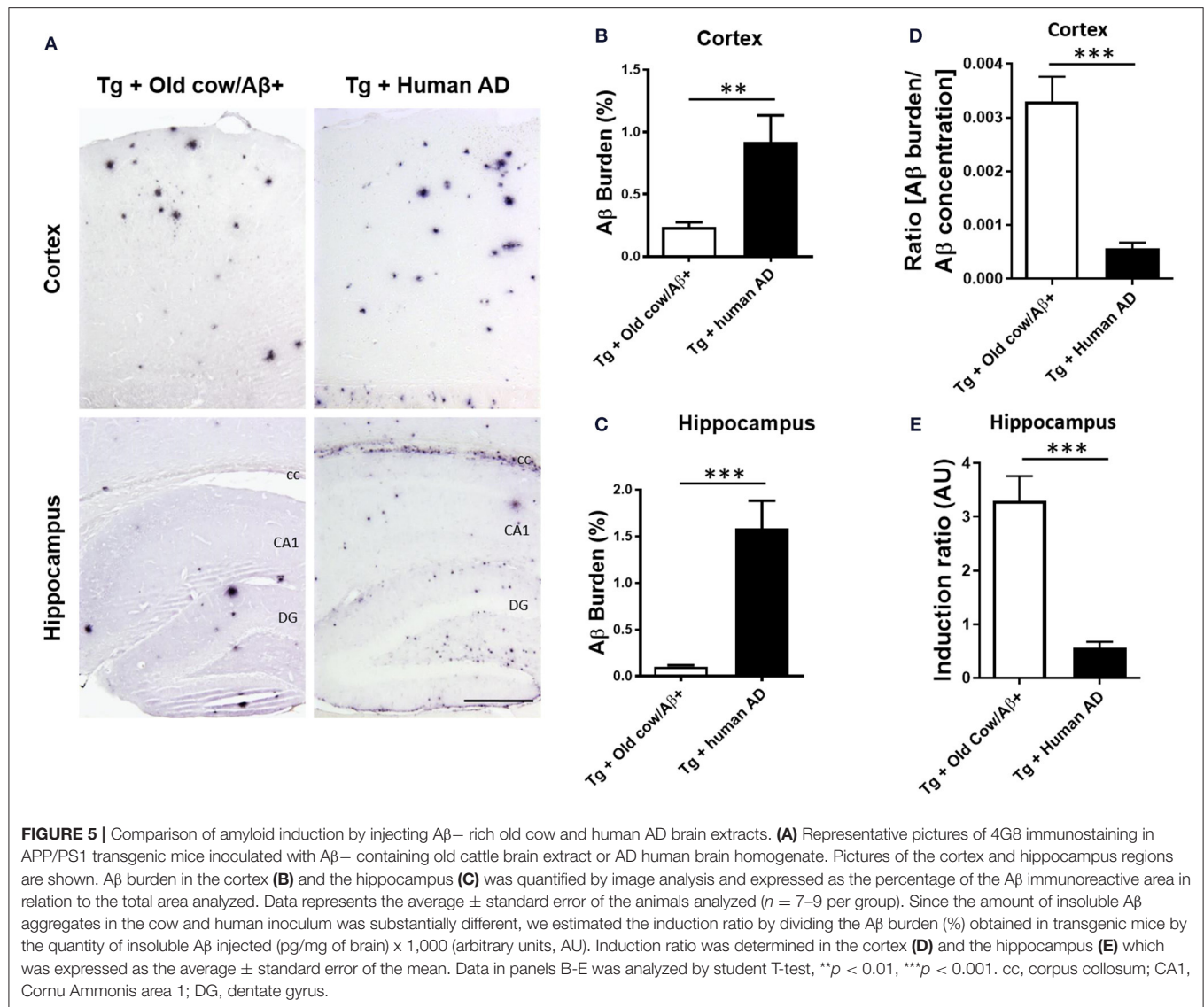
DISCUSSION

The prion-like induction and spreading of misfolded protein aggregates implicated in several protein misfolding disorders is a recently recognized process with potentially important implications to understand the etiology and progression of



these diseases and the development of novel strategies for therapeutic intervention (Prusiner, 2012; Soto, 2012; Walker and Jucker, 2015). The prion principle of disease transmission posits that a misfolded protein aggregate is able to transfer biological information by converting the normal form of the protein into more of the abnormal, disease-associated form. This process initiates the progressive generation of misfolded protein aggregates that spread to other areas of the brain and accumulate over time to produce brain damage and disease. The prion-like transmission of the pathological folding—operating at the molecular and cellular levels—is probably at the root of the spreading of damage throughout the brain that is characteristic of neurodegenerative diseases (Moreno-Gonzalez and Soto, 2011; Thal et al., 2014; Walker and Jucker, 2015). However, in prion diseases transmission also occurs among different individuals in which prions act as *bona fide* infectious agents to spread disease in animal or human populations. Moreover, in the case of prions the disease can be transmitted across animals from different species (Béringue et al., 2008), with the landmark case being the generation of a new human disease, termed variant Creutzfeldt-Jakob disease, produced by exposure to cattle affected by bovine spongiform encephalopathy (Collinge et al., 1996; Bruce et al., 1997; Scott et al., 1999). Evidence gathered over the past 10 years has demonstrated that both protein aggregates implicated in AD (Aβ and tau) can propagate under experimental conditions as prions (Prusiner, 2012; Soto, 2012; Morales et al., 2015a,b; Walker and Jucker, 2015).

The main goal of our study was to investigate whether cattle present AD-like lesions in the brain, and if these pathological features display prion-like seeding activity. For this purpose, we characterized the brains from many cows at different ages for the presence of amyloid deposits and subsequently the ability of those aggregates to induce amyloid pathology in a mouse model of amyloid deposition. The results of this study show



that some old cows spontaneously develop amyloid deposits in their brain. Interestingly, these deposits were similar to those present in human cases of AD. Out of the 63 cattle brain samples analyzed, nine of them (14.3%) displayed typical A β aggregates in the analyzed areas. Therefore, appearance of amyloid deposits in cattle brain appears at a frequency comparable to the prevalence of AD pathological abnormalities in humans, since it is estimated that AD affects about 6% of people 65 years and older, and the incidence doubles every 5 years. Of course, many more elderly non-demented people display amyloid pathology in their brains, a condition that is usually considered as pre-clinical or prodromal AD (Tagliavini et al., 1988; Price et al., 2009).

Cattle brains were also analyzed for hyperphosphorylated tau (ptau) and tangle formation. We found that only three specimens had elevated levels of ptau using AT8 antibody. These brains

were not used as inoculum for the intracerebral inoculation study to specifically evaluate the effect of A β aggregates. We cannot exclude that brains could also contain other types of amyloid seeds including tau oligomers that we were unable to detect. Although tau aggregates can modulate A β toxicity, it has been reported that they are not able to induce A β aggregation (Bloom, 2014; Nisbet et al., 2015). This, together with the use of APP mice, allows evaluating the seeding capability of A β using complete brain homogenates, excluding the effect of potential other seeds present in the inoculum.

Although behavioral or cognitive abnormalities were not analyzed in cows, the amount of A β deposits observed parallels pre-clinical AD. Importantly, brain extracts from old cows containing A β aggregates were able to significantly increase amyloid deposition when injected intra-cerebrally into a double transgenic mouse model of AD amyloidosis. Though the total

level of pathological induction was lower than the one produced by inoculation of AD brain homogenates, the cow material showed a higher promotion activity than human tissue when the rate of induction was corrected by the amount of A β aggregates injected. This surprising result suggests that cattle aggregates are better seeds than their human counterparts. The most likely explanation for this result is that cattle deposits are smaller, less compact and contain smaller amounts of other components compared to human aggregates, which presumably remain deposited in the brain for much longer periods of time. This interpretation is supported by our previous observations showing that brain tissue from people affected by mild cognitive impairment (MCI), which is considered a pre-clinical form of AD, produced significantly higher A β induction than tissue from established AD patients (Duran-Aniotz et al., 2013). Moreover, Jucker and colleagues have shown that small, soluble A β oligomers are better seeds *in vivo* than large fibrillar aggregates (Langer et al., 2011). We have recently published data demonstrating that AD patients displaying different amyloid pathology induce different pathological features in the same transgenic models used in this study (Duran-Aniotz et al., 2021). In that line, the distinctive pathology observed between cattle and human AD patients may be responsible of their dissimilar seeding activity. It could well be that these differences are due to the fact that cattle develop different strain(s) of A β , which are able to accelerate aggregation with smaller amounts of the original seeds or more efficiently. A more in-depth study would be needed to determine the presence of a different A β strain in cattle.

The prion-like transmission of A β aggregates has been extensively reported in animal models and likely plays an important role in the progressive spreading of pathological abnormalities throughout the brain (Moreno-Gonzalez and Soto, 2011; Thal et al., 2014; Walker and Jucker, 2015). Nevertheless, whether this phenomenon ever operates in the inter-individual transmission of disease pathology in humans remains highly debatable. Recent studies have provided evidence for the induction of A β aggregation in people receiving human pituitary-derived growth hormone (Jaunmuktane et al., 2015; Ritchie et al., 2017). However, when the risk of AD development, and not only amyloid pathology, was studied no evidence was found for disease transmission (Irwin et al., 2013). The findings of our current study suggest that A β aggregates present in the brains of old cattle are competent to seed amyloid deposition *in vivo*. This induction has also been observed with other protein aggregates such as AA amyloid (Rising et al., 2021). However, the potential transmission of A β cattle-derived seeds to humans is unlikely, considering that repeated oral administration of AD brain extracts to susceptible mice failed to accelerate pathological features (Morales et al., 2021). The results presented in this manuscript suggest that aged

cattle are susceptible to develop pathological features similar to AD, and that misfolded A β present in their brain is seeding competent.

DATA AVAILABILITY STATEMENT

The raw data supporting the conclusions of this article will be made available by the authors on reasonable request.

ETHICS STATEMENT

The studies involving human participants were reviewed and approved by Institutional Review Board, The University of Texas Health Science Center at Houston. Informed consent was obtained by the National Disease Research Interchange (NDRI). The animal study was reviewed and approved by Committee of Animal Use for Research, The University of Texas Health Science Center at Houston.

AUTHOR CONTRIBUTIONS

IM-G designed the experiments, participated in animal manipulation, performed the histological, biochemical, image, and statistical analyses, prepared the figures, and wrote the manuscript. GEIII participated in animal manipulation and performed the histological analysis. RM participated in animal manipulation and participated in the experimental design. CD-A performed histological, image, and statistical analysis. GEJr participated in histological analysis. MM and MP provided cattle samples and performed their initial neuropathological analysis. CS supervised the entire project, designed the research plan, and wrote the manuscript. All authors read and approved the final manuscript.

FUNDING

This work was partially funded by the Alzheimer's Association (NIRP-12-257323 to IM-G, AARGD-18-566576 to RM), the Spanish Ministry of Science and Innovation PID2019-107090RA-I00 and Ramon y Cajal Program RYC-2017-21879 (IM-G), the National Institutes of Health RF1AG072491 (RM) and 3P01AI077774-09S1 to CS, and an award from the Mitchell Foundation (CS) 2018-AARG-591107, ANID/FONDEF ID20II10152, ANID/FONDECYT 1210622, and Anillo ACT210096 to CD-A.

SUPPLEMENTARY MATERIAL

The Supplementary Material for this article can be found online at: <https://www.frontiersin.org/articles/10.3389/fnagi.2021.815361/full#supplementary-material>

REFERENCES

- Beekes, M., Thomzig, A., Schulz-Schaeffer, W. J., and Burger, R. (2014). Is there a risk of prion-like disease transmission by Alzheimer- or Parkinson-associated protein particles? *Acta Neuropathol.* 128, 463–476. doi: 10.1007/s00401-014-1324-9
- Béringue, V., Vilotte, J. L., and Laude, H. (2008). Prion agent diversity and species barrier. *Vet. Res.* 39, 47. doi: 10.1051/vetres:2008024

- Bloom, G. S. (2014). Amyloid- β and Tau: The trigger and bullet in Alzheimer disease pathogenesis. *JAMA Neurol.* 71, 505–508. doi: 10.1001/jamaneurol.2013.5847
- Bruce, M. E., Will, R. G., Ironside, J. W., McConnell, I., Drummond, D., Suttie, A., et al. (1997). Transmissions to mice indicate that “new variant” CJD is caused by the BSE agent. *Nature.* 389, 498–501. doi: 10.1038/39057
- Caughey, B., and Lansbury, P. T. (2003). Protofibrils, pores, fibrils, and neurodegeneration: separating the responsible protein aggregates from the innocent bystanders. *Annu. Rev. Neurosci.* 26, 267–298. doi: 10.1146/annurev.neuro.26.010302.081142
- Chiti, Z., Knutsen, O. M., Betmouni, S., and Greene, J. R. T. (2006). An integrated, temporal study of the behavioural, electrophysiological and neuropathological consequences of murine prion disease. *Neurobiol. Dis.* 22, 363–373. doi: 10.1016/j.nbd.2005.12.002
- Collinge, J. (2016). Mammalian prions and their wider relevance in neurodegenerative diseases. *Nature.* 217–26. doi: 10.1038/nature20415
- Collinge, J., Sidle, K. C., Meads, J., Ironside, J., and Hill, A. F. (1996). Molecular analysis of prion strain variation and the aetiology of “new variant” CJD. *Nature.* 383, 685–690. doi: 10.1038/383685a0
- Costassa, E. V., Fiorini, M., Zanusso, G., Peletto, S., Acutis, P., and Baioni, E. (2016). Characterization of amyloid- β deposits in bovine brains. *J. Alzheimer's Dis.* 51, 875. doi: 10.3233/JAD-151007
- Duran-Aniotz, C., Morales, R., Moreno-Gonzalez, I., Hu, P. P., Fedynyshyn, J., and Soto, C. (2014). Aggregate-depleted brain fails to induce Abeta deposition in a mouse model of Alzheimer's disease. *PLoS ONE.* 9, e89014. doi: 10.1371/journal.pone.0089014
- Duran-Aniotz, C., Morales, R., Moreno-Gonzalez, I., Hu, P. P., and Soto, C. (2013). Brains from non-Alzheimer's individuals containing amyloid deposits accelerate Abeta deposition in vivo. *Acta Neuropathol. Commun.* 1, 76. doi: 10.1186/2051-5960-1-76
- Duran-Aniotz, C., Moreno-Gonzalez, I., Gamez, N., Perez-Urrutia, N., Vegas-Gomez, L., and Soto, C. (2021). Amyloid pathology arrangements in Alzheimer's disease brains modulate in vivo seeding capability. *Acta Neuropathol. Commun.* 9, 1–13. doi: 10.1186/s40478-021-01155-0
- Eisele, Y. S., Obermüller, U., Heilbronner, G., Baumann, F., Kaeser, S. A., and Wolburg, H. (2010). Peripherally applied Abeta-containing inoculates induce cerebral beta-amyloidosis. *Science.* 330, 980–982. doi: 10.1126/science.1194516
- Fernández-Borges, N., Eraña, H., Elezgarai, S. R., Harrathi, C., Gayosso, M., and Castilla, J. (2013). Infectivity versus seeding in neurodegenerative diseases sharing a prion-like mechanism. *Int. J. Cell Biol.* 2013, 583498. doi: 10.1155/2013/583498
- Fritsch, S. K., Langer, F., Kaeser, S. A., Maia, L. F., Portelius, E., and Pinotsi, D. (2014). Highly potent soluble amyloid-beta seeds in human Alzheimer brain but not cerebrospinal fluid. *Brain.* 137, 2909–2915. doi: 10.1093/brain/awu255
- Gomez-Isla, T., Spires, T., and Calignon A. D., and Hyman, B. T. (2008). Neuropathology of Alzheimer's disease. *Handb. Clin. Neurol.* 89, 233–243. doi: 10.1016/S0072-9752(07)01222-5
- Huang, Y., and Mucke, L. (2012). Alzheimer mechanisms and therapeutic strategies. *Cell.* 148, 1204–1222. doi: 10.1016/j.cell.2012.02.040
- Irwin, D. J., Abrams, J. Y., Schonberger, L. B., Leschek, E. W., Mills, J. L., and Lee, V. M. Y. (2013). Evaluation of potential infectivity of Alzheimer and Parkinson disease proteins in recipients of cadaver-derived human growth hormone. *JAMA Neurol.* 70, 462–468. doi: 10.1001/jamaneurol.2013.1933
- Jankowsky, J. L., Fadale, D. J., Anderson, J., Xu, G. M., Gonzales, V., and Jenkins, N. A. (2004). Mutant presenilins specifically elevate the levels of the 42 residue beta-amyloid peptide in vivo: evidence for augmentation of a 42-specific gamma secretase. *Hum. Mol. Genet.* 13, 159–170. doi: 10.1093/hmg/ddh019
- Jaunmuktane, Z., Mead, S., Ellis, M., Wadsworth, J. D., Nicoll, A. J., and Kenny, J. (2015). Evidence for human transmission of amyloid-beta pathology and cerebral amyloid angiopathy. *Nature.* 525, 247–250. doi: 10.1038/nature15369
- Johnstone, E. M., Chaney, M. O., Norris, F. H., Pascual, R., and Little, S. P. (1991). Conservation of the sequence of the Alzheimer's disease amyloid peptide in dog, polar bear and five other mammals by cross-species polymerase chain reaction analysis. *Brain Res. Mol. Brain Res.* 10, 299–305. doi: 10.1016/0169-328X(91)90088-F
- Kane, M. D., Lipinski, W. J., Callahan, M. J., Bian, F., and Durham, R. (2000). Evidence for seeding of beta -amyloid by intracerebral infusion of Alzheimer brain extracts in beta -amyloid precursor protein-transgenic mice. *J. Neurosci.* 20, 3606–11. doi: 10.1523/JNEUROSCI.20-10-03606.2000
- Langer, F., Eisele, Y. S., Fritsch, S. K., Staufenbiel, M., Walker, L. C., and Jucker, M. (2011). Soluble Abeta seeds are potent inducers of cerebral beta-amyloid deposition. *J. Neurosci.* 31, 14488–14495. doi: 10.1523/JNEUROSCI.3088-11.2011
- Masters, C. L., and Selkoe, D. J. (2012). Biochemistry of amyloid-protein and amyloid deposits in Alzheimer disease. *Cold Spring Harb.* 2, a006262. doi: 10.1101/cshperspect.a006262
- Meyer-Luehmann, M., Coomaraswamy, J., Bolmont, T., Kaeser, S., Schaefer, C., and Kilger, E. (2006). Exogenous induction of cerebral beta-amyloidogenesis is governed by agent and host. *Science.* 313, 1781–1784. doi: 10.1126/science.1131864
- Morales, R., Bravo-Alegria, J., Duran-Aniotz, C., and Soto, C. (2015a). Titration of biologically active amyloid- β seeds in a transgenic mouse model of Alzheimer's disease. *Sci. Reports.* 5, 1–8. doi: 10.1038/srep09349
- Morales, R., Bravo-Alegria, J., Moreno-Gonzalez, I., Duran-Aniotz, C., Gamez, N., and Edwards, G. (2021). Transmission of cerebral amyloid pathology by peripheral administration of misfolded A β aggregates. *Mol. Psychiatry.* 2021, 1–12. doi: 10.1038/s41380-021-01150-w
- Morales, R., Callegari, K., and Soto, C. (2015b). Prion-like features of misfolded A β and tau aggregates. *Virus Res.* 207, 106–112. doi: 10.1016/j.virusres.2014.12.031
- Morales, R., Duran-Aniotz, C., Castilla, J., Estrada, L. D., and Soto, C. (2011). De novo induction of Amyloid-beta deposition in vivo. *Mol. Psych.* 17, 1347–53. doi: 10.1038/mp.2011.120
- Moreno-Gonzalez, I., and Soto, C. (2011). Misfolded protein aggregates: mechanisms, structures and potential for disease transmission. *Semin. Cell Dev. Biol.* 22, 482–487. doi: 10.1016/j.semcdb.2011.04.002
- Moreno-Gonzalez, I., and Soto, C. (2018). Natural animal models of neurodegenerative protein misfolding diseases. *Curr. Pharm. Des.* 18. doi: 10.2174/138161212799315768
- Nisbet, R. M., Polanco, J. C., Ittner, L. M., and Götz, J. (2015). Tau aggregation and its interplay with amyloid- β . *Acta Neuropathol.* 3, 207–220. doi: 10.1007/s00401-014-1371-2
- Price, J. L., McKeel D. W. Jr., Buckles, V. D., Roe, C. M., Xiong, C., Grundman M., et al. (2009). Neuropathology of nondemented aging: presumptive evidence for preclinical Alzheimer disease. *NeurobiolAging.* 30, 1026–1036. doi: 10.1016/j.neurobiolaging.2009.04.002
- Prusiner, S. B. (1998). The prion diseases. *Brain Pathol.* 8, 499–513. doi: 10.1111/j.1750-3639.1998.tb00171.x
- Prusiner, S. B. (2012). Cell biology. A unifying role for prions in neurodegenerative diseases. *Science.* 336, 1511–1513. doi: 10.1126/science.1222951
- Rising, A., Gherardi, P., Chen, G., Johansson, J., Oskarsson, M. E., and Westermark, G. T. (2021). AA amyloid in human food chain is a possible biohazard. *Sci Reports.* 11, 21069. doi: 10.1038/s41598-021-00588-w
- Ritchie, D. L., Adlard, P., Peden, A. H., Lowrie, S., Le Grice, M., and Burns, K. (2017). Amyloid- β accumulation in the CNS in human growth hormone recipients in the UK. *Acta Neuropathol.* 134, 221–240. doi: 10.1007/s00401-017-1703-0
- Rosen, R. F., Fritz, J. J., Dooyema, J., Cintron, A. F., Hamaguchi, T., and Lah, J. J. (2011). Exogenous seeding of cerebral beta-amyloid deposition in betaAPP-transgenic rats. *J. Neurochem.* 120, 660–666. doi: 10.1111/j.1471-4159.2011.07551.x
- Scott, M. R., Will, R., Ironside, J., Nguyen, H. O., Tremblay, P., DeArmond, S. J., et al. (1999). Compelling transgenic evidence for transmission of bovine spongiform encephalopathy prions to humans. *Proc Natl Acad Sci U S A.* 96, 15137–15142. doi: 10.1073/pnas.96.26.15137
- Soto, C. (2003). Unfolding the role of protein misfolding in neurodegenerative diseases. *Nat. Rev. Neurosci.* 4, 49–60. doi: 10.1038/nrn1007
- Soto, C. (2012). Transmissible proteins: expanding the prion heresy. *Cell.* 149, 968–77. doi: 10.1016/j.cell.2012.05.007
- Soto, C., Estrada, L., and Castilla, J. (2006). Amyloids, prions and the inherent infectious nature of misfolded protein aggregates. *Trends Biochem. Sci.* 31, 150–155. doi: 10.1016/j.tibs.2006.01.002
- Stöhr, J., Watts, J. C., Mensinger, Z. L., Oehler, A., Grillo, S. K., DeArmond, S. J., et al. (2012). Purified and synthetic Alzheimer's amyloid beta (A β) prions. *Proc. Natl. Acad. Sci. U S A.* 109, 11025–30. doi: 10.1073/pnas.1206555109

- Tagliavini, F., Giaccone, G., Frangione, B., and Bugiani, O. (1988). Preamyloid deposits in the cerebral cortex of patients with Alzheimer's disease and nondemented individuals. *NeurosciLett.* 93, 191–196. doi: 10.1016/0304-3940(88)90080-8
- Thal, D. R., Attems, J., and Ewers, M. (2014). Spreading of amyloid, tau, and microvascular pathology in alzheimer's disease: Findings from neuropathological and neuroimaging studies. *J. Alzheimer's Dis.* S421–S429. doi: 10.3233/JAD-141461
- Walker, L. C., and Jucker, M. (2015). Neurodegenerative diseases: expanding the prion concept. *Annu. Rev. Neurosci.* 38, 87–103. doi: 10.1146/annurev-neuro-071714-033828
- Walker, L. C., Levine, 3rd H., Mattson, M. P., and Jucker, M. (2006). Inducible proteopathies. *Trends Neurosci.* 29, 438–443. doi: 10.1016/j.tins.2006.06.010
- Watts, J. C., Giles, K., Grillo, S. K., Lemus, A., DeArmond, S. J., Prusiner, S. B. (2011). Bioluminescence imaging of Aβ deposition in bigenic mouse models of Alzheimer's disease. *Proc. Natl. Acad. Sci. U S A.* 108, 2528–2533. doi: 10.1073/pnas.1019034108

Conflict of Interest: The authors declare that the research was conducted in the absence of any commercial or financial relationships that could be construed as a potential conflict of interest.

Publisher's Note: All claims expressed in this article are solely those of the authors and do not necessarily represent those of their affiliated organizations, or those of the publisher, the editors and the reviewers. Any product that may be evaluated in this article, or claim that may be made by its manufacturer, is not guaranteed or endorsed by the publisher.

Copyright © 2022 Moreno-Gonzalez, Edwards, Morales, Duran-Aniotz, Escobedo, Marquez, Pumarola and Soto. This is an open-access article distributed under the terms of the Creative Commons Attribution License (CC BY). The use, distribution or reproduction in other forums is permitted, provided the original author(s) and the copyright owner(s) are credited and that the original publication in this journal is cited, in accordance with accepted academic practice. No use, distribution or reproduction is permitted which does not comply with these terms.

Frontiers in Aging Neuroscience

Explores the mechanisms of central nervous system aging and age-related neural disease

The third most-cited journal in the field of geriatrics and gerontology, with a focus on understanding the mechanistic processes associated with central nervous system aging.

Discover the latest Research Topics

[See more →](#)

Frontiers

Avenue du Tribunal-Fédéral 34
1005 Lausanne, Switzerland
frontiersin.org

Contact us

+41 (0)21 510 17 00
frontiersin.org/about/contact

